frontiers | Research Topics

The role of GABA-shift in neurodevelopment and psychiatric disorders

Edited by
Lorenz S. Neuwirth, Abdeslem El Idrissi, Atsuo Fukuda and Werner Kilb

Published in
Frontiers in Molecular Neuroscience

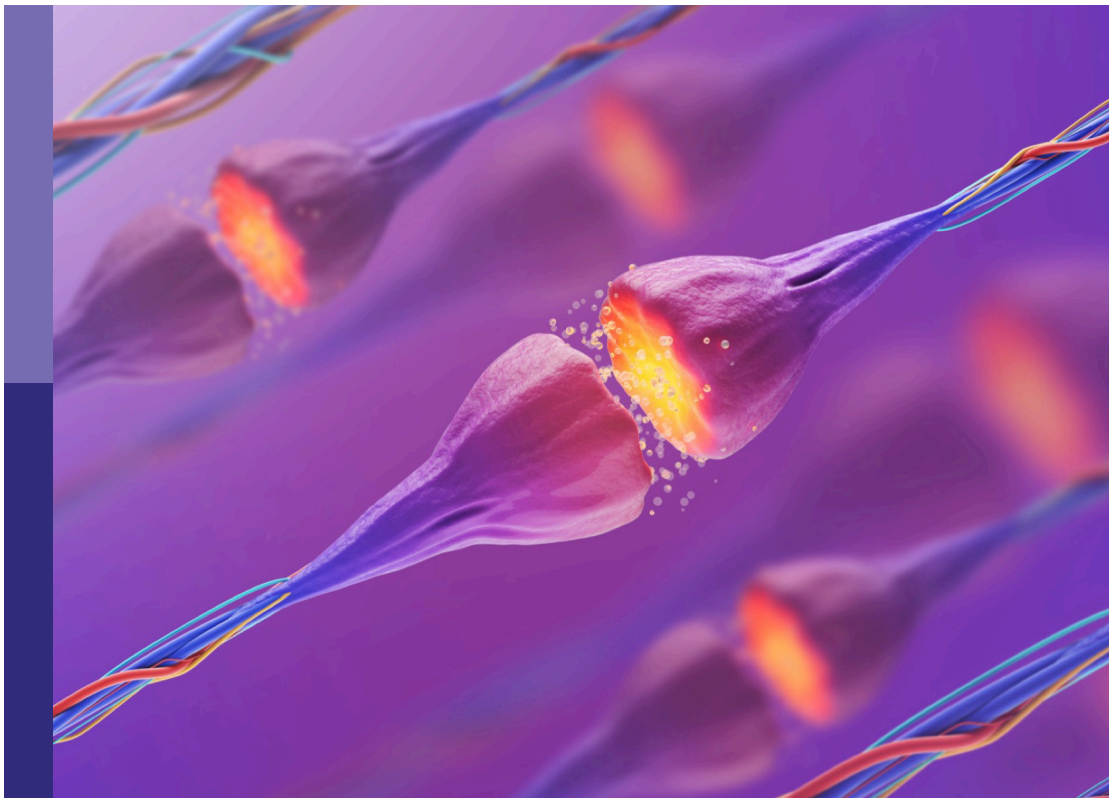

ISSN 1664-8714
ISBN 978-2-83251-918-9
DOI 10.3389/978-2-83251-918-9

About Frontiers

Frontiers is more than just an open access publisher of scholarly articles: it is a pioneering approach to the world of academia, radically improving the way scholarly research is managed. The grand vision of Frontiers is a world where all people have an equal opportunity to seek, share and generate knowledge. Frontiers provides immediate and permanent online open access to all its publications, but this alone is not enough to realize our grand goals.

Frontiers journal series

The Frontiers journal series is a multi-tier and interdisciplinary set of open-access, online journals, promising a paradigm shift from the current review, selection and dissemination processes in academic publishing. All Frontiers journals are driven by researchers for researchers; therefore, they constitute a service to the scholarly community. At the same time, the *Frontiers journal series* operates on a revolutionary invention, the tiered publishing system, initially addressing specific communities of scholars, and gradually climbing up to broader public understanding, thus serving the interests of the lay society, too.

Dedication to quality

Each Frontiers article is a landmark of the highest quality, thanks to genuinely collaborative interactions between authors and review editors, who include some of the world's best academicians. Research must be certified by peers before entering a stream of knowledge that may eventually reach the public - and shape society; therefore, Frontiers only applies the most rigorous and unbiased reviews. Frontiers revolutionizes research publishing by freely delivering the most outstanding research, evaluated with no bias from both the academic and social point of view. By applying the most advanced information technologies, Frontiers is catapulting scholarly publishing into a new generation.

What are Frontiers Research Topics?

Frontiers Research Topics are very popular trademarks of the *Frontiers journals series*: they are collections of at least ten articles, all centered on a particular subject. With their unique mix of varied contributions from Original Research to Review Articles, Frontiers Research Topics unify the most influential researchers, the latest key findings and historical advances in a hot research area.

Find out more on how to host your own Frontiers Research Topic or contribute to one as an author by contacting the Frontiers editorial office: frontiersin.org/about/contact

The role of GABA-shift in neurodevelopment and psychiatric disorders

Topic editors

Lorenz S. Neuwirth — State University of New York at Old Westbury, United States
Abdeslem El Idrissi — The City University of New York, United States
Atsuo Fukuda — Hamamatsu University School of Medicine, Japan
Werner Kilb — Johannes Gutenberg University Mainz, Germany

Citation

Neuwirth, L. S., El Idrissi, A., Fukuda, A., Kilb, W., eds. (2023). *The role of GABA-shift in neurodevelopment and psychiatric disorders*. Lausanne: Frontiers Media SA.
doi: 10.3389/978-2-83251-918-9

Table of contents

frontiers | Frontiers in Molecular Neuroscience

TYPE Editorial
PUBLISHED 28 February 2023
DOI 10.3389/fnmol.2023.1162689

OPEN ACCESS

EDITED AND REVIEWED BY
Clive R. Bramham,
University of Bergen, Norway

*CORRESPONDENCE
Lorenz S. Neuwirth
✉ neuwirthl@oldwestbury.edu
Abdeslem El Idrissi
✉ abdeslem.elidrissi@csi.cuny.edu
Atsuo Fukuda
✉ axfukuda@hama-med.ac.jp
Werner Kilb
✉ wkilb@uni-mainz.de

SPECIALTY SECTION
This article was submitted to Neuroplasticity and Development, a section of the journal Frontiers in Molecular Neuroscience

RECEIVED 09 February 2023
ACCEPTED 10 February 2023
PUBLISHED 28 February 2023

CITATION
Neuwirth LS, El Idrissi A, Fukuda A and Kilb W (2023) Editorial: The role of GABA-shift in neurodevelopment and psychiatric disorders. *Front. Mol. Neurosci.* 16:1162689. doi: 10.3389/fnmol.2023.1162689

Editorial: The role of GABA-shift in neurodevelopment and psychiatric disorders

Lorenz S. Neuwirth[1,2]*, Abdeslem El Idrissi[3,4]*, Atsuo Fukuda[5]* and Werner Kilb[6]*

[1]Department of Psychology, SUNY Old Westbury, Old Westbury, NY, United States, [2]SUNY Neuroscience Research Institute, SUNY Old Westbury, Old Westbury, NY, United States, [3]Center for Developmental Neuroscience, The College of Staten Island (CUNY), Staten Island, NY, United States, [4]Department of Biology, The College of Staten Island (CUNY), Staten Island, NY, United States, [5]Department of Neurophysiology, Hamamatsu University School of Medicine, Hamamatsu, Japan, [6]Institute of Physiology, University Medical Center, Johannes Gutenberg University, Mainz, Germany

KEYWORDS

GABA, $GABA_A$ receptor ($GABA_AR$), KCC2, NKCC1, Cl^- homeostasis

Editorial on the Research Topic
The role of GABA-shift in neurodevelopment and psychiatric disorders

The main inhibitory neurotransmitter in the mature brain, GABA, has the unique feature that post-synaptic responses upon it's interaction with $GABA_A$ receptors can change their direction in response to alterations in the intracellular Cl^- concentration. This GABA-shift plays an important role during early neurodevelopment and has been implicated in a variety of neuropathological conditions. The mechanisms behind the GABA-shift are mediated by changes in the expression and functions of key transporters for Cl^- and bicarbonate, in particular, Cl^- transporters NKCC1 (i.e., mediating Cl^- import) and KCC2 (i.e., mediating Cl^- extrusion). The current Research Topic sought to provide a forum for reviewing recent progress in this fascinating field and to collect recent studies investigating the role of the GABA-shift in neurodevelopment and in the etiology of neurological diseases.

The current Research Topic comprises five review articles and seven original research articles. The review articles provide an update on features of the GABA-shift, spanning from the structural basis of its regulation, *via* its role during neurodevelopment up to new perspectives for the etiology and treatment of neurological disorders. The original research articles focus on the role of Cl^- homeostasis under physiological conditions or in neurological disorders and present new experimental methods to determine the reversal potential of GABA.

A thorough introduction into the molecular basis of Cl^- homeostasis and regulation is provided by the review article of Hartmann and Nothwang, which provides an update on the structural basis underlying the regulation of KCC2 and NKCC1. The authors characterize phosphorylation sites on both transporters and describe the functional consequences of phosphorylation/dephosphorylation at these sites. They conclude that the intracellular loop between the α8 and α9 helix represents a region of particular importance for the functional regulation of KCC2. The review article by Kilb emphasizes that depolarizing GABAergic responses are not excitatory *per se* and provides a theoretical framework and experimental findings determining whether GABAergic depolarizations are inhibitory or excitatory. A more global review on GABAergic neurodevelopment is provided by Warm et al., summarizing the role of GABAergic interneuron populations in the functional maturation of the cerebral cortex and further describing the mutual interaction between maturation of the GABAergic system and cortical network activity. The remaining two review articles focus on the role of the GABA-shift in neurological and neuropsychiatric diseases. Hui et al.

discusses how the developmental shift from excitatory-to-inhibitory GABAergic actions is altered in neurodevelopmental and neuropsychiatric disorders. They concentrate on the cell signaling and regulatory mechanisms underlying this GABA-shift and discuss how the GABA-shift influences interactions between GABAergic interneurons and other cell types in the developing brain and thereby contributes to neurodevelopment. Finally, they briefly outline recent progress on targeting NKCC1 and KCC2 as a therapeutic strategy against neurodevelopmental and neuropsychiatric disorders. More specifically, Huang et al. concentrated on the role of the GABAergic system in post-traumatic stress disorders (PSTD) and reviewed changes of the GABAergic system in PTSD based on imaging and pharmacological results from both preclinical and clinical studies and derived putative pharmacological targets that might be helpful in the future treatment of PTSD.

The original research article of Vazetdinova et al. reported the accuracy of cell-attached recordings to determine important cellular physiological parameters, which established that cell-attached recordings of cortical and hippocampal neurons can be used to reliably determine the GABA reversal potential and other physiologically relevant parameters. Therefore, cell-attached recordings can be used to investigate the GABA-shift, because they don't artificially disturb the intracellular Cl^- concentration. Two original research reports deal with the role of hyperpolarized GABAergic responses in GABAergic interneurons for the control of cortical excitability. Zavalin et al. reported that depletion of KCC2 in Dlx5-lineage neurons, which targets several types of GABAergic interneurons including parvalbumin-positive interneurons (PV-INs), induces a massive change in the distribution of GABA interneuron subpopulations, a high incidence of spontaneous seizures, and a high rate of premature death in juvenile animals. In contrast to their initial hypothesis, they did not observe migration deficits or disturbed laminar organization of interneurons, indicating that the adverse effects should occur later. Alternatively, they observed a milder phenotype in mice if KCC2 expression was obsolete only in PV-INs. In line with this, Herrmann et al. reported that a Cre-mediated disruption of KCC2 specifically in PV-INs led to the expected shift in the GABA reversal potential and a higher frequency of inhibitory post-synaptic potentials, indicating a disinhibition of PV-INs. In addition, these animals displayed a reduced seizure threshold with the occurrence of increased spontaneous seizures and an upregulation of pro-apoptotic genes in parvalbumin-positive interneurons.

At several locations in the adult brain, the developmental GABA-shift does not occur and GABA maintains a depolarizing action until adulthood. One of these regions is the hypothalamic medial eminence, involved in the hypothalamic-pituitary-adrenal (HPA) axis of corticosterone release. Yesmin et al. investigated the GABAergic network in this area and observed that a subpopulation of GABAergic neurons directly project to the axon terminals from CRH neurons. The conditional deletion of NKCC1 from the CRH axon terminals results in significantly lower corticosterone levels, demonstrating the important role of depolarizing GABAergic responses in the HPA axis and may serve as an early pathological trigger for later psychiatric issues.

Three additional articles revealed that modification of GABAergic system elements can led to persisting alterations in the excitability unrestricted to the GABAergic system. Sinha et al. reported that a depletion of WNK3, a developmentally expressed member of the WNK-family that regulates Cl^- homeostasis *via* phosphorylation of NKCC1 and KCC2, results in slightly higher intracellular Cl- concentrations. However, the authors observed that other neuronal properties determining excitability (e.g., K^+-channel expression) are also altered in the WNK3 knockout animals, but that this effect can be ameliorated by an overexpression of KCC2, suggesting that the interactive function of WNK3 is probably the maintenance and development of both intrinsic and synaptic excitabilities. A comparable interaction between the GABAergic synaptic system and intrinsic neuronal excitability was reported by Hosoi et al., who investigated the role of taurine, an important agonist of the GABAergic system during early development and a modulator of WNK and hence Cl^- homeostasis, on the excitability of matured neurons. They report an obvious alteration of firing properties in differentiated Layer 2/3 pyramidal neurons of taurine-depleted animals. Lastly, Qin et al. discloses that inhibition of σ1- receptors, an orphan-receptor associated to depression-like phenotypes, reduces the expression of the $GABA_A$ receptor subunits α1, α2, β2, and β3 in the nucleus accumbens. The resulting reduction in GABAergic transmission contributes to the impaired long-term depression and a depression-like phenotype in these mice.

In summary, the current Research Topic summarizes recent opinions on advancing our understanding of the mechanisms and functional consequences of the GABA-shift from the last three decades, but also provides evidence that changes in the GABAergic responses, either acute or during early developmental stages, can lead to persistent functional changes in the nervous system by affecting the GABA-shift and other subsequent processes that move beyond the GABAergic system completing the full integration of the mature brain.

Author contributions

All authors listed have made a substantial, direct, and intellectual contribution to the work and approved it for publication.

Conflict of interest

The authors declare that the research was conducted in the absence of any commercial or financial relationships that could be construed as a potential conflict of interest.

Publisher's note

frontiers in Molecular Neuroscience

REVIEW
published: 24 November 2021
doi: 10.3389/fnmol.2021.747835

When Are Depolarizing GABAergic Responses Excitatory?

*Werner Kilb**

Institute of Physiology, University Medical Center of the Johannes Gutenberg-University Mainz, Mainz, Germany

The membrane responses upon activation of GABA(A) receptors critically depend on the intracellular Cl^- concentration ($[Cl^-]_i$), which is maintained by a set of transmembrane transporters for Cl^-. During neuronal development, but also under several pathophysiological conditions, the prevailing expression of the Cl^- loader NKCC1 and the low expression of the Cl^- extruder KCC2 causes elevated $[Cl^-]_i$, which result in depolarizing GABAergic membrane responses. However, depolarizing GABAergic responses are not necessarily excitatory, as GABA(A) receptors also reduces the input resistance of neurons and thereby shunt excitatory inputs. To summarize our knowledge on the effect of depolarizing GABA responses on neuronal excitability, this review discusses theoretical considerations and experimental studies illustrating the relation between GABA conductances, GABA reversal potential and neuronal excitability. In addition, evidences for the complex spatiotemporal interaction between depolarizing GABAergic and glutamatergic inputs are described. Moreover, mechanisms that influence $[Cl^-]_i$ beyond the expression of Cl^- transporters are presented. And finally, several *in vitro* and *in vivo* studies that directly investigated whether GABA mediates excitation or inhibition during early developmental stages are summarized. In summary, these theoretical considerations and experimental evidences suggest that GABA can act as inhibitory neurotransmitter even under conditions that maintain substantial depolarizing membrane responses.

Keywords: chloride homeostasis, NKCC1, KCC2, SLC12A2, SLC12A5, gaba receptor, neuronal development

OPEN ACCESS

Edited by:
Andreas Vlachos,
University of Freiburg, Germany

Reviewed by:
Imre Vida,
Charité University Medicine Berlin, Germany
Corette J. Wierenga,
Utrecht University, Netherlands

***Correspondence:**
Werner Kilb
wkilb@uni-mainz.de

Specialty section:
This article was submitted to Neuroplasticity and Development, a section of the journal Frontiers in Molecular Neuroscience

Received: *26 July 2021*
Accepted: *28 October 2021*
Published: *24 November 2021*

Citation:
Kilb W (2021) When Are Depolarizing GABAergic Responses Excitatory? Front. Mol. Neurosci. 14:747835. doi: 10.3389/fnmol.2021.747835

INTRODUCTION

About 30–40 years ago it was first published that $GABA_A$ receptors can mediate depolarizing and even excitatory membrane responses in the immature brain (Mueller et al., 1983; Ben-Ari et al., 1989; Luhmann and Prince, 1991), in contrast to the general textbook knowledge that GABA mediates inhibitory and mostly hyperpolarizing neurotransmission in the CNS. In the following decades, it has been shown that depolarizing GABAergic membrane responses play an essential role for cortical development (Ben-Ari, 2002; Owens and Kriegstein, 2002; Kirmse and Holthoff, 2020) and that such depolarizing GABAergic responses can be re-attained under pathophysiological conditions like trauma, stroke or epilepsy (Jaenisch et al., 2010; Dzhala et al., 2012; Kaila et al., 2014; Liu et al., 2020).

The main molecular mechanisms underlying these depolarizing membrane responses have in the meantime been unraveled (Blaesse et al., 2009; Loscher et al., 2013; Watanabe and Fukuda, 2015; Virtanen et al., 2020) and the existence of depolarizing GABAergic responses had been demonstrated *in vivo* (Kirmse et al., 2015; Valeeva et al., 2016; Murata and Colonnese, 2020). Thus evidences indicate that the direction of GABAergic membrane responses shows a striking modification during neurodevelopment and under pathophysiological conditions, a process termed "GABA-shift". Regarding the physiological consequences of this "GABA-shift" it is, however, important to consider that depolarizing GABAergic responses can mediate inhibition already during early postnatal development (Khalilov et al., 1999; Kolbaev et al., 2011a; Kirmse et al., 2015; Valeeva et al., 2016) and that inhibitory responses in the adult CNS can be accompanied by GABAergic depolarizations (Andersen et al., 1980; Misgeld et al., 1982; Staley and Mody, 1992). To provide a current concept of the functional impact of depolarizing GABAergic responses, I summarize in this review theoretical considerations and experimental studies that illustrate how the relation between GABA conductances, GABA reversal potential and membrane potential changes determines the impact of GABA on neuronal excitability. In addition, I review studies that directly investigated whether GABA mediates excitation during early developmental stages.

Cl^- AND HCO_3^- SET THE PACE FOR THE EFFECTS OF $GABA_A$ RECEPTORS

The flux of the hydrophilic Cl^- ions across the hydrophobic plasma membrane occurs exclusively *via* integral membrane proteins that mediate Cl^- transport. Passive Cl^- fluxes are mediated by a heterogeneous set of anion channels that are more or less specific for Cl^- ions (Duran et al., 2010; Jentsch and Pusch, 2018), including the $GABA_A$ receptor (Farrant and Kaila, 2007). The passive Cl^- fluxes through these anion channels follow the electromotive force for Cl^- ions (EMF_{Cl}), which depends on the difference between the Cl^- equilibrium potential (E_{Cl}) and the membrane potential (E_m). In consequence, hyperpolarizing or depolarizing GABAergic responses require that the intracellular Cl^- concentration ($[Cl^-]_i$) is not in an equilibrium state. Active transmembrane transport is required for accumulation or depletion of Cl^- from cells (Huebner and Holthoff, 2013; Kaila et al., 2014). In the absence of such active transport processes $[Cl^-]_i$ follows a passive distribution, which due to the negative E_m is set at low millimolar concentrations under physiological conditions (given by the Nernst equation). Either primary active Cl^- transport, *via* an ATP-dependent Cl^- pump, or secondary active transport, coupling Cl^- transport to the transport of another ions along their gradient, is required to obtain $[Cl^-]_i$ below or above this passive distribution. The major proteins that mediate secondary active transmembrane Cl^- transport are Na^+-dependent K^+/Cl^--cotransporters (NKCC), K^+/Cl^--cotransporters (KCC) and Cl^-/HCO_3^--antiporters (Payne et al., 2003; Blaesse et al., 2009; **Figure 1**), whereas there is currently little evidence for a neuronal Cl^--dependent ATPase or Cl^- pump (Gerencser and Zhang, 2003). The most important Cl^- loader in neurons is NKCC1 (SLC12A2), an ubiquitously expressed Cl^- transporter that utilizes the inwardly directed Na^+ gradient to mediate an electroneutral import of Cl^- ions (and K^+ ions) into cells (Russell, 2000; Virtanen et al., 2020). The main transporter responsible for the low $[Cl^-]_i$ of mature neurons is KCC2 (SLC12A5; Rivera et al., 1999; Lee et al., 2005), which uses the outwardly directed K^+ gradient to extrude Cl^-. In addition, the isoforms KCC1, KCC3, and KCC4 were expressed in some neuron populations, but these isoforms can also be found in non-neuronal tissue (Becker et al., 2003). The anion exchanger (AE3) mediates the counter-transport of one Cl^- with one HCO_3^-, thus leading to Cl^- accumulation at physiological pH values (Gonzalez-Islas et al., 2009; Pfeffer et al., 2009). The contribution of Na^+-dependent Cl^-/HCO_3^--antiporters, which mediate Cl^- extrusion, to neuronal $[Cl^-]_i$ homeostasis is less clear (Huebner and Holthoff, 2013). And finally, Misgeld and coworkers demonstrated that the combination of voltage-dependent Cl^- channels with depolarizing E_m transients can also lead to an elevated $[Cl^-]_i$ (Titz et al., 2003).

$GABA_A$ receptors also have a considerable HCO_3^- permeability (Farrant and Kaila, 2007; Blaesse et al., 2009). The relative HCO_3^- permeability of $GABA_A$ receptors is between 0.18 and 0.44 of the Cl^- permeability (Bormann et al., 1987; Fatima-Shad and Barry, 1993). Due to the rather positive equilibrium potential for HCO_3^- (E_{HCO3}), which is around −10 mV, the HCO_3^- fluxes always add a depolarizing component to the GABAergic current (Rivera et al., 2005; Huebner and Holthoff, 2013). The high E_{HCO3} is a consequence of the low intracellular HCO_3^- concentration ($[HCO_3^-]_i$), which is on one hand maintained by secondary active HCO_3^- uptake *via* electroneutral and electrogenic Na^+/HCO_3^- symporters (Sinning et al., 2011; Huebner and Holthoff, 2013). On the other hand, the $[HCO_3^-]_i$ is directly linked to the intracellular pH (pH_i) *via* the carbonic anhydrase (Sinning and Hübner, 2013). Thus at physiological pH values between 7.0 and 7.4 (Ruffin et al., 2014), which is maintained by aforementioned Na^+/HCO_3^- symporters and the Na^+/H^+ exchanger (Ruffin et al., 2014), $[HCO_3^-]_i$ values of ca. 14 mM can be estimated (Lombardi et al., 2019). In consequence, E_{GABA} is typically positive to E_{Cl}, albeit the contribution of E_{HCO3} to E_{GABA} becomes smaller with higher $[Cl^-]_i$ (Farrant and Kaila, 2007). During massive GABAergic stimulation, e.g., during epileptic seizures, the stable depolarizing drive of the GABAergic HCO_3^- currents will enhance activity-dependent Cl^- uptake and thus directly contributes to the generation of GABAergic excitation under this conditions (Kaila et al., 1997; Ruusuvuori et al., 2004).

EXPRESSION PROFILE OF Cl^- LOADERS AND Cl^- EXTRUDERS (AND WHY THIS DOES NOT TELL EVERYTHING ABOUT GABA ACTIONS)

During development the different Cl^--transporters are differentially expressed in the nervous system (Blaesse et al., 2009;

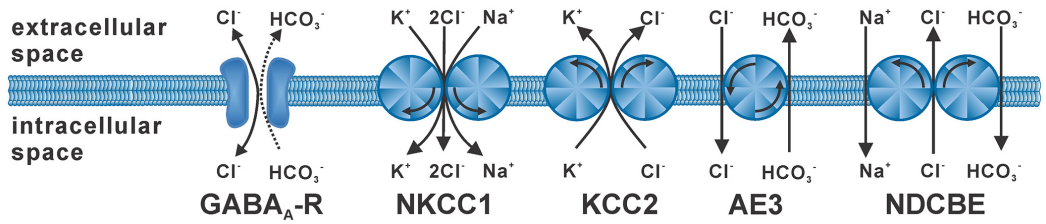

FIGURE 1 | Stoichiometry and typical operation of secondary active Cl^- transporters. The $GABA_A$ receptor ($GABA_A$-R) mediates mainly Cl^- fluxes and to a lesser extent HCO_3^- fluxes. NKCC1 mediates uptake of two Cl^- ions with of one K^+ and one Na^+ ion. KCC2 mediates extrusion of one Cl^- with one K^+ ion. The anion-exchanger (AE3) is supposed to mediate uptake of one Cl^- ion in antiport with one HCO_3^- ion. The Na^+-dependent Cl^-/HCO_3^- exchanger (NDCBE) utilizes the Na^+ gradient to extrude Cl^- ions.

Huebner and Holthoff, 2013; Kaila et al., 2014; Kirmse et al., 2018). The expression levels of NKCC1 vary significantly between neuronal cell types and between different developmental or functional states of individual neurons (Watanabe and Fukuda, 2015; Virtanen et al., 2020).

Experimental studies show that NKCC1 expression either declines (Plotkin et al., 1997) or increases (Clayton et al., 1998) during development. Therefore, no general statements about the trend of NKCC1 expression level during development could be made (Virtanen et al., 2020). In contrast, the expression of KCC2 has been tightly correlated to the developmental downregulation of $[Cl^-]_i$. Suppression of functional KCC2 expression increases neuronal $[Cl^-]_i$ (Rivera et al., 1999; Pellegrino et al., 2011), whereas enhancing the functional expression of KCC2 during early developmental stages leads to a reduced neuronal $[Cl^-]_i$ (Lee et al., 2005). The expression of KCC2 occurs typically delayed to the expression of NKCC1 (Lu et al., 1999; Rivera et al., 1999; Stein et al., 2004), with the temporal profile of KCC2 expression depending on brain structures (Watanabe and Fukuda, 2015), cortical layers (Li et al., 2002; Shimizu-Okabe et al., 2002), and neuronal cell types (Ikeda et al., 2003; Clarkson and Herbison, 2006). In particular, GABAergic interneurons seem to display systematically more depolarized GABA reversal potentials (E_{GABA}) than glutamatergic or principle neurons in the amygdala and neocortex (Martina et al., 2001), the cerebellum (Chavas and Marty, 2003), and in the hippocampus (Elgueta and Bartos, 2019; Otsu et al., 2020). For the hippocampus this has directly been related to a lower KCC2 expression in the GABAergic interneurons (Elgueta and Bartos, 2019). There are also evidences that the expression ratio between NKCC1 and KCC2 can be different in distinct compartments of the same cell (Virtanen et al., 2020). The most striking example is the axon initial segment, in which GABAergic synapses mediate depolarizing responses with putative excitatory effect (Szabadics et al., 2006; Khirug et al., 2008), which has been linked to the delayed shift in the expression ration of Cl^- transporter expression in this compartment (Rinetti-Vargas et al., 2017). The observation of a somatodencritic $[Cl^-]_i$ gradient (Kuner and Augustine, 2000; Elgueta and Bartos, 2019) suggest a variable NKCC1/KCC2 expression ratio within dendritic membranes.

A variety of pathophysiological conditions are also linked to massive changes in the $[Cl^-]_i$ -homeostasis (Kaila et al., 2014). It has been shown that depolarizing GABAergic responses and/or an high NKCC1/KCC2 expression ration can be re-attained for example after traumatic (Toyoda et al., 2003; Dzhala et al., 2012) or ischemic (Jaenisch et al., 2010) insults, in peri-tumor regions (Pallud et al., 2014; Campbell et al., 2015) and as cause or consequence of epilepsy (Fujiwara-Tsukamoto et al., 2003; Aronica et al., 2007; Huberfeld et al., 2007; Buchin et al., 2016; Burman et al., 2019; Liu et al., 2020). The putative switch in GABAergic responses from excitation to inhibition related to this alterations can aggravate the clinical consequences of these neuropathologies (Kaila et al., 2014).

However, it should always be kept in mind that both KCC2 and NKCC1 are highly regulated proteins (Russell, 2000; Blaesse et al., 2009; Kaila et al., 2014). For example it has been demonstrated that membrane trafficking and functional expression of KCC2 is tightly controlled by the sonic hedgehog pathway, neuronal-restricted silencing element or the neurotrophin BDNF (Karadsheh and Delpire, 2001; Rivera et al., 2002; Delmotte et al., 2020). In addition, the activity of KCC2 can be modulated by phosphorylation (Wake et al., 2007; Banke and Gegelashvili, 2008) and thereby neurotransmitters can directly interfere with the $[Cl^-]_i$ homeostasis (Banke and Gegelashvili, 2008; Inoue et al., 2012; Yang et al., 2015). Thus the $[Cl^-]_i$ is clearly regulated beyond the expression ratio of Cl^- transporters.

The situation is made even more complicated by the fact that $[Cl^-]_i$, is also directly influenced by GABAergic activity *via* Cl^- fluxes across $GABA_A$ receptors (Wright et al., 2011; Raimondo et al., 2012; Branchereau et al., 2016). This is not only relevant for high, pathophysiological activity patterns, but also for physiological levels of neuronal activity (Gonzalez-Islas et al., 2010; Kolbaev et al., 2011b; Currin et al., 2020). In-silico experiments show that these activity-dependent $[Cl^-]_i$ changes are influenced by the dendritic morphology, membrane properties as well as the kinetics of GABAergic inputs, $[Cl^-]_i$ homeostasis and $[HCO_3^-]_i$ homeostasis (Doyon et al., 2016a; Mohapatra et al., 2016; Düsterwald et al., 2018; Lombardi et al., 2019). In addition, such activity-dependent $[Cl^-]_i$ transients are augmented by coincident glutamatergic inputs (Halbhuber et al., 2019; Lombardi et al., 2021). Thus the impact of neuronal

activity on $[Cl^-]_i$ is probably particularly relevant under *in vivo* situations, where an ongoing "bombardment" with GABAergic and glutamatergic synaptic inputs has been suggested (Steriade, 2001).

In summary, these facts demonstrate that, although an increasing KCC2 expression is correlated to a $[Cl^-]_i$ decline during neuronal development, the precise $[Cl^-]_i$, and thus the GABAergic effects cannot be directly estimated from the general expression level of KCC2. In particular, results from *in vitro* experiments may overestimate the *in vivo* levels of $[Cl^-]_i$ in immature neurons (and underestimate them in adult neurons), because the influence of neuronal activity on $[Cl^-]_i$ is negligible due to the limited activity in the *in vitro* preparations.

RELATION BETWEEN $[Cl^-]_i$, GABAergic MEMBRANE RESPONSES AND EXCITATION/INHIBITION

The $[Cl^-]_i$ is a main factor that determines EMF_{Cl} and thus the direction and size of Cl^- fluxes through the anion-pore of $GABA_A$ receptors (Farrant and Kaila, 2007). As mentioned before, HCO_3^- fluxes contribute to GABAergic membrane responses, because $GABA_A$ receptors have a considerable HCO_3^- permeability (Farrant and Kaila, 2007). EMF_{HCO3} is directed outwards and therefore HCO_3^- efflux adds a depolarizing component to GABAergic responses. Whereas the HCO_3^- fluxes shift GABA responses in depolarizing direction for low $[Cl^-]_i$, their contribution is relatively small at higher $[Cl^-]_i$ (Farrant and Kaila, 2007). Because of its mostly minor contribution and in order to make the following considerations more concise, HCO_3^--fluxes will not be taken into account in the remainder of this review. Nevertheless, the (small) depolarizing HCO_3^--currents *via* $GABA_A$ receptors will slightly enhance the excitatory potency of GABAergic effects.

When considering the effect of GABA on neuronal excitability, one should keep in mind that GABA can mediate inhibition by two mechanisms (Farrant and Kaila, 2007): first, by hyperpolarization, which increases the difference between E_m and the AP threshold (**Figure 2A**, left traces), and second by a decreased membrane resistivity upon $GABA_A$ receptor activation (**Figure 2A**, right traces), which shunts excitatory synaptic inputs (Edwards, 1990; Staley and Mody, 1992; Farrant and Kaila, 2007). However, in reality both effects act in parallel (**Figure 2B**). To predict the effects of GABA on the excitability, it is necessary to delineate how both mechanisms are related to $[Cl^-]_i$. If EMF_{Cl^-} is negative (i.e., $[Cl^-]_i$ is below the passive distribution) activation of $GABA_A$ receptors will induce a Cl^- influx and thus hyperpolarize the membrane. Such a membrane hyperpolarization, together with the membrane shunting, will increases the amount of excitatory synaptic currents required to cross the AP threshold. Thus it is obvious that under low $[Cl^-]_i$ conditions $GABA_A$ receptors mediate an inhibitory effect on neuronal membranes. It is sometimes considered that at higher $[Cl^-]_i$ GABA receptors mediate an opposite effect, because the depolarizing GABAergic responses shift E_m towards AP threshold. However, under this condition the excitatory influence of this depolarizing effect is opposed by the reduction in the membrane resistivity, which in parallel shunts excitatory postsynaptic potentials (Edwards, 1990; Staley and Mody, 1992; Egawa and Fukuda, 2013). Thereby depolarizing GABAergic responses can also reduce excitatory influence and thus mediate inhibition (**Figure 2B**). The central question arising from these considerations is: Which GABAergic membrane depolarization is required to mediate an excitatory response, i.e., to increase the probability to trigger an AP?

Theoretically, this question can be easily addressed by calculating the membrane depolarization and the shunting effect that are caused by a given GABAergic conductance. The maximal GABAergic depolarization is, in accordance with Ohm's law, given by the product of the GABAergic current (I_{GABA}) and the input resistance (R_{Input}). I_{GABA} is given by the product of EMF_{Cl} (when the GABAergic HCO_3^- permeability is neglected) and g_{GABA}. A combination of these functions define the relation between g_{GABA} and EMF_{Cl} and can be used to estimate under which conditions GABA responses itself can reach AP threshold and trigger APs (**Figure 2C**).

However, this situation does not reflect the physiologically relevant situation. More relevant is the question whether subthreshold GABAergic depolarizations can attenuate or augment the excitatory effect of additional excitatory synaptic inputs. In this respect it must be considered that the increase in g_{GABA}, which is necessarily linked to the depolarization, also reduces the membrane resistivity and thus shunts excitatory synaptic inputs. The impact of both effects on the excitability can be estimated in a simplified model for E_m (which neglects the HCO_3^- conductance of $GABA_A$ receptors) as follows:

$$E_m = \frac{RT}{F} * ln \left(\frac{g_{Na}^{pas}[Na^+]_e + g_K^{pas}[K^+]_e + g_{GABA}[Cl^-]_i + g_{AMPA}[Na^+]_e + g_{AMPA}[K^+]_e}{g_{Na}^{pas}[Na^+]_i + g_K^{pas}[K^+]_i + g_{GABA}[Cl^-]_e + g_{AMPA}[Na^+]_i + g_{AMPA}[K^+]_i} \right)$$

(with g_{Na}^{pas} and g_K^{pas} as passive membrane conductance for Na^+ and K^+, g_{GABA} and g_{AMPA} as conductance of GABA and AMPA receptors, and $[X^+]_i$ and $[X^+]_e$ as intra- and extracellular concentration of the ion X^+, respectively). Note that at this moment we use a rather simple model that neglects capacitive currents, the time course of GABAergic and glutamatergic conductances, as well as spatial integration (Gidon and Segev, 2012). Thus this formula describes only the interaction of stationary GABAergic and glutamatergic conductances.

Using this formula, the g_{Glu} value leading to a depolarization that equals the AP threshold (E_{Thr}) can be calculated as follows:

$$g_{Glu}^{Thr} = \frac{e^F g_K^{pas}[K^+]_e - g_K^{pas}[K^+]_i + e^F g_{Na}^{pas}[Na^+]_e - g_K^{pas}[Na^+]_i + e^F g_{GABA}[Cl^-]_i - g_{GABA}[Cl^-]_e}{[Na^+]_i + [K^+]_i - e^F[K^+]_a - e^F[Na^+]_a}$$

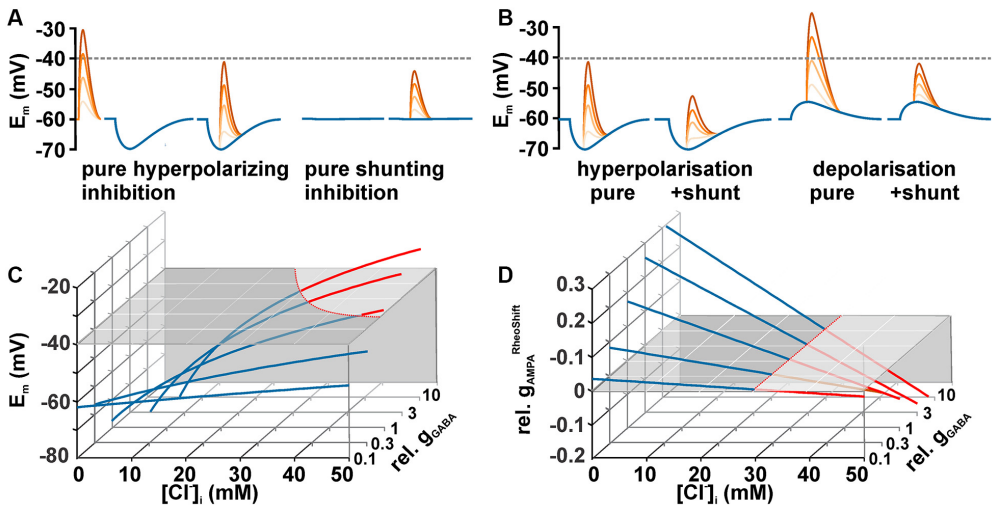

FIGURE 2 | Dependency between $[Cl^-]_i$ and GABAergic actions. **(A)** Schematic diagrams illustrating the two exemplary effects of GABAergic inputs (blue traces) on glutamatergic inputs (red traces) of different intensities. A GABAergic hyperpolarization augments the distance between peak glutamate depolarization and the AP threshold (hyperpolarizing inhibition). At a passive Cl^--distribution GABA does not affect E_m, but the decreased membrane resistivity induced by GABA reduced the peak glutamate depolarization (shunting inhibition). The dashed line represents a hypothetical action potential threshold. **(B)** Schematic diagrams illustrating that the combination of the membrane potential shift with the shunting effect caused by the decreased membrane resistivity augments the effect of a hyperpolarization inhibition (left traces) and can lead to inhibition even at depolarizing GABAergic membrane responses (right traces). **(C)** $[Cl^-]_i$-dependency of the membrane potential (E_m) calculated for five different GABAergic conductances (g_{GABA}, normalized to g_{Input}) under stationary conditions (see main text for details). The gray plane represents AP threshold. Note that considerable g_{GABA} in combination with high $[Cl^-]_i$ is needed for a suprathreshold GABAergic depolarization. **(D)** Dependency of $g_{AMPA}{}^{Rheoshift}$ (normalized to g_{Input}, ; $g_{AMPA}{}^{Rheoshift} = g_{AMPA}$ in presence of GABA minus g_{AMPA} in absence of GABA) on $[Cl^-]_i$ and g_{GABA}. Red traces indicate excitatory and blue traces inhibitory GABAergic effects. Note that $g_{GABA}{}^{Rheoshift}$ becomes negative at identical $[Cl^-]_i$ independent of g_{GABA}.

$$with\ e^F = 10^{\frac{E_{Thr}}{-61mv}}\ (\text{for a given T of } 37^\circ C)$$

These threshold g_{Glu} values (g_{Glu}^{Thr}) describe the excitatory conductance required to just reach AP threshold. To quantify the GABAergic effect on the excitability, g_{Glu}^{Thr} determined in the absence of GABA (i.e., $g_{GABA} = 0$) is subtracted from g_{Glu}^{Thr} determined in the presence of GABA. This value is termed GABAergic rheobase shift ($g_{Glu}^{Rheoshift}$). Negative $g_{Glu}^{Rheoshift}$ values characterize an excitatory GABAergic action (less g_{Glu} is required to induce APs). Intriguingly, GABA mediates an excitatory action, independent of the g_{GABA} values, for all $[Cl^-]_i \geq 29.5$ mM in the exemplary simulated neuron used for **Figure 2D**. Note that this $[Cl^-]_i$ corresponds to an E_{GABA} that is identical to the AP threshold of −40 mV used in this model. This relation suggests that GABA mediate an excitation whenever E_{GABA} is positive to AP threshold. This theoretical suggestion is in line with previous assumptions that GABA mediate an excitatory effect as long as E_{GABA} is above AP threshold (Ben-Ari, 2002; Owens and Kriegstein, 2002) and it was replicated in patch-clamp experiments (Kolbaev et al., 2011a).

However, as already mentioned the previous considerations are clearly an oversimplification as they: (i) neglect additional voltage gated conductances that contribute to excitability (Valeeva et al., 2010); and (ii) represent only stationary conductances in a quasi one-dimensional situation ignoring the consequences of the temporal relation between GABA and glutamatergic inputs (Gao et al., 1998; Gulledge and Stuart, 2003) and the complex neuronal topologies (Jadi et al., 2012; Spruston et al., 2016) on spatiotemporal properties of GABAergic inhibition/excitation.

To understand the influence of temporal relation between GABA and glutamatergic inputs on the excitability, it is important to consider that the GABAergic membrane depolarization outlasts the GABAergic conductance increase (**Figure 3A**). The amplitude of a glutamatergic excitatory postsynaptic potential (ePSP) drops by shunting effects when it was evoked in synchrony to the GABAergic input. However, when the glutamatergic input was stimulated during the late phase of the GABAergic depolarization (when the GABAergic conductance ceases, but the GABAergic depolarization is still present), temporal summation lead to an increased peak voltage of the compound postsynaptic potential (PSP; **Figure 3B**). Thereby, GABA can mediate a substantial inhibitory effect on synchronously occurring glutamatergic inputs, while the longer lasting depolarization can enhance the amplitude of delayed ePSPs and thus mediate excitation (**Figure 3C**). Such a temporal shunting-to-excitation sequence has already been shown *in vitro* (Gao et al., 1998; Gulledge and Stuart, 2003; Bracci and Panzeri, 2006). This finding also implies that for excitatory inputs that occur with a substantial delay after the GABA input mainly the GABAergic depolarization is effective and thus an excitatory effect can be imposed whenever E_{GABA} is positive to RMP. In consequence, GABA may more probably have an excitatory effect when GABA inputs are not temporally correlated to glutamatergic inputs, e.g., for tonic GABAergic

inhibition (Song et al., 2011; Kolbaev et al., 2012). On the other hand, when GABA and glutamate inputs are temporally highly correlated, e.g., at feedback, feedforward, or lateral inhibition, GABA mediates a reliable inhibition as long as E_{GABA} is below AP threshold.

To address the role of complex neuronal topologies on the GABAergic effect, it must be considered: (i) that $GABA_A$ receptor activation influences the length and time constant of membranes and (ii) that the GABAergic effect depends on the spatial relation between the GABAergic and the glutamatergic inputs. A simple NEURON-based in-silico simulation demonstrate that a GABAergic PSPs showed the typical decline in the amplitude with increasing dendritic distance (**Figure 4A**), which reflects the length constant within a linear neuronal structure (Rall, 1989). On the other hand, the membrane shunting effect demonstrated a more complex behavior (Gulledge and Stuart, 2003; Gidon and Segev, 2012). If the GABA synapse is located between the soma and the excitatory glutamatergic input ("on-path", Gidon and Segev, 2012) a stable attenuation of the ePSP amplitude occurs (**Figure 4B**). But when the GABA synapse is distal to the AMPA synapse ("off-path"), the shunting declines rather fast (**Figure 4B**). To estimate whether GABA has an excitatory or inhibitory influence, the interaction between the wide spreading depolarizing effect (**Figure 4A**) and the complex spatial profile of shunting inhibition (**Figure 4B**) is fundamental. The co-stimulation of a depolarizing GABA synapse which is co-localized to an AMPA synapse mediate an inhibitory effect (**Figure 4C**), suggesting a dominance of the shunting effect. With increasing distance between the GABA and the AMPA synapse the shunting effect was attenuated and the excitatory potential of the GABAergic depolarization dominates, leading to an excitatory effect of the co-stimulation (**Figure 4C**). Thus even under mild depolarizing conditions found in dendrites of mature cortical pyramidal cells (Kuner and Augustine, 2000) GABAergic stimulation in the remote dendritic compartment can mediate an excitatory response (Gulledge and Stuart, 2003).

Of note, these findings have some implication for the inhibition mediated by GABA receptors. The typical perisomatic GABAergic inputs of parvalbumin-positive basket interneurons (Freund, 2003; Elgueta and Bartos, 2019) will mediate a stable inhibitory effect, even at depolarizing GABAergic responses, since they can effectively shunt ePSPs. In contrast, for GABAergic synapses located in the dendritic periphery, e.g., from hippocampal O-LM interneurons (Somogyi and Klausberger, 2005) or neocortical Martinotti interneurons (Ascoli et al., 2008; Gidon and Segev, 2012), depolarizing GABA responses can more easily mediate an excitatory effect on glutamatergic inputs from distant sites in the dendrite.

In summary, the action of GABA did not only depend on the ratio between E_{GABA} and the AP threshold, but also on the spatiotemporal relation between the GABAergic and glutamatergic inputs. Thus, under physiological conditions depolarizing GABAergic inputs can mediate in the same cell excitation as well as inhibition, depending on the exact spatiotemporal relation between both inputs. Thus it is difficult or even impossible to make general predictions for a global effect of depolarizing GABAergic responses. However, from the published observations one can presume: (i) that at sufficiently high E_{GABA} above the AP threshold reliable excitation is mediated by $GABA_A$ receptors; (ii) that at intermediate E_{GABA} levels GABA mediates a dominant inhibitory effect for spatially and temporally correlated inputs; and (iii) that the effect of GABA on delayed or spatially separated inputs can be excitatory under this conditions. Thus the typical GABAergic feedforward or feedback loops with perisomatic terminals will already mediate inhibition, even at higher $[Cl^-]_I$ that are typical during development (Farrant and Kaila, 2007; Blaesse et al., 2009). In addition, these synapses will be rather resistant to activity-dependent $[Cl^-]_i$ increases (Wright et al., 2011; Doyon et al., 2016b; Lombardi et al., 2018). In contrast, other modes of GABAergic mechanisms are more prone to mediate an excitatory influence at rather moderate $[Cl^-]_i$ increases.

EXAMPLES FOR EXCITATORY AND INHIBITORY GABAergic EFFECTS IN THE IMMATURE CNS

With all of the information provided above, one of the major questions remaining is, of course, whether the depolarizing $GABA_A$ receptor-mediated responses in the immature CNS (Ben Ari et al., 2012) have a net excitatory or inhibitory effect.

Several *in vitro* studies demonstrate that activation of $GABA_A$ receptors can mediate excitatory inputs in immature neurons. For example, it was demonstrated that hippocampal giant depolarizations critically depend on tonic depolarizing GABAergic currents (Ben-Ari et al., 1989; Sipila et al., 2005). Gramicidin-perforated or cell-attached patch-clamp experiments, which both did not artificially alter $[Cl^-]_i$ and thus allow estimating the physiological GABA responses, demonstrated suprathreshold GABAergic responses in neocortical (Dammerman et al., 2000; Hanganu et al., 2002; Rheims et al., 2008; Sava et al., 2014), hippocampal (Khazipov et al., 1997; Leinekugel et al., 1997; Sauer and Bartos, 2010; Valeeva et al., 2013), and hypothalamic neurons (Wang et al., 2001). And finally, optogenetic activation of GABAergic interneurons *in vitro* increases the frequency of neocortical and hippocampal EPSCs (Valeeva et al., 2016), as well as synchronous network activity (Flossmann et al., 2019), demonstrating a direct excitatory effect of GABA in neuronal networks. Excitatory GABAergic actions have also been found in mature neurons for distant off-path GABAergic inputs (Gulledge and Stuart, 2003).

In contrast to these reports of excitatory GABAergic actions, several *in vitro* studies also demonstrate that GABAergic stimulation can mediate inhibition already in early postnatal neurons (Agmon et al., 1996; Khalilov et al., 1999; Lamsa et al., 2000). The frequent observations that inhibition of $GABA_A$ receptors provoke epileptiform discharges in the immature CNS (Khalilov et al., 1999; Wells et al., 2000; Richter et al., 2010; Kolbaev et al., 2012; Sharopov et al., 2019) also suggest that GABA may mediate a net inhibitory effect in immature hippocampal and neocortical networks. However, depolarizing

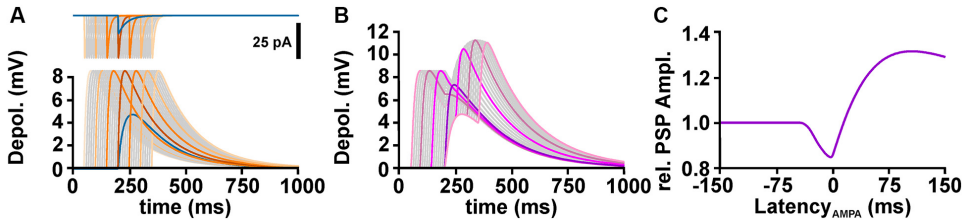

FIGURE 3 | Temporal profile of GABAergic shunting and GABAergic depolarizing effects on excitatory glutamatergic inputs. **(A)** The upper traces illustrate GABAergic (blue line) and glutamatergic (orange and gray lines) currents provided at latencies between −150 and +150 ms. The lower traces illustrate the postsynaptic potentials (PSPs) evoked by these currents. Note that the PSPs outlast the synaptic currents. **(B)** Compound PSPs induced by the co-stimulation of GABA and glutamate synapses, with the glutamatergic inputs provided at latencies between −150 and +150 ms. **(C)** Peak amplitude of compound PSP, normalized to the glutamatergic PSP in the absence of GABA, plotted against the latency between AMPA and GABA stimuli, as shown in **(B)**. Note that the compound PSP amplitude drops if glutamatergic synapses are activated within a narrow interval around coincident stimulation, but increases when AMPA receptors are stimulated several ms after the GABA input.

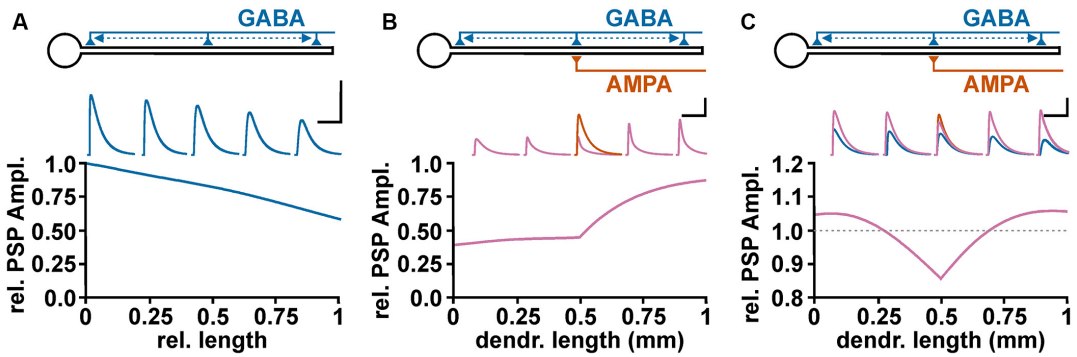

FIGURE 4 | Spatial profile of GABAergic depolarization and GABAergic shunting effects on excitatory glutamatergic inputs. **(A)** Relative amplitude of GABAergic PSPs, as measured at the soma, upon activation of a depolarizing GABA synapse (E_{GABA} = −52 mV) at different dendritic positions. The voltage traces above graph illustrate GABAergic PSPs at 0%, 25%, 50%, 75%, and 100% of the dendritic length. Scale bar in **(A–C)** is 5 mV/500 ms. **(B)** Profile of the GABAergic shunting effect on glutamatergic inputs, calculated by normalizing the amplitude of the compound PSPs obtained in the presence of GABA (purple traces) to the EPSC amplitude obtained in the absence of GABA inputs (orange trace). In these experiments the shunting effect was isolated by maintaining E_{GABA} at resting membrane potential. Note that GABA synapses located proximally to the AMPA synapse ("on-path") mediate a stable shunting effect, while for GABA synapses distal to the AMPA synapse ("off-path") the shunting effect declines rather fast. **(C)** Effect of a depolarizing GABAergic input (E_{GABA} = −52 mV) at different positions along the dendrite on the peak compound PSP amplitude during co-stimulation The blue traces represent purely GABAergic PSPs, the orange trace the glutamatergic PSP, and the purple traces the compound PSPs upon co-activation of AMPA and GABA synapses. Note that GABA inputs mediate an inhibitory effect when co-localized with the AMPA synapse, while at more distant on-path and off-path synapses an excitatory effect is observed.

GABAergic responses has been suggested to significantly contribute to epilepsy in the immature CNS (Dzhala and Staley, 2003; Dzhala et al., 2005; Khalilov et al., 2005; Nardou et al., 2009, 2013). This discrepancy most probably reflects the complexity of functional consequences of depolarizing GABAergic responses. Notably, *in vitro* experiments demonstrated that weak GABAergic stimulation can promote excitation, whereas stronger GABAergic currents mediate inhibition (Khalilov et al., 1999; Winkler et al., 2019), indicating that the balance between GABAergic depolarization and shunt determines the net effect. In line with the aforementioned spatiotemporal dependency of GABAergic effects, it has been observed in the immature hippocampus that synaptic $GABA_A$ receptors mediate an anticonvulsive and tonic $GABA_A$ receptors a proconvulsive effect (Kolbaev et al., 2012). In summary, these experiments promote the view that it depends, in addition to the $[Cl^-]_i$, on the properties and mode of GABAergic stimulation whether GABA has a pro- or anticonvulsive effect.

However, the *in vitro* experiments summarized above represent fairly artificial conditions that may severely interfere with $[Cl^-]_i$ homeostasis. The slicing procedures used for the generation of most *in vitro* preparation represent a traumatic insult, which alters the expression and function of NKCC1 and/or KCC2 and led to an increased $[Cl^-]_i$ in many neurons within such preparations (Dzhala et al., 2012). In addition, neuronal activity, and thus most probably also the frequency of GABAergic inputs, is massively reduced in most *in vitro* preparations (Steriade, 2001). However, the frequency of GABAergic inputs massively influences $[Cl^-]_i$ and lead in immature neurons to a reduction of their high $[Cl^-]_i$ (Kolbaev et al., 2011b; Wright et al., 2011; Lombardi et al., 2018). Thus,

in vitro condition may systematically overestimate the excitatory capacity of $GABA_A$ receptors. Thus it is essential that the effect of GABA in immature nervous systems must also be investigated under *in vivo* conditions.

Seminal *in vivo* experiments addressing the functional responses of GABA on cortical neurons during early developmental stages demonstrated that exogenously applied GABA indeed mediates depolarizing membrane responses, but that these responses reduce neuronal activity in the developing neocortex (Kirmse et al., 2015). In line with these results, optogenetic activation of GABAergic interneurons *in vivo* decreases the frequency of neocortical and hippocampal EPSCs already at early developmental stages (Valeeva et al., 2016), demonstrating a direct inhibitory effect of GABA on neuronal networks. Interestingly, this *in vivo* result is opposing the observation made in the same study under *in vitro* conditions, emphasizing the limitations of conclusions drawn from *in vitro* experiments. Also the observations that the GABA antagonist gabazine enhances the frequency of spindle bust oscillation in the early postnatal neocortex *in vivo* (Minlebaev et al., 2007), and that GABAergic agonists attenuate epileptiform activity *in vivo* (Isaev et al., 2005) already suggest a putative inhibitory role of GABA at this developmental stage.

On the other hand, recent studies demonstrated that activation of GABAergic interneurons *in vivo* can also enhance network activity in the immature hippocampus, suggesting that also under *in vivo* conditions GABA may exert an excitatory effect in this region. Using DREADD as well as optogenetic approaches, it was demonstrated that activation of GABAergic interneurons enhances and inhibition of GABAergic interneurons suppresses network activity in hippocampus of non-anesthetized 3 day old mice pups (Murata and Colonnese, 2020). This effect reversed to GABAergic inhibition already at the 7th postnatal day (Murata and Colonnese, 2020). Comparable results are observed when depolarizing GABAergic responses during early development are minimized by a conditional NKCC1 knockout in pyramidal neurons. In these animals the spontaneous correlated network activity in the hippocampus was attenuated (Graf et al., 2021), suggesting a putative excitatory effect of depolarizing GABAergic responses in the immature hippocampus. However, in line with the previous *in vivo* studies on neocortical areas these two *in vivo* study demonstrated for the visual cortex that activation of GABAergic interneurons mediates inhibition already at the 3rd postnatal day (Murata and Colonnese, 2020) and that a conditional NKCC1 knockout in pyramidal neurons of the visual cortex has no effect on the typical network activity (Graf et al., 2021).

CONCLUSION

While it is obvious that the effect of $GABA_A$ receptor activation critically depends on the $[Cl^-]_i$, and thus on the expression and function of Cl^- transporters, theoretical consideration and many experimental findings indicate that the effect of GABA on the excitability cannot reliably be predicted only from the expression ratio of Cl^- transporters or the $[Cl^-]_i$. Several additional parameters determine whether GABA mediate excitation or inhibition at a given $[Cl^-]_i$. Recent experimental evidences suggest that GABA probably mediates inhibition already in the immature cortex, whereas it may contribute to excitation in the immature hippocampus. However, these experiments can, of course, not predict GABAergic effects during fetal stages or in brain structures that have not been investigated yet.

AUTHOR CONTRIBUTIONS

WK conceptualized and wrote this manuscript.

FUNDING

WK received funding from the Deutsche Forschungsgemeinschaft (DFG-grant Ki835/3).

ACKNOWLEDGMENTS

WK thanks Heiko J. Luhmann, Anne Sinning, Peter Jedlicka, and Atsuo Fukuda for intense discussion on this topic. The valuable contribution of Aniello Lombardi, Sergey Kolbaev, Katharina Achilles, Lisa Halbhuber, Akihito Okabe, Chigusa Shimizu-Okabe, Ileana Hanganu-Opatz, Junko Yamada, Salim Sharopov, Daniel Richter, Bogdan Sava, Haiyan Sun, Sigrid Stroh-Kaffei, Violetta Steinbrecher, and Beate Krumm to the experimental evaluation of the complex relation between $GABA_A$ receptors and the $[Cl^-]_i$ is highly acknowledged.

REFERENCES

Agmon, A., Hollrigel, G., and O'Dowd, D. K. (1996). Functional GABAergic synaptic connection in neonatal mouse barrel cortex. *J. Neurosci.* 16, 4684–4695. doi: 10.1523/JNEUROSCI.16-15-04684.1996

Andersen, P., Dingledine, R., Gjerstad, L., Langmoen, I. A., and Laursen, A. M. (1980). Two different responses of hippocampal pyramidal cells to application of gamma-amino butyric acid. *J. Physiol.* 305, 279–296. doi: 10.1113/jphysiol.1980.sp013363

Aronica, E., Boer, K., Redeker, S., Spliet, W. G. M., van Rijen, P. C., Troost, D., et al. (2007). Differential expression patterns of chloride transporters, Na^+-K^+-$2Cl^-$-cotransporter and K^+-Cl^--cotransporter, in epilepsy-associated malformations of cortical development. *Neuroscience* 145, 185–196. doi: 10.1016/j.neuroscience.2006.11.041

Ascoli, G. A., Alonso-Nanclares, L., Anderson, S. A., Barrionuevo, G., Benavides-Piccione, R., Burkhalter, A., et al. (2008). Petilla terminology: nomenclature of features of GABAergic interneurons of the cerebral cortex. *Nat. Rev. Neurosci.* 9, 557–568. doi: 10.1038/nrn2402

Banke, T. G., and Gegelashvili, G. (2008). Tonic activation of group I mGluRs modulates inhibitory synaptic strength by regulating KCC2 activity. *J. Physiol.* 586, 4925–4934. doi: 10.1113/jphysiol.2008.157024

Becker, M., Nothwang, H. G., and Friauf, E. (2003). Differential expression pattern of chloride transporters NCC, NKCC2, KCC1, KCC3, KCC4 and AE3 in the developing rat auditory brainstem. *Cell Tissue Res.* 312, 155–165. doi: 10.1007/s00441-003-0713-5

Ben-Ari, Y. (2002). Excitatory actions of GABA during development: the nature of the nurture. *Nat. Rev. Neurosci.* 3, 728–739. doi: 10.1038/nrn920

Ben-Ari, Y., Cherubini, E., Corradetti, R., and Gaiarsa, J.-L. (1989). Giant synaptic potentials in immature rat CA3 hippocampal neurones. *J. Physiol.* 416, 303–325. doi: 10.1113/jphysiol.1989.sp017762

Ben Ari, Y., Woodin, M. A., Sernagor, E., Cancedda, L., Vinay, L., Rivera, C., et al. (2012). Refuting the challenges of the developmental shift of polarity of GABA actions: GABA more exciting than ever!. *Front. Cell. Neurosci.* 6:35. doi: 10.3389/fncel.2012.00035

Blaesse, P., Airaksinen, M. S., Rivera, C., and Kaila, K. (2009). Cation-chloride cotransporters and neuronal function. *Neuron* 61, 820–838. doi: 10.1016/j.neuron.2009.03.003

Bormann, J., Hamill, O. P., and Sakmann, B. (1987). Mechanism of anion permeation through channels gated by glycine and gamma-aminobutyric acid in mouse cultured spinal neurones. *J. Physiol.* 385, 243–286. doi: 10.1113/jphysiol.1987.sp016493

Bracci, E., and Panzeri, S. (2006). Excitatory GABAergic effects in striatal projection neurons. *J. Neurophysiol.* 95, 1285–1290. doi: 10.1152/jn.00598.2005

Branchereau, P., Cattaert, D., Delpy, A., and Allain, A. (2016). Depolarizing GABA/glycine synaptic events switch from excitation to inhibition during frequency increases. *Sci. Rep.* 6:21753. doi: 10.1038/srep21753

Buchin, A., Chizhov, A., Huberfeld, G., Miles, R., and Gutkin, B. S. (2016). Reduced efficacy of the KCC2 cotransporter promotes epileptic oscillations in a subiculum network model. *J. Neurosci.* 36, 11619–11633. doi: 10.1523/JNEUROSCI.4228-15.2016

Burman, R. J., Selfe, J. S., Lee, J. H., Van Den Berg, M., Calin, A., Codadu, N. K., et al. (2019). Excitatory GABAergic signalling is associated with benzodiazepine resistance in status epilepticus. *Brain* 142, 3482–3501. doi: 10.1093/brain/awz283

Campbell, S. L., Robel, S., Cuddapah, V. A., Robert, S., Buckingham, S. C., Kahle, K. T., et al. (2015). GABAergic disinhibition and impaired KCC2 cotransporter activity underlie tumor-associated epilepsy. *Glia* 63, 23–36. doi: 10.1002/glia.22730

Chavas, J., and Marty, A. (2003). Coexistence of excitatory and inhibitory GABA synapses in the cerebellar interneuron network. *J. Neurosci.* 23, 2019–2031. doi: 10.1523/JNEUROSCI.23-06-02019.2003

Clarkson, J., and Herbison, A. E. (2006). Development of GABA and glutamate signaling at the GnRH neuron in relation to puberty. *Mol. Cell. Endocrinol.* 254–255, 32–38. doi: 10.1016/j.mce.2006.04.036

Clayton, G. H., Owens, G. C., Wolff, J. S., and Smith, R. L. (1998). Ontogeny of cation-Cl^- cotransporter expression in rat neocortex. *Brain Res. Dev. Brain Res.* 109, 281–292. doi: 10.1016/s0165-3806(98)00078-9

Currin, C. B., Trevelyan, A. J., Akerman, C. J., and Raimondo, J. V. (2020). Chloride dynamics alter the input-output properties of neurons. *PLoS Comput. Biol.* 16:e1007932. doi: 10.1371/journal.pcbi.1007932

Dammerman, R. S., Flint, A. C., Noctor, S., and Kriegstein, A. R. (2000). An excitatory GABAergic plexus in developing neocortical layer 1. *J. Neurophysiol.* 84, 428–434. doi: 10.1152/jn.2000.84.1.428

Delmotte, Q., Hamze, M., Medina, I., Buhler, E., Zhang, J., Belgacem, Y. H., et al. (2020). Smoothened receptor signaling regulates the developmental shift of GABA polarity in rat somatosensory cortex. *J. Cell Sci.* 133:jcs247700. doi: 10.1242/jcs.247700

Doyon, N., Prescott, S. A., and De Koninck, Y. (2016a). Mild KCC2 hypofunction causes inconspicuous chloride dysregulation that degrades neural coding. *Front. Cell. Neurosci.* 9:516. doi: 10.3389/fncel.2015.00516

Doyon, N., Vinay, L., Prescott, S. A., and De Koninck, Y. (2016b). Chloride regulation: a dynamic equilibrium crucial for synaptic inhibition. *Neuron* 89, 1157–1172. doi: 10.1016/j.neuron.2016.02.030

Duran, C., Thompson, C. H., Xiao, Q., and Hartzell, H. C. (2010). Chloride channels: often enigmatic, rarely predictable. *Annu. Rev. Physiol.* 72, 95–121. doi: 10.1146/annurev-physiol-021909-135811

Düsterwald, K. M., Currin, C. B., Burman, R. J., Akerman, C. J., Kay, A. R., and Raimondo, J. V. (2018). Biophysical models reveal the relative importance of transporter proteins and impermeant anions in chloride homeostasis. *eLife* 7:e39575. doi: 10.7554/eLife.39575

Dzhala, V. I., and Staley, K. J. (2003). Excitatory actions of endogenously released GABA contribute to initiation of ictal epileptiform activity in the developing hippocampus. *J. Neurosci.* 23, 1840–1846. doi: 10.1523/JNEUROSCI.23-05-01840.2003

Dzhala, V. I., Talos, D. M., Sdrulla, D. A., Brumback, A. C., Mathews, G. C., Benke, T. A., et al. (2005). NKCC1 transporter facilitates seizures in the developing brain. *Nat. Med.* 11, 1205–1213. doi: 10.1038/nm1301

Dzhala, V., Valeeva, G., Glykys, J., Khazipov, R., and Staley, K. (2012). Traumatic alterations in GABA signaling disrupt hippocampal network activity in the developing brain. *J. Neurosci.* 32, 4017–4031. doi: 10.1523/JNEUROSCI.5139-11.2012

Edwards, D. H. (1990). Mechanisms of depolarizing inhibition at the crayfish giant motor synapse. I. Electrophysiology. *J. Neurophysiol.* 64, 532–540. doi: 10.1152/jn.1990.64.2.532

Egawa, K., and Fukuda, A. (2013). Pathophysiological power of improper tonic GABAAconductances in mature and immature models. *Front. Neural Circuits* 7:170. doi: 10.3389/fncir.2013.00170

Elgueta, C., and Bartos, M. (2019). Dendritic inhibition differentially regulates excitability of dentate gyrus parvalbumin-expressing interneurons and granule cells. *Nat. Commun.* 10:5561. doi: 10.1038/s41467-019-13533-3

Farrant, M., and Kaila, K. (2007). The cellular, molecular and ionic basis of GABA(A) receptor signalling. *Prog. Brain Res.* 160, 59–87. doi: 10.1016/S0079-6123(06)60005-8

Fatima-Shad, K., and Barry, P. H. (1993). Anion permeation in GABA- and glycine-gated channels of mammalian cultured hippocampal neurons. *Proc. Biol. Sci.* 253, 69–75. doi: 10.1098/rspb.1993.0083

Flossmann, T., Kaas, T., Rahmati, V., Kiebel, S. J., Witte, O. W., Holthoff, K., et al. (2019). Somatostatin interneurons promote neuronal synchrony in the neonatal hippocampus. *Cell Rep.* 26, 3173–3182.e5. doi: 10.1016/j.celrep.2019.02.061

Freund, T. F. (2003). Interneuron Diversity series: Rhythm and mood in perisomatic inhibition. *Trends Neurosci.* 26, 489–495. doi: 10.1016/S0166-2236(03)00227-3

Fujiwara-Tsukamoto, Y., Isomura, Y., Nambu, A., and Takada, M. (2003). Excitatory gaba input directly drives seizure-like rhythmic synchronization in mature hippocampal CA1 pyramidal cells. *Neuroscience* 119, 265–275. doi: 10.1016/s0306-4522(03)00102-7

Gao, X. B., Chen, G., and Van Den Pol, A. N. (1998). GABA-dependent firing of glutamate-evoked action potentials at AMPA/kainate receptors in developing hypothalamic neurons. *J. Neurophysiol.* 79, 716–726. doi: 10.1152/jn.1998.79.2.716

Gerencser, G. A., and Zhang, J. L. (2003). Existence and nature of the chloride pump. *Biochim. Biophys. Acta* 1618, 133–139. doi: 10.1016/j.bbamem.2003.09.013

Gidon, A., and Segev, I. (2012). Principles governing the operation of synaptic inhibition in dendrites. *Neuron* 75, 330–341. doi: 10.1016/j.neuron.2012.05.015

Gonzalez-Islas, C., Chub, N., Garcia-Bereguiain, M. A., and Wenner, P. (2010). GABAergic synaptic scaling in embryonic motoneurons is mediated by a shift in the chloride reversal potential. *J. Neurosci.* 30, 13016–13020. doi: 10.1523/JNEUROSCI.1659-10.2010

Gonzalez-Islas, C., Chub, N., and Wenner, P. (2009). NKCC1 and AE3 appear to accumulate chloride in embryonic motoneurons. *J. Neurophysiol.* 101, 507–518. doi: 10.1152/jn.90986.2008

Graf, J., Zhang, C., Marguet, S. L., Herrmann, T., Flossmann, T., Hinsch, R., et al. (2021). A limited role of NKCC1 in telencephalic glutamatergic neurons for developing hippocampal network dynamics and behavior. *Proc. Natl. Acad. Sci. U S A* 118:e2014784118. doi: 10.1073/pnas.2014784118

Gulledge, A. T., and Stuart, G. J. (2003). Excitatory actions of GABA in the cortex. *Neuron* 37, 299–309. doi: 10.1016/s0896-6273(02)01146-7

Halbhuber, L., Achtner, C., Luhmann, H. J., Sinning, A., and Kilb, W. (2019). Coincident activation of glutamate receptors enhances GABAA receptor-induced ionic plasticity of the intracellular Cl^--concentration in dissociated neuronal cultures. *Front. Cell. Neurosci.* 13:497. doi: 10.3389/fncel.2019.00497

Hanganu, I. L., Kilb, W., and Luhmann, H. J. (2002). Functional synaptic projections onto subplate neurons in neonatal rat somatosensory cortex. *J. Neurosci.* 22, 7165–7176. doi: 10.1523/JNEUROSCI.22-16-07165.2002

Huberfeld, G., Wittner, L., Clemenceau, S., Baulac, M., Kaila, K., Miles, R., et al. (2007). Perturbed chloride homeostasis and GABAergic signaling in human temporal lobe epilepsy. *J. Neurosci.* 27, 9866–9873. doi: 10.1523/JNEUROSCI.2761-07.2007

Huebner, C. A., and Holthoff, K. (2013). Anion transport and GABA signaling. *Front. Cell. Neurosci.* 7:177. doi: 10.3389/fncel.2013.00177

Ikeda, M., Toyoda, H., Yamada, J., Okabe, A., Sato, K., Hotta, Y., et al. (2003). Differential development of cation-chloride cotransporters and Cl-homeostasis contributes to differential GABAergic actions between developing rat visual cortex and dorsal lateral geniculate nucleus. *Brain Res.* 984, 149–159. doi: 10.1016/s0006-8993(03)03126-3

Inoue, K., Furukawa, T., Kumada, T., Yamada, J., Wang, T., Inoue, R., et al. (2012). Taurine inhibits K^+-Cl^- cotransporter KCC2 to regulate embryonic Cl^- homeostasis *via* with-no-lysine (WNK) protein kinase signaling pathway. *J. Biol. Chem.* 287, 20839–20850. doi: 10.1074/jbc.M111.319418

Isaev, D., Isaeva, E., Khazipov, R., and Holmes, G. L. (2005). Anticonvulsant action of GABA in the high potassium-low magnesium model of ictogenesis in the neonatal rat hippocampus *in vivo* and *in vitro*. *J. Neurophysiol.* 94, 2987–2992. doi: 10.1152/jn.00138.2005

Jadi, M., Polsky, A., Schiller, J., and Mel, B. W. (2012). Location-dependent effects of inhibition on local spiking in pyramidal neuron dendrites. *PLoS Comput. Biol.* 8:e1002550. doi: 10.1371/journal.pcbi.1002550

Jaenisch, N., Witte, O. W., and Frahm, C. (2010). Downregulation of potassium chloride cotransporter KCC2 after transient focal cerebral ischemia. *Stroke* 41, e151–e159. doi: 10.1161/STROKEAHA.109.570424

Jentsch, T. J., and Pusch, M. (2018). CLC chloride channels and transporters: Structure, function, physiology and disease. *Physiol. Rev.* 98, 1493–1590. doi: 10.1152/physrev.00047.2017

Kaila, K., Lamsa, K., Smirnov, S., Taira, T., and Voipio, J. (1997). Long-lasting GABA-mediated depolarization evoked by high-frequency stimulation in pyramidal neurons of rat hippocampal slice is attributable to a network-driven, bicarbonate-dependent K+ transient. *J. Neurosci.* 17, 7662–7672. doi: 10.1523/JNEUROSCI.17-20-07662.1997

Kaila, K., Price, T. J., Payne, J. A., Puskarjov, M., and Voipio, J. (2014). Cation-chloride cotransporters in neuronal development, plasticity and disease. *Nat. Rev. Neurosci.* 15, 637–654. doi: 10.1038/nrn3819

Karadsheh, M. F., and Delpire, E. (2001). Neuronal restrictive silencing element is found in the KCC2 gene: molecular basis for KCC2-specific expression in neurons. *J. Neurophysiol.* 85, 995–997. doi: 10.1152/jn.2001.85.2.995

Khalilov, I., Dzhala, V., Ben-Ari, Y., and Khazipov, R. (1999). Dual role of GABA in the neonatal rat hippocampus. *Dev. Neurosci.* 21, 310–319. doi: 10.1159/000017380

Khalilov, I., Le Van Quyen, M., Gozlan, H., and Ben-Ari, Y. (2005). Epileptogenic actions of GABA and fast oscillations in the developing hippocampus. *Neuron* 48, 787–796. doi: 10.1016/j.neuron.2005.09.026

Khazipov, R., Leinekugel, X., Khalilov, I., Gaiarsa, J. L., and Ben-Ari, Y. (1997). Synchronization of GABAergic interneuronal network in CA3 subfield of neonatal rat hippocampal slices. *J. Physiol.* 498, 763–772. doi: 10.1113/jphysiol.1997.sp021900

Khirug, S., Yamada, J., Afzalov, R., Voipio, J., Khiroug, L., and Kaila, K. (2008). GABAergic depolarization of the axon initial segment in cortical principal neurons is caused by the Na-K-2Cl cotransporter NKCC1. *J. Neurosci.* 28, 4635–4639. doi: 10.1523/JNEUROSCI.0908-08.2008

Kirmse, K., and Holthoff, K. (2020). "Chloride transporter activities shape early brain circuit development," in *Neuronal Chloride Transporters in Health and Disease*, ed X. Tang (London, UK: Academic Press), 59–88.

Kirmse, K., Hübner, C. A., Isbrandt, D., Witte, O. W., and Holthoff, K. (2018). GABAergic transmission during brain development: multiple effects at multiple stages. *Neuroscientist* 24, 36–53. doi: 10.1177/1073858417701382

Kirmse, K., Kummer, M., Kovalchuk, Y., Witte, O. W., Garaschuk, O., and Holthoff, K. (2015). GABA depolarizes immature neurons and inhibits network activity in the neonatal neocortex *in vivo*. *Nat. Commun.* 6:7750. doi: 10.1038/ncomms8750

Kolbaev, S. N., Achilles, K., Luhmann, H. J., and Kilb, W. (2011a). Effect of depolarizing GABA A-mediated membrane responses on excitability of cajal-retzius cells in the immature rat neocortex. *J. Neurophysiol.* 106, 2034–2044. doi: 10.1152/jn.00699.2010

Kolbaev, S. N., Luhmann, H. J., and Kilb, W. (2011b). Activity-dependent scaling of GABAergic excitation by dynamic Cl^- changes in Cajal-Retzius cells. *Pflugers Arch.* 461, 557–565. doi: 10.1007/s00424-011-0935-4

Kolbaev, S. N., Sharopov, S., Dierkes, P. W., Luhmann, H. J., and Kilb, W. (2012). Phasic GABAA-receptor activation is required to suppress epileptiform activity in the CA3 region of the immature rat hippocampus. *Epilepsia* 53, 888–896. doi: 10.1111/j.1528-1167.2012.03442.x

Kuner, T., and Augustine, G. J. (2000). A genetically encoded ratiometric indicator for chloride: capturing chloride transients in cultured hippocampal neurons. *Neuron* 27, 447–459. doi: 10.1016/s0896-6273(00)00056-8

Lamsa, K., Palva, J. M., Ruusuvuori, E., Kaila, K., and Taira, T. (2000). Synaptic GABA(A) activation inhibits AMPA-kainate receptor-mediated bursting in the newborn (P0–P2) rat hippocampus. *J. Neurophysiol.* 83, 359–366. doi: 10.1152/jn.2000.83.1.359

Lee, H., Chen, C. X., Liu, Y. J., Aizenman, E., and Kandler, K. (2005). KCC2 expression in immature rat cortical neurons is sufficient to switch the polarity of GABA responses. *Eur. J. Neurosci.* 21, 2593–2599. doi: 10.1111/j.1460-9568.2005.04084.x

Leinekugel, X., Medina, I., Khalilov, I., Ben-Ari, Y., and Khazipov, R. (1997). Ca2+ oscillations mediated by the synergistic excitatory actions of GABA(A) and NMDA receptors in the neonatal hippocampus. *Neuron* 18, 243–255. doi: 10.1016/s0896-6273(00)80265-2

Li, H., Tornberg, J., Kaila, K., Airaksinen, M. S., and Rivera, C. (2002). Patterns of cation-chloride cotransporter expression during embryonic rodent CNS development. *Eur. J. Neurosci.* 16, 2358–2370. doi: 10.1046/j.1460-9568.2002.02419.x

Liu, R., Wang, J., Liang, S., Zhang, G., and Yang, X. (2020). Role of NKCC1 and KCC2 in epilepsy: from expression to function. *Front. Neurol.* 10:1407. doi: 10.3389/fneur.2019.01407

Lombardi, A., Jedlicka, P., Luhmann, H. J., and Kilb, W. (2018). Giant depolarizing potentials trigger transient changes in the intracellular Cl^- concentration in CA3 pyramidal neurons of the immature mouse hippocampus. *Front. Cell. Neurosci.* 12:420. doi: 10.3389/fncel.2018.00420

Lombardi, A., Jedlicka, P., Luhmann, H. J., and Kilb, W. (2019). Interactions between membrane resistance, GABA-A receptor properties, bicarbonate dynamics and Cl^--transport shape activity-dependent changes of intracellular Cl^- concentration. *Int. J. Mol. Sci.* 20:1416. doi: 10.3390/ijms20061416

Lombardi, A., Jedlicka, P., Luhmann, H. J., and Kilb, W. (2021). Coincident glutamatergic depolarizations enhance GABAA receptor-dependent Cl^- influx in mature and suppress Cl^- efflux in immature neurons. *PLoS Comput. Biol.* 17:e1008573. doi: 10.1371/journal.pcbi.1008573

Loscher, W., Puskarjov, M., and Kaila, K. (2013). Cation-chloride cotransporters NKCC1 and KCC2 as potential targets for novel antiepileptic and antiepileptogenic treatments. *Neuropharmacology* 69, 62–74. doi: 10.1016/j.neuropharm.2012.05.045

Lu, J., Karadsheh, M., and Delpire, E. (1999). Developmental regulation of the neuronal-specific isoform of K-Cl cotransporter KCC2 in postnatal rat brains. *J. Neurobiol.* 39, 558–568.

Luhmann, H. J., and Prince, D. A. (1991). Postnatal maturation of the GABAergic system in rat neocortex. *J. Neurophysiol.* 65, 247–263. doi: 10.1152/jn.1991.65.2.247

Martina, M., Royer, B., and Pare, D. (2001). Cell-type-specific GABA responses and chloride homeostasis in the cortex and amygdala. *J. Neurophysiol.* 86, 2887–2895. doi: 10.1152/jn.2001.86.6.2887

Minlebaev, M., Ben-Ari, Y., and Khazipov, R. (2007). Network mechanisms of spindle-burst oscillations in the neonatal rat barrel cortex *in vivo*. *J. Neurophysiol.* 97, 692–700. doi: 10.1152/jn.00759.2006

Misgeld, U., Wagner, A., and Ohno, T. (1982). Depolarizing IPSPs and depolarization by GABA of rat neostriatum cells *in vitro*. *Exp. Brain Res.* 45, 108–114. doi: 10.1007/BF00235769

Mohapatra, N., Tonnesen, J., Vlachos, A., Kuner, T., Deller, T., Nagerl, U. V., et al. (2016). Spines slow down dendritic chloride diffusion and affect short-term ionic plasticity of GABAergic inhibition. *Sci. Rep.* 6:23196. doi: 10.1038/srep23196

Mueller, A. L., Chesnut, R. M., and Schwartzkroin, P. A. (1983). Actions of GABA in developing rabbit hippocampus: an *in vitro* study. *Neurosci. Lett.* 39, 193–198. doi: 10.1016/0304-3940(83)90076-9

Murata, Y., and Colonnese, M. T. (2020). GABAergic interneurons excite neonatal hippocampus *in vivo*. *Sci. Adv.* 6:eaba1430. doi: 10.1126/sciadv.aba1430

Nardou, R., Ben-Ari, Y., and Khalilov, I. (2009). Bumetanide, an NKCC1 antagonist, does not prevent formation of epileptogenic focus but blocks epileptic focus seizures in immature rat hippocampus. *J. Neurophysiol.* 101, 2878–2888. doi: 10.1152/jn.90761.2008

Nardou, R., Ferrari, D. C., and Ben-Ari, Y. (2013). Mechanisms and effects of seizures in the immature brain. *Semin. Fetal Neonatal Med.* 18, 175–184. doi: 10.1016/j.siny.2013.02.003

Otsu, Y., Donneger, F., Schwartz, E. J., and Poncer, J. C. (2020). Cation-chloride cotransporters and the polarity of GABA signalling in mouse hippocampal parvalbumin interneurons. *J. Physiol.* 598, 1865–1880. doi: 10.1113/JP279221

Owens, D. F., and Kriegstein, A. R. (2002). Is there more to GABA than synaptic inhibition? *Nat. Rev. Neurosci.* 3, 715–727. doi: 10.1038/nrn919

Pallud, J., Le Van Quyen, M., Bielle, F., Pellegrino, C., Varlet, P., Labussiere, M., et al. (2014). Cortical GABAergic excitation contributes to epileptic activities around human glioma. *Sci. Transl. Med.* 6:244ra89. doi: 10.1126/scitranslmed.3008065

Payne, J. A., Rivera, C., Voipio, J., and Kaila, K. (2003). Cation-chloride co-transporters in neuronal communication, development and trauma. *Trends Neurosci.* 26, 199–206. doi: 10.1016/S0166-2236(03)00068-7

Pellegrino, C., Gubkina, O., Schaefer, M., Becq, H., Ludwig, A., Mukhtarov, M., et al. (2011). Knocking down of the KCC2 in rat hippocampal neurons increases intracellular chloride concentration and compromises neuronal survival. *J. Physiol.* 589, 2475–2496. doi: 10.1113/jphysiol.2010.203703

Pfeffer, C. K., Stein, V., Keating, D. J., Maier, H., Rinke, I., Rudhard, Y., et al. (2009). NKCC1-dependent GABAergic excitation drives synaptic network maturation during early hippocampal development. *J. Neurosci.* 29, 3419–3430. doi: 10.1523/JNEUROSCI.1377-08.2009

Plotkin, M. D., Snyder, E. Y., Hebert, S. C., and Delpire, E. (1997). Expression of the Na-K-2Cl cotransporter is developmentally regulated in postnatal rat brains: A possible mechanism underlying GABA's excitatory role in immature brain. *J. Neurobiol.* 33, 781–795. doi: 10.1002/(sici)1097-4695(19971120)33:6<781::aid-neu6>3.0.co;2-5

Raimondo, J. V., Markram, H., and Akerman, C. J. (2012). Short-term ionic plasticity at GABAergic synapses. *Front. Synaptic Neurosci.* 4:5. doi: 10.3389/fnsyn.2012.00005

Rall, W. (1989). "Cable theory for dendritic neurons," in *Methods in Neuronal Modeling*, eds K. Koch and I. Segev (Cambridge, MA: MIT Press), 9–92.

Rheims, S., Minlebaev, M., Ivanov, A., Represa, A., Khazipov, R., Holmes, G. L., et al. (2008). Excitatory GABA in rodent developing neocortex *in vitro*. *J. Neurophysiol.* 100, 609–619. doi: 10.1152/jn.90402.2008

Richter, D., Luhmann, H. J., and Kilb, W. (2010). Intrinsic activation of $GABA_A$ receptors suppresses epileptiform activity in the cerebral cortex of immature mice. *Epilepsia* 51, 1483–1492. doi: 10.1111/j.1528-1167.2010.02591.x

Rinetti-Vargas, G., Phamluong, K., Ron, D., and Bender, K. J. (2017). Periadolescent maturation of GABAergic hyperpolarization at the axon initial segment. *Cell Rep.* 20, 21–29. doi: 10.1016/j.celrep.2017.06.030

Rivera, C., Li, H., Thomas-Crusells, J., Lahtinen, H., Viitanen, T., Nanobashvili, A., et al. (2002). BDNF-induced TrkB activation down-regulates the K^+-Cl^- cotransporter KCC2 and impairs neuronal Cl^- extrusion. *J. Cell Biol.* 159, 747–752. doi: 10.1083/jcb.200209011

Rivera, C., Voipio, J., and Kaila, K. (2005). Two developmental switches in GABAergic signalling: the K^+-Cl^- cotransporter KCC2 and carbonic anhydrase CAVII. *J. Physiol.* 562, 27–36. doi: 10.1113/jphysiol.2004.077495

Rivera, C., Voipio, J., Payne, J. A., Ruusuvuori, E., Lahtinen, H., Lamsa, K., et al. (1999). The K^+/Cl^- co-transporter KCC2 renders GABA hyperpolarizing during neuronal maturation. *Nature* 397, 251–255. doi: 10.1038/16697

Ruffin, V. A., Salameh, A. I., Boron, W. F., and Parker, M. D. (2014). Intracellular pH regulation by acid-base transporters in mammalian neurons. *Front. Physiol.* 5:43. doi: 10.3389/fphys.2014.00043

Russell, J. M. (2000). Sodium-potassium-chloride cotransport. *Physiol. Rev.* 80, 211–276. doi: 10.1152/physrev.2000.80.1.211

Ruusuvuori, E., Li, H., Huttu, K., Palva, J. M., Smirnov, S., Rivera, C., et al. (2004). Carbonic anhydrase isoform VII acts as a molecular switch in the development of synchronous gamma-frequency firing of hippocampal CA1 pyramidal cells. *J. Neurosci.* 24, 2699–2707. doi: 10.1523/JNEUROSCI.5176-03.2004

Sauer, J. F., and Bartos, M. (2010). Recruitment of early postnatal parvalbumin-positive hippocampal interneurons by GABAergic excitation. *J. Neurosci.* 30, 110–115. doi: 10.1523/JNEUROSCI.4125-09.2010

Sava, B. A., Chen, R., Sun, H., Luhmann, H. J., and Kilb, W. (2014). Taurine activates GABAergic networks in the neocortex of immature mice. *Front. Cell. Neurosci.* 8:26. doi: 10.3389/fncel.2014.00026

Sharopov, S., Winkler, P., Uehara, R., Lombardi, A., Halbhuber, L., Okabe, A., et al. (2019). Allopregnanolone augments epileptiform activity of an *in vitro* mouse hippocampal preparation in the first postnatal week. *Epilepsy Res.* 157:106196. doi: 10.1016/j.eplepsyres.2019.106196

Shimizu-Okabe, C., Yokokura, M., Okabe, A., Ikeda, M., Sato, K., Kilb, W., et al. (2002). Layer-specific expression of Cl^- transporters and differential $[Cl^-]i$ in newborn rat cortex. *Neuroreport* 13, 2433–2437. doi: 10.1097/00001756-200212200-00012

Sinning, A., and Hübner, C. A. (2013). Minireview: PH and synaptic transmission. *FEBS Lett.* 587, 1923–1928. doi: 10.1016/j.febslet.2013.04.045

Sinning, A., Liebmann, L., Kougioumtzes, A., Westermann, M., Bruehl, C., and Hübner, C. A. (2011). Synaptic glutamate release is modulated by the Na^+-driven Cl^-/HCO_3^- exchanger Slc4a8. *J. Neurosci.* 31, 7300–7311. doi: 10.1523/JNEUROSCI.0269-11.2011

Sipila, S. T., Huttu, K., Soltesz, I., Voipio, J., and Kaila, K. (2005). Depolarizing GABA acts on intrinsically bursting pyramidal neurons to drive giant depolarizing potentials in the immature hippocampus. *J. Neurosci.* 25, 5280–5289. doi: 10.1523/JNEUROSCI.0378-05.2005

Somogyi, P., and Klausberger, T. (2005). Defined types of cortical interneurone structure space and spike timing in the hippocampus. *J. Physiol.* 562, 9–26. doi: 10.1113/jphysiol.2004.078915

Song, I., Savtchenko, L., and Semyanov, A. (2011). Tonic excitation or inhibition is set by GABAA conductance in hippocampal interneurons. *Nat. Commun.* 2:376. doi: 10.1038/ncomms1377

Spruston, N., Stuart, G., and Häusser, M. (2016). "Principles of dendritic integration," in *Dendrites*, eds G. Stuart, N. Spruston and M. Häusser (Oxford, UK: Oxford Scholarship), 351–398.

Staley, K. J., and Mody, I. (1992). Shunting of excitatory input to dentate gyrus granule cells by a depolarizing GABA(A) receptor-mediated postsynaptic conductance. *J. Neurophysiol.* 68, 197–212. doi: 10.1152/jn.1992.68.1.197

Stein, V., Hermans-Borgmeyer, I., Jentsch, T. J., and Hubner, C. A. (2004). Expression of the KCl cotransporter KCC2 parallels neuronal maturation and the emergence of low intracellular chloride. *J. Comp. Neurol.* 468, 57–64. doi: 10.1002/cne.10983

Steriade, M. (2001). *The Intact and Sliced Brain.* Cambridge: MIT Press.

Szabadics, J., Varga, C., Molnár, G., Oláh, S., Barzó, P., and Tamás, G. (2006). Excitatory effect of GABAergic axo-axonic cells in cortical microcircuits. *Science* 311, 233–235. doi: 10.1126/science.1121325

Titz, S., Hans, M., Kelsch, W., Lewen, A., Swandulla, D., and Misgeld, U. (2003). Hyperpolarizing inhibition develops without trophic support by GABA in cultured rat midbrain neurons. *J. Physiol.* 550, 719–730. doi: 10.1113/jphysiol.2003.041863

Toyoda, H., Ohno, K., Yamada, J., Ikeda, M., Okabe, A., Sato, K., et al. (2003). Induction of NMDA and GABAA receptor-mediated Ca^{2+} oscillations with KCC2 mRNA downregulation in injured facial motoneurons. *J. Neurophysiol.* 89, 1353–1362. doi: 10.1152/jn.00721.2002

Valeeva, G., Abdullin, A., Tyzio, R., Skorinkin, A., Nikolski, E., Ben-Ari, Y., et al. (2010). Temporal coding at the immature depolarizing gabaergic synapse. *Front. Cell. Neurosci.* 4:17. doi: 10.3389/fncel.2010.00017

Valeeva, G., Tressard, T., Mukhtarov, M., Baude, A., and Khazipov, R. (2016). An optogenetic approach for investigation of excitatory and inhibitory network GABA actions in mice expressing channelrhodopsin-2 in GABAergic neurons. *J. Neurosci.* 36, 5961–5973. doi: 10.1523/JNEUROSCI.3482-15.2016

Valeeva, G., Valiullina, F., and Khazipov, R. (2013). Excitatory actions of GABA in the intact neonatal rodent hippocampus *in vitro*. *Front. Cell. Neurosci.* 7:20. doi: 10.3389/fncel.2013.00020

Virtanen, M. A., Uvarov, P., Hübner, C. A., and Kaila, K. (2020). NKCC1, an elusive molecular target in brain development: making sense of the existing data. *Cells* 9:2607. doi: 10.3390/cells9122607

Wake, H., Watanabe, M., Moorhouse, A. J., Kanematsu, T., Horibe, S., Matsukawa, N., et al. (2007). Early changes in KCC2 phosphorylation in response to neuronal stress result in functional downregulation. *J. Neurosci.* 27, 1642–1650. doi: 10.1523/JNEUROSCI.3104-06.2007

Wang, Y. F., Gao, X. B., and Van Den Pol, A. N. (2001). Membrane properties underlying patterns of GABA-dependent action potentials in developing mouse hypothalamic neurons. *J. Neurophysiol.* 86, 1252–1265. doi: 10.1152/jn.2001.86.3.1252

Watanabe, M., and Fukuda, A. (2015). Development and regulation of chloride homeostasis in the central nervous system. *Front. Cell. Neurosci.* 9:371. doi: 10.3389/fncel.2015.00371

Wells, J. E., Porter, J. T., and Agmon, A. (2000). GABAergic inhibition suppresses paroxysmal network activity in the neonatal rodent hippocampus and neocortex. *J. Neurosci.* 20, 8822–8830. doi: 10.1523/JNEUROSCI. 20-23-08822.2000

Winkler, P., Luhmann, H. J., and Kilb, W. (2019). Taurine potentiates the anticonvulsive effect of the GABA A agonist muscimol and pentobarbital in the immature mouse hippocampus. *Epilepsia* 60, 464–474. doi: 10.1111/epi.14651

Wright, R., Raimondo, J. V., and Akerman, C. J. (2011). Spatial and Temporal Dynamics in the Ionic Driving Force for GABA(A) Receptors. *Neural Plast.* 2011:728395. doi: 10.1155/2011/728395

Yang, B., Rajput, P. S., Kumar, U., and Sastry, B. R. (2015). Regulation of GABA equilibrium potential by mGluRs in rat hippocampal CA1 neurons. *PLoS One* 10:e0138215. doi: 10.1371/journal.pone.0138215

Conflict of Interest: The author declares that the research was conducted in the absence of any commercial or financial relationships that could be construed as a potential conflict of interest.

frontiers in Molecular Neuroscience

REVIEW
published: 03 January 2022
doi: 10.3389/fnmol.2021.807969

Gabaergic Interneurons in Early Brain Development: Conducting and Orchestrated by Cortical Network Activity

*Davide Warm†, Jonas Schroer† and Anne Sinning**

Institute of Physiology, University Medical Center of the Johannes Gutenberg University, Mainz, Germany

Throughout early phases of brain development, the two main neural signaling mechanisms—excitation and inhibition—are dynamically sculpted in the neocortex to establish primary functions. Despite its relatively late formation and persistent developmental changes, the GABAergic system promotes the ordered shaping of neuronal circuits at the structural and functional levels. Within this frame, interneurons participate first in spontaneous and later in sensory-evoked activity patterns that precede cortical functions of the mature brain. Upon their subcortical generation, interneurons in the embryonic brain must first orderly migrate to and settle in respective target layers before they can actively engage in cortical network activity. During this process, changes at the molecular and synaptic level of interneurons allow not only their coordinated formation but also the pruning of connections as well as excitatory and inhibitory synapses. At the postsynaptic site, the shift of GABAergic signaling from an excitatory towards an inhibitory response is required to enable synchronization within cortical networks. Concomitantly, the progressive specification of different interneuron subtypes endows the neocortex with distinct local cortical circuits and region-specific modulation of neuronal firing. Finally, the apoptotic process further refines neuronal populations by constantly maintaining a controlled ratio of inhibitory and excitatory neurons. Interestingly, many of these fundamental and complex processes are influenced—if not directly controlled—by electrical activity. Interneurons on the subcellular, cellular, and network level are affected by high frequency patterns, such as spindle burst and gamma oscillations in rodents and delta brushes in humans. Conversely, the maturation of interneuron structure and function on each of these scales feeds back and contributes to the generation of cortical activity patterns that are essential for the proper peri- and postnatal development. Overall, a more precise description of the conducting role of interneurons in terms of how they contribute to specific activity patterns—as well as how specific activity patterns impinge on their maturation as orchestra members—will lead to a better understanding of the physiological and pathophysiological development and function of the nervous system.

Keywords: cortex, development, activity patterns, interneuron, GABA shift, apoptosis, migration, synaptogenesis

OPEN ACCESS

Edited by:
Atsuo Fukuda,
Hamamatsu University School of Medicine, Japan

Reviewed by:
Matthew T. Colonnese,
George Washington University, United States
Miao He,
Fudan University, China

***Correspondence:**
Anne Sinning
asinning@uni-mainz.de

†These authors have contributed equally to this work

Specialty section:
This article was submitted to Neuroplasticity and Development, a section of the journal Frontiers in Molecular Neuroscience

Received: *02 November 2021*
Accepted: *06 December 2021*
Published: *03 January 2022*

Citation:
Warm D, Schroer J and Sinning A (2022) GABAergic Interneurons in Early Brain Development: Conducting and Orchestrated by Cortical Network Activity. Front. Mol. Neurosci. 14:807969. doi: 10.3389/fnmol.2021.807969

INTRODUCTION

During early development, mammalian brains can be functionally characterized by the progressive emergence of distinct cortical activity patterns which are essential for the establishment of basic functions of the cerebral cortex (Blankenship and Feller, 2010; Kilb et al., 2011; Kirkby et al., 2013). Underlying this dynamic change in neuronal activity, among other developmental processes, is the structural and functional maturation of the two main signaling principles of neurons: excitation and inhibition (Egorov and Draguhn, 2013; Luhmann et al., 2016; Teppola et al., 2019). While glutamatergic signaling is established already within early, embryonic stages in rodents and humans (Monyer et al., 1994; Bagasrawala et al., 2017), the maturation of the GABAergic system extends into the postnatal period of most mammals. Starting with the formation of the first GABAergic synapse (Khazipov et al., 2001), the maturation of the inhibitory system coincides with the emergence of correlated oscillatory activity patterns, such as spindle burst and gamma oscillations in newborn rodents or delta brushes in prenatal humans (Luhmann and Khazipov, 2018). Here, the thalamus contributes significantly to the generation of these early cortical oscillations (Minlebaev et al., 2011; Yang et al., 2013; Murata and Colonnese, 2016), which conversely also modulate thalamic activity within a cortico-thalamic feedback loop (Yang et al., 2013; Martini et al., 2021). Furthermore, the maturation of the adult inhibitory GABAergic system is still not complete when cortical activity evolves to its final more de-correlated activity state that underlies its later complex functions (Golshani et al., 2009; Rochefort et al., 2009).

Although the contribution of GABA signaling to cortical activities during the perinatal phases is not fully understood, it is often speculated that GABAergic interneurons critically modulate the output of neuronal circuits in the form of spontaneous and sensory-driven activity (Bonifazi et al., 2009; Butt et al., 2017). In general, the importance of distinct cortical activity patterns during cortical development is emphasized by their necessity for and coherent emergence with higher cognitive function (Tort et al., 2009; Bosman et al., 2012). Consistently, in sensory cortical areas during the postnatal period of rodents, stereotypical spontaneous and evoked activity patterns concurrently develop with respective sensory modalities (Rochefort et al., 2009; Yang et al., 2009; Colonnese et al., 2010; Ackman and Crair, 2014; Martini et al., 2021). However, the source of spontaneous activity is still a matter of ongoing research, as well as the root cause and type of evoked activity which varies depending on the region and time point of perinatal development.

Yet, undoubtedly, neuronal activity itself is a key regulator of many—if not all—developmental processes in the cortex. Thus, it comes to no surprise that neuronal activity also strongly impacts the maturation of the GABAergic system, from the cellular to the network level, and fine-tunes excitation/inhibition balance (Turrigiano and Nelson, 2004; Takesian and Hensch, 2013). Besides cortical activity, thalamic inputs also play a role in interneuron maturation on the level of the cortex (Pouchelon et al., 2014; Marques-Smith et al., 2016), while interneurons in turn function as a gate for the thalamus by effecting cortical network activity (Yang et al., 2013; Martini et al., 2021). Therefore, the GABAergic system must permit sufficient excitation to engage in cortical activity and still provide the needed inhibition to prevent over-excitation. In this respect, it is worth mentioning that a certain level of freedom in the excitation/inhibition balance is needed, especially for the establishment of the sensory cortical system during early development (Masquelier et al., 2009; Deidda et al., 2015; Wosniack et al., 2021). Both the GABAergic system and neuronal activity are fulfilling important functions during these critical periods, as discussed in more detail elsewhere (Sale et al., 2010; Reha et al., 2020).

In this article, the focus will be on the interdependency of the maturation of the GABAergic system and cortical network activity throughout the perinatal and postnatal development of the rodent cortex. For this purpose, we will review how neuronal activity impacts the maturation of the GABAergic system on the subcellular (mostly synaptic) level, on the cellular and on the network level and discuss how the maturation on each of these scales feeds back on cortical activity, thus impacting the function of the mature cortex. Finally, we will describe the physiological implications of this interdependency and highlight open questions in this field of research.

THE INTERPLAY OF ACTIVITY AND PERINATAL CHANGES OF GABAergic SYSTEM AT THE SUBCELLULAR LEVEL

Before becoming the main inhibitory neurotransmitter in the mature brain, GABA exerts mainly excitatory function in immature neurons (Luhmann and Prince, 1991; Leinekugel et al., 1995; Rheims et al., 2008; Kirmse et al., 2015) and is suggested to regulate spontaneous activity during development (Ben-Ari, 2002; Le Magueresse and Monyer, 2013; Kirmse et al., 2015). In turn, the neuronal activity itself is a key regulator of the subcellular processes that underlie this developmental change in GABA signaling—like the expression of chloride transporters (Fiumelli et al., 2005), GABA-receptor expression, and GABAergic synaptogenesis (Ganguly et al., 2001; Wardle and Poo, 2003; see also **Figure 1** for overview).

GABA-Receptor Signaling

At the postsynaptic side, GABA exerts its function *via* ionotropic $GABA_A$-receptors and metabotropic $GABA_B$-receptors. $GABA_A$-receptors are a heterogenous group of chloride channels with rapid kinetics. Each of them is formed by a heteromeric complex that consists of five of a possible 19 different subunits (α1–6, β1–3, γ1–3, π, θ, δ, ε, Kumada and Fukuda, 2020). Differences in localization of $GABA_A$-receptors lead to two major forms of GABAergic inhibition: phasic inhibition and tonic inhibition. Where the former is mediated by synaptic, low affinity $GABA_A$-receptors, the latter is facilitated by high affinity, extrasynaptic $GABA_A$-receptors (Kumada and Fukuda, 2020). The expression of $GABA_A$-receptor subunits changes with development: some subunits display a consistent increase in expression levels with

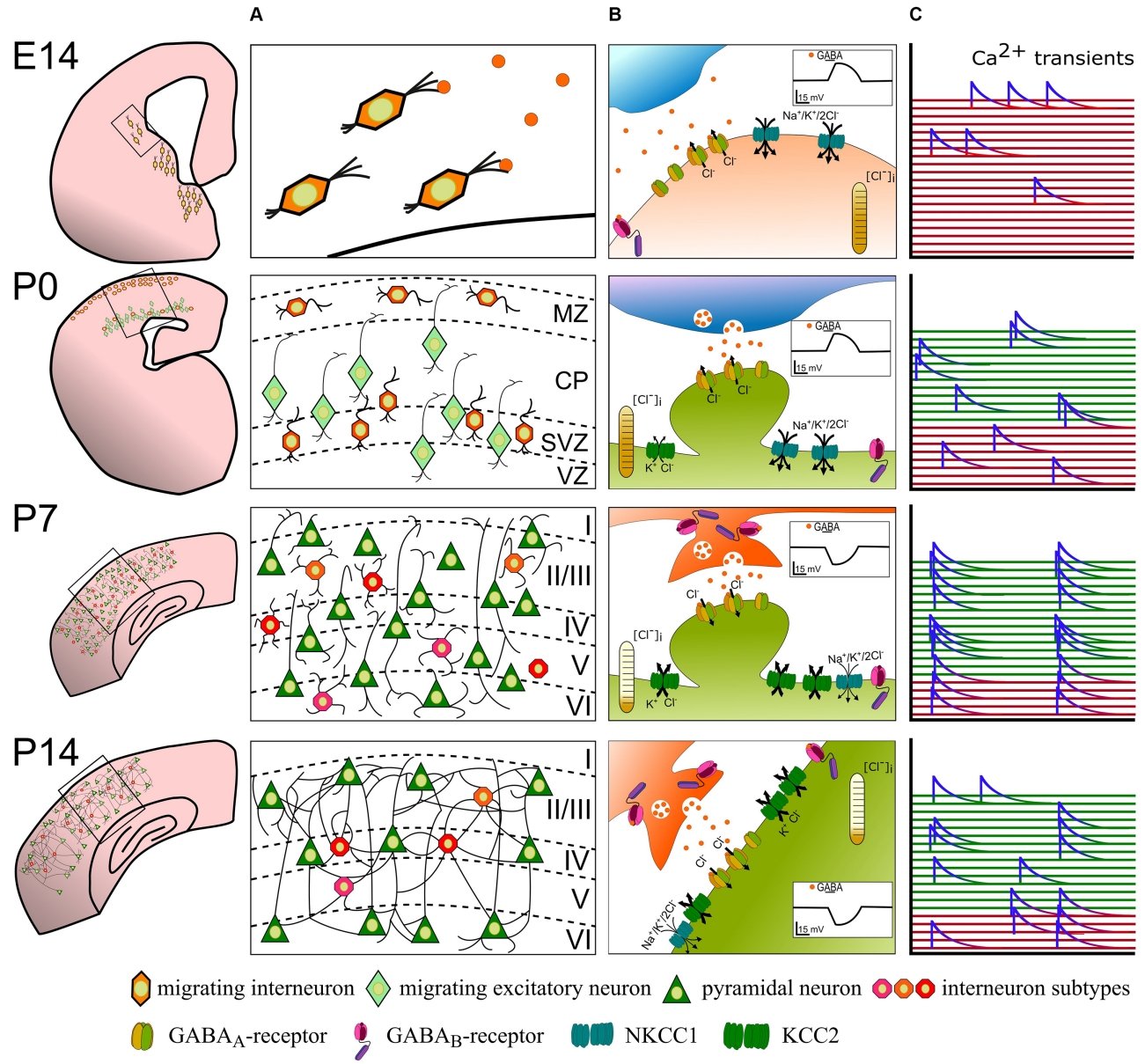

FIGURE 1 | The developmental sequence of perinatal changes in **(A)** positioning and integration of nascent interneurons, **(B)** synaptic GABA signaling, and **(C)** interneuron participation in network activity in the rodent cortex. At E14, GABAergic interneuron precursors tangentially migrate from the ganglionic eminences into the cortex and ambient GABA acts as a chemoattractant. Binding of GABA to $GABA_A$-receptors at this stage depolarizes recipient interneurons and likely contributes to sporadic, uncorrelated Ca^{2+} transients (red). Around birth (P0), immature GABAergic interneurons are found in the marginal zone and migrate radially concomitant with pyramidal neurons. Here, GABA acts as a Stop and Go signal mainly through $GABA_A$-receptors. At this developmental stage, GABA is still excitatory and contributes to uncorrelated Ca^{2+} transients in GABAergic interneurons (red traces) and immature pyramidal neurons (green traces). At the end of the 1st postnatal week (P7), layering of the cortex is mostly complete and maturing neurons already begin to form synapses. Vesicular released GABA hyperpolarizes the postsynaptic cell *via* postsynaptic $GABA_A$- and binds to extra- and pre-synaptic $GABA_B$-receptors. Highly synchronous spontaneous activity in interneurons and pyramidal neurons is a hallmark of this developmental phase. By P14, excess neurons were depleted through developmental apoptosis and stable functional, also perisomatic connections have developed. The cation-chloride transporter profile is fully matured and GABA receptor signaling fulfills its mostly inhibitory function. Spontaneous and sensory-evoked activity shifts to a more decorrelated state.

age (e.g., α1, β1, β2, δ) whereas others instead show a peak, followed by a decline (e.g., α2, α3, α5, β3, γ3, Laurie et al., 1992). Although a large portion of $GABA_A$ receptor subunits is only found in postmigratory neurons, others (α2, α3, β1, β3, γ1, γ2) are already detectable in the germinal zone and in migrating neurons in the marginal zone and the cortical plate (Araki et al., 1992; Laurie et al., 1992; Poulter et al., 1992; Van Eden et al., 1995). The early timing of the expression profile supports an

effective role of GABAergic signaling before synaptogenesis, i.e., during interneuron migration and maturation of GABAergic synapses.

In contrast to the ionotropic $GABA_A$-receptors, the metabotropic $GABA_B$-receptors consist of two distinct subunits (B1 and B2). Subunit B1 is expressed in two isoforms: namely, B1a and B1b, which require the dimerization with a B2 subunit to form functional heteromeric $GABA_B$-receptors (Terunuma, 2018). Once the receptor is activated by ligand binding on the extracellular domain of the B1 subunit, a G-protein mediated signaling cascade is started which opens K^+ channels at the post- and Ca^{2+} channels at the presynaptic site. In this way, $GABA_B$ receptor mediated inhibition leads to hyperpolarization of the postsynaptic neuron and/or to reduced release probability of neurotransmitters in the synaptic cleft. In rodents, $GABA_B$ receptors are expressed as early as embryonic day 14 (López-Bendito et al., 2002) and reach their expression level peak in the first postnatal week (Turgeon and Albin, 1994; Behuet et al., 2019). Furthermore, it was shown that the different $GABA_B$ subunits have distinct expression levels with $GABA_{B1}$ playing a more important role during prenatal development of the rat (Li et al., 2004). In addition, $GABA_{B1}$-receptors are expressed in migrating neurons in the lower intermediate zone, where GABA not only enhances $GABA_B$-receptor expression but also works as a chemo-attractant that promotes motility of migrating neurons (Behar et al., 2001). $GABA_B$ receptors are found in dendritic spines and dendritic shafts at extrasynaptic and perisynaptic sites during postnatal development (López-Bendito et al., 2002). Moreover, in the postnatal stage, activity-dependent secretion of brain-derived neurotrophic factor (BDNF) is mainly mediated by activation of $GABA_B$-receptors, which then promote the development of perisomatic GABAergic synapses (Fiorentino et al., 2009).

Taken together, the results on GABA receptor signaling during brain development illustrate the importance of $GABA_A$-receptor activity for corticogenesis, interneuron migration, and for modulation of synaptic transmission (Cancedda et al., 2007; Patrizi et al., 2008; Fuchs et al., 2013) and indicate a potentially important but largely unresolved role for $GABA_B$-receptors.

Facilitating the Chloride Gradient: The Cotransporters NKKC1 and KCC2

Activation of mature postsynaptic $GABA_A$ receptors typically leads to a fast hyperpolarization through anion influx, predominantly by Cl^- (Kaila, 1994; Olsen and Sieghart, 2009). However, during brain development, GABA plays a critical role as an excitatory drive relevant for the proper development and establishment of neuronal circuits (Ben-Ari, 2002; Rheims et al., 2008). In fact, in the immature brain $GABA_A$-receptor activation leads to depolarization of neurons due to the high intracellular Cl^- concentration (Rivera et al., 1999; Yamada et al., 2004; Rheims et al., 2008; Kirmse et al., 2015). The intracellular concentration is mostly set by two main cation-chloride cotransporters Na^+-K^+-$2Cl^-$-Cotransporter 1 (NKCC1)—a chloride-importer—and K^+-Cl^--cotransporter 2 (KCC2)—a chloride extruder, which play a pivotal role in the polarity of GABAergic action (Rivera et al., 1999; Yamada et al., 2004; Achilles et al., 2007; Rheims et al., 2008; Kirmse et al., 2015). In immature cortical neurons, intracellular chloride is significantly higher than in mature neurons due to the predominant expression of NKCC1 over KCC2. The developmental change in chloride-cotransporter expression, which occurs within the first postnatal week in the rodent cortex (Shimizu-Okabe et al., 2002), is hence effectively reversing GABA action from depolarizing to hyperpolarizing (Rivera et al., 1999; Shimizu-Okabe et al., 2002; Yamada et al., 2004; Rheims et al., 2008). Studies in various animal models have shown that this switch occurs at different time points within different species and have brain region-specific effects (Leinekugel et al., 1995; Reith and Sillar, 1999; Saint-Amant and Drapeau, 2000; Eilers et al., 2001; Gao and Van Den Pol, 2001; Murata and Colonnese, 2020). It also could be demonstrated that the precise time point of the switch is not strictly determined by the genetic program, but might be influenced by neurotrophic factors and neuronal activity (Ganguly et al., 2001; Wardle and Poo, 2003). For example, repetitive fast postsynaptic excitation influences KCC2 expression and therefore affects the chloride reversal potential (Fiumelli et al., 2005). Also, GABA itself can be crucial for the determination of the time point of shift. In the turtle retina, under blockade of $GABA_A$ receptors at the developmental time point of the shift, GABA action remains excitatory, through inhibition of KCC2 upregulation (Leitch et al., 2005). On the other hand, experiments in hippocampal slice and dissociated hippocampal cultures do not support a GABA and/or activity dependency of the switch from de- to hyperpolarizing (Ludwig et al., 2003; Titz et al., 2003). Unfortunately, studies aiming to assess the role of activity for the expression of NKCC1 are still difficult to interpret, likely because of broad technical difficulties (Virtanen et al., 2020). A recent study, in which NKCC1 is selectively knocked-out in telencephalic glutamatergic neurons, showed that in the visual cortex NKCC1 is not necessary for the establishment of fully functional networks in adult mice (Graf et al., 2021). Conceptually this is in line with another recent study, in which GABAergic activation did not produce excitation in postsynaptic neurons in the visual cortex of 3 days old mice (Murata and Colonnese, 2020). Supporting brain region specific differences in GABAergic synaptic transmission, glutamatergic hippocampal neurons lacking NKCC1 display significantly lower intracellular chloride concentrations. Despite the alterations in correlated spontaneous activity during development and slightly altered network dynamics in the hippocampus of adult mice, these knock-out mice are perfectly capable of performing hippocampus-dependent behavioral tasks (Graf et al., 2021). However, it remains unclear whether changes in network dynamics are an acute effect of NKCC1 loss, or rather an adaptation to ensure proper functionality in NKCC1 knock-out mouse lines. In support of the latter hypothesis, an earlier study showed that the complete loss of NKCC1 prevents excitation *via* GABA in hippocampal CA3 neurons, nevertheless, these mice still display typical network activity patterns as seen under physiological conditions (Sipilä et al., 2009). In contrast, another constitutive NKCC1 knock-out mouse line shows impairments in early hippocampal activity patterns and delayed maturation of the network (Pfeffer et al., 2009).

GABAergic Signaling Before and During Synaptogenesis

On a structural level, GABAergic synapses are among the first synapses that are formed in the developing brain (Tyzio et al., 1999; Khazipov et al., 2001; Rymar and Sadikot, 2007). Immature neurons in the hippocampus as well as in the neocortex first receive GABAergic before glutamatergic input (Ben-Ari, 2006; Wang and Kriegstein, 2008). In the neocortex of newborn mice GABAergic vesicle abundance is relatively low and only during the following days the expression of GABAergic synaptic markers increases gradually until it reaches a plateau at the end of the 2nd postnatal week (Minelli et al., 2003). However, not only does the number of GABAergic vesicles increase, but also their overall distribution changes within the developing cortex. While GABAergic vesicles can only be detected in the marginal zone in newborn mice, their distribution gradually extends deeper into the neocortex until finally covering all cortical layers at the end of the second postnatal week (Minelli et al., 2003). Despite the maturation of GABAergic vesicles late in the first postnatal week (Minelli et al., 2003), GABA positive cells can already be found even in the deeper layer of the neocortex at birth (Takayama and Inoue, 2010). These findings support a role of GABAergic signaling before the onset of synaptogenesis, i.e., extrasynaptic transmission. In line with this, GAD67 (the main GABA-producing enzyme isoform) and $GABA_A$ receptors can already be detected as early as E17 in the ventricular zone (Ma and Barker, 1995) and throughout the cortical plate (van den Berghe et al., 2013). Paracrine release of GABA was demonstrated to occur in different cell types during development, e.g., in immature neurons, but also in endothelial cells (Taylor and Gordon-Weeks, 1991; Gao and Van Den Pol, 2000; Li et al., 2018). In the latter, partial or complete loss of GABA release during embryogenesis leads to impairment of long-distance migration and positioning of cortical interneurons (Li et al., 2018). In the adult cortex, astrocytes express the GABA transporter GAT1 and thus influence the excitatory and inhibitory transmission through the paracrine spread of GABA (Minelli et al., 1995; Barakat and Bordey, 2002). However, whether or not astrocytes are also a source of GABA during development is yet not clear.

Maturation of GABAergic Synapses

Neuronal activity e.g., *via* the depolarization of immature neurons, is a key regulator in synaptogenesis. *in vitro* and *in vivo* studies show that the excitatory effect of GABA during early development is essential for the normal maturation of dendritic spines (Hensch et al., 1998; Cancedda et al., 2007; Chattopadhyaya et al., 2007; Wang and Kriegstein, 2008; Pfeffer et al., 2009; Oh et al., 2016; Flossmann et al., 2019). In line with an important role for $GABA_A$-receptor-mediated activity during the establishment of neural circuits, the development of synapses between somatostatin-positive (SST) interneurons and pyramidal cells in the hippocampus is NKCC1-dependent (Pfeffer et al., 2009; Flossmann et al., 2019). However, not only GABA-induced activity is required for the proper maturation of GABAergic interneurons, but also, NMDA receptor activity affects the regulation of GABAergic synaptogenesis (Cserép et al., 2012; Gu et al., 2016; Hanson et al., 2019). Tonic NMDA-mediated neuronal activity is important for the maturation and correct integration of parvalbumin-positive (PV) interneurons into the developing cortical network (Hanson et al., 2019). In early development, NMDA-receptors are co-localized with $GABA_A$-receptors at the postsynaptic site (Cserép et al., 2012), where NMDA-receptors act as upstream signaling molecules essential for GABAergic synaptogenesis *via* Ca^{2+} transient and calmodulin signaling (Gu et al., 2016). Conversely, $GABA_A$-receptor activation is sufficient to remove the voltage-dependent Mg^{2+} blockade and thus activate NMDA-receptors (Wang and Kriegstein, 2008). The mutual interplay between $GABA_A$- and NMDA-receptors is thus shown to play an important role in the emergence of spontaneous synchronous activity and the correct balance between excitation and inhibition (E/I) in the neocortex (Wang and Kriegstein, 2008). Of note, also AMPA-receptor expression at the postsynaptic site can be affected by GABAergic action, such that AMPA-receptor levels are downregulated in glutamatergic/GABAergic-mixed synapses (Fattorini et al., 2019). Thereby, a proper E/I balance is ensured and a potential neuroprotective effect is exerted in the developing brain (Fattorini et al., 2019). $GABA_A$-receptors fulfill important functions for GABAergic synapse development not only on the functional but also on the structural level (Chattopadhyaya et al., 2007; Deng et al., 2007; Fuchs et al., 2013; Oh et al., 2016). Along this line, GABA release from SST interneurons leads to the expression of the scaffolding protein gephyrin and dendritic spine formation by recruitment and activation of $GABA_A$ receptors in layer 2/3 cortical pyramidal neurons in neonatal mice (Oh et al., 2016). Accordingly, conditionally knocking-out GAD67 in PV basket cells results in less terminal branching, smaller boutons size, and hence, fewer and deficient synaptic contacts (Chattopadhyaya et al., 2007). Depletion of GAD65, the smaller isoform of the GAD protein, leads to impaired formation of cortical networks and over-responsiveness in the visual cortex (Hensch et al., 1998) while overexpression of GAD67 leads to faster perisomatic innervation (Chattopadhyaya et al., 2007). Together, these findings suggest that GABA regulates perisynaptic contact formation during the maturation of neural circuits (Chattopadhyaya et al., 2007) and imply that suppression of electrical activity leads to fewer synaptic contacts *via* reduced GABA levels (Chattopadhyaya et al., 2004). On the other hand, mice with disturbed GABA homeostasis also display less activity (Fiorentino et al., 2009). This raises the question of whether GABA action on synaptogenesis should be mostly considered as an activity-independent mechanism.

THE INTERPLAY OF ACTIVITY AND PERINATAL CHANGES OF GABAergic SYSTEM AT THE CELLULAR AND NETWORK LEVEL

Not only the maturation of the GABAergic system at the subcellular level is affected by, but also the maturation of

the single (inter-)neuron and network level activity shows an activity-dependence. While, on the other hand, network composition in general—and especially the activity of GABAergic subpopulations—significantly influence cortical activity during the postnatal period of rodents (Le Magueresse and Monyer, 2013; Kepecs and Fishell, 2014; Tremblay et al., 2016; for an overview see also **Figure 2**). Inversely, cortical activity is not only the most relevant cortical output function, but also has an important feedback role as a key regulating factor for many processes at the cellular and network level during early brain development (Luhmann et al., 2016; Okujeni and Egert, 2019). In this way (and as can be seen in **Figure 2**), cortical activity and especially the activity of interneurons themselves critically control several key steps in the development of GABAergic neurons on the network level, including migration, wiring, and programmed cell death.

Neurogenesis and Proliferation of Interneuron Precursors

In chronological order, the first step to consider is the embryonic generation of GABAergic interneurons, i.e., the neurogenesis and proliferation of interneuron precursor cells in the ventral telencephalon—in particular the medial and caudal ganglionic eminences (MGE and CGE, respectively), with a minor contribution of the preoptic area and the lateral ganglionic eminence (POA and LGE; Gelman and Marín, 2010; Sultan et al., 2013). Expression of homeobox transcription factors of the Dlx family is of essential importance for GABAergic precursors proliferation, as well as for the differentiation of interneurons (Petryniak et al., 2007). Additionally, both processes are activity-dependent. The proliferation of neuronal progenitors, in general, has been shown to be influenced by spontaneous calcium activity (Weissman et al., 2004; Malmersjö et al., 2013). Meanwhile, spontaneous calcium activity in parallel also critically impacts the further specification of neuronal phenotypes (Ciccolini et al., 2003; Borodinsky et al., 2004), which is no surprise considering the tight link between neuronal gene expression and neuronal activity (Flavell and Greenberg, 2008). In this regard, it should be highlighted that the increasing complexity of activity patterns in developing neurons that follows the occurrence of simple calcium transients in progenitor cells also offers a higher order complexity on the level of gene regulation (Tyssowski et al., 2018). Activity-dependent regulation of the proliferation and differentiation of neural stem cells and oligodendrocyte precursors has also been shown in the postnatal brain (Káradóttir and Kuo, 2018). Thus, neuronal activity is not only an import modulator determining the extent and type of interneurons during development but also remains important in adult neuro- and gliogenesis. Moreover, *via* the direct action of synaptically released GABA (Andäng et al., 2008) as well as through cortical activity that is in turn significantly influenced by GABAergic neuronal population sizes (Modol et al., 2020), cross-talk of interneuron proliferation and cortical activity should be carefully considered as a regulatory mechanism that shapes neuronal circuitry.

Migration of Interneurons

Upon their generation, interneurons need to migrate from their places of origin in the subpallium along the subventricular and marginal zone to reach their final place of destination in the postnatal cortex. This location is spatially characterized by a distinct radial position within a certain cortical region and also a distinct laminar location within a certain cortical layer (Faux et al., 2012). Early experiments *in vitro* have already shown that migration of immature neurons is generally dependent on spontaneous calcium activity (Komuro and Rakic, 1996; Komuro and Kumada, 2005). These experiments were later confirmed *in vivo*, where the pharmacological or genetic reduction of activity also altered the migration of excitatory and inhibitory neurons (Heck et al., 2007; De Marco García et al., 2011). In addition to this effect of neuronal activity on migration, one has to note that various neurotransmitters—including GABA—act as chemoattractants for targeting migratory streams and thus, can directly modulate neuronal migration (Behar et al., 2000; Inada et al., 2011). Since GABA release itself is regulated in an activity-dependent manner, this implies a further level of regulation on account of this (Luhmann et al., 2015). Further, more recent studies show that silencing neuronal activity e.g., by the overexpression of the Kir2.1 channel, results in mispositioning of specific interneuron subpopulations by affecting the expression of Dlx genes (De Marco García et al., 2011). This suggests that genetic programs initiated at the progenitor stage are modulated during development by activity (Bando et al., 2016; Hurni et al., 2017). Nevertheless, the experimental disentangling of direct causal links between activity and differentiation, migration, and/or integration of interneurons remains challenging and requires the careful analysis of subtype-specific differences in these relationships (Bugeon et al., 2021). Moreover, the simultaneous maturation of the inhibitory GABAergic response from its immature excitatory function (Ben-Ari, 2002) with the migration of interneurons adds another layer to the complex and multidimensional regulation needed for the correct laminar positioning of interneurons. The importance of which is also experimentally supported by the halt of neuronal motility induced by upregulation of KCC2 or pharmacological interference with $GABA_A$ receptor function (Heck et al., 2007; Bortone and Polleux, 2009).

Thus, activity on the single interneuron level but also on the network level critically regulates the migration of immature neurons. However, the extent to which spatial and temporal changes in the migration of interneurons impacts cortical activity and function needs further investigations, especially since interneuron migration is tightly linked to the specification of interneurons (Lim et al., 2018b).

Specification of Interneuron Subtypes

In the neocortex, the vast majority of GABAergic cells are represented by local circuit interneurons, which are traditionally classified as aspiny neurons (Lodato and Arlotta, 2015). All GABAergic interneurons produce GABA, the hyperpolarizing action of which in the mature brain accounts for their definition as inhibitory neurons. GABAergic neurons form a heterogeneous

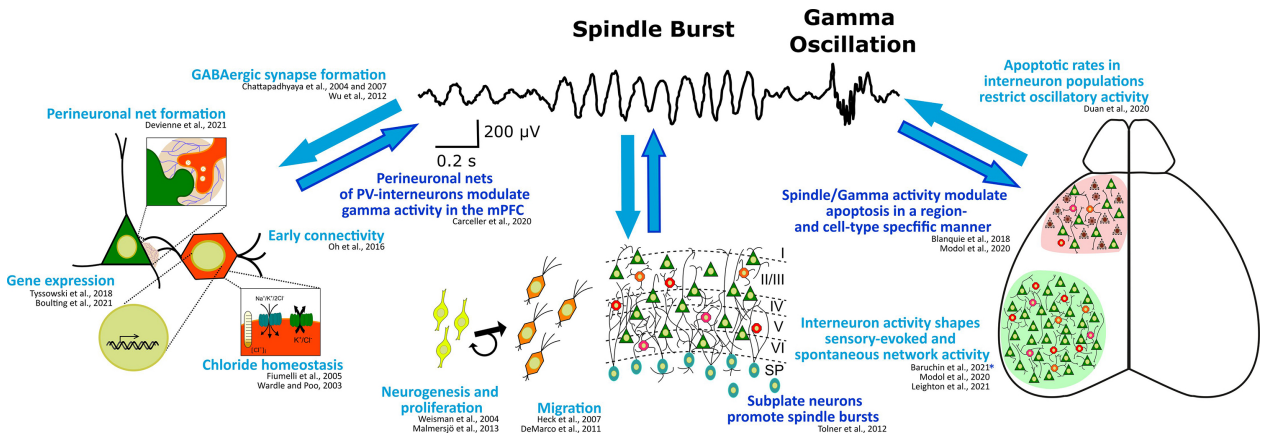

FIGURE 2 | Interdependence of (oscillatory) cortical network activity and development of the GABAergic system at the subcellular, cellular, and network level. Known regulation of or by high frequency spindle burst and gamma activity are highlighted in dark blue. Exemplary references to experimental evidence supporting these processes are listed. *Note, this study suggests that somatostatin interneurons contribute to the early processing of sensory information in a way, that their activity affects spindle burst activity possibly through the plastic arrangement of thalamic innervation to the neocortex.

population, of which classification is an ongoing effort that encompasses several morphological, electrophysiological, molecular, connectivity, and transcriptomic properties (Kepecs and Fishell, 2014). The broadest and most widely adopted classification relies on molecular markers, two of which (namely: parvalbumin and somatostatin) label around 70% of cortical interneurons. The remaining 30% are instead identified by a handful of markers, among which the most prevalent one is the serotonin receptor 5hT3aR. Other markers—such as the vasointestinal peptide (VIP), reelin (RELN), cholecystokinin (CCK), and calretinin (CR)—label smaller subclasses.

The maturation of subtype-specific properties of inhibitory interneurons mainly occurs during the first weeks of postnatal development in rodents and the different types of interneurons become only observable after the migration is complete at the end of the 1st postnatal week (Lim et al., 2018b). Whether the lineage specification is already predetermined during the embryonic stage or is (partially) acquired during the postnatal period through a microenvironment-mediated influence is still a matter of debate (Wamsley and Fishell, 2017; Lim et al., 2018a). However, it is becoming evident that activity-dependent mechanisms impinge on cellular properties of interneurons, such as morphology, synapse specificity, and connectivity (De Marco García et al., 2011; Dehorter et al., 2015). Indeed, many supporting findings are coming out from studies that manipulate or abolish the activity of certain cell-type precursors (MGE or CGE derived) (Chattopadhyaya et al., 2004, 2007; De Marco García et al., 2011). Some of these findings suggest an activity-dependent regulation of molecular and electrophysiological properties of different interneuron subtypes (Miller et al., 2011; Dehorter et al., 2015) and thereby contribute to subtype-specific differences in gene expression (Batista-Brito et al., 2008; Paul et al., 2017), which have now been resolved with increasing depth (Joglekar et al., 2021; Scala et al., 2021). Furthermore, the onset and duration of these activity modulations have differential effects on the different interneurons subtypes, reflecting the timeline with which they differentiate from the respective ganglionic eminences (Wamsley and Fishell, 2017). Mostly early maturational aspects of MGE- and CGE-derived interneuron specification are hereby discussed, since general morphological and electrophysiological characteristics that distinguish the different interneuron subpopulations are extensively described elsewhere (Gelman and Marín, 2010; Rudy et al., 2011; Pfeffer et al., 2013; Lim et al., 2018a; Fishell and Kepecs, 2020).

Early Maturation of MGE-Derived Interneurons

In the rodent cortex, the earliest developing interneurons are SST and PV interneurons originating from the MGE. As mentioned before, the first GABAergic neurons start to populate the cortical plate very early in development, already between E9.5 and E12.5 in deep cortical laminas (Miyoshi et al., 2007). At first, SST interneurons are generated from the dorsal division of MGE. Around E17.5, they are found in the deep layer of the cortical plate (Miyoshi and Fishell, 2011), whereas at the end of the 1st postnatal week, they are visible across all cortical layers (Liguz-Lecznar et al., 2016). During early postnatal days, SST interneurons play transient and instrumental functions in shaping neural circuits in the cortex. At P4–6 in the mouse somatosensory cortex, SST interneurons receive dense innervation from the thalamus, and in turn, give inputs to pyramidal cells, spiny stellate cells, and recently migrated prospective PV neurons (Marques-Smith et al., 2016; Tuncdemir et al., 2016). Remarkably, these connections are fundamental for the proper formation of thalamo-cortical feedforward circuits (Tuncdemir et al., 2016), the coordinated activation of PV cells (Modol et al., 2020), and functional topography (Duan et al., 2020), since conditional ablation or silencing of SST neurons drastically impairs these processes. Conversely, it has been shown that the functional maturation of SST interneurons is delayed if afferent excitatory inputs from pyramidal neurons are decreased at early (P1) rather than later (P8) postnatal stages

(Pan et al., 2019). Furthermore, besides direct synaptic inputs, it was recently shown that SST interneurons also exert a paracrine role through the release of synaptogenic extracellular matrix proteins such as collagen XIX (Su et al., 2020). During the 2nd postnatal week, SST interneurons are involved in the control of sensory-evoked activity, such as spontaneous retinally-driven activity in the visual cortex (Leighton et al., 2021), or multi-whisking activity in the barrel cortex (Kastli et al., 2020). In line with these findings, conditional silencing of SST interneurons leads to a decrease in spontaneous spindle-burst activity and abolished facilitation in sensory adaptation (Baruchin et al., 2021).

Later on, PV neurons originate from the ventral division of MGE (Bandler et al., 2017) and start to radially migrate between E18 and P2, not reaching their final position until P6 (Bartholome et al., 2020). Between the 2nd and the 4th week, cortical PV neurons start expressing PV and defining ion channel composition that characterizes their peculiar electrophysiological properties (Bartholome et al., 2020). Upon arrival into the cortical layer, a particular type of extracellular matrix dubbed the perineuronal net (PNN), plays a critical role in the correct settling of PV interneurons by influencing their connectivity. The PNN can control synaptic plasticity by preventing spine formation (Vo et al., 2013). In support of this, degradation of PNNs leads to reduced gamma activity in juvenile mice (Carceller et al., 2020), which is in line with recent discovery linking PV to gamma activity (Bitzenhofer et al., 2020) and the finding that altered PNNs lead to abnormal activity (Wingert and Sorg, 2021). In addition to the role of PNNs, other molecular mechanisms can influence PV development, such as tonic activation of NMDA receptor (Hanson et al., 2019), BDNF (Lau et al., 2021), or retinoic acid (Larsen et al., 2019), whose receptor expression is also dependent on activity.

Early Maturation of CGE-Derived Interneuron

In the rodent brain, CGE-derived interneurons are produced at first at E12.5, reaching a peak around E16.5 (Miyoshi et al., 2010). Unlike MGE-derived cortical interneurons, they do not populate the cortex in an inside-out manner, but the vast majority are located in superficial cortical layers, and only acquire their final position around P4 (Miyoshi et al., 2010). Remarkably, the integration into the neocortex of CGE-derived interneurons depends on serotonin signaling (Murthy et al., 2014): impairment of which leads to their mispositioning (Frazer et al., 2015). Although it has been shown that a common feature of most, if not all, CGE-derived interneurons is the expression of the serotonin ionotropic receptor 5HT3aR (Lee et al., 2010) most of our understanding nonetheless remains built upon traditional molecular markers that identify specific subclasses (Tremblay et al., 2016). Of these, the best characterized is probably the VIP interneuron subclass, which accounts for around 40% of all CGE-derived interneurons, and the reelin subclass which labels around 60% of them (Wamsley and Fishell, 2017). However, our knowledge on the early developmental phases of CGE-derived interneurons is still limited and, only recently, CGE-specific transcriptional factors and activity-dependent mechanisms began to be explored (De Marco García et al., 2011; Miyoshi et al., 2015; Wei et al., 2019). Of note, it was shown that Prox1 is fundamental for the acquisition of CGE-derived interneuron properties both in the embryonic and postnatal stage (Miyoshi et al., 2015), with its conditional knock-out during early postnatal days leading to impairment of excitatory inputs onto the VIP multipolar subtype (Stachniak et al., 2021). Remarkably, it has been shown that network activity critically affects the proper morphological development of CR-positive VIP bipolar cells and RELN interneurons, but not that of CCK-positive VIP multipolar interneurons (De Marco García et al., 2011, 2015). Thus, activity and genetic program might act in a subtype-specific manner onto CGE-derived interneuron developmental steps. Finally, with the introduction of subtype-specific driver Cre-lines early functions and regulatory mechanisms have also begun to be studied in more depth (Taniguchi et al., 2011). In the barrel cortex, for example, VIP interneurons show a transient preferential response to multi-whisking that is lost during the 3rd postnatal week (Kastli et al., 2020), and their conditional silencing influence the onset of active whisking (Baruchin et al., 2021).

Connectivity Within GABAergic Populations and Across Transient Neuronal Populations

Interneurons are not only integrated into nascent and mature cortical networks *via* chemical synapses—of which many previously discussed pre- and postsynaptic GABAergic elements critically impact the emergence of cortical activity but also *via* gap junctions which are ubiquitous in the cortex. Gap junctions form connections mainly amongst GABAergic interneurons of the same functional class, but also across functionally distinct classes in the mature and immature cortex (Peinado et al., 1993; Hatch et al., 2017). Interestingly, gap junctions are generally described to be essential for oscillatory activity (Tchumatchenko and Clopath, 2014; Pernelle et al., 2018) and bidirectional activity-dependent plasticity is shown (Haas et al., 2016). Yet, the concise contribution of electrical coupling to distinct activity patterns during peri- and postnatal development remains unknown. Integration of GABAergic interneurons into developing cortical circuits *via* chemical synapses can be measured as spontaneous and evoked GABAergic inputs onto cortical plate neurons in the rodent cortex as early as E19 and P3, respectively (Owens et al., 1999; Daw et al., 2007). Instead, functional synaptic connections between GABAergic interneurons have only been shown after P4 in the visual cortex (Pangratz-Fuehrer and Hestrin, 2011). Prior to this, transient cortical populations already show GABAergic inputs (Kilb and Luhmann, 2001; Soda et al., 2003). However, the contribution of interneurons towards GABAergic signaling to transient cell populations like Cajal Retzius neurons, or subplate neurons that precede the integration of GABAergic cells into immature but persistent cortical circuits—is the subject of ongoing research (Molnár et al., 2020). The prerequisite for the functional integration of GABAergic interneurons is the maturation of their electrophysiological as well as their morphological features at the presynapse, but also the maturation of GABAergic synapses on the postsynaptic side of the recipient

cells. This includes the aforementioned expression of GABAergic receptors and the setting of chloride and bicarbonate gradients. As discussed above, this structural and functional maturation of the GABAergic synapse occurs in an largely activity-independent manner (le Magueresse et al., 2011). Not only does neuronal activity influence the initial formation of perisomatic synapses by interneurons (Chattopadhyaya et al., 2004), but it also remains a key influencer of plastic changes on the structure and function of GABAergic synapses in the adult brain (Flores and Méndez, 2014). On the other side of the coin, many important key cortical functions depend on the proper integration of GABAergic interneurons into the cortical network, like selectivity of sensory modalities, gain control, range modulation and plasticity of cortical circuits, regulation of firing rates and bursting activity with high temporal precision, generation and synchronization of cortical rhythms, as well as the maintenance of the excitatory and inhibitory balance (Tremblay et al., 2016; Fishell and Kepecs, 2020).

Developmental Apoptosis

Besides genetic programs, trophic support, and pro- and anti-apoptotic factors, neuronal activity also has a major impact on cell death and survival rates in the developing cortical network (Blanquie et al., 2017a; Wong and Marín, 2019). Here, increases in neuronal activity are associated with elevated survival rates in principal neurons and interneurons, whereas blockade or attenuation of activity is generally associated with higher apoptotic rates (Ruijter et al., 1991; Ikonomidou et al., 1999; Heck et al., 2008; Southwell et al., 2012). However, cell-type-specific peculiarities exist, for example in the transient cell population of Cajal Retzius neurons, where activity even fulfills an antithetic pro-apoptotic function (Del Río et al., 1995; Blanquie et al., 2017b). Whether this effect of activity for the survival of developing neurons is controlled by a cell-autonomous process or by network-dependent mechanisms is the subject of current investigations (Southwell et al., 2012; Blanquie et al., 2017c; Wong et al., 2018). Most recent evidence suggests that not only the level of neuronal activity but also the temporal pattern of activity affects neuronal survival rates *in vivo* (Blanquie et al., 2017c) and *in vitro* (Wong Fong Sang et al., 2021). This also applies to interneurons, as different evidence supports that positive or negative alterations in network activity result in a respective change of survival rates in GABAergic interneurons (Wong et al., 2018; Duan et al., 2020; Bitzenhofer et al., 2021). Notably, the most potent neuroprotective patterns highlighted within these studies are of a high-frequency oscillatory nature and resemble activity which typically occurs at the end of the 1st postnatal week *in vivo* (Yang et al., 2009; Luhmann and Khazipov, 2018) or is reflected *in vitro* by reminiscent patterns such as recurrent bursts (Wagenaar et al., 2006; Sun et al., 2010). Interestingly, GABAergic neurons themselves are essential for the modulation of these cortical activity patterns (Bonifazi et al., 2009; Isaacson and Scanziani, 2011; Modol et al., 2020). Thus, as far as the understanding of the mutual dependency of activity and apoptosis in interneurons goes until now, cortical activity acts as a master regulator of apoptotic rates in both interneurons and pyramidal neurons (Wong et al., 2018), even in a region-specific manner (Blanquie et al., 2017c). Herewith, activity-dependent regulation of developmental cell death can be seen as a *bona fide* homeostatic system (Blanquie et al., 2017a; Causeret et al., 2018) with the GABAergic interneurons in the perfect position to orchestrate this cortical activity set point (Duan et al., 2020).

How Do Dynamic Changes in the GABAergic Neuron Fraction During Perinatal Development Affect Network Activity in the Developing Cortex?

The sequential generation, migration, and apoptotic removal of interneurons during early brain development eventually influence GABAergic population sizes in the mature cortex, but also cause a dynamic variation in the absolute GABAergic neuron population size in the cortex during the developmental phase. Yet, the relative GABAergic neuron fraction is maintained throughout the embryonic and postnatal development and into adulthood (Sahara et al., 2012). Experimental manipulations of excitation/inhibition ratio are effectively compensated for, either through adjustments in the number of connections (Sukenik et al., 2021) or changes in synaptic strength (Southwell et al., 2012). Similar adaptive mechanisms also stabilize cortical inhibition on the network level under physiological (Southwell et al., 2012; Field et al., 2020; Romagnoni et al., 2020) and pathophysiological conditions (Hunt et al., 2013). Thus, in line with the dispensability of NKCC1-mediated depolarizing GABA responses for the establishment of cortical activity patterns (Graf et al., 2021), cortical networks adapt surprisingly well to alterations in the relative GABAergic fraction (Liu, 2004; Sukenik et al., 2021) and thereby keep the network activity level and patterning mostly stable. Both phenomena—specifically the stable expression of network activity despite the physiological changes in absolute GABAergic population during development, but also the tight homeostatic regulation of activity upon pathological or experimental perturbations of the GABAergic system—emphasize the importance of network activity as the most relevant output function. At the same time, these findings do not exclude that the developmental changes in interneuron function and network composition cause *per se* physiologically relevant difference in this output, i.e., merging network activity patterns throughout development and differences in activity patterns across models (Luhmann et al., 2016). Deciphering the multi-layered developmental processes in GABA signaling discussed above is necessary for the future assessment of the exact contribution of these processes to cortical activity patterns seen during development and in adult cortical networks. Certain partly-transient network structures, such as clustered GABAergic assemblies (Tuncdemir et al., 2016; Modol et al., 2020), subplate neurons (Kanold and Shatz, 2006; Molnár et al., 2020), and subcortical thalamic regions (Minlebaev et al., 2011; Yang et al., 2013; Murata and Colonnese, 2016), are surely essential and thus not dispensable for the establishment of cortical network activity and function during early brain development (Tolner et al., 2012).

CONCLUSION AND OUTLOOK

Immature cortical networks have a unique capacity to stabilize their network activity, even if strong changes in GABA signaling are introduced e.g., by alterations in the absolute number of GABAergic interneurons in neocortical cultures (Sukenik et al., 2021; Xing et al., 2021), genetic changes of total GABA content in the brain (Tamamaki et al., 2003), or modulations of chloride homeostasis (Pfeffer et al., 2009; Graf et al., 2021). This stability underlines the great source of plasticity of the neuronal system in general, but is especially remarkable given the suggested key function of GABAergic interneurons for the balancing of excitation and inhibition, and thus coordinating network activity during development (Bonifazi et al., 2009; Le Magueresse and Monyer, 2013; Modol et al., 2020; Baruchin et al., 2021). By and large, GABAergic interneurons keep this crucial role in mature networks with some critical modifications (Markram et al., 2004; Bartos et al., 2007; Tremblay et al., 2016). While it is well accepted that GABAergic neuron-mediated inhibition is essential for the regulation of synchronized oscillations in adult cortical networks (Klausberger and Somogyi, 2008; Gonzalez-Burgos et al., 2010), the functional role of interneurons during development is still less clear. It remains to be seen, if the activity of distinct interneuron subclasses during development is crucial *per se* for brain development, as suggested by recent studies (Modol et al., 2020; Baruchin et al., 2021; Leighton et al., 2021), or if only certain network activity patterns must be played in distinct cortical compartments or temporal windows for proper brain development-regardless of the GABAergic contribution. Interestingly, a prolonged developmental timeline for GABAergic interneurons is an amplified trait in higher order gyrencephalic mammals, which suggests that a protracted development of interneurons through neurogenesis, neuronal migration, and network integration is a mechanism for increased complexity and cognitive flexibility in cortex function (Kim and Paredes, 2021).

In view of the above, the association of pathophysiological changes in interneuron function or excitation/inhibition balance with neurological and psychological conditions in humans are to be expected and have been well described (Marín, 2012; Nelson and Valakh, 2015). With pharmacological GABAergic modulators such as benzodiazepines as first-line treatment options in acute epileptic emergencies in children and adults (Glauser et al., 2016), the direct intervention with $GABA_A$ receptor signaling is already common practice in the clinic and will likely profit from future advances in this field of research. Additionally, the absence of certain activity patterns during critical developmental periods, to which GABAergic interneurons significantly contribute, is associated with unfavorable outcomes in humans and animal models (Ranasinghe et al., 2015; Whitehead et al., 2016). Thus, scientific progress will likely also provide important insights to the clinically relevant questions: (I) how pre- and early postnatal pathophysiological insults (e.g., *in utero* inflammation/infection, perinatal hypoxia-ischemia); or (II) certain drugs that impact GABAergic signaling (e.g., medications or drug abuse during pregnancy) change spontaneous activity; (III) how these activity changes ultimately affect clinical outcomes; and (IV) which clinical interventions could be advisable (ter Horst et al., 2004; Iyer et al., 2014).

Besides the manifold developmental changes in both interneuron function and cortical activity which are described in this review, in addition to the pathophysiological changes in this mutual interaction (described in more detail elsewhere; Marín, 2012), makes it more and more evident that physiological conditions—as well as anatomical and even subcellular compartment location—critically impact the contribution of GABA signaling to neuronal activity, and *vice versa* (Raimondo et al., 2017; Düsterwald et al., 2018). While current research in this field has already begun to understand these subcellular effects of ionic plasticity (Blaesse et al., 2009) and coincidence membrane depolarization (Doyon et al., 2011; Raimondo et al., 2012) on network activity in the adult brain (Jedlička and Backus, 2006; Raimondo et al., 2017), the relevance of subcellular as well as regional or state-dependent differences in GABA signaling and their impact on cortical network activity during development, remains largely unexploited. Hence, the final portrait of interneurons as replaceable or unique orchestra members and/or designated conductors of cortical activity within the orchestra line-up of the immature cortex remains a vibrant field of research with many open questions. We are only beginning to understand: (I) how interneuron subpopulations and subcellular processes contribute to spontaneous and evoked activity patterns on the network level; (II) how the GABAergic contribution differs across functionally distinct cortical regions and converging periods of development; and (III) how cortical network activity eventually feeds back on nascent interneuron function. However, it is becoming more evident that cortical network activity should be considered as the most significant output in development or, in the figurative sense, as the most sonorous symphony that the heterogenous orchestra of the developing neocortex has to play.

AUTHOR CONTRIBUTIONS

DW and JS contributed equally to this manuscript. All authors contributed to the article and approved the submitted version.

FUNDING

This study was supported by funding from the Deutsche Forschungsgemeinschaft (DFG) to AS (CRC 1080, A01), a FTN stipend to DW, and intramural funding to AS (Stufe1).

ACKNOWLEDGMENTS

We thank Heiko J. Luhmann and all members of the Institute of Physiology Mainz for their continuous support as well as Davide Bassetti, Elena Nigi, and Celine Gallagher for helpful comments on the manuscript.

REFERENCES

Achilles, K., Okabe, A., Ikeda, M., Shimizu-Okabe, C., Yamada, J., Fukuda, A., et al. (2007). Kinetic properties of Cl^- uptake mediated by Na^+-dependent K^+-$2Cl^-$ cotransport in immature rat neocortical neurons. *J. Neurosci.* 27, 8616–8627. doi: 10.1523/JNEUROSCI.5041-06.2007

Ackman, J. B., and Crair, M. C. (2014). Role of emergent neural activity in visual map development. *Curr. Opin. Neurobiol.* 24, 166–175. doi: 10.1016/j.conb.2013.11.011

Andäng, M., Hjerling-Leffler, J., Moliner, A., Lundgren, T. K., Castelo-Branco, G., Nanou, E., et al. (2008). Histone H2AX-dependent $GABA_A$ receptor regulation of stem cell proliferation. *Nature* 451, 460–464. doi: 10.1038/nature06488

Araki, T., Kiyama, H., and Tohyama, M. (1992). $GABA_A$ Receptor subunit messenger RNAs show differential expression during cortical development in the rat brain. *Neuroscience* 51, 583–591. doi: 10.1016/0306-4522(92)90298-g

Bagasrawala, I., Memi, F., Radonjić, N. V., and Zecevic, N. (2017). N-methyl d-aspartate receptor expression patterns in the human fetal cerebral cortex. *Cereb. Cortex* 27, 5041–5053. doi: 10.1093/cercor/bhw289

Bandler, R. C., Mayer, C., and Fishell, G. (2017). Cortical interneuron specification: the juncture of genes, time and geometry. *Curr. Opin. Neurobiol.* 42, 17–24. doi: 10.1016/j.conb.2016.10.003

Bando, Y., Irie, K., Shimomura, T., Umeshima, H., Kushida, Y., Kengaku, M., et al. (2016). Control of spontaneous Ca^{2+} transients is critical for neuronal maturation in the developing neocortex. *Cereb. Cortex* 26, 106–117. doi: 10.1093/cercor/bhu180

Barakat, L., and Bordey, A. (2002). GAT-1 and reversible GABA transport in Bergmann glia in slices. *J. Neurophysiol.* 88, 1407–1419. doi: 10.1152/jn.2002.88.3.1407

Bartholome, O., de la Brassinne Bonardeaux, O., Neirinckx, V., and Rogister, B. (2020). A composite sketch of fast-spiking parvalbumin-positive neurons. *Cereb. Cortex Commun.* 1, 1–15. doi: 10.1093/texcom/tgaa026

Bartos, M., Vida, I., and Jonas, P. (2007). Synaptic mechanisms of synchronized gamma oscillations in inhibitory interneuron networks. *Nat. Rev. Neurosci.* 8, 45–56. doi: 10.1038/nrn2044

Baruchin, L. J., Ghezzi, F., Kohl, M. M., and Butt, S. J. B. (2021). Contribution of interneuron subtype-specific gabaergic signaling to emergent sensory processing in mouse somatosensory whisker barrel cortex. *Cereb. Cortex* 2021:bhab363. doi: 10.1093/cercor/bhab363

Batista-Brito, R., MacHold, R., Klein, C., and Fishell, G. (2008). Gene expression in cortical interneuron precursors is prescient of their mature function. *Cereb. Cortex* 18, 2306–2317. doi: 10.1093/cercor/bhm258

Behar, T. N., Schaffner, A. E., Scott, C. A., Greene, C. L., and Barker, J. L. (2000). GABA receptor antagonists modulate postmitotic cell migration in slice cultures of embryonic rat cortex. *Cereb. Cortex* 10, 899–909. doi: 10.1093/cercor/10.9.899

Behar, T. N., Smith, S. V., Kennedy, R. T., Mckenzi, J. M., Maric, I., and Barker, J. L. (2001). $GABA_B$ receptors mediate motility signals for migrating embryonic cortical cells. *Cereb. Cortex* 11, 744–753. doi: 10.1093/cercor/11.8.744

Behuet, S., Cremer, J. N., Cremer, M., Palomero-Gallagher, N., Zilles, K., and Amunts, K. (2019). Developmental changes of glutamate and GABA receptor densities in wistar rats. *Front. Neuroanat.* 13:100. doi: 10.3389/fnana.2019.00100

Ben-Ari, Y. (2002). Excitatory actions of GABA during development: the nature of the nurture. *Nat. Rev. Neurosci.* 3, 728–739. doi: 10.1038/nrn920

Ben-Ari, Y. (2006). Basic developmental rules and their implications for epilepsy in the immature brain. *Epileptic Disord.* 8, 91–102.

Bitzenhofer, S. H., Pöpplau, J. A., Chini, M., Marquardt, A., and Hanganu-Opatz, I. L. (2021). A transient developmental increase in prefrontal activity alters network maturation and causes cognitive dysfunction in adult mice. *Neuron* 109, 1350–1364.e6. doi: 10.1016/j.neuron.2021.02.011

Bitzenhofer, S. H., Pöpplau, J. A., and Hanganu-Opatz, I. L. (2020). Gamma activity accelerates during prefrontal development. *eLife* 9:e56795. doi: 10.7554/eLife.56795

Blaesse, P., Airaksinen, M. S., Rivera, C., and Kaila, K. (2009). Cation-chloride cotransporters and neuronal function. *Neuron* 61, 820–838. doi: 10.1016/j.neuron.2009.03.003

Blankenship, A. G., and Feller, M. B. (2010). Mechanisms underlying spontaneous patterned activity in developing neural circuits. *Nat. Rev. Neurosci.* 11, 18–29. doi: 10.1038/nrn2759

Blanquie, O., Kilb, W., Sinning, A., and Luhmann, H. J. (2017a). Homeostatic interplay between electrical activity and neuronal apoptosis in the developing neocortex. *Neuroscience* 358, 190–200. doi: 10.1016/j.neuroscience.2017.06.030

Blanquie, O., Liebmann, L., Hübner, C. A., Luhmann, H. J., and Sinning, A. (2017b). NKCC1-mediated GABAergic signaling promotes postnatal cell death in neocortical cajal-retzius cells. *Cereb. Cortex* 27, 1644–1659. doi: 10.1093/cercor/bhw004

Blanquie, O., Yang, J. W., Kilb, W., Sharopov, S., Sinning, A., and Luhmann, H. J. (2017c). Electrical activity controls area-specific expression of neuronal apoptosis in the mouse developing cerebral cortex. *eLife* 6:e27696. doi: 10.7554/eLife.27696

Bonifazi, P., Goldin, M., Picardo, M. A., Jorquera, I., Cattani, A., Bianconi, G., et al. (2009). GABAergic hub neurons orchestrate synchrony in developing hippocampal networks. *Science* 326, 1419–1424. doi: 10.1126/science.1175509

Borodinsky, L. N., Root, C. M., Cronin, J. A., Sann, S. B., Gu, X., and Spitzer, N. C. (2004). Activity-dependent homeostatic specification of transmitter expression in embryonic neurons. *Nature* 429, 523–530. doi: 10.1038/nature02518

Bortone, D., and Polleux, F. (2009). KCC2 expression promotes the termination of cortical interneuron migration in a voltage-sensitive calcium-dependent manner. *Neuron* 62, 53–71. doi: 10.1016/j.neuron.2009.01.034

Bosman, C. A., Schoffelen, J. M., Brunet, N., Oostenveld, R., Bastos, A. M., Womelsdorf, T., et al. (2012). Attentional stimulus selection through selective synchronization between monkey visual areas. *Neuron* 75, 875–888. doi: 10.1016/j.neuron.2012.06.037

Bugeon, S., Haubold, C., Ryzynski, A., Cremer, H., and Platel, J. C. (2021). Intrinsic neuronal activity during migration controls the recruitment of specific interneuron subtypes in the postnatal mouse olfactory bulb. *J. Neurosci.* 41, 2630–2644. doi: 10.1523/JNEUROSCI.1960-20.2021

Butt, S. J., Stacey, J. A., Teramoto, Y., and Vagnoni, C. (2017). A role for GABAergic interneuron diversity in circuit development and plasticity of the neonatal cerebral cortex. *Curr. Opin. Neurobiol.* 43, 149–155. doi: 10.1016/j.conb.2017.03.011

Cancedda, L., Fiumelli, H., Chen, K., and Poo, M. M. (2007). Excitatory GABA action is essential for morphological maturation of cortical neurons *in vivo*. *J. Neurosci.* 27, 5224–5235. doi: 10.1523/JNEUROSCI.5169-06.2007

Carceller, H., Guirado, R., Ripolles-Campos, E., Teruel-Marti, V., and Nacher, J. (2020). Perineuronal nets regulate the inhibitory perisomatic input onto parvalbumin interneurons and γ activity in the prefrontal cortex. *J. Neurosci.* 40, 5008–5018. doi: 10.1523/JNEUROSCI.0291-20.2020

Causeret, F., Coppola, E., and Pierani, A. (2018). Cortical developmental death: selected to survive or fated to die. *Curr. Opin. Neurobiol.* 53, 35–42. doi: 10.1016/j.conb.2018.04.022

Chattopadhyaya, B., Di Cristo, G., Higashiyama, H., Knott, G. W., Kuhlman, S. J., Welker, E., et al. (2004). Experience and activity-dependent maturation of perisomatic GABAergic innervation in primary visual cortex during a postnatal critical period. *J. Neurosci.* 24, 9598–9611. doi: 10.1523/JNEUROSCI.1851-04.2004

Chattopadhyaya, B., Di Cristo, G., Wu, C. Z., Knott, G., Kuhlman, S., Fu, Y., et al. (2007). GAD67-mediated GABA synthesis and signaling regulate inhibitory synaptic innervation in the visual cortex. *Neuron* 54, 889–903. doi: 10.1016/j.neuron.2007.05.015

Ciccolini, F., Collins, T. J., Sudhoelter, J., Lipp, P., Berridge, M. J., and Bootman, M. D. (2003). Local and global spontaneous calcium events regulate neurite outgrowth and onset of GABAergic phenotype during neural precursor differentiation. *J. Neurosci.* 23, 103–111. doi: 10.1523/JNEUROSCI.23-01-00103.2003

Colonnese, M. T., Kaminska, A., Minlebaev, M., Milh, M., Bloem, B., Lescure, S., et al. (2010). A conserved switch in sensory processing prepares developing neocortex for vision. *Neuron* 67, 480–498. doi: 10.1016/j.neuron.2010.07.015

Cserép, C., Szabadits, E., Szonyi, A., Watanabe, M., Freund, T. F., and Nyiri, G. (2012). NMDA receptors in GABAergic synapses during postnatal development. *PLoS One* 7:e37753. doi: 10.1371/journal.pone.0037753

Daw, M. I., Ashby, M. C., and Isaac, J. T. R. (2007). Coordinated developmental recruitment of latent fast spiking interneurons in layer IV barrel cortex. *Nat. Neurosci.* 10, 453–461. doi: 10.1038/nn1866

De Marco García, N. V., Karayannis, T., and Fishell, G. (2011). Neuronal activity is required for the development of specific cortical interneuron subtypes. *Nature* 472, 351–355. doi: 10.1038/nature09865

De Marco García, N. V., Priya, R., Tuncdemir, S. N., Fishell, G., and Karayannis, T. (2015). Sensory inputs control the integration of neurogliaform interneurons into cortical circuits. *Nat. Neurosci.* 18, 393–403. doi: 10.1038/nn.3946

Dehorter, N., Ciceri, G., Bartolini, G., Lim, L., Del Pino, I., and Marín, O. (2015). Tuning of fast-spiking interneuron properties by an activity-dependent transcriptional switch. *Science* 349, 1216–1220. doi: 10.1126/science.aab3415

Deidda, G., Allegra, M., Cerri, C., Naskar, S., Bony, G., Zunino, G., et al. (2015). Early depolarizing GABA controls critical-period plasticity in the rat visual cortex. *Nat. Neurosci.* 18, 87–96. doi: 10.1038/nn.3890

Del Río, J. A., Martinez, A., Fonseca, M., Auladell, C., and Soriano, E. (1995). Glutamate-like immunoreactivity and fate of cajal-retzius cells in the murine cortex as identified with calretinin antibody. *Cereb. Cortex* 5, 13–21. doi: 10.1093/cercor/5.1.13

Deng, L., Yao, J., Fang, C., Dong, N., Luscher, B., and Chen, G. (2007). Sequential postsynaptic maturation governs the temporal order of gabaergic and glutamatergic synaptogenesis in rat embryonic cultures. *J. Neurosci.* 27, 10860–10869. doi: 10.1523/JNEUROSCI.2744-07.2007

Doyon, N., Prescott, S. A., Castonguay, A., Godin, A. G., Kröger, H., and de Koninck, Y. (2011). Efficacy of synaptic inhibition depends on multiple, dynamically interacting mechanisms implicated in chloride homeostasis. *PLoS Comput. Biol.* 7:e1002149. doi: 10.1371/journal.pcbi.1002149

Duan, Z. R. S., Che, A., Chu, P., Modol, L., Bollmann, Y., Babij, R., et al. (2020). GABAergic restriction of network dynamics regulates interneuron survival in the developing cortex. *Neuron* 105, 75–92.e5. doi: 10.1016/j.neuron.2019.10.008

Düsterwald, K. M., Currin, C. B., Burman, R. J., Akerman, C. J., Kay, A. R., and Raimondo, J. V. (2018). Biophysical models reveal the relative importance of transporter proteins and impermeant anions in chloride homeostasis. *eLife* 7:e39575. doi: 10.7554/eLife.39575

Egorov, A. V., and Draguhn, A. (2013). Development of coherent neuronal activity patterns in mammalian cortical networks: common principles and local hetereogeneity. *Mech. Dev.* 130, 412–423. doi: 10.1016/j.mod.2012.09.006

Eilers, J., Plant, T. D., Marandi, N., and Konnerth, A. (2001). GABA-mediated Ca^{2+} signalling in developing rat cerebellar Purkinje neurones. *J. Physiol.* 536, 429–437. doi: 10.1111/j.1469-7793.2001.0429c.xd

Fattorini, G., Ripoli, C., Cocco, S., Spinelli, M., Mattera, A., Grassi, C., et al. (2019). Glutamate/GABA co-release selectively influences postsynaptic glutamate receptors in mouse cortical neurons. *Neuropharmacology* 161:107737. doi: 10.1016/j.neuropharm.2019.107737

Faux, C., Rakic, S., Andrews, W., and Britto, J. M. (2012). Neurons on the move: migration and lamination of cortical interneurons. *NeuroSignals* 20, 168–189. doi: 10.1159/000334489

Field, R. E., D'amour, J. A., Tremblay, R., Miehl, C., Rudy, B., Gjorgjieva, J., et al. (2020). Heterosynaptic plasticity determines the set point for cortical excitatory-inhibitory balance. *Neuron* 106, 842–854.e4. doi: 10.1016/j.neuron.2020.03.002

Fiorentino, H., Kuczewski, N., Diabira, D., Ferrand, N., Pangalos, M. N., Porcher, C., et al. (2009). $GABA_B$ receptor activation triggers BDNF release and promotes the maturation of GABAergic synapses. *J. Neurosci.* 29, 11650–11661. doi: 10.1523/JNEUROSCI.3587-09.2009

Fishell, G., and Kepecs, A. (2020). Interneuron types as attractors and controllers. *Annu. Rev. Neurosci.* 43, 1–30. doi: 10.1146/annurev-neuro-070918-050421

Fiumelli, H., Cancedda, L., and Poo, M. M. (2005). Modulation of GABAergic transmission by activity *via* postsynaptic Ca^{2+}-dependent regulation of KCC2 function. *Neuron* 48, 773–786. doi: 10.1016/j.neuron.2005.10.025

Flavell, S. W., and Greenberg, M. E. (2008). Signaling mechanisms linking neuronal activity to gene expression and plasticity of the nervous system. *Annu. Rev. Neurosci.* 31, 563–590. doi: 10.1146/annurev.neuro.31.060407.125631

Flores, C. E., and Méndez, P. (2014). Shaping inhibition: activity dependent structural plasticity of GABAergic synapses. *Front. Cell. Neurosci.* 8:327. doi: 10.3389/fncel.2014.00327

Flossmann, T., Kaas, T., Rahmati, V., Kiebel, S. J., Witte, O. W., Holthoff, K., et al. (2019). Somatostatin interneurons promote neuronal synchrony in the neonatal hippocampus. *Cell Rep.* 26, 3173–3182.e5. doi: 10.1016/j.celrep.2019.02.061

Frazer, S., Otomo, K., and Dayer, A. (2015). Early-life serotonin dysregulation affects the migration and positioning of cortical interneuron subtypes. *Transl. Psychiatry* 5:e644. doi: 10.1038/tp.2015.147

Fuchs, C., Abitbol, K., Burden, J. J., Mercer, A., Brown, L., Iball, J., et al. (2013). $GABA_A$ receptors can initiate the formation of functional inhibitory GABAergic synapses. *Eur. J. Neurosci.* 38, 3146–3158. doi: 10.1111/ejn.12331

Ganguly, K., Schinder, A. F., Wong, S. T., and Poo, M. M. (2001). GABA itself promotes the developmental switch of neuronal GABAergic responses from excitation to inhibition. *Cell* 105, 521–532. doi: 10.1016/s0092-8674(01)00341-5

Gao, X. B., and Van Den Pol, A. N. (2000). GABA release from mouse axonal growth cones. *J. Physiol.* 523, 629–637. doi: 10.1111/j.1469-7793.2000.t01-1-00629.x

Gao, X. B., and Van Den Pol, A. N. (2001). GABA, not glutamate, a primary transmitter driving action potentials in developing hypothalamic neurons. *J. Neurophysiol.* 85, 425–434. doi: 10.1152/jn.2001.85.1.425

Gelman, D. M., and Marín, O. (2010). Generation of interneuron diversity in the mouse cerebral cortex. *Eur. J. Neurosci.* 31, 2136–2141. doi: 10.1111/j.1460-9568.2010.07267.x

Glauser, T., Shinnar, S., Gloss, D., Alldredge, B., Arya, R., Bainbridge, J., et al. (2016). Evidence-based guideline: treatment of convulsive status epilepticus in children and adults: report of the guideline committee of the american epilepsy society. *Epilepsy Curr.* 16, 48–61. doi: 10.5698/1535-7597-16.1.48

Golshani, P., Gonçalves, J. T., Khoshkhoo, S., Mostany, R., Smirnakis, S., and Portera-Cailliau, C. (2009). Internally mediated developmental desynchronization of neocortical network activity. *J. Neurosci.* 29, 10890–10899. doi: 10.1523/JNEUROSCI.2012-09.2009

Gonzalez-Burgos, G., Hashimoto, T., and Lewis, D. A. (2010). Alterations of cortical GABA neurons and network oscillations in schizophrenia. *Curr. Psychiatry Rep.* 12, 335–344. doi: 10.1007/s11920-010-0124-8

Graf, J., Zhang, C., Marguet, S. L., Herrmann, T., Flossmann, T., Hinsch, R., et al. (2021). A limited role of NKCC1 in telencephalic glutamatergic neurons for developing hippocampal network dynamics and behavior. *Proc. Natl. Acad. Sci. U S A* 118:e2014784118. doi: 10.1073/pnas.2014784118

Gu, X., Zhou, L., and Lu, W. (2016). An NMDA receptor-dependent mechanism underlies inhibitory synapse development. *Cell Rep.* 14, 471–478. doi: 10.1016/j.celrep.2015.12.061

Haas, J. S., Greenwald, C. M., and Pereda, A. E. (2016). Activity-dependent plasticity of electrical synapses: increasing evidence for its presence and functional roles in the mammalian brain. *BMC Cell Biol.* 17:14. doi: 10.1186/s12860-016-0090-z

Hanson, E., Armbruster, M., Lau, L. A., Sommer, M. E., Klaft, Z. J., Swanger, S. A., et al. (2019). Tonic activation of GluN2C/GluN2D-containing NMDA receptors by ambient glutamate facilitates cortical interneuron maturation. *J. Neurosci.* 39, 3611–3626. doi: 10.1523/JNEUROSCI.1392-18.2019

Hatch, R. J., Mendis, G. D. C., Kaila, K., Reid, C. A., and Petrou, S. (2017). Gap junctions link regular-spiking and fast-spiking interneurons in layer 5 somatosensory cortex. *Front. Cell. Neurosci.* 11:204. doi: 10.3389/fncel.2017.00204

Heck, N., Golbs, A., Riedemann, T., Sun, J.-J., Lessmann, V., and Luhmann, H. J. (2008). Activity-dependent regulation of neuronal apoptosis in neonatal mouse cerebral cortex. *Cereb. Cortex* 18, 1335–1349. doi: 10.1093/cercor/bhm165

Heck, N., Kilb, W., Reiprich, P., Kubota, H., Furukawa, T., Fukuda, A., et al. (2007). GABA-A receptors regulate neocortical neuronal migration *in vitro* and *in vivo*. *Cereb. Cortex* 17, 138–148. doi: 10.1093/cercor/bhj135

Hensch, T. K., Fagiolini, M., Mataga, N., Stryker, M. P., Baekkeskov, S., and Kash, S. F. (1998). Local GABA circuit control of experience-dependent plasticity in developing visual cortex. *Science* 282, 1504–1508. doi: 10.1126/science.282.5393.1504

Hunt, R. F., Girskis, K. M., Rubenstein, J. L., Alvarez-Buylla, A., and Baraban, S. C. (2013). GABA progenitors grafted into the adult epileptic brain control seizures and abnormal behavior. *Nat. Neurosci.* 16, 692–697. doi: 10.1038/nn.3392

Hurni, N., Kolodziejczak, M., Tomasello, U., Badia, J., Jacobshagen, M., Prados, J., et al. (2017). Transient cell-intrinsic activity regulates the migration and laminar positioning of cortical projection neurons. *Cereb. Cortex* 27, 3052–3063. doi: 10.1093/cercor/bhx059

Ikonomidou, C., Bosch, F., Miksa, M., Bittigau, P., Vöckler, J., Dikranian, K., et al. (1999). Blockade of NMDA receptors and apoptotic neurodegeneration in the developing brain. *Science* 283, 70–74. doi: 10.1126/science.283.5398.70

Inada, H., Watanabe, M., Uchida, T., Ishibashi, H., Wake, H., Nemoto, T., et al. (2011). GABA regulates the multidirectional tangential migration of GABAergic interneurons in living neonatal mice. *PLoS One* 6:e27048. doi: 10.1371/journal.pone.0027048

Isaacson, J. S., and Scanziani, M. (2011). How inhibition shapes cortical activity. *Neuron* 72, 231–243. doi: 10.1016/j.neuron.2011.09.027

Iyer, K. K., Roberts, J. A., Metsäranta, M., Finnigan, S., Breakspear, M., and Vanhatalo, S. (2014). Novel features of early burst suppression predict outcome after birth asphyxia. *Ann. Clin. Transl. Neurol.* 1, 209–214. doi: 10.1002/acn3.32

Jedlička, P., and Backus, K. H. (2006). Inhibitory transmission, activity-dependent ionic changes and neuronal network oscillations. *Physiol. Res.* 55, 139–149.

Joglekar, A., Prjibelski, A., Mahfouz, A., Collier, P., Lin, S., Schlusche, A. K., et al. (2021). A spatially resolved brain region- and cell type-specific isoform atlas of the postnatal mouse brain. *Nat. Commun.* 12:463. doi: 10.1038/s41467-020-20343-5

Kaila, K. (1994). Ionic basis of $GABA_A$ receptor channel function in the nervous system. *Prog. Neurobiol.* 42, 489–537. doi: 10.1016/0301-0082(94)90049-3

Kanold, P. O., and Shatz, C. J. (2006). Subplate neurons regulate maturation of cortical inhibition and outcome of ocular dominance plasticity. *Neuron* 51, 627–638. doi: 10.1016/j.neuron.2006.07.008

Káradóttir, R. T., and Kuo, C. T. (2018). Neuronal activity-dependent control of postnatal neurogenesis and gliogenesis. *Annu. Rev. Neurosci.* 41, 139–161. doi: 10.1146/annurev-neuro-072116-031054

Kastli, R., Vighagen, R., van der Bourg, A., Argunsah, A. Ö., Iqbal, A., Voigt, F. F., et al. (2020). Developmental divergence of sensory stimulus representation in cortical interneurons. *Nat. Commun.* 11:5729. doi: 10.1038/s41467-020-19427-z

Kepecs, A., and Fishell, G. (2014). Interneuron cell types are fit to function. *Nature* 505, 318–326. doi: 10.1038/nature12983

Khazipov, R., Esclapez, M., Caillard, O., Bernard, C., Khalilov, I., Tyzio, R., et al. (2001). Early development of neuronal activity in the primate hippocampus in utero. *J. Neurosci.* 21, 9770–9781. doi: 10.1523/JNEUROSCI.21-24-09770.2001

Kilb, W., and Luhmann, H. J. (2001). Spontaneous GABAergic postsynaptic currents in Cajal-Retzius cells in neonatal rat cerebral cortex. *Eur. J. Neurosci.* 13, 1387–1390. doi: 10.1046/j.0953-816x.2001.01514.x

Kilb, W., Kirischuk, S., and Luhmann, H. J. (2011). Electrical activity patterns and the functional maturation of the neocortex. *Eur. J. Neurosci.* 34, 1677–1686. doi: 10.1111/j.1460-9568.2011.07878.x

Kim, J. Y., and Paredes, M. F. (2021). Implications of extended inhibitory neuron development. *Int. J. Mol. Sci.* 22:5113. doi: 10.3390/ijms22105113

Kirkby, L. A., Sack, G. S., Firl, A., and Feller, M. B. (2013). A role for correlated spontaneous activity in the assembly of neural circuits. *Neuron* 80, 1129–1144. doi: 10.1016/j.neuron.2013.10.030

Kirmse, K., Kummer, M., Kovalchuk, Y., Witte, O. W., Garaschuk, O., and Holthoff, K. (2015). GABA depolarizes immature neurons and inhibits network activity in the neonatal neocortex *in vivo*. *Nat. Commun.* 6:7750. doi: 10.1038/ncomms8750

Klausberger, T., and Somogyi, P. (2008). Neuronal diversity and temporal dynamics: the unity of hippocampal circuit operations. *Science* 321, 53–57. doi: 10.1126/science.1149381

Komuro, H., and Kumada, T. (2005). Ca^{2+} transients control CNS neuronal migration. *Cell Calcium* 37, 387–393. doi: 10.1016/j.ceca.2005.01.006

Komuro, H., and Rakic, P. (1996). Intracellular Ca^{2+} fluctuations modulate the rate of neuronal migration. *Neuron* 17, 275–285. doi: 10.1016/s0896-6273(00)80159-2

Kumada, T., and Fukuda, A. (2020). "Multimodal $GABA_A$ receptor functions in the development of the central nervous system," in *Synapse Development and Maturation*, (Cambridge, MA: Elsevier), 323–343. doi: 10.1016/b978-0-12-823672-7.00014-4

Larsen, R., Proue, A., Scott, E. P., Christiansen, M., and Nakagawa, Y. (2019). The thalamus regulates retinoic acid signaling and development of parvalbumin interneurons in postnatal mouse prefrontal cortex. *eNeuro* 6:30868103. doi: 10.1523/ENEURO.0018-19.2019

Lau, C. G., Zhang, H., and Murthy, V. N. (2021). Deletion of TrkB in parvalbumin interneurons alters cortical neural dynamics. *J. Cell. Physiol.* doi: 10.1002/jcp.30571. [Online ahead of print].

Laurie, D. J., Wisden, W., and Seeburg, P. H. (1992). The distribution of thirteen GABA(A) receptor subunit mRNAs in the rat brain. III. embryonic and postnatal development. *J. Neurosci.* 12, 4151–4172. doi: 10.1523/JNEUROSCI.12-11-04151.1992

le Magueresse, C., Alfonso, J., Khodosevich, K., Martín, Á. A. A., Bark, C., and Monyer, H. (2011). "Small axonless neurons": postnatally generated neocortical interneurons with delayed functional maturation. *J. Neurosci.* 31, 16731–16747. doi: 10.1523/JNEUROSCI.4273-11.2011

Le Magueresse, C., and Monyer, H. (2013). GABAergic interneurons shape the functional maturation of the cortex. *Neuron* 77, 388–405. doi: 10.1016/j.neuron.2013.01.011

Leighton, A. H., Cheyne, J. E., Houwen, G. J., Maldonado, P. P., De Winter, F., Levelt, C. N., et al. (2021). Somatostatin interneurons restrict cell recruitment to retinally driven spontaneous activity in the developing cortex. *Cell Rep.* 36:109316. doi: 10.1016/j.celrep.2021.109316

Leinekugel, X., Tseeb, V., Ben-Ari, Y., and Bregestovski, P. (1995). Synaptic $GABA_A$ activation induces Ca^{2+} rise in pyramidal cells and interneurons from rat neonatal hippocampal slices. *J. Physiol.* 487, 319–329. doi: 10.1113/jphysiol.1995.sp020882

Leitch, E., Coaker, J., Young, C., Mehta, V., and Sernagor, E. (2005). GABA type-A activity controls its own developmental polarity switch in the maturing retina. *J. Neurosci.* 25, 4801–4805. doi: 10.1523/JNEUROSCI.0172-05.2005

Lee, S., Hjerling-Leffler, J., Zagha, E., Fishell, G., and Rudy, B. (2010). The largest group of superficial neocortical GABAergic interneurons expresses ionotropic serotonin receptors. *J. Neurosci.* 30, 16796–16808. doi: 10.1523/JNEUROSCI.1869-10.2010

Li, S., Kumar, P., Joshee, S., Kirschstein, T., Subburaju, S., Khalili, J. S., et al. (2018). Endothelial cell-derived GABA signaling modulates neuronal migration and postnatal behavior. *Cell Res.* 28, 221–248. doi: 10.1038/cr.2017.135

Li, S., Park, M. S., and Kim, M. O. (2004). Prenatal alteration and distribution of the $GABA_{B1}$ and $GABA_{B2}$ receptor subunit mRNAs during rat central nervous system development. *Brain Res. Dev. Brain Res.* 150, 141–150. doi: 10.1016/j.devbrainres.2004.03.009

Liguz-Lecznar, M., Urban-Ciecko, J., and Kossut, M. (2016). Somatostatin and somatostatin-containing neurons in shaping neuronal activity and plasticity. *Front. Neural Circuits* 10:48. doi: 10.3389/fncir.2016.00048

Lim, L., Mi, D., Llorca, A., and Marín, O. (2018a). Development and functional diversification of cortical interneurons. *Neuron* 100, 294–313. doi: 10.1016/j.neuron.2018.10.009

Lim, L., Pakan, J. M. P., Selten, M. M., Marques-Smith, A., Llorca, A., Bae, S. E., et al. (2018b). Optimization of interneuron function by direct coupling of cell migration and axonal targeting. *Nat. Neurosci.* 21, 920–931. doi: 10.1038/s41593-018-0162-9

Liu, G. (2004). Local structural balance and functional interaction of excitatory and inhibitory synapses in hippocampal dendrites. *Nat. Neurosci.* 7, 373–379. doi: 10.1038/nn1206

Lodato, S., and Arlotta, P. (2015). Generating neuronal diversity in the mammalian cerebral cortex. *Annu. Rev. Cell Dev. Biol.* 31, 699–720. doi: 10.1146/annurev-cellbio-100814-125353

López-Bendito, G., Shigemoto, R., Kulik, A., Paulsen, O., Fairén, A., and Luján, R. (2002). Expression and distribution of metabotropic GABA receptor subtypes $GABA_B$R1 and $GABA_B$R2 during rat neocortical development. *Eur. J. Neurosci.* 15, 1766–1778. doi: 10.1046/j.1460-9568.2002.02032.x

Ludwig, A., Li, H., Saarma, M., Kaila, K., and Rivera, C. (2003). Developmental up-regulation of KCC2 in the absence of GABAergic and glutamatergic transmission. *Eur. J. Neurosci.* 18, 3199–3206. doi: 10.1111/j.1460-9568.2003.03069.x

Luhmann, H. J., Fukuda, A., and Kilb, W. (2015). Control of cortical neuronal migration by glutamate and GABA. *Front. Cell. Neurosci.* 9:4. doi: 10.3389/fncel.2015.00004

Luhmann, H. J., and Khazipov, R. (2018). Neuronal activity patterns in the developing barrel cortex. *Neuroscience* 368, 256–267. doi: 10.1016/j.neuroscience.2017.05.025

Luhmann, H. J., and Prince, D. A. (1991). Postnatal maturation of the GABAergic system in rat neocortex. *J. Neurophysiol.* 65, 247–263. doi: 10.1152/jn.1991.65.2.247

Luhmann, H. J., Sinning, A., Yang, J. W., Reyes-Puerta, V., Stüttgen, M. C., Kirischuk, S., et al. (2016). Spontaneous neuronal activity in developing neocortical networks: from single cells to large-scale interactions. *Front. Neural Circuits* 10:40. doi: 10.3389/fncir.2016.00040

Ma, W., and Barker, J. L. (1995). Complementary expressions of transcripts encoding GAD67 and GABA(A) receptor α4, β1 and γ1 subunits in the proliferative zone of the embryonic rat central nervous system. *J. Neurosci.* 15, 2547–2560. doi: 10.1523/JNEUROSCI.15-03-02547.1995

Malmersjö, S., Rebellato, P., Smedler, E., Planert, H., Kanatani, S., Liste, I., et al. (2013). Neural progenitors organize in small-world networks to promote cell proliferation. *Proc. Natl. Acad. Sci. U S A* 110, E1524–E1532. doi: 10.1073/pnas.1220179110

Marín, O. (2012). Interneuron dysfunction in psychiatric disorders. *Nat. Rev. Neurosci.* 13, 107–120. doi: 10.1038/nrn3155

Markram, H., Toledo-Rodriguez, M., Wang, Y., Gupta, A., Silberberg, G., and Wu, C. (2004). Interneurons of the neocortical inhibitory system. *Nat. Rev. Neurosci.* 5, 793–807. doi: 10.1038/nrn1519

Marques-Smith, A., Lyngholm, D., Kaufmann, A. K., Stacey, J. A., Hoerder-Suabedissen, A., Becker, E. B. E., et al. (2016). A transient translaminar GABAergic interneuron circuit connects thalamocortical recipient layers in neonatal somatosensory cortex. *Neuron* 89, 536–549. doi: 10.1016/j.neuron.2016.01.015

Martini, F. J., Guillamón-Vivancos, T., Moreno-Juan, V., Valdeolmillos, M., and López-Bendito, G. (2021). Spontaneous activity in developing thalamic and cortical sensory networks. *Neuron* 109, 2519–2534. doi: 10.1016/j.neuron.2021.06.026

Masquelier, T., Hugues, E., Deco, G., and Thorpe, S. J. (2009). Oscillations, phase-of-firing coding and spike timing-dependent plasticity: an efficient learning scheme. *J. Neurosci.* 29, 13484–13493. doi: 10.1523/JNEUROSCI.2207-09.2009

Miller, M. N., Okaty, B. W., Kato, S., and Nelson, S. B. (2011). Activity-dependent changes in the firing properties of neocortical fast-spiking interneurons in the absence of large changes in gene expression. *Dev. Neurobiol.* 71, 62–70. doi: 10.1002/dneu.20811

Minelli, A., Alonso-Nanclares, L., Edwards, R. H., Defelipe, J., and Conti, F. (2003). Postnatal development of the vesicular GABA transporter in rat cerebral cortex. *Neuroscience* 117, 337–346. doi: 10.1016/s0306-4522(02)00864-3

Minelli, A., Brecha, N. C., Karschin, C., DeBiasi, S., and Conti, F. (1995). GAT-1, a high-affinity GABA plasma membrane transporter, is localized to neurons and astroglia in the cerebral cortex. *J. Neurosci.* 15, 7734–7746. doi: 10.1523/JNEUROSCI.15-11-07734.1995

Minlebaev, M., Colonnese, M., Tsintsadze, T., Sirota, A., and Khazipov, R. (2011). Early gamma oscillations synchronize developing thalamus and cortex. *Science* 334, 226–229. doi: 10.1126/science.1210574

Miyoshi, G., Butt, S. J. B., Takebayashi, H., and Fishell, G. (2007). Physiologically distinct temporal cohorts of cortical interneurons arise from telencephalic Olig2-expressing precursors. *J. Neurosci.* 27, 7786–7798. doi: 10.1523/JNEUROSCI.1807-07.2007

Miyoshi, G., and Fishell, G. (2011). GABAergic interneuron lineages selectively sort into specific cortical layers during early postnatal development. *Cereb. Cortex* 21, 845–852. doi: 10.1093/cercor/bhq155

Miyoshi, G., Hjerling-Leffler, J., Karayannis, T., Sousa, V. H., Butt, S. J. B., Battiste, J., et al. (2010). Genetic fate mapping reveals that the caudal ganglionic eminence produces a large and diverse population of superficial cortical interneurons. *J. Neurosci.* 30, 1582–1594. doi: 10.1523/JNEUROSCI.4515-09.2010

Miyoshi, G., Young, A., Petros, T., Karayannis, T., Chang, M. M. K., Lavado, A., et al. (2015). Prox1 regulates the subtype-specific development of caudal ganglionic eminence-derived GABAergic cortical interneurons. *J. Neurosci.* 35, 12869–12889. doi: 10.1523/JNEUROSCI.1164-15.2015

Modol, L., Bollmann, Y., Tressard, T., Baude, A., Che, A., Duan, Z. R. S., et al. (2020). Assemblies of perisomatic GABAergic neurons in the developing barrel cortex. *Neuron* 105, 93–105.e4. doi: 10.1016/j.neuron.2019.10.007

Molnár, Z., Luhmann, H. J., and Kanold, P. O. (2020). Transient cortical circuits match spontaneous and sensory-driven activity during development. *Science* 370:eabb2153. doi: 10.1126/science.abb2153

Monyer, H., Burnashev, N., Laurie, D. J., Sakmann, B., and Seeburg, P. H. (1994). Developmental and regional expression in the rat brain and functional properties of four NMDA receptors. *Neuron* 12, 529–540. doi: 10.1016/0896-6273(94)90210-0

Murata, Y., and Colonnese, M. T. (2016). An excitatory cortical feedback loop gates retinal wave transmission in rodent thalamus. *eLife* 5:e18816. doi: 10.7554/eLife.18816

Murata, Y., and Colonnese, M. T. (2020). GABAergic interneurons excite neonatal hippocampus *in vivo*. *Sci. Adv.* 6:eaba1430. doi: 10.1126/sciadv.aba1430

Murthy, S., Niquille, M., Hurni, N., Limoni, G., Frazer, S., Chameau, P., et al. (2014). Serotonin receptor 3A controls interneuron migration into the neocortex. *Nat. Commun.* 5:5524. doi: 10.1038/ncomms6524

Nelson, S. B., and Valakh, V. (2015). Excitatory/inhibitory balance and circuit homeostasis in autism spectrum disorders. *Neuron* 87, 684–698. doi: 10.1016/j.neuron.2015.07.033

Oh, W. C., Lutzu, S., Castillo, P. E., and Kwon, H. B. (2016). *De novo* synaptogenesis induced by GABA in the developing mouse cortex. *Science* 353, 1037–1040. doi: 10.1126/science.aaf5206

Okujeni, S., and Egert, U. (2019). Self-organization of modular network architecture by activity-dependent neuronal migration and outgrowth. *eLife* 8:e47996. doi: 10.7554/eLife.47996

Olsen, R. W., and Sieghart, W. (2009). $GABA_A$ receptors: subtypes provide diversity of function and pharmacology. *Neuropharmacology* 56, 141–148. doi: 10.1016/j.neuropharm.2008.07.045

Owens, D. F., Liu, X., and Kriegstein, A. R. (1999). Changing properties of GABA(A) receptor-mediated signaling during early neocortical development. *J. Neurophysiol.* 82, 570–583. doi: 10.1152/jn.1999.82.2.570

Pan, N. C., Fang, A., Shen, C., Sun, L., Wu, Q., and Wang, X. (2019). Early excitatory activity-dependent maturation of somatostatin interneurons in cortical layer 2/3 of mice. *Cereb. Cortex* 29, 4107–4118. doi: 10.1093/cercor/bhy293

Pangratz-Fuehrer, S., and Hestrin, S. (2011). Synaptogenesis of electrical and GABAergic synapses of fast-spiking inhibitory neurons in the neocortex. *J. Neurosci.* 31, 10767–10775. doi: 10.1523/JNEUROSCI.6655-10.2011

Patrizi, A., Scelfo, B., Viltono, L., Briatore, F., Fukaya, M., Watanabe, M., et al. (2008). Synapse formation and clustering of neuroligin-2 in the absence of $GABA_A$ receptors. *Proc. Natl. Acad. Sci. U S A* 105, 13151–13156. doi: 10.1073/pnas.0802390105

Paul, A., Crow, M., Raudales, R., He, M., Gillis, J., and Huang, Z. J. (2017). Transcriptional architecture of synaptic communication delineates GABAergic neuron identity. *Cell* 171, 522–539.e20. doi: 10.1016/j.cell.2017.08.032

Peinado, A., Yuste, R., and Katz, L. C. (1993). Extensive dye coupling between rat neocortical neurons during the period of circuit formation. *Neuron* 10, 103–114. doi: 10.1016/0896-6273(93)90246-n

Pernelle, G., Nicola, W., and Clopath, C. (2018). Gap junction plasticity as a mechanism to regulate network-wide oscillations. *PLoS Comput. Biol.* 14:e1006025. doi: 10.1371/journal.pcbi.1006025

Petryniak, M. A., Potter, G. B., Rowitch, D. H., and Rubenstein, J. L. R. (2007). Dlx1 and Dlx2 control neuronal versus oligodendroglial cell fate acquisition in the developing forebrain. *Neuron* 55, 417–433. doi: 10.1016/j.neuron.2007.06.036

Pfeffer, C. K., Stein, V., Keating, D. J., Maier, H., Rinke, I., Rudhard, Y., et al. (2009). NKCC1-dependent GABAergic excitation drives synaptic network maturation during early hippocampal development. *J. Neurosci.* 29, 3419–3430. doi: 10.1523/JNEUROSCI.1377-08.2009

Pfeffer, C. K., Xue, M., He, M., Huang, Z. J., and Scanziani, M. (2013). Inhibition of inhibition in visual cortex: the logic of connections between molecularly distinct interneurons. *Nat. Neurosci.* 16, 1068–1076. doi: 10.1038/nn.3446

Pouchelon, G., Gambino, F., Bellone, C., Telley, L., Vitali, I., Lüscher, C., et al. (2014). Modality-specific thalamocortical inputs instruct the identity of postsynaptic L4 neurons. *Nature* 511, 471–474. doi: 10.1038/nature13390

Poulter, M. O., Barker, J. L., O'Carroll, A. M., Lolait, S. J., and Mahan, L. C. (1992). Differential and transient expression of GABA(A) receptor α-subunit mRNAs in the developing rat CNS. *J. Neurosci.* 12, 2888–2900. doi: 10.1523/JNEUROSCI.12-08-02888.1992

Raimondo, J. V., Markram, H., and Akerman, C. J. (2012). Short-term ionic plasticity at GABAergic synapses. *Front. Synaptic Neurosci.* 4:5. doi: 10.3389/fnsyn.2012.00005

Raimondo, J. V., Richards, B. A., and Woodin, M. A. (2017). Neuronal chloride and excitability - the big impact of small changes. *Curr. Opin. Neurobiol.* 43, 35–42. doi: 10.1016/j.conb.2016.11.012

Ranasinghe, S., Or, G., Wang, E. Y., Ievins, A., McLean, M. A., Niell, C. M., et al. (2015). Reduced cortical activity impairs development and plasticity after neonatal hypoxia ischemia. *J. Neurosci.* 35, 11946–11959. doi: 10.1523/JNEUROSCI.2682-14.2015

Reha, R. K., Dias, B. G., Nelson, C. A., Kaufer, D., Werker, J. F., Kolbh, B., et al. (2020). Critical period regulation across multiple timescales. *Proc. Natl. Acad. Sci. U S A* 117, 23242–23251. doi: 10.1073/pnas.1820836117

Reith, C. A., and Sillar, K. T. (1999). Development and role of $GABA_A$ receptor-mediated synaptic potentials during swimming in postembryonic *Xenopus laevis* tadpoles. *J. Neurophysiol.* 82, 3175–3187. doi: 10.1152/jn.1999.82.6.3175

Rheims, S., Minlebaev, M., Ivanov, A., Represa, A., Khazipov, R., Holmes, G. L., et al. (2008). Excitatory GABA in rodent developing neocortex *in vitro*. *J. Neurophysiol.* 100, 609–619. doi: 10.1152/jn.90402.2008

Rivera, C., Voipio, J., Payne, J. A., Ruusuvuori, E., Lahtinen, H., Lamsa, K., et al. (1999). The K^+/Cl^- co-transporter KCC2 renders GABA hyperpolarizing during neuronal maturation. *Nature* 397, 251–255. doi: 10.1038/16697

Rochefort, N. L., Garaschuk, O., Milos, R. I., Narushima, M., Marandi, N., Pichler, B., et al. (2009). Sparsification of neuronal activity in the visual cortex at eye-opening. *Proc. Natl. Acad. Sci. U S A* 106, 15049–15054. doi: 10.1073/pnas.0907660106

Romagnoni, A., Colonnese, M. T., Touboul, J. D., and Gutkin, B. S. (2020). Progressive alignment of inhibitory and excitatory delay may drive a rapid developmental switch in cortical network dynamics. *J. Neurophysiol.* 123, 1583–1599. doi: 10.1152/jn.00402.2019

Rudy, B., Fishell, G., Lee, S. H., and Hjerling-Leffler, J. (2011). Three groups of interneurons account for nearly 100% of neocortical GABAergic neurons. *Dev. Neurobiol.* 71, 45–61. doi: 10.1002/dneu.20853

Ruijter, J. M., Baker, R. E., De Jong, B. M., and Romijn, H. J. (1991). Chronic blockade of bioelectric activity in neonatal rat cortex grown *in vitro*: morphological effects. *Int. J. Dev. Neurosci.* 9, 331–333. doi: 10.1016/0736-5748(91)90054-p

Rymar, V. V., and Sadikot, A. F. (2007). Laminar fate of cortical GABAergic interneurons is dependent on both birthdate and phenotype. *J. Comp. Neurol.* 501, 369–380. doi: 10.1002/cne.21250

Sahara, S., Yanagawa, Y., O'Leary, D. D. M., and Stevens, C. F. (2012). The fraction of cortical GABAergic neurons is constant from near the start of cortical neurogenesis to adulthood. *J. Neurosci.* 32, 4755–4761. doi: 10.1523/JNEUROSCI.6412-11.2012

Saint-Amant, L., and Drapeau, P. (2000). Motoneuron activity patterns related to the earliest behavior of the zebrafish embryo. *J. Neurosci.* 20, 3964–3972. doi: 10.1523/JNEUROSCI.20-11-03964.2000

Sale, A., Berardi, N., Spolidoro, M., Baroncelli, L., and Maffei, L. (2010). GABAergic inhibition in visual cortical plasticity. *Front. Cell. Neurosci.* 4:10. doi: 10.3389/fncel.2010.00010

Scala, F., Kobak, D., Bernabucci, M., Bernaerts, Y., Cadwell, C. R., Castro, J. R., et al. (2021). Phenotypic variation of transcriptomic cell types in mouse motor cortex. *Nature* 598, 144–150. doi: 10.1038/s41586-020-2907-3

Shimizu-Okabe, C., Yokokura, M., Okabe, A., Ikeda, M., Sato, K., Kilb, W., et al. (2002). Layer-specific expression of Cl^- transporters and differential $[Cl^-]_i$ in newborn rat cortex. *Neuroreport* 13, 2433–2437. doi: 10.1097/00001756-200212200-00012

Sipilä, S. T., Huttu, K., Yamada, J., Afzalov, R., Voipio, J., Blaesse, P., et al. (2009). Compensatory enhancement of intrinsic spiking upon NKCC1 disruption in neonatal hippocampus. *J. Neurosci.* 29, 6982–6988. doi: 10.1038/s41467-021-22339-1

Soda, T., Nakashima, R., Watanabe, D., Nakajima, K., Pastan, I., and Nakanishi, S. (2003). Segregation and coactivation of developing neocortical layer 1 neurons. *J. Neurosci.* 23, 6272–6279. doi: 10.1523/JNEUROSCI.23-15-06272.2003

Southwell, D. G., Paredes, M. F., Galvao, R. P., Jones, D. L., Froemke, R. C., Sebe, J. Y., et al. (2012). Intrinsically determined cell death of developing cortical interneurons. *Nature* 491, 109–113. doi: 10.1038/nature11523

Stachniak, T. J., Kastli, R., Hanley, O., Argunsah, A. Ö., van der Valk, E. G. T., Kanatouris, G., et al. (2021). Postmitotic Prox1 expression controls the final specification of cortical VIP interneuron subtypes. *J. Neurosci.* 41, 8150–8162. doi: 10.1523/JNEUROSCI.1021-21.2021

Su, J., Basso, D., Iyer, S., Su, K., Wei, J., and Fox, M. A. (2020). Paracrine role for somatostatin interneurons in the assembly of perisomatic inhibitory synapses. *J. Neurosci.* 40, 7421–7435. doi: 10.1523/JNEUROSCI.0613-20.2020

Sukenik, N., Vinogradov, O., Weinreb, E., Segal, M., Levina, A., and Moses, E. (2021). Neuronal circuits overcome imbalance in excitation and inhibition by adjusting connection numbers. *Proc. Natl. Acad. Sci. U S A* 118:e2018459118. doi: 10.1073/pnas.2018459118

Sultan, K. T., Brown, K. N., and Shi, S. H. (2013). Production and organization of neocortical interneurons. *Front. Cell. Neurosci.* 7:221. doi: 10.1073/pnas.2018459118

Sun, J. J., Kilb, W., and Luhmann, H. J. (2010). Self-organization of repetitive spike patterns in developing neuronal networks *in vitro*. *Eur. J. Neurosci.* 32, 1289–1299. doi: 10.1111/j.1460-9568.2010.07383.x

Takayama, C., and Inoue, Y. (2010). Developmental localization of potassium chloride co-transporter 2 (KCC2), GABA and vesicular GABA transporter (VGAT) in the postnatal mouse somatosensory cortex. *Neurosci. Res.* 67, 137–148. doi: 10.1016/j.neures.2010.02.010

Takesian, A. E., and Hensch, T. K. (2013). Balancing plasticity/stability across brain development. *Prog Brain Res.* 207, 3–34. doi: 10.1016/B978-0-444-63327-9.00001-1

Tamamaki, N., Yanagawa, Y., Tomioka, R., Miyazaki, J. I., Obata, K., and Kaneko, T. (2003). Green fluorescent protein expression and colocalization with calretinin, parvalbumin and somatostatin in the GAD67-GFP knock-in mouse. *J. Comp. Neurol.* 467, 60–79. doi: 10.1002/cne.10905

Taniguchi, H., He, M., Wu, P., Kim, S., Paik, R., Sugino, K., et al. (2011). A resource of cre driver lines for genetic targeting of GABAergic neurons in cerebral cortex. *Neuron* 71, 995–1013. doi: 10.1016/j.neuron.2011.07.026

Taylor, J., and Gordon-Weeks, P. R. (1991). Calcium-independent γ-aminobutyric acid release from growth cones: role of γ-aminobutyric acid transport. *J. Neurochem.* 56, 273–280. doi: 10.1111/j.1471-4159.1991.tb02592.x

Tchumatchenko, T., and Clopath, C. (2014). Oscillations emerging from noise-driven steady state in networks with electrical synapses and subthreshold resonance. *Nat. Commun.* 5:5512. doi: 10.1038/ncomms6512

Teppola, H., Aćimović, J., and Linne, M. L. (2019). Unique features of network bursts emerge from the complex interplay of excitatory and inhibitory receptors in rat neocortical networks. *Front. Cell. Neurosci.* 13:377. doi: 10.3389/fncel.2019.00377

Terunuma, M. (2018). Diversity of structure and function of $GABA_B$ receptors: a complexity of $GABA_B$-mediated signaling. *Proc. Jpn. Acad. Ser. B Phys. Biol. Sci.* 94, 390–411. doi: 10.2183/pjab.94.026

ter Horst, H. J., Sommer, C., Bergman, K. A., Fock, J. M., van Weerden, T. W., and Bos, A. F. (2004). Prognostic significance of amplitude-integrated EEG during the first 72 hours after birth in severely asphyxiated neonates. *Pediatr. Res.* 55, 1026–1033. doi: 10.1203/01.pdr.0000127019.52562.8c

Titz, S., Hans, M., Kelsch, W., Lewen, A., Swandulla, D., and Misgeld, U. (2003). Hyperpolarizing inhibition develops without trophic support by GABA in cultured rat midbrain neurons. *J. Physiol.* 550, 719–730. doi: 10.1113/jphysiol.2003.041863

Tolner, E. A., Sheikh, A., Yukin, A. Y., Kaila, K., and Kanold, P. O. (2012). Subplate neurons promote spindle bursts and thalamocortical patterning in the neonatal rat somatosensory cortex. *J. Neurosci.* 32, 692–702. doi: 10.1523/JNEUROSCI.1538-11.2012

Tort, A. B. L., Komorowski, R. W., Manns, J. R., Kopell, N. J., and Eichenbaum, H. (2009). Theta-gamma coupling increases during the learning of item-context associations. *Proc. Natl. Acad. Sci. U S A* 106, 20942–20947. doi: 10.1073/pnas.0911331106

Tremblay, R., Lee, S., and Rudy, B. (2016). GABAergic interneurons in the neocortex: from cellular properties to circuits. *Neuron* 91, 260–292. doi: 10.1016/j.neuron.2016.06.033

Tuncdemir, S. N., Wamsley, B., Stam, F. J., Osakada, F., Goulding, M., Callaway, E. M., et al. (2016). Early somatostatin interneuron connectivity

mediates the maturation of deep layer cortical circuits. *Neuron* 89, 521–535. doi: 10.1016/j.neuron.2015.11.020

Turgeon, S. M., and Albin, R. L. (1994). Postnatal ontogeny of $GABA_B$ binding in rat brain. *Neuroscience* 62, 601–613. doi: 10.1016/0306-4522(94)90392-1

Turrigiano, G. G., and Nelson, S. B. (2004). Homeostatic plasticity in the developing nervous system. *Nat. Rev. Neurosci.* 5, 97–107. doi: 10.1038/nrn1327

Tyssowski, K. M., DeStefino, N. R., Cho, J. H., Dunn, C. J., Poston, R. G., Carty, C. E., et al. (2018). Different neuronal activity patterns induce different gene expression programs. *Neuron* 98, 530–546.e11. doi: 10.1016/j.neuron.2018.04.001

Tyzio, R., Represa, A., Jorquera, I., Ben-Ari, Y., Gozlan, H., and Aniksztejn, L. (1999). The establishment of GABAergic and glutamatergic synapses on CA1 pyramidal neurons is sequential and correlates with the development of the apical dendrite. *J. Neurosci.* 19, 10372–10382. doi: 10.1523/JNEUROSCI.19-23-10372.1999

van den Berghe, V., Stappers, E., Vandesande, B., Dimidschstein, J., Kroes, R., Francis, A., et al. (2013). Directed migration of cortical interneurons depends on the cell-autonomous action of sip1. *Neuron* 77, 70–82. doi: 10.1016/j.neuron.2012.11.009

Van Eden, C. G., Parmar, R., Lichtensteiger, W., and Schlumpf, M. (1995). Laminar distribution of $GABA_A$ receptor α1, β2 and γ2 subunit mRNAs in the granular and agranular frontal cortex of the rat during pre- and postnatal development. *Cereb. Cortex* 5, 234–246. doi: 10.1093/cercor/5.3.234

Virtanen, M. A., Uvarov, P., Hübner, C. A., and Kaila, K. (2020). NKCC1, an elusive molecular target in brain development: making sense of the existing data. *Cells* 9:2607. doi: 10.3390/cells9122607

Vo, T., Carulli, D., Ehlert, E. M. E., Kwok, J. C. F., Dick, G., Mecollari, V., et al. (2013). The chemorepulsive axon guidance protein semaphorin3A is a constituent of perineuronal nets in the adult rodent brain. *Mol. Cell. Neurosci.* 56, 186–200. doi: 10.1016/j.mcn.2013.04.009

Wagenaar, D. A., Pine, J., and Potter, S. M. (2006). An extremely rich repertoire of bursting patterns during the development of cortical cultures. *BMC Neurosci.* 7:11. doi: 10.1186/1471-2202-7-11

Wamsley, B., and Fishell, G. (2017). Genetic and activity-dependent mechanisms underlying interneuron diversity. *Nat. Rev. Neurosci.* 18, 299–309. doi: 10.1038/nrn.2017.30

Wang, D. D., and Kriegstein, A. R. (2008). GABA regulates excitatory synapse formation in the neocortex *via* NMDA receptor activation. *J. Neurosci.* 28, 5547–5558. doi: 10.1523/JNEUROSCI.5599-07.2008

Wardle, R. A., and Poo, M. M. (2003). Brain-derived neurotrophic factor modulation of GABAergic synapses by postsynaptic regulation of chloride transport. *J. Neurosci.* 23, 8722–8732. doi: 10.1523/JNEUROSCI.23-25-08722.2003

Wei, S., Du, H., Li, Z., Tao, G., Xu, Z., Song, X., et al. (2019). Transcription factors Sp8 and Sp9 regulate the development of caudal ganglionic eminence-derived cortical interneurons. *J. Comp. Neurol.* 527, 2860–2874. doi: 10.1002/cne.24712

Weissman, T. A., Riquelme, P. A., Ivic, L., Flint, A. C., and Kriegstein, A. R. (2004). Calcium waves propagate through radial glial cells and modulate proliferation in the developing neocortex. *Neuron* 43, 647–661. doi: 10.1016/j.neuron.2004.08.015

Whitehead, K., Pressler, R., and Fabrizi, L. (2016). Characteristics and clinical significance of delta brushes in the EEG of premature infants. *Clin. Neurophysiol. Pract.* 2, 12–18. doi: 10.1016/j.cnp.2016.11.002

Wingert, J. C., and Sorg, B. A. (2021). Impact of perineuronal nets on electrophysiology of parvalbumin interneurons, principal neurons and brain oscillations: a review. *Front. Synaptic Neurosci.* 13:673210. doi: 10.3389/fnsyn.2021.673210

Wong Fong Sang, I. E., Schroer, J., Halbhuber, L., Warm, D., Yang, J. W., Luhmann, H. J., et al. (2021). Optogenetically controlled activity pattern determines survival rate of developing neocortical neurons. *Int. J. Mol. Sci.* 22:6575. doi: 10.3390/ijms22126575

Wong, F. K., Bercsenyi, K., Sreenivasan, V., Portalés, A., Fernández-Otero, M., and Marín, O. (2018). Pyramidal cell regulation of interneuron survival sculpts cortical networks. *Nature* 557, 668–673. doi: 10.1038/s41586-018-0139-6

Wong, F. K., and Marín, O. (2019). Developmental cell death in the cerebral cortex. *Annu. Rev. Cell Dev. Biol.* 35, 523–542. doi: 10.1146/annurev-cellbio-100818-125204

Wosniack, M. E., Kirchner, J. H., Chao, L. Y., Zabouri, N., Lohmann, C., and Gjorgjieva, J. (2021). Adaptation of spontaneous activity in the developing visual cortex. *eLife* 10:e61619. doi: 10.7554/eLife.61619

Xing, W., de Lima, A. D., and Voigt, T. (2021). The structural E/I balance constrains the early development of cortical network activity. *Front. Cell. Neurosci.* 15:687306. doi: 10.3389/fncel.2021.687306

Yamada, J., Okabe, A., Toyoda, H., Kilb, W., Luhmann, H. J., and Fukuda, A. (2004). Cl- uptake promoting depolarizing GABA actions in immature rat neocortical neurones is mediated by NKCC1. *J. Physiol.* 557, 829–841. doi: 10.1113/jphysiol.2004.062471

Yang, J. W., An, S., Sun, J. J., Reyes-Puerta, V., Kindler, J., Berger, T., et al. (2013). Thalamic network oscillations synchronize ontogenetic columns in the newborn rat barrel cortex. *Cereb. Cortex* 23, 1299–1316. doi: 10.1093/cercor/bhs103

Yang, J. W., Hanganu-Opatz, I. L., Sun, J. J., and Luhmann, H. J. (2009). Three patterns of oscillatory activity differentially synchronize developing neocortical networks *in vivo*. *J. Neurosci.* 29, 9011–9025. doi: 10.1523/JNEUROSCI.5646-08.2009

Conflict of Interest: The authors declare that the research was conducted in the absence of any commercial or financial relationships that could be construed as a potential conflict of interest.

Publisher's Note: All claims expressed in this article are solely those of the authors and do not necessarily represent those of their affiliated organizations, or those of the publisher, the editors and the reviewers. Any product that may be evaluated in this article, or claim that may be made by its manufacturer, is not guaranteed or endorsed by the publisher.

frontiers in Molecular Neuroscience

ORIGINAL RESEARCH
published: 03 February 2022
doi: 10.3389/fnmol.2021.807090

Disruption of KCC2 in Parvalbumin-Positive Interneurons Is Associated With a Decreased Seizure Threshold and a Progressive Loss of Parvalbumin-Positive Interneurons

*Tanja Herrmann, Melanie Gerth, Ralf Dittmann, Daniel Pensold†, Martin Ungelenk, Lutz Liebmann and Christian A. Hübner**

Institute of Human Genetics, University Hospital Jena, Jena, Germany

OPEN ACCESS

Edited by:
Lorenz S. Neuwirth, SUNY Old Westbury, United States

Reviewed by:
Mark Beenhakker, University of Virginia, United States
Ludovic Tricoire, Université Pierre et Marie Curie, France

***Correspondence:**
Christian A. Hübner
Christian.huebner@med.uni-jena.de

†Present address:
Daniel Pensold, Division of Functional Epigenetics, Institute of Zoology (Biology 2), RWTH Aachen University, Aachen, Germany

Specialty section:
This article was submitted to Brain Disease Mechanisms, a section of the journal Frontiers in Molecular Neuroscience

Received: *01 November 2021*
Accepted: *20 December 2021*
Published: *03 February 2022*

Citation:
Herrmann T, Gerth M, Dittmann R, Pensold D, Ungelenk M, Liebmann L and Hübner CA (2022) Disruption of KCC2 in Parvalbumin-Positive Interneurons Is Associated With a Decreased Seizure Threshold and a Progressive Loss of Parvalbumin-Positive Interneurons. Front. Mol. Neurosci. 14:807090. doi: 10.3389/fnmol.2021.807090

$GABA_A$ receptors are ligand-gated ion channels, which are predominantly permeable for chloride. The neuronal K-Cl cotransporter KCC2 lowers the intraneuronal chloride concentration and thus plays an important role for GABA signaling. KCC2 loss-of-function is associated with seizures and epilepsy. Here, we show that KCC2 is expressed in the majority of parvalbumin-positive interneurons (PV-INs) of the mouse brain. PV-INs receive excitatory input from principle cells and in turn control principle cell activity by perisomatic inhibition and inhibitory input from other interneurons. Upon Cre-mediated disruption of KCC2 in mice, the polarity of the GABA response of PV-INs changed from hyperpolarization to depolarization for the majority of PV-INs. Reduced excitatory postsynaptic potential-spike (E-S) coupling and increased spontaneous inhibitory postsynaptic current (sIPSC) frequencies further suggest that PV-INs are disinhibited upon disruption of KCC2. *In vivo*, PV-IN-specific KCC2 knockout mice display a reduced seizure threshold and develop spontaneous sometimes fatal seizures. We further found a time dependent loss of PV-INs, which was preceded by an up-regulation of pro-apoptotic genes upon disruption of KCC2.

Keywords: KCC2, GABA, interneuron, epilepsy, inhibition

INTRODUCTION

Brain function depends on highly interconnected networks of excitatory pyramidal neurons and inhibitory interneurons. The latter are predominantly locally projecting neurons, which release GABA to refine and shape circuit output by modulating the gain, timing, tuning, bursting properties of pyramidal cell firing, and selective filtering of synaptic excitation (Roux and Buzsaki, 2015). GABAergic interneurons account for roughly 20-30% of the overall neuronal population in the mammalian cerebral cortex (Hendry et al., 1987) and can be classified by different features. The most common classification is based on the expression of different molecular markers such as parvalbumin (PV), calbindin, somatostatin, and others (Markram et al., 2004). PV-positive interneurons (PV-INs) are the most common subtype (Celio, 1986) and are characterized by a fast-spiking phenotype, low input resistance and high-amplitude rapid after-hyperpolarization

(Hu et al., 2014). They can be further divided into basket cells, which innervate the soma and proximal dendrites, and chandelier cells that synapse onto the axon initial segment. GABAergic interneuron subtypes not only target different domains of pyramidal cells but also other interneurons (Gibson et al., 1999; Blatow et al., 2003; Hu et al., 2011; Jiang et al., 2013; Pfeffer et al., 2013). If interneuron function is impaired, this can affect higher brain functions and may result in seizures (Liu et al., 2014).

The polarity of the response to GABA critically depends on the intraneuronal chloride concentration. The intraneuronal chloride concentration $[Cl^-]_i$ is mainly determined by the interplay between the Na^+-dependent KCl-cotransporter NKCC1, which uses the Na^+ gradient to raise $[Cl^-]_i$, and the Na^+-independent KCl-cotransporter KCC2, which uses the K^+-gradient to lower $[Cl^-]_i$ (Payne et al., 1996, 2003; Blaesse et al., 2009; Kilb, 2012; Luhmann et al., 2014; Virtanen et al., 2020). The GABA-mediated hyperpolarizing chloride current is typically established during the first postnatal weeks in rodents (Rivera et al., 1999; Hubner et al., 2001; Ben-Ari et al., 2012). Mice with a total deletion of *Slc12a5* (*Kcc2*) die immediately after birth because of a failure to breathe (Hubner et al., 2001), while hypomorphic mice, which express about 5–8% of wild-type KCC2 protein levels, exhibit spontaneous generalized seizures and die before the third postnatal week (Woo et al., 2002). Notably, KCC2 loss-of-function mutations in humans are associated with inherited febrile seizures, severe genetic generalized epilepsy and epilepsy of infancy with migrating focal seizures (Hubner, 2014; Kahle et al., 2014; Puskarjov et al., 2014; Kahle et al., 2016; Saitsu et al., 2016; Di Cristo et al., 2018).

Here, we addressed the role of KCC2 in PV-INs. We show that the targeted disruption of KCC2 under control of the PV-promoter in mice results in a reduced seizure threshold with progressive loss of PV-INs. *In vitro*, the response of PV-INs to GABA was converted from hyperpolarizing to depolarizing. In agreement, network dependent GABA release was increased. The transcriptional profiling of PV-INs isolated from these mice suggest that stress related pathway may trigger apoptosis.

RESULTS

KCC2 Is Broadly Expressed in PV-Positive Neurons

PV-INs constitute ∼2.6% of overall neurons in the CA1 region of the hippocampus and ∼40% of GABAergic neocortical neurons (Rudy et al., 2011). To visualize PV-expressing cells we mated mice expressing Cre-recombinase under control of the PV promoter (PV-Cre) (Hippenmeyer et al., 2005) with a tdTomato reporter line (tdTomato) (Madisen et al., 2010) to obtain mice expressing tdTomato in PV-INs (WT^{PV} mice) (**Figures 1A,B**). In brain sections from 8-week-old WT^{PV} mice nearly all cells expressing tdTomato also stained for PV (**Supplementary Figure 1A**). When we stained such brain sections for KCC2, we observed that the vast majority of tdTomato-positive neurons also stained for KCC2 (75.46 ± 2.412%). This included PV-INs of the hippocampus (**Figure 1C**), the somatosensory cortex (**Figure 1D**) as well as Purkinje cells in the cerebellum (**Figure 1E**).

These data confirm that the majority of PV-positive neurons express KCC2.

Disruption of KCC2 Under the Control of the PV-promoter Increases Seizure Susceptibility

Previously, we reported that Cre-recombinase mediated deletion of exons 2-5 of the floxed *Kcc2* allele ($Kcc2^{flox/flox}$) results in a *Kcc2* knockout (KO) allele (Seja et al., 2012). To disrupt KCC2 in PV-INs we mated the floxed *Kcc2* line with the WT^{PV} line (Hippenmeyer et al., 2005), which also carried the tdTomato transgene (**Figure 2A**). Cre-positive mice carrying one floxed *Kcc2* allele did not show any obvious abnormalities (data not shown). Homozygous $Kcc2^{flox/flox}$/PV-Cre/tdTomato (KCC2 KO^{PV}) mice were born from heterozygous matings at the expected ratio. Staining of brain sections dissected from 8-week-old mice (**Figure 2B**) revealed that roughly 80% of the tdTomato-labeled cells in somatosensory cortex showed robust labeling for KCC2 in WT^{PV} mice, while only less than 20% of the tdTomato-positive cells labeled for KCC2 in KCC2 KO^{PV} mice (**Figure 2C**). Similar results were obtained for the hippocampus (**Supplementary Figures 1B,C**).

At 8 weeks of age almost 80% of the KCC2 KO^{PV} mice spread their hind-limbs when lifted by the tail, which was a very rare finding in control mice (**Figures 2D,E**). Fifteen weeks later, the hind-limb spreading was a consistent finding in KCC2 KO^{PV} mice. The Rotarod analysis showed significant motor impairments in KCC2 KO^{PV} mice, which started between 6 and 8 weeks of age (**Supplementary Figure 2A**). Because of the progressive motor impairments, we assessed mice in a fear conditioning paradigm, which is largely independent of motor functions. While both genotypes remembered the conditioned stimulus and the context of the aversive stimulus, KCC2 KO^{PV} mice displayed an increased anxiety-like behavior (**Supplementary Figure 2B**). In agreement, systemic corticosterone levels were increased in 8-week-old KCC2 KO^{PV} mice (**Supplementary Figure 2C**).

Notably, KCC2 KO^{PV} mice also showed a delayed increase in bodyweight from 8 weeks of age onward (**Figure 2F**) and the lethality drastically increased with almost no KCC2 KO^{PV} mouse surviving beyond 8 months of age (**Figure 2G**).

Repetitively, animal caretakers reported spontaneous seizures in KCC2 KO^{PV} mice, which were first noticed at 8 weeks of age with an age-dependent increase of such events. Some seizures ended fatally, thus at least in part explaining the high lethality of KCC2 KO^{PV} mice.

To assess the seizure susceptibility in a quantitative manner, we challenged 8-week-old KCC2 KO^{PV} and control mice with 80 mg/kg bodyweight pilocarpine after priming with 423 mg/kg lithium chloride i.p. 18 h before the challenge

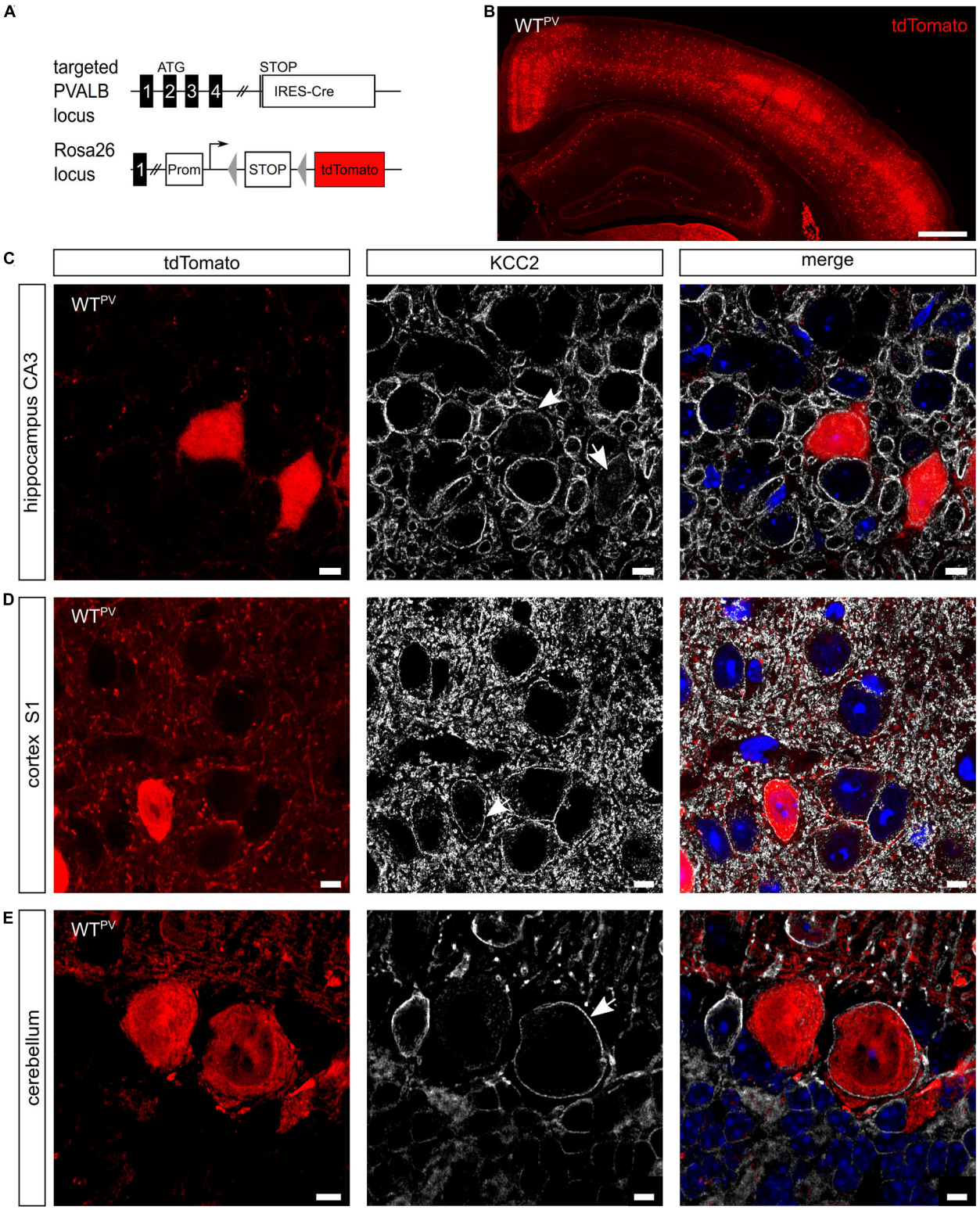

FIGURE 1 | KCC2 is broadly expressed in PV-INs. **(A)** To label PV-INs we mated a mouse line expressing Cre-recombinase under the control of the PV promoter (PV-Cre) (Hippenmeyer et al., 2005) with a tdTomato reporter line (Madisen et al., 2010). Cre-mediated excision of the STOP cassette results in the expression of tdTomato. **(B)** Coronal section of the cortex and the hippocampus of an 8-week-old mouse transgenic for Cre-recombinase and the tdTomato allele (WT^{PV}). Scale bars 500 μm. **(C–E)** Brain sections from WT^{PV} mice were stained for KCC2. tdTomato-positive neurons in the hippocampus **(C)**, somatosensory cortex **(D)**, and cerebellum **(E)** displayed a clear KCC2 signal at the plasma membrane (arrows). Nuclei were counterstained with DAPI. Scale bars 10 μm.

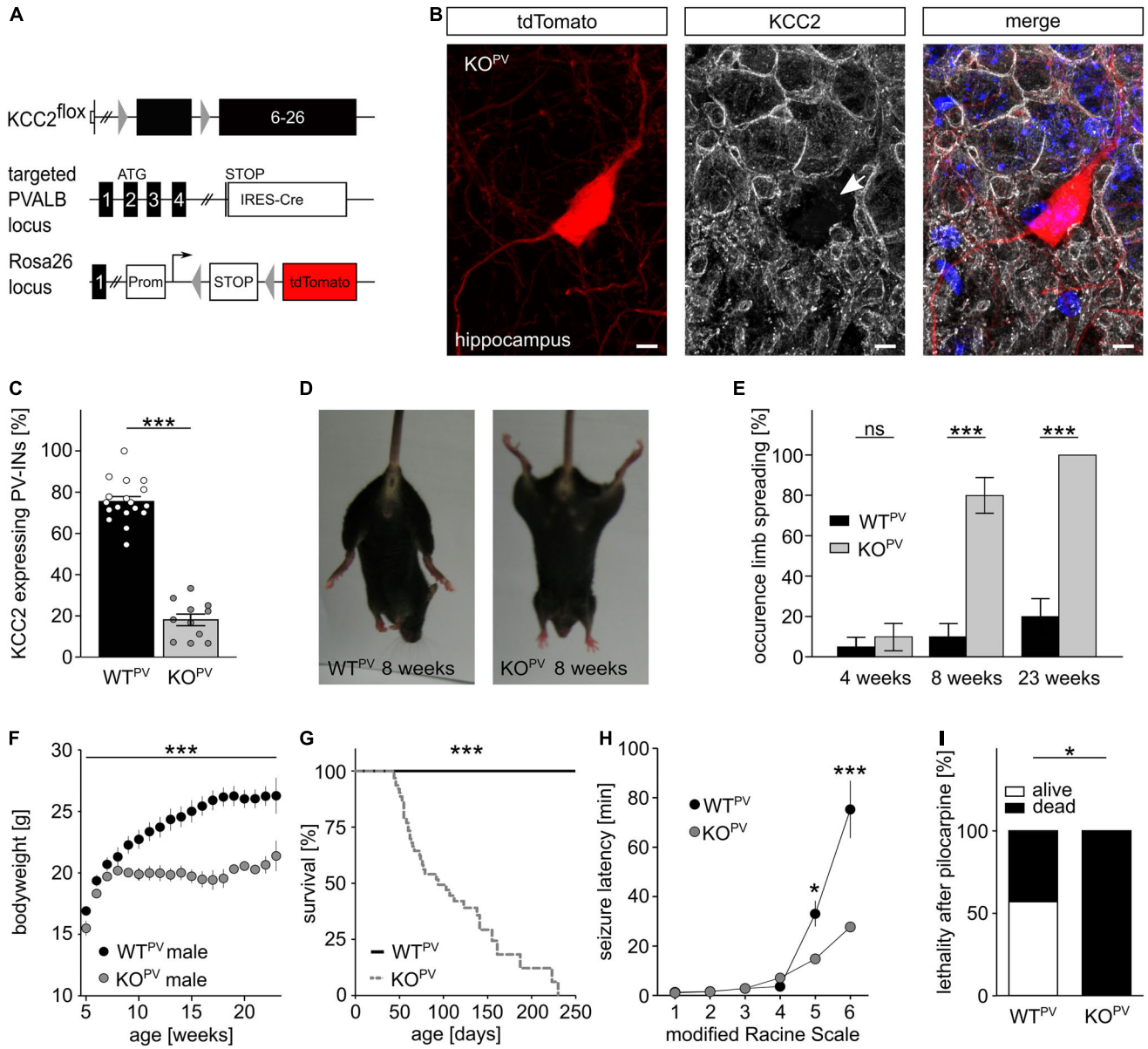

FIGURE 2 | Fatal epileptic activity upon disruption of KCC2 in PV-INs. **(A–C)** We mated our floxed *Kcc2* line (*Kcc2*$^{flox/flox}$) (Seja et al., 2012) with WT^{PV} mice to delete exons 2-5 of the *KCC2* gene **(A)**. The KCC2-labeled section of an 8-week-old *KCC2*$^{flox/flox}$/PV-Cre/tdTomato (KCC2 KO^{PV}) mouse shows that the disruption of KCC2 was effective in the majority of tdTomato-labeled interneurons (arrow) **(B)**. Scale bars 5 μm. The quantification of KCC2-labeled tdTomato-positive neurons in cortex of WT^{PV} and KCC2 KO^{PV} mice confirms the deletion of KCC2 in most PV-INs at 8 weeks of age **(C)**. The ratio of tdTomato-positive with a clear plasma membrane labeling for KCC2 and the total number of tdTomato-positive cells was determined for the somatosentory cortex (WT: 75.5 ± 2.4%; KO: 18.1 ± 2.8%; quantification from n = 9 sections and N = 3 mice; Student's unpaired t-test; ***$p < 0.001$). **(D,E)** KCC2 KO^{PV} mice spread their hind limbs **(D)**. Quantification of hind limb spreading in WT^{PV} and KCC2 KO^{PV} mice at different ages (N = 20/20 mice, Kruskal-Wallis Test; *post hoc* Dunn's multiple comparison; ns not significant; ***$p < 0.001$). **(F)** The gain in body weight is decreased in KCC2 KO^{PV} mice (N = 10/9 mice; 2-way ANOVA; Bonferroni post-test; ***$p < 0.0001$). **(G)** KCC2 KO^{PV} animals have a shortened life span with a mean survival of 94 days (N = 66/44 mice; Mantel-Cox Test; ***$p < 0.0001$). **(H,I)** 8-week-old WT^{PV} and KCC2 KO^{PV} mice were challenged with pilocarpine after LiCl sensitization to induce epileptic seizures. All challenged animals developed generalized tonic-clonic seizures. The seizure threshold was decreased in KCC2 KO^{PV} mice compared to WT^{PV} mice (N = 6/6 mice; 2-way ANOVA; Bonferroni post-test; ***$p = 0.0003$) and the seizure related lethality increased (I) (N = 6/6; 2-way ANOVA; Bonferroni post-test; *$p = 0.037$).

(Lodato et al., 2011). Latencies for the loss of postural control and the onset of generalized tonic-clonic seizures were drastically reduced in KCC2 KO^{PV} mice (**Figure 2H**). While the duration of Racine levels 4 and 5 was significantly shortened, the duration of Racine level 3 was prolonged (**Supplementary Figures 2D,E**). Moreover, the pilocarpine-induced seizures were always lethal in KCC2 KO^{PV} mice, while more than half of the control mice survived pilocarpine-induced seizures (**Figure 2I**).

Taken together, the disruption of KCC2 under control of the PV-promoter increases the seizure susceptibility.

KCC2 Controls the Polarity of GABAergic Responses in PV-Positive Interneurons

Resting membrane potential and basic passive membrane properties like membrane resistance and capacity were not altered in PV-INs of 8-week-old KCC2 KO^{PV} mice (**Figure 3A**). Neither the action potential threshold and height (**Figure 3B**) nor action potential half-width and amplitudes of fast after-hyperpolarizations (fAHP) differed between genotypes (**Figure 3C**). Also the action potential frequency in response to current injections did not differ between genotypes (**Figure 3D**). Thus, the basic excitability of PV-INs was not altered upon disruption of KCC2.

To scrutinize the role of KCC2 for the regulation of the intracellular chloride concentration and thus GABA signaling we used a tight cell patch approach without affecting transmembrane ionic gradients (Perkins, 2006) and tested the polarity of GABA responses in tdTomato labeled interneurons in CA1 of acute brain slices dissected from 8-week-old WT^{PV} mice. Consistent with a role of KCC2 for GABA responses in PV-positive interneurons, 9 from 10 cells in acute brain slices of control mice displayed a hyperpolarizing response, while it was depolarizing in 9 out of 11 cells for KCC2 KO^{PV} mice (**Figure 3E**).

We used field recordings to assess the consequences of the disruption of KCC2 in PV-INs for network excitability (**Figure 4A**). While the paired-pulse ratio was not changed in the *stratum radiatum* (**Figure 4B**), it was diminished for short interstimulus intervals in the *stratum pyramidale* of

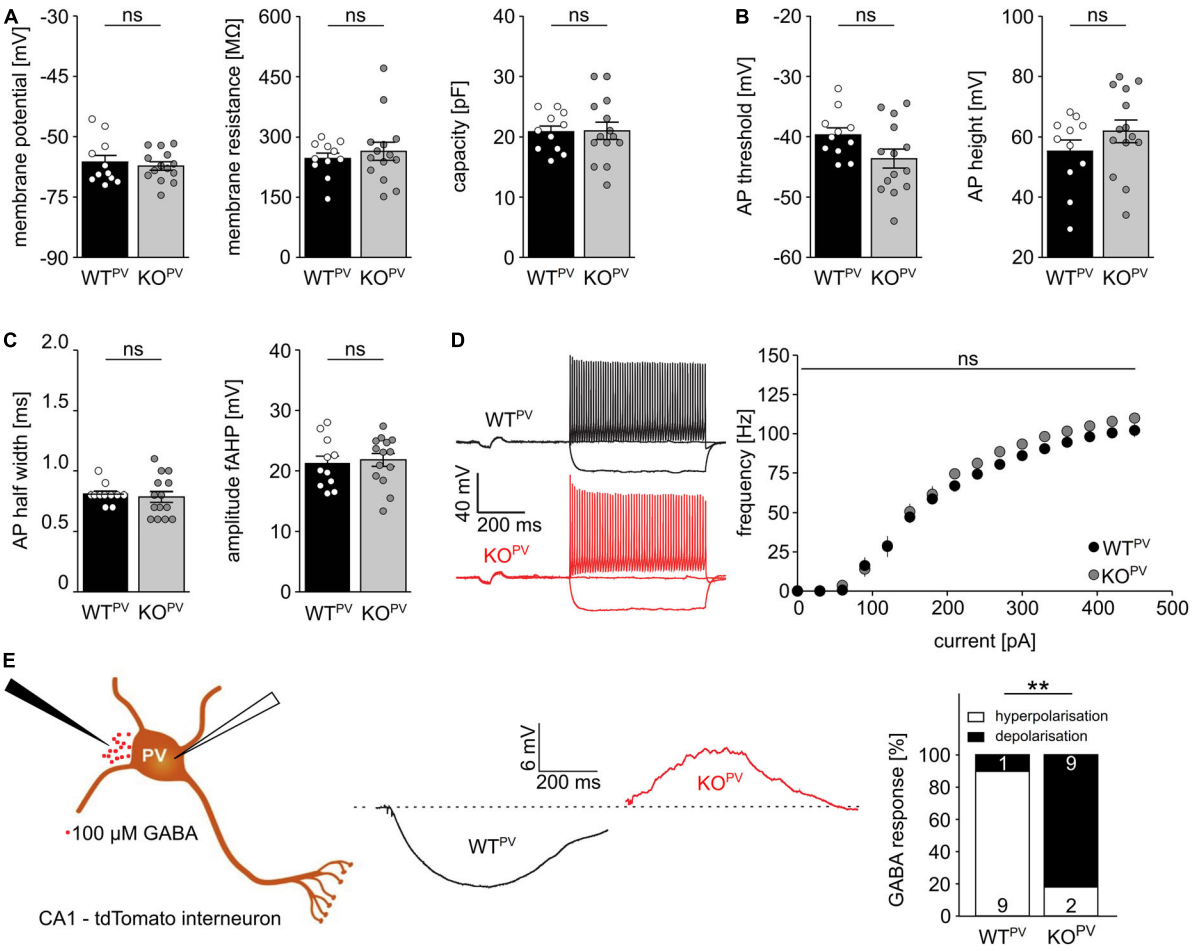

FIGURE 3 | Disruption of KCC2 does not change the intrinsic excitability of PV-INs but changes the polarity of their GABA response. **(A)** Intrinsic properties such as resting membrane potential, membrane resistance and capacity are not altered in the absence of KCC2 (n = 11/14 cells from N = 5/6 mice; unpaired Student's t-test; ns not significant). **(B)** Action potential (AP) threshold and amplitude are as well unchanged in the absence of KCC2 (n = 11/14 cells from N = 5/6 mice; unpaired Student's t-test; ns not significant). **(C)** Action potential half width (left) and fast after-hyperpolarization (fAHP) (right) of PV-INs is similar in WT^{PV} and KO^{PV} (n = 11/14 cells from N = 5/6 mice; unpaired Student's t-test; ns not significant). **(D)** The spike frequency upon current injection is not altered by disruption of KCC2 (n = 11/14 cells from N = 5/6 mice; 2-way ANOVA; Bonferroni post-test; ns not significant). **(E)** 100 mM GABA puffs were applied to tight seal (> 4 GΩ) patched tdTomato-labeled interneurons in the CA1 region of acute brain sections of 8-week-old WT^{PV} and KCC2 KO^{PV} mice (n = 10/11 cells from N = 5/6 mice; Fisher's exact test; $^{**}p$ = 0.0019).

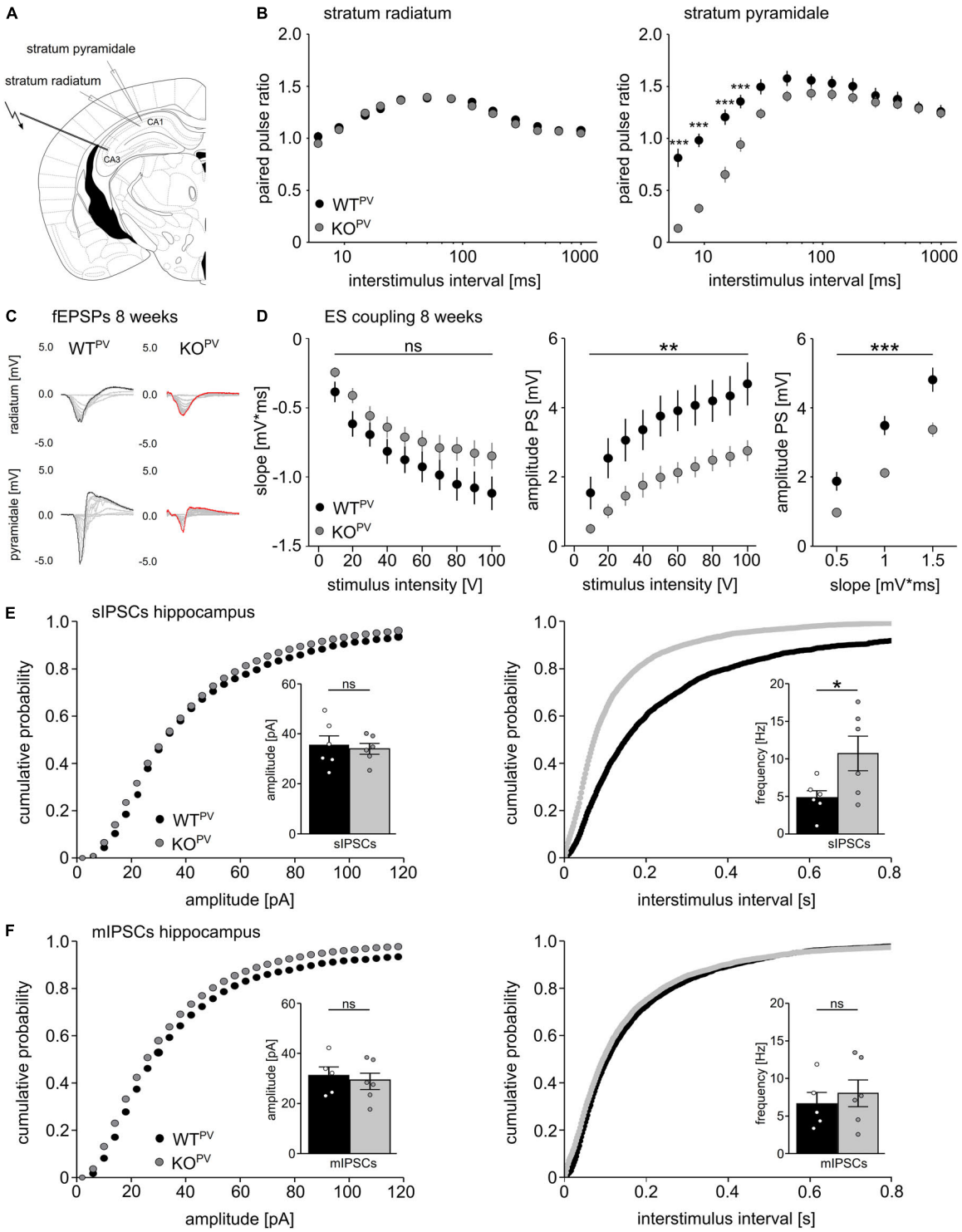

FIGURE 4 | Disinhibition of PV-INs upon disruption of KCC2. **(A)** Position of stimulus and recording electrodes for field recordings in the *stratum pyramidale* and *radiatum* of CA1. **(B)** Paired-pulse ratios are reduced in the *stratum pyramidale* (n = 28/24 cells from N = 9/9 mice), but not in the *stratum radiatum* (n = 35/34 cells from N = 11/11 mice) of KCC2 KO^{PV} mice (2-way ANOVA repeated measure; Bonferroni post-test; ***$p < 0.0001$). **(C)** Representative examples of fESPs recorded in the *stratum radiatum* and *stratum pyramidale* in KCC2 WT^{PV} and KCC2 KO^{PV} mice. **(D)** E-S-coupling is diminished in 8-week-old KCC2 KO^{PV} mice (n = 14/17 slices from N = 4/4 mice, 2-way ANOVA repeated measure; Bonferroni post-test; **p = 0.008; ***$p < 0.0001$). **(E)** The frequency, but not the amplitude of spontaneous inhibitory post synaptic currents (sIPSCs) is increased in CA1 pyramidal neurons in KCC2 KO^{PV} mice (N = 6/6 mice, unpaired Student's t-test; Kolmogorov-Smirnov test; ns not significant; *p = 0.0398). **(F)** Miniature inhibitory postsynaptic currents (mIPSCs) upon tetrodotoxin (TTX) inhibition of spontaneous network driven events are not changed in 8-week-old KCC2 KO^{PV} mice (N = 6/6 mice; unpaired Student's t-test; Kolmogorov-Smirnov test; ns not significant).

CA1 in 8-week-old KCC2 KO^{PV} mice (**Figure 4C**). This is compatible with increased GABAergic inhibition, because the response to the second stimulus at short intervals is limited via $GABA_A$ dependent feed forward inhibition, while for intervals between 100–125 ms activation of presynaptic $GABA_B$ autoreceptor activation dominates (Davies et al., 1990; Steffensen and Henriksen, 1991).

While slopes of extracellular recordings of field excitatory postsynaptic potentials (fEPSPs) recorded in the *stratum pyramidale* in response to a single stimulation of Schaffer collaterals did not differ between genotypes, amplitudes of population spikes and E-S coupling were decreased in KCC2 KO^{PV} mice (**Figure 4D**).

Next, we patched CA1 pyramidal cells and measured spontaneous GABA release in acute slices of 8-week-old control and KCC2 KO^{PV} mice. The frequency of spontaneous inhibitory postsynaptic currents (sIPSCs) was clearly increased in KCC2 KO^{PV} mice (**Figure 4E**). When we blocked spontaneous action potentials with tetrodotoxin (TTX), miniature inhibitory postsynaptic currents (mIPSCs) did not differ between genotypes (**Figure 4F**). Similar results were obtained for the motor cortex and the somatosensory cortex (**Supplementary Figure 3**).

Taken together, these data suggest that PV-INs are disinhibited in the absence of KCC2.

Progressive Loss of PV-Positive Interneurons Upon Disruption of KCC2

When we re-assessed E-S coupling in the CA1 of acute brain slices obtained from 23-week-old mice, E-S coupling was increased in KCC2 KO^{PV} compared to WT^{PV} mice (**Figures 5A,B**). This finding suggested that GABAergic inhibition may be compromised in older KCC2 KO^{PV} mice. We hence wondered whether loss of KCC2 may affect the long-term maintenance of PV-INs. Therefore, we counted the number of tdTomato-labeled interneurons in the cortex and the hippocampus of 8- and 23-week-old control and KCC2 KO^{PV} mice (**Figure 5C**). In the somatosensory cortex (S1) we found no difference in the number of tdTomato-labeled interneurons at 8 weeks of age, while the number was clearly reduced in 23-week-old KCC2 KO^{PV} mice (**Figures 5D,E**). In the retrosplenial cortex (RSP), we observed a slight decrease already at 8 weeks of age, which was even more pronounced at 23 weeks (**Figure 5F**). A loss of PV-INs was also evident in the hippocampus of KCC2 KO^{PV} mice at 23 weeks of age (**Figure 5G**). The remaining PV-INs in CA1 also showed some structural abnormalities as evidenced by less basal dendrites compared to WT^{PV} mice (**Figure 5H**). Overall, the architecture of neurites appeared to be altered in older KCC2 KO^{PV} mice (**Supplementary Figure 4**).

Perineuronal Networks Decrease in KCC2 KO^{PV} Mice

Many PV-INs are ensheathed by perineuronal nets (PNN) (Wen et al., 2018; Carceller et al., 2020; **Figure 6A**), extracellular matrix (ECM) assemblies that can be easily detected by lectins such as the *Wisteria floribunda agglutinin* (WFA). PNNs regulate the intrinsic properties of the encapsulated neurons and thus aid the fast-spiking of PV-INs (Chaunsali et al., 2021). The loss of PNNs has been associated with diseases such as Alzheimer (Crapser et al., 2020) and epilepsy (Tewari et al., 2018; Chaunsali et al., 2021). Notably, WFA signals per area were drastically decreased in the hippocampus and in the somatosensory and retrosplenial cortex of 23-week-old KCC2 KO^{PV} mice (**Figure 6B**). The percentage of WFA-positive tdTomato-cells was also reduced in 23-week-old KCC2 KO^{PV} mice but not at 8 weeks of age (**Figures 6C,D**). Moreover, the WFA labeling of individual tdTomato-positive cells was reduced in 23-week-old KCC2 KO^{PV} mice indicating that the loss of PNNs precedes the loss PV-INs (**Figures 6D,E**).

Previously, it was described that seizures induce the expression of glial fibrillary acidic protein (GFAP) in astrocytes (Steward et al., 1992; Coulter and Steinhauser, 2015; Steinhauser et al., 2016; Siracusa et al., 2019; Sanz and Garcia-Gimeno, 2020). Indeed, GFAP immunoreactivity was strongly induced in 23-week-old KCC2 KO^{PV} mice (**Figures 6F,G**).

These data show profound structural changes in brains of 23-week-old KCC2 KO^{PV} mice.

Transcriptional Profiling of PV-Positive Interneurons Upon Disruption of KCC2

To get further clues about the loss of PV-positive interneurons, we FACS sorted tdTomato-positive and negative neurons from WT^{PV} and KCC2 KO^{PV} mice at 23 weeks of age. As described recently (Pensold et al., 2020), we combined mechanical and trypsin/collagenase-based enzymatic dissociation of brain tissue with *Percoll* density gradient centrifugation. The transcriptome of tdTomato-negative neurons isolated from 23-week-old control and KCC2 KO^{PV} mice did not show major differences in the KEGG pathway term enrichment analysis as well as *Panther - Gene List Analysis* (**Figure 7A**).

Comparison of the transcriptome of tdTomato-positive interneurons isolated from 23-week-old control and KCC2 KO^{PV} mice revealed major changes in genes involved in PI3K-Akt signaling and MAPK signaling (**Figures 7B,C**), some of which have been linked with epilepsy previously (Berdichevsky et al., 2013; Pernice et al., 2016; Carter et al., 2017). Several transcripts of apoptosis related genes including the death receptors FAS and Tnfrsf10b (tumor necrosis factor receptor superfamily, member 10b) and caspases were upregulated in KCC2 KO^{PV} mice, suggesting that the loss of PV-INs is preceded by activation of pro-apoptotic pathways. We also found differences for transcripts of cell-cell contact and ECM-related genes in PV-INs isolated from KCC2 KO^{PV} mice. As reported previously following status epilepticus (Dubey et al., 2017), transcripts of matrix metalloproteinases such as *MMP3*, *ADAMTS5*, *ADAMTS8*, and *ADAMTS9* were induced (**Figure 7D**).

MATERIALS AND METHODS

Animals

Mice were maintained on a C57BL/6 background and were housed in plastic cages at a 12 h day-night rhythm with constant temperature and humidity. Animals had access to food and water

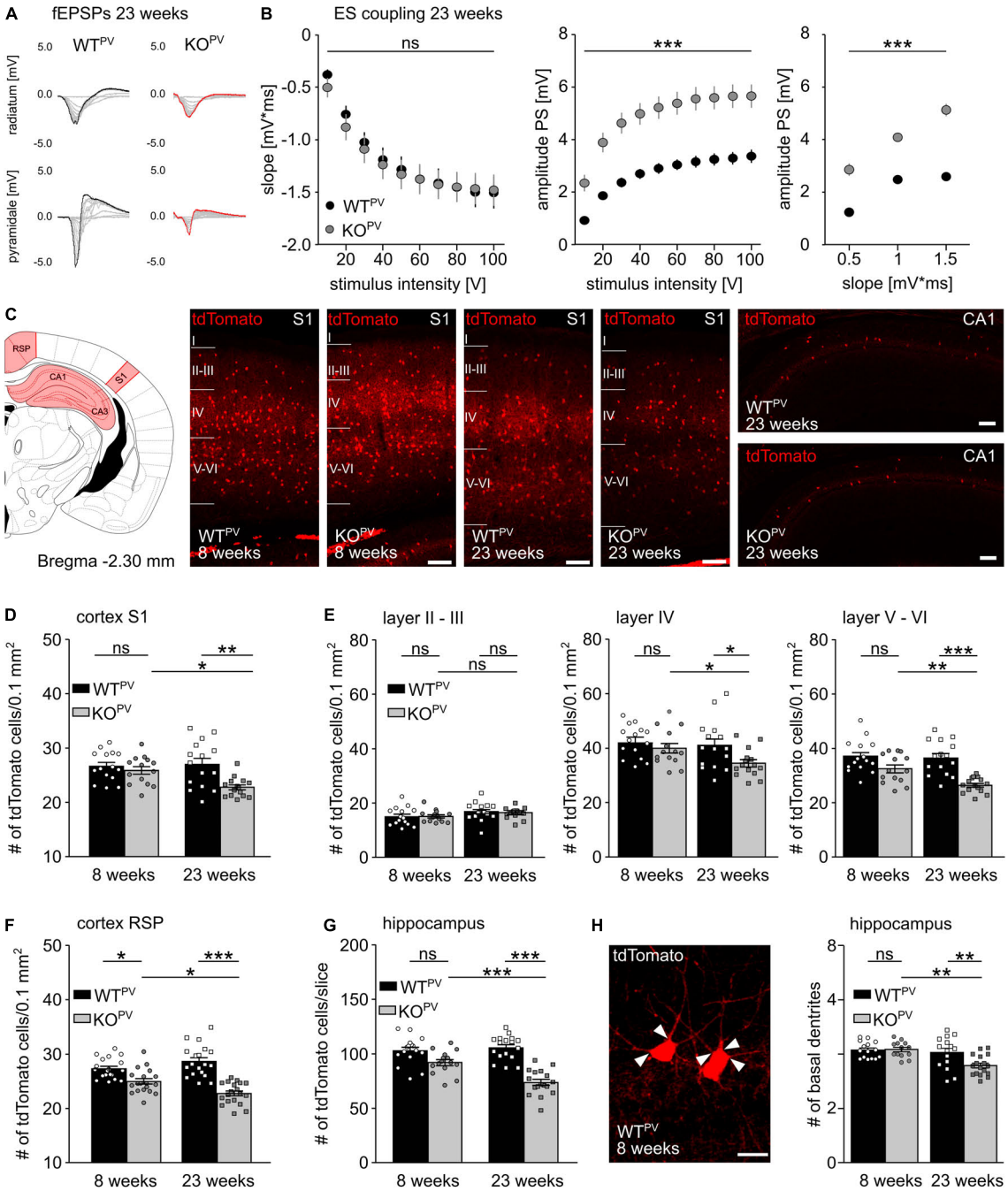

FIGURE 5 | Loss of PV-INs in KCC2 KO^{PV} mice. **(A)** Representative examples of fEPSPs recorded in the *stratum radiatum* and *stratum pyramidale* of 23-week-old WT^{PV} and KCC2 KO^{PV} mice. **(B)** E-S-coupling is increased in 23-week-old KCC2 KO^{PV} mice (n = 24/33 slices from N = 5/5 mice; 2-way ANOVA repeated measure; Bonferroni post-test; ***$p < 0.0001$). **(C)** Illustration of the brain regions (red) for the quantification of tdTomato-positive neurons. Representative images of tdTomato-positive cells from the somatosensory cortex (S1) of WT^{PV} (left) and KCC2 KO^{PV} (right) mice at 23 weeks of age and hippocampus CA1 of 23-week-old mice. Scale bars 100 μm. **(D)** Number of tdTomato-positive cells per 0.1 mm^2 of a 30 μm thick section of S1 of 8- and 23-week-old KCC2 WT^{PV} and KO^{PV} mice (n = 15/15 slices; N = 5/5 mice; 1-way ANOVA; Bonferroni post-test; *$p < 0.05$; **$p < 0.01$). **(E)** Number of tdTomato-positive cells per 0.1 mm^2 and layer of a 30 μm thick section of S1 (n = 15/15 slices; N = 5/5 mice; 1-way ANOVA; Bonferroni post-test; ns not significant; *$p < 0.05$; **$p < 0.01$; ***$p < 0.001$). **(F)** Number of tdTomato-positive cells per 0.1mm^2 of a 30 μm thick section of the retrosplenial cortex (RSP) of 8- and 23-week-old WT^{PV} and KCC2 KO^{PV} mice (n = 17/15 slices; N = 5/5 mice; 1-way ANOVA; Bonferroni post-test; *$p < 0.05$; ***$p < 0.0001$). **(G)** Quantification of tdTomato-positive cells in a 30 μm thick hippocampal section (Bregma -2.3 mm, 1 hemisphere) of 8- and 23-week-old WT^{PV} and KCC2 KO^{PV} mice (n = 15/15 slices; N = 5/5 mice; 1-way ANOVA; Bonferroni post-test; ***$p < 0.0001$). Individual numbers for D-G are provided in **Supplementary Table 1**. **(H)** The number of basal dendrites (arrowheads) of tdTomato-positive neurons in the hippocampus is slightly decreased in 23-week-old KCC2 KO^{PV} mice (WT 8 weeks: 4.2 ± 0.1; KO 8 weeks: 4.2 ± 0.1; WT 23 weeks: 4.1 ± 0.2; KO 23 weeks: 3.6 ± 0.1; n = 15/15 slices from N = 5/5 mice; 1-way ANOVA; Bonferroni's multiple comparison test; **$p < 0,001$).

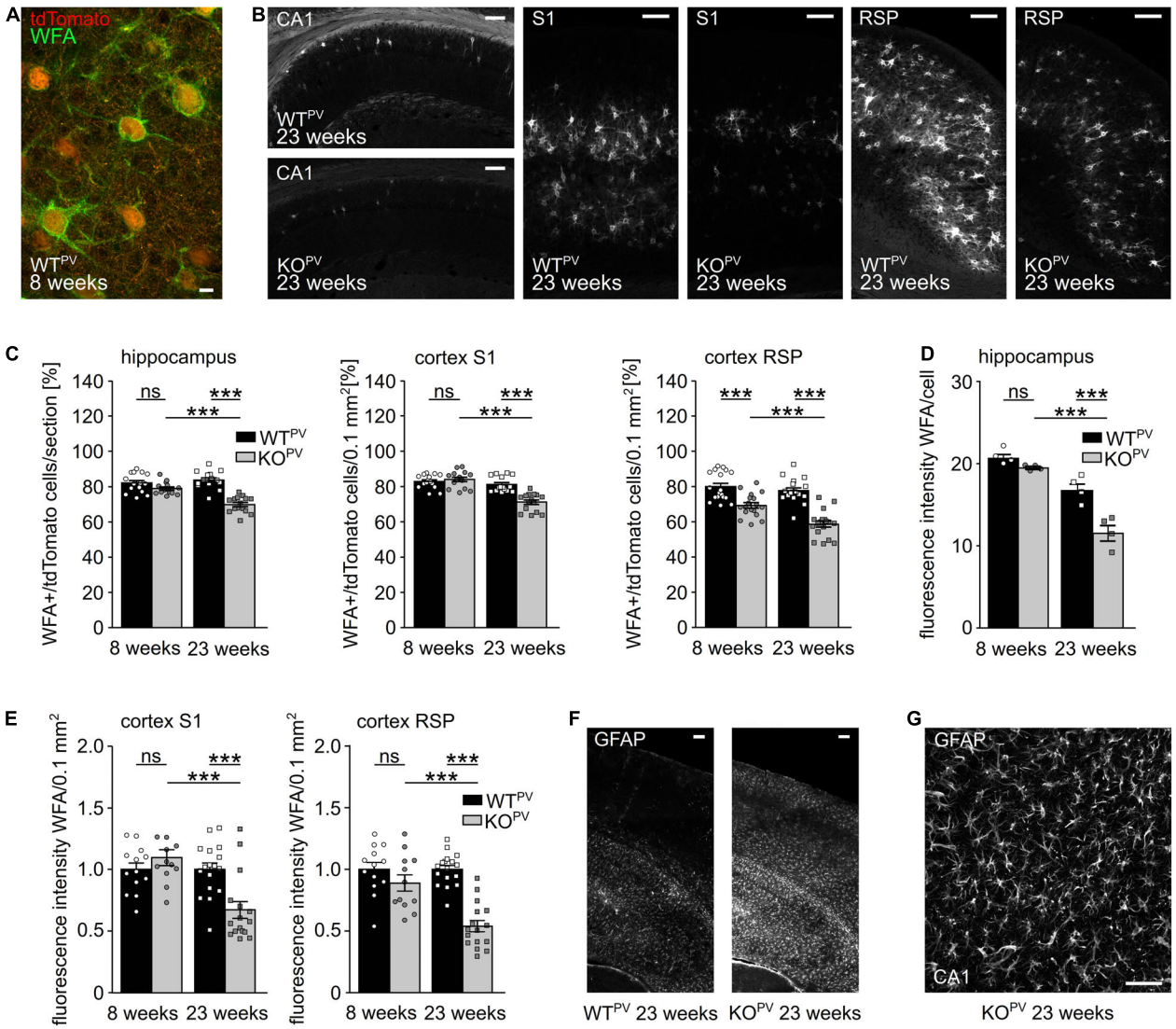

FIGURE 6 | Perineuronal networks (PNN) decrease in KCC2 KO^{PV} mice. **(A)** Representative WFA stainings of the somatosensory cortex of a WT^{PV} mouse at the age of 8 weeks. Scale bar 5 μm. **(B)** Representative WFA stainings of the hippocampus (left), the S1 (middle) and RSP cortex (right) of WT^{PV} and KCC2 KO^{PV} mice at 23 weeks of age. Scale bars 100 μm. **(C)** Quantification of WFA^{+}/tdTomato cells in the hippocampus (left), S1 (middle), and RSP (right) cortex of WT^{PV} and KCC2 KO^{PV} mice at the age of 8 and 23 weeks shows a reduced proportion of ensheathed PV-INs in older KO^{PV} mice (n = 15/15 slices, N = 5/5 mice; 1-way ANOVA; Bonferroni's multiple comparison test; ns not significant; ***$p < 0.001$). **(D,E)** WFA signal intensity per individual cell in the hippocampus (D) (n = 12/9 slices; N = 4/3 mice; 1-way ANOVA; Bonferroni post-test; ns not significant; ***$p < 0.0001$). WFA signal intensity per 0.1 mm^2 in the S1 cortex (left) and RSP (right) decreases over time in KCC2 KO^{PV} mice (n = 13/15 slices; N = 5/5 mice; 1-way ANOVA Bonferroni post-test; ns not significant; ***$p < 0.0001$). **(F)** Representative GFAP staining of the cortex and hippocampus of WT^{PV} and KCC2 KO^{PV} at the age of 23 weeks. Scale bar 100 μm. **(G)** Close up of GFAP -stained reactive astrocytes in CA3 in KCC2 KO^{PV}. Scale bar 50 μm.

ad libitum. The body weight of the mice was measured weekly between 4 and 25 weeks of age. Hind limb spreading was scored at 4, 8, and 23 weeks of age. All animal experiments were approved by the Thüringer Landesamt für Lebensmittelsicherheit und Verbraucherschutz (TLLV). Two different mouse lines were used in the following experiments: PV-KCC2 and PV-tomato-KCC2.

Cell-type specific knockouts were obtained by mating a floxed KCC2 line reported previously (Seja et al., 2012) with PV-Cre mice (B6;129P2-Pvalbtm1(cre)Arbr/J) (Hippenmeyer et al., 2005). For labeling of PV-positive interneurons these mice were mated with the B6.Cg-Gt(ROSA)26Sortm14(CAG-tdTomato)Hze/J line (Madisen et al., 2010). All breeders were homozygous for tdTomato. Male heterozygous floxed Cre-negative KCC2 mice were mated with heterozygous floxed Cre-positive female KCC2 mice. For KCC2 genotyping we used a forward primer 5′-TCT GCC TGG AAC ACT CTC CTG C-3′ and reverse primer 5′-CAA CCT GAA CTC CCA AGG ATA CCC-3′ to amplify a 420 bp WT allele and a 465 bp *floxed* allele. For PV-Cre genotyping the primers 5′-AACAGCAGCGAGCCCGAGTAGTG-3′; 5′-TAA GAA CTA

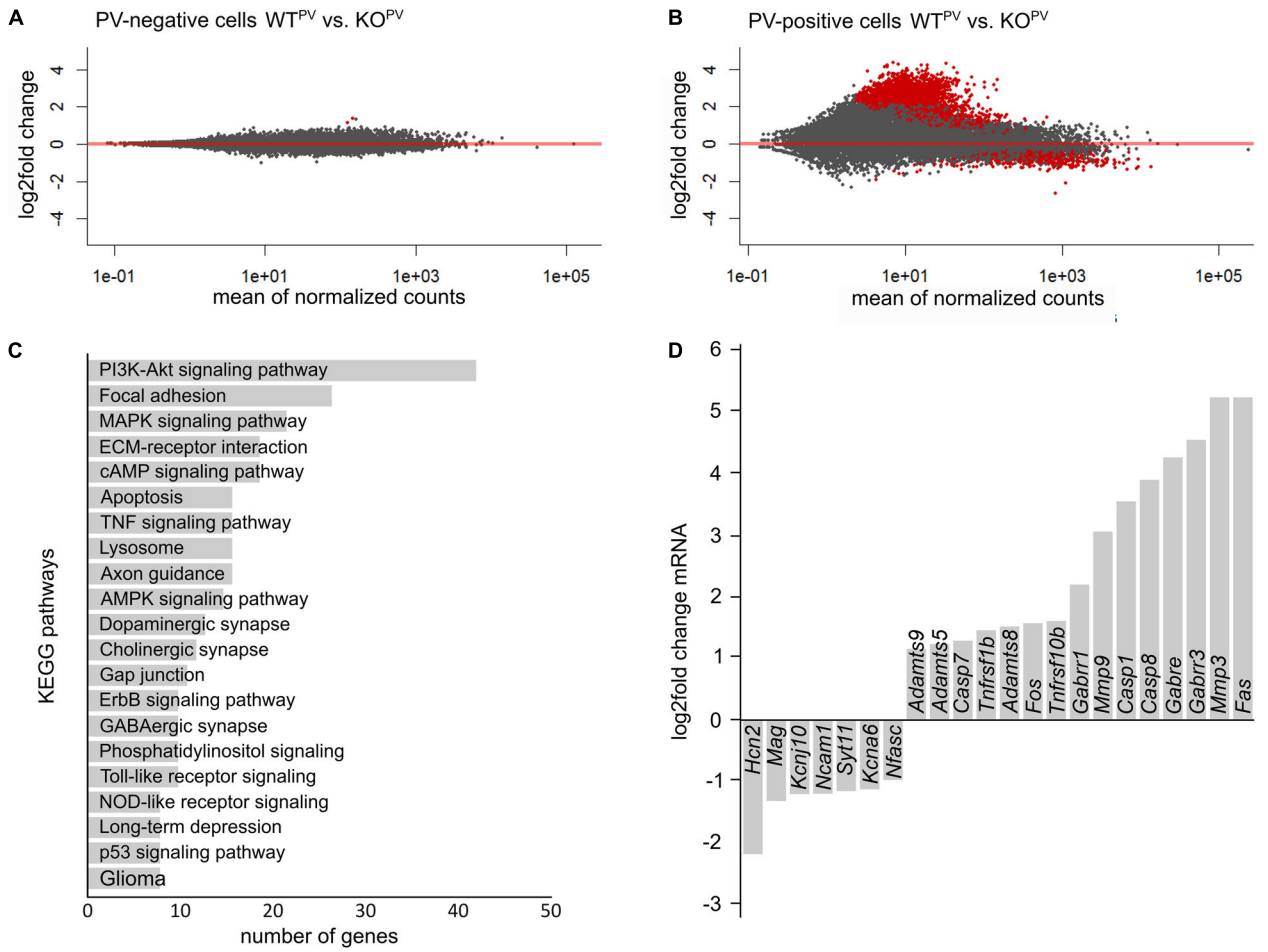

FIGURE 7 | Transcriptional profiling of PV-INs. **(A,B)** MA-plot illustrating differentially expressed genes in PV-negative **(A)** and PV-positive **(B)** cells isolated from 23-week-old WT^{PV} and KCC2 KO^{PV} mice (n = 4/4 experiment; N = 8/8 mice (brains from 2 mice of the same genotype were pooled per experiment); red dots $p < 0.05$; Benjamini adjusted). **(C)** KEGG pathway enrichment analysis of 1,126 differentially expressed genes ($p < 0.05$; Benjamini adjusted). **(D)** Selected differentially expressed genes in PV-INs of KCC2 KO^{PV} mice.

GAC CCA GGG TAC AAT G-3′; 5′-AAA CGT TGA TGC CGG TGA ACG TGC-3′ and 5′-TAA CAT TCT CCC ACC GTC AGT ACG-3′ were used to amplify a 388 bp WT allele and a 214 bp Cre allele. For tdTomato genotyping we used the WT primer 5′-AAG GGA GCT GCA GTG GAG TA-3′ and 5′- CCG AAA ATC TGT GGG AAG TC-3′ to amplify a 297 bp WT allele and the *knock-in* primers 5′-GGC ATT AAA GCA GCG TAT CC-3′ and 5′-CTG TTC CTG TAC GGC ATG G-3′ to amplify a 196 bp fragment.

Immunofluorescence

Brains were dissected after transcardial perfusion with ice-cold 4% PFA/PBS and post-fixed in 4%PFA/PBS overnight. The tissue was subsequently immersed in 15% sucrose/PBS and 30% sucrose/PBS for cryoprotection. Brain tissue was cut into free-floating 30 μm thick sections with a sliding microtome (Leica). Sections were rinsed in PBS. 0.25% (v/v) Triton X-100 in 1 × PBS was used to permeabilize cells. After blocking with NGS (normal Goat serum; Vector Laboratories), the sections were incubated overnight at 4°C with the following primary antibodies: rabbit anti-KCC2 (Millipore, 07-432) 1:1,000, rabbit anti-Parvalbumin (Svant, PV25) 1:1,000, mouse anti-Parvalbumin (Svant, PV235) 1:2,000, mouse anti-GFAP (Millipore MAB360) 1:500 and rabbit anti-GABA (Sigma A2052) 1:1,000. To detect PNNs, we used Flourescein labeled Wisteria Floribunda Lectin (WFA, Vector Labs, FL-1351) in a dilution of 1:200. Corresponding secondary antibodies were obtained from Invitrogen (dilution 1:2,000). Nuclei were stained with DAPI 1:10,000 (Invitrogen). Sections were mounted with Fluoromount-G (Southern Biotech). Images were acquired with a Zeiss LSM 880 Airyscan confocal microscope. Z-projections with average intensities processed with ImageJ are shown. The acquisition parameters and image processing were identical for all genotypes. 3 consecutive slices (Bregma -2.3) were analyzed for quantification of cell numbers.

Seizure Threshold

To determine the seizure threshold, 8-week-old mice were pre-treated with 423 mg/kg lithium chloride (intraperitoneally (i.p.), Sigma, L9650). 18 h later we injected 1 mg/kg Methylscopolamine

(Sigma, S8502). Seizures were induced 30 min later by intraperitoneal injection of 80 mg/kg pilocarpine (Sigma, P6503). Seizures were scored for 3 h according to a modified Racine scale: 0 (no changes, normal behavior), 1 (behavioral arrest, motionless starring, orofacial automatism), 2 (head nodding), 3 (lordotic posture, chewing), 4 (rearing), 5 (falling, loss of postural control), 6 (generalized tonic-clonic activity, complete loss of control). Surviving animals were sacrificed 4 weeks later (Racine, 1972).

Behavioral Tests

The motor performance was tested by RotaRod analysis at 6, 8, and 12 weeks of age. The RotaRod apparatus (3375-4R; TSE Systems, Germany) consisted of a striated rod providing a good grip (diameter: 3 cm), separated in four compartments (width: 8.5 cm) and located 27.2 cm above the floor grid. Mice were placed on the rod for 30 sec without rotation followed by 120 s of low speed rotation at 4 rpm. Subsequently, the mice were tested in 3 trials for 5 min (4–40 rpm). At each trial, the latency to fall was recorded.

Fear conditioning: Mice were placed in a chamber (d 17 × w 17 × h 25 cm, plexiglas wall, 4 lux light, 70% ethanol, fan speed 100%) and allowed to explore the surrounding area for 180 s. A tone was applied for the following 20 s (9 kHz, volume 20%, 80 dB) paired with a foot shock (unconditioned stimulus, 0.7 mA for 2 s) applied in the last 2 s via the metal grid. After additional 60 s, mice were replaced into their home cages. After 24 h, the cued test was performed to assess the tone-shock association. Mice were placed in a differently shaped box with altered color pattern (Caro patterned wall, white floor), lighting (2 lux), odor (3% acetic acid), and fan speed (50%). Mice were allowed to explore the new area for 180 s before the tone was applied for 180 s. After additional 60 s, mice were transferred into their home cages and allowed to relax for 2 h. After 2 h, they were placed in the same context as during acquisition (Plexiglas walls, metal grid floor, lightening 4 lux, odor 70% ethanol, fan speed 100%), and observed for 180 s. Animals were video recorded throughout for automatic detection of freezing behavior by the ANY-maze software (Stoelting). For freezing detection, videos were analyzed manually. Freezing time is presented as percentage of the investigated 60 s intervals (Kamprath and Wotjak, 2004; Fanselow and Poulos, 2005; Smith et al., 2007).

Corticosterone Levels

To minimize stress, the animals were housed in sets of two and handling of the mice was avoided10 days prior to blood collection. At the day of blood collection, the animals were placed in a quiet environment. In a separate room, mice were rapidly decapitated and trunk blood collected 2 to 3 h before the end of the light cycle, when systemic corticosterone (CORT) levels peak (Helen and Atkinson, 1997). The blood was then centrifuged at 5,000 rpm for 5 min; the serum was collected and stored at −80°C until CORT analysis was performed.

Serum CORT levels were measured using an enzyme immunoassay kit (# 900-097; Enzo Life Sciences) according to the manufacturer's instructions. The sensitivity of the assay was 27 pg/ml; all samples were run in the same assay to avoid inter-assay variability. Sample size was 8–9 mice/group. The samples were diluted 1:40 in ELISA buffer and run in duplicates. Every plate included wells with negative controls (Blank, NSB), positive controls (Total Activity TA, Maximum binding Bo) and standards #1 - #5 (#1: 20,000 pg/mL; #2: 4,000 pg/mL; #3: 800 pg/mL; #4: 160 pg/mL; #5 32 pg/mL). The ELISA plate reader was normalized against blank wells and optical density read at 405 nm with correction at 580 nm. Average net Optical Density (OD) bound for each standard and sample was calculated by subtracting the average NSB OD from the average OD bound: Average net OD = average bound OD – average NSB OD. The binding was calculated as a percentage of the maximum binding wells (Bo): Percent bound = net OD/net Bo OD * 100. Plotting a graph with the standard absorbance value as the dependent variable (*Y*-axis) and CORT concentration as the independent variable (*X*-axis) results in a standard curve. The standard curve was fitted with the exponential regression function: $y = a^*x2 + b^*x + c$. Solving for x determines the concentration of the sample.

Electrophysiological Analysis

Slice Preparation for Electrophysiology

After decapitation of mice (8-10 weeks or 23 weeks of age) the brain was quickly isolated, placed in ice-cold artificial cerebrospinal fluid (aCSF: 120 mM NaCl, 3.5 mM KCl, 1.3 mM $MgSO_4$ x 7 H_2O, 12.5 mM NaH_2PO_4 x H_2O, 2.5 mM $CaCl_2$ x 2 H_2O, 10 mM Glucose, 25 mM $NaHCO_3$; gassed with 5% CO_2, 95% O_2) and cut into horizontal slices with a vibroslicer (VT 1000S, Leica instruments) as described previously (Liebmann et al., 2009). Slices (350 μm) were stored at RT in aCSF for at least 1 h until use.

Field Potential Recordings

After equilibration, the slices were transferred to an interface recording chamber. Slices were allowed to adapt to recording conditions for 1 h (oxygenated aCSF, 32°C, flow 2-3 mL/min). Parallel bipolar stimulating electrodes with a tip separation of 75 μm (PI2ST30.1A3, Science Products) were placed onto glutamatergic Schaffer collaterals of the hippocampus CA3 region to stimulate CA1 pyramidal neurons. Upon stimulation (pulse duration 50 μs), field excitatory postsynaptic potentials (fEPSPs) were recorded using glass microelectrodes (2-5 MΩ, filled with aCSF) impaled into the *stratum pyramidale* or the *stratum radiatum* of the hippocampal CA1 region. Slopes of fEPSPs and amplitudes of population spikes (PS) were analyzed. Data of field potential recordings were collected with an extracellular amplifier (EXT-02, NPI), low pass filtered at 4 kHz and digitally stored with a sample frequency of 10 kHz. Data acquisition and analysis of population spike (PS) amplitudes were performed using the software Signal (Cambridge Electronic Design, United Kingdom). To determine the maximal population spike amplitude or the maximal slope of fEPSP, the stimulus intensity was gradually increased (0-50 V, 5 V increment) for each experiment (interstimulus interval 30 s). The relationship between stimulus intensity and the evoked response was fitted by a sigmoid function: $R_{(i)} = R_{max}/[1 + exp((i_h\text{-}i)/i_c)]$, where $R_{(i)}$ is the response at intensity (i), R_{max} is the maximal response, i_h is the intensity at which a half-maximal response was observed and i_c is the intensity required to change the response e-fold. After determination of the half-maximal stimulus intensity,

paired-pulse stimuli were applied with interstimulus intervals of 15, 20, 30, 50, 80, 120, 180, 280, 430, 650, and 1,000 ms. To assess fEPSP-PS coupling, slopes of fEPSP recorded in the *stratum radiatum* and the amplitudes of the simultaneously recorded corresponding PS in the *stratum pyramidale* were correlated. For a comparison between genotypes, mean PS amplitudes within fEPSP slope bins of 0.5 mV/ms were calculated.

Patch Clamp Recordings

Recordings of miniature inhibitory postsynaptic currents (IPSCs) in pyramidal neurons of the hippocampal area CA1 were performed in a submerged recording chamber mounted on an upright microscope (BX51WI, Olympus). Slices were continuously superfused with gassed aCSF (2-3 ml/min, 32°C, pH 7.3) as described previously (Sinning et al., 2011). IPSCs were recorded at a holding potential of -70 mV for at least 5 min in aCSF. Data analysis was performed off-line, with the detection threshold levels set to 5 pA for IPSCs. Recordings were performed using a CsCl-based intracellular solution (in mM): 122 CsCl, 8 NaCl, 0.2 $MgCl_2$, 10 HEPES, 2 EGTA, 2 Mg-ATP, 0.5 Na-GTP, 10 QX-314 [N-(2,6-dimethyl-phenylcarbamoyl-methyl) triethylammonium bromide], pH adjusted to 7.3 with CsOH. dl-APV (30 μM, Tocris Bioscience), CNQX disodium salt (10 μM, Tocris Bioscience) were added to the perfusate. After 5 min recording of sIPSCs, extracellular solution containing 0.5 μM tetrodotoxin was washed in and 5 min mIPSCs were recorded. The following parameters were determined: frequency, peak amplitude, time constant of decay (τ), half-width, and electrical charge transfer. To investigate intrinsic properties of PV-interneurons of the CA1, action potential properties and spike frequency were recorded under current clamp conditions. Prolonged current steps (600 ms) were applied from the resting membrane potential in the range of 0 to 560 pA with 40 pA increments. Patch pipettes were filled with (in mM): 140 K-methane-sulfonate, 10 HEPES, 0.1 EGTA, 4 Mg-ATP and 0.3 Na-GTP, pH 7.3.

For testing of a depolarizing or hyperpolarizing effect of GABA, tight seals (> 4 GΩ) were established in PV-INs (Otsu et al., 2020). Therefore, pipettes (4-7 MΩ impedance) were filled with HEPES buffered aCSF. The change of the membrane potential in response to pressure application of GABA (100 μM, 100 ms, 5 psi) using the Toohey Spritzer Pressure System (Toohey Company) were recorded under current clamp conditions. The action potential half-width was determined as the duration of the action potential at the voltage halfway between threshold and the peak. The amplitude of the fast after-hyperpolarization (fAHP) was determined as the delta between minimum voltage within 2 ms after the action potential peak subtracted and the threshold voltage. The Software pClamp 10 (Molecular Devices) was used for the analysis of IPSCs and current clamp recordings.

Dissection of Neurons and Cell Sorting

For the analysis of the transcriptome of PV-positive interneurons, animals at the age of 23 weeks were sacrificed by cervical dislocation and decapitated. The brain was quickly removed with sterile instruments and placed in Gray's Balanced Salt Solution with glucose (GBSS/Glc: 137.93 mM NaCl, 3.66 mM KCl, 2.702 mM $NaHCO_3$, 1.03 mM $CaCl_2$, 0.28 mM $MgSO_4x7H_2O$, 0.84 mM Na_2HPO_4, 0.22 mM KH_2PO_4, 5.56 mM glucose; pH 7.4; sterile filtered) on ice. The cortex and the hippocampus were dissected in GBSS/Glc on ice. The tissue was cut into small pieces (1 – 2 mm^3) with a sterile razor blade and transferred into falcons in a sterile environment. After washing (gentle shaking; wash medium 98.2 ml HBSS w/o Ca and Mg; 700 μl 1M HEPES; 1 ml Penicillin-Streptomycin; 100 μl 65% glucose) the tissue was incubated for 5 min with 0.25% Trypsin/EDTA (Thermo Fisher Scientific; 4.5 ml 0.25% Trypsin/EDTA, 50 μl Penicillin-Streptomycin, 50 μl 1M HEPES, 500 μl 50% trehalose) for 30 min at 37°C. Pre-incubated DNAse (AplliChem, 50 μl, 4 μg/μl, 600 U) was added to the mix. A washing step with 2.1 ml trypsin stop-medium (40 ml DMEM/F12, 5 ml FBS, 500 μl Penicillin-Streptomycin, 5 ml 50% trehalose) led to the inactivation of trypsin. 900 μl collagenase type 2 (Worthington, 10 mg/ml in HBSS) was added to the medium and the tissue was incubated again for 25 min at 37°C. After another washing step with warm trypsin stop-medium and 3.63 μl 0.5 M EDTA, the samples were left on ice to cool down and finally resuspended in 1.5 ml trypsin stop-medium. Sterile coated (Sigmacote®) Pasteur pipettes with three different opening diameters (large, medium and small) were used to homogenize the tissue (pipetted up and down max 20 times). The lysate was centrifuged at 4°C (5 min, 160 rcf) and resuspended in 4 ml wash-buffer/trehalose (36 ml HBSS w/o Ca and Mg, 280 μl 1M HEPES, 400 μl Penicillin-Streptomycin, 40 μl 65% Glucose, 4 ml 50% trehalose). After another centrifugation step (4°C, 5 min, 160 rcf), the pellet was resuspended in 4 ml 30% Percoll™ (GE Healthcare, 7.5 ml Percoll™, 15 ml PBS, 2.5 ml 50% trehalose) for a density gradient centrifugation (4°C, 13 min, 600 rcf). The supernatant and the cell waste were discarded in order to resuspend the pellet in 1.0 ml wash-buffer/trehalose. Pellets were resuspended in 1.0 ml wash-buffer/trehalose and sorted (Pensold et al., 2020).

Cell suspensions prepared from the cortical hemispheres and hippocampi of 23-week-old mice were subjected to fluorescence-activated cell sorting (FACS). Following addition of DAPI, cells were sorted using an ARIA III FACS sorter (BD Biosciences, United States) with a maximal flow rate of six. The tdTomato reporter was excited by a laser (excitation 554 nm, emission 581 nm). Living cells were sorted based on a distinctive tdTomato signal. Two populations were sorted: tdTomato-positive (+) cells and tdTomato-negative (−) cells. The different cell populations (Co-tomato$^+$; Co-tomato$^-$; HC-tomato$^+$; HC-tomato$^-$) were collected in 1xPBS with 2% FBS and centrifuged (4°C; 10 min; 1,000 g). The supernatant was discarded and the cells were lysed in 150 μl TRIzol™ Reagent (Thermo Fisher Scientific) and then frozen (−80°C) for further processing.

RNA Isolation and Sequencing

RNA was isolated and purified using the Direct-zol™ RNA MicroPrep Kit from Zymo Research. All samples were processed according to the manufacturer's protocol and checked for integrity by capillary gel electrophoresis (Bioanalyzer, Agilent Technologies, Inc., United States). The RNA samples were stored at −80°C.

Total RNA of cells and native controls were used in biological triplicates to perform whole transcriptome analysis. Library preparation for RNA-Seq was performed using the SMARTer® Stranded Total RNA-Seq Kit v2 - Pico Input Mammalian (Takara, Cat# 634412) including rRNA-depletion and further processed according to the manufacturer's protocol. The concentrations of final cDNA libraries were determined using the Qubit 2.0 fluorometer (Invitrogen) (average 20 ng/μl) and quality checked with a Bioanalyzer (Agilent 2100 Bioanalyzer) high sensitivity DNA assay. cDNA libraries were amplified and sequenced on an Illumina NextSeq 550 system (high-output, paired-end, read length 151 nt; San Diego, CA, United States). Overall, 24 samples were sequenced, yielding between 26.2 and 105.6 million paired-end reads per sample. One sample with only 1.6 million reads was considered to be a drop-out and retained from further analysis.

After demultiplexing, the quality of the resulting FASTQ files was monitored using FastQC (https://www.bioinformatics.babraham.ac.uk/projects/fastqc/). The reads were individually mapped to the murine reference primary assembly mm10 using STAR_2.5.0c (Dobin et al., 2013) with default parameters and using additionally the –quantMode GeneCounts. Resulting ReadsPerGene tables were processed with an in house R-pipeline and differentially expression analysis carried out based on DESeq2 v.1.16.1[1]. Genes in the PV-KCC2 RNA sequencing data were considered differentially expressed with a Benjamini-Hochberg adjusted p value $p < 0.05$ and a $|\log fc| > 0{,}5$. Gene lists were submitted to the *Database for Annotation, Visualization and Integrated Discovery1* (DAVID) for Gene Ontology (GO) or KEGG Pathway term enrichment analysis. Results of GO enrichment analysis were visualized in a bar diagram including the respective Benjamini-Hochberg corrected p-value, the number of genes and the enrichment fold change included in a certain term. All raw read data were deposited at ArrayExpress under accession E-MATB-11147.

Statistics

For statistical analysis, raw data were analyzed for normal distribution with the Kolmogorov-Smirnov test or with graphical analysis using the box-plot and QQ-plot. If appropriate, we used 1-way ANOVA, 2-way ANOVA, Student's t test (unpaired), Kruskal-Wallis Test, Mantel-Cox Test and Fisher's exact test. P values of less than 0.05 were considered significant. For all data, means with SEM are shown.

Study Approval

All animal experiments were approved by our local institutions (TLV UKJ-17-006; 02-069/16).

DISCUSSION

PV-INs play a major role to control the timing of pyramidal cell activity (Pouille and Scanziani, 2001), for the generation of rhythmic activities as well as the coupling of principal cells into functional assemblies (Klausberger and Somogyi, 2008; Agetsuma et al., 2018). They receive excitatory input from principal cells and GABAergic input from local (Gulyas et al., 1996) and long-range projecting (Freund and Antal, 1988) interneurons. Our immunolabeling of brain sections dissected from 8-week-old WT^{PV} mice shows that the majority of PV-INs in the hippocampus express KCC2. This is in agreement with data obtained for adult rat brains, where somata and radially running dendrites labelled for KCC2 and PV in the *strata oriens*, *radiatum* and *lacunosum moleculare* (Gulyas et al., 2001). PV-INs in the mouse cortex also label for KCC2.

Intrinsic properties such as resting membrane potential and basic passive membrane properties including membrane resistance and capacity of PV-INs were not altered in KCC2 KO^{PV} mice. This suggests that the previous finding that KCC2 affects pyramidal cell excitability through its interaction with Task-3 potassium channels (Goutierre et al., 2019) does not apply to PV-positive interneurons. Nevertheless, KCC2 appears to have an important role for the GABA response of hippocampal PV-INs, because its pharmacological inhibition depolarized the reversal potential of $GABA_A$ receptor mediated currents in mice (Otsu et al., 2020). To evaluate the polarity of synaptic potentials in PV-INs we used a similar minimally invasive approach and performed cell-attached current clamp recordings from PV-positive CA1 interneurons in acute brain slices thus avoiding major perturbations of ion gradients (Perkins, 2006; Kirmse et al., 2015; Otsu et al., 2020) and found a hyperpolarizing response in the majority of PV-INs in 8-10-week-old WT^{PV} mice. Notably, a mostly depolarizing response was reported for PV-INs in 6-week-old control mice (Otsu et al., 2020). This may suggest that the maturation of the transmembrane chloride gradient in mice extends beyond 6 weeks of age.

Although most PV-INs showed a depolarizing response in KCC2 KO^{PV} mice, a depolarizing GABA response can still result in inhibition due to membrane resistance shunting (Staley and Mody, 1992; Kirmse et al., 2015). Decreased E-S coupling and diminished paired pulse facilitation in acute brain slices, however, suggest that PV-INs are disinhibited in KCC2 KO^{PV} mice. In agreement the sIPSC frequency recorded from principal cells was increased in KCC2 KO^{PV} mice, while frequencies and amplitudes of mIPSCs upon block of spontaneous events by tetrodotoxin were independent of the genotype.

Recent studies highlighted that the activity of GABAergic interneurons is controlled by GABA-mediated synaptic inhibition, which can produce oscillatory synchrony in interneuron networks (Traub et al., 1996; Wang and Buzsáki, 1996; Bartos et al., 2007; Khazipov, 2016). Inhibitory neurons can specifically suppress the firing of other inhibitory neurons (Pfeffer et al., 2009; Pi et al., 2013). Such disinhibition can lead to the selective amplification of local processing. Thus, adding to the diversity of GABAergic interneuron classes and their differential recruitment by specific patterns of excitatory input, inhibition of inhibitory GABA neurons markedly expands the range of mechanisms by which they regulate cortical network function (Kepecs and Fishell, 2014).

It is well accepted that failure of the inhibitory restraint provided by GABAergic interneurons can underlie seizure initiation and propagation in both animal models and in humans (Trevelyan et al., 2006; Schevon et al., 2012). This

[1]https://bioconductor.org/packages/release/bioc/html/DESeq2.html

may also explain, why acute blockade of GABA receptors rapidly initiates seizure activity (Treiman, 2001) and drugs that increase synaptic GABA by inhibiting GABA catabolism act as effective anticonvulsants (Sills and Rogawski, 2020). Also Dravet syndrome, which is caused by inactivating mutations of the voltage gated sodium channel Nav1.1 (Claes et al., 2001; Tran et al., 2020), likely results from dampened excitability of interneurons thus decreasing the inhibitory control of the network (Yu et al., 2006). Here, we show that disinhibiting PV-INs by disrupting KCC2, which increases the GABAergic drive, decreases the seizure susceptibility, which at first sight might be counterintuitive. Increases in interneuron activity, however, can render GABA responses of the target cells depolarizing due to chloride accumulation (Payne et al., 2003; Khazipov et al., 2004; Magloire et al., 2019). Such excitatory GABA effects due to chloride accumulation may contribute to seizure induction (Cossart et al., 2005; Palma et al., 2006; Kaila and Miles, 2010; Gonzalez et al., 2018; Klein et al., 2018) because PV-INs are able to synchronize network activity (Jiruska et al., 2013; Khazipov, 2016).

Remarkably, interneurons are particularly sensitive to seizure-related damage (Sloviter Robert, 1987; de Lanerolle et al., 1989; Cossart et al., 2001; Bartos et al., 2007). Among the most vulnerable interneurons in human temporal lobe epilepsy and related animal models are those expressing PV (Bouilleret et al., 2000). As a matter of fact, we found a time-dependent decrease in PV-INs in KCC2 KO^{PV} mice. This may further increase the excitability of the network as evidenced by the decreased E-S coupling in 23-week-old KCC2 KO^{PV} mice and thus aggravate epilepsy. Indeed, focal ablation of GABAergic interneurons can cause hyperexcitability and repetitive seizures (Drexel et al., 2017; Spampanato and Dudek, 2017).

To get further clues we analyzed the transcriptional profile of PV-INs from WT^{PV} and KCC2 KO^{PV} mice. In agreement with the progressive loss of PNNs in KCC2 KO^{PV} transcripts of several metalloproteinases were up-regulated, which contribute to the remodeling of the ECM and synaptic circuit remodeling (Ferrer-Ferrer and Dityatev, 2018). More importantly, we also identified major changes in PI3K-AKT and p38-MAPK signaling. A dysregulation of the PI3K-AKT pathway is known for several disorders of the central nervous system such as Parkinson's disease (Khwanraj et al., 2016), ischemic brain injury (Zhang et al., 2015) as well as epilepsy (Roy et al., 2015). Although PI3K-AKT is generally known for cell survival, it can also trigger apoptosis by its ability to increase reactive oxygen species and to suppress antioxidant enzymes (Los et al., 2009).

MAPKs play a pivotal role in converting extracellular stimuli into a wide range of cellular responses, including cell growth, migration, proliferation, differentiation, and apoptosis (Wada and Penninger, 2004). In particular, p38-MAPK signaling plays a key role to balance cell survival and death in response to both extracellular and intracellular stresses in a cell context-specific and cell type-specific manner, which can eventually converge on caspase activation as key effectors of apoptosis (Devanand Sarkar et al., 2002; Porras et al., 2004). Altogether, these transcriptional changes suggest that the progressive loss of PV-INs in KCC2 KO^{PV} mice is mediated via apoptosis.

The knowledge how individual neuron subtypes are affected by epilepsy and how individual subtypes contribute to epileptogenesis is very limited. Here we show a prominent role of PV-INs. Fatal spontaneous seizures, which were incidentally observed in KCC2 KO^{PV} mice starting from roughly 8 weeks of age, likely explain the high lethality of KCC2 KO^{PV} mice. Other factors, however, may contribute as well, because PV-INs are broadly expressed and involved in different neuronal circuits. For a systematic analysis of the onset, frequency and outcome of spontaneous seizures chronic electroencephalogram recordings are desirably for future analyses. Such data will shed additional light on the role of PV-INs for the pathophysiology of seizures and are necessary, in order to better understand disease etiology and discover new targets for diagnostics and treatment.

DATA AVAILABILITY STATEMENT

The raw data supporting the conclusions of this article will be made available by the authors, without undue reservation.

ETHICS STATEMENT

The animal study was reviewed and approved by Landesverwaltungsamt Thüringen. Written informed consent was obtained from the owners for the participation of their animals in this study.

AUTHOR CONTRIBUTIONS

TH, MG, RD, DP, MU, and LL performed experiments and analyzed data. CH interpreted data, initiated and supervised the study and wrote the manuscript. All authors contributed to the article and approved the submitted version.

FUNDING

This study was funded by the BMBF (ACROBAT 01EW1706) and Priority Program 1665 (HU 800/8–1/2) to CH.

SUPPLEMENTARY MATERIAL

The Supplementary Material for this article can be found online at: https://www.frontiersin.org/articles/10.3389/fnmol.2021.807090/full#supplementary-material

Supplementary Figure 1 | TdTomato-labeled cells in brain sections of PV-Cre/tdTomato mice stain for PV. **(A)** Representative images from hippocampus and S1 of a brain section of an 8-week-old PV-Cre/tdTomato mouse stained for PV (green). Scale bar 100 μm. **(B)** Representative KCC2 and DAPI staining from the CA3 region of the hippocampus of 8-week-old WT^{PV} and KO^{PV} mice. Scale bars 5 μm. **(C)** The quantification of KCC2-labeled tdTomato-positive neurons in the hippocampus of WT^{PV} and KCC2 KO^{PV} mice confirms the deletion of KCC2 in most PV-INs at 8 weeks of age. KCC2 expressing tdTomato labeled cells were counted in CA1 (WT: 80.3 ± 1.9%; KO: 21.3 ± 3.1%) and CA3 (WT: 83.6 ± 2.1%; KO: 19.5 ± 1.61%) quantification from n = 9 sections and N = 3 mice; Student's unpaired t-test; $^{***}p < 0.001$).

Supplementary Figure 2 | Motor impairment and increased anxiety in KCC2 KO^{PV} mice. **(A)** The Rotarod analysis at 6, 8, and 12 weeks of age shows a progressive decline of motor functions in KCC2 KO^{PV} mice (N = 15/16 mice; 2-way ANOVA; Bonferroni's post-test; *** $p < 0.0001$). **(B)** Cued and contextual fear conditioning test in 8-week-old WT^{PV} and KCC2 KO^{PV} mice. Freezing behavior during the test was measured as an index of fear memory. For acquisition mice were placed into a conditioning chamber and were given pairings of a tone and an electric foot-shock. After 24 h mice were either exposed to a different chamber with presentation of the auditory cue (cued test) or the same context as for acquisition (context test). Both genotypes remembered the conditioned stimulus and the context of the aversive stimulus. KCC2 KO^{PV} mice displayed an increased anxiety-like behavior (2-way ANOVA; Bonferroni post-test; *$p > 0.05$; **$p < 0.001$; ***$p < 0.0001$). **(C)** The serum corticosterone concentration is elevated in 8-week-old KCC2 KO^{PV} mice (N = 8/9 mice; unpaired Student's t-test; *$p = 0.016$). **(D)** Duration of each Racine level after pilocarpine injection (N = 6/6; 2-way ANOVA; Bonferroni post-test; ns not significant; *$p > 0.05$; **$p < 0.001$). **(E)** Survival of WT^{PV} and KO^{PV} mice after pilocarpine injection (N = 6/6; Mantel-Cox Test; *$p = 0.0337$).

Supplementary Figure 3 | Disinhibition of cortical PV-INs upon disruption of KCC2. **(A,B)** Paired-pulse ratios are reduced in the motor cortex (A; n = 35/32 slices from N = 12/9 mice) and somatosensory cortex (B; n = 34/33 slices from N = 13/11 mice) of KCC2 KO^{PV} mice (2-way ANOVA repeated measure; Bonferroni post-test; *$p > 0.05$; **$p < 0.001$; ***$p < 0.0001$). **(C)** The frequency but not the amplitude of spontaneous inhibitory post synaptic currents (sIPSCs) is increased in the somatosensory cortex of KCC2 KO^{PV} mice (N = 6/6 mice; unpaired Student's t-test; Kolmogorov-Smirnov test; ns not significant; *$p = 0.0137$). **(D)** Miniature inhibitory postsynaptic currents (mIPSCs) upon tetrodotoxin (TTX) inhibition are not changed in 8-week-old KCC2 KO^{PV} mice (N = 6/6 mice; unpaired Student's t-test; Kolmogorov-Smirnov test; ns not significant).

Supplementary Figure 4 | Altered neurites in 23-week-old KCC2 KO^{PV} mice. TdTomato-signals from S1 (left), the retrospenial (RSP) cortex (middle), and the hippocampus of WT^{PV} (upper) and KCC2 KO^{PV} (lower) brain sections. Scale bars 100 μm.

Supplementary Table 1 | Individual numbers for the quantification of tdTomato-positive cells displayed in **Figures 5D–G**.

REFERENCES

Agetsuma, M., Hamm, J. P., Tao, K., Fujisawa, S., and Yuste, R. (2018). Parvalbumin-positive interneurons regulate neuronal ensembles in visual cortex. *Cereb. Cortex* 28, 1831–1845. doi: 10.1093/cercor/bhx169

Bartos, M., Vida, I., and Jonas, P. (2007). Synaptic mechanisms of synchronized gamma oscillations in inhibitory interneuron networks. *Nat. Rev. Neurosci.* 8, 45–56. doi: 10.1038/nrn2044

Ben-Ari, Y., Khalilov, I., Kahle, K. T., and Cherubini, E. (2012). The GABA excitatory/inhibitory shift in brain maturation and neurological disorders. *Neuroscientist* 18, 467–486. doi: 10.1177/1073858412438697

Berdichevsky, Y., Dryer, A. M., Saponjian, Y., Mahoney, M. M., Pimentel, C. A., Lucini, C. A., et al. (2013). PI3K-Akt signaling activates mTOR-mediated epileptogenesis in organotypic hippocampal culture model of post-traumatic epilepsy. *J. Neurosci.* 33, 9056–9067. doi: 10.1523/JNEUROSCI.3870-12.2013

Blaesse, P., Airaksinen, M. S., Rivera, C., and Kaila, K. (2009). Cation-chloride cotransporters and neuronal function. *Neuron* 61, 820–838. doi: 10.1016/j.neuron.2009.03.003

Blatow, M., Rozov, A., Katona, I., Hormuzdi, S. G., Meyer, A. H., Whittington, M. A., et al. (2003). A novel network of multipolar bursting interneurons generates theta frequency oscillations in neocortex. *Neuron* 38, 805–817. doi: 10.1016/s0896-6273(03)00300-3

Bouilleret, V., Loup, F., Kiener, T., Marescaux, C., and Fritschy, J.-M. (2000). Early loss of interneurons and delayed subunit-specific changes in GABAA-receptor expression in a mouse model of mesial temporal lobe epilepsy. *Hippocampus* 10, 305–324. doi: 10.1002/1098-1063(2000)10:3<305::AID-HIPO11>3.0.CO;2-I

Carceller, H., Guirado, R., Ripolles-Campos, E., Teruel-Marti, V., and Nacher, J. (2020). Perineuronal nets regulate the inhibitory perisomatic input onto parvalbumin interneurons and gamma activity in the prefrontal cortex. *J. Neurosci.* 40, 5008–5018. doi: 10.1523/JNEUROSCI.0291-20.2020

Carter, A. N., Born, H. A., Levine, A. T., Dao, A. T., Zhao, A. J., Lee, W. L., et al. (2017). Wortmannin attenuates seizure-induced hyperactive PI3K/Akt/mTOR signaling, impaired memory, and spine dysmorphology in rats. *eNeuro* 4, ENEURO.0354-16.2017. doi: 10.1523/ENEURO.0354-16.2017

Celio, M. R. (1986). Parvalbumin in most gamma-aminobutyric acid-containing neurons of the rat cerebral cortex. *Science* 231, 995–997. doi: 10.1126/science.3945815

Chaunsali, L., Tewari, B. P., and Sontheimer, H. (2021). Perineuronal net dynamics in the pathophysiology of epilepsy. *Epilepsy Curr.* 21, 273–281. doi: 10.1177/15357597211018688

Claes, L., Del-Favero, J., Ceulemans, B., Lagae, L., Van Broeckhoven, C., and De Jonghe, P. (2001). De novo mutations in the sodium-channel gene SCN1A cause severe myoclonic epilepsy of infancy. *Am. J. Hum. Genet.* 68, 1327–1332.

Cossart, R., Bernard, C., and Ben-Ari, Y. (2005). Multiple facets of GABAergic neurons and synapses: multiple fates of GABA signalling in epilepsies. *Trends Neurosci.* 28, 108–115. doi: 10.1016/j.tins.2004.11.011

Cossart, R., Dinocourt, C., Hirsch, J. C., Merchan-Perez, A., De Felipe, J., Ben-Ari, Y., et al. (2001). Dendritic but not somatic GABAergic inhibition is decreased in experimental epilepsy. *Nat. Neurosci.* 4, 52–62. doi: 10.1038/82900

Coulter, D. A., and Steinhauser, C. (2015). Role of astrocytes in epilepsy. *Cold Spring Harb. Perspect. Med.* 5:a022434.

Crapser, J. D., Spangenberg, E. E., Barahona, R. A., Arreola, M. A., Hohsfield, L. A., and Green, K. N. (2020). Microglia facilitate loss of perineuronal nets in the Alzheimer's disease brain. *EBioMedicine* 58:102919. doi: 10.1016/j.ebiom.2020.102919

Davies, C. H., Davies, S. N., and Collingridge, G. L. (1990). Paired-pulse depression of monosynaptic GABA-mediated inhibitory postsynaptic responses in rat hippocampus. *J. Physiol.* 424, 513–531. doi: 10.1113/jphysiol.1990.sp018080

de Lanerolle, N. C., Kim, J. H., Robbins, R. J., and Spencer, D. D. (1989). Hippocampal interneuron loss and plasticity in human temporal lobe epilepsy. *Brain Res.* 495, 387–395. doi: 10.1016/0006-8993(89)90234-5

Di Cristo, G., Awad, P. N., Hamidi, S., and Avoli, M. (2018). KCC2, epileptiform synchronization, and epileptic disorders. *Prog. Neurobiol.* 162, 1–16. doi: 10.1016/j.pneurobio.2017.11.002

Dobin, A., Davis, C. A., Schlesinger, F., Drenkow, J., Zaleski, C., Jha, S., et al. (2013). STAR: ultrafast universal RNA-seq aligner. *Bioinformatics* 29, 15–21. doi: 10.1093/bioinformatics/bts635

Drexel, M., Romanov, R. A., Wood, J., Weger, S., Heilbronn, R., Wulff, P., et al. (2017). Selective silencing of hippocampal parvalbumin interneurons induces development of recurrent spontaneous limbic seizures in mice. *J. Neurosci.* 37, 8166–8179. doi: 10.1523/JNEUROSCI.3456-16.2017

Dubey, D., Mcrae, P. A., Rankin-Gee, E. K., Baranov, E., Wandrey, L., Rogers, S., et al. (2017). Increased metalloproteinase activity in the hippocampus following status epilepticus. *Epilepsy Res.* 132, 50–58. doi: 10.1016/j.eplepsyres.2017.02.021

Fanselow, M. S., and Poulos, A. M. (2005). The neuroscience of mammalian associative learning. *Annu. Rev. Psychol.* 56, 207–234. doi: 10.1146/annurev.psych.56.091103.070213

Ferrer-Ferrer, M., and Dityatev, A. (2018). Shaping synapses by the neural extracellular matrix. *Front. Neuroanat.* 12:40. doi: 10.3389/fnana.2018.00040

Freund, T. F., and Antal, M. (1988). GABA-containing neurons in the septum control inhibitory interneurons in the hippocampus. *Nature* 336, 170–173. doi: 10.1038/336170a0

Gibson, J. R., Beierlein, M., and Connors, B. W. (1999). Two networks of electrically coupled inhibitory neurons in neocortex. *Nature* 402, 75–79. doi: 10.1038/47035

Gonzalez, O. C., Shiri, Z., Krishnan, G. P., Myers, T. L., Williams, S., Avoli, M., et al. (2018). Role of KCC2-dependent potassium efflux in 4-aminopyridine-induced epileptiform synchronization. *Neurobiol. Dis.* 109, 137–147. doi: 10.1016/j.nbd.2017.10.011

Goutierre, M., Al Awabdh, S., Donneger, F., Francois, E., Gomez-Dominguez, D., Irinopoulou, T., et al. (2019). KCC2 Regulates neuronal excitability and

hippocampal activity via interaction with task-3 channels. *Cell Rep* 28, 91–103.e7. doi: 10.1016/j.celrep.2019.06.001

Gulyas, A. I., Hajos, N., and Freund, T. F. (1996). Interneurons containing calretinin are specialized to control other interneurons in the rat hippocampus. *J. Neurosci.* 16, 3397–3411. doi: 10.1523/JNEUROSCI.16-10-03397.1996

Gulyas, A. I., Sik, A., Payne, J. A., Kaila, K., and Freund, T. F. (2001). The KCl cotransporter, KCC2, is highly expressed in the vicinity of excitatory synapses in the rat hippocampus. *Eur. J. Neurosci.* 13, 2205–2217. doi: 10.1046/j.0953-816x.2001.01600.x

Helen, C., and Atkinson, B. J. W. (1997). Circadian variation in basal plasma corticosterone and adrenocorticotropin in the rat: sexual dimorphism and changes across the estrous cycle. *Endocrinology* 138, 3842–3848. doi: 10.1210/endo.138.9.5395

Hendry, S. H., Schwark, H. D., Jones, E. G., and Yan, J. (1987). Numbers and proportions of GABA-immunoreactive neurons in different areas of monkey cerebral cortex. *J. Neurosci.* 7, 1503–1519. doi: 10.1523/JNEUROSCI.07-05-01503.1987

Hippenmeyer, S., Vrieseling, E., Sigrist, M., Portmann, T., Laengle, C., Ladle, D. R., et al. (2005). A developmental switch in the response of DRG neurons to ETS transcription factor signaling. *PLoS Biol.* 3:e159. doi: 10.1371/journal.pbio.0030159

Hu, H., Gan, J., and Jonas, P. (2014). Interneurons. fast-spiking, parvalbumin(+) GABAergic interneurons: from cellular design to microcircuit function. *Science* 345:1255263. doi: 10.1126/science.1255263

Hu, H., Ma, Y., and Agmon, A. (2011). Submillisecond firing synchrony between different subtypes of cortical interneurons connected chemically but not electrically. *J. Neurosci.* 31, 3351–3361. doi: 10.1523/JNEUROSCI.4881-10.2011

Hubner, C. A. (2014). The KCl-cotransporter KCC2 linked to epilepsy. *EMBO Rep.* 15, 732–733. doi: 10.15252/embr.201439039

Hubner, C. A., Stein, V., Hermans-Borgmeyer, I., Meyer, T., Ballanyi, K., and Jentsch, T. J. (2001). Disruption of KCC2 reveals an essential role of K-Cl cotransport already in early synaptic inhibition. *Neuron* 30, 515–524. doi: 10.1016/s0896-6273(01)00297-5

Jiang, X., Wang, G., Lee, A. J., Stornetta, R. L., and Zhu, J. J. (2013). The organization of two new cortical interneuronal circuits. *Nat. Neurosci.* 16, 210–218. doi: 10.1038/nn.3305

Jiruska, P., De Curtis, M., Jefferys, J. G., Schevon, C. A., Schiff, S. J., and Schindler, K. (2013). Synchronization and desynchronization in epilepsy: controversies and hypotheses. *J. Physiol.* 591, 787–797. doi: 10.1113/jphysiol.2012.239590

Kahle, K. T., Khanna, A. R., Duan, J., Staley, K. J., Delpire, E., and Poduri, A. (2016). The KCC2 cotransporter and human epilepsy: getting excited about inhibition. *Neuroscientist* 22, 555–562. doi: 10.1177/1073858416645087

Kahle, K. T., Merner, N. D., Friedel, P., Silayeva, L., Liang, B., Khanna, A., et al. (2014). Genetically encoded impairment of neuronal KCC2 cotransporter function in human idiopathic generalized epilepsy. *EMBO Rep.* 15, 766–774. doi: 10.15252/embr.201438840

Kaila, K., and Miles, R. (2010). Chloride homeostasis and GABA signaling in temporal lobe epilepsy. *Epilepsia* 51, 52–52.

Kamprath, K., and Wotjak, C. T. (2004). Nonassociative learning processes determine expression and extinction of conditioned fear in mice. *Learn. Mem.* 11, 770–786. doi: 10.1101/lm.86104

Kepecs, A., and Fishell, G. (2014). Interneuron cell types are fit to function. *Nature* 505, 318–326. doi: 10.1038/nature12983

Khazipov, R. (2016). GABAergic Synchronization in Epilepsy. *Cold Spring Harb. Perspect. Med.* 6:a022764. doi: 10.1101/cshperspect.a022764

Khazipov, R., Khalilov, I., Tyzio, R., Morozova, E., Ben-Ari, Y., and Holmes, G. L. (2004). Developmental changes in GABAergic actions and seizure susceptibility in the rat hippocampus. *Eur. J. Neurosci.* 19, 590–600. doi: 10.1111/j.0953-816x.2003.03152.x

Khwanraj, K., Madlah, S., Grataitong, K., and Dharmasaroja, P. (2016). Comparative mRNA expression of eEF1A isoforms and a PI3K/Akt/mTOR pathway in a Cellular model of Parkinson's disease. *Parkinsons Dis.* 2016:8716016. doi: 10.1155/2016/8716016

Kilb, W. (2012). Development of the GABAergic system from birth to adolescence. *Neuroscientist* 18, 613–630. doi: 10.1177/1073858411422114

Kirmse, K., Kummer, M., Kovalchuk, Y., Witte, O. W., Garaschuk, O., and Holthoff, K. (2015). GABA depolarizes immature neurons and inhibits network activity in the neonatal neocortex in vivo. *Nat. Commun.* 6:7750.

Klausberger, T., and Somogyi, P. (2008). Neuronal diversity and temporal dynamics: the unity of hippocampal circuit operations. *Science* 321, 53–57. doi: 10.1126/science.1149381

Klein, P. M., Lu, A. C., Harper, M. E., Mckown, H. M., Morgan, J. D., and Beenhakker, M. P. (2018). Tenuous inhibitory GABAergic signaling in the reticular thalamus. *J. Neurosci.* 38, 1232–1248. doi: 10.1523/JNEUROSCI.1345-17.2017

Liebmann, L., Karst, H., and Joels, M. (2009). Effects of corticosterone and the beta-agonist isoproterenol on glutamate receptor-mediated synaptic currents in the rat basolateral amygdala. *Eur. J. Neurosci.* 30, 800–807. doi: 10.1111/j.1460-9568.2009.06882.x

Liu, Y.-Q., Yu, F., Liu, W.-H., He, X.-H., and Peng, B.-W. (2014). Dysfunction of hippocampal interneurons in epilepsy. *Neurosci. Bull.* 30, 985–998. doi: 10.1007/s12264-014-1478-4

Lodato, S., Tomassy, G. S., De Leonibus, E., Uzcategui, Y. G., Andolfi, G., Armentano, M., et al. (2011). Loss of COUP-TFI alters the balance between caudal ganglionic eminence- and medial ganglionic eminence-derived cortical interneurons and results in resistance to epilepsy. *J. Neurosci.* 31, 4650–4662. doi: 10.1523/JNEUROSCI.6580-10.2011

Los, M., Maddika, S., Erb, B., and Schulze-Osthoff, K. (2009). Switching Akt: from survival signaling to deadly response. *Bioessays* 31, 492–495. doi: 10.1002/bies.200900005

Luhmann, H. J., Kirischuk, S., Sinning, A., and Kilb, W. (2014). Early GABAergic circuitry in the cerebral cortex. *Curr. Opin. Neurobiol.* 26, 72–78. doi: 10.1016/j.conb.2013.12.014

Madisen, L., Zwingman, T. A., Sunkin, S. M., Oh, S. W., Zariwala, H. A., Gu, H., et al. (2010). A robust and high-throughput cre reporting and characterization system for the whole mouse brain. *Nat. Neurosci.* 13, 133–140. doi: 10.1038/nn.2467

Magloire, V., Cornford, J., Lieb, A., Kullmann, D. M., and Pavlov, I. (2019). KCC2 overexpression prevents the paradoxical seizure-promoting action of somatic inhibition. *Nat. Commun.* 10:1225.

Markram, H., Toledo-Rodriguez, M., Wang, Y., Gupta, A., Silberberg, G., and Wu, C. (2004). Interneurons of the neocortical inhibitory system. *Nat. Rev. Neurosci.* 5, 793–807. doi: 10.1038/nrn1519

Otsu, Y., Donneger, F., Schwartz, E. J., and Poncer, J. C. (2020). Cation-chloride cotransporters and the polarity of GABA signalling in mouse hippocampal parvalbumin interneurons. *J. Physiol.* 598, 1865–1880. doi: 10.1113/JP279221

Palma, E., Amici, M., Sobrero, F., Spinelli, G., Di Angelantonio, S., Ragozzino, D., et al. (2006). Anomalous levels of Cl- transporters in the hippocampal subiculum from temporal lobe epilepsy patients make GABA excitatory. *Proc. Natl. Acad. Sci. U.S.A.* 103, 8465–8468. doi: 10.1073/pnas.0602979103

Payne, J. A., Rivera, C., Voipio, J., and Kaila, K. (2003). Cation–chloride co-transporters in neuronal communication, development and trauma. *Trends Neurosci.* 26, 199–206. doi: 10.1016/S0166-2236(03)00068-7

Payne, J. A., Stevenson, T. J., and Donaldson, L. F. (1996). Molecular characterization of a putative K-Cl cotransporter in rat brain. A neuronal-specific isoform. *J. Biol. Chem.* 271, 16245–16252.

Pensold, D., Reichard, J., Van Loo, K. M. J., Ciganok, N., Hahn, A., Bayer, C., et al. (2020). DNA methylation-mediated modulation of endocytosis as potential mechanism for synaptic function regulation in murine inhibitory cortical interneurons. *Cereb. Cortex* 30, 3921–3937. doi: 10.1093/cercor/bhaa009

Perkins, K. L. (2006). Cell-attached voltage-clamp and current-clamp recording and stimulation techniques in brain slices. *J. Neurosci. Methods* 154, 1–18. doi: 10.1016/j.jneumeth.2006.02.010

Pernice, H. F., Schieweck, R., Kiebler, M. A., and Popper, B. (2016). mTOR and MAPK: from localized translation control to epilepsy. *BMC Neurosci.* 17:73. doi: 10.1186/s12868-016-0308-1

Pfeffer, C. K., Stein, V., Keating, D. J., Maier, H., Rinke, I., Rudhard, Y., et al. (2009). NKCC1-dependent GABAergic excitation drives synaptic network maturation during early hippocampal development. *J. Neurosci.* 29, 3419–3430. doi: 10.1523/JNEUROSCI.1377-08.2009

Pfeffer, C. K., Xue, M., He, M., Huang, Z. J., and Scanziani, M. (2013). Inhibition of inhibition in visual cortex: the logic of connections between molecularly distinct interneurons. *Nat. Neurosci.* 16, 1068–1076. doi: 10.1038/nn.3446

Pi, H. J., Hangya, B., Kvitsiani, D., Sanders, J. I., Huang, Z. J., and Kepecs, A. (2013). Cortical interneurons that specialize in disinhibitory control. *Nature* 503, 521–524. doi: 10.1038/nature12676

Porras, A., Zuluaga, S., Black, E., Valladares, A., Alvarez, A. M., Ambrosino, C., et al. (2004). P38 alpha mitogen-activated protein kinase sensitizes cells to apoptosis induced by different stimuli. *Mol. Biol. Cell* 15, 922–933. doi: 10.1091/mbc.e03-08-0592

Pouille, F., and Scanziani, M. (2001). Enforcement of temporal fidelity in pyramidal cells by somatic feed-forward inhibition. *Science* 293, 1159–1163. doi: 10.1126/science.1060342

Puskarjov, M., Seja, P., Heron, S. E., Williams, T. C., Ahmad, F., Iona, X., et al. (2014). A variant of KCC2 from patients with febrile seizures impairs neuronal Cl- extrusion and dendritic spine formation. *EMBO Rep.* 15, 723–729. doi: 10.1002/embr.201438749

Racine, R. J. (1972). Modification of seizure activity by electrical stimulation. II. Motor seizure. *Electroencephalogr. Clin. Neurophysiol.* 32, 281–294.

Rivera, C., Voipio, J., Payne, J. A., Ruusuvuori, E., Lahtinen, H., Lamsa, K., et al. (1999). The K+/Cl- co-transporter KCC2 renders GABA hyperpolarizing during neuronal maturation. *Nature* 397, 251–255. doi: 10.1038/16697

Roux, L., and Buzsaki, G. (2015). Tasks for inhibitory interneurons in intact brain circuits. *Neuropharmacology* 88, 10–23. doi: 10.1016/j.neuropharm.2014.09.011

Roy, A., Skibo, J., Kalume, F., Ni, J., Rankin, S., Lu, Y., et al. (2015). Mouse models of human PIK3CA-related brain overgrowth have acutely treatable epilepsy. *Elife* 4:e12703. doi: 10.7554/eLife.12703

Rudy, B., Fishell, G., Lee, S., and Hjerling-Leffler, J. (2011). Three groups of interneurons account for nearly 100% of neocortical GABAergic neurons. *Dev. Neurobiol.* 71, 45–61. doi: 10.1002/dneu.20853

Saitsu, H., Watanabe, M., Akita, T., Ohba, C., Sugai, K., Ong, W. P., et al. (2016). Impaired neuronal KCC2 function by biallelic SLC12A5 mutations in migrating focal seizures and severe developmental delay. *Sci. Rep.* 6:30072. doi: 10.1038/srep30072

Sanz, P., and Garcia-Gimeno, M. A. (2020). Reactive glia inflammatory signaling pathways and epilepsy. *Int. J. Mol. Sci.* 21:4096. doi: 10.3390/ijms21114096

Sarkar, D., Su, Z. Z., Lebedeva, I. V., Sauane, M., Gopalkrishnan, R. V., Valerie, K., et al. (2002). mda-7 (IL-24) mediates selective apoptosis in human melanoma cells by inducing the coordinated overexpression of the gadd family of genes by means of p38 MAPK. *Proc. Natl. Acad. Sci. U.S.A.* 99, 10054–10059. doi: 10.1073/pnas.152327199

Schevon, C. A., Weiss, S. A., Mckhann, G. Jr., Goodman, R. R., Yuste, R., Emerson, R. G., et al. (2012). Evidence of an inhibitory restraint of seizure activity in humans. *Nat. Commun.* 3:1060. doi: 10.1038/ncomms2056

Seja, P., Schonewille, M., Spitzmaul, G., Badura, A., Klein, I., Rudhard, Y., et al. (2012). Raising cytosolic Cl- in cerebellar granule cells affects their excitability and vestibulo-ocular learning. *EMBO J.* 31, 1217–1230. doi: 10.1038/emboj.2011.488

Sills, G. J., and Rogawski, M. A. (2020). Mechanisms of action of currently used antiseizure drugs. *Neuropharmacology* 168:107966. doi: 10.1016/j.neuropharm.2020.107966

Sinning, A., Liebmann, L., Kougioumtzes, A., Westermann, M., Bruehl, C., and Hubner, C. A. (2011). Synaptic glutamate release is modulated by the Na+ -driven Cl^-/HCO_3– exchanger Slc4a8. *J. Neurosci.* 31, 7300–7311. doi: 10.1523/JNEUROSCI.0269-11.2011

Siracusa, R., Fusco, R., and Cuzzocrea, S. (2019). Astrocytes: role and functions in brain pathologies. *Front. Pharmacol.* 10:1114. doi: 10.3389/fphar.2019.01114

Sloviter Robert, S. (1987). Decreased hippocampal inhibition and a selective loss of interneurons in experimental epilepsy. *Science* 235, 73–76. doi: 10.1126/science.2879352

Smith, D. R., Gallagher, M., and Stanton, M. E. (2007). Genetic background differences and nonassociative effects in mouse trace fear conditioning. *Learn. Mem.* 14, 597–605. doi: 10.1101/lm.614807

Spampanato, J., and Dudek, F. E. (2017). Targeted interneuron ablation in the mouse hippocampus can cause spontaneous recurrent seizures. *eNeuro* 4, ENEURO.130-ENEURO.117. doi: 10.1523/ENEURO.0130-17.2017

Staley, K. J., and Mody, I. (1992). Shunting of excitatory input to dentate gyrus granule cells by a depolarizing GABAA receptor-mediated postsynaptic conductance. *J. Neurophysiol.* 68, 197–212. doi: 10.1152/jn.1992.68.1.197

Steffensen, S. C., and Henriksen, S. J. (1991). Effects of baclofen and bicuculline on inhibition in the fascia dentata and hippocampus regio superior. *Brain Res.* 538, 46–53. doi: 10.1016/0006-8993(91)90374-5

Steinhauser, C., Grunnet, M., and Carmignoto, G. (2016). Crucial role of astrocytes in temporal lobe epilepsy. *Neuroscience* 323, 157–169. doi: 10.1016/j.neuroscience.2014.12.047

Steward, O., Torre, E. R., Tomasulo, R., and Lothman, E. (1992). Seizures and the regulation of astroglial gene expression. *Epilepsy Res. Suppl.* 7, 197–209.

Tewari, B. P., Chaunsali, L., Campbell, S. L., Patel, D. C., Goode, A. E., and Sontheimer, H. (2018). Perineuronal nets decrease membrane capacitance of peritumoral fast spiking interneurons in a model of epilepsy. *Nat. Commun.* 9:4724.

Tran, C. H., Vaiana, M., Nakuci, J., Somarowthu, A., Goff, K. M., Goldstein, N., et al. (2020). Interneuron desynchronization precedes seizures in a mouse model of dravet syndrome. *J. Neurosci.* 40, 2764–2775. doi: 10.1523/JNEUROSCI.2370-19.2020

Traub, R. D., Whittington, M. A., Colling, S. B., Buzsáki, G., and Jefferys, J. G. (1996). Analysis of gamma rhythms in the rat hippocampus in vitro and in vivo. *J. Physiol.* 493(Pt 2), 471–484. doi: 10.1113/jphysiol.1996.sp021397

Treiman, D. M. (2001). GABAergic mechanisms in epilepsy. *Epilepsia* 42, 8–12. doi: 10.1046/j.1528-1157.2001.042suppl.3008.x

Trevelyan, A. J., Sussillo, D., Watson, B. O., and Yuste, R. (2006). Modular propagation of epileptiform activity: evidence for an inhibitory veto in neocortex. *J. Neurosci.* 26, 12447–12455. doi: 10.1523/JNEUROSCI.2787-06.2006

Virtanen, M. A., Uvarov, P., Hubner, C. A., and Kaila, K. (2020). NKCC1, an elusive molecular target in brain development: making sense of the existing data. *Cells* 9:2607. doi: 10.3390/cells9122607

Wada, T., and Penninger, J. M. (2004). Mitogen-activated protein kinases in apoptosis regulation. *Oncogene* 23, 2838–2849.

Wang, X. J., and Buzsáki, G. (1996). Gamma oscillation by synaptic inhibition in a hippocampal interneuronal network model. *J. Neurosci.* 16, 6402–6413. doi: 10.1523/JNEUROSCI.16-20-06402.1996

Wen, T. H., Binder, D. K., Ethell, I. M., and Razak, K. A. (2018). The perineuronal 'Safety' Net? perineuronal net abnormalities in neurological disorders. *Front. Mol. Neurosci.* 11:270. doi: 10.3389/fnmol.2018.00270

Woo, N. S., Lu, J., England, R., Mcclellan, R., Dufour, S., Mount, D. B., et al. (2002). Hyperexcitability and epilepsy associated with disruption of the mouse neuronal-specific K-Cl cotransporter gene. *Hippocampus* 12, 258–268. doi: 10.1002/hipo.10014

Yu, F. H., Mantegazza, M., Westenbroek, R. E., Robbins, C. A., Kalume, F., Burton, K. A., et al. (2006). Reduced sodium current in GABAergic interneurons in a mouse model of severe myoclonic epilepsy in infancy. *Nat. Neurosci.* 9, 1142–1149. doi: 10.1038/nn1754

Zhang, W., Liu, J., Hu, X., Li, P., Leak, R. K., Gao, Y., et al. (2015). n-3 Polyunsaturated fatty acids reduce neonatal hypoxic/ischemic brain injury by promoting phosphatidylserine formation and Akt signaling. *Stroke* 46, 2943–2950. doi: 10.1161/STROKEAHA.115.010815

Conflict of Interest: The authors declare that the research was conducted in the absence of any commercial or financial relationships that could be construed as a potential conflict of interest.

Publisher's Note: All claims expressed in this article are solely those of the authors and do not necessarily represent those of their affiliated organizations, or those of the publisher, the editors and the reviewers. Any product that may be evaluated in this article, or claim that may be made by its manufacturer, is not guaranteed or endorsed by the publisher.

frontiers in Molecular Neuroscience

ORIGINAL RESEARCH
published: 16 March 2022
doi: 10.3389/fnmol.2022.826427

Loss of KCC2 in GABAergic Neurons Causes Seizures and an Imbalance of Cortical Interneurons

*Kirill Zavalin[1], Anjana Hassan[1], Cary Fu[2], Eric Delpire[3] and Andre H. Lagrange[1,4]**

[1] Department of Neurology, School of Medicine, Vanderbilt University, Nashville, TN, United States, [2] Department of Pediatrics, Vanderbilt University Medical Center, Nashville, TN, United States, [3] Department of Anesthesiology, School of Medicine, Vanderbilt University, Nashville, TN, United States, [4] Department of Neurology, Tennessee Valley Healthcare – Veterans Affairs (TVH VA), Medical Center, Nashville, TN, United States

OPEN ACCESS

Edited by:
Atsuo Fukuda, Hamamatsu University School of Medicine, Japan

Reviewed by:
Xavier Leinekugel, Institut National de la Santé et de la Recherche Médicale (INSERM), France
Graziella DiCristo, Université de Montréal, Canada

***Correspondence:**
Andre H. Lagrange
andre.h.lagrange@vumc.org

Specialty section:
This article was submitted to Neuroplasticity and Development, a section of the journal Frontiers in Molecular Neuroscience

Received: *30 November 2021*
Accepted: *21 February 2022*
Published: *16 March 2022*

Citation:
Zavalin K, Hassan A, Fu C, Delpire E and Lagrange AH (2022) Loss of KCC2 in GABAergic Neurons Causes Seizures and an Imbalance of Cortical Interneurons. Front. Mol. Neurosci. 15:826427. doi: 10.3389/fnmol.2022.826427

K-Cl transporter KCC2 is an important regulator of neuronal development and neuronal function at maturity. Through its canonical transporter role, KCC2 maintains inhibitory responses mediated by γ-aminobutyric acid (GABA) type A receptors. During development, late onset of KCC2 transporter activity defines the period when depolarizing GABAergic signals promote a wealth of developmental processes. In addition to its transporter function, KCC2 directly interacts with a number of proteins to regulate dendritic spine formation, cell survival, synaptic plasticity, neuronal excitability, and other processes. Either overexpression or loss of KCC2 can lead to abnormal circuit formation, seizures, or even perinatal death. GABA has been reported to be especially important for driving migration and development of cortical interneurons (IN), and we hypothesized that properly timed onset of KCC2 expression is vital to this process. To test this hypothesis, we created a mouse with conditional knockout of KCC2 in Dlx5-lineage neurons (Dlx5 KCC2 cKO), which targets INs and other post-mitotic GABAergic neurons in the forebrain starting during embryonic development. While KCC2 was first expressed in the INs of layer 5 cortex, perinatal IN migrations and laminar localization appeared to be unaffected by the loss of KCC2. Nonetheless, the mice had early seizures, failure to thrive, and premature death in the second and third weeks of life. At this age, we found an underlying change in IN distribution, including an excess number of somatostatin neurons in layer 5 and a decrease in parvalbumin-expressing neurons in layer 2/3 and layer 6. Our research suggests that while KCC2 expression may not be entirely necessary for early IN migration, loss of KCC2 causes an imbalance in cortical interneuron subtypes, seizures, and early death. More work will be needed to define the specific cellular basis for these findings, including whether they are due to abnormal circuit formation versus the sequela of defective IN inhibition.

Keywords: KCC2, interneuron, excitatory GABA, excitatory/inhibitory balance, development, somatostatin interneuron, parvalbumin interneuron, seizure

INTRODUCTION

For over a decade, K-Cl transporter KCC2 has been in a spotlight of attention due to multiple important roles it plays in regulation of CNS development and neuronal function in adult CNS. This protein serves a number of functions, including cytoskeletal dynamics, dendrite regulation, and ion channel trafficking. However, by far the most widely published function of KCC2 is its "canonical" role to help regulate the neuronal membrane Cl^- gradient, which in turn maintains inhibitory responses to γ-aminobutyric acid (GABA). Mutations that impair KCC2 function are associated with schizophrenia, autism spectrum disorders (Merner et al., 2015), and several seizure types (Kahle et al., 2014; Saitsu et al., 2016; Saito et al., 2017) in human patients. In rodents, full KCC2 knockout animals die at birth (Hübner et al., 2001), and knockout of one of two isoforms, KCC2b, dies in the third postnatal week from seizures (Woo et al., 2002). Moreover, mutations in KCC2 that impair its ability to extrude Cl^- without otherwise affecting expression likewise result in epilepsy phenotypes (Watanabe et al., 2019).

A prominent hypothesis in the field is that KCC2 prevents seizures by maintaining inhibitory responses through GABA type A receptors (GABARs) (Huberfeld et al., 2007; Kahle et al., 2008; Silayeva et al., 2015). GABARs are pentameric ligand-gated Cl^- channels and the primary source of inhibitory neurotransmission in the adult CNS (Engin et al., 2018). Activation of GABARs inhibits neurons by hyperpolarizing the neuronal membrane due to an influx of Cl^-, which relies on a low neuronal $[Cl^-]$. KCC2 transporter activity helps maintain this low neuronal $[Cl^-]$ (Rivera et al., 1999; Zhu et al., 2005; Di Cristo et al., 2018; Akita and Fukuda, 2020; Otsu et al., 2020), though the importance of KCC2 in setting the neuronal $[Cl^-]$ has been debated in favor of alternative mechanisms, such as distribution of impermeable anionic charges (Delpire and Staley, 2014; Glykys et al., 2017). Nonetheless, KCC2 is vital in facilitating Cl^- transport to this setpoint and maintaining low internal $[Cl^-]$. Elimination of KCC2 in neurons results in higher intracellular $[Cl^-]$ and inability to rapidly extrude Cl^- upon Cl^- loading, such as during prolonged periods of activity (Di Cristo et al., 2018; Dzhala and Staley, 2021).

In the developing brain, GABA acts contrastingly to its function in adult CNS by stimulating multiple processes of neuronal development (Platel et al., 2010; Luhmann et al., 2015; Wu and Sun, 2015). Immature neurons do not strongly express KCC2, but express a Na-K-Cl transporter NKCC1, which increases internal $[Cl^-]$, often resulting in depolarizing responses that increase neuronal excitability and may elicit intracellular calcium transients (Kaila et al., 2014; Schulte et al., 2018), though whether GABAergic depolarization is always able to directly excite developing neurons *in vivo* remains a matter of debate (Kirmse et al., 2015; Valeeva et al., 2016; Murata and Colonnese, 2020; Kilb, 2021; Ben-Ari and Cherubini, 2022). This increased excitability caused by altered Cl^- homeostasis has been shown to be necessary for many of the developmental processes driven by GABA (Ge et al., 2006; Cancedda et al., 2007; Allene et al., 2008; Bortone and Polleux, 2009; Inada et al., 2011; Young et al., 2012; Griguoli and Cherubini, 2017; Fukuda, 2020; Peerboom and Wierenga, 2021).

Studies show that onset of KCC2 expression is a regulator of neuronal development (Dehorter et al., 2012; Llano et al., 2020; Peerboom and Wierenga, 2021), which is likely mediated by both transporter and transport-independent functions. For instance, the onset of KCC2 expression coincides with the transition to inhibitory GABA responses (Dehorter et al., 2012; Fukuda, 2020; Murata and Colonnese, 2020; Kilb, 2021) and is tightly coupled to precede emergence of GABAergic synaptic activity (Kobayashi et al., 2008). At the same time, this point marks the cessation of developmental programs driven by depolarizing GABA at appropriate postnatal timepoints. Independently of its transporter function, KCC2 facilitates a number of processes that are central to circuit development, such as actin re-arrangement/formation of dendritic spines and plasticity of glutamatergic synapses (Llano et al., 2020), and may be an anti-apoptotic factor regulating neuronal survival (Horn et al., 2010; Mavrovic et al., 2020; Virtanen et al., 2021).

Several groups have proposed that migration and possibly other developmental processes in cortical interneurons (INs) are terminated by KCC2 expression (Bortone and Polleux, 2009; Inamura et al., 2012; Zechel et al., 2016; Peerboom and Wierenga, 2021). Though INs comprise only ∼20% of cortical neurons, they are the only GABAergic neurons in cortex, and are critical to regulating activity of cortical circuits through a variety of mechanisms (Takada et al., 2014). This diversity of inhibitory signaling is mediated by a number of functionally distinct subtypes, such as parvalbumin (PV) and somatostatin (SST) INs, which have different birth origins (Wonders and Anderson, 2006; Lim et al., 2018) and properties at maturity (Markram et al., 2004; Kepecs and Fishell, 2014; Williams and Riedemann, 2021). Deficits in IN development and function underlie neurologic and psychiatric disorders, such as epilepsy (Bozzi et al., 2012; Righes Marafiga et al., 2021), schizophrenia, bipolar disorder, and autism spectrum disorders (Rossignol, 2011; Marin, 2012; Ruden et al., 2021).

The INs are born in subpallial ganglionic eminences and rely on GABAergic signaling to migrate through striatum to cortex, and then tangentially along cortical migratory zones before settling throughout the cortical layers. Drugs that modulate GABARs or disrupt the Cl^- electrochemical gradient interfere with IN migration (Cuzon et al., 2006; Bortone and Polleux, 2009; Inada et al., 2011). INs are vital to some forms of nascent cortical network activity, including "giant depolarizing potentials" *ex vivo* (Allene et al., 2008), which have been shown to help incorporate neurons into functional circuits in hippocampal studies (Griguoli and Cherubini, 2017). These observations compound with the aforementioned developmental studies in other neuronal types, indicating that KCC2 expression may be crucial to regulating multiple aspects of IN development, but requires further examination *in vivo*.

We hypothesized that well-timed expression of KCC2 is vital for regulating IN development. Indeed, we found KCC2 is expressed remarkably early in life in layer 5 cortical INs. To test our hypothesis, we created a conditional knockout mouse that lacks KCC2 in INs (Dlx5 KCC2 cKO). Contrary to our initial hypothesis, we found no major differences in perinatal migration or laminar localization of INs in KCC2 KO mice. Nonetheless, the mice had early seizures, failure to thrive, and premature

death similar to a full KCC2b knockout. We found that KCC2 disruption produced a layer-specific imbalance of IN subtypes. We hypothesize that together with defective synaptic inhibition, this imbalance contributes to Dlx5:KCC2 cKO pathology.

RESULTS

Cortical Interneurons Precociously Express KCC2

Like previous reports, we found that strong cortical expression of KCC2 only begins after the first postnatal week of life. Expression of KCC2 is nearly absent in perinatal cortex, and intermediate and marginal zone, being restricted mainly to a select number of cells within layer 5. To identify these cells, we used transgenic Dlx5:cre-IRES-EGFP mice, where the Dlx5 promoter drives cre and fluorescent GFP reporter expression exclusively in GABAergic neurons within forebrain. Because many INs lose Dlx5 expression with maturity (data not shown), we additionally used the Ai14 cre-inducible tdTomato reporter for permanent labeling. We collected cortical brain sections of P0 mice expressing these reporters and stained them with the KCC2 antibody. We found that at this timepoint, INs are the only cells in cortex that express KCC2, as plasmalemmal KCC2 immunoreactivity was only seen in cells with somatic expression of the tdTomato reporter (**Figure 1**).

This finding is in line with previous work suggesting that Cl^- transporters regulate even the earliest stages of IN development, including migration. We hypothesized that precocious KCC2 expression is important for development and emerging circuit function of INs. We created a conditional knockout mouse (Dlx5 KCC2 cKO) that lacks expression of KCC2 in Dlx5-lineage neurons. This was done by breeding Dlx5:cre-IRES-EGFP line with a line that has *lox*P sites surrounding exon 5 of *Slc12a5*. Expression of cre in a cell typically results in full loss of KCC2 expression (Mavrovic et al., 2020). Mice were also bred to include a cre-driven Ai14 tdTomato reporter to track Dlx5-expressing INs. In Dlx5 KCC2 cKO cortex, KCC2 immunoreactivity is completely absent at P0 (**Figure 2**), confirming that KCC2 expression in neonatal cortex is exclusive to INs. At P13 and P19, expression of KCC2 is comparable in wild-type and Dlx5 KCC2 cKO cortices, which attests to unaffected KCC2 expression in principal neurons. However, brain structures that are predominantly populated by Dlx5-lineage neurons have a profound loss of KCC2 expression at all timepoints. This includes medium spiny neurons of the striatum, neurons of reticular nucleus of the thalamus (**Figure 2A** and **Supplementary Figure 1**), and granule cells of the olfactory bulb (**Supplementary Figure 2**).

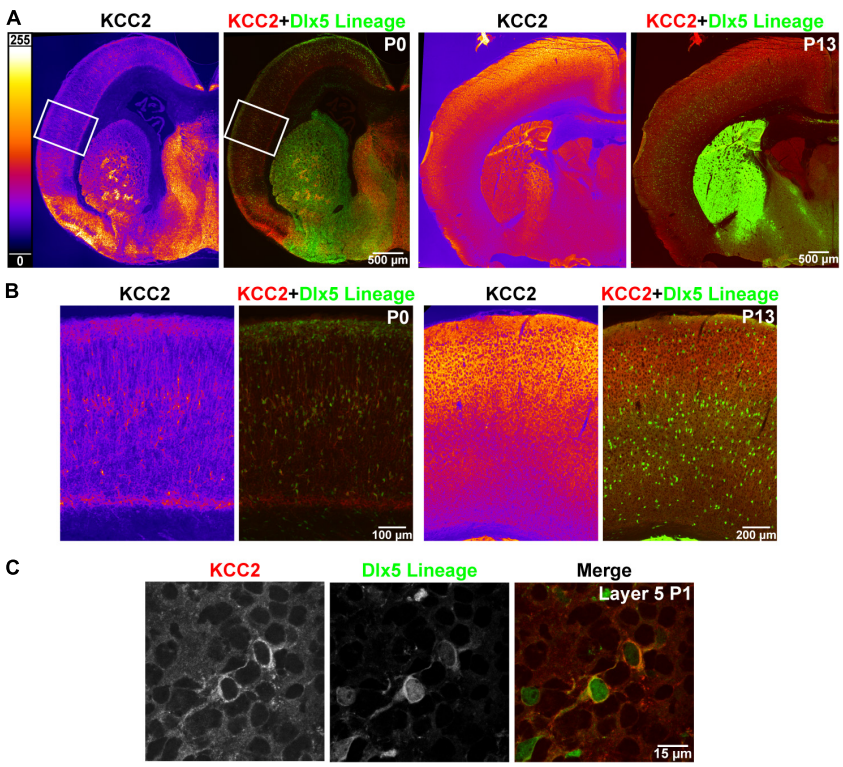

FIGURE 1 | Precocious expression of KCC2 in layer 5 INs. **(A)** KCC2 immunoreactivity in P0 and P13 WT cortex (orange heatmap images) and its overlay with Dlx5:cre tdTomato reporter, which marks cortical interneurons (KCC2 red, Dlx5 reporter green). **(B)** Magnified areas of P0 cortex indicated by a white rectangle in **(A)** and matching images of barrel field cortex at P13. **(C)** Confocal images from layer 5 showing plasmalemmal KCC2 expression in two WT cells expressing a Dlx5 GFP reporter.

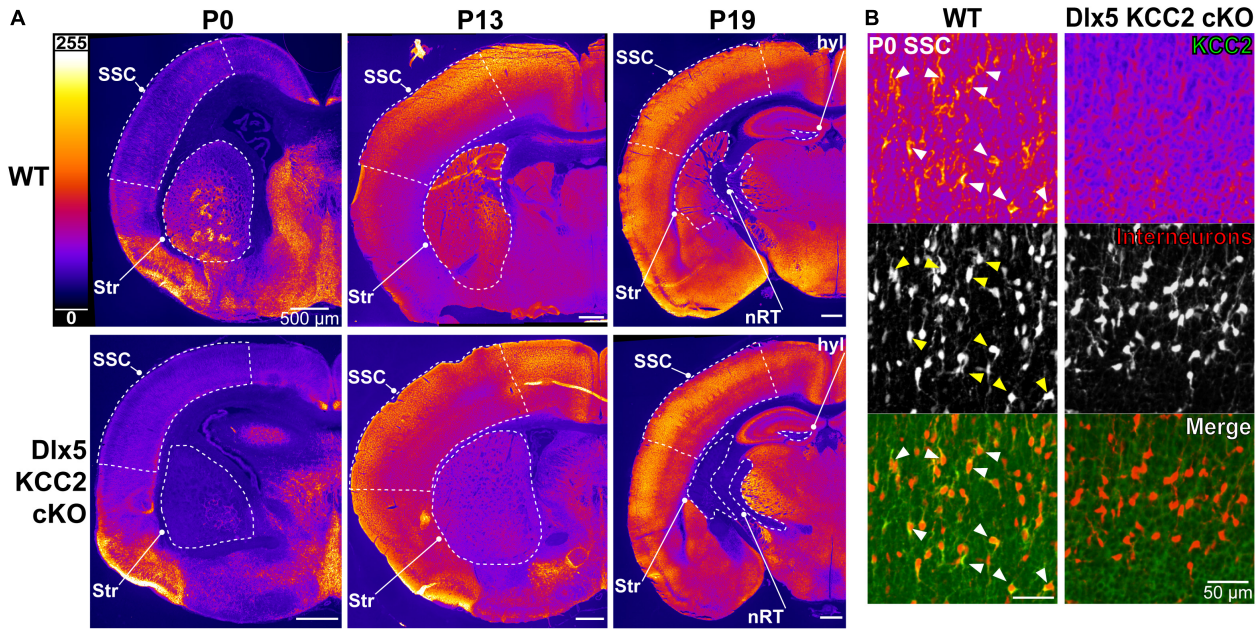

FIGURE 2 | Loss of KCC2 expression in INs of Dlx5 KCC2 cKO. **(A)** KCC2 expression in WT (top row) and Dlx5 KCC2 cKO (bottom row) cortical hemisections at P0, P13, and P19. Note lack of KCC2 immunoreactivity in somatosensory cortex (SSC) of Dlx5 KCC2 cKO at P0, but not at later ages. Loss of immunoreactivity persists in striatum (Str), hippocampal hilus (hyl), and reticular nucleus of thalamus (nRT). Regions of interest are outlined by a dashed white line. **(B)** Close-up images showing loss of plasmalemmal KCC2 immunoreactivity in INs marked by cre tdTomato reporter (KCC2 green, INs red). Arrows point out several examples of KCC2-expressing INs in WT.

Changes in Interneuron Distribution in Dlx5 KCC2 cKO Mouse

Multiple studies demonstrate that GABA provides the impetus for migration of INs in the marginal zone (Cuzon et al., 2006; Inada et al., 2011), and that the onset of KCC2 expression coincides with the timepoint when INs reach their final intracortical locations and stop migrating (Bortone and Polleux, 2009; Inada et al., 2011; Inamura et al., 2012). Therefore, we hypothesized that INs in Dlx5 KCC2 cKO mice would remain in a prolonged migratory state, producing an altered cortical distribution of INs. Migrating INs first enter the cortex laterally and then migrate in the marginal zone and intermediate zone toward more dorsomedial areas. Upon entering the cortical plate, they first populate deep cortical layers before superficial layers. Prolonged migration could then shift IN distribution to enrich areas that form later in development, such as superficial cortical layers and medial cortex.

To evaluate if this shift occurs in Dlx5 KCC2 cKO, we quantified IN distribution during the final stages of cortical migration at P0. Surprisingly, we did not find an enrichment of INs in the migratory marginal zone, nor did we observe a shift in IN distribution among cortical layers or between the medial and lateral regions of Dlx5 KCC2 cKO cortex (**Figure 3A**).

Normal Distribution of Birth-Dated Interneurons

Normal cortical development involves several different cell types, each of which may develop at different rates. While IN distribution at P0 appeared normal, we hypothesized that loss of KCC2 may disrupt the tempo of IN migration, causing INs to end migration out of phase with other circuit-forming processes in perinatal cortex. Therefore, we used a birth dating procedure, labeling newborn INs with EdU at E13.5 and determining their location at P0. Normally, some E13.5-born INs are still migrating at P0, while others have entered the cortical plate (**Figure 3B**), allowing us to test for a delayed exit from the migratory zones and for shifts in IN distribution. Somewhat surprisingly, we found no difference in the density of migrating E13.5-born INs between wild-type and KO mice (**Figure 3B**). Contrary to our hypothesis, INs in Dlx5 KCC2 cKO were distributed similarly to wild-type, both when comparing regions along the mediolateral axis and across cortical layers (**Figure 3**). For both WT and Dlx5 KCC2 cKO, there were more EdU+ INs in deeper layers of medial cortex than lateral cortex, in line with lateral-to-medial sequence of development for both principal neurons and INs (Smart, 1984), though these medial-to-lateral differences were much more subtle for INs than for all other EdU+ cells. These results indicate that despite loss of KCC2, INs could exit migratory streams in a timely manner and navigate to their typical positions.

Dlx5 KCC2 cKO Have Failure to Thrive, Seizures and Early Death

Despite appearing relatively normal at birth, the Dlx5 KCC2 cKO mice exhibited a severe failure to thrive phenotype at later ages. While Dlx5 KCC2 cKO pups are born at expected Mendelian ratios, and no pups died prenatally, Dlx5 KCC2 cKO pups had

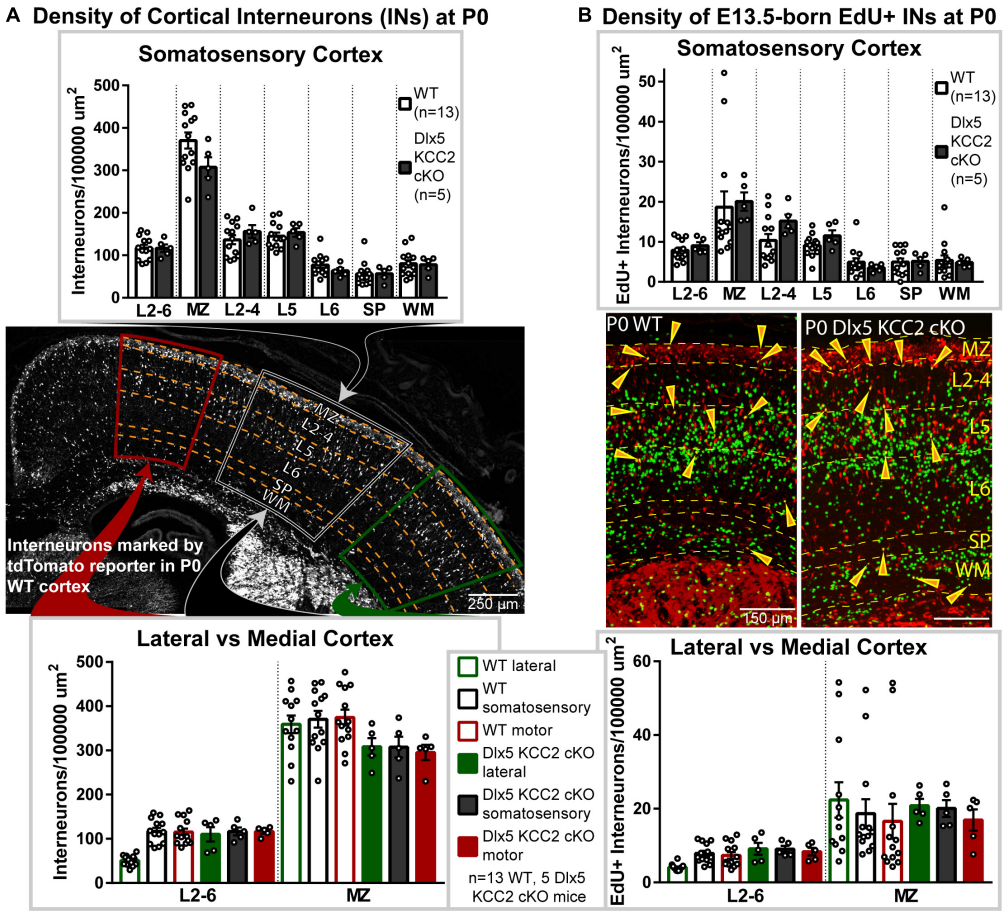

FIGURE 3 | Interneuronal loss of KCC2 does not alter perinatal IN migration. **(A)** Distribution of INs, marked by tdTomato cre reporter, in P0 Dlx5 KCC2 cKO and age-matched WT. Top graph compares cortical layers of somatosensory cortex, and bottom compares medial and lateral cortex. Center image shows exemplar distribution of INs in P0 WT cortex with labels of layers/regions used for comparison. **(B)** Distribution of E13.5-labeled EdU+ INs in P0 Dlx5 KCC2 cKO and age-matched WT. EdU was injected into G13.5 pregnant dams, and distribution of EdU+ INs (shown in center images) was compared between Dlx5 KCC2 cKO and WT in cortical layers of somatosensory cortex (top graph), and between lateral and medial cortex (bottom graph). For both **(A,B)**, no significant differences found by one-way ANOVA with Sidak's multiple comparisons. Comparisons were also made between individual layers of medial and lateral cortex with no differences found (data not shown). For **(A,B)**, *n* = 13 WT and 5 Dlx5 KCC2 cKO mice. Abbreviations: (MZ), marginal zone; (L2-4), layers 2-4; (L5), layer 5; (L6), layer 6; (layers 2-6), L2-6; (SP), subplate; (WM), white matter.

reduced body weight and body length than their littermates, were mildly hypoglycemic, had occasional spontaneous seizures, and died in the third to fourth postnatal weeks (**Figures 4A–D**). Previous work has sometimes found that genetic disruption of GABAergic signaling can produce unexpected anatomic defects, such as the cleft palate found in *Gabrb3* knockout mice (Culiat et al., 1995). Both Dlx5 and KCC2 have relatively limited areas of tissue expression, and the combination of these two makes it unlikely that our genetic model has severely disrupted KCC2 expression outside the nervous system. Nonetheless, we performed necropsy and found no obvious anatomical or histological defects in any of the major organ systems. The palatal structures form normally in Dlx5 KCC2 cKO, and Dlx5 KCC2 cKO pups can be observed feeding and display a "milk spot" of consumed milk in their stomach. Thus, we believe Dlx5 KCC2 cKO pups have no physical impediment to feeding. Therefore, we expect that failure to thrive and early death is due to a developmental or neurological condition. We did not find any gross differences in brain morphology of P17 Dlx5 KCC2 cKO mice, and vGlut2 (**Supplementary Figure 3**) immunofluorescence showed a grossly normal laminar pattern of somatosensory cortex.

Spontaneous Seizures and Induced-Seizure Susceptibility in Dlx5 KCC2 cKO Mouse

There is extensive literature on KCC2 dysfunction with epilepsy, and our mice had occasional epileptic seizures. Therefore, we decided to more formally evaluate seizure susceptibility of Dlx5 KCC2 cKO by inducing generalized tonic-clonic seizures in P4–P5 and P10 pups with flurothyl. These ages were chosen based on the fact that KCC2 expression is relatively low in non-INs at P5 and earlier, but more diffusely expressed

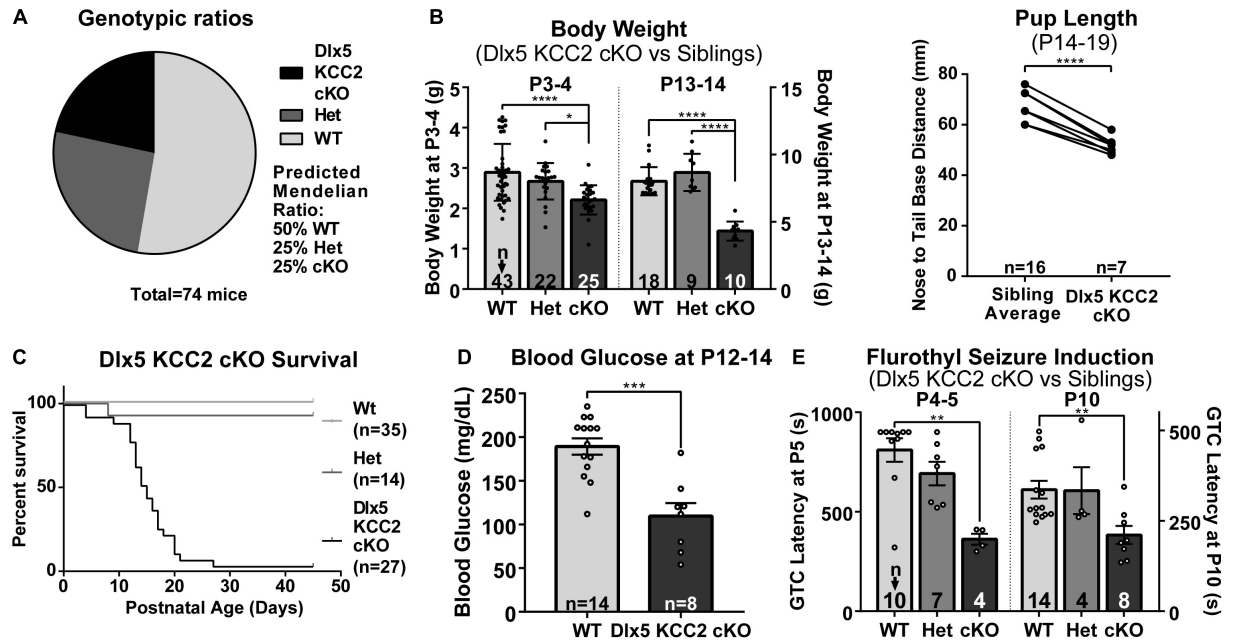

FIGURE 4 | Dlx5 KCC2 cKO mice exhibit failure to thrive and seizures. **(A–C)** Graphs showing that Dlx5 KCC2 cKO pups are born at expected 25% Mendelian ratio **(A)**, but have decreased weight and length **(B)**, and die in the postnatal period **(C)**. One-way ANOVA with Sidak's multiple comparisons: *P < 0.05, ****P < 0.0001. For body length, paired comparisons against an average of matched littermate lengths were done using a ratio paired T-test, ****P < 0.0001. **(D)** Mild hypoglycemia in Dlx5 KCC2 cKO pups. T-test: ***P < 0.001. **(E)** Susceptibility of Dlx5 KCC2 cKO pups to faster onset of flurothyl-induced generalized tonic clonic seizures (GTC) at P4–P5 and P10. Kruskal–Wallis non-parametric ANOVA: **P < 0.01. The number of mice examined is indicated by n values in each panel. For bar graphs, these are listed at the bottom of each bar.

after P10 (Takayama and Inoue, 2010). We found that from an early postnatal age, Dlx5 KCC2 cKO pups developed seizures significantly faster than their wild-type and heterozygous littermates (**Figure 4E**). Moreover, video monitoring revealed that Dlx5 KCC2 cKO pups frequently wandered out of the nest and exhibited spontaneous seizures (**Supplementary Movie 1**) much like the global KCC2b knockout mice (Woo et al., 2002). Finally, we used overnight video monitoring to help clarify the cause for early death in the Dlx5 KCC2 cKO mice. These recordings were done in the animal's home cage with their mothers and littermates. Therefore, we could not visualize the entire cage all night. Nonetheless, in 6 out of 9 monitored cases with early death, Dlx5 KCC2 cKO pups experienced a violent and prolonged seizure the night before their death (**Supplementary Movie 1**). These findings lead us to believe that loss of KCC2 in Dlx5 lineage causes mice to have seizures that disturb normal pup behavior and eventually lead to their death.

Increased Interneuron Density in Layer 5 at P12–14, but Unchanged Somatic Inhibition in Pyramidal Cells

The seizure phenotype of Dlx5 KCC2 cKO suggested a deficiency in IN function in Dlx5 KCC2 cKO pups, a potential origin of which is altered IN distribution. Despite a normal distribution of INs at P0, a shift could occur later due to altered cell-type specific survival. Therefore, we evaluated IN distribution in P12–14 barrel cortex, as early death precluded rigorous examination of later ages. At P12–14, we detected a ∼30% increase in density of layer 5 INs (**Figure 5**).

We therefore hypothesized that excess IN density in layer 5 would cause disrupted inhibition in that layer. Contrary to this hypothesis, we recorded normal frequency of sIPSCs from layer 5 pyramidal neurons (**Figure 6**), as well as normal amplitude and total charge transfer, and a slightly faster decay than WT.

Changes in Parvalbumin and Somatostatin Subtypes

By recording from layer 5 pyramidal somata, our slice physiology experiments were biased toward measuring disruption in intralaminar parvalbumin (PV)-expressing basket cell input. One reason for unaltered sIPSCs in layer 5 may be because Dlx5 KCC2 cKO affected non-PV cells. The majority of layer 5 INs express either PV or somatostatin (SST), so we evaluated whether either of these populations is selectively affected in Dlx5 KCC2 cKO. Per expectation, SST and PV immunostaining labeled non-overlapping populations, fully co-localized with our IN reporter, and each labeled about 30% of tdTomato+ INs (**Figure 7A**). Because parvalbumin expression begins at mature developmental stages, numbers of PV+ INs significantly varied between P12–14 animals due to slight differences in their age and development. Therefore, we made paired comparisons of PV+ IN densities between siblings, but a grouped comparison of SST+ INs. We found that at P12–14, SST+ INs showed a modest, but

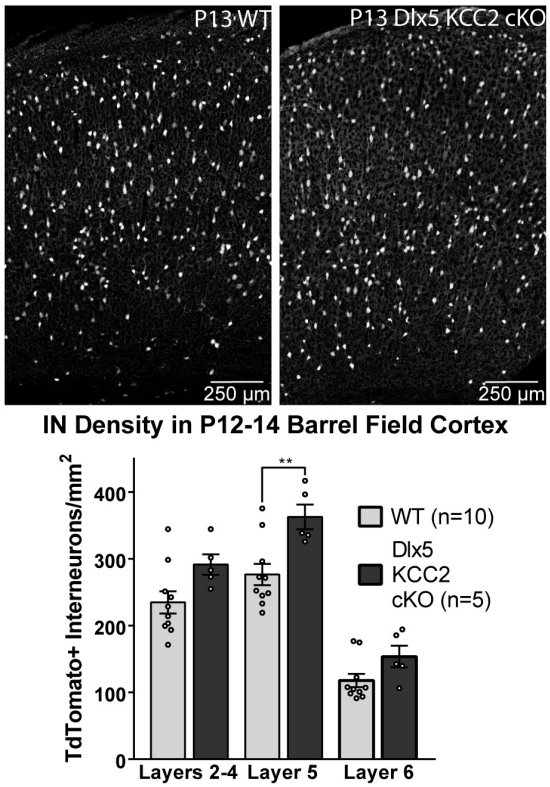

FIGURE 5 | Increase in Layer 5 INs in P12–14 Dlx5 KCC2 cKO Cortex. Bar graph shows densities of INs, labeled by cre reporter, by different layers of barrel field cortex in P12–14 WT, heterozygote, and Dlx5 KCC2 cKO. Images show examples of IN reporter expression in WT and Dlx5 KCC2 cKO cortex. One-way ANOVA with Sidak's multiple comparisons: $^{**}P < 0.01$. $n = 10$ WT, 5 Dlx5 KCC2 cKO mice.

significant density increase in L5 and were comparable to wild-type siblings in other layers of somatosensory cortex (**Figure 7B**), although this finding was not preserved in the small subset of Dlx5 KCC2 cKO that survived until P18–20 (**Supplementary Figure 4**). On the other hand, there was a significant decrease in density of PV+ INs in layers 2–4, layer 6, but not layer 5 in somatosensory cortex at P12–14 (**Figure 7C**). We therefore concluded that Dlx5 KCC2 cKO mice suffer a layer-specific PV and SST IN disruption.

However, whether the change in PV and SST INs significantly contributes to Dlx5 KCC2 cKO pathology was unclear due to potential confounding effects from other GABAergic cells affected by KCC2 loss. Thus, we next investigated whether loss of KCC2 in a more restricted population of INs would result in a similar phenotype to Dlx5 KCC2 cKO using Nkx2.1 driven cre expression to inactivate KCC2 in medial ganglionic eminence (MGE) precursors (Nkx2.1 KCC2 cKO). Nkx2.1-cre is minimally active in caudal ganglionic eminence, thus targeting fewer IN subtypes than Dlx5, being primarily limited to SST and PV INs within cortex (Xu et al., 2008). Nkx2.1 KCC2 cKO pups also died at or before weaning, indicating that relatively selective loss of KCC2 in PV and SST INs can bring about a pathology similar to Dlx5 KCC2 cKO (**Figure 7D**).

Normal Composition of GABAergic Synapses

We also wanted to assess for changes in the number and composition of inhibitory synapses in our Dlx5 KCC2 cKO mice. Depolarizing GABA is reported to guide synaptogenesis, including that of GABAergic synapses. The number or composition of GABAergic synapses could thus be altered in Dlx5 KCC2 cKO, which could underlie the seizure phenotype. For this reason, we looked for changes in density of GABAergic synapses by counting vGAT puncta, which mark presynaptic terminals, and found comparable densities in each layer of somatosensory cortex in WT and Dlx5 KCC2 cKO (**Supplementary Figure 5**). Furthermore, we found no gross differences in expression of $GABA_A$ receptor subunits (**Supplementary Figure 6**), which undergoes a dramatic shift during development and imparts significant changes to synaptic signals.

Parvalbumin KCC2 cKO Mouse Has Milder Phenotype Than Dlx5 KCC2 cKO Mouse

We hypothesized that a significant portion of Dlx5 KCC2 cKO phenotype arises from loss of KCC2 in PV INs. These INs provide somatic inhibition to local pyramidal neurons and serve as primary mediators of local feedforward and feedback inhibition, such as in the thalamocortical circuit. A change in the number or excitability of these cells would hinder feedforward and feedback inhibitory regulation of the cortical circuit, and could lead to seizures that we observe in Dlx5 KCC2 cKO. We observed a decrease in cortical PV+ cell density in the Dlx5 KCC2 cKO mouse. Moreover, a significant decrease of PV+ cells is reported in hippocampus of global KCC2b knockout (Woo et al., 2002). To distinguish the contribution of PV-driven pathology to Dlx5 KCC2 cKO mouse phenotype, we created a conditional KCC2 knockout using the parvalbumin promoter, which restricts KCC2 loss to maturing PV interneurons starting from the second postnatal week, but leaves perinatal immature PV neurons and other INs types unaffected. Unlike Dlx5 KCC2 cKO mice, the PV KCC2 cKO mice had normal pup weight and survived to adulthood, though adult weight of PV KCC2 cKO was slightly lower than wildtype littermates (**Figures 8B,C**). Moreover, the density of PV INs, labeled by the cre reporter, appeared comparable to heterozygote control (**Figure 8A**). PV KCC2 cKO mice develop flurothyl-induced seizures with the same latency as wild-type littermates (**Figure 8D**), but have a high likelihood of fatality, as 4 out of the 6 tested PV KCC2 cKO mice died shortly following the seizure. PV KCC2 cKO mice also developed an adult-onset motor phenotype, marked by reduction of muscle tone and tremor when moving limbs (**Supplementary Movie 2**). The phenotype of Dlx5 KCC2 cKO mice thus arises from early and pan-IN loss of KCC2, and is not driven solely by PV INs.

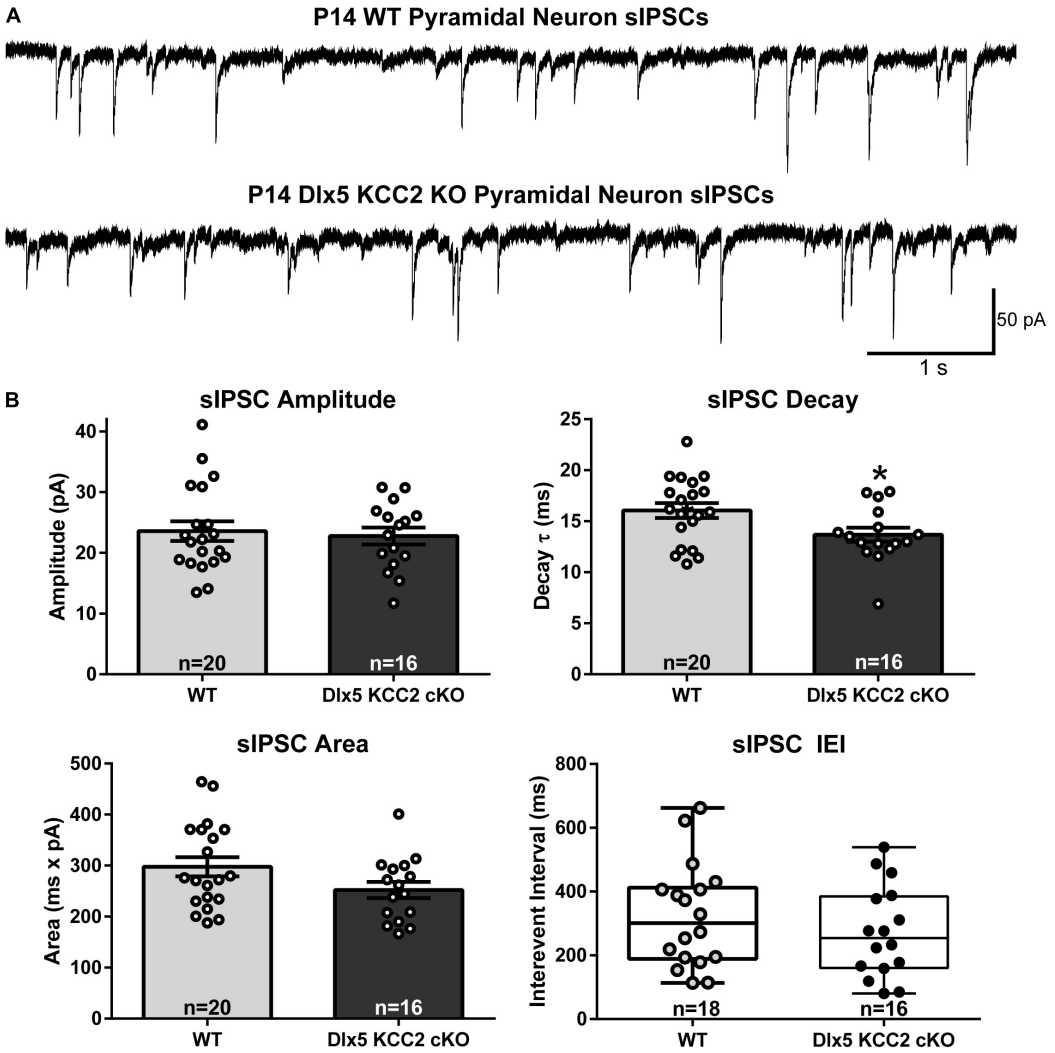

FIGURE 6 | Normal sIPSC frequency, faster decay in pyramidal neurons in KO. **(A)** Sample recordings of spontaneous IPSCs in layer 5 pyramidal neurons in barrel cortex of P12–14 WT and Dlx5 KCC2 cKO. **(B)** Amplitude, area, decay (mean ± SEM), and inter-event interval (IEI, box and whisker plot showing median, 25/75 percentile, and maximum/minimum) of spontaneous IPSCs in layer 5 pyramidal neurons in barrel cortex of P12–14 WT and Dlx5 KCC2 cKO. *T*-test: $^*P < 0.05$. Non-parametric Mann–Whitney test was used for IEI only. *n* values at the bottom of each bar/box and whisker plot indicate the number of cells recorded, taken from ≥5 mice, for each group.

DISCUSSION

KCC2 is an important regulator of neuronal development, particularly for INs, where timely expression of KCC2 has been hypothesized to stop IN migration. We demonstrated that cortical expression of KCC2 in INs begins as early as in the embryonic period, which is well-timed to terminate IN migration and subsequent early circuit formation. To investigate the role of KCC2 in development of INs, we created the conditional Dlx5 KCC2 cKO mouse that lacks KCC2 in forebrain GABAergic neurons. We showed that despite loss of KCC2 expression, INs migrated to their normal cortical destinations in the perinatal period without obvious delay. Nonetheless, the Dlx5 KCC2 cKO mice have failure to thrive and spontaneous seizures leading to early death around the third week of life. Potentially, this pathology is related to layer and subtype-specific imbalance of IN distribution, though subcortical effects of the Dlx5 KCC2 cKO, which were not the focus of this investigation, might also be a contributing factor.

KCC2 is clearly highly important to IN function. The seizure pathology and failure to thrive of Dlx5 KCC2 cKO mice is very similar to a global KCC2b knockout mouse, suggesting that much of the previously mentioned KCC2b global knockout pathology is an interneuronopathy. Though we observed a mild hypoglycemia in Dlx5 KCC2 cKO, blood glucose levels of Dlx5 KCC2 cKO remained higher than those reported to cause seizures (Schauwecker, 2012). This is in line with observations in KCC2b global knockout, which has a malnutrition phenotype, but rescuing this phenotype with supplemental feeding does not prevent seizures nor death, though it does temporarily rescue

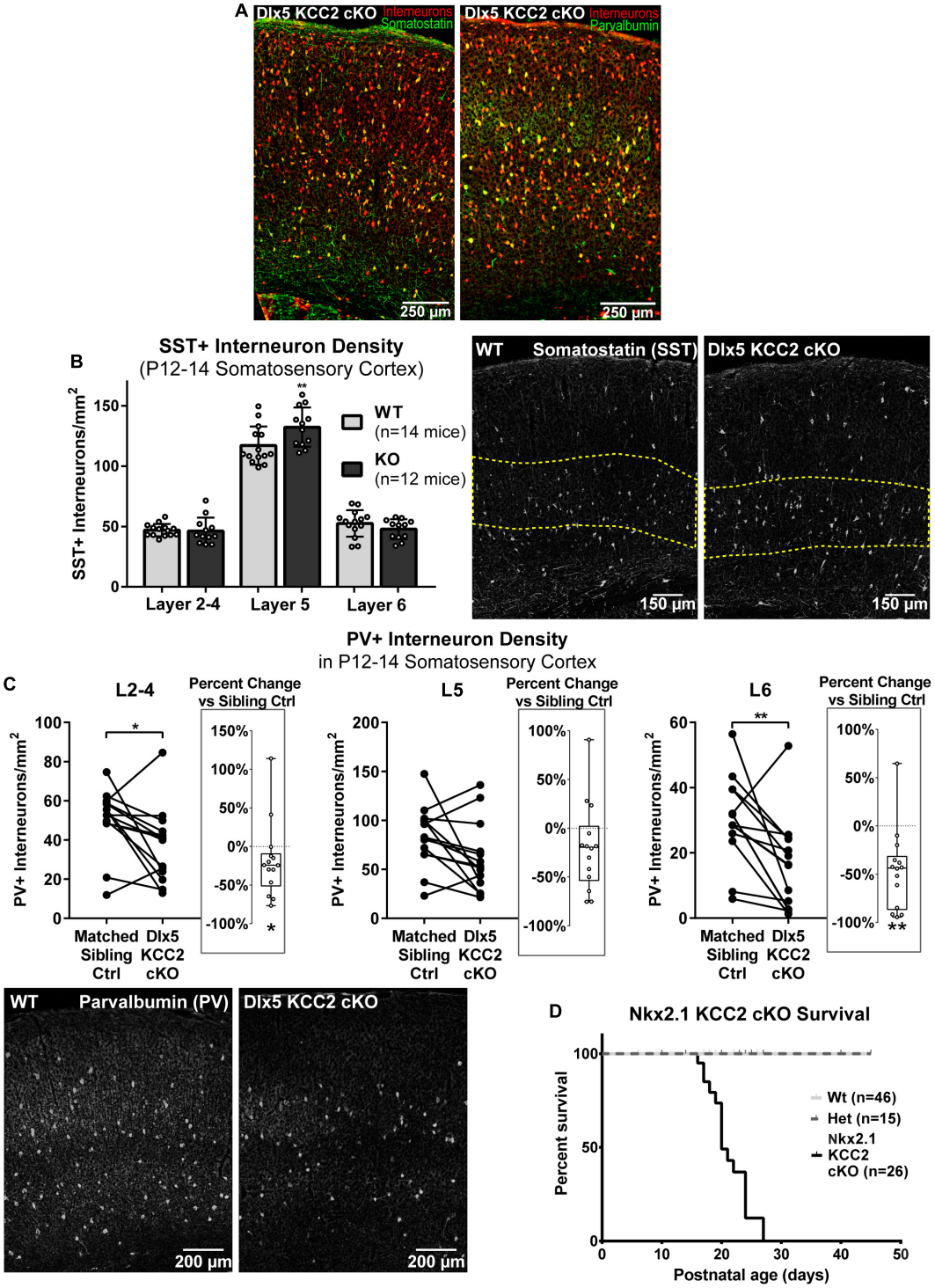

FIGURE 7 | Altered distribution of somatostatin and parvalbumin INs in maturing cortex of Dlx5 KCC2 cKO. **(A)** Images showing complete co-localization of SST (left, green) and PV (right, green) immunopositive neurons with Ai14 cre reporter used to label INs (red) in P13 barrel field cortex. **(B)** Average density with SEM of SST+ cells in different layers of P12–14 somatosensory cortex with exemplary images of SST immunolabeling. Yellow dashed line demarcates layer 5. n = 14 WT, 12 Dlx5 KCC2 cKO mice. One-way ANOVA with Sidak's multiple comparisons: $^{**}P < 0.01$. **(C)** Paired comparisons of density of PV+ cells in layers 2–4 (L2–4), 5 (L5), and 6 (L6) in P12–14 somatosensory cortex of Dlx5 KCC2 cKO and control littermates, with exemplary images of PV immunolabeling. Box and whisker plots in each graph plot percent difference change in each littermate pair, n = 12 littermate mouse pairs. Wilcoxon matched-pairs signed rank test, $^{**}P < 0.01$, $^{*}P < 0.05$. **(D)** Survival plot of Nkx2.1 KCC2 knockout, conditional only to PV and SST INs. n = 46 WT, 15 heterozygote, 26 Nkx2.1 KCC2 knockout mice.

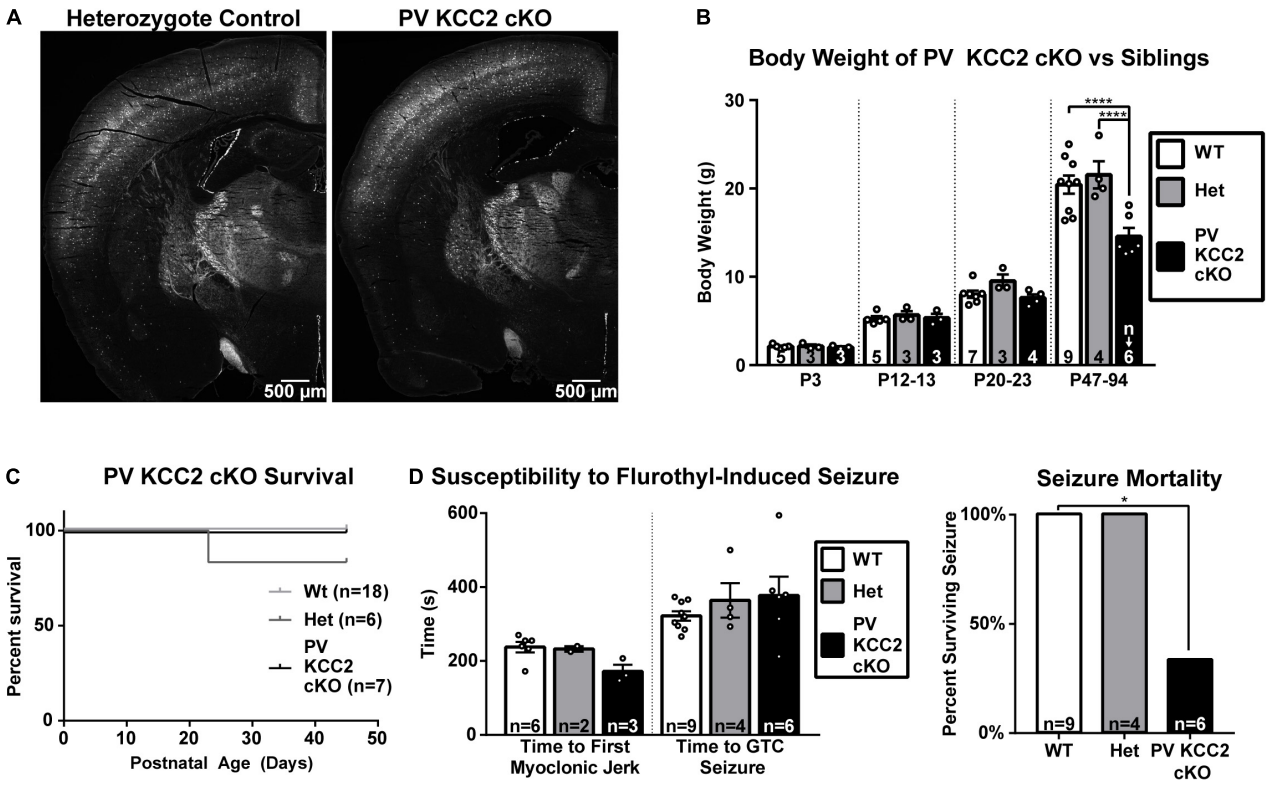

FIGURE 8 | Selective loss of KCC2 in parvalbumin neurons does not cause seizure susceptibility nor failure to thrive. **(A)** PV INs labeled by Ai14 cre reporter in hemisections of P64 PV KCC2 cKO and sibling control. **(B)** Body weight of PV KCC2 cKO. One-way ANOVA with Sidak's multiple comparisons: $^{****}P < 0.0001$. Note normal PV KCC2 cKO body weight until adulthood, when it is slightly diminished. **(C)** Postnatal survival is unaffected in PV KCC2 cKO. **(D)** Seizure susceptibility (right) measured by time to first myoclonic jerk and generalized tonic clonic seizure (left) and seizure mortality (right) resulting from flurothyl seizure induction in PV KCC2 cKO mice. Note that PV KCC2 cKO do not exhibit faster onset of induced seizures, but are highly likely to die from them. Chi squared with Yates' correction: $^{*}P < 0.05$. The number of mice examined is indicated by *n* values in each panel. For bar graphs, these are listed at the bottom of each bar.

weight loss. Therefore, we believe seizures in both mice originate from malfunctioning INs.

At the outset of this study, we hypothesized the transporter function of KCC2 to be a regulator of IN development. Early GABA signaling promotes many aspects of neuronal development, and changes in that system can lead to abnormal circuit formation. Developmental processes like neurite arborization (Chattopadhyaya et al., 2007) and IN migration (Cuzon et al., 2006; Inada et al., 2011) are excessive if GABA levels or signaling are increased. Conversely, migration is stalled and morphological development is stunted when GABA is diminished by drugs, reduction in GABA synthesis (Cuzon et al., 2006; Inada et al., 2011), or made prematurely hyperpolarizing by KCC2 expression (Cancedda et al., 2007; Bortone and Polleux, 2009). Moreover, intrinsic mechanisms regulating transporter activity, such as KCC2 expression and post-translational modifications (Fukuda and Watanabe, 2019), allow neurons to interpret a similar developmental environment in a manner appropriate to each neuron's stage of maturity. For instance, individual maturing INs leave a migratory zone while other INs, surrounded by the same cues, continue migrating. For these reasons, the onset of endogenous KCC2 expression was thought to carry out an important regulatory role by defining a cell-autonomous temporal window for developmental processes, especially termination of IN migration. Contrary to this hypothesis, our experiments demonstrate that IN migration occurs normally when KCC2 is deleted. We conclude that the onset of KCC2 expression is not the sole determinant of the exit from migration, and other compensatory mechanisms must be in place to transition INs to a mature, post-migratory state. However, our observations are limited by the timepoints that we chose for our experiments. It is possible that KCC2 loss causes transient migratory defects or movement speed, but not location of migratory INs on a population level. These changes would best be detected by more thorough means: time-lapse imaging of migratory INs or measurements of cortical IN distribution throughout many timepoints.

It is striking that deleterious effects of KCC2 loss impact Dlx5 KCC2 cKO mice at an early age, with small weight and seizure susceptibility detectable as early as P4–P5, when KCC2 expression in cortex is low (Takayama and Inoue, 2010) and generally restricted to INs. At this age, *in vitro* studies report that GABA is depolarizing to pyramidal neurons (Rheims et al., 2008), and that giant depolarizing potentials (GDPs) that are driven by GABA help incorporate deep layer neurons into functional circuits (Allene et al., 2008; Griguoli and Cherubini, 2017).

One might speculate that seizure susceptibility at P4–P5 could indicate increased IN activity and increased GDP output, as well as globally increased activity. However, by P10–P14, pyramidal neurons express KCC2, and GABA-driven GDPs have largely disappeared. The fact that we still see seizure susceptibility at this age suggests that IN-specific knockout may cause a change in network formation that persists even after GABA becomes mostly inhibitory in the brain. At the same time, we cannot rule out the possibility that hyperexcitable interneurons, independent of any developmental effects, are the source of seizures and early death in our Dlx5 KCC2 cKO mice. This might be answered using an inducible, interneuron-specific promoter to knockout KCC2 later in life. However, this is beyond the scope of the current paper.

While our initial hypotheses were based on the literature showing that KCC2 and depolarizing GABA regulate IN development, it is important to note that the KCC2 function is not limited to Cl^- transport. A rapidly growing body of literature suggests that KCC2 may also regulate neuronal development and function through a number of protein-protein interactions. The most well-studied is regulation of dendritic spine formation and long-term synaptic plasticity through direct protein/protein interactions with β-pix and/or the cytoskeletal protein 4.1N (Li et al., 2007; Llano et al., 2015, 2020), and regulation of AMPA receptor trafficking through transport-independent cofilin phosphorylation (Gauvain et al., 2011; Chevy et al., 2015). Furthermore, KCC2 expression is associated with apoptosis. Premature overexpression of KCC2 disrupted brain development through a transport-independent interaction with the cytoskeleton-associated protein 4.1N (Horn et al., 2010), while loss of KCC2 leads to excessive perinatal apoptosis (Mavrovic et al., 2020), and KCC2 overexpression and pharmacological block lead to apoptosis in mature neurons (Kontou et al., 2021). Studies of protein/protein interactions and work using transporter-deficient KCC2 mutants have revealed a previously unsuspected array of activity through interactions through membrane and cytoskeletal proteins (Llano et al., 2020), such as kainate receptors (Mahadevan et al., 2014), β-Pix (Llano et al., 2015), KCNK9 channels (Goutierre et al., 2019), gephyrin (Al Awabdh et al., 2021), $GABA_B$ receptors (Wright et al., 2017), and Neto2 (Ivakine et al., 2013). Some of these interactions have effects independent of GABAergic signaling, such as increasing neuronal excitability through downregulating KCNK9 expression (Goutierre et al., 2019). Other interactions currently appear to be mechanisms for regulating transporter activity of KCC2 (Ivakine et al., 2013; Mahadevan et al., 2014), but likely have additional effects. This field is still in its infancy, and much of this work has targeted exclusively glutamatergic neurons. Therefore, the extent to which these interactions regulate IN development and function is yet to be determined.

A question still remains of whether synapses or neurite arbors of INs developed differently in Dlx5 KCC2 cKO. INs do not form significant dendritic spines and are less likely to rely on some of the scaffolding roles of KCC2. Therefore, we did not investigate glutamatergic synapses of INs. However, KCC2 may still be involved in formation and plasticity of glutamatergic synapses in INs, which a follow-up study might investigate. On the other hand, GABA has been shown to promote neurite arborization and synaptogenesis of GABAergic synapses in multiple neuronal types (Gascon et al., 2006; Ge et al., 2006; Bouzigues et al., 2007; Cancedda et al., 2007; Chattopadhyaya et al., 2007; Oh et al., 2016; Brady et al., 2018) and recently, an interaction between KCC2 and GABAergic synapse scaffolding protein gephyrin has been demonstrated (Al Awabdh et al., 2021). Nonetheless, we found unremarkable expression of synaptic proteins and sIPSCs in layer 5 pyramidal neurons, suggesting normal development of GABAergic synapses in Dlx5 KCC2 cKO cortex. Possibly, KCC2 does not affect synaptic development of INs, despite the circumstances that suggest involvement. For example, synaptogenesis of glutamatergic and GABAergic synapses within the lateral superior olive is not affected by loss of KCC2, despite coincident onset of KCC2 expression and critical window of synapse formation (Lee et al., 2016). However, it may also be true that more subtle changes in synapse formation occur, since our analysis can only detect gross changes in GABAergic synapses. To thoroughly investigate effects of KCC2 loss on IN synaptogenesis/neurite formation, a follow-up study is needed, focusing on the morphology of neuronal arbors as well as the density, localization, and composition of inhibitory synapses. Moreover, since INs are morphologically diverse, the study must selectively analyze IN subtypes and cortical layer locations.

While IN migration was unaffected, loss of KCC2 increased IN density in layer 5 at 2 weeks of age. Considering normal IN migration and perinatal IN counts, this was presumably due to increased cell survival. If this effect is mediated by a prolonged period depolarizing GABA, it contrasts with previous studies. Only exceptionally strong alterations in GABAergic excitation were shown to affect cell survival (Represa and Ben-Ari, 2005), primarily causing decreased neuron numbers. For example, application of a high concentration of GABAergic agonist muscimol caused death of GABAergic neurons in 3D cultures (Honegger et al., 1998); in contrast, embryonic application of GABAergic antagonist also caused loss of PV INs (Luk and Sadikot, 2001). Increased survival could be mediated by increased expression of neurotrophins (Ceni et al., 2014), such as BDNF, in response to GABAergic depolarization (Obrietan et al., 2002; Fukuchi et al., 2014; Brady et al., 2018). However, while limited studies show that neurotrophins are produced by INs (Biane et al., 2014; Barreda Tomás et al., 2020) and regulate certain aspects of IN development/plasticity (Jones et al., 1994; Polleux et al., 2002; Jin et al., 2003; Patz et al., 2004), their role in IN survival is not known. Independently of transport function of KCC2, both overexpression and loss of KCC2 have also been reported to promote apoptosis during development (Horn et al., 2010; Mavrovic et al., 2020). Somewhat more consistent with our findings, recent work in hippocampal pyramidal cells showed that KCC2 loss promotes apoptosis after 18 days *in vitro*, but not at 3 days, which is a more relevant timeframe for most of our work (Kontou et al., 2021). Interestingly, despite an increase in layer 5 INs, we did not observe a change in inhibitory synaptic input received by pyramidal neurons. It is possible that while IN numbers changed, the number of synapses remained constant through compensation. Alternatively, our recordings were done at room temperature and may have missed changes seen at more physiologically relevant temperatures, though there is no

a priori reason to think this is the case. Recordings from WT and KO tissue were done at the same temperatures, and the scant literature regarding temperature dependence of KCC2 shows that it is likely insensitive (Woodin et al., 2003) or suppressed at higher temperatures (Hartmann and Nothwang, 2011). An equally plausible explanation is that whole cell recordings reflect perisomatic input, which is chiefly provided by PV INs, which were present at normal density in layer 5 of Dlx5 KCC2 cKO. Therefore, while SST INs were increased in layer 5, they may have not influenced whole cell recordings due to their typical projection to distal dendrites.

Additionally, outside of layer 5, we found that loss of KCC2 caused a pronounced loss of PV+ INs, similar to what has been reported in the global KCC2b knockout (Woo et al., 2002). Impaired development or dysfunction of PV INs have also been associated with epilepsy (Jiang et al., 2016). PV INs regulate cortical excitation and oscillatory activity, and in pathologic conditions, seizure initiation and spreading often depends on PV IN activity (Jiang et al., 2016; Anstotz et al., 2021), where PV INs can either promote seizures by synchronizing circuit firing or prevent seizure spreading through inhibition. Given the loss of PV+ INs both in Dlx5 KCC2 cKO and global KCC2b knockout, we hypothesize PV IN dysfunction may play an important role in the observed phenotypes. However, it is unclear whether the loss of PV+ INs reflects neuronal death, thereby decreasing cortical inhibition, or simply lost parvalbumin protein expression. Though the mechanism is not known, reduced parvalbumin expression is associated with a number of psychiatric disorders (ASD, schizophrenia) (Filice et al., 2020; Ruden et al., 2021) and can cause increased network synchronization/enhanced PV IN output by enhancing facilitation and shortening delayed transmitter release in INs that are deficient in PV expression (Collin et al., 2005; Muller et al., 2007; Manseau et al., 2010; Orduz et al., 2013).

It is possible the seizures and early death in our mice arise from pan-interneuronal dysfunction due to the loss of KCC2. We tested whether cell-restricted loss of KCC2 in mature PV INs was sufficient to cause a significant pathology similar to IN-wide KCC2 loss by using a mouse with PV-specific conditional KCC2 knockout. Since PV gene expression in cortex is absent before the second postnatal week (Alcántara et al., 1993; del Rio et al., 1994), the PV KCC2 cKO animals have normal KCC2 expression during development, but loss of KCC2 in mature PV neurons. The PV KCC2 cKO mouse did not have the seizure susceptibility, failure to thrive pathology, nor prominent PV IN loss. Therefore, the seizures and premature death we observe in Dlx5 KCC2 cKO after P10 does not solely arise from hyperexcitability in mature PV INs. This could suggest that PV neurons do not play a role in the phenotype of our Dlx5 KCC2 cKO mice. However, another possibility is that the effects of KCC2-knockout are specific to the perinatal period. Interneuron dysfunction in the early postnatal period may produce developmentally-specific derangement of circuit formation and function through a variety of mechanisms, including early network oscillation/GDP synchronization and activity-dependent growth factor release (Jin et al., 2003; Patz et al., 2004; Biane et al., 2014; Brady et al., 2018). This interpretation is also supported by seizure susceptibility of Dlx5 KCC2 cKO mice at P4–5. Development of IN subtypes is tightly interdependent through complex and nuanced mechanisms (Duan et al., 2020). For instance, SST INs play a vital role in orchestrating the establishment of PV-neuron feed-forward inhibition in perinatal thalamocortical circuits (Tuncdemir et al., 2016). Moreover, MGE-derived interneurons form spatially segregated neuronal assemblies with excitatory neurons, before large scale circuits become established. Loss of this GABAergic input disrupts normal apoptosis, leading to excess survival of SST and PV INs (Duan et al., 2020). In Dlx5 KCC2 cKO, changes in inhibition and synchrony due to hyperexcitability of INs in Dlx5 KCC2 cKO could likewise lead to changes in SST and PV IN densities.

To conclude, we found that KCC2 is vital for IN development and function, but despite models in the field, is not the primary cue for terminating IN migration. Deficits in IN distribution specific to cortical layers and IN subtype-specific deficits in IN distribution likely underlie the seizures suffered by Dlx5 KCC2 cKO, but further studies targeting physiology and structure of INs, as well as temporally restricting KCC2 loss, would uncover the full breadth of developmental and physiological deficits contributing to this phenotype.

MATERIALS AND METHODS

Animal Husbandry

The Tg(mI56i-cre-EGFP)1Kc (Dlx5/6-Cre-IRES-EGFP) (Stenman et al., 2003), Tg(Nkx2-1-cre)2S and (Nkx2.1-cre), Pvalb$^{TM1(cre)Arbr}$ (PV-cre), and Gt(ROSA)26Sor$^{TM14(CAG-tdTomato)Hze}$ (Ai14) (Madisen et al., 2010) mice were acquired from Jackson laboratories (Stock #007914, 008661, 008069, and 023724, respectively). The KCC2 flox mouse was created and contributed by Dr. Eric Delpire. In this mouse, *lox*P sites flank exon 5 of *Slc12a5*, and expression of cre in a cell results in excision of exon 5, premature stop codon, and complete KCC2 knockout (Mavrovic et al., 2020). PV-cre, Nkx2.1-cre, and Ai14 were maintained in C57/Bl6 background, while Dlx5/6-cre-IRES-EGFP and KCC2 flox were in FVB background, resulting in mixed B6/FVB mice for majority of Dlx5 KCC2 cKO experiments.

Weight and Length Measurement

Body weight was measured by placing a pup into a plastic beaker or large weight boat on a scale. Body length was measured by anesthetizing pups with isoflurane, and suspending them vertically by the tail. Nose tip to tail base length was measured against a ruler. Pups that were anesthetized for body length measurement were not used in subsequent studies.

Genotyping, PCR and Primers

Genomic DNA extraction and PCR were performed on mouse biopsy tissue (tail or toe if P0–P7, ear lobe if P12+) using Sigma REDExtract-N-Amp Tissue PCR kit Catalog#: XNAT-100RXN (Sigma, St. Louis, MO, United States). Target bands were distinguished by electrophoresis on a 2% agarose gel stained with

SYBR Safe DNA gel stain from Invitrogen Cat# P/N S33102 and visualized using Bio-Rad Gel Doc EZ.

For genotyping our Ai14-tdTomato mice, we used the following primers: WT forward 5′-AAGGGAGCTGCAGT GGAGTA-3′; WT reverse 5′-CCGAAAATCTGTGGGAAGTC-3′; Ai14 forward 5′-CTGTTCCTGTACGGCATGG-3′; Ai14 reverse 5′-GGCATTAAAGCAGCGTATCC-3′. The reaction conditions were 94°C for 5 min, (94°C for 15 s, 65°C for 1 min, 72°C for 30 s) × 36 cycles, 72°C for 2 min. Product bands were 297 bp WT, 196 bp Ai14 positive.

For genotyping our floxed KCC2 mice, we used the following primers: forward 5′-TTACACAAGTACTGCCGGTCCATTG-3′; reverse 5′-GCCTCAAGGCTATGTGTAAAGACTCA-3′. The reaction conditions were 94°C for 5 min, (92°C for 30 s, 62°C for 30 s, 72°C for 30 s) × 40 cycles. Product bands were 230 bp WT, 282 bp KCC2 floxed.

For genotyping our Dlx5:Cre-IRES-EGFP and PV-cre mice, we used the following primers targeting the Cre sequence forward 5′-GCATTACCGGTCGATGCAACGAGTGATGAG-3′; reverse 5′-GAGTGAACGAACCTGGTCGAAATCAGTGCG-3′. The reaction conditions were 94°C for 3 min, (94°C for 30 s, 68°C for 30 s, 72°C for 1 min) × 36 cycles. Product band was 408 bp.

Blood Glucose Measurement

Blood glucose was measured with OneTouch glucometer as per manufacturer instruction using blood from the right atrium taken during non-survival tissue collection.

Pathology Core Work-Up

Histological analysis was performed by Vanderbilt Pathology Core. Four male P17 mice (2 Dlx5 KCC2 cKO, 2 WT siblings) were analyzed grossly, histologically, and by complete blood count. Mice were euthanized with carbon dioxide. Blood was collected via intracardiac puncture and placed in an EDTA tube. Complete blood count was performed on the Forcyte Hematology Analyzer (Oxford Science, Oxford, CT United States). Gross necropsy was performed, and a complete set of tissues were collected and submerged in 10% neutral buffered formalin for 48 h fixation. Tissues were processed routinely, embedded in paraffin, sectioned at 5 microns and stained with hematoxylin and eosin. Additionally, sections of the brain were stained with Fluro-Jade.

Tissue Collection and Preparation

Tissue for immunohistochemistry and fluorophore imaging was collected and fixed either by brief or heavy fixation. For brief fixation, mice were anesthetized, and brains were dissected and immersed in 4% paraformaldehyde (PFA) for 15 min. For heavy fixation, mice were anesthetized, transcardially perfused with PBS, then 4% PFA. The brains were then dissected and immersed in 4% PFA overnight at 4°C. After brief or heavy fixation, brains were washed in PBS, transferred to 30% sucrose solution for a week at 4°C for cryoprotection, blocked, immersed in OCT compound, and flash-frozen in liquid nitrogen. Coronal sections containing barrel cortex were sectioned at 20 μm on a Leica cryostat and stored at −80°C.

Immunohistochemistry

For most applications, we used briefly fixed tissue, but heavily fixed tissue was used for parvalbumin and sometimes somatostatin staining with inclusion of comparable controls. The slides were dried for 30 min, then incubated in 4% PFA for 5 min. For heavily fixed tissue only, there were then two PBS washes, and unmasking for 30 min in 50 mM Na-Citrate at 80°C. Both briefly and heavily fixed tissue was then washed (PBS + 0.1% Triton X-100), blocked overnight at 4°C in blocking solution (PBS + 0.5% Triton X-100 + 8% horse serum), washed, incubated overnight at 4°C in primary antibody (**Table 1**) in blocking solution, washed, incubated overnight at 4°C in secondary antibody (**Table 2**) in blocking solution, washed, dried, and mounted/coverslipped in hard-setting Vectashield or Prolong Gold mounting medium with DAPI. Sections were allowed to cure for at least 30 min, then stored at 4°C and imaged within 2 weeks. When visualizing fluorophores without immunohistochemistry, sections were thawed and mounted/coverslipped.

EdU-Labeling Interneurons

Pregnant mouse dams were injected at E13.5 with 1 mg EdU/10 g body weight, delivered as 10 mg/mL solution of 5-Ethynyl-2′-deoxyuridine (EdU, from Carbosynth) in 0.9% sodium chloride saline. Brain tissue was collected from P0 pups by anesthetizing pups, decapitation, 30 min immersion of the head in 4% PFA, and further processing/cryosectioning as outlined earlier in the protocol. To label EdU, slide-mounted sections were rinsed in PBS thrice (rinsed), permeabilized in PBS + 0.5% Triton X-100, rinsed, incubated for 5 min in CLICK reaction cocktail [4 mM $CuSO_4$ pentahydrate, 5 μM Sulfo-Cyanine 5 Azide (Lumiprobe #A3330), 100 mM sodium ascorbate in Tris-buffered saline], rinsed, dried for 30 min, and mounted/coverslipped using Prolong Gold with DAPI.

TABLE 1 | List of primary antibodies used.

Target	Host	Vendor name	Catalog #	Dilution	Type
KCC2	Rb	EMD-Millipore/Upstate	07-432	1:250	IgG
Parvalbumin	Ms	Sigma	P3088	1:250	IgG
Somatostatin	Rb	Santa Cruz	Sc-13099	1:250	IgG
vGAT	Gp	SYSY	131-004	1:250	IgG
vGlut2	Ms	Neuromab/UC Davis	75-067	1:500	IgG
Gephyrin	Ms	SYSY	147021	1:250	IgG_{1K}
α1 GABA-A receptor	Rb	Millipore	06-868	1:500	IgG
α2 GABA-A receptor	Rb	Abcam	ab72445	1:250	IgG
α3 GABA-A receptor	Rb	Alomone	AGA-003	1:500	IgG
α4 GABA-A receptor	Rb	Novus	NB300-194	1:500	IgG
α5 GABA-A receptor	Rb	Millipore	AB9678	1:250	IgG
β2 GABA-A receptor	Rb	Millipore	AB5561	1:250	IgG
β3 GABA-A receptor	Rb	Novus	NB300-199	1:250	IgG
δ GABA-A receptor	Rb	R&D Systems	PPS090	1:250	IgG
γ2 GABA-A receptor	Rb	Synaptic Systems	224-003	1:250	IgG

Host species abbreviations are: Rb, rabbit; Ms, mouse; Gp, Guinea Pig.

TABLE 2 | List of secondary antibodies used.

Target	Fluorophore	Host	Vendor name	Catalog #	Dilution
Anti-Rabbit IgG (H + L)	Cy3	Donkey	Jackson ImmunoResearch	711-165-152	1:250-1000
Anti-Rabbit IgG (H + L) anti-Mouse	Cy5	Donkey	Jackson ImmunoResearch	711-165-152	1:100-500
Anti-Mouse IgG (H + L)	Cy3	Donkey	Jackson ImmunoResearch	715-165-150	1:250-500
Anti-Mouse (H + L)	Alexa-647	Donkey	Jackson ImmunoResearch	715-605-150	1:250
Anti-Mouse (H + L)	Cy5	Donkey	Jackson ImmunoResearch	715-605-150	1:100-250
Anti-Guinea Pig IgG (H + L)	Alexa-488	Donkey	Jackson ImmunoResearch	706-545-148	1:100-250
Anti-Guinea Pig IgG (H + L)	Cy3	Donkey	Jackson ImmunoResearch	706-165-148	1:100-250

Image Acquisition and Analysis

Brain sections were imaged using a Leica DM 6000 epifluorescent microscope equipped with a DFC365 FX digital camera and a computer running Leica LAS X software (Leica, Buffalo Grove, IL, United States). Images were acquired using 5 and 10× objectives. Images were stitched using Fiji ImageJ software stitching plugin (Preibisch et al., 2009): stitching-grid/collection stitching, 30% overlap, maximum intensity fusion method with subpixel accuracy. The resulting fused images were saved as 8-bit tagged image files (TIFs). Confocal images were taken using a Leica TCS SPE/DM2500 microscope with 63× oil immersion objective and a computer running Leica LAS software.

Image analysis and editing was done using Fiji ImageJ. For immunohistochemistry images that compare expression intensity, images were acquired with similar settings and minimally edited. For KCC2/reporter co-localization, projections from confocal image stacks were made using Fiji ImageJ. Brain regions were identified using Paxinos (2007) and Schambra and Schambra (2008). When needed, marginal zone and subplate were further identified using Bayer and Altman (1990) and Qu et al. (2016). Cortical layers were defined using DAPI staining of our tissue. For separate analysis, these regions were segregated into regions of interest (ROIs). EdU+, TdTomato+ cells, PV+ cells, and SST+ cells were counted manually using the cell counter plugin. Counts of TdTomato+ cells and VGAT+ particles were done by manually setting a threshold for each image that distinguished cells/particles from background, and then automatically counting particles with the "analyze particles" feature. These automatic IN counts were compared to be consistent with manual counts. Density was calculated as number of cells/particles divided by ROI area.

Electrophysiology

P12–P14 mice were anesthetized and transcardially perfused with cold, oxygenated cutting solution, consisting of: 200 mM sucrose, 1.9 mM KCl, 1.2 mM NaH_2PO_4, 6 mM $MgCl_2$, 0.5 mM $CaCl_2$, 10 mM glucose, 25 mM $NaHCO_3$ (305 mOsm, pH 7.4). Mice were then decapitated, their brains were dissected, blocked, and coronal slices were sectioned at 300 μm on a Leica VT1200S vibratome in cold, oxygenated cutting solution. Slices were then recovered for 30 min at 34°C and 1 hr at room temperature (20–21°C) in aCSF, consisting of: 125 mM NaCl, 2.5 mM KCl, 1.25 mM NaH_2PO_4, 1.3 mM $MgCl_2$, 0.2 mM $CaCl_2$, 10 mM glucose, 25 mM $NaHCO_3$ (305 mOsm, pH 7.4). Recordings were performed in a chamber perfused with 20–21°C oxygenated aCSF, perfused at a rate of 2.0 mL/min. Pyramidal neurons of layer 5 of barrel field cortex was targeted based on anatomical location, visible barrels, and cellular morphology. Neurons were patched with 3–5 MΩ glass electrodes filled with internal solution containing: 150 mM CsCl, 1 mM $MgCl_2$, 10 mM HEPES, 0.1 mM $CaCl_2$, 1.1 mM EGTA, and 2 mM Na_2ATP (285 mOsm, pH 7.4) and clamped at −70 mV. Whole-cell recordings were acquired using an Axon MultiClamp 700B amplifier, filtered at 2 kHz, digitized at 10 kHz with Digidata 1440A, and recorded with ClampeX 10.4 software. sIPSCs were recorded with 10 μM NBQX and 50 μM APV in aCSF and analyzed with miniAnalysis software with event threshold set at 15 pA. Series resistance (R_a) was uncorrected, and recordings were discarded if R_a was over 25 MΩ or changed by more than 15% over the course of a recording. For IPSC kinetics analysis, events with a rise time of more than 3 ms were discarded due to space-clamp concerns. Medians of amplitude, rise time, decay, area, and interevent interval were calculated for each cell and used for WT vs. Dlx5 KCC2 cKO comparison.

Flurothyl Seizure Induction

Mice were placed individually into an airtight, clear acrylic chamber with internal volume of 2 L. A 10% (v/v) solution of flurothyl (bis-2,2,2-trifluoroethyl ether, Sigma-Aldrich) dissolved in 95% ethanol was delivered via precision syringe pump at a rate of 100 μL/min through a port in the chamber lid onto an absorbent pad in a tray suspended from the underside of the lid. The onset of seizure was defined as the point at which the mouse started convulsing with loss of postural control. The time latency (in seconds) to the onset of seizure was measured from the first drop of flurothyl onto the filter paper. The chamber was vented and cleansed of all flurothyl residue between trials. All flurothyl trials were video recorded for later review. The experimenter remained blinded to animal genotypes throughout all phases of data acquisition.

Video Monitoring

Cages of dams with litters containing Dlx5 KCC2 cKO pups were nightly monitored for seizure activity using an infrared DVC 24.0 megapixel HD camera at 720 p/30 fps and VGA/30 fps settings, positioned in front of the cage in the mouse housing facility. Whenever a pup died, we reviewed the previous night's recordings, looking for pups venturing from the nest and convulsing. Litters were checked daily for dead pups. The camera captured the entirety of the cage, but pups in the nest or buried

in bedding were occluded from view. WT littermates were kept in the cages with Dlx5 KCC2 cKO to keep conditions as close to normal, and minimize stress and subsequent seizure provocation. Dlx5 KCC2 cKO pups were identified by their smaller size. Unlike Dlx5 KCC2 cKO pups, WT pups seldom left the nest in the first two postnatal weeks, which made it easy to observe the Dlx5 KCC2 cKO. Seizure activity was judged based on observable clonus.

Data Analysis and Statistics

All numerical data was stored in data tables using Microsoft Excel 2016. Statistical analysis and graph preparation was done in GraphPad Prism 7.0. All bar graphs display an average with standard error of the mean. Statistical tests and graph types used are described in the legend of each figure.

DATA AVAILABILITY STATEMENT

The raw data supporting the conclusions of this article will be made available by the authors, without undue reservation.

ETHICS STATEMENT

The animal study was reviewed and approved by Vanderbilt's Institutional Animal Care and Use Committee.

AUTHOR CONTRIBUTIONS

KZ, ED, and AL contributed to the conception and design of the study. ED contributed the KCC2 flox mouse, which he created. KZ did most of the experiments, performed statistical analysis, made most of the figures, and wrote the first draft of the manuscript, which was significantly revised together with AL. AH helped with designing and conducting histology experiments and animal husbandry and molecular biology for this project, optimized and performed GABAA receptor subunit and VGluT2 immunostaining experiments, and made **Supplementary Figure 3**. CF contributed as a collaborator by conceiving, designing, and performing the flurothyl seizure experiments and Nkx2.1 Dlx5 cKO survival experiments, as well as doing statistical analysis, figures, and writing methods for these sections (panels in **Figures 4**, **7**). All authors contributed to manuscript revision, read, and approved the submitted version.

FUNDING

This work was supported by several grants. AL was funded by Veteran Affairs Merit grant I01 BX001189. ED was funded by National Institutes of Health grant DK093501 and by grant 17CVD05 from the Leducq Foundation.

SUPPLEMENTARY MATERIAL

The Supplementary Material for this article can be found online at: https://www.frontiersin.org/articles/10.3389/fnmol.2022.826427/full#supplementary-material

REFERENCES

Akita, T., and Fukuda, A. (2020). Intracellular Cl^- dysregulation causing and caused by pathogenic neuronal activity. *Pflügers Arch.* 472, 977–987. doi: 10.1007/s00424-020-02375-4

Al Awabdh, S., Donneger, F., Goutierre, M., Séveno, M., Vigy, O., Weinzettl, P., et al. (2021). Gephyrin interacts with the K-Cl co-transporter KCC2 to regulate its surface expression and function in cortical neurons. *J. Neurosci.* 42, 166–182. doi: 10.1523/jneurosci.2926-20.2021

Alcántara, S., Ferrer, I., and Soriano, E. (1993). Postnatal development of parvalbumin and calbindin D28K immunoreactivities in the cerebral cortex of the rat. *Anat. Embryol.* 188, 63–73. doi: 10.1007/BF00191452

Allene, C., Cattani, A., Ackman, J. B., Bonifazi, P., Aniksztejn, L., Ben Ari, Y., et al. (2008). Sequential generation of two distinct synapse-driven network patterns in developing neocortex. *J. Neurosci.* 28, 12851–12863.

Anstotz, M., Fiske, M. P., and Maccaferri, G. (2021). Impaired KCC2 function triggers interictal-like activity driven by parvalbumin-expressing interneurons in the isolated subiculum in vitro. *Cereb. Cortex* 31, 4681–4698. doi: 10.1093/cercor/bhab115

Barreda Tomás, F. J., Turko, P., Heilmann, H., Trimbuch, T., Yanagawa, Y., Vida, I., et al. (2020). BDNF expression in cortical GABAergic interneurons. *Int. J. Mol. Sci.* 21:1567. doi: 10.3390/ijms21051567

Bayer, S. A., and Altman, J. (1990). Development of layer I and the subplate in the rat neocortex. *Exp. Neurol.* 107, 48–62. doi: 10.1016/0014-4886(90)90062-w

Ben-Ari, Y., and Cherubini, E. (2022). The GABA polarity shift and bumetanide treatment: making sense requires unbiased and undogmatic analysis. *Cells* 11:396.

Biane, J., Conner, J. M., and Tuszynski, M. H. (2014). Nerve growth factor is primarily produced by GABAergic neurons of the adult rat cortex. *Front. Cell. Neurosci.* 8:220. doi: 10.3389/fncel.2014.00220

Bortone, D., and Polleux, F. (2009). KCC2 expression promotes the termination of cortical interneuron migration in a voltage-sensitive calcium-dependent manner. *Neuron* 62, 53–71.

Bouzigues, C., Morel, M., Triller, A., and Dahan, M. (2007). Asymmetric redistribution of GABA receptors during GABA gradient sensing by nerve growth cones analyzed by single quantum dot imaging. *Proc. Natl. Acad. Sci. U.S.A.* 104, 11251–11256. doi: 10.1073/pnas.0702536104

Bozzi, Y., Casarosa, S., and Caleo, M. (2012). Epilepsy as a neurodevelopmental disorder. *Front. Psychiatry* 3:19. doi: 10.3389/fpsyt.2012.00019

Brady, M. L., Pilli, J., Lorenz-Guertin, J. M., Das, S., Moon, C. E., Graff, N., et al. (2018). Depolarizing, inhibitory GABA type A receptor activity regulates GABAergic synapse plasticity via ERK and BDNF signaling. *Neuropharmacology* 128, 324–339. doi: 10.1016/j.neuropharm.2017.10.022

Cancedda, L., Fiumelli, H., Chen, K., and Poo, M. M. (2007). Excitatory GABA action is essential for morphological maturation of cortical neurons in vivo. *J.Neurosci.* 27, 5224–5235.

Ceni, C., Unsain, N., Zeinieh, M. P., and Barker, P. A. (2014). Neurotrophins in the regulation of cellular survival and death. *Handb. Exp. Pharmacol.* 220, 193–221. doi: 10.1007/978-3-642-45106-5_8

Chattopadhyaya, B., Di Cristo, G., Wu, C. Z., Knott, G., Kuhlman, S., Fu, Y., et al. (2007). GAD67-mediated GABA synthesis and signaling regulate inhibitory synaptic innervation in the visual cortex. *Neuron* 54, 889–903.

Chevy, Q., Heubl, M., Goutierre, M., Backer, S., Moutkine, I., Eugène, E., et al. (2015). KCC2 gates activity-driven AMPA receptor traffic through cofilin

phosphorylation. *J. Neurosci.* 35, 15772–15786. doi: 10.1523/jneurosci.1735-15.2015

Collin, T., Chat, M., Lucas, M. G., Moreno, H., Racay, P., Schwaller, B., et al. (2005). Developmental changes in parvalbumin regulate presynaptic Ca^{2+} signaling. *J. Neurosci.* 25, 96–107. doi: 10.1523/JNEUROSCI.3748-04.2005

Culiat, C. T., Stubbs, L. J., Woychik, R. P., Russell, L. B., Johnson, D. K., and Rinchik, E. M. (1995). Deficiency of the beta 3 subunit of the type A gamma-aminobutyric acid receptor causes cleft palate in mice. *Nat. Genet.* 11, 344–346. doi: 10.1038/ng1195-344

Cuzon, V. C., Yeh, P. W., Cheng, Q., and Yeh, H. H. (2006). Ambient GABA promotes cortical entry of tangentially migrating cells derived from the medial ganglionic eminence. *Cereb. Cortex* 16, 1377–1388.

Dehorter, N., Vinay, L., Hammond, C., and Ben-Ari, Y. (2012). Timing of developmental sequences in different brain structures: physiological and pathological implications. *Eur. J. Neurosci.* 35, 1846–1856. doi: 10.1111/j.1460-9568.2012.08152.x

del Rio, J., de Lecea, L., Ferrer, I., and Soriano, E. (1994). The development of parvalbumin-immunoreactivity in the neocortex of the mouse. *Dev. Brain Res.* 81, 247–259. doi: 10.1016/0165-3806(94)90311-5

Delpire, E., and Staley, K. J. (2014). Novel determinants of the neuronal Cl^- concentration. *J. Physiol.* 592, 4099–4114. doi: 10.1113/jphysiol.2014.275529

Di Cristo, G., Awad, P. N., Hamidi, S., and Avoli, M. (2018). KCC2, epileptiform synchronization, and epileptic disorders. *Prog. Neurobiol.* 162, 1–16. doi: 10.1016/j.pneurobio.2017.11.002

Duan, Z. R. S., Che, A., Chu, P., Modol, L., Bollmann, Y., Babij, R., et al. (2020). GABAergic restriction of network dynamics regulates interneuron survival in the developing cortex. *Neuron* 105, 75–92.e5. doi: 10.1016/j.neuron.2019.10.008

Dzhala, V. I., and Staley, K. J. (2021). KCC2 chloride transport contributes to the termination of ictal epileptiform activity. *eNeuro* 8:ENEURO.0208-20.2020. doi: 10.1523/eneuro.0208-20.2020

Engin, E., Benham, R. S., and Rudolph, U. (2018). An emerging circuit pharmacology of GABAA receptors. *Trends Pharmacol. Sci.* 39, 710–732. doi: 10.1016/j.tips.2018.04.003

Filice, F., Janickova, L., Henzi, T., Bilella, A., and Schwaller, B. (2020). The parvalbumin hypothesis of autism spectrum disorder. *Front. Cell. Neurosci.* 14:577525. doi: 10.3389/fncel.2020.577525

Fukuchi, M., Kirikoshi, Y., Mori, A., Eda, R., Ihara, D., Takasaki, I., et al. (2014). Excitatory GABA induces BDNF transcription via CRTC1 and phosphorylated CREB-related pathways in immature cortical cells. *J. Neurochem.* 131, 134–146. doi: 10.1111/jnc.12801

Fukuda, A. (2020). Chloride homeodynamics underlying modal shifts in cellular and network oscillations. *Neurosci. Res.* 156, 14–23. doi: 10.1016/j.neures.2020.02.010

Fukuda, A., and Watanabe, M. (2019). Pathogenic potential of human SLC12A5 variants causing KCC2 dysfunction. *Brain Res.* 1710, 1–7. doi: 10.1016/j.brainres.2018.12.025

Gascon, E., Dayer, A. G., Sauvain, M. O., Potter, G., Jenny, B., De Roo, M., et al. (2006). GABA regulates dendritic growth by stabilizing lamellipodia in newly generated interneurons of the olfactory bulb. *J. Neurosci.* 26, 12956–12966. doi: 10.1523/JNEUROSCI.4508-06.2006

Gauvain, G., Chamma, I., Chevy, Q., Cabezas, C., Irinopoulou, T., Bodrug, N., et al. (2011). The neuronal K-Cl cotransporter KCC2 influences postsynaptic AMPA receptor content and lateral diffusion in dendritic spines. *Proc. Natl. Acad. Sci. U.S.A.* 108, 15474–15479. doi: 10.1073/pnas.1107893108

Ge, S., Goh, E. L., Sailor, K. A., Kitabatake, Y., Ming, G. L., and Song, H. (2006). GABA regulates synaptic integration of newly generated neurons in the adult brain. *Nature* 439, 589–593.

Glykys, J., Dzhala, V., Egawa, K., Kahle, K. T., Delpire, E., and Staley, K. (2017). Chloride dysregulation, seizures, and cerebral edema: a relationship with therapeutic potential. *Trends Neurosci.* 40, 276–294. doi: 10.1016/j.tins.2017.03.006

Goutierre, M., Awabdh, S. A., Donneger, F., François, E., Gomez-Dominguez, D., Irinopoulou, T., et al. (2019). KCC2 regulates neuronal excitability and hippocampal activity via interaction with task-3 channels. *Cell Rep.* 28, 91–103.e7. doi: 10.1016/j.celrep.2019.06.001

Griguoli, M., and Cherubini, E. (2017). Early correlated network activity in the hippocampus: its putative role in shaping neuronal circuits. *Front. Cell. Neurosci.* 11:255. doi: 10.3389/fncel.2017.00255

Hartmann, A.-M., and Nothwang, H. G. (2011). Opposite temperature effect on transport activity of KCC2/KCC4 and N(K)CCs in HEK-293 cells. *BMC Res. Notes* 4:526. doi: 10.1186/1756-0500-4-526

Honegger, P., Pardo, B., and Monnet-Tschudi, F. (1998). Muscimol-induced death of GABAergic neurons in rat brain aggregating cell cultures. *Brain Res. Dev. Brain Res.* 105, 219–225. doi: 10.1016/s0165-3806(97)00194-6

Horn, Z., Ringstedt, T., Blaesse, P., Kaila, K., and Herlenius, E. (2010). Premature expression of KCC2 in embryonic mice perturbs neural development by an ion transport-independent mechanism. *Eur. J. Neurosci.* 31, 2142–2155. doi: 10.1111/j.1460-9568.2010.07258.x

Huberfeld, G., Wittner, L., Clemenceau, S., Baulac, M., Kaila, K., Miles, R., et al. (2007). Perturbed chloride homeostasis and GABAergic signaling in human temporal lobe epilepsy. *J. Neurosci.* 27, 9866–9873. doi: 10.1523/JNEUROSCI.2761-07.2007

Hübner, C. A., Stein, V., Hermans-Borgmeyer, I., Meyer, T., Ballanyi, K., and Jentsch, T. J. (2001). Disruption of KCC2 reveals an essential role of K-Cl cotransport already in early synaptic inhibition. *Neuron* 30, 515–524. doi: 10.1016/S0896-6273(01)00297-5

Inada, H., Watanabe, M., Uchida, T., Ishibashi, H., Wake, H., Nemoto, T., et al. (2011). GABA regulates the multidirectional tangential migration of GABAergic interneurons in living neonatal mice. *PLoS One* 6:e27048. doi: 10.1371/journal.pone.0027048

Inamura, N., Kimura, T., Tada, S., Kurahashi, T., Yanagida, M., Yanagawa, Y., et al. (2012). Intrinsic and extrinsic mechanisms control the termination of cortical interneuron migration. *J. Neurosci.* 32, 6032–6042. doi: 10.1523/JNEUROSCI.3446-11.2012

Ivakine, E. A., Acton, B. A., Mahadevan, V., Ormond, J., Tang, M., Pressey, J. C., et al. (2013). Neto2 is a KCC2 interacting protein required for neuronal Cl^-regulation in hippocampal neurons. *Proc. Natl. Acad. Sci. U.S.A.* 110, 3561–3566. doi: 10.1073/pnas.1212907110

Jiang, X., Lachance, M., and Rossignol, E. (2016). Involvement of cortical fast-spiking parvalbumin-positive basket cells in epilepsy. *Prog. Brain Res.* 226, 81–126.

Jin, X., Hu, H., Mathers, P. H., and Agmon, A. (2003). Brain-derived neurotrophic factor mediates activity-dependent dendritic growth in nonpyramidal neocortical interneurons in developing organotypic cultures. *J. Neurosci.* 23, 5662–5673. doi: 10.1523/jneurosci.23-13-05662.2003

Jones, K. R., Fariñas, I., Backus, C., and Reichardt, L. F. (1994). Targeted disruption of the BDNF gene perturbs brain and sensory neuron development but not motor neuron development. *Cell* 76, 989–999. doi: 10.1016/0092-8674(94)90377-8

Kahle, K. T., Merner, N. D., Friedel, P., Silayeva, L., Liang, B., Khanna, A., et al. (2014). Genetically encoded impairment of neuronal KCC2 cotransporter function in human idiopathic generalized epilepsy. *EMBO Rep.* 15, 766–774. doi: 10.15252/embr.201438840

Kahle, K. T., Staley, K. J., Nahed, B. V., Gamba, G., Hebert, S. C., Lifton, R. P., et al. (2008). Roles of the cation-chloride cotransporters in neurological disease. *Nat. Clin. Pract. Neurol.* 4, 490–503. doi: 10.1038/ncpneuro0883

Kaila, K., Price, T. J., Payne, J. A., Puskarjov, M., and Voipio, J. (2014). Cation-chloride cotransporters in neuronal development, plasticity and disease. *Nat. Rev. Neurosci.* 15, 637–654. doi: 10.1038/nrn3819

Kepecs, A., and Fishell, G. (2014). Interneuron cell types are fit to function. *Nature* 505, 318–326. doi: 10.1038/nature12983

Kilb, W. (2021). When are depolarizing GABAergic responses excitatory? *Front. Mol. Neurosci.* 14:747835. doi: 10.3389/fnmol.2021.747835

Kirmse, K., Kummer, M., Kovalchuk, Y., Witte, O. W., Garaschuk, O., and Holthoff, K. (2015). GABA depolarizes immature neurons and inhibits network activity in the neonatal neocortex in vivo. *Nat. Commun.* 6:7750. doi: 10.1038/ncomms8750

Kobayashi, M., Hamada, T., Kogo, M., Yanagawa, Y., Obata, K., and Kang, Y. (2008). Developmental profile of GABAA-mediated synaptic transmission in pyramidal cells of the somatosensory cortex. *Eur. J. Neurosci.* 28, 849–861. doi: 10.1111/j.1460-9568.2008.06401.x

Kontou, G., Josephine Ng, S. F., Cardarelli, R. A., Howden, J. H., Choi, C., Ren, Q., et al. (2021). KCC2 is required for the survival of mature neurons but not for their development. *J. Biol. Chem.* 296:100364. doi: 10.1016/j.jbc.2021.100364

Lee, H., Bach, E., Noh, J., Delpire, E., and Kandler, K. (2016). Hyperpolarization-independent maturation and refinement of GABA/glycinergic connections in the auditory brain stem. *J. Neurophysiol.* 115, 1170–1182. doi: 10.1152/jn.00926.2015

Li, H., Khirug, S., Cai, C., Ludwig, A., Blaesse, P., Kolikova, J., et al. (2007). KCC2 interacts with the dendritic cytoskeleton to promote spine development. *Neuron* 56, 1019–1033. doi: 10.1016/j.neuron.2007.10.039

Lim, L., Mi, D., Llorca, A., and Marin, O. (2018). Development and functional diversification of cortical interneurons. *Neuron* 100, 294–313. doi: 10.1016/j.neuron.2018.10.009

Llano, O., Rivera, C., and Ludwig, A. (2020). "Chapter 6 – KCC2 regulates dendritic spine development," in *Neuronal Chloride Transporters in Health and Disease*, ed. X. Tang (Cambridge, MA: Academic Press), 103–132.

Llano, O., Smirnov, S., Soni, S., Golubtsov, A., Guillemin, I., Hotulainen, P., et al. (2015). KCC2 regulates actin dynamics in dendritic spines via interaction with beta-PIX. *J. Cell Biol.* 209, 671–686. doi: 10.1083/jcb.201411008

Luhmann, H. J., Fukuda, A., and Kilb, W. (2015). Control of cortical neuronal migration by glutamate and GABA. *Front. Cell. Neurosci.* 9:4. doi: 10.3389/fncel.2015.00004

Luk, K. C., and Sadikot, A. F. (2001). GABA promotes survival but not proliferation of parvalbumin-immunoreactive interneurons in rodent neostriatum: an in vivo study with stereology. *Neuroscience* 104, 93–103. doi: 10.1016/s0306-4522(01)00038-0

Madisen, L., Zwingman, T. A., Sunkin, S. M., Oh, S. W., Zariwala, H. A., Gu, H., et al. (2010). A robust and high-throughput Cre reporting and characterization system for the whole mouse brain. *Nat. Neurosci.* 13, 133–140.

Mahadevan, V., Pressey, J. C., Acton, B. A., Uvarov, P., Huang, Michelle, Y., et al. (2014). Kainate receptors coexist in a functional complex with KCC2 and regulate chloride homeostasis in hippocampal neurons. *Cell Rep.* 7, 1762–1770. doi: 10.1016/j.celrep.2014.05.022

Manseau, F., Marinelli, S., Mendez, P., Schwaller, B., Prince, D. A., Huguenard, J. R., et al. (2010). Desynchronization of neocortical networks by asynchronous release of GABA at autaptic and synaptic contacts from fast-spiking interneurons. *PLoS Biol.* 8:e1000492. doi: 10.1371/journal.pbio.1000492

Marin, O. (2012). Interneuron dysfunction in psychiatric disorders. *Nat. Rev. Neurosci.* 13, 107–120. doi: 10.1038/nrn3155

Markram, H., Toledo-Rodriguez, M., Wang, Y., Gupta, A., Silberberg, G., and Wu, C. (2004). Interneurons of the neocortical inhibitory system. *Nat. Rev. Neurosci.* 5, 793–807. doi: 10.1038/nrn1519

Mavrovic, M., Uvarov, P., Delpire, E., Vutskits, L., Kaila, K., and Puskarjov, M. (2020). Loss of non-canonical KCC2 functions promotes developmental apoptosis of cortical projection neurons. *EMBO Rep.* 21:e48880. doi: 10.15252/embr.201948880

Merner, N. D., Chandler, M. R., Bourassa, C., Liang, B., Khanna, A. R., Dion, P., et al. (2015). Regulatory domain or CpG site variation in SLC12A5, encoding the chloride transporter KCC2, in human autism and schizophrenia. *Front. Cell. Neurosci.* 9:386. doi: 10.3389/fncel.2015.00386

Muller, M., Felmy, F., Schwaller, B., and Schneggenburger, R. (2007). Parvalbumin is a mobile presynaptic Ca^{2+} buffer in the calyx of Held that accelerates the decay of Ca^{2+} and short-term facilitation. *J. Neurosci.* 27, 2261–2271. doi: 10.1523/JNEUROSCI.5582-06.2007

Murata, Y., and Colonnese, M. T. (2020). GABAergic interneurons excite neonatal hippocampus in vivo. *Sci. Adv.* 6:eaba1430. doi: 10.1126/sciadv.aba1430

Obrietan, K., Gao, X.-B., and Van Den Pol, A. N. (2002). Excitatory actions of GABA increase BDNF expression via a MAPK-CREB–dependent mechanism—a positive feedback circuit in developing neurons. *J. Neurophysiol.* 88, 1005–1015. doi: 10.1152/jn.2002.88.2.1005

Oh, W. C., Lutzu, S., Castillo, P. E., and Kwon, H.-B. (2016). De novo synaptogenesis induced by GABA in the developing mouse cortex. *Science* 353, 1037–1040. doi: 10.1126/science.aaf5206

Orduz, D., Bischop, D. P., Schwaller, B., Schiffmann, S. N., and Gall, D. (2013). Parvalbumin tunes spike-timing and efferent short-term plasticity in striatal fast spiking interneurons. *J. Physiol.* 591, 3215–3232. doi: 10.1113/jphysiol.2012.250795

Otsu, Y., Donneger, F., Schwartz, E. J., and Poncer, J. (2020). Cation-chloride cotransporters and the polarity of GABA signalling in mouse hippocampal parvalbumin interneurons. *J. Physiol.* 598, 1865–1880. doi: 10.1113/jp279221

Patz, S., Grabert, J., Gorba, T., Wirth, M. J., and Wahle, P. (2004). Parvalbumin expression in visual cortical interneurons depends on neuronal activity and TrkB ligands during an early period of postnatal development. *Cereb. Cortex* 14, 342–351. doi: 10.1093/cercor/bhg132

Paxinos, G. (2007). *Atlas of the Developing Mouse Brain at E17.5, P0 and P6*. Amsterdam: Elsevier.

Peerboom, C., and Wierenga, C. J. (2021). The postnatal GABA shift: a developmental perspective. *Neurosci. Biobehav. Rev.* 124, 179–192. doi: 10.1016/j.neubiorev.2021.01.024

Platel, J.-C., Stamboulian, S., Nguyen, I., and Bordey, A. (2010). Neurotransmitter signaling in postnatal neurogenesis: the first leg. *Brain Res. Rev.* 63, 60–71. doi: 10.1016/j.brainresrev.2010.02.004

Polleux, F., Whitford, K. L., Dijkhuizen, P. A., Vitalis, T., and Ghosh, A. (2002). Control of cortical interneuron migration by neurotrophins and PI3-kinase signaling. *Development* 129, 3147–3160.

Preibisch, S., Saalfeld, S., and Tomancak, P. (2009). Globally optimal stitching of tiled 3D microscopic image acquisitions. *Bioinformatics* 25, 1463–1465. doi: 10.1093/bioinformatics/btp184

Qu, G. J., Ma, J., Yu, Y. C., and Fu, Y. (2016). Postnatal development of GABAergic interneurons in the neocortical subplate of mice. *Neuroscience* 322, 78–93. doi: 10.1016/j.neuroscience.2016.02.023

Represa, A., and Ben-Ari, Y. (2005). Trophic actions of GABA on neuronal development. *Trends Neurosci.* 28, 278–283. doi: 10.1016/j.tins.2005.03.010

Rheims, S., Minlebaev, M., Ivanov, A., Represa, A., Khazipov, R., Holmes, G. L., et al. (2008). Excitatory GABA in rodent developing neocortex in vitro. *J. Neurophysiol* 100, 609–619. doi: 10.1152/jn.90402.2008

Righes Marafiga, J., Vendramin Pasquetti, M., and Calcagnotto, M. E. (2021). GABAergic interneurons in epilepsy: more than a simple change in inhibition. *Epilepsy Behav.* 121(Pt B):106935. doi: 10.1016/j.yebeh.2020.106935

Rivera, C., Voipio, J., Payne, J. A., Ruusuvuori, E., Lahtinen, H., Lamsa, K., et al. (1999). The K^+/Cl^- co-transporter KCC2 renders GABA hyperpolarizing during neuronal maturation. *Nature* 397, 251–255. doi: 10.1038/16697

Rossignol, E. (2011). Genetics and function of neocortical GABAergic interneurons in neurodevelopmental disorders. *Neural Plast.* 2011:649325. doi: 10.1155/2011/649325

Ruden, J. B., Dugan, L. L., and Konradi, C. (2021). Parvalbumin interneuron vulnerability and brain disorders. *Neuropsychopharmacology* 46, 279–287. doi: 10.1038/s41386-020-0778-9

Saito, T., Ishii, A., Sugai, K., Sasaki, M., and Hirose, S. (2017). A de novo missense mutation in SLC12A5 found in a compound heterozygote patient with epilepsy of infancy with migrating focal seizures. *Clin. Genet.* 92, 654–658. doi: 10.1111/cge.13049

Saitsu, H., Watanabe, M., Akita, T., Ohba, C., Sugai, K., Ong, W. P., et al. (2016). Impaired neuronal KCC2 function by biallelic SLC12A5 mutations in migrating focal seizures and severe developmental delay. *Sci. Rep.* 6:30072. doi: 10.1038/srep30072

Schambra, U. B., and Schambra, U. B. (2008). *Prenatal Mouse Brain Atlas*, 2nd Edn. New York, NY: Springer.

Schauwecker, P. E. (2012). The effects of glycemic control on seizures and seizure-induced excitotoxic cell death. *BMC Neurosci.* 13:94. doi: 10.1186/1471-2202-13-94

Schulte, J. T., Wierenga, C. J., and Bruining, H. (2018). Chloride transporters and GABA polarity in developmental, neurological and psychiatric conditions. *Neurosci. Biobehav. Rev.* 90, 260–271. doi: 10.1016/j.neubiorev.2018.05.001

Silayeva, L., Deeb, T. Z., Hines, R. M., Kelley, M. R., Munoz, M. B., Lee, H. H., et al. (2015). KCC2 activity is critical in limiting the onset and severity of status epilepticus. *Proc. Natl. Acad. Sci. U.S.A.* 112, 3523–3528. doi: 10.1073/pnas.1415126112

Smart, I. H. (1984). Histogenesis of the mesocortical area of the mouse telencephalon. *J. Anat.* 138(Pt 3), 537–552.

Stenman, J., Toresson, H., and Campbell, K. (2003). Identification of two distinct progenitor populations in the lateral ganglionic eminence: implications for striatal and olfactory bulb neurogenesis. *J. Neurosci.* 23, 167–174. doi: 10.1523/JNEUROSCI.23-01-00167.2003

Takada, N., Pi, H. J., Sousa, V. H., Waters, J., Fishell, G., Kepecs, A., et al. (2014). A developmental cell-type switch in cortical interneurons leads to a selective defect in cortical oscillations. *Nat. Commun.* 5:5333. doi: 10.1038/ncomms6333

Takayama, C., and Inoue, Y. (2010). Developmental localization of potassium chloride co-transporter 2 (KCC2), GABA and vesicular GABA transporter (VGAT) in the postnatal mouse somatosensory cortex. *Neurosci. Res.* 67, 137–148. doi: 10.1016/j.neures.2010.02.010

Tuncdemir, S. N., Wamsley, B., Stam, F. J., Osakada, F., Goulding, M., Callaway, E. M., et al. (2016). Early somatostatin interneuron connectivity mediates the maturation of deep layer cortical circuits. *Neuron* 89, 521–535. doi: 10.1016/j.neuron.2015.11.020

Valeeva, G., Tressard, T., Mukhtarov, M., Baude, A., and Khazipov, R. (2016). An optogenetic approach for investigation of excitatory and inhibitory network GABA actions in mice expressing channelrhodopsin-2 in GABAergic neurons. *J. Neurosci.* 36, 5961–5973. doi: 10.1523/jneurosci.3482-15.2016

Virtanen, M. A., Uvarov, P., Mavrovic, M., Poncer, J. C., and Kaila, K. (2021). The multifaceted roles of KCC2 in cortical development. *Trends Neurosci.* 44, 378–392. doi: 10.1016/j.tins.2021.01.004

Watanabe, M., Zhang, J., Mansuri, M. S., Duan, J., Karimy, J. K., Delpire, E., et al. (2019). Developmentally regulated KCC2 phosphorylation is essential for dynamic GABA-mediated inhibition and survival. *Sci. Signal.* 12:eaaw9315. doi: 10.1126/scisignal.aaw9315

Williams, R. H., and Riedemann, T. (2021). Development, diversity, and death of MGE-derived cortical interneurons. *Int. J. Mol. Sci.* 22:9297. doi: 10.3390/ijms22179297

Wonders, C. P., and Anderson, S. A. (2006). The origin and specification of cortical interneurons. *Nat. Rev. Neurosci.* 7, 687–696. doi: 10.1038/nrn1954

Woo, N. S., Lu, J., England, R., McClellan, R., Dufour, S., Mount, D. B., et al. (2002). Hyperexcitability and epilepsy associated with disruption of the mouse neuronal-specific K-Cl cotransporter gene. *Hippocampus* 12, 258–268.

Woodin, M. A., Ganguly, K., and Poo, M.-M. (2003). Coincident pre- and postsynaptic activity modifies GABAergic synapses by postsynaptic changes in Cl^- transporter activity. *Neuron* 39, 807–820. doi: 10.1016/S0896-6273(03)00507-5

Wright, R., Newey, S. E., Ilie, A., Wefelmeyer, W., Raimondo, J. V., Ginham, R., et al. (2017). Neuronal chloride regulation via KCC2 is modulated through a $GABA_B$ receptor protein complex. *J. Neurosci.* 37, 5447–5462. doi: 10.1523/jneurosci.2164-16.2017

Wu, C., and Sun, D. (2015). GABA receptors in brain development, function, and injury. *Metab. Brain Dis.* 30, 367–379. doi: 10.1007/s11011-014-9560-1

Xu, Q., Tam, M., and Anderson, S. A. (2008). Fate mapping Nkx2.1-lineage cells in the mouse telencephalon. *J. Comp. Neurol.* 506, 16–29. doi: 10.1002/cne.21529

Young, S. Z., Taylor, M. M., Wu, S., Ikeda-Matsuo, Y., Kubera, C., and Bordey, A. (2012). NKCC1 knockdown decreases neuron production through GABAA-regulated neural progenitor proliferation and delays dendrite development. *J. Neurosci.* 32, 13630–13638. doi: 10.1523/jneurosci.2864-12.2012

Zechel, S., Nakagawa, Y., and Ibanez, C. F. (2016). Thalamo-cortical axons regulate the radial dispersion of neocortical GABAergic interneurons. *Elife* 5:e20770. doi: 10.7554/eLife.20770

Zhu, L., Lovinger, D., and Delpire, E. (2005). Cortical neurons lacking KCC2 expression show impaired regulation of intracellular chloride. *J. Neurophysiol.* 93, 1557–1568.

Conflict of Interest: The authors declare that the research was conducted in the absence of any commercial or financial relationships that could be construed as a potential conflict of interest.

Publisher's Note: All claims expressed in this article are solely those of the authors and do not necessarily represent those of their affiliated organizations, or those of the publisher, the editors and the reviewers. Any product that may be evaluated in this article, or claim that may be made by its manufacturer, is not guaranteed or endorsed by the publisher.

frontiers | Frontiers in Molecular Neuroscience

REVIEW
published: 08 July 2022
doi: 10.3389/fnmol.2022.893111

How Staying Negative Is Good for the (Adult) Brain: Maintaining Chloride Homeostasis and the GABA-Shift in Neurological Disorders

Kelvin K. Hui[1,2*†‡], *Thomas E. Chater*[3*†‡], *Yukiko Goda*[3,4†] *and Motomasa Tanaka*[5†]

[1] Department of Developmental and Molecular Biology, Albert Einstein College of Medicine, Bronx, NY, United States, [2] Institute for Aging Research, Albert Einstein College of Medicine, Bronx, NY, United States, [3] Laboratory for Synaptic Plasticity and Connectivity, RIKEN Center for Brain Science, Wako, Japan, [4] Synapse Biology Unit, Okinawa Institute for Science and Technology Graduate University, Onna, Japan, [5] Laboratory for Protein Conformation Diseases, RIKEN Center for Brain Science, Wako, Japan

OPEN ACCESS

Edited by:
Werner Kilb,
Johannes Gutenberg University
Mainz, Germany

Reviewed by:
Kiyoshi Egawa,
Hokkaido University, Japan
Anna-Maria Hartmann,
Carl von Ossietzky University
of Oldenburg, Germany

***Correspondence:**
Kelvin K. Hui
kelvin.hui@alum.utoronto.ca
Thomas E. Chater
thomas.chater@riken.jp

†ORCID:
Kelvin K. Hui
orcid.org/0000-0003-2699-4536
Thomas E. Chater
orcid.org/0000-0001-6133-0001
Yukiko Goda
orcid.org/0000-0003-0352-9498
Motomasa Tanaka
orcid.org/0000-0002-2994-7703

‡These authors have contributed equally to this work

Specialty section:
This article was submitted to Neuroplasticity and Development, a section of the journal Frontiers in Molecular Neuroscience

Received: 10 March 2022
Accepted: 10 June 2022
Published: 08 July 2022

Citation:
Hui KK, Chater TE, Goda Y and Tanaka M (2022) How Staying Negative Is Good for the (Adult) Brain: Maintaining Chloride Homeostasis and the GABA-Shift in Neurological Disorders.
Front. Mol. Neurosci. 15:893111.
doi: 10.3389/fnmol.2022.893111

Excitatory-inhibitory (E-I) imbalance has been shown to contribute to the pathogenesis of a wide range of neurodevelopmental disorders including autism spectrum disorders, epilepsy, and schizophrenia. GABA neurotransmission, the principal inhibitory signal in the mature brain, is critically coupled to proper regulation of chloride homeostasis. During brain maturation, changes in the transport of chloride ions across neuronal cell membranes act to gradually change the majority of GABA signaling from excitatory to inhibitory for neuronal activation, and dysregulation of this GABA-shift likely contributes to multiple neurodevelopmental abnormalities that are associated with circuit dysfunction. Whilst traditionally viewed as a phenomenon which occurs during brain development, recent evidence suggests that this GABA-shift may also be involved in neuropsychiatric disorders due to the "dematuration" of affected neurons. In this review, we will discuss the cell signaling and regulatory mechanisms underlying the GABA-shift phenomenon in the context of the latest findings in the field, in particular the role of chloride cotransporters NKCC1 and KCC2, and furthermore how these regulatory processes are altered in neurodevelopmental and neuropsychiatric disorders. We will also explore the interactions between GABAergic interneurons and other cell types in the developing brain that may influence the GABA-shift. Finally, with a greater understanding of how the GABA-shift is altered in pathological conditions, we will briefly outline recent progress on targeting NKCC1 and KCC2 as a therapeutic strategy against neurodevelopmental and neuropsychiatric disorders associated with improper chloride homeostasis and GABA-shift abnormalities.

Keywords: potassium chloride cotransporter-2 (KCC2), Na^+-K^+-$2Cl^-$ cotransporter-1 (NKCC1), neuropsychiatric disorders (NPD), neurodevelopmental disorders (NDD), chloride homeostasis, GABA-shift

INTRODUCTION

The predominant form of neurotransmission in the brain occurs at chemical synapses where presynaptic neurons release neurotransmitters that bind to receptors on postsynaptic neurons. A major type of postsynaptic receptors are ion channels which allow the selective influx or efflux of monovalent (Na^+, K^+, and Cl^-) or divalent (Ca^{2+}) ions into and out of postsynaptic neurons.

For any particular ion, the direction of flow is dictated by the electrochemical gradient, and the difference in concentrations of ions across the membrane results in a membrane potential. In the adult brain, the opening of ion channels permeable to cations such as Na^+ and Ca^{2+} drives the membrane potential toward the threshold potential (depolarization) through their entry into the cell. Increased permeability for Cl^- anions and their cell entry, in contrast, hyperpolarizes the cell to drive the membrane potential further away from the threshold potential, and reduces the chance of the cell firing an action potential.

The primary inhibitory neurotransmitter in the central nervous system (CNS), γ-aminobutyric acid (GABA), activates ionotropic $GABA_A$ receptors that are permeable to chloride, and the maintenance of intracellular and extracellular chloride concentrations ($[Cl^-]_i$ and $[Cl^-]_e$, respectively) is crucial for effective GABAergic neurotransmission. The intracellular chloride concentration ($[Cl^-]_i$) relative to its extracellular concentration is generally lower in the mature brain than in the immature brain, and thus the opening of $GABA_A$ receptors results in the influx of chloride ions into the postsynaptic neuron and hyperpolarizes it (Fukuda et al., 1998; Kuner and Augustine, 2000). Since disruptions in the excitation-inhibition (E-I) balance has been strongly linked to a number of neurological disorders such as epilepsy and autism spectrum disorder (ASD) (Fritschy, 2008; Nelson and Valakh, 2015), and inhibition critically depends on chloride levels, there has been much research interest in recent years to determine whether and how impairments in chloride homeostasis contribute to these pathologies.

Neuronal chloride homeostasis is maintained primarily by K^+-Cl^- cotransporter-2 (KCC2) (Jarolimek et al., 1999; Kakazu et al., 1999; Rivera et al., 1999; Hübner et al., 2001b) and Na^+-K^+-$2Cl^-$ cotransporter-1 (NKCC1) (Kakazu et al., 1999; Lu et al., 1999), which act to export and import Cl^- out of and into the cell, respectively. Because cells normally have a high $[K^+]_i$, KCC2 is able to transport the chloride ion (along with K^+) against its concentration gradient in order to maintain a low $[Cl^-]_i$ (Payne et al., 1996). Similarly, NKCC1 uses the electrochemical gradient of Na^+ to move K^+ and Cl^- into the cell (Gamba et al., 1994; **Figure 1A**).

During the development and maturation of the nervous system, intracellular chloride levels in neurons change dramatically in concentration, from 37 mM at E18, to 12 mM at P16, however it should be noted that such measurements are not trivial (Owens et al., 1996; Arosio and Ratto, 2014). This initial higher $[Cl^-]_i$ in immature neurons causes a chloride efflux when $GABA_A$ receptors are activated and ultimately results in membrane depolarization, thus effectively making GABA signaling excitatory in nature in the immature nervous system. While depolarizing responses are typically excitatory, there are counter-examples of GABA acting to depolarize cells leading to inhibition of network activity (for example see Kirmse et al., 2015). During early postnatal neurodevelopment, changes in expression of KCC2 and NKCC1 are believed to reduce the intracellular chloride concentration, thereby causing GABAergic neurotransmission to become inhibitory (Kakazu et al., 1999; Rivera et al., 1999; Yamada et al., 2004). In human neocortices, their expressions reach adult levels between postconceptional week (PCW) 40–50 (but see Sedmak et al., 2015 for an example of continuing postnatal increases), while in rodent hippocampus and cortex these changes primarily occur during the second week following birth (Rivera et al., 1999; Dzhala et al., 2005). The drop of $[Cl^-]_i$ was largely attributed by earlier studies to the downregulation of NKCC1 in neurons as they mature (Plotkin et al., 1997; Hübner et al., 2001a; Yamada et al., 2004), although the exact expression pattern of NKCC1 still remains somewhat controversial (Virtanen et al., 2020). Subsequent studies have revealed that KCC2 upregulation, in particular the KCC2b isoform, likely plays a prominent role for the observed GABA-shift in the cortex during brain maturation (Rivera et al., 1999; Dzhala et al., 2005; Zhu et al., 2005; Uvarov et al., 2007). This is complicated, however, by observations of functionally inactive KCC2 in immature neuronal populations related to subcellular localization, oligomerization, and phosphorylation status (Balakrishnan et al., 2003; Khirug et al., 2005; Blaesse et al., 2006), thus suggesting that expression alone may not necessarily imply transporter function. Despite some controversies surrounding their specific contributions to the GABA-shift during brain development, KCC2 and NKCC1 both act to maintain a low intracellular chloride level in mature neurons, and thus ensure inward Cl^- flow upon $GABA_A$ receptor activation.

THE EFFECTS OF GABA DURING DEVELOPMENT

Diverse Roles of GABA Prior to the GABA-Shift

Before discussing the GABA-shift in details, let us first describe the diverse roles of GABAergic signaling during normal neurodevelopment. The transition of highly plastic young brain into the relatively stable adult state involves multiple sets of overlapping processes (**Figure 1B**). These include the laying down of perineuronal nets, the buildup of extracellular matrix (Hensch, 2005), the refinement of excitatory and inhibitory neuronal networks, and the topic of this review: the change of GABA acting as a depolarizing, excitatory neurotransmitter to a hyperpolarizing inhibitory one. It is worth paying attention to the different roles demanded of the mature and immature nervous system, and how GABA acts on each in turn. In the developing nervous system, depolarizing GABA promotes calcium entry into cells (Leinekugel et al., 1995), which in turn triggers various signaling cascades leading to neurite outgrowth and synapse development (see below). Moreover, excitatory GABAergic synaptic activity combines with glutamatergic inputs to drive waves of activity called giant depolarizing potentials (GDPs) that can then shape synaptic connectivity (Ben-Ari et al., 1989). Notably, deficits in GDPs have been linked to neuropsychiatric disorders (Griguoli and Cherubini, 2017).

Interestingly, the GABA-shift is still retained in brain-derived organoids (Zafeiriou et al., 2020) and appears to be a widespread and robust phenomenon in developing neuronal systems across species. It has not been confirmed that the GABA-shift occurs in humans, however there is immunohistochemical evidence

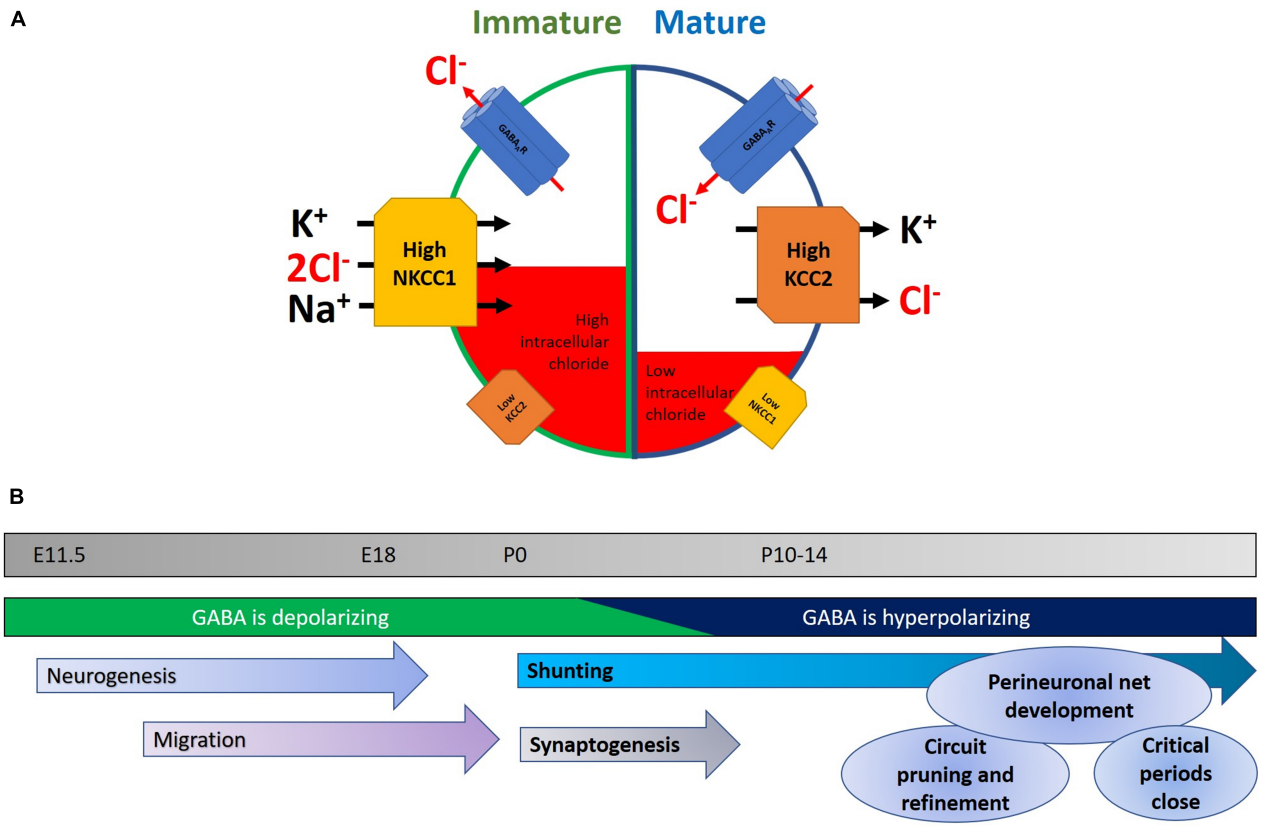

FIGURE 1 | (A) Developmental changes in NKCC1 and KCC2 within neurons. In immature neurons, NKCC1 is expressed at high levels and is stabilized at neuronal plasma membranes, where it transports chloride into the cell, along with potassium and sodium. A concomitant low level of KCC2 expression keeps intracellular chloride levels high. The net result of this is that opening of $GABA_A$ receptors results in an efflux of chloride, leading to neuronal depolarization and a higher probability of neuronal activity. Later in development, the GABA-shift in neurons is primarily characterized by an upregulation of KCC2, potentially accompanied by a downregulation of NKCC1. This mature state is characterized by lower levels of intracellular chloride, and consequently chloride enters the cell upon GABAergic activity, and hyperpolarizes the neuron, reducing the likelihood of action potential generation. **(B)** Timeline highlighting some key events during early development. Normal development of the nervous system is characterized by a series of stages in which neurons are born, migrate to their final location, and then begin to make synapses. Early in the program, depolarizing GABA helps in aspects of neurogenesis, migration, and elevating activity in the nascent network. As the GABA-shift switches GABA to being hyperpolarizing, this coincides with the onset of an increase in glutamatergic synaptic drive. Later in development, interneuronal activity and structure continue to be refined with the formation of perineuronal nets and the closure of critical periods.

suggesting that human cortical GABAergic development follows a similar course (Pinto et al., 2010).

GABA signaling is active in the developing neuronal network prior to the formation of synapses (Andäng et al., 2008; Wang and Kriegstein, 2008). Following the first wave of synaptogenesis, synaptic GABA responses have been detected before birth in both hippocampus and cortex prior to the formation of excitatory inputs in both rat and mouse tissues (LoTurco et al., 1995; Owens et al., 1996, 1999; Demarque et al., 2002; Gozlan and Ben-Ari, 2003). At the time of birth, GABAergic inputs into CA1 neurons are formed before glutamatergic ones, and appear as the apical dendrite arborizes (Tyzio et al., 1999).

During these early stages, depolarizing GABA signals modulate multiple temporally-overlapping aspects of network development, including the migration of young neurons (Behar et al., 1996, 1998, 2000; Denter et al., 2010; see Barker et al., 1998; Luhmann et al., 2015 for review) to proliferation (both promoting or inhibiting proliferation dependent on the cell type/brain region, see Haydar et al., 2000 for examples of both). Once the components of the network are in place, then depolarizing GABA acts to drive neurite outgrowth, and subsequently promote synapse formation. An early study demonstrated that mouse neuroblastoma cultures treated with GABA had an increase in neurite length and branching (Eins et al., 1983) and this has been repeated across a diverse range of cell types (reviewed in Sernagor et al., 2010). The capacity for GABA to promote neurite development in the cortex (Cancedda et al., 2007) has been shown to depend on chloride homeostasis as inhibiting NKCC1 with the loop diuretic bumetanide reduces dendritic arbor complexity (Wang and Kriegstein, 2011) and furthermore knockdown of NKCC1 slows the development of dendritic arbors (Young et al., 2012). Similarly, GABA has been demonstrated to drive dendritic arborization in the hippocampus (Gascon et al., 2006; Ge et al., 2006; Duveau et al., 2011). Critically, the potentiating effects of GABA on neurite complexity are limited to depolarizing GABA and no longer observed after the GABA-shift

(Maric et al., 2001), which suggest that the delayed or extended GABA-shift may result in overgrowth in neuronal arbors and a state of hyperconnectivity.

Earlier work on the depolarizing nature of GABA in young tissue was somewhat controversial (see Holmgren et al., 2010; Zilberter et al., 2010; Mukhtarov et al., 2011; Dzhala et al., 2012; reviewed in Bregestovski and Bernard, 2012; and rebutted in Ben-Ari et al., 2012) due to potential artifacts associated with *in vitro* slice preparations and the difficulty of making *in vivo* measurements of $[Cl^-]_i$. A recent optogenetic approach, where ChR2 was expressed in interneurons (Valeeva et al., 2016), strengthens the case that GABA can be directly depolarizing in the early network. In this study, *in vitro* stimulation of ChR2-expressing interneurons drove a marked increase in EPSC frequency, whereas the same stimulation *in vivo* in anesthetized animals led to a small decrease in EPSC frequency. Nonetheless, even in young neurons, GABA may still act to reduce postsynaptic activity by shunting excitatory currents (Khalilov et al., 1999; Wells et al., 2000), further complicating the picture.

Finally, the network undergoes a large burst in synapse formation during the final stages of depolarizing GABA, with GABA-dependent excitation acting to facilitate the generation of new synapses, both in the hippocampus and cortex (Ben-Ari et al., 1997; Griguoli and Cherubini, 2017), by helping relieve the Mg^{2+} block of NMDARs. Locally applied GABA alone is sufficient to generate new synapses during development (Oh et al., 2016). On the contrary, Salmon et al. (2020) found that blocking $GABA_A$ receptors immediately prior to the GABA-shift (in mouse organotypic hippocampal slice cultures) increases the number of glutamatergic synapses formed. However, the authors also assessed the effect of bumetanide inhibition of NKCC1 on excitatory synapse numbers; they found that even under these conditions, GABA inhibition still increased excitatory synaptic density.

Altogether, the downstream effects of GABA on aspects of brain organization and function differ across the GABA-shift. Let us next discuss how the beginning and end of this process is controlled.

Timing of the GABA-Shift

When exactly does the GABA-shift happen? Interestingly, the exact timing of the switch from depolarizing to hyperpolarizing GABA varies substantially across neuronal type, species, brain region, and even sexes. The shift happens earlier in cortex than in hippocampus (Murata and Colonnese, 2020), earlier and longer-lasting in females than in males (Kyrozis et al., 2006; Nuñez and McCarthy, 2007; Galanopoulou, 2008; but reversed in cerebral cortex, see Roux et al., 2018), and earlier in GABAergic neurons compared to pyramidal cells (although this is also controversial, see Banke and McBain, 2006; Sauer and Bartos, 2010 for opposing examples). Presumably, the regulation of NKCC1 and KCC2 expression pattern that are unique to each experimental context being examined (cell type, brain region, animal sex, and species) contribute to variations in the shift of the actions of GABA.

Throughout the developing nervous system, spontaneous endogenous waves of activity play a profound role in shaping the network connectivity and function. For example, in rodents, eye opening happens over a brief period of one to two days during the second week of life, at a time when the visual network is already functional. Does the depolarizing nature of GABA in the young brain help this process? Interestingly, a recent study (Ge et al., 2021) demonstrated a role for retinal waves in guiding the formation of direction-selective visual network by simulating a naturalistic pattern of optic flow. This occurred at a similar developmental period (P8–11) to the GABA-shift during which rodent retina are either undergoing the GABA-shift (Vu et al., 2000) or have just finished it (Zhang et al., 2005). Previous work in retina has demonstrated also that the switch from depolarizing to hyperpolarizing GABA coincides with the end of the propagating retinal waves, with a role for the regulation of KCC2 (Vu et al., 2000; Sernagor et al., 2003). On the contrary, however, another study has found that intravitreous injection of a $GABA_A$ blocker (bicuculine) from birth to P15-18 did not prevent the development of direction-selective circuitry (Sun et al., 2011), raising questions about the necessity of depolarizing GABA for the proper visual network development.

As we have discussed above, given the highly variable timing of the GABA-shift, it is perhaps not surprising that the experimental evidence is mixed as to the identity of the signals that determine the start and end of the GABA-shift. Using rat hippocampal cultures, one study found that blockade of $GABA_A$ receptors prevented the increases in KCC2, and thus delayed the GABA-shift (Ganguly et al., 2001); whilst another study, using mouse cultured neurons and organotypic slices, found no contribution of $GABA_A$ signaling to the changes in KCC2 (Ludwig et al., 2003). These studies broadly agreed on some points, namely that blocking excitatory neurotransmission (using APV and CNQX) had no effect on the course of the GABA-shift, and that blockade of neuronal spiking with tetrodotoxin (TTX) did not inhibit the GABA-shift. Notably, Khirug et al. (2005) reported that cultured mouse hippocampal neurons showed a step-like change in KCC2 activity after two weeks in culture between DIV 13 and 14, whilst acute slices showed instead a gradual increase from P5 to 14.

In some preparations, neuronal activity does seem to be a critical part of the GABA-shift mechanism. In turtle retina, spontaneous activity begins well before hatching, and the end of spontaneous activity corresponds with KCC2 upregulation (Sernagor et al., 2003). Moreover, dark-rearing turtles delays the GABA-shift, with a correspondingly weaker KCC2 expression. Further work in turtle retina has demonstrated that at least in this model, $GABA_A$ activity is required for the switch (Leitch et al., 2005). Similar to the study by Ganguly et al. (2001), the chronic blockade of $GABA_A$ signaling in turtle retina prevented the switch. On the contrary, a study using mouse retina found that the GABA-shift normally could be detected between P7-9, which was complete by P9-11, and that mouse retinal explants cultured in blockers of $GABA_{A/B/C}$ signaling still underwent the GABA-shift (Barkis et al., 2010). In fact, the same study subsequently blocked nearly all activity using a combination of drugs including TTX and glutamatergic signaling and still observed the GABA-shift.

What could be the triggers of the GABA-shift? Barkis et al. (2010) found that retinal ganglion cells (RGCs) cultured alone failed to make the switch. Importantly, the impaired switch was

rescued by co-culturing with cells from the superior colliculus, suggesting a diffusible factor originating from other cell types as a required component, while the possible contribution of brain-derived neurotrophic factor (BDNF) could be excluded. On the contrary, the BDNF precursor pro-BDNF has been shown to regulate KCC2 levels (Riffault et al., 2016), keeping it low during development. Intriguingly, BDNF itself, either exogenously applied (Ludwig et al., 2011) or using a BDNF-overexpressing mouse model (Aguado et al., 2003), increases KCC2 levels despite KCC2 levels being unaffected in *Bdnf* knockout (KO) mice (Puskarjov et al., 2015) (see below for further discussion on BDNF-dependent signaling that regulates KCC2 and NKCC1). Liu et al. (2006) have identified a role for cholinergic signaling in controlling the GABA switch in chick ciliary ganglion, where spontaneous nicotinic cholinergic activity modulates transporter levels, and thus the balance of Cl^- across the membrane. Taken as a whole, the evidence largely points to the regulation of KCC2 as being the primary driver behind the onset of the GABA-shift, but the identities of the upstream signal and the basis for cell-type specificity remain to be fully elucidated.

Another example of a potential molecular player in triggering the GABA-shift is the oxytocin receptor, activation of which promotes cell surface expression of KCC2 and stabilizes it at the cell membrane (Leonzino et al., 2016). Neurons from oxytocin receptor KO mice show a delayed GABA-shift, which nevertheless fully completes a few days later than control animals. Additionally, in these cultures NKCC1 levels were not different in KO cells, again consistently with KCC2 being the key player (Leonzino et al., 2016). It is worth mentioning here that there is another, transient GABA-shift during childbirth, that is also triggered by oxytocin, and acts to protect the fetus against anoxic episodes (Tyzio et al., 2006). Interestingly, the target for this transient GABA-shift has been suggested to be in fact NKCC1 activity and not KCC2, thus demonstrating that under certain conditions NKCC1 can dramatically influence GABA-shift behavior. It is worth mentioning that other candidates have been proposed to explain the suppression of neuronal activity during birth (for example vasopressin, see Spoljaric et al., 2017)].

Finally, another aspect of the GABA-shift concerns the developmental change in the $GABA_A$ receptor activity itself. $GABA_A$ receptors are large pentameric channels composed of a mixture of α, β, and γ subunits, often accompanied by the accessory δ and ρ subunits (Hevers and Lüddens, 1998). An early study that characterized $GABA_A$ receptor subunit mRNA levels in rat brain tissue found a change in the α subunit at around P8, from α2/3 to α1 in several brain regions (Laurie et al., 1992). Similarly, immunohistochemical studies suggest that α1 expression ramps up following birth and is still increasing at around the time of the GABA-shift (Fritschy et al., 1994; Davis et al., 2000) with a concomitant decrease in α2 levels. Importantly, $GABA_A$ receptors containing α1 subunits are more sensitive to GABA than those containing α2/3 (Wafford et al., 1993; Ebert et al., 1994; Hevers and Lüddens, 1998) and as such, the switch in the receptor subunit composition may serve to exaggerate the GABA-shift.

CELL SIGNALING PATHWAYS AND MECHANISMS AFFECTING KCC2 AND NKCC1 EXPRESSION AND FUNCTION

Genetic and Epigenetic Regulation of NKCC1 and KCC2 Expression

A number of genetic and epigenetic mechanisms regulating KCC2 expression have been identified thus far (**Figure 2A**). KCC2 is encoded by the *SLC12A5* gene to produce two isoforms (KCC2a and KCC2b), both of which are expressed only in neuronal cells (Payne et al., 1996; Uvarov et al., 2007). This is principally mediated by a 1.4 kb promoter fragment and two RE1-Silencing Transcription factor (REST)/Neuron-Restrictive Silencer Factor (NRSF) repressor elements identified in its 5′ promoter region and the first intron of the KCC2b isoform (Yeo et al., 2009). Notably, the 1.4 kb promoter fragment alone is sufficient to restrict KCC2 expression in neuronal cells (Uvarov et al., 2005), and the fragment contains binding sites for transcription factors such as Early growth response 4 (Egr4) (Uvarov et al., 2006) and Upstream stimulating factors 1 and 2 (USF-1/2) (Markkanen et al., 2008), suggesting these as key factors in controlling neuronal expression.

Given its role in mediating chloride homeostasis and consequently the direction of Cl^- flow triggered by $GABA_A$ receptor signaling, it is not surprising that the regulation of KCC2 expression also depends on the maturation status of the neuron of interest. For instance, as mentioned above, BDNF is known to regulate KCC2 expression. In particular, BDNF enhances KCC2 expression in immature neurons but suppresses it in mature neurons (Rivera et al., 2002, 2004; Aguado et al., 2003; Wake et al., 2007; Shulga et al., 2008; Boulenguez et al., 2010; Ludwig et al., 2011). Such opposing effects appear to be mediated via distinct pathways as BDNF activates expression in immature neurons via the ERK1/2 pathway and Egr4 (Ludwig et al., 2011), whereas its inhibitory effects on KCC2 expression in mature neurons depends on a signaling cascade involving Src homology domain containing transforming protein/FGF receptor substrate 2 (Shc/FRS-2), phospholipase C γ (PLC-γ), and cAMP response element-binding protein CREB (Rivera et al., 2004). The regulation of KCC2 by BDNF is further complicated by the effects of its precursor form (pro-BDNF), which can also suppress KCC2 expression via binding to the p75 neurotrophin receptor ($p75^{NTR}$) (Rivera et al., 2002; Riffault et al., 2016). Thus, the overall effects of BDNF and pro-BDNF on KCC2 expression likely depends on the combinatorial expression patterns of BDNF/pro-BDNF and their respective receptors in the developing brain. Notably, this is further supported by the observations that $p75^{NTR}$ is highly expressed during development (Yang et al., 2014; Menshanov et al., 2015; Winnubst et al., 2015) and that BDNF/pro-BDNF are involved in various activity-dependent changes in neurons (Gubellini et al., 2005; Langlois et al., 2013; Yang et al., 2014).

In contrast, much less is currently known about the regulation of NKCC1 expression (encoded by the *SLC12A2* gene), but both BDNF and oxytocin have been observed to downregulate its expression (Ceanga et al., 2010; Eftekhari et al., 2014;

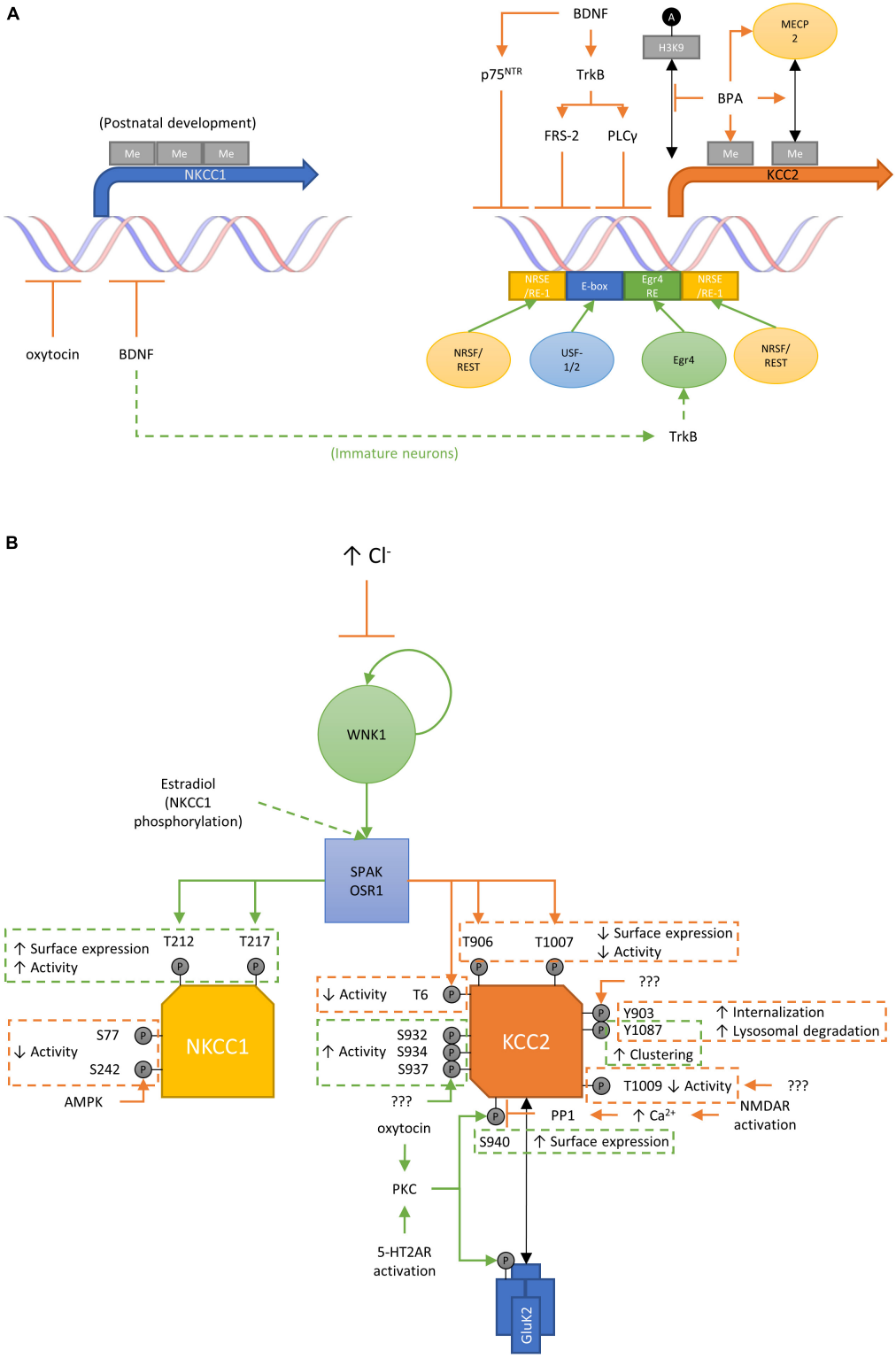

FIGURE 2 | (A) Transcriptional and epigenetic mechanisms involved in regulating KCC2 and NKCC1 expression. Transcriptional regulatory elements including NRSE/RE-1, E-box, and Erg4 RE are involved in regulating the expression of KCC2 and NKCC1 by various stimuli such as oxytocin and BDNF-TrkB/p75^{NTR} signaling. Additional regulatory mechanisms including DNA methylation and histone acetylation have also been demonstrated for KCC2 regulation. Given the association of chromatin regulators and other proteins that regulate gene expression with various neurodevelopmental disorders such as ASD, it will be of interest to determine how the expression of KCC2 and NKCC1, and ultimately the GABA-shift, may be affected in those pathologic conditions. A, acetylation; Me, DNA

(Continued)

FIGURE 2 | methylation. **(B)** Phospho-regulatory network by WNK/SPAK/OSR1 and other kinases to modulate KCC2 and NKCC1 activity. WNK kinases function both as a sensor and effector of intracellular chloride concentrations as their catalytic activities are influenced by the direct binding of Cl^- ions. SPAK/OSR1 are phosphorylated by WNK kinases and in turn can phosphorylate KCC2 and NKCC1 proteins. Numerous phosphorylation sites have been identified on KCC2 and NKCC1, which ultimately modulate their activities directly or by influencing their surface expression or degradation. Other phosphorylation sites have been identified on KCC2 and NKCC1 (discussed in main text) but were found to have no effects on transporter functionality and/or surface expression. P, phosphorylation.

Tyzio et al., 2014). The factors required to maintain high NKCC1 expression in immature neurons however remains to be identified.

In addition, although much less is known about epigenetic regulation of *SLC12A2* and *SLC12A5*, several recent studies have also demonstrated that the expressions of NKCC1 and KCC2 may be modulated via epigenetic mechanisms. Exposure of cultured developing human and rat cortical neurons to Bisphenol A (BPA), a possible chemical toxicant used in the production of a wide range of consumer products linked to increased incidence of neurodevelopmental disorders (Nesan and Kurrasch, 2019), was found to delay the KCC2 expression and increase $[Cl^-]_i$ during neuronal maturation (Yeo et al., 2013). BPA treatment was observed to alter both the methyl-CpG binding protein 2 (MECP2) binding to the KCC2 promoter and its histone H3K9 acetylation. Furthermore, DNA methylation of the KCC2 regulatory region was found to be increased by BPA treatment while the administration of a DNA methyltransferase inhibitor partially rescued the reduction of KCC2 expression caused by BPA. Consistent with other studies using chemical or genetic HDAC inhibition (Yeo et al., 2009; Hou et al., 2018; Ouyang et al., 2019), this study also found *Hdac1/2* knockdown to increase *SLC12A5* mRNA levels and rescue the BPA-induced KCC2 downregulation (Yeo et al., 2013). Conversely, DNA methylation of the NKCC1 promoter region increases significantly during postnatal neurodevelopment and *in vitro* DNA methylation of the NKCC1 promoter region reduces NKCC1 expression (Lee H. A. et al., 2010). Together, these studies point to possible epigenetic mechanisms regulating KCC2 and NKCC1 expression to mediate the GABA-shift during neurodevelopment.

WNK-SPAK/OSR1 Pathway Regulates KCC2/NKCC1 Functions

Aside from the transcriptional mechanisms described above, KCC2 and NKCC1 are also regulated via post-translational modifications that modulate their surface expression and activity levels. While other kinases have been shown to regulate NKCC1 and KCC2, the with-no-lysine (K) (WNK)-serine/threonine protein kinase 39 (SPAK)/OSR1 oxidative stress-responsive 1 (OSR1) pathway is a principal regulator for both transporters to coordinate their activities based on intracellular chloride concentrations (Alessi et al., 2014; Shekarabi et al., 2017).

Of all four WNK isoforms (WNK1-4) in the human genome, WNK1 is believed to be the principal WNK kinase in the human CNS (Shekarabi et al., 2013). This is supported by the observation that *WNK1* mutations result in an autosomal recessive disease characterized by congenital pain insensitivity (Shekarabi et al., 2008). WNK kinases effectively function as intracellular chloride sensors, through Cl^- binding to their catalytic domains in an inhibitory manner that suppress their autophosphorylation and kinase activity (Piala et al., 2014). Active WNK kinases phosphorylate SPAK and OSR1 (Moriguchi et al., 2005), which in turn directly phosphorylate KCC2 and NKCC1 to suppress and enhance their activities, respectively (Pacheco-Alvarez et al., 2006; Vitari et al., 2006; de los Heros et al., 2014; **Figure 2B**). When $[Cl^-]_i$ is low, chloride-unbound WNK kinases are active and consequently suppress KCC2 (to reduce Cl^- export) and increase NKCC1 activation (to enhance Cl^- import). In contrast, WNK kinases are inhibited by high $[Cl^-]_i$, thereby reversing these changes to enhance KCC2-mediated Cl^- export while suppressing further import by NKCC1.

Specifically, activated SPAK/OSR1 targets threonine residues T906 and T1007 (all residue numbers refer to human sequences) located on the C-terminal intracellular domain of KCC2 (de los Heros et al., 2014), which significantly suppress its Cl^- transport activity (Rinehart et al., 2009). Notably, while these sites were partially phosphorylated in neonatal mouse brains, there was no evidence of their phosphorylation from adult brains, thus providing fully active KCC2 to export chloride ions to maintain the inhibitory nature of GABAergic signaling. Moreover, a separate study directly implicated the WNK1-SPAK/OSR1 signaling pathway in modulating KCC2 function and GABA activity by enhancing its phosphorylation at these two sites in immature neurons (Friedel et al., 2015). Specifically, the authors observed that *in utero* knockdown of *Wnk1* resulted in lower $[Cl^-]_i$ and a hyperpolarizing shift for GABA specifically in immature neurons (P3-5), as there were no observable effects on mature neurons (P30). These findings thus support a role for WNK kinases in maintaining the high intracellular chloride concentration necessary for GABA to have depolarizing effects in the immature brain and may potentially be involved in regulating the GABA-shift. As described above, WNK kinases in theory should be inhibited by the high $[Cl^-]_i$ present in immature neurons and in turn reduce KCC2 phosphorylation to enhance Cl^- export. However, although *Wnk1* knockdown was found to reduce $[Cl^-]_i$ in immature neurons, Friedel et al. (2015) did observe higher T906 and T1007 phosphorylation on KCC2 in immature neurons compared to their mature counterparts; thus suggesting that either the WNK-SPAK/OSR1 pathway remained sufficiently active despite the high $[Cl^-]_i$ in immature neurons or that additional kinases are at work during this stage. Further studies comparing the WNK-SPAK/OSR1 pathway between immature and mature neurons are necessarily to fully delineate the importance of this pathway to $[Cl^-]_i$ regulation and the GABA-shift during neurodevelopment. More recently, two groups independently produced knock-in mice with phosphomimetic mutations in these two phosphorylation sites (i.e., T906E

and T1007E) to evaluate their physiologic significance. The authors observed reduced postnatal survival of homozygous mutants due to respiratory arrest and epileptic seizures (Watanabe et al., 2019), while heterozygotes displayed abnormal ASD-like impairments in ultrasonic vocalization and social behavior (Pisella et al., 2019), thereby demonstrating further the physiological importance of these two phosphorylation sites. Pharmacologically, *N*-ethylmaleimide (NEM) was found to activate KCC2 activity by enhancing the phosphorylation and dephosphorylation of S940 (to be discussed below) and T1007, respectively, to stabilize its surface expression (Conway et al., 2017). It was revealed that NEM mediates its effects on KCC2 by reducing WNK-dependent SPAK phosphorylation (S373) and depends on the dephosphorylation of T1007 on KCC2 as the overexpression of the T1007E phosphomimic mutant abolished the effects of NEM on KCC2 activity. Conversely, experiments using knock-in mice with alanine replacement at these phosphorylation sites demonstrated that they are critical to the timing of the GABA-shift (Moore et al., 2019). Moreover, the S906A/T1007A mutations altered social behaviors and led to slight enhancements in specific cognitive functions (Moore et al., 2019), while also protecting against chemoconvulsant-induced seizures (Moore et al., 2018). In addition, the WNK-SPAK/OSR1 pathway is also known to phosphorylate the N-terminal T6 of KCC2a, which is missing in KCC2b due to alternative splicing of exon-1a (Uvarov et al., 2007; Markkanen et al., 2017). Similar to its C-terminal counterparts (T906 and T1007), phosphorylation of T6 by SPAK was found to reduce its transporter activity (Markkanen et al., 2017).

In contrast, the activity of NKCC1 is enhanced by the phosphorylation of T203, T207, T212, T217, and T230 by the WNK-SPAK/OSR1 pathway (Darman and Forbush, 2002; Flemmer et al., 2002; Kahle et al., 2005; Vitari et al., 2006). Specifically, it was demonstrated that T217 phosphorylation is necessary for NKCC1 activity while the other sites serve modulatory roles (Darman and Forbush, 2002). Thus, through the coordinated phosphorylation of KCC2 and NKCC1, the WNK-SPAK/OSR1 pathway serves to monitor $[Cl^-]_i$ and alter KCC2/NKCC1 activities to maintain an optimal intracellular chloride concentration. This control of KCC2/NKCC1 activity by the WNK-SPAK/OSR1 pathway is primarily achieved by influencing the surface expression of these two cotransporters on the cell membrane (Rinehart et al., 2009).

In addition to modulation by the WNK-SPAK/OSR1 pathway, the activities of KCC2 and NKCC1 are also regulated by other phosphorylation events. The phosphorylation of KCC2 at serine residue S940 is mediated by protein kinase C (PKC) and enhances its surface expression to increase overall transporter activity. The physiological importance of this phosphorylation site was revealed as knock-in mice incapable of S940 phosphorylation (i.e., S940A mutants) exhibit ASD-like deficits in social behaviors and cognitive functions (Moore et al., 2019), while also showing accelerated onset of status epilepticus and lethality from chemical-induced seizure activity (Silayeva et al., 2015). As for its regulatory signaling, both oxytocin and 5-hydroxytryptamine type 2A receptor activation are known to increase KCC2 activity by promoting S940 phosphorylation via PKC-dependent mechanisms (Lee et al., 2007; Bos et al., 2013; Leonzino et al., 2016). Notably, PKC can also indirectly influence KCC2 surface expression by enhancing complex formation between KCC2 and kainate receptors via the phosphorylation of subunit GluK2 (Mahadevan et al., 2014; Pressey et al., 2017; Garand et al., 2019). Conversely, S940 dephosphorylation can be triggered by calcium influx via NMDA receptors through the actions of protein phosphatase 1 (PP1) (Lee et al., 2011).

Aside from these serine and threonine residues, KCC2 tyrosine phosphorylation at Y903 and Y1087 have also been observed by as yet unidentified tyrosine kinases. These C-terminal phosphorylation sites are believed to enhance KCC2 internalization and lysosomal degradation (Lee H. H. C. et al., 2010), as the phosphorylation-incompetent Y903F/Y1087F mutant showed increases in both total and surface KCC2 expression (Lee H. H. C. et al., 2010). Notably, Strange et al. (2000) had originally drew similar conclusions about Y1087 phosphorylation as they observed the phosphomimic Y1087D mutation to completely abolish KCC2 activity in *Xenopus* oocytes without any changes in surface expression of the mutants. It remains unclear, however, how phosphorylated Y1087 could directly impact KCC2 activity. In addition, other groups have also found the Y1087D variant to disrupt KCC2 activity in subsequent studies (Akerman and Cline, 2006; Pellegrino et al., 2011). By contrast, an independent study using the same aspartate substitution at Y1087 but considered it as a non-phosphorylatable mutant concluded that Y1087 phosphorylation activates KCC2 activity by influencing its distribution on the cell membrane and regulating its clustering (Watanabe et al., 2009). Notably, the authors also used genistein or lavendustin A, and sodium vanadate as tyrosine kinase inhibitor and tyrosine phosphatase inhibitor, respectively, to manipulate Y1087 phosphorylation status to examine its effects; it must be taken into consideration that these compounds are non-specific and therefore KCC2 Y1087 phosphorylation-independent effects cannot be dismissed. Given this, and that aspartate (as well as glutamate) substitutions are typically considered as phosphomimics rather than a non-phosphorylatable state, the findings by Watanabe et al. (2009) may in fact be in agreement with the previous studies about the effects of Y1087 phosphorylation even though the precise molecular mechanism underlying its influence on KCC2 function remains largely unknown. Apart from Y903 and Y1087, additional phosphorylation sites at both the N- (S25, S26, S31, and T34) and C-termini (S932, S934, S937, T999, T1009, S1022, S1025, and S1026) have been identified to date (Weber et al., 2014; Cordshagen et al., 2018). Using alanine and aspartate mutants, the authors demonstrated S932D, S934D, S937D, and T1009A substitutions to enhance KCC2 functions, whereas mutations at the other sites had no effects. Importantly, the S932D, S934D, S937D, and T1009A mutations did not influence surface expression of KCC2 and thus suggested that the effects were directly on its transport activity.

As for NKCC1, AMPK has been shown to phosphorylate it at S77 and S242, which in turn suppresses its activity (Sid et al., 2010; Fraser et al., 2014). In both studies, AMPK was shown by both groups to directly phosphorylate N-terminal fragments of NKCC1 *in vitro* using recombinant proteins.

While phosphorylation of NKCC1 at these sites appear to be AMPK-dependent, additional studies are necessary to determine whether they occur and are mediated directly by AMPK *in vivo*, especially in the context of neural cells, given the contrasting evidence from these and other groups (Sid et al., 2010; Miraucourt et al., 2016; King et al., 2019). Altogether, the above studies reveal the dynamic regulation of KCC2 and NKCC1 activity at multiple levels by phosphorylation.

KCC2 glycosylation has also been observed on at least six residues (N283, N291, N310, N328, N338, and N339) and are believed to regulate its membrane targeting (Agez et al., 2017). Notably, three KCC2 mutations associated with severe early-onset epileptic encephalopathy (L311H, L426P, and G551D) have been shown to reduce glycosylation and surface expression (Stödberg et al., 2015).

It is clear that the correct expression, surface targeting, and phosphorylation status of NKCC1 and KCC2 are critically important for healthy circuit development and function, but how does this impact the myriad of different cell types in the brain? We will discuss this topic next.

INTERACTIONS BETWEEN DIFFERENT CELL TYPES DURING THE GABA-SHIFT

GABA-Shift and Interneuronal Development

Changes in the balance of chloride across neuronal membranes are not expected to strongly affect postsynaptic neuronal activity unless there is concomitant release of GABA from presynaptic inhibitory neurons. The development of the inhibitory network has been widely studied across brain regions (review by Kubota et al., 2016; Lim et al., 2018; Ferrer and García, 2022), and mistimed development or inappropriate levels of inhibitory neuronal activity has been linked to multiple pathological states, with epilepsy being the primary example, but also schizophrenia and autism (reviewed by Marín, 2012; Chu and Anderson, 2015). The mammalian cortex contains a wide range of inhibitory neurons (Petilla Interneuron Nomenclature Group et al., 2008), and they change in number throughout development and past the end of the GABA-shift (for more details on interneuronal development we refer the reader to Gonchar et al., 2008; Bartolini et al., 2013; Ouellet and de Villers-Sidani, 2014). The activity and development of the interneuronal network is implicated in various aspects of circuit maturation, including ending critical periods (Hensch, 2005) and dynamically modulating axonal pruning and dendritic spine formation (Anderson et al., 1995).

Interneuronal development proceeds in stages, beginning at neurogenesis, followed by migration, and finally embedding into and modulating the circuit (Lim et al., 2018). This process is still ongoing throughout the period of the GABA shift, with some subpopulations of interneurons becoming mature earlier than others. Interestingly, the developmental period of the inhibitory neuronal network is temporally extended in larger animals such as humans, and this may contribute to the high levels of cognitive flexibility exhibited by these creatures, whilst also leaving them susceptible to many of the disease states that arise from imprecise GABAergic activity (Kim and Paredes, 2021).

Glial Contributions to Chloride Regulation

Currently, one critical missing piece of the puzzle is the contribution of glial cell types to the shift in GABA's effect. The presence of astrocytes has been shown to increase the speed of the GABA-shift *in vitro* (Li et al., 1998), however it is difficult to repeat this kind of experiment *in vivo*. Expression of NKCC1 and KCC2 can act to regulate neuronal intracellular [Cl^-] levels, but functions of the network critically depend also on the ionic balance of the extracellular milieu for which astrocytes play a central role, particularly of potassium levels (see Hertz and Chen, 2016; Bellot-Saez et al., 2017 for review). In support of such a role, dysfunction in glial potassium homeostasis has pathological downstream effects on neuronal activity (Robel and Sontheimer, 2016). The KCC2 protein requires a low extracellular potassium concentration to carry chloride out of the cell. There is a substantial body of evidence indicating that astrocytes are largely responsible for the clearance of extracellular K^+ following bouts of neuronal activity (Hertz, 1965; Ransom et al., 2000; Wang et al., 2012), either by local uptake or redistribution and buffering throughout the gap-junction connected astrocyte network. Astrocytes can also clear GABA from the extracellular milieu through GAT1-3 expression and activity (Boddum et al., 2016), and themselves express GABA receptors (MacVicar et al., 1989; Boisvert et al., 2018). Moreover, there is a wealth of data demonstrating that GABA signals can bidirectionally modulate astrocytic calcium levels (Doengi et al., 2009; Matos et al., 2018; Yu et al., 2018), which in turn controls the release of ATP and other gliotransmitters (Kang et al., 1998; Liu et al., 2004; Serrano et al., 2006). Neuronal activity, extracellular Cl^- levels, and astrocytic Cl^- have been demonstrated to be dynamically linked, and neuronal activity can trigger the release of Cl^- from astrocytes into the extracellular space, where it contributes to subsequent GABAergic activity (Egawa et al., 2013). Astrocytes and GABAergic neurons are known to signal to one another (for examples of interneuron to astrocyte, see Mariotti et al., 2018; Mederos et al., 2021; for astrocyte to interneuron, see Shigetomi et al., 2012; reviewed in Mederos and Perea, 2019) in a manner that appears to be specific to particular classes of GABAergic interneurons (Mariotti et al., 2018; Matos et al., 2018), adding an extra layer of complexity to the system.

NKCC1 is expressed in murine astrocytes (Su et al., 2002) and astrocytic internal Cl^- levels remains high throughout development, at around 30–50 mM in cultures (Bekar and Walz, 2002) and brain slices (Untiet et al., 2017). *In vivo* measurements have proven tricky, however (see Arosio and Ratto, 2014 for review). Although NKCC1 levels are largely stable in astrocytes, under various pathological conditions NKCC1 expression can be upregulated, undergoes phosphorylation, and is stabilized at the astrocytic plasma membrane (Jayakumar and Norenberg, 2010). Astrocytes from *Slc12a2* KO mice are unable to regulate their volume in response to a hyperkalemic (75 mM K^+)

challenge (Su et al., 2002), and NKCC1 has been implicated in astrocytic swelling in pathological conditions such as ischemia and brain edema caused by liver dysfunction (Yan et al., 2001; Jayakumar et al., 2008; reviewed in Jayakumar and Norenberg, 2010). Astrocytic NKCC1 is upregulated in response to trauma (Jayakumar et al., 2011) and both inhibiting NKCC1 activity pharmacologically with bumetanide or genetically with an anti-NKCC1 siRNA significantly reduces trauma-induced increase in astrocytic volume. It is worth mentioning that the *Slc12a2* KO mouse is viable (Delpire et al., 1999; Dixon et al., 1999; Flagella et al., 1999); however, the loss of the NKCC1 protein causes deficits in neuronal proliferation (Magalhães and Rivera, 2016) and exacerbates the severity of a mouse model of epilepsy (Hampel et al., 2021), amongst other issues. Whereas neuronal loss of NKCC1 appears to be compensated for at the network level (Sipila et al., 2009), the consequences on glia are much less clear. In adult tissue, NKCC1 has been implicated in astrocytic responses to neuronal potentiation (Henneberger et al., 2020), helping coordinate the withdrawal of fine astrocytic processes from synapses. All of the above indicates that deficits in NKCC1 astrocytic expression, function, or surface trafficking may all have pathological consequences. Nevertheless, experimental evidence using astrocytic-specific knockdown or knockout of NKCC1 are currently lacking. As discussed below, NKCC1 has joined the long-list of proteins whose mutation or absence in humans is linked to diseases (reviewed in Koumangoye et al., 2020), although it remains unclear how the loss of NKCC1 function in the affected individuals may have influenced the GABA-shift during their development. In fact, very little is known about the consequences of disrupted astrocytic NKCC1 expression or function on the GABA-shift, and this is a ripe field for study.

Conversely, how about the role of glia in the case of KCC2? Multiple studies have demonstrated a link between chronic inflammatory pain and KCC2 downregulation in the spinal cord (Coull et al., 2003, 2005; Okada-Ogawa et al., 2015; Tsuruga et al., 2016). Interestingly, the trigger for changes in neuronal KCC2 levels seems to be BDNF that is potentially released from nearby glia. Originally, microglia were thought to be the culprits; however, recent evidence suggests astrocytic signaling to be important for regulating both KCC2 and NKCC1. There is further evidence for a more direct role of astrocytes in modulating KCC2 levels. IL-6 released from astrocytes can elevate BDNF expression, and this in turn triggers downregulation of KCC2 in a model of neuropathic pain (Kitayama et al., 2016). It remains unclear if the source of this BDNF is neuronal or astrocytic, or potentially both.

GABA-SHIFT DEFECTS IN NEURODEVELOPMENTAL AND NEUROPSYCHIATRIC DISORDERS

Effects of *SLC12A2* and *SLC12A5* Mutations and Chromatin Dysregulation

Due to their critical role in maintaining chloride homeostasis and consequently the GABA-shift during brain development, it is not surprising that a number of studies have revealed changes in KCC2 and NKCC1 in patients with various neurodevelopmental and neuropsychiatric disorders.

Several recent studies have identified mutations in *SLC12A5* from children affected by epilepsy in infancy with migrating focal seizures (EIMFS) (**Table 1**; Stödberg et al., 2015; Saitsu et al., 2016; Saito et al., 2017). The loss-of-function mutations

TABLE 1 | Mutations in *SLC12A5* and *SLC12A2* identified from patients with neurodevelopmental and neuropsychiatric disorders.

Gene	Mutation	Pathology	Reference
SLC12A5 (KCC2)	R952H	IGE	Kahle et al., 2014
		Febril seizures	Puskarjov et al., 2014
		ASD	Merner et al., 2015
		SZ	Merner et al., 2015
	R1049C	IGE	Kahle et al., 2014
		ASD	Merner et al., 2015
	R1048W	ASD	Merner et al., 2015
	L331H	EIMFS	Stödberg et al., 2015
	L426P	EIMFS	Stödberg et al., 2015
	G551D	EIMFS	Stödberg et al., 2015
	E50_Q93del (exon 3, 44 aa deletion)	EIMFS	Saitsu et al., 2016
	A191V	EIMFS	Saitsu et al., 2016
	W318S	EIMFS	Saitsu et al., 2016
	S323P	EIMFS	Saitsu et al., 2016
	M415V	EIMFS	Saitsu et al., 2016
	S748del	EIMFS	Saitsu et al., 2016
	S399L	EIMFS	Saito et al., 2017
	R880L	EIMFS	Saito et al., 2017
	V473I	IGE	Till et al., 2019
SLC12A2 (NKCC1)	V1026Ffs*2	Seizure-like episodes (multisystem dysfunction)	Delpire et al., 2016
	L863F	MAEP	Marchese et al., 2016
	c.2617-2A > G (cDNA)	ID	Anazi et al., 2017
	Exons 2-7 (22kb deletion)	Kilquist syndrome	Macnamara et al., 2019
	H186Afs*17	Severe global developmental delay	McNeill et al., 2020
	V327A	Cortical dysplasia (multiple congenital anomalies)	McNeill et al., 2020
	N376I	Spastic paraparesis and delay of speech and gross motor development	McNeill et al., 2020
	A379L	ASD and ID	McNeill et al., 2020
	R410Q	ASD and mild ID	McNeill et al., 2020
	W892*	Global developmental delay, autism, motor stereotypy and hypotonia	McNeill et al., 2020
	c.2006-1G > A (exon 13 deleted) c.1431delT (exon 8 frameshift)	ID with encephalopathy	Stödberg et al., 2020

*ASD, autism spectrum disorder; EIMFS, epilepsy of infancy with migrating focal seizures; ID, intellectual disability; IGE, idiopathic generalized epilepsy; MAEP, macrocephaly autism–epilepsy phenotype; SZ, schizophrenia; *STOP codon.*

(L311H, L426P, and G551D as mentioned above) identified by Stödberg et al. (2015), reduce KCC2 surface expression in neurons accompanied by depolarized chloride equilibrium potential (E_{Cl}), thereby potentially reducing $GABA_A$R-mediated hyperpolarization compared to neurons carrying wild-type KCC2 protein. In a separate study (Saitsu et al., 2016), two of the mutations identified from EIMFS patients (E50_Q93del and M415V) significantly elevated E_{Cl} even though no changes in KCC2 cell surface expression were observed. Electrophysiological recordings demonstrated that the presence of these mutations suppressed the ability of the transporter to extrude chloride from the cell's interior, and overexpression of E50_Q93del and M415V mutants of KCC2 resulted in elevated intracellular chloride concentrations. Furthermore, another study found a distinct mutation (R952H) in KCC2 from patients from an Australian family with febrile seizures that similarly disrupted chloride homeostasis by reducing KCC2 surface expression and function (Puskarjov et al., 2014). Another group also found the same mutation (R952H) along with R1049C to associate with idiopathic generalized epilepsy (IGE) (Kahle et al., 2014). Notably, the authors detected a reduction of S940 phosphorylation in the mutant proteins, previously demonstrated to enhance KCC2 surface expression by reducing its internalization (Lee et al., 2007). More recently, the R952H and R1049C mutations in *SLC12A5* were also found in ASD (Merner et al., 2015). In addition, the same study identified the R1048W mutation in ASD patients, likely to cause similar disruption in KCC2 expression and function as R1049C due to their proximity. Notably, exome sequencing data suggest that ASD patients are more likely than healthy controls to have synonymous mutations predicted to create or disrupt CpG sites, thereby potentially affecting gene expression via alterations in DNA methylation patterns. Aside from these mutations affecting KCC2, recent studies have also identified multiple *SLC12A2* mutations in patients affected by various neurodevelopmental disorders (**Table 1**; Delpire et al., 2016; Marchese et al., 2016; Anazi et al., 2017; Macnamara et al., 2019; McNeill et al., 2020; Stödberg et al., 2020). The pathogenic effects of these mutations on NKCC1 expression or functions, however, remain largely unknown.

Recent studies have also observed altered *SLC12A5* and *SLC12A2* expression in patients. Consistent with their opposing roles in maintaining chloride homeostasis and GABA-shift, whereas NKCC1 protein levels were observed to be increased in patients with temporal lobe epilepsy (TLE) (Sen et al., 2007), *SLC12A5* (KCC2) mRNA expression was found to be downregulated (Huberfeld et al., 2007). In addition, patients with tuberous sclerosis or type IIb cortical dysplasia, both of which are common causes of refractory epilepsy, also displayed changes in KCC2 and NKCC1 expression and levels (Talos et al., 2012; Ruffolo et al., 2016).

As described above, previous studies suggest that the expression of KCC2 and NKCC1 can be regulated via epigenetic mechanisms. Notably, a strong link between disrupted chromatin regulation and neurodevelopmental disorders has been implicated in recent years (Hui et al., 2018). Specifically, mutations in a number of chromatin regulators have been associated with neurodevelopmental disorders such as Rett syndrome (*MECP2*), intellectual disability (*CHD1*, *CHD2*, *CHD7*, *CHD8*, *ATRX,* and *KDM5C*), epilepsy (*CHD1*, *CHD2*, *CHD7*, *CHD8*) (Consortium et al., 2013), and ASD (*MECP2*, *CHD1, CHD2*, *CHD3*, *CHD7*, *CHD8*, *MBD1*, *MACROD2*, *H2AFY*, *ARID1B*, *SMARCC1*, *SMARCC2*, and *JMJD1C*) (reviewed in LaSalle, 2013). Two recent studies found *KCC2* RNA expression to be significantly reduced in Rett syndrome patients (Gogliotti et al., 2018; Hinz et al., 2019). At the protein level, KCC2 levels were reduced in cerebrospinal fluid collected from patients with Rett syndrome without a change in NKCC1 levels, thereby disturbing the KCC2/NKCC1 ratio (Duarte et al., 2013). It will be of particular interest to examine how KCC2 and NKCC1 expression are altered in patients carrying mutations in the other chromatin regulators and determine how potential disruptions of the GABA-shift may contribute to those neurodevelopmental disorders.

GABA-Shift Abnormalities Due to "Dematuration" in Neuropsychiatric Disorders Such as Schizophrenia, Bipolar Disorder, and Major Depressive Disorder

Recent studies have also identified alterations of NKCC1 and/or KCC2 expression in patient-derived brain samples or animal models of neuropsychiatric disorders such as SZ and bipolar disorder (BD). For example, a significant reduction in KCC2 expression and thus an reducing trend for the KCC2/NKCC1 transcript ratio (as NKCC1 mRNA levels were not different between patients and controls) were observed in the hippocampi of SZ patients, suggesting the possibility of an immature GABA-shift (Hyde et al., 2011). Consistent with this, a separate group also observed reduced protein levels of KCC2 in the dorsal lateral prefrontal cortex of SZ patients (Sullivan et al., 2015). A follow-up study of alternative KCC2 transcripts further identified increased expression of transcript EXON6B (with a new exon 6) in SZ patients but the same transcript was reduced in patients with major depressive disorder (MDD), while other alternatively spliced transcripts examined including AK098371 (truncated KCC2 transcript), EXON2B (with a new exon 2), and ΔEXON6 (with exon 6 deletion) were not found to be different (Tao et al., 2012). In contrast, Morita et al. (2014) identified reduced expression of various alternatively spliced transcripts of NKCC1 (NKCC1b and 1-2a) in SZ patients compared to healthy controls. Although it is unclear how these alternative transcripts may affect overall KCC2 and NKCC1 functions, the studies highlight the potential involvement for differentially spliced KCC2 and NKCC1 transcripts in SZ and MDD pathophysiology.

SLC12A5 and *SLC12A2* mutations have also been identified in SZ patients, including the R952H mutation in *SLC12A5* described above (Merner et al., 2015). The same group later identified a Y199C mutation in the *SLC12A2* gene specifically in SZ patients but not in ASD nor intellectual disability (ID) patients (Merner et al., 2016). Functional analysis of this NKCC1 mutant revealed an increase in its transporter activity, thus potentially altering

chloride homeostasis and consequently GABAergic signaling in affected neurons. In addition, increased expression of OSR1 and WNK3 were detected in SZ patients compared to healthy controls (Arion and Lewis, 2010), thus potentially altering KCC2 and NKCC1 phospho-regulation and ultimately disturbing the GABA-shift. Similar to changes in KCC2 and NKCC1 expression discussed above, it remains to be determined how precisely these alterations are involved in pathophysiology, given that neuropsychiatric disorders do not typically manifest until late adolescence or early adulthood even though the mutations have been present during neurodevelopment.

To this end, it is of interest that several studies have recently identified transcriptomic signatures of "immaturity" in the dentate gyri and prefrontal cortices of adult patients with ASD, SZ, or BD (Gandal et al., 2012; Walton et al., 2012; Hagihara et al., 2014; Murano et al., 2019), suggestive of a reversal of the mature state ("dematuration"). Nevertheless, interpretation of the observations in dentate gyri are complicated by the fact that it is a major site of adult neurogenesis and thus the changes may reflect a difference in the process or the state of developmental maturation rather than signifying dematuration *per se*. Furthermore, multiple studies have also observed immature morphological and functional properties in neurons of SZ animal models or mutant animals exhibiting behavioral deficits relevant to neuropsychiatric disorders (Miyakawa et al., 2003; Yamasaki et al., 2008; Ohira et al., 2013; Shin et al., 2013; Takao et al., 2013; Kobayashi et al., 2014; Zhao et al., 2018; Sawada et al., 2020). Given the importance of the GABA-shift from excitatory to inhibitory during brain development and maturation, any disruptions in this process or even its reversal in the form of dematuration of neuronal phenotypes could potentially have profound effects on brain network activity and contribute to neurological disorders. Interestingly, a state of neuronal dematuration can be induced by different types of stimuli such as inflammation, hyperactivity, and drug treatment (Kobayashi et al., 2010, 2012; Takao et al., 2013). In parallel, various studies have shown that KCC2 and NKCC1 expression, phosphorylation status, or function could be affected by various types of stress (Hewitt et al., 2009; Sarkar et al., 2011; Miller and Maguire, 2014; Corradini et al., 2017; Furukawa et al., 2017; Hu et al., 2017) and may coincide with a disruption of neuronal maturation or the induction of a dematuration process. For example, maternal immune activation (MIA) by the injection of double stranded RNA poly(I:C) was found to alter the KCC2/NKCC1 ratio via a proinflammatory cytokine-dependent mechanism, and consequently delay the GABA-shift (Corradini et al., 2017). An independent study found that a similar MIA effectively abolished the GABA-shift and maintained GABA as an excitatory signal (Fernandez et al., 2018). Interestingly, a NKCC1-specific inhibitor was able to restore the hyperpolarizing actions of GABA in hippocampal slices from poly(I:C)-treated animals, thus highlighting the involvement of disrupted KCC2/NKCC1-mediated chloride homeostasis in the neurological deficits caused by MIA. More importantly, such findings indicate that pharmacologic intervention is possible and could have therapeutic benefits for certain patients with neurodevelopmental and neuropsychiatric disorders that have disturbed GABA-shifts.

GENETIC AND PHARMACOLOGIC APPROACHES TO MODULATE KCC2 AND NKCC1 EXPRESSION TO RECTIFY NEUROLOGICAL CONDITIONS ASSOCIATED WITH HYPEREXCITABILITY AND EXCITATORY-INHIBITORY IMBALANCE

In addition to the above study that demonstrated the beneficial effects of NKCC1-specific inhibitor bumetanide, commonly used clinically as a diuretic, it has been shown to be a useful treatment in mouse models of SZ (Kim et al., 2021), Down Syndrome (DS) (Deidda et al., 2015), Rett Syndrome (Banerjee et al., 2016), 22q11.2 deletion (DiGeorge) syndrome (Amin et al., 2017), neonatal epilepsy (Dzhala et al., 2005), and ID (Maset et al., 2021). More recent studies have further identified a novel therapeutic molecule known as ARN23746 (Savardi et al., 2020; Borgogno et al., 2021) and a series of KCC2 expression-enhancing compounds (KEECs) to be effective against the core symptoms exhibited by DS and ASD mouse models (Tang et al., 2019). Whereas ARN23746 targets NKCC1 selectively (thus limiting off-target diuretic side effects exhibited by bumetanide), the KEECs act via distinct cell signaling pathways [activation of the sirtuin 1 (SIRT1) or transient receptor potential cation channel subfamily V member 1 (TRPV1) pathways, or inhibition of fms-like tyrosine kinase 3 (FLT3) or glycogen synthase kinase 3β (GSK3β) pathways] to upregulate KCC2 expression at both mRNA and protein levels. In addition, anti-NKCC1 gene therapy or positive modulation of KCC2 overexpression by IGF1 and oxytocin have also been shown to be useful in treating cognitive deficits in a DS (Parrini et al., 2021) and Rett Syndrome mouse models (Tang et al., 2016; Bertoni et al., 2021), respectively.

Thus far, clinical trials have provided mixed results for the use of the NKCC1 blocker bumetanide to help reduce ASD symptoms in patients. While there have been reports hinting at successes in correcting for some symptoms in open-label pilot studies (Lemonnier and Ben-Ari, 2010; Hadjikhani et al., 2018; Fernell et al., 2021) and randomized double-blind clinical trials (NCT01078714 and NCT03156153) (Lemonnier et al., 2012, 2017; Zhang et al., 2020; Dai et al., 2021), other studies (NCT03715153, NCT03715166, and 2014-001560-35) have failed to show significant differences compared to placebo in their primary outcome measures (Sprengers et al., 2020; Crutel et al., 2021; Georgoula et al., 2022). Similarly, there are contrasting findings from small scale studies which attempt to treat patients with other types of neurodevelopmental and neuropsychiatric disorders such as epilepsy, fragile X syndrome, and schizophrenia using bumetanide (Eftekhari et al., 2013; Lemonnier et al., 2016; Rahmanzadeh et al., 2017; Soul et al., 2021), clearly highlighting the need for larger studies to definitively verify its effects. A particular issue with bumetanide potentially hindering its beneficial effects in these trials is its poor penetration into

the CNS. Fortunately, the aforementioned ARN23746 appears to have a better *in vivo* pharmacokinetic profile in mice as compared to bumetanide (Savardi et al., 2020), thus offering a glimpse of hope that ARN23746 and its derivatives may have more potent effects in human patients. Furthermore, in dealing with complex disorders such as ASD and schizophrenia in which the precise pathogenic cause is typically unknown for each patient, pharmacologic strategies such as bumetanide may simply not be effective for every patient since it is likely that only a subpopulation are experiencing E-I imbalance due to a dysregulated GABA-shift. As such, brain organoids derived from patient-specific induced pluripotent stem cells (iPSCs) (Zafeiriou et al., 2020) could be used to screen for patients with pathologic alterations in the GABA-shift to determine whether they are likely going to benefit from NKCC1 inhibitors. Finally, another issue with understanding the potentially negative consequences of disrupted NKCC1 function and its contribution to GABA-shift is the widespread expression of the protein (as well as its relatives like NKCC2, for example), and the resulting broad spectrum of problems that may occur throughout the body when they are inhibited. Thus, continued efforts to identify new therapeutic molecules such as ARN23746 and KEECs which do not have peripheral effects like bumetanide may prove to be fruitful.

CONCLUSION

This review has attempted to lay out the changes that occur in GABAergic signaling during early development, with a particular focus on the GABA-shift, both in how it proceeds in healthy tissue, and how it is disrupted in various pathological states. Abnormalities in the progression of the GABA-shift have been linked to several neurodevelopmental and neuropsychiatric disorders. Potential therapeutic targets typically focus on a handful of proteins: the transporters that move Cl^- across the neuronal membrane, and regulators of those proteins, such as WNK kinases. The balance of Cl^- across the membrane is primarily regulated by KCC2 and NKCC1, and as such, they are prime targets for pharmacological modulation. However, the widespread expression of NKCC1 in other tissues of the body complicates the utility of the pharmacological approach for therapy. Furthermore, our understanding of disturbances in the normal GABA-shift is hampered by the high variability: it happens at different times, in different cell types, that may be intermingled within a particular brain region. Moreover, in human cases with a mutated or missing chloride transporter, it is not clear how much of a patient's symptoms may be attributable to an abnormal GABA-shift, and how much is related to ongoing network dysfunction. Further research is required to understand the pathological consequences of a mis-timed or incomplete GABA-shift, and treatment options, whilst currently available, are limited.

A better grasp of the factors that control the GABA-shift during development may provide a greater understanding of what happens in the process of dematuration within the adult network. What are the exact triggers for the onset and successful completion of the GABA-shift? The impact and participation of different cell types in the GABA-shift, and the ongoing maintenance of GABAergic signaling, and both intra- and extracellular chloride regulation is an extremely important topic, and the extent of the contribution of glial cells remains a topic of much interest.

AUTHOR CONTRIBUTIONS

KH and TC conceptualized and wrote the manuscript. YG and MT provided intellectual input and edited the manuscript. All authors contributed to the article and approved the submitted version.

FUNDING

This work was supported by the RIKEN Center for Brain Science, Japan Agency for Medical Research and Development (AMED; JP21wm0525014h, JP15dm0207001, and 21gm1410009h to MT), Core-to-Core Program (JPJSCCA20220007 to YG) by Japan Society for the Promotion of Science (JSPS), Grants-in-Aid for Transformative Research Area (A) (21H05257 to MT) from Ministry of Education, Culture, Sports, Science and Technology (MEXT, Japan), and Japan Epilepsy Research Foundation (to MT).

REFERENCES

Agez, M., Schultz, P., Medina, I., Baker, D. J., Burnham, M. P., Cardarelli, R. A., et al. (2017). Molecular architecture of potassium chloride co-transporter KCC2. *Sci. Rep.* 7:16452. doi: 10.1038/s41598-017-15739-1

Aguado, F., Carmona, M. A., Pozas, E., Aguiloì, A., Martiìnez-Guijarro, F. J., Alcantara, S., et al. (2003). BDNF regulates spontaneous correlated activity at early developmental stages by increasing synaptogenesis and expression of the K+/Cl− co-transporter KCC2. *Development* 130, 1267–1280. doi: 10.1242/dev.00351

Akerman, C. J., and Cline, H. T. (2006). Depolarizing GABAergic Conductances regulate the balance of excitation to inhibition in the developing retinotectal circuit *in vivo*. *J. Neurosci.* 26, 5117–5130. doi: 10.1523/jneurosci.0319-06.2006

Alessi, D. R., Zhang, J., Khanna, A., Hochdorfer, T., Shang, Y., and Kahle, K. T. (2014). The WNK-SPAK/OSR1 pathway: master regulator of cation-chloride cotransporters. *Sci. Signal.* 7:re3. doi: 10.1126/scisignal.2005365

Amin, H., Marinaro, F., Tonelli, D. D. P., and Berdondini, L. (2017). Developmental excitatory-to-inhibitory GABA-polarity switch is disrupted in 22q11.2 deletion syndrome: a potential target for clinical therapeutics. *Sci. Rep.* 7:15752. doi: 10.1038/s41598-017-15793-9

Anazi, S., Maddirevula, S., Salpietro, V., Asi, Y. T., Alsahli, S., Alhashem, A., et al. (2017). Expanding the genetic heterogeneity of intellectual disability. *Hum. Genet.* 136, 1419–1429. doi: 10.1007/s00439-017-1843-2

Andäng, M., Hjerling-Leffler, J., Moliner, A., Lundgren, T. K., Castelo-Branco, G., Nanou, E., et al. (2008). Histone H2AX-dependent GABA(A) receptor regulation of stem cell proliferation. *Nature* 451, 460–464. doi: 10.1038/nature06488

Anderson, S. A., Classey, J. D., Condé, F., Lund, J. S., and Lewis, D. A. (1995). Synchronous development of pyramidal neuron dendritic spines and parvalbumin-immunoreactive chandelier neuron axon terminals in layer III of

monkey prefrontal cortex. *Neuroscience* 67, 7–22. doi: 10.1016/0306-4522(95)00051-j

Arion, D., and Lewis, D. A. (2010). Altered expression of regulators of the cortical chloride transporters NKCC1 and KCC2 in schizophrenia. *Arch. Gen. Psychiatry* 68, 21–31. doi: 10.1001/archgenpsychiatry.2010.114

Arosio, D., and Ratto, G. M. (2014). Twenty years of fluorescence imaging of intracellular chloride. *Front. Cell. Neurosci.* 8:258. doi: 10.3389/fncel.2014.00258

Balakrishnan, V., Becker, M., Löhrke, S., Nothwang, H. G., Güresir, E., and Friauf, E. (2003). Expression and function of chloride transporters during development of inhibitory neurotransmission in the auditory Brainstem. *J. Neurosci.* 23, 4134–4145. doi: 10.1523/jneurosci.23-10-04134.2003

Banerjee, A., Rikhye, R. V., Breton-Provencher, V., Tang, X., Li, C., Li, K., et al. (2016). Jointly reduced inhibition and excitation underlies circuit-wide changes in cortical processing in Rett syndrome. *Proc. Natl. Acad. Sci. U.S.A.* 113, E7287–E7296. doi: 10.1073/pnas.1615330113

Banke, T. G., and McBain, C. J. (2006). GABAergic Input onto CA3 hippocampal interneurons remains shunting throughout development. *J. Neurosci.* 26, 11720–11725. doi: 10.1523/jneurosci.2887-06.2006

Barker, J. L., Behar, T., Li, Y. X., Liu, Q. Y., Ma, W., Maric, D., et al. (1998). GABAergic cells and signals in CNS development. *Perspect. Dev. Neurobiol.* 5, 305–322.

Barkis, W. B., Ford, K. J., and Feller, M. B. (2010). Non–cell-autonomous factor induces the transition from excitatory to inhibitory GABA signaling in retina independent of activity. *Proc. Natl. Acad. Sci. U.S.A.* 107, 22302–22307. doi: 10.1073/pnas.1008775108

Bartolini, G., Ciceri, G., and Marín, O. (2013). Integration of gabaergic interneurons into cortical cell assemblies: lessons from embryos and adults. *Neuron* 79, 849–864. doi: 10.1016/j.neuron.2013.08.014

Behar, T., Li, Y., Tran, H., Ma, W., Dunlap, V., Scott, C., et al. (1996). GABA stimulates chemotaxis and chemokinesis of embryonic cortical neurons via calcium-dependent mechanisms. *J. Neurosci.* 16, 1808–1818. doi: 10.1523/jneurosci.16-05-01808.1996

Behar, T. N., Schaffner, A. E., Scott, C. A., Greene, C. L., and Barker, J. L. (2000). GABA receptor antagonists modulate postmitotic cell migration in slice cultures of embryonic rat cortex. *Cereb. Cortex* 10, 899–909. doi: 10.1093/cercor/10.9.899

Behar, T. N., Schaffner, A. E., Scott, C. A., O'Connell, C., and Barker, J. L. (1998). Differential response of cortical plate and ventricular zone cells to GABA as a Migration Stimulus. *J. Neurosci.* 18, 6378–6387. doi: 10.1523/jneurosci.18-16-06378.1998

Bekar, L. K., and Walz, W. (2002). Intracellular chloride modulates A-type potassium currents in astrocytes. *Glia* 39, 207–216. doi: 10.1002/glia.10096

Bellot-Saez, A., Kékesi, O., Morley, J. W., and Buskila, Y. (2017). Astrocytic modulation of neuronal excitability through K+ spatial buffering. *Neurosci. Biobehav. Rev.* 77, 87–97. doi: 10.1016/j.neubiorev.2017.03.002

Ben-Ari, Y., Khazipov, R., Leinekugel, X., Caillard, O., and Gaiarsa, J.-L. (1997). GABAA, NMDA and AMPA receptors: a developmentally regulated 'ménage à trois'. *Trends Neurosci.* 20, 523–529. doi: 10.1016/s0166-2236(97)01147-8

Ben-Ari, Y., Woodin, M. A., Sernagor, E., Cancedda, L., Vinay, L., Rivera, C., et al. (2012). Refuting the challenges of the developmental shift of polarity of GABA actions: GABA more exciting than ever! *Front. Cell. Neurosci.* 6:35. doi: 10.3389/fncel.2012.00035

Ben-Ari, Y., Cherubini, E., Corradetti, R., and Gaiarsa, J. L. (1989). Giant synaptic potentials in immature rat CA3 hippocampal neurones. *J. Physiol.* 416, 303–325. doi: 10.1113/jphysiol.1989.sp017762

Bertoni, A., Schaller, F., Tyzio, R., Gaillard, S., Santini, F., Xolin, M., et al. (2021). Oxytocin administration in neonates shapes hippocampal circuitry and restores social behavior in a mouse model of autism. *Mol. Psychiatry* 26, 7582–7595. doi: 10.1038/s41380-021-01227-6

Blaesse, P., Guillemin, I., Schindler, J., Schweizer, M., Delpire, E., Khiroug, L., et al. (2006). Oligomerization of KCC2 correlates with development of inhibitory neurotransmission. *J. Neurosci.* 26, 10407–10419. doi: 10.1523/jneurosci.3257-06.2006

Boddum, K., Jensen, T. P., Magloire, V., Kristiansen, U., Rusakov, D. A., Pavlov, I., et al. (2016). Astrocytic GABA transporter activity modulates excitatory neurotransmission. *Nat. Commun.* 7:13572. doi: 10.1038/ncomms13572

Boisvert, M. M., Erikson, G. A., Shokhirev, M. N., and Allen, N. J. (2018). The aging astrocyte transcriptome from multiple regions of the mouse brain. *Cell Rep.* 22, 269–285. doi: 10.1016/j.celrep.2017.12.039

Borgogno, M., Savardi, A., Manigrasso, J., Turci, A., Portioli, C., Ottonello, G., et al. (2021). Design, synthesis, *in vitro* and *in vivo* characterization of selective NKCC1 Inhibitors for the Treatment of Core Symptoms in Down Syndrome. *J. Med. Chem.* 64, 10203–10229. doi: 10.1021/acs.jmedchem.1c00603

Bos, R., Sadlaoud, K., Boulenguez, P., Buttigieg, D., Liabeuf, S., Brocard, C., et al. (2013). Activation of 5-HT2A receptors upregulates the function of the neuronal K-Cl cotransporter KCC2. *Proc. Natl. Acad. Sci. U.S.A.* 110, 348–353. doi: 10.1073/pnas.1213680110

Boulenguez, P., Liabeuf, S., Bos, R., Bras, H., Jean-Xavier, C., Brocard, C., et al. (2010). Down-regulation of the potassium-chloride cotransporter KCC2 contributes to spasticity after spinal cord injury. *Nat. Med.* 16, 302–307. doi: 10.1038/nm.2107

Bregestovski, P., and Bernard, C. (2012). Excitatory GABA: how a correct observation may turn out to be an experimental artifact. *Front. Pharmacol.* 3:65. doi: 10.3389/fphar.2012.00065

Cancedda, L., Fiumelli, H., Chen, K., and Poo, M.-M. (2007). Excitatory GABA action is essential for morphological maturation of cortical neurons *in vivo*. *J. Neurosci.* 27, 5224–5235. doi: 10.1523/jneurosci.5169-06.2007

Ceanga, M., Spataru, A., and Zagrean, A.-M. (2010). Oxytocin is neuroprotective against oxygen–glucose deprivation and reoxygenation in immature hippocampal cultures. *Neurosci. Lett.* 477, 15–18. doi: 10.1016/j.neulet.2010.04.024

Chu, J., and Anderson, S. A. (2015). Development of Cortical Interneurons. *Neuropsychopharmacology* 40, 16–23. doi: 10.1038/npp.2014.171

Consortium, E., Project, E. P., Allen, A. S., Berkovic, S. F., Cossette, P., Delanty, N., et al. (2013). De novo mutations in epileptic encephalopathies. *Nature* 501, 217–221. doi: 10.1038/nature12439

Conway, L. C., Cardarelli, R. A., Moore, Y. E., Jones, K., McWilliams, L. J., Baker, D. J., et al. (2017). N-Ethylmaleimide increases KCC2 cotransporter activity by modulating transporter phosphorylation. *J. Biol. Chem.* 292, 21253–21263. doi: 10.1074/jbc.m117.817841

Cordshagen, A., Busch, W., Winklhofer, M., Nothwang, H. G., and Hartmann, A.-M. (2018). Phosphoregulation of the intracellular termini of K+-Cl− cotransporter 2 (KCC2) enables flexible control of its activity. *J. Biol. Chem.* 293, 16984–16993. doi: 10.1074/jbc.ra118.004349

Corradini, I., Focchi, E., Rasile, M., Morini, R., Desiato, G., Tomasoni, R., et al. (2017). Maternal immune activation delays excitatory-to-inhibitory gamma-aminobutyric acid switch in offspring. *Biol. Psychiatry* 83, 680–691. doi: 10.1016/j.biopsych.2017.09.030

Coull, J. A. M., Beggs, S., Boudreau, D., Boivin, D., Tsuda, M., Inoue, K., et al. (2005). BDNF from microglia causes the shift in neuronal anion gradient underlying neuropathic pain. *Nature* 438, 1017–1021. doi: 10.1038/nature04223

Coull, J. A. M., Boudreau, D., Bachand, K., Prescott, S. A., Nault, F., Sík, A., et al. (2003). Trans-synaptic shift in anion gradient in spinal lamina I neurons as a mechanism of neuropathic pain. *Nature* 424, 938–942. doi: 10.1038/nature01868

Crutel, V., Lambert, E., Penelaud, P.-F., Severo, C. A., Fuentes, J., Rosier, A., et al. (2021). Bumetanide oral liquid formulation for the treatment of children and adolescents with autism spectrum disorder: design of two phase III Studies (SIGN Trials). *J. Autism Dev. Disord.* 51, 2959–2972. doi: 10.1007/s10803-020-04709-8

Dai, Y., Zhang, L., Yu, J., Zhou, X., He, H., Ji, Y., et al. (2021). Improved symptoms following bumetanide treatment in children aged 3-6 years with autism spectrum disorder: a randomized, double-blind, placebo-controlled trial. *Sci. Bull.* 66, 1591–1598. doi: 10.1016/j.scib.2021.01.008

Darman, R. B., and Forbush, B. (2002). A regulatory locus of phosphorylation in the N Terminus of the Na-K-Cl Cotransporter, NKCC1. *J. Biol. Chem.* 277, 37542–37550. doi: 10.1074/jbc.m206293200

Davis, A. M., Penschuck, S., Fritschy, J. M., and McCarthy, M. M. (2000). Developmental switch in the expression of GABA(A) receptor subunits alpha(1) and alpha(2) in the hypothalamus and limbic system of the rat. *Brain Res. Dev. Brain Res.* 119, 127–138. doi: 10.1016/s0165-3806(99)00150-9

de los Heros, P., Alessi, D. R., Gourlay, R., Campbell, D. G., Deak, M., Macartney, T. J., et al. (2014). The WNK-regulated SPAK/OSR1 kinases directly

phosphorylate and inhibit the K+–Cl− co-transporters. *Biochem. J.* 458, 559–573. doi: 10.1042/bj20131478

Deidda, G., Parrini, M., Naskar, S., Bozarth, I. F., Contestabile, A., and Cancedda, L. (2015). Reversing excitatory GABAAR signaling restores synaptic plasticity and memory in a mouse model of Down syndrome. *Nat. Med.* 21, 318–326. doi: 10.1038/nm.3827

Delpire, E., Lu, J., England, R., Dull, C., and Thorne, T. (1999). Deafness and imbalance associated with inactivation of the secretory Na-K-2Cl co-transporter. *Nat. Genet.* 22, 192–195. doi: 10.1038/9713

Delpire, E., Wolfe, L., Flores, B., Koumangoye, R., Schornak, C. C., Omer, S., et al. (2016). A patient with multisystem dysfunction carries a truncation mutation in human SLC12A2, the gene encoding the Na-K-2Cl cotransporter, NKCC1. *Cold Spring Harb. Mol. Case Stud.* 2:a001289. doi: 10.1101/mcs.a001289

Demarque, M., Represa, A., Becq, H., Khalilov, I., Ben-Ari, Y., and Aniksztejn, L. (2002). Paracrine intercellular communication by a Ca2+- and SNARE-independent release of GABA and glutamate prior to synapse formation. *Neuron* 36, 1051–1061. doi: 10.1016/s0896-6273(02)01053-x

Denter, D. G., Heck, N., Riedemann, T., White, R., Kilb, W., and Luhmann, H. J. (2010). GABAC receptors are functionally expressed in the intermediate zone and regulate radial migration in the embryonic mouse neocortex. *Neuroscience* 167, 124–134. doi: 10.1016/j.neuroscience.2010.01.049

Dixon, M. J., Gazzard, J., Chaudhry, S. S., Sampson, N., Schulte, B. A., and Steel, K. P. (1999). Mutation of the Na-K-Cl Co-Transporter Gene Slc12a2 Results in Deafness in Mice. *Hum. Mol. Genet.* 8, 1579–1584. doi: 10.1093/hmg/8.8.1579

Doengi, M., Hirnet, D., Coulon, P., Pape, H.-C., Deitmer, J. W., and Lohr, C. (2009). GABA uptake-dependent Ca(2+) signaling in developing olfactory bulb astrocytes. *Proc. Natl. Acad. Sci. U.S.A.* 106, 17570–17575. doi: 10.1073/pnas.0809513106

Duarte, S. T., Armstrong, J., Roche, A., Ortez, C., Pérez, A., O'Callaghan, M., et al. (2013). Abnormal expression of cerebrospinal fluid cation chloride cotransporters in patients with rett syndrome. *PLoS One* 8:e68851. doi: 10.1371/journal.pone.0068851

Duveau, V., Laustela, S., Barth, L., Gianolini, F., Vogt, K. E., Keist, R., et al. (2011). Spatiotemporal specificity of GABAA receptor-mediated regulation of adult hippocampal neurogenesis. *Eur. J. Neurosci.* 34, 362–373. doi: 10.1111/j.1460-9568.2011.07782.x

Dzhala, V., Valeeva, G., Glykys, J., Khazipov, R., and Staley, K. (2012). Traumatic alterations in GABA signaling disrupt hippocampal network activity in the developing brain. *J. Neurosci.* 32, 4017–4031. doi: 10.1523/jneurosci.5139-11.2012

Dzhala, V. I., Talos, D. M., Sdrulla, D. A., Brumback, A. C., Mathews, G. C., Benke, T. A., et al. (2005). NKCC1 transporter facilitates seizures in the developing brain. *Nat. Med.* 11, 1205–1213. doi: 10.1038/nm1301

Ebert, B., Wafford, K. A., Whiting, P. J., Krogsgaard-Larsen, P., and Kemp, J. A. (1994). Molecular pharmacology of gamma-aminobutyric acid type A receptor agonists and partial agonists in oocytes injected with different alpha, beta, and gamma receptor subunit combinations. *Mol. Pharmacol.* 46, 957–963.

Eftekhari, S., Habibabadi, J. M., Ziarani, M. N., Fesharaki, S. S. H., Gharakhani, M., Mostafavi, H., et al. (2013). Bumetanide reduces seizure frequency in patients with temporal lobe epilepsy. *Epilepsia* 54, e9–e12. doi: 10.1111/j.1528-1167.2012.03654.x

Eftekhari, S., Mehrabi, S., Soleimani, M., Hassanzadeh, G., Shahrokhi, A., Mostafavi, H., et al. (2014). BDNF modifies hippocampal KCC2 and NKCC1 expression in a temporal lobe epilepsy model. *Acta Neurobiol. Exp.* 74, 276–287.

Egawa, K., Yamada, J., Furukawa, T., Yanagawa, Y., and Fukuda, A. (2013). Cl− homeodynamics in gap junction-coupled astrocytic networks on activation of GABAergic synapses. *J. Physiol.* 591, 3901–3917. doi: 10.1113/jphysiol.2013.257162

Eins, S., Spoerri, P. E., and Heyder, E. (1983). GABA or sodium-bromide-induced plasticity of neurites of mouse neuroblastoma cells in culture. *Cell Tissue Res.* 229, 457–460. doi: 10.1007/bf00214987

Fernandez, A., Dumon, C., Guimond, D., Tyzio, R., Bonifazi, P., Lozovaya, N., et al. (2018). The GABA developmental shift is abolished by maternal immune activation already at birth. *Cereb. Cortex* 29, 3982–3992. doi: 10.1093/cercor/bhy279

Fernell, E., Gustafsson, P., and Gillberg, C. (2021). Bumetanide for autism: open-label trial in six children. *Acta Paediatr.* 110, 1548–1553. doi: 10.1111/apa.15723

Ferrer, C., and García, N. V. D. M. (2022). The role of inhibitory interneurons in circuit assembly and refinement across sensory cortices. *Front. Neural Circuits* 16:866999. doi: 10.3389/fncir.2022.866999

Flagella, M., Clarke, L. L., Miller, M. L., Erway, L. C., Giannella, R. A., Andringa, A., et al. (1999). Mice lacking the Basolateral Na-K-2Cl cotransporter have impaired epithelial chloride secretion and are profoundly deaf. *J. Biol. Chem.* 274, 26946–26955. doi: 10.1074/jbc.274.38.26946

Flemmer, A. W., Giménez, I., Dowd, B. F. X., Darman, R. B., and Forbush, B. (2002). Activation of the Na-K-Cl Cotransporter NKCC1 detected with a phospho-specific antibody. *J. Biol. Chem.* 277, 37551–37558. doi: 10.1074/jbc.m206294200

Fraser, S. A., Davies, M., Katerelos, M., Gleich, K., Choy, S.-W., Steel, R., et al. (2014). Activation of AMPK reduces the co-transporter activity of NKCC1. *Mol. Membr. Biol.* 31, 95–102. doi: 10.3109/09687688.2014.902128

Friedel, P., Kahle, K. T., Zhang, J., Hertz, N., Pisella, L. I., Buhler, E., et al. (2015). WNK1-regulated inhibitory phosphorylation of the KCC2 cotransporter maintains the depolarizing action of GABA in immature neurons. *Sci. Signal.* 8:ra65. doi: 10.1126/scisignal.aaa0354

Fritschy, J.-M. (2008). Epilepsy, E/I balance and GABAA receptor plasticity. *Front. Mol. Neurosci.* 1:5. doi: 10.3389/neuro.02.005.2008

Fritschy, J. M., Paysan, J., Enna, A., and Mohler, H. (1994). Switch in the expression of rat GABAA-receptor subtypes during postnatal development: an immunohistochemical study. *J. Neurosci.* 14, 5302–5324. doi: 10.1523/JNEUROSCI.14-09-05302.1994

Fukuda, A., Tanaka, M., Yamada, Y., Muramatsu, K., Shimano, Y., and Nishino, H. (1998). Simultaneous optical imaging of intracellular Cl− in neurons in different layers of rat neocortical slices: advantages and limitations. *Neurosci. Res.* 32, 363–371. doi: 10.1016/s0168-0102(98)00099-6

Furukawa, M., Tsukahara, T., Tomita, K., Iwai, H., Sonomura, T., Miyawaki, S., et al. (2017). Neonatal maternal separation delays the GABA excitatory-to-inhibitory functional switch by inhibiting KCC2 expression. *Biochem. Biophy. Res. Commun.* 493, 1243–1249. doi: 10.1016/j.bbrc.2017.09.143

Galanopoulou, A. S. (2008). Dissociated gender-specific effects of recurrent seizures on GABA Signaling in CA1 Pyramidal Neurons: role of GABAA Receptors. *J. Neurosci.* 28, 1557–1567. doi: 10.1523/jneurosci.5180-07.2008

Gamba, G., Miyanoshita, A., Lombardi, M., Lytton, J., Lee, W. S., Hediger, M. A., et al. (1994). Molecular cloning, primary structure, and characterization of two members of the mammalian electroneutral sodium-(potassium)-chloride cotransporter family expressed in kidney. *J. Biol. Chem.* 269, 17713–17722. doi: 10.1016/s0021-9258(17)32499-7

Gandal, M. J., Nesbitt, A. M., McCurdy, R. M., and Alter, M. D. (2012). Measuring the maturity of the fast-spiking interneuron transcriptional program in autism, schizophrenia, and bipolar disorder. *PLoS One* 7:e41215. doi: 10.1371/journal.pone.0041215

Ganguly, K., Schinder, A. F., Wong, S. T., and Poo, M. (2001). GABA itself promotes the developmental switch of neuronal GABAergic responses from excitation to inhibition. *Cell* 105, 521–532. doi: 10.1016/s0092-8674(01)00341-5

Garand, D., Mahadevan, V., and Woodin, M. A. (2019). Ionotropic and metabotropic kainate receptor signalling regulates Cl− homeostasis and GABAergic inhibition. *J. Physiol.* 597, 1677–1690. doi: 10.1113/jp276901

Gascon, E., Dayer, A. G., Sauvain, M.-O., Potter, G., Jenny, B., Roo, M. D., et al. (2006). GABA regulates dendritic growth by stabilizing lamellipodia in newly generated interneurons of the olfactory bulb. *J. Neurosci.* 26, 12956–12966. doi: 10.1523/jneurosci.4508-06.2006

Ge, S., Goh, E. L. K., Sailor, K. A., Kitabatake, Y., Ming, G., and Song, H. (2006). GABA regulates synaptic integration of newly generated neurons in the adult brain. *Nature* 439, 589–593. doi: 10.1038/nature04404

Ge, X., Zhang, K., Gribizis, A., Hamodi, A. S., Sabino, A. M., and Crair, M. C. (2021). Retinal waves prime visual motion detection by simulating future optic flow. *Science* 373:eabd0830. doi: 10.1126/science.abd0830

Georgoula, C., Ferrin, M., Pietraszczyk-Kedziora, B., Hervas, A., Marret, S., Oliveira, G., et al. (2022). A Phase III Study of Bumetanide Oral Liquid Formulation for the Treatment of Children and Adolescents Aged Between 7 and 17 Years with Autism Spectrum Disorder (SIGN 1 Trial): participant

Baseline Characteristics. *Child Psychiatry Hum. Dev.* [Epub ahead of print]. doi: 10.1007/s10578-022-01328-5

Gogliotti, R., Fisher, N., Stansley, B., Jones, C., Lindsley, C., Conn, J., et al. (2018). Total RNA-sequencing of Rett syndrome autopsy samples identifies the M4 muscarinic receptor as a novel therapeutic target. *J. Pharmacol. Exp. Ther.* 365, 291–300. doi: 10.1124/jpet.117.246991

Gonchar, Y., Wang, Q., and Burkhalter, A. (2008). Multiple distinct subtypes of GABAergic neurons in mouse visual cortex identified by triple immunostaining. *Front. Neuroanat.* 1:3. doi: 10.3389/neuro.05.003.2007

Gozlan, H., and Ben-Ari, Y. (2003). Interneurons are the Source and the Targets of the First Synapses Formed in the Rat Developing Hippocampal Circuit. *Cereb. Cortex* 13, 684–692. doi: 10.1093/cercor/13.6.684

Griguoli, M., and Cherubini, E. (2017). Early correlated network activity in the hippocampus: its putative role in shaping neuronal circuits. *Front. Cell. Neurosci.* 11:255. doi: 10.3389/fncel.2017.00255

Gubellini, P., Ben-Ari, Y., and Gaïarsa, J.-L. (2005). Endogenous neurotrophins are required for the induction of GABAergic long-term potentiation in the neonatal rat hippocampus. *J. Neurosci.* 25, 5796–5802. doi: 10.1523/jneurosci.0824-05.2005

Hadjikhani, N., Johnels, J. Å, Lassalle, A., Zürcher, N. R., Hippolyte, L., Gillberg, C., et al. (2018). Bumetanide for autism: more eye contact, less amygdala activation. *Sci. Rep.* 8:3602. doi: 10.1038/s41598-018-21958-x

Hagihara, H., Ohira, K., Takao, K., and Miyakawa, T. (2014). Transcriptomic evidence for immaturity of the prefrontal cortex in patients with schizophrenia. *Mol. Brain* 7:41. doi: 10.1186/1756-6606-7-41

Hampel, P., Johne, M., Gailus, B., Vogel, A., Schidlitzki, A., Gericke, B., et al. (2021). Deletion of the Na-K-2Cl cotransporter NKCC1 results in a more severe epileptic phenotype in the intrahippocampal kainate mouse model of temporal lobe epilepsy. *Neurobiol. Dis.* 152:105297. doi: 10.1016/j.nbd.2021.105297

Haydar, T. F., Wang, F., Schwartz, M. L., and Rakic, P. (2000). Differential modulation of proliferation in the neocortical ventricular and subventricular zones. *J. Neurosci.* 20, 5764–5774. doi: 10.1523/jneurosci.20-15-05764.2000

Henneberger, C., Bard, L., Panatier, A., Reynolds, J. P., Kopach, O., Medvedev, N. I., et al. (2020). ltp induction boosts glutamate spillover by driving withdrawal of Perisynaptic Astroglia. *Neuron* 108, 919–936.e11. doi: 10.1016/j.neuron.2020.08.030

Hensch, T. K. (2005). Critical period mechanisms in developing visual cortex. *Curr. Top. Dev. Biol.* 69, 215–237. doi: 10.1016/s0070-2153(05)69008-4

Hertz, L. (1965). Possible role of neuroglia: a potassium-Mediated Neuronal – Neuroglial – Neuronal Impulse Transmission System. *Nature* 206, 1091–1094. doi: 10.1038/2061091a0

Hertz, L., and Chen, Y. (2016). Importance of astrocytes for potassium ion (K+) homeostasis in brain and glial effects of K+ and its transporters on learning. *Neurosci. Biobehav. Rev.* 71, 484–505. doi: 10.1016/j.neubiorev.2016.09.018

Hevers, W., and Lüddens, H. (1998). The diversity of GABAA receptors: pharmacological and electrophysiological properties of GABAA channel subtypes. *Mol. Neurobiol.* 18, 35–86. doi: 10.1007/bf02741459

Hewitt, S. A., Wamsteeker, J. I., Kurz, E. U., and Bains, J. S. (2009). Altered chloride homeostasis removes synaptic inhibitory constraint of the stress axis. *Nat. Neurosci.* 12, 438–443. doi: 10.1038/nn.2274

Hinz, L., Barrufet, J. T., and Heine, V. M. (2019). KCC2 expression levels are reduced in post mortem brain tissue of Rett syndrome patients. *Acta Neuropathol. Commun.* 7:196. doi: 10.1186/s40478-019-0852-x

Holmgren, C. D., Mukhtarov, M., Malkov, A. E., Popova, I. Y., Bregestovski, P., and Zilberter, Y. (2010). Energy substrate availability as a determinant of neuronal resting potential, GABA signaling and spontaneous network activity in the neonatal cortex *in vitro*. *J. Neurochem.* 112, 900–912. doi: 10.1111/j.1471-4159.2009.06506.x

Hou, X., Weng, Y., Wang, T., Ouyang, B., Li, Y., Song, Z., et al. (2018). Suppression of HDAC2 in spinal cord alleviates mechanical hyperalgesia and restores KCC2 expression in a rat model of bone cancer pain. *Neuroscience* 377, 138–149. doi: 10.1016/j.neuroscience.2018.02.026

Hu, D., Yu, Z.-L., Zhang, Y., Han, Y., Zhang, W., Lu, L., et al. (2017). Bumetanide treatment during early development rescues maternal separation-induced susceptibility to stress. *Sci. Rep.* 7:11878. doi: 10.1038/s41598-017-12183-z

Huberfeld, G., Wittner, L., Clemenceau, S., Baulac, M., Kaila, K., Miles, R., et al. (2007). Perturbed chloride homeostasis and GABAergic signaling in human temporal lobe epilepsy. *J. Neurosci.* 27, 9866–9873. doi: 10.1523/jneurosci.2761-07.2007

Hübner, C. A., Stein, V., Hermans-Borgmeyer, I., Meyer, T., Ballanyi, K., and Jentsch, T. J. (2001b). Disruption of KCC2 reveals an essential role of K-Cl Cotransport Already in Early Synaptic Inhibition. *Neuron* 30, 515–524. doi: 10.1016/s0896-6273(01)00297-5

Hübner, C. A., Lorke, D. E., and Hermans-Borgmeyer, I. (2001a). Expression of the Na-K-2Cl-cotransporter NKCC1 during mouse development. *Mech. Dev.* 102, 267–269. doi: 10.1016/s0925-4773(01)00309-4

Hui, K., Katayama, Y., Nakayama, K. I., Nomura, J., and Sakurai, T. (2018). Characterizing vulnerable brain areas and circuits in mouse models of autism: towards understanding pathogenesis and new therapeutic approaches. *Neurosci. Biobehav. Rev.* 110, 77–91. doi: 10.1016/j.neubiorev.2018.08.001

Hyde, T. M., Lipska, B. K., Ali, T., Mathew, S. V., Law, A. J., Metitiri, O. E., et al. (2011). Expression of GABA signaling molecules KCC2, NKCC1, and GAD1 in cortical development and schizophrenia. *J. Neurosci.* 31, 11088–11095. doi: 10.1523/jneurosci.1234-11.2011

Jarolimek, W., Lewen, A., and Misgeld, U. (1999). A Furosemide-Sensitive K+–Cl-cotransporter counteracts intracellular Cl− accumulation and depletion in cultured rat midbrain neurons. *J. Neurosci.* 19, 4695–4704. doi: 10.1523/jneurosci.19-12-04695.1999

Jayakumar, A. R., Liu, M., Moriyama, M., Ramakrishnan, R., Forbush, B., Reddy, P. V. B., et al. (2008). Na-K-Cl cotransporter-1 in the mechanism of ammonia-induced astrocyte swelling. *J. Biol. Chem.* 283, 33874–33882. doi: 10.1074/jbc.m804016200

Jayakumar, A. R., and Norenberg, M. D. (2010). The Na–K–Cl Co-transporter in astrocyte swelling. *Metab. Brain Dis.* 25, 31–38. doi: 10.1007/s11011-010-9180-3

Jayakumar, A. R., Panickar, K. S., Curtis, K. M., Tong, X. Y., Moriyama, M., and Norenberg, M. D. (2011). Na-K-Cl cotransporter-1 in the mechanism of cell swelling in cultured astrocytes after fluid percussion injury. *J. Neurochem.* 117, 437–448. doi: 10.1111/j.1471-4159.2011.07211.x

Kahle, K. T., Merner, N. D., Friedel, P., Silayeva, L., Liang, B., Khanna, A., et al. (2014). Genetically encoded impairment of neuronal KCC2 cotransporter function in human idiopathic generalized epilepsy. *EMBO Rep.* 15, 766–774. doi: 10.15252/embr.201438840

Kahle, K. T., Rinehart, J., de los Heros, P., Louvi, A., Meade, P., Vazquez, N., et al. (2005). WNK3 modulates transport of Cl− in and out of cells: implications for control of cell volume and neuronal excitability. *Proc. Natl. Acad. Sci. U.S.A.* 102, 16783–16788. doi: 10.1073/pnas.0508307102

Kakazu, Y., Akaike, N., Komiyama, S., and Nabekura, J. (1999). Regulation of intracellular chloride by cotransporters in developing lateral superior olive neurons. *J. Neurosci.* 19, 2843–2851. doi: 10.1523/jneurosci.19-08-02843.1999

Kang, J., Jiang, L., Goldman, S. A., and Nedergaard, M. (1998). Astrocyte-mediated potentiation of inhibitory synaptic transmission. *Nat. Neurosci.* 1, 683–692. doi: 10.1038/3684

Khalilov, I., Dzhala, V., Ben-Ari, Y., and Khazipov, R. (1999). Dual Role of GABA in the neonatal rat hippocampus. *Dev. Neurosci.* 21, 310–319. doi: 10.1159/000017380

Khirug, S., Huttu, K., Ludwig, A., Smirnov, S., Voipio, J., Rivera, C., et al. (2005). Distinct properties of functional KCC2 expression in immature mouse hippocampal neurons in culture and in acute slices. *Eur. J. Neurosci.* 21, 899–904. doi: 10.1111/j.1460-9568.2005.03886.x

Kim, H. R., Rajagopal, L., Meltzer, H. Y., and Martina, M. (2021). Depolarizing GABAA current in the prefrontal cortex is linked with cognitive impairment in a mouse model relevant for schizophrenia. *Sci. Adv.* 7:eaba5032. doi: 10.1126/sciadv.aba5032

Kim, J.-Y., and Paredes, M. F. (2021). Implications of extended inhibitory neuron development. *Int. J. Mol. Sci.* 22:5113. doi: 10.3390/ijms22105113

King, S. J., Bunz, M., Chappell, A., Scharl, M., Docherty, M., Jung, B., et al. (2019). AMPK mediates inhibition of electrolyte transport and NKCC1 activity by reactive oxygen species. *Am. J. Physiol. Gastrointest. Liver Physiol.* 317, G171–G181. doi: 10.1152/ajpgi.00317.2018

Kirmse, K., Kummer, M., Kovalchuk, Y., Witte, O. W., Garaschuk, O., and Holthoff, K. (2015). GABA depolarizes immature neurons and inhibits network activity in the neonatal neocortex *in vivo*. *Nat. Commun.* 6:7750. doi: 10.1038/ncomms8750

Kitayama, T., Morita, K., Motoyama, N., and Dohi, T. (2016). Down-regulation of zinc transporter-1 in astrocytes induces neuropathic pain via the brain-derived neurotrophic factor - K+-Cl− co-transporter-2 signaling pathway in the mouse spinal cord. *Neurochem. Int.* 101, 120–131. doi: 10.1016/j.neuint.2016.11.001

Kobayashi, K., Haneda, E., Higuchi, M., Suhara, T., and Suzuki, H. (2012). Chronic fluoxetine selectively upregulates dopamine D1-like receptors in the hippocampus. *Neuropsychopharmacology* 37, 1500–1508. doi: 10.1038/npp.2011.335

Kobayashi, K., Ikeda, Y., Sakai, A., Yamasaki, N., Haneda, E., Miyakawa, T., et al. (2010). Reversal of hippocampal neuronal maturation by serotonergic antidepressants. *Proc. Natl. Acad. Sci. U.S.A.* 107, 8434–8439. doi: 10.1073/pnas.0912690107

Kobayashi, M., Nakatani, T., Koda, T., Matsumoto, K., Ozaki, R., Mochida, N., et al. (2014). Absence of BRINP1 in mice causes increase of hippocampal neurogenesis and behavioral alterations relevant to human psychiatric disorders. *Mol. Brain* 7:12. doi: 10.1186/1756-6606-7-12

Koumangoye, R., Bastarache, L., and Delpire, E. (2020). NKCC1: newly found as a human disease-causing ion transporter. *Function* 2:zqaa028. doi: 10.1093/function/zqaa028

Kubota, Y., Karube, F., Nomura, M., and Kawaguchi, Y. (2016). The diversity of cortical inhibitory synapses. *Front. Neural Circuits* 10:27. doi: 10.3389/fncir.2016.00027

Kuner, T., and Augustine, G. J. (2000). A genetically encoded ratiometric indicator for chloride capturing chloride transients in cultured hippocampal neurons. *Neuron* 27, 447–459. doi: 10.1016/s0896-6273(00)00056-8

Kyrozis, A., Chudomel, O., Moshé, S. L., and Galanopoulou, A. S. (2006). Sex-dependent maturation of GABAA receptor-mediated synaptic events in rat substantia nigra reticulata. *Neurosci. Lett.* 398, 1–5. doi: 10.1016/j.neulet.2005.12.018

Langlois, A., Diabira, D., Ferrand, N., Porcher, C., and Gaiarsa, J.-L. (2013). NMDA-Dependent Switch of proBDNF Actions on Developing GABAergic Synapses. *Cereb. Cortex* 23, 1085–1096. doi: 10.1093/cercor/bhs071

LaSalle, J. (2013). Autism genes keep turning up chromatin. *OA Autism* 1:14. doi: 10.13172/2052-7810-1-2-610

Laurie, D., Wisden, W., and Seeburg, P. (1992). The distribution of thirteen GABAA receptor subunit mRNAs in the rat brain. III. Embryonic and postnatal development. *J. Neurosci.* 12, 4151–4172.

Lee, H. H. C., Deeb, T. Z., Walker, J. A., Davies, P. A., and Moss, S. J. (2011). NMDA receptor activity downregulates KCC2 resulting in depolarizing GABAA receptor–mediated currents. *Nat. Neurosci.* 14, 736–743. doi: 10.1038/nn.2806

Lee, H. A., Hong, S., Kim, J., and Jang, I. (2010). Possible involvement of DNA methylation in NKCC1 gene expression during postnatal development and in response to ischemia. *J. Neurochem.* 114, 520–529. doi: 10.1111/j.1471-4159.2010.06772.x

Lee, H. H. C., Jurd, R., and Moss, S. J. (2010). Tyrosine phosphorylation regulates the membrane trafficking of the potassium chloride co-transporter KCC2. *Mol. Cell. Neurosci.* 45, 173–179. doi: 10.1016/j.mcn.2010.06.008

Lee, H. H. C., Walker, J. A., Williams, J. R., Goodier, R. J., Payne, J. A., and Moss, S. J. (2007). Direct Protein Kinase C-dependent Phosphorylation Regulates the Cell Surface Stability and Activity of the Potassium Chloride Cotransporter KCC2. *J. Biol. Chem.* 282, 29777–29784. doi: 10.1074/jbc.m705053200

Leinekugel, X., Tseeb, V., Ben-Ari, Y., and Bregestovski, P. (1995). Synaptic GABAA activation induces Ca2+ rise in pyramidal cells and interneurons from rat neonatal hippocampal slices. *J. Physiol.* 487, 319–329. doi: 10.1113/jphysiol.1995.sp020882

Leitch, E., Coaker, J., Young, C., Mehta, V., and Sernagor, E. (2005). GABA type-A activity controls its own developmental polarity switch in the maturing retina. *J. Neurosci.* 25, 4801–4805. doi: 10.1523/jneurosci.0172-05.2005

Lemonnier, E., and Ben-Ari, Y. (2010). The diuretic bumetanide decreases autistic behaviour in five infants treated during 3 months with no side effects. *Acta Paediatr.* 99, 1885–1888. doi: 10.1111/j.1651-2227.2010.01933.x

Lemonnier, E., Degrez, C., Phelep, M., Tyzio, R., Josse, F., Grandgeorge, M., et al. (2012). A randomised controlled trial of bumetanide in the treatment of autism in children. *Transl. Psychiatry* 2:e202. doi: 10.1038/tp.2012.124

Lemonnier, E., Lazartigues, A., and Ben-Ari, Y. (2016). Treating Schizophrenia with the diuretic bumetanide: a case report. *Clin. Neuropharmacol.* 39, 115–117. doi: 10.1097/wnf.0000000000000136

Lemonnier, E., Villeneuve, N., Sonie, S., Serret, S., Rosier, A., Roue, M., et al. (2017). Effects of bumetanide on neurobehavioral function in children and adolescents with autism spectrum disorders. *Transl. Psychiatry* 7:e1056. doi: 10.1038/tp.2017.10

Leonzino, M., Busnelli, M., Antonucci, F., Verderio, C., Mazzanti, M., and Chini, B. (2016). The Timing of the Excitatory-to-Inhibitory GABA switch is regulated by the oxytocin receptor via KCC2. *Cell Rep.* 15, 96–103. doi: 10.1016/j.celrep.2016.03.013

Li, Y., Schaffner, A. E., Walton, M. K., and Barker, J. L. (1998). Astrocytes regulate developmental changes in the chloride ion gradient of embryonic rat ventral spinal cord neurons in culture. *J. Physiol.* 509, 847–858. doi: 10.1111/j.1469-7793.1998.847bm.x

Lim, L., Mi, D., Llorca, A., and Marín, O. (2018). Development and functional diversification of cortical interneurons. *Neuron* 100, 294–313. doi: 10.1016/j.neuron.2018.10.009

Liu, Q., Xu, Q., Arcuino, G., Kang, J., and Nedergaard, M. (2004). Astrocyte-mediated activation of neuronal kainate receptors. *Proc. Natl. Acad. Sci. U.S.A.* 101, 3172–3177. doi: 10.1073/pnas.0306731101

Liu, Z., Neff, R. A., and Berg, D. K. (2006). Sequential interplay of nicotinic and GABAergic signaling guides neuronal development. *Science* 314, 1610–1613. doi: 10.1126/science.1134246

LoTurco, J. J., Owens, D. F., Heath, M. J. S., Davis, M. B. E., and Kriegstein, A. R. (1995). GABA and glutamate depolarize cortical progenitor cells and inhibit DNA synthesis. *Neuron* 15, 1287–1298. doi: 10.1016/0896-6273(95)90008-x

Lu, J., Karadsheh, M., and Delpire, E. (1999). Developmental regulation of the neuronal-specific isoform of K-CL cotransporter KCC2 in postnatal rat brains. *J. Neurobiol.* 39, 558–568.

Ludwig, A., Li, H., Saarma, M., Kaila, K., and Rivera, C. (2003). Developmental up-regulation of KCC2 in the absence of GABAergic and glutamatergic transmission. *Eur. J. Neurosci.* 18, 3199–3206. doi: 10.1111/j.1460-9568.2003.03069.x

Ludwig, A., Uvarov, P., Soni, S., Thomas-Crusells, J., Airaksinen, M. S., and Rivera, C. (2011). Early Growth Response 4 Mediates BDNF Induction of Potassium Chloride Cotransporter 2 Transcription. *J. Neurosci.* 31, 644–649. doi: 10.1523/jneurosci.2006-10.2011

Luhmann, H. J., Fukuda, A., and Kilb, W. (2015). Control of cortical neuronal migration by glutamate and GABA. *Front. Cell. Neurosci.* 9:4. doi: 10.3389/fncel.2015.00004

Macnamara, E. F., Koehler, A. E., D'Souza, P., Estwick, T., Lee, P., Vezina, G., et al. (2019). Kilquist syndrome: a novel syndromic hearing loss disorder caused by homozygous deletion of SLC12A2. *Hum. Mutat.* 40, 532–538. doi: 10.1002/humu.23722

MacVicar, B., Tse, F., Crichton, S., and Kettenmann, H. (1989). GABA-activated Cl− channels in astrocytes of hippocampal slices. *J. Neurosci.* 9, 3577–3583. doi: 10.1523/jneurosci.09-10-03577.1989

Magalhães, A. C., and Rivera, C. (2016). NKCC1-deficiency results in abnormal proliferation of neural progenitor cells of the lateral ganglionic eminence. *Front. Cell. Neurosci.* 10:200. doi: 10.3389/fncel.2016.00200

Mahadevan, V., Pressey, J. C., Acton, B. A., Uvarov, P., Huang, M. Y., Chevrier, J., et al. (2014). Kainate receptors coexist in a functional complex with KCC2 and regulate chloride homeostasis in hippocampal neurons. *Cell Rep.* 7, 1762–1770. doi: 10.1016/j.celrep.2014.05.022

Marchese, M., Valvo, G., Moro, F., Sicca, F., and Santorelli, F. M. (2016). Targeted Gene Resequencing (Astrochip) to explore the tripartite synapse in autism–epilepsy phenotype with macrocephaly. *Neuromol. Med.* 18, 69–80. doi: 10.1007/s12017-015-8378-2

Maric, D., Liu, Q. Y., Maric, I., Chaudry, S., Chang, Y. H., Smith, S. V., et al. (2001). GABA expression dominates neuronal lineage progression in the embryonic rat neocortex and facilitates neurite outgrowth via GABA(A) autoreceptor/Cl− channels. *J. Neurosci.* 21, 2343–2360. doi: 10.1523/JNEUROSCI.21-07-02343.2001

Marín, O. (2012). Interneuron dysfunction in psychiatric disorders. *Nat. Rev. Neurosci.* 13, 107–120. doi: 10.1038/nrn3155

Mariotti, L., Losi, G., Lia, A., Melone, M., Chiavegato, A., Gómez-Gonzalo, M., et al. (2018). Interneuron-specific signaling evokes distinctive somatostatin-mediated responses in adult cortical astrocytes. *Nat. Commun.* 9:82. doi: 10.1038/s41467-017-02642-6

Markkanen, M., Ludwig, A., Khirug, S., Pryazhnikov, E., Soni, S., Khiroug, L., et al. (2017). Implications of the N-terminal heterogeneity for the neuronal K-Cl cotransporter KCC2 function. *Brain Res.* 1675, 87–101. doi: 10.1016/j.brainres.2017.08.034

Markkanen, M., Uvarov, P., and Airaksinen, M. S. (2008). Role of upstream stimulating factors in the transcriptional regulation of the neuron-specific K–Cl cotransporter KCC2. *Brain Res.* 1236, 8–15. doi: 10.1016/j.brainres.2008.08.007

Maset, A., Galla, L., Francia, S., Cozzolino, O., Capasso, P., Goisis, R. C., et al. (2021). Altered Cl− homeostasis hinders forebrain GABAergic interneuron migration in a mouse model of intellectual disability. *Proc. Natl. Acad. Sci. U.S.A.* 118:e2016034118. doi: 10.1073/pnas.2016034118

Matos, M., Bosson, A., Riebe, I., Reynell, C., Vallée, J., Laplante, I., et al. (2018). Astrocytes detect and upregulate transmission at inhibitory synapses of somatostatin interneurons onto pyramidal cells. *Nat. Commun.* 9:4254. doi: 10.1038/s41467-018-06731-y

McNeill, A., Iovino, E., Mansard, L., Vache, C., Baux, D., Bedoukian, E., et al. (2020). SLC12A2 variants cause a neurodevelopmental disorder or cochleovestibular defect. *Brain* 143, 2380–2387. doi: 10.1093/brain/awaa176

Mederos, S., and Perea, G. (2019). Monitoring interneuron-astrocyte signaling and its consequences on synaptic transmission. *Methods Mol. Biol.* 1938, 117–129. doi: 10.1007/978-1-4939-9068-9_9

Mederos, S., Sánchez-Puelles, C., Esparza, J., Valero, M., Ponomarenko, A., and Perea, G. (2021). GABAergic signaling to astrocytes in the prefrontal cortex sustains goal-directed behaviors. *Nat. Neurosci.* 24, 82–92. doi: 10.1038/s41593-020-00752-x

Menshanov, P. N., Lanshakov, D. A., and Dygalo, N. N. (2015). proBDNF is a Major product of bdnf Gene Expressed in the Perinatal Rat Cortex. *Physiol. Res.* 64, 925–934. doi: 10.33549/physiolres.932996

Merner, N. D., Chandler, M. R., Bourassa, C., Liang, B., Khanna, A. R., Dion, P., et al. (2015). Regulatory domain or CpG site variation in SLC12A5, encoding the chloride transporter KCC2, in human autism and schizophrenia. *Front. Cell. Neurosci.* 9:386. doi: 10.3389/fncel.2015.00386

Merner, N. D., Mercado, A., Khanna, A. R., Hodgkinson, A., Bruat, V., Awadalla, P., et al. (2016). Gain-of-function missense variant in SLC12A2, encoding the bumetanide-sensitive NKCC1 cotransporter, identified in human schizophrenia. *J. Psychiatr. Res.* 77, 22–26. doi: 10.1016/j.jpsychires.2016.02.016

Miller, S., and Maguire, J. (2014). Deficits in KCC2 and activation of the HPA axis lead to depressionlike behavior following social defeat. *Horm. Stud.* 2, 1–10. doi: 10.7243/2052-8000-2-2

Miraucourt, L. S., Tsui, J., Gobert, D., Desjardins, J.-F., Schohl, A., Sild, M., et al. (2016). Endocannabinoid signaling enhances visual responses through modulation of intracellular chloride levels in retinal ganglion cells. *eLife* 5:e15932. doi: 10.7554/elife.15932

Miyakawa, T., Leiter, L. M., Gerber, D. J., Gainetdinov, R. R., Sotnikova, T. D., Zeng, H., et al. (2003). Conditional calcineurin knockout mice exhibit multiple abnormal behaviors related to schizophrenia. *Proc. Natl. Acad. Sci. U.S.A.* 100, 8987–8992. doi: 10.1073/pnas.1432926100

Moore, Y. E., Conway, L. C., Wobst, H. J., Brandon, N. J., Deeb, T. Z., and Moss, S. J. (2019). Developmental Regulation of KCC2 phosphorylation has long-term impacts on cognitive function. *Front. Mol. Neurosci.* 12:173. doi: 10.3389/fnmol.2019.00173

Moore, Y. E., Deeb, T. Z., Chadchankar, H., Brandon, N. J., and Moss, S. J. (2018). Potentiating KCC2 activity is sufficient to limit the onset and severity of seizures. *Proc. Natl. Acad. Sci. U.S.A.* 115, 10166–10171. doi: 10.1073/pnas.1810134115

Moriguchi, T., Urushiyama, S., Hisamoto, N., Iemura, S., Uchida, S., Natsume, T., et al. (2005). WNK1 Regulates Phosphorylation of Cation-Chloride-coupled Cotransporters via the STE20-related Kinases, SPAK and OSR1. *J. Biol. Chem.* 280, 42685–42693. doi: 10.1074/jbc.m510042200

Morita, Y., Callicott, J. H., Testa, L. R., Mighdoll, M. I., Dickinson, D., Chen, Q., et al. (2014). Characteristics of the cation cotransporter NKCC1 in human brain: alternate transcripts, expression in development, and potential relationships to brain function and schizophrenia. *J. Neurosci.* 34, 4929–4940. doi: 10.1523/jneurosci.1423-13.2014

Mukhtarov, M., Ivanov, A., Zilberter, Y., and Bregestovski, P. (2011). Inhibition of spontaneous network activity in neonatal hippocampal slices by energy substrates is not correlated with intracellular acidification. *J. Neurochem.* 116, 316–321. doi: 10.1111/j.1471-4159.2010.07111.x

Murano, T., Hagihara, H., Tajinda, K., Matsumoto, M., and Miyakawa, T. (2019). Transcriptomic immaturity inducible by neural hyperexcitation is shared by multiple neuropsychiatric disorders. *Commun. Biol.* 2:32. doi: 10.1038/s42003-018-0277-2

Murata, Y., and Colonnese, M. T. (2020). GABAergic interneurons excite neonatal hippocampus in vivo. *Sci. Adv.* 6:eaba1430. doi: 10.1126/sciadv.aba1430

Nelson, S. B., and Valakh, V. (2015). Excitatory/inhibitory balance and circuit homeostasis in autism spectrum disorders. *Neuron* 87, 684–698. doi: 10.1016/j.neuron.2015.07.033

Nesan, D., and Kurrasch, D. M. (2019). Gestational exposure to common endocrine disrupting chemicals and their impact on neurodevelopment and behavior. *Annu. Rev. Physiol.* 82, 177–202. doi: 10.1146/annurev-physiol-021119-034555

Nuñez, J. L., and McCarthy, M. M. (2007). Evidence for an extended duration of GABA-mediated excitation in the developing male versus female hippocampus. *Dev. Neurobiol.* 67, 1879–1890. doi: 10.1002/dneu.20567

Oh, W. C., Lutzu, S., Castillo, P. E., and Kwon, H.-B. (2016). De novo synaptogenesis induced by GABA in the developing mouse cortex. *Science* 353, 1037–1040. doi: 10.1126/science.aaf5206

Ohira, K., Kobayashi, K., Toyama, K., Nakamura, H. K., Shoji, H., Takao, K., et al. (2013). Synaptosomal-associated protein 25 mutation induces immaturity of the dentate granule cells of adult mice. *Mol. Brain* 6:12. doi: 10.1186/1756-6606-6-12

Okada-Ogawa, A., Nakaya, Y., Imamura, Y., Kobayashi, M., Shinoda, M., Kita, K., et al. (2015). Involvement of medullary GABAergic system in extraterritorial neuropathic pain mechanisms associated with inferior alveolar nerve transection. *Exp. Neurol.* 267, 42–52. doi: 10.1016/j.expneurol.2015.02.030

Ouellet, L., and de Villers-Sidani, E. (2014). Trajectory of the main GABAergic interneuron populations from early development to old age in the rat primary auditory cortex. *Front. Neuroanat.* 8:40. doi: 10.3389/fnana.2014.00040

Ouyang, B., Chen, D., Hou, X., Wang, T., Wang, J., Zou, W., et al. (2019). Normalizing HDAC2 Levels in the Spinal Cord Alleviates Thermal and Mechanical Hyperalgesia After Peripheral Nerve Injury and Promotes GAD65 and KCC2 Expression. *Front. Neurosci.* 13:346. doi: 10.3389/fnins.2019.00346

Owens, D. F., Boyce, L. H., Davis, M. B. E., and Kriegstein, A. R. (1996). Excitatory GABA responses in embryonic and neonatal cortical slices demonstrated by gramicidin perforated-patch recordings and calcium imaging. *J. Neurosci.* 16, 6414–6423. doi: 10.1523/jneurosci.16-20-06414.1996

Owens, D. F., Liu, X., and Kriegstein, A. R. (1999). Changing Properties of GABA A Receptor–mediated signaling during early neocortical development. *J. Neurophysiol.* 82, 570–583. doi: 10.1152/jn.1999.82.2.570

Pacheco-Alvarez, D., Cristóbal, P. S., Meade, P., Moreno, E., Vazquez, N., Muñoz, E., et al. (2006). The Na+:Cl− cotransporter is activated and phosphorylated at the amino-terminal domain upon intracellular chloride depletion. *J. Biol. Chem.* 281, 28755–28763. doi: 10.1074/jbc.m603773200

Parrini, M., Naskar, S., Alberti, M., Colombi, I., Morelli, G., Rocchi, A., et al. (2021). Restoring neuronal chloride homeostasis with anti-NKCC1 gene therapy rescues cognitive deficits in a mouse model of Down syndrome. *Mol. Ther.* 29, 3072–3092. doi: 10.1016/j.ymthe.2021.05.023

Payne, J. A., Stevenson, T. J., and Donaldson, L. F. (1996). Molecular characterization of a putative K-Cl cotransporter in rat brain. A neuronal-specific isoform. *J. Biol. Chem.* 271, 16245–16252. doi: 10.1074/jbc.271.27.16245

Pellegrino, C., Gubkina, O., Schaefer, M., Becq, H., Ludwig, A., Mukhtarov, M., et al. (2011). Knocking down of the KCC2 in rat hippocampal neurons increases intracellular chloride concentration and compromises neuronal survival. *J. Physiol.* 589, 2475–2496. doi: 10.1113/jphysiol.2010.203703

Petilla Interneuron Nomenclature Group, Ascoli, G. A., Alonso-Nanclares, L., Anderson, S. A., Barrionuevo, G., Benavides-Piccione, R., et al. (2008). Petilla terminology: nomenclature of features of GABAergic interneurons of the cerebral cortex. *Nat. Rev. Neurosci.* 9, 557–568. doi: 10.1038/nrn2402

Piala, A. T., Moon, T. M., Akella, R., He, H., Cobb, M. H., and Goldsmith, E. J. (2014). Chloride Sensing by WNK1 involves inhibition of autophosphorylation. *Sci. Signal.* 7:ra41. doi: 10.1126/scisignal.2005050

Pinto, J. G. A., Hornby, K. R., Jones, D. G., and Murphy, K. M. (2010). Developmental Changes in GABAergic mechanisms in human visual cortex across the lifespan. *Front. Cell. Neurosci.* 4:16. doi: 10.3389/fncel.2010.00016

Pisella, L. I., Gaiarsa, J.-L., Diabira, D., Zhang, J., Khalilov, I., Duan, J., et al. (2019). Impaired regulation of KCC2 phosphorylation leads to neuronal network dysfunction and neurodevelopmental pathology. *Sci. Signal.* 12:eaay0300. doi: 10.1126/scisignal.aay0300

Plotkin, M. D., Snyder, E. Y., Hebert, S. C., and Delpire, E. (1997). Expression of the Na-K-2Cl cotransporter is developmentally regulated in postnatal rat brains: a possible mechanism underlying GABA's excitatory role in immature brain. *J. Neurobiol.* 33, 781–795. doi: 10.1002/(sici)1097-4695(19971120)33:6\<781::aid-neu6\>3.0.co;2-5

Pressey, J. C., Mahadevan, V., Khademullah, C. S., Dargaei, Z., Chevrier, J., Ye, W., et al. (2017). A kainate receptor subunit promotes the recycling of the neuron-specific K+-Cl− co-transporter KCC2 in hippocampal neurons. *J. Biol. Chem.* 292, 6190–6201. doi: 10.1074/jbc.m116.767236

Puskarjov, M., Ahmad, F., Khirug, S., Sivakumaran, S., Kaila, K., and Blaesse, P. (2015). BDNF is required for seizure-induced but not developmental up-regulation of KCC2 in the neonatal hippocampus. *Neuropharmacology* 88, 103–109. doi: 10.1016/j.neuropharm.2014.09.005

Puskarjov, M., Seja, P., Heron, S. E., Williams, T. C., Ahmad, F., Iona, X., et al. (2014). A variant of KCC2 from patients with febrile seizures impairs neuronal Cl− extrusion and dendritic spine formation. *EMBO Rep.* 15, 723–729. doi: 10.1002/embr.201438749

Rahmanzadeh, R., Shahbazi, A., Ardakani, M. K., Mehrabi, S., Rahmanzade, R., and Joghataei, M. T. (2017). Lack of the effect of bumetanide, a selective NKCC1 inhibitor, in patients with schizophrenia: a double-blind randomized trial. *Psychiatry Clin. Neurosci.* 71, 72–73. doi: 10.1111/pcn.12475

Ransom, C. B., Ransom, B. R., and Sontheimer, H. (2000). Activity-dependent extracellular K+ accumulation in rat optic nerve: the role of glial and axonal Na+ pumps. *J. Physiol.* 522, 427–442. doi: 10.1111/j.1469-7793.2000.00427.x

Riffault, B., Kourdougli, N., Dumon, C., Ferrand, N., Buhler, E., Schaller, F., et al. (2016). Pro-Brain-Derived Neurotrophic Factor (proBDNF)-Mediated p75NTR Activation Promotes Depolarizing Actions of GABA and Increases Susceptibility to Epileptic Seizures. *Cereb. Cortex* 28, 510–527. doi: 10.1093/cercor/bhw385

Rinehart, J., Maksimova, Y. D., Tanis, J. E., Stone, K. L., Hodson, C. A., Zhang, J., et al. (2009). Sites of Regulated Phosphorylation that Control K-Cl Cotransporter Activity. *Cell* 138, 525–536. doi: 10.1016/j.cell.2009.05.031

Rivera, C., Li, H., Thomas-Crusells, J., Lahtinen, H., Viitanen, T., Nanobashvili, A., et al. (2002). BDNF-induced TrkB activation down-regulates the K+–Cl− cotransporter KCC2 and impairs neuronal Cl− extrusion. *J. Cell Biol.* 159, 747–752. doi: 10.1083/jcb.200209011

Rivera, C., Voipio, J., Payne, J. A., Ruusuvuori, E., Lahtinen, H., Lamsa, K., et al. (1999). The K+/Cl− co-transporter KCC2 renders GABA hyperpolarizing during neuronal maturation. *Nature* 397, 251–255. doi: 10.1038/16697

Rivera, C., Voipio, J., Thomas-Crusells, J., Li, H., Emri, Z., Sipilä, S., et al. (2004). Mechanism of activity-dependent downregulation of the neuron-specific K-Cl Cotransporter KCC2. *J. Neurosci.* 24, 4683–4691. doi: 10.1523/jneurosci.5265-03.2004

Robel, S., and Sontheimer, H. (2016). Glia as drivers of abnormal neuronal activity. *Nat. Neurosci.* 19, 28–33. doi: 10.1038/nn.4184

Roux, S., Lohof, A., Ben-Ari, Y., Poulain, B., and Bossu, J.-L. (2018). Maturation of GABAergic transmission in cerebellar purkinje cells is sex dependent and altered in the valproate model of autism. *Front. Cell. Neurosci.* 12:232. doi: 10.3389/fncel.2018.00232

Ruffolo, G., Iyer, A., Cifelli, P., Roseti, C., Mühlebner, A., van Scheppingen, J., et al. (2016). Functional aspects of early brain development are preserved in tuberous sclerosis complex (TSC) epileptogenic lesions. *Neurobiol. Dis.* 95, 93–101. doi: 10.1016/j.nbd.2016.07.014

Saito, T., Ishii, A., Sugai, K., Sasaki, M., and Hirose, S. (2017). A de novo missense mutation in SLC12A5 found in a compound heterozygote patient with epilepsy of infancy with migrating focal seizures. *Clin. Genet.* 92, 654–658. doi: 10.1111/cge.13049

Saitsu, H., Watanabe, M., Akita, T., Ohba, C., Sugai, K., Ong, W. P., et al. (2016). Impaired neuronal KCC2 function by biallelic SLC12A5 mutations in migrating focal seizures and severe developmental delay. *Sci. Rep.* 6:30072. doi: 10.1038/srep30072

Salmon, C. K., Pribiag, H., Gizowski, C., Farmer, W. T., Cameron, S., Jones, E. V., et al. (2020). Depolarizing GABA transmission restrains activity-dependent glutamatergic synapse formation in the developing hippocampal circuit. *Front. Cell. Neurosci.* 14:36. doi: 10.3389/fncel.2020.00036

Sarkar, J., Wakefield, S., MacKenzie, G., Moss, S. J., and Maguire, J. (2011). Neurosteroidogenesis is required for the physiological response to stress: role of neurosteroid-sensitive GABAA receptors. *J. Neurosci.* 31, 18198–18210. doi: 10.1523/jneurosci.2560-11.2011

Sauer, J.-F., and Bartos, M. (2010). Recruitment of early postnatal parvalbumin-positive hippocampal interneurons by GABAergic Excitation. *J. Neurosci.* 30, 110–115. doi: 10.1523/jneurosci.4125-09.2010

Savardi, A., Borgogno, M., Narducci, R., Sala, G. L., Ortega, J. A., Summa, M., et al. (2020). Discovery of a small molecule drug candidate for selective NKCC1 inhibition in brain disorders. *Chem* 6, 2073–2096. doi: 10.1016/j.chempr.2020.06.017

Sawada, T., Chater, T. E., Sasagawa, Y., Yoshimura, M., Fujimori-Tonou, N., Tanaka, K., et al. (2020). Developmental excitation-inhibition imbalance underlying psychoses revealed by single-cell analyses of discordant twins-derived cerebral organoids. *Mol. Psychiatry* 25, 2695–2711. doi: 10.1038/s41380-020-0844-z

Sedmak, G., Jovanov-Milošević, N., Puskarjov, M., Ulamec, M., Krušlin, B., Kaila, K., et al. (2015). Developmental expression patterns of KCC2 and functionally associated molecules in the human brain. *Cereb. Cortex* 26, 4574–4589. doi: 10.1093/cercor/bhv218

Sen, A., Martinian, L., Nikolic, M., Walker, M. C., Thom, M., and Sisodiya, S. M. (2007). Increased NKCC1 expression in refractory human epilepsy. *Epilepsy Res.* 74, 220–227. doi: 10.1016/j.eplepsyres.2007.01.004

Sernagor, E., Chabrol, F., Bony, G., and Cancedda, L. (2010). GABAergic control of neurite outgrowth and remodeling during development and adult neurogenesis: general rules and differences in diverse systems. *Front. Cell. Neurosci.* 4:11. doi: 10.3389/fncel.2010.00011

Sernagor, E., Young, C., and Eglen, S. J. (2003). Developmental modulation of retinal wave dynamics: shedding light on the GABA saga. *J. Neurosci.* 23, 7621–7629. doi: 10.1523/jneurosci.23-20-07621.2003

Serrano, A., Haddjeri, N., Lacaille, J.-C., and Robitaille, R. (2006). GABAergic network activation of glial cells underlies hippocampal heterosynaptic depression. *J. Neurosci.* 26, 5370–5382. doi: 10.1523/jneurosci.5255-05.2006

Shekarabi, M., Girard, N., Rivière, J.-B., Dion, P., Houle, M., Toulouse, A., et al. (2008). Mutations in the nervous system–specific HSN2 exon of WNK1 cause hereditary sensory neuropathy type II. *J. Clin. Invest.* 118, 2496–2505. doi: 10.1172/jci34088

Shekarabi, M., Lafrenière, R. G., Gaudet, R., Laganière, J., Marcinkiewicz, M. M., Dion, P. A., et al. (2013). Comparative analysis of the expression profile of Wnk1 and Wnk1/Hsn2 Splice variants in developing and adult mouse tissues. *PLoS One* 8:e57807. doi: 10.1371/journal.pone.0057807

Shekarabi, M., Zhang, J., Khanna, A. R., Ellison, D. H., Delpire, E., and Kahle, K. T. (2017). WNK kinase signaling in ion homeostasis and human disease. *Cell Metab.* 25, 285–299. doi: 10.1016/j.cmet.2017.01.007

Shigetomi, E., Tong, X., Kwan, K. Y., Corey, D. P., and Khakh, B. S. (2012). TRPA1 channels regulate astrocyte resting calcium and inhibitory synapse efficacy through GAT-3. *Nat. Neurosci.* 15, 70–80. doi: 10.1038/nn.3000

Shin, R., Kobayashi, K., Hagihara, H., Kogan, J. H., Miyake, S., Tajinda, K., et al. (2013). The immature dentate gyrus represents a shared phenotype of mouse models of epilepsy and psychiatric disease. *Bipolar Disord.* 15, 405–421. doi: 10.1111/bdi.12064

Shulga, A., Thomas-Crusells, J., Sigl, T., Blaesse, A., Mestres, P., Meyer, M., et al. (2008). Posttraumatic GABAA-Mediated [Ca2+]i Increase is essential for the induction of brain-derived neurotrophic factor-dependent survival of mature central neurons. *J. Neurosci.* 28, 6996–7005. doi: 10.1523/jneurosci.5268-07.2008

Sid, B., Miranda, L., Vertommen, D., Viollet, B., and Rider, M. H. (2010). Stimulation of human and mouse erythrocyte Na+–K+–2Cl− cotransport by osmotic shrinkage does not involve AMP-activated protein kinase, but is associated with STE20/SPS1-related proline/alanine-rich kinase activation. *J. Physiol.* 588, 2315–2328. doi: 10.1113/jphysiol.2009.185900

Silayeva, L., Deeb, T. Z., Hines, R. M., Kelley, M. R., Munoz, M. B., Lee, H. H. C., et al. (2015). KCC2 activity is critical in limiting the onset and severity of status

epilepticus. *Proc. Natl. Acad. Sci. U.S.A.* 112, 3523–3528. doi: 10.1073/pnas.1415126112

Sipila, S. T., Huttu, K., Yamada, J., Afzalov, R., Voipio, J., Blaesse, P., et al. (2009). Compensatory Enhancement of Intrinsic Spiking upon NKCC1 Disruption in Neonatal Hippocampus. *J. Neurosci.* 29, 6982–6988. doi: 10.1523/jneurosci.0443-09.2009

Soul, J. S., Bergin, A. M., Stopp, C., Hayes, B., Singh, A., Fortuno, C. R., et al. (2021). A pilot randomized, controlled, double-blind trial of bumetanide to treat neonatal seizures. *Ann. Neurol.* 89, 327–340. doi: 10.1002/ana.25959

Spoljaric, A., Seja, P., Spoljaric, I., Virtanen, M. A., Lindfors, J., Uvarov, P., et al. (2017). Vasopressin excites interneurons to suppress hippocampal network activity across a broad span of brain maturity at birth. *Proc. Natl. Acad. Sci. U.S.A.* 114, E10819–E10828. doi: 10.1073/pnas.1717337114

Sprengers, J. J., van Andel, D. M., Zuithoff, N. P. A., Keijzer-Veen, M. G., Schulp, A. J. A., Scheepers, F. E., et al. (2020). Bumetanide for Core Symptoms of Autism Spectrum Disorder (BAMBI): a single center, double-blinded, participant-randomized, placebo-controlled, phase-2 superiority trial. *J. Am. Acad. Child Adolesc. Psychiatry* 60, 865–876. doi: 10.1016/j.jaac.2020.07.888

Stödberg, T., Magnusson, M., Lesko, N., Wredenberg, A., Munoz, D. M., Stranneheim, H., et al. (2020). SLC12A2 mutations cause NKCC1 deficiency with encephalopathy and impaired secretory epithelia. *Neurol. Genet.* 6:e478. doi: 10.1212/nxg.0000000000000478

Stödberg, T., McTague, A., Ruiz, A. J., Hirata, H., Zhen, J., Long, P., et al. (2015). Mutations in SLC12A5 in epilepsy of infancy with migrating focal seizures. *Nat. Commun.* 6:8038. doi: 10.1038/ncomms9038

Strange, K., Singer, T. D., Morrison, R., and Delpire, E. (2000). Dependence of KCC2 K-Cl cotransporter activity on a conserved carboxy terminus tyrosine residue. *Am. J. Physiol. Cell Physiol.* 279, C860–C867. doi: 10.1152/ajpcell.2000.279.3.c860

Su, G., Kintner, D. B., Flagella, M., Shull, G. E., and Sun, D. (2002). Astrocytes from Na+-K+-Cl-cotransporter-null mice exhibit absence of swelling and decrease in EAA release. *Am. J. Physiol. Cell Physiol.* 282, C1147–C1160. doi: 10.1152/ajpcell.00538.2001

Sullivan, C. R., Funk, A. J., Shan, D., Haroutunian, V., and McCullumsmith, R. E. (2015). Decreased chloride channel expression in the dorsolateral prefrontal cortex in schizophrenia. *PLoS One* 10:e0123158. doi: 10.1371/journal.pone.0123158

Sun, L., Han, X., and He, S. (2011). Direction-selective circuitry in rat retina develops independently of GABAergic, cholinergic and action potential activity. *PLoS One* 6:e19477. doi: 10.1371/journal.pone.0019477

Takao, K., Kobayashi, K., Hagihara, H., Ohira, K., Shoji, H., Hattori, S., et al. (2013). Deficiency of Schnurri-2, an MHC enhancer binding protein, induces mild chronic inflammation in the brain and confers molecular, neuronal, and behavioral phenotypes related to schizophrenia. *Neuropsychopharmacology* 38, 1409–1425. doi: 10.1038/npp.2013.38

Talos, D. M., Sun, H., Kosaras, B., Joseph, A., Folkerth, R. D., Poduri, A., et al. (2012). Altered inhibition in tuberous sclerosis and type IIb cortical dysplasia. *Ann. Neurol.* 71, 539–551. doi: 10.1002/ana.22696

Tang, X., Drotar, J., Li, K., Clairmont, C. D., Brumm, A. S., Sullins, A. J., et al. (2019). Pharmacological enhancement of KCC2 gene expression exerts therapeutic effects on human Rett syndrome neurons and Mecp2 mutant mice. *Sci. Transl. Med.* 11:eaau0164. doi: 10.1126/scitranslmed.aau0164

Tang, X., Kim, J., Zhou, L., Wengert, E., Zhang, L., Wu, Z., et al. (2016). KCC2 rescues functional deficits in human neurons derived from patients with Rett syndrome. *Proc. Natl. Acad. Sci. U.S.A.* 113, 751–756. doi: 10.1073/pnas.1524013113

Tao, R., Li, C., Newburn, E. N., Ye, T., Lipska, B. K., Herman, M. M., et al. (2012). Transcript-specific associations of SLC12A5 (KCC2) in human prefrontal cortex with development, schizophrenia, and affective disorders. *J. Neurosci.* 32, 5216–5222. doi: 10.1523/jneurosci.4626-11.2012

Till, Á, Szalai, R., Hegyi, M., Kövesdi, E., Büki, G., Hadzsiev, K., et al. (2019). [A rare form of ion channel gene mutation identified as underlying cause of generalized epilepsy]. *Orv. Hetil.* 160, 835–838. doi: 10.1556/650.2019.31404

Tsuruga, K., Hashimoto, T., Kato, R., Kato, R., Uchida, Y., Hase, T., et al. (2016). Plantar injection of formalin in rats reduces the expression of a potassium chroride cotransporter KCC2 in the spinal cord and a kinase inhibitor suppresses this reduction. *Biomed. Res.* 37, 243–249. doi: 10.2220/biomedres.37.243

Tyzio, R., Cossart, R., Khalilov, I., Minlebaev, M., Hübner, C. A., Represa, A., et al. (2006). Maternal oxytocin triggers a transient inhibitory switch in GABA signaling in the fetal brain during delivery. *Science* 314, 1788–1792. doi: 10.1126/science.1133212

Tyzio, R., Nardou, R., Ferrari, D. C., Tsintsadze, T., Shahrokhi, A., Eftekhari, S., et al. (2014). Oxytocin-mediated GABA inhibition during delivery attenuates autism pathogenesis in rodent offspring. *Science* 343, 675–679. doi: 10.1126/science.1247190

Tyzio, R., Represa, A., Jorquera, I., Ben-Ari, Y., Gozlan, H., and Aniksztejn, L. (1999). The establishment of GABAergic and glutamatergic synapses on CA1 pyramidal neurons is sequential and correlates with the development of the apical dendrite. *J. Neurosci.* 19, 10372–10382. doi: 10.1523/JNEUROSCI.19-23-10372.1999

Untiet, V., Kovermann, P., Gerkau, N. J., Gensch, T., Rose, C. R., and Fahlke, C. (2017). Glutamate transporter-associated anion channels adjust intracellular chloride concentrations during glial maturation. *Glia* 65, 388–400. doi: 10.1002/glia.23098

Uvarov, P., Ludwig, A., Markkanen, M., Pruunsild, P., Kaila, K., Delpire, E., et al. (2007). A Novel N-terminal Isoform of the Neuron-specific K-Cl Cotransporter KCC2. *J. Biol. Chem.* 282, 30570–30576. doi: 10.1074/jbc.m705095200

Uvarov, P., Ludwig, A., Markkanen, M., Rivera, C., and Airaksinen, M. S. (2006). Upregulation of the Neuron-Specific K+/Cl− Cotransporter Expression by Transcription Factor Early Growth Response 4. *J. Neurosci.* 26, 13463–13473. doi: 10.1523/jneurosci.4731-06.2006

Uvarov, P., Pruunsild, P., Timmusk, T., and Airaksinen, M. S. (2005). Neuronal K+/Cl− co-transporter (KCC2) transgenes lacking neurone restrictive silencer element recapitulate CNS neurone-specific expression and developmental up-regulation of endogenous KCC2 gene. *J. Neurochem.* 95, 1144–1155. doi: 10.1111/j.1471-4159.2005.03434.x

Valeeva, G., Tressard, T., Mukhtarov, M., Baude, A., and Khazipov, R. (2016). An Optogenetic Approach for Investigation of Excitatory and Inhibitory Network GABA Actions in Mice Expressing Channelrhodopsin-2 in GABAergic Neurons. *J. Neurosci.* 36, 5961–5973. doi: 10.1523/jneurosci.3482-15.2016

Virtanen, M. A., Uvarov, P., Hübner, C. A., and Kaila, K. (2020). NKCC1, an elusive molecular target in brain development: making sense of the existing data. *Cells* 9:2607. doi: 10.3390/cells9122607

Vitari, A. C., Thastrup, J., Rafiqi, F. H., Deak, M., Morrice, N. A., Karlsson, H. K. R., et al. (2006). Functional interactions of the SPAK/OSR1 kinases with their upstream activator WNK1 and downstream substrate NKCC1. *Biochem. J.* 397, 223–231. doi: 10.1042/bj20060220

Vu, T. Q., Payne, J. A., and Copenhagen, D. R. (2000). Localization and developmental expression patterns of the neuronal K-Cl cotransporter (KCC2) in the rat retina. *J. Neurosci.* 20, 1414–1423. doi: 10.1523/JNEUROSCI.20-04-01414.2000

Wafford, K. A., Bain, C. J., Whiting, P. J., and Kemp, J. A. (1993). Functional comparison of the role of gamma subunits in recombinant human gamma-aminobutyric acidA/benzodiazepine receptors. *Mol. Pharmacol.* 44, 437–442.

Wake, H., Watanabe, M., Moorhouse, A. J., Kanematsu, T., Horibe, S., Matsukawa, N., et al. (2007). Early Changes in KCC2 Phosphorylation in Response to Neuronal Stress Result in Functional Downregulation. *J. Neurosci.* 27, 1642–1650. doi: 10.1523/jneurosci.3104-06.2007

Walton, N. M., Zhou, Y., Kogan, J. H., Shin, R., Webster, M., Gross, A. K., et al. (2012). Detection of an immature dentate gyrus feature in human schizophrenia/bipolar patients. *Transl. Psychiatry* 2:e135. doi: 10.1038/tp.2012.56

Wang, D. D., and Kriegstein, A. R. (2008). GABA regulates excitatory synapse formation in the neocortex via NMDA receptor activation. *J. Neurosci.* 28, 5547–5558. doi: 10.1523/jneurosci.5599-07.2008

Wang, D. D., and Kriegstein, A. R. (2011). Blocking Early GABA Depolarization with Bumetanide Results in Permanent Alterations in Cortical Circuits and Sensorimotor Gating Deficits. *Cereb. Cortex* 21, 574–587. doi: 10.1093/cercor/bhq124

Wang, F., Smith, N. A., Xu, Q., Fujita, T., Baba, A., Matsuda, T., et al. (2012). Astrocytes modulate neural network activity by Ca^2+-dependent uptake of extracellular K+. *Sci. Signal.* 5:ra26. doi: 10.1126/scisignal.2002334

Watanabe, M., Wake, H., Moorhouse, A. J., and Nabekura, J. (2009). Clustering of Neuronal K+-Cl− Cotransporters in Lipid Rafts by Tyrosine Phosphorylation. *J. Biol. Chem.* 284, 27980–27988. doi: 10.1074/jbc.m109.043620

Watanabe, M., Zhang, J., Mansuri, M. S., Duan, J., Karimy, J. K., Delpire, E., et al. (2019). Developmentally regulated KCC2 phosphorylation is essential for dynamic GABA-mediated inhibition and survival. *Sci. Signal.* 12:eaaw9315. doi: 10.1126/scisignal.aaw9315

Weber, M., Hartmann, A.-M., Beyer, T., Ripperger, A., and Nothwang, H. G. (2014). A Novel Regulatory Locus of Phosphorylation in the C Terminus of the Potassium Chloride Cotransporter KCC2 That Interferes with N-Ethylmaleimide or Staurosporine-mediated Activation. *J. Biol. Chem.* 289, 18668–18679. doi: 10.1074/jbc.m114.567834

Wells, J. E., Porter, J. T., and Agmon, A. (2000). GABAergic inhibition suppresses paroxysmal network activity in the neonatal rodent hippocampus and neocortex. *J. Neurosci.* 20, 8822–8830. doi: 10.1523/jneurosci.20-23-08822.2000

Winnubst, J., Cheyne, J. E., Niculescu, D., and Lohmann, C. (2015). Spontaneous activity drives local synaptic plasticity *in vivo*. *Neuron* 87, 399–410. doi: 10.1016/j.neuron.2015.06.029

Yamada, J., Okabe, A., Toyoda, H., Kilb, W., Luhmann, H. J., and Fukuda, A. (2004). Cl− uptake promoting depolarizing GABA actions in immature rat neocortical neurones is mediated by NKCC1. *J. Physiol.* 557, 829–841. doi: 10.1113/jphysiol.2004.062471

Yamasaki, N., Maekawa, M., Kobayashi, K., Kajii, Y., Maeda, J., Soma, M., et al. (2008). Alpha-CaMKII deficiency causes immature dentate gyrus, a novel candidate endophenotype of psychiatric disorders. *Mol. Brain* 1:6. doi: 10.1186/1756-6606-1-6

Yan, Y., Dempsey, R. J., and Sun, D. (2001). Na+-K+-Cl− Cotransporter in Rat Focal Cerebral Ischemia. *J. Cereb. Blood Flow Metab.* 21, 711–721. doi: 10.1097/00004647-200106000-00009

Yang, J., Harte-Hargrove, L. C., Siao, C.-J., Marinic, T., Clarke, R., Ma, Q., et al. (2014). proBDNF negatively regulates neuronal remodeling, synaptic transmission, and synaptic plasticity in hippocampus. *Cell Rep.* 7, 796–806. doi: 10.1016/j.celrep.2014.03.040

Yeo, M., Berglund, K., Augustine, G., and Liedtke, W. (2009). Novel Repression of Kcc2 Transcription by REST–RE-1 controls developmental switch in neuronal chloride. *J. Neurosci.* 29, 14652–14662. doi: 10.1523/jneurosci.2934-09.2009

Yeo, M., Berglund, K., Hanna, M., Guo, J. U., Kittur, J., Torres, M. D., et al. (2013). Bisphenol A delays the perinatal chloride shift in cortical neurons by epigenetic effects on the Kcc2 promoter. *Proc. Natl. Acad. Sci. U.S.A.* 110, 4315–4320. doi: 10.1073/pnas.1300959110

Young, S. Z., Taylor, M. M., Wu, S., Ikeda-Matsuo, Y., Kubera, C., and Bordey, A. (2012). NKCC1 knockdown decreases neuron production through GABAA-regulated neural progenitor proliferation and delays dendrite development. *J. Neurosci.* 32, 13630–13638. doi: 10.1523/jneurosci.2864-12.2012

Yu, X., Taylor, A. M. W., Nagai, J., Golshani, P., Evans, C. J., Coppola, G., et al. (2018). Reducing astrocyte calcium signaling *in vivo* alters striatal microcircuits and causes repetitive behavior. *Neuron* 99, 1170–1187.e9. doi: 10.1016/j.neuron.2018.08.015

Zafeiriou, M.-P., Bao, G., Hudson, J., Halder, R., Blenkle, A., Schreiber, M.-K., et al. (2020). Developmental GABA polarity switch and neuronal plasticity in Bioengineered Neuronal Organoids. *Nat. Commun.* 11:3791. doi: 10.1038/s41467-020-17521-w

Zhang, L., Huang, C.-C., Dai, Y., Luo, Q., Ji, Y., Wang, K., et al. (2020). Symptom improvement in children with autism spectrum disorder following bumetanide administration is associated with decreased GABA/glutamate ratios. *Transl. Psychiatry* 10:9. doi: 10.1038/s41398-020-0692-2

Zhang, L.-L., Pathak, H. R., Coulter, D. A., Freed, M. A., and Vardi, N. (2005). Shift of intracellular chloride concentration in ganglion and amacrine cells of developing mouse retina. *J. Neurophysiol.* 95, 2404–2416. doi: 10.1152/jn.00578.2005

Zhao, X.-F., Kohen, R., Parent, R., Duan, Y., Fisher, G. L., Korn, M. J., et al. (2018). PlexinA2 Forward Signaling through Rap1 GTPases regulates dentate gyrus development and schizophrenia-like behaviors. *Cell Rep.* 22, 456–470. doi: 10.1016/j.celrep.2017.12.044

Zhu, L., Lovinger, D., and Delpire, E. (2005). Cortical Neurons Lacking KCC2 expression show impaired regulation of intracellular chloride. *J. Neurophysiol.* 93, 1557–1568. doi: 10.1152/jn.00616.2004

Zilberter, Y., Zilberter, T., and Bregestovski, P. (2010). Neuronal activity in vitro and the in vivo reality: the role of energy homeostasis. *Trends Pharmacol. Sci.* 31, 394–401. doi: 10.1016/j.tips.2010.06.005

Conflict of Interest: The authors declare that the research was conducted in the absence of any commercial or financial relationships that could be construed as a potential conflict of interest.

frontiers | Frontiers in Molecular Neuroscience

TYPE Review
PUBLISHED 22 July 2022
DOI 10.3389/fnmol.2022.964488

OPEN ACCESS

EDITED BY
Atsuo Fukuda,
Hamamatsu University School of Medicine, Japan

REVIEWED BY
Sabine Levi,
Institut National de la Santé et de la Recherche Médicale (INSERM), France
Pavel Uvarov,
University of Helsinki, Finland

*CORRESPONDENCE
Anna-Maria Hartmann
anna.maria.hartmann@uol.de

SPECIALTY SECTION
This article was submitted to Neuroplasticity and Development, a section of the journal Frontiers in Molecular Neuroscience

RECEIVED 08 June 2022
ACCEPTED 06 July 2022
PUBLISHED 22 July 2022

CITATION
Hartmann A-M and Nothwang HG (2022) NKCC1 and KCC2: Structural insights into phospho-regulation. *Front. Mol. Neurosci.* 15:964488. doi: 10.3389/fnmol.2022.964488

NKCC1 and KCC2: Structural insights into phospho-regulation

Anna-Maria Hartmann[1,2]* and Hans Gerd Nothwang[1,2,3]

[1]Division of Neurogenetics, School of Medicine and Health Sciences, Carl von Ossietzky University Oldenburg, Oldenburg, Germany, [2]Research Center for Neurosensory Sciences, Carl von Ossietzky University Oldenburg, Oldenburg, Germany, [3]Center of Excellence Hearing4all, Carl von Ossietzky University Oldenburg, Oldenburg, Germany

Inhibitory neurotransmission plays a fundamental role in the central nervous system, with about 30–50% of synaptic connections being inhibitory. The action of both inhibitory neurotransmitter, gamma-aminobutyric-acid (GABA) and glycine, mainly relies on the intracellular Cl^- concentration in neurons. This is set by the interplay of the cation chloride cotransporters NKCC1 (Na^+, K^+, Cl^- cotransporter), a main Cl^- uptake transporter, and KCC2 (K^+, Cl^- cotransporter), the principle Cl^- extruder in neurons. Accordingly, their dysfunction is associated with severe neurological, psychiatric, and neurodegenerative disorders. This has triggered great interest in understanding their regulation, with a strong focus on phosphorylation. Recent structural data by cryogenic electron microscopy provide the unique possibility to gain insight into the action of these phosphorylations. Interestingly, in KCC2, six out of ten (60%) known regulatory phospho-sites reside within a region of 134 amino acid residues (12% of the total residues) between helices α8 and α9 that lacks fixed or ordered three-dimensional structures. It thus represents a so-called intrinsically disordered region. Two further phospho-sites, Tyr^{903} and Thr^{906}, are also located in a disordered region between the ß8 strand and the α8 helix. We make the case that especially the disordered region between helices α8 and α9 acts as a platform to integrate different signaling pathways and simultaneously constitute a flexible, highly dynamic linker that can survey a wide variety of distinct conformations. As each conformation can have distinct binding affinities and specificity properties, this enables regulation of $[Cl^-]_i$ and thus the ionic driving force in a history-dependent way. This region might thus act as a molecular processor underlying the well described phenomenon of ionic plasticity that has been ascribed to inhibitory neurotransmission. Finally, it might explain the stunning long-range effects of mutations on phospho-sites in KCC2.

KEYWORDS

CCC, structure, phosphorylation, conformational changes, synaptic inhibition, intrinsically disordered region, neurological diseases

Abbreviations: CCC, cation chloride cotransporter; KCC, K^+, Cl^-cotransporter, NKCC, Na^+, K^+, Cl^- cotransporter, GABA, gamma-aminobutyric acid, TM, transmembrane domain.

Introduction

Information transfer in the brain requires a homeostatic control of neuronal firing rate (Turrigiano and Nelson, 2004; Eichler and Meier, 2008). Therefore, a functional balance between excitatory and inhibitory synapses (E-I balance) is established during development and maintained throughout life (Turrigiano and Nelson, 2004; Eichler and Meier, 2008). Excitatory synaptic transmission is mainly mediated through glutamatergic synapses and inhibitory synaptic transmission by GABAergic and glycinergic signaling (Eichler and Meier, 2008). The inhibitory neurotransmitters GABA (gamma aminobutyric acid) and glycine mainly bind to ionotropic $GABA_A$ and glycine receptors ($GABA_AR$ and GlyR), correspondingly (Bormann et al., 1987). GABA is the main inhibitory neurotransmitter in both the brain and spinal cord, since $GABA_AR$ are widely expressed in these tissues [reviewed in Möhler (2006)]. Glycine is mainly present in the brainstem and spinal cord, where it acts on a variety of neurons involved in motor and sensory function [reviewed in Rahmati et al. (2018)]. In mature neurons, the binding of the inhibitory neurotransmitters results in Cl^- influx due to a low intracellular Cl^- ($[Cl^-]_i$) concentration and thus to hyperpolarizing inhibitory post-synaptic potentials (**Figure 1**). In contrast, in immature neurons, binding of GABA and glycine to their respective ionotropic receptors leads to an efflux of Cl^- due to a high $[Cl^-]_i$ (Cherubini et al., 1990, 1991; Luhmann and Prince, 1991; Zhang et al., 1991; Ehrlich et al., 1999; Ben-Ari et al., 2007; Rahmati et al., 2018; **Figure 1**). This results in a depolarizing action. The developmental shift from depolarization to hyperpolarization (D/H shift) occurs during early postnatal life (Blaesse et al., 2009; Kaila et al., 2014) and is present throughout the nervous system (e.g., cortex, hippocampus, hypothalamus, brainstem, and spinal cord) (Ben-Ari et al., 1983; Cherubini et al., 1990; Luhmann and Prince, 1991; Wu et al., 1992; Kandler and Friauf, 1995; Owens et al., 1996; Rohrbough and Spitzer, 1996; Ehrlich et al., 1999). However, the timing of the D/H shift can differ between species such as precocial (e.g., guinea pig, prenatal D/H shift) and altricial (e.g., rat and mice, postnatal D/H shift) species (Rivera et al., 1999). Furthermore, even within a species, timing differences exist between different neuronal populations (Löhrke et al., 2005).

Important players to regulate the D/H shift are the secondary active membrane transporters NKCC1 (sodium potassium chloride cotransporter 1) and KCC2 (potassium chloride cotransporter 2) (Delpire, 2000; Payne et al., 2003; Moore et al., 2017; Virtanen et al., 2021). Both transporters mediate the Cl^- coupled transport of K^+ with or without Na^+ across the plasma membrane. In immature neurons, NKCC1 is one of the main Cl^- uptake transporter, maintaining a high $[Cl^-]_i$ (**Figure 1**; Sung et al., 2000; Ikeda et al., 2004; Dzhala et al., 2005; Achilles et al., 2007). In mature neurons, KCC2 is the essential Cl^- extruder that lowers $[Cl^-]_i$ and thus enables fast hyperpolarizing post-synaptic inhibition due to Cl^- influx (Kaila, 1994; Rivera et al., 1999). NKCC1 is also expressed in mature neurons, but the mRNA expression developmentally changes from a neuronal pattern at birth to a glial pattern (esp. oligodendrocytes and their precursors, endothelial cells, astrocytes and microglia) in adult mouse brain (Hübner et al., 2001a; Su et al., 2001; Wang et al., 2003; Zhang et al., 2014; Henneberger et al., 2020; Virtanen et al., 2020; Tóth et al., 2022). In glia cells, NKCC1 regulates for instance the proliferation and maturation of oligodendrocyte precursor cells in the adult mouse cerebellar white mater (Zonouzi et al., 2015) and modulates the microglial phenotype and inflammatory response (Tóth et al., 2022).

The physiological relevance of NKCC1 and KCC2 is corroborated by the phenotypes present in knock-out mice. Mice with disruption of the gene *Slc12a2* encoding both NKCC1 splice variants (NKCC1a and NKCCb) are viable, but suffer from deafness, pain perception, and male infertility (Randall et al., 1997; Delpire et al., 1999; Delpire and Mount, 2002). Mice with disruption of the gene *Slc12a5* that encodes both splice variants of KCC2 (KCC2a and KCC2b) die shortly after birth due to severe motor deficits that also affect respiration (Hübner et al., 2001b; Uvarov et al., 2007).

Several other plasma membrane Cl^- channels and transporters are present to regulate Cl^- homeostasis in neurons [see review: (Rahmati et al., 2018)]. These include the voltage-gated Cl^- channels (e.g., ClC-1 to 3), Ca^{2+} activated Cl^- channels (TMEM16 family, anoctamins), the pH sensitive Cl^- channels and transporters of the *SLC4* family [Na^+-independent Cl^-/HCO^{3-} exchangers (e.g., AE3) and Na^+-dependent Cl^-/HCO^{3-} exchangers (e.g., NCBE and NDCBE)], and *SLC26* family [e.g., anion exchange transporter (*SLC26A7*) and sodium independent sulfate anion transporter (*SLC26A11*)] and glutamate-activated Cl^- channels (EAAT4) (Blaesse et al., 2009; Rahmati et al., 2018; Kilb, 2020). In this review, we will focus on the secondary active transporters NKCC1 and KCC2.

Ionic plasticity

Inhibitory neurotransmission mediated by $GABA_A$ or glycine receptors is somewhat unique in that its function can be relatively easily modified *via* changes to the ionic driving force. In mature neurons, a low $[Cl^-]_i$ results in E_{Cl} being slightly hyperpolarized with respect to the neuronal resting membrane potential V_{rest} (**Figure 1**). In P12 auditory neurons of the lateral superior olive, for instance, $[Cl^-]_i$ is 8 ± 5 mM, and in cortical pyramidal neurons cultured for 21 days, it is 7.3 ± 0.2 mM (Balakrishnan et al., 2003; Zhu et al., 2005). In such conditions, $GABA_A$ or glycine receptor activation results in an inward Cl^- gradient that reduces excitability by pulling the membrane potential away from threshold. This decreases the probability of action potential generation. However, even

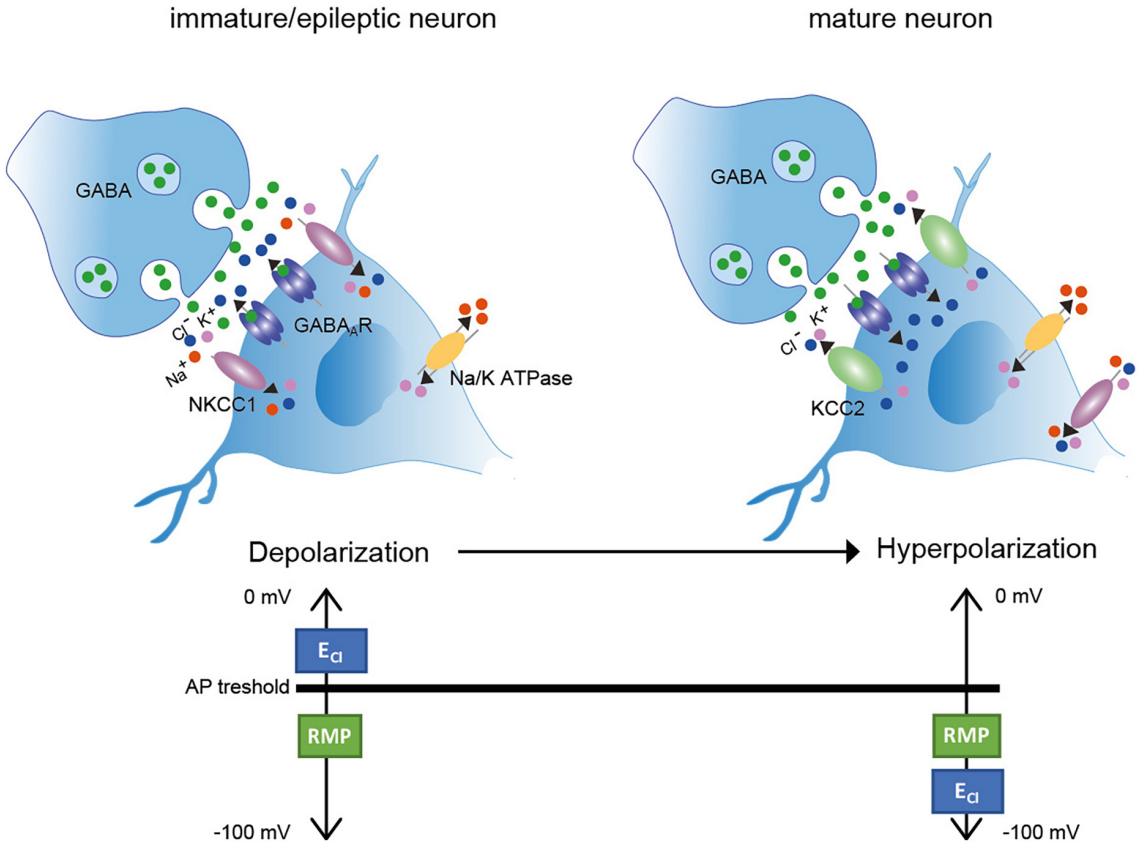

FIGURE 1
Depolarization/Hyperpolarization shift in inhibitory neurons (Left). In immature neurons, high transport activity of NKCC1 results in increased $[Cl^-]_i$. Binding of the inhibitory neurotransmitter GABA to $GABA_A$ receptors results in Cl^- outward currents and thus depolarization. Here, the E_{Cl-} is more depolarized than the AP threshold (Right). In mature neurons, KCC2 activity is increased resulting in decreased $[Cl^-]_i$. Binding of the inhibitory neurotransmitter GABA to its receptor results in Cl^- inward currents and thus hyperpolarization. E_{Cl-} is here hyperpolarized according to the resting membrane potential. AP: action potential; RMP: resting membrane potential. Green dots: GABA; red dots: Na^+; purple dots: K^+; blue dots: Cl^-. Figure modified from Moore et al. (2017).

relatively small increases in $[Cl^-]_i$ will depolarize E_{Cl} toward V_{rest} (Currin et al., 2020). This significantly reduces or even eliminates hyperpolarizing inhibition thus affecting the input-out function of neurons and modify or even degenerate neuronal function (Currin et al., 2020). Computational models of a mature CA1 pyramidal neuron revealed that shifting the reversal potential of GABA (E_{GABA}) by only ∼2.5 mM (∼ to 5 mV from −75 to −70 mV) results in an increase in action potential firing by 39% (Saraga et al., 2008). Further increase in Cl^-can even invert the polarity of $GABA_A$ or glycine receptor mediated currents from hyperpolarizing to depolarizing. On the other hand, extraordinary decreases in neuronal Cl^- with functional relevance have also been observed. Auditory neurons of the superior paraolivary nucleus possess an extremely negative E_{Cl}, which increases the magnitude of hyperpolarizing currents. This is required to trigger hyperpolarization-activated non-specific cationic and T-type calcium currents to promote rebound spiking to signal when a sound ceases (Kopp-Scheinpflug et al., 2011).

Changes in the ionic driving force for Cl^- have been observed on different time scales. The developmental D/H shift occurs on the long term and results in the general observation of hyperpolarizing action of GABA or glycine in the mature brain. More dynamic, short-term alterations have also been reported (Woodin et al., 2003; Khirug et al., 2005; Lamsa et al., 2010; Chamma et al., 2012; Doyon et al., 2016). These changes often occur in a way that relates to the history of synaptic activity. Coincident pre- and post-synaptic spiking results in mature hippocampal neurons in a shift of E_{GABA} toward more positive values (Woodin et al., 2003; Ormond and Woodin, 2009). This change in $[Cl^-]_i$ in the post-synaptic neurons was synapse specific and dependent on KCC2 activity, as revealed by furosemide application (Woodin et al., 2003). In immature hippocampal neurons, coincident activity was reported to result in both a hyperpolarized E_{GABA} (Balena and Woodin, 2008) or a depolarized E_{GABA} (Xu et al., 2008). This difference might be attributed to differences in the system used (cultured neurons vs. hippocampal slices) or in the protocols. In both studies,

pharmacological approaches related the change in E_{GABA} to changes in the activity of NKCC1.

These examples of short-term plasticity that involves changes in the ionic driving force for post-synaptic ionotropic receptors have been referred to as ionic plasticity (Rivera et al., 2005) or ionic shift plasticity (Lamsa et al., 2010). These changes are directly related to the history of activity at inhibitory synapses and likely include rapid post-translational modifications of NKCC1 and KCC2.

Perturbed $[Cl^-]_i$ related diseases

The easy modification of the effect of GABA and glycine *via* changes in the ionic driving force for Cl^- makes inhibitory neurotransmission prone to disease causing alterations. Indeed, perturbation of $[Cl^-]_i$ is associated with a long and still growing list of neurological, psychiatric, and neurodegenerative disorders including epilepsy, neuropathic pain, spasticity, schizophrenia, autism spectrum disorder, brain trauma, ischemic insults, Rett Syndrome and Parkinson's disease (Rivera et al., 2002; Coull et al., 2003; Huberfeld et al., 2007; Papp et al., 2008; Shulga et al., 2008; Boulenguez et al., 2010; Kim et al., 2012; Kahle et al., 2014; Puskarjov et al., 2014; Tyzio et al., 2014; Merner et al., 2015; Ben-Ari, 2017; Pisella et al., 2019; Savardi et al., 2021). These disorders are often associated with increased activity of NKCC1 and/or decreased activity of KCC2 promoting $GABA_AR$ mediated membrane depolarization and excitation (**Figure 1**; Kaila et al., 2014; Mahadevan and Woodin, 2016; Ben-Ari, 2017; Moore et al., 2017; Fukuda and Watanabe, 2019; Tillman and Zhang, 2019; Liu et al., 2020; Savardi et al., 2021). In patients with temporal lobe epilepsy, a subset of neurons in the subiculum in the hippocampus displayed depolarizing up to excitatory GABAergic response that correlated with decreased KCC2 expression and upregulation of NKCC1 (Cohen et al., 2002; Palma et al., 2006; Huberfeld et al., 2007; Muñoz et al., 2007; Moore et al., 2017). Contradictory, recent finding in NKCC1 knock out mice showed that deletion of NKCC1 results in more severe epileptic phenotype in the intrahippocampal kainate mouse model of temporal lobe epilepsy (Hampel et al., 2021). Thus, NKCC1 role in epilepsy is still not completely understood.

Concerning KCC2, several human pathogenic variants are associated with epilepsy, schizophrenia, and autism spectrum disorder (**Figure 2**). These include the heterozygous missense mutations of Arg to His at positions 952 (Arg^{952His}; numbering according to KCC2b) and 1049 ($Arg^{1049His}$) that are associated with febrile seizures and/or idiopathic generalized seizure and decreased KCC2 activity (Kahle et al., 2014; Puskarjov et al., 2014; Merner et al., 2015). Substitution of Arg^{952His} was also found to be associated with schizophrenia (Merner et al., 2015, 2016). In addition, three autosomal recessive heterozygous mutations (Leu^{288His}, Leu^{403Pro}, and Gly^{528Asp}) were identified in children of two unrelated families, which are associated with epilepsy of infancy with migrating focal seizures (Stödberg et al., 2015). Two children had compound heterozygous mutations of Leu^{403Pro} and Gly^{528Asp} and the other child had a homozygous Leu^{288His} mutation (Stödberg et al., 2015). Leu^{403Pro} and Gly^{528Asp} both result in loss-of-function and Leu^{288His} decreases KCC2 activity (Stödberg et al., 2015). Saitsu et al. (2016) also discovered six heterozygous compound KCC2 variants ($E50\_Q93^{del}$, Ala^{191Val}, Ser^{323Pro}, Met^{415Val}, Trp^{318Ser}, and Ser^{748del}) that are associated with this disorder (Saitsu et al., 2016). Analysis of $E50\_Q93^{del}$ and Met^{415Val} revealed that each of the mutations strongly decreases KCC2 activity, whereas Ala^{191Val} and Ser^{323Pro} moderately impair KCC2 function. Co-transfection of $E50\_Q93^{del}$ with Ala^{191Val} or Met^{415Val} with Ser^{323Pro} significantly decreases KCC2 activity (Saitsu et al., 2016).

In schizophrenia, an enhanced NKCC1/KCC2 expression ratio was shown to increase $[Cl^-]_i$ (Arion and Lewis, 2011; Hyde et al., 2011; Ben-Ari, 2017). Substitution of Arg^{952His} is associated with schizophrenia and results in decreased KCC2 activity (**Figure 2**; Merner et al., 2015). Additionally, the human pathogenic NKCC1 variant Tyr^{199Cys}, which enhances its activity, is associated with this disorder (**Figure 3**; Merner et al., 2016).

In autism spectrum disorder, downregulation of KCC2 and upregulation of NKCC1 were observed in several brain regions (Savardi et al., 2021). Application of bumetanide, a specific NKCC inhibitor, markedly improves visual contact, sensory behavior, rigidity and memory performance in preclinical trials (Lemonnier and Ben-Ari, 2010; Lemonnier et al., 2012, 2017; Hadjikhani et al., 2015, 2018). This suggests an association of NKCC1 with autism spectrum disorder. This is supported by two human pathogenic variants (Ala^{379Leu} and Arg^{410Gln}) that are linked to this disorder and intellectual disabilities (McNeill et al., 2020; Adadey et al., 2021). Both mutations impair NKCC1 function (McNeill et al., 2020), indicating a developmental defect. Unfortunately, bumetanide has a poor blood-brain barrier permeability and two recent phase 3 clinical trials using bumetanide in the treatment of ASD in children and adults showed no effectiveness (Löscher and Kaila, 2021). Concerning KCC2, three human pathogenic variants (Arg^{952His}, $Arg^{1048Trp}$, and $Arg^{1049Cys}$) have also been linked to it (Merner et al., 2016). Both Arg^{952His} and $Arg^{1049Cys}$ impair KCC2 function; functional data for $Arg^{1048Trp}$ are not yet available (Kahle et al., 2014).

Several NKCC1 human pathogenic variants are furthermore associated with multisystem dysfunction (Val^{1026F} fs^{*2}), spastic quadriparesis ($His^{186fs17}$ frameshift mutant), spastic paraparesis (Asn^{376Ile}) and minor developmental delay (W892*) (Delpire et al., 2016; McNeill et al., 2020; Adadey et al., 2021). Finally, NKCC1 exon 21 variants are linked to hearing impairment (Glu^{979Lys}, Glu^{980Val}, Glu^{980Lys}) and hearing loss (Asp^{981Tyr}, Pro^{988Ser}, Pro^{988Thr}, and 2930-2A > G) (Morgan et al., 2020;

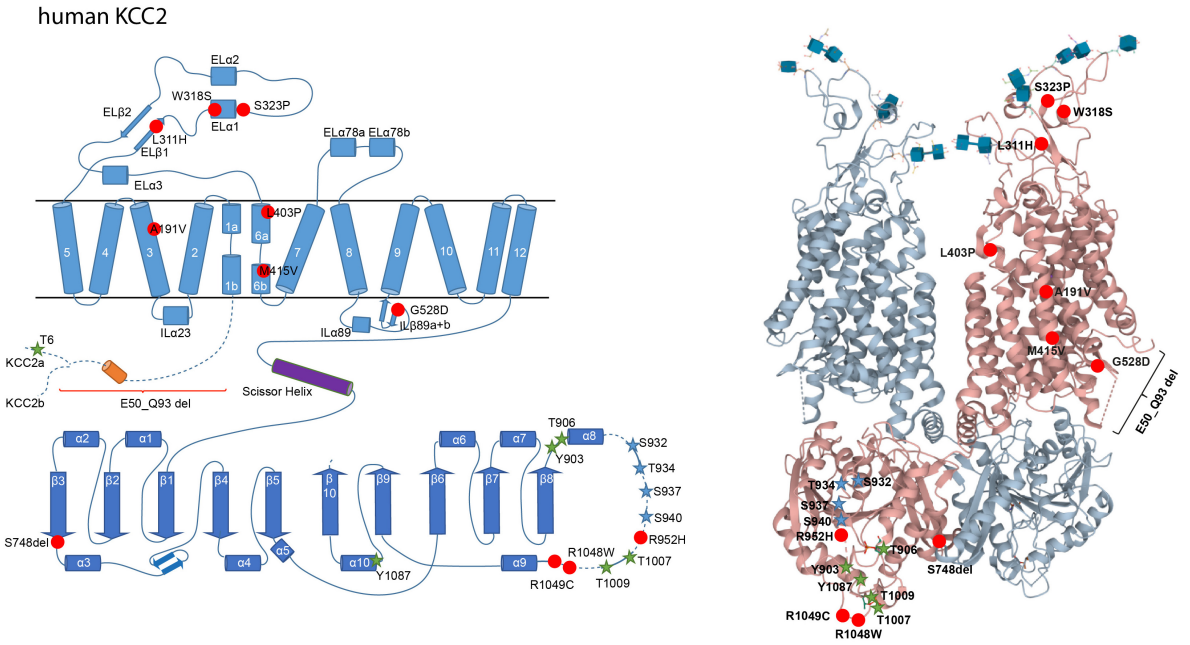

FIGURE 2
Structural organization of human KCC2. 2-dimensional (left) and 3-dimensional (right) organization of human KCC2 according to Chi X. et al. (2020) (PDB: 6m23). KCC2 consists of 12 transmembrane domains (TMs) and two intracellular termini. A large extracellular loop is located between transmembrane domains 5 and 6 (EL3) and five N-glycosylation sites (blue cubes, left). Phosphorylation sites that increase KCC2 activity upon dephosphorylation are marked as green stars (Thr^{6} in KCC2a, Thr^{906}, Tyr^{903}, Thr^{1007}, Thr^{1009}, and Tyr^{1087}). Phosphorylation sites that increase KCC2 activity upon phosphorylation are marked as blue stars (Ser^{932}, Thr^{934}, Ser^{937}, Ser^{940}). Human pathogenic variants of KCC2 associated with epilepsy, autism-spectrum disorder, and schizophrenia are depicted as red dots (Ala^{191Val}, Leu^{311His}, Trp^{318Ser}, Ser^{323Pro}, Leu^{403Pro}, Met^{415Val}, Gly^{528Asp}, Arg^{952His}, $Arg^{1048Trp}$, Arg^{1049C}, Ser^{748del}). Annotation of amino acid residues is according to human KCC2b. The 3D reconstruction of KCC2 was generated using cryo-EM (Chi X. et al., 2020). 3D visualization was performed using Mol* Viewer in PDB (Sehnal et al., 2021).

Mutai et al., 2020; Adadey et al., 2021; Koumangoye et al., 2021; Vanniya et al., 2022). The mutation 2930-2A > G has an effect on splicing leading to loss of exon 21 (Mutai et al., 2020). All of these mutations impair NKCC1 function (Delpire et al., 2016; McNeill et al., 2020; Mutai et al., 2020; Adadey et al., 2021). The human pathogenic variants Ala^{327Val} and $Thr^{1144Asn}$ outside exon 21 are also associated with hearing impairment (McNeill et al., 2020; Adadey et al., 2021). These sensory impairments, however, rather reflects perturbed K^+ recycling in the inner ear than an imbalance in neurotransmission.

To sum up, dysregulation of NKCC1 and KCC2 result in an imbalance of excitation/inhibition that is associated with several neurological and psychiatric disorders.

Phospho-regulation of NKCCs and KCCs

Modulation of Cl^- extrusion constitute promising new strategies for treating these debilitating diseases. Phosphorylation has emerged as the major means to rapidly and reversibly modulate intrinsic transport activity, cell surface stability, and plasma membrane trafficking of NKCC1 and KCC2 (Kahle et al., 2013). So far, four to five phospho-sites with a regulatory effect on transport activity have been identified in the N-terminus of NKCC1 (Thr^{203}, Thr^{207}, Thr^{212}, and Thr^{217} in human NKCC1; Thr^{175}, Thr^{179}, Thr^{184}, Thr^{189}, and Thr^{202} in shark NKCC1) (Muzyamba et al., 1999; Flemmer et al., 2002; Gagnon et al., 2006; Vitari et al., 2006; Hartmann and Nothwang, 2014). For KCC2, the number of regulatory phospho-sites that affect transport activity due to (de)phosphorylation is even higher with one regulatory phospho-site in the N-terminus (Thr^{6} in KCC2a) and nine phospho-sites in the C-terminus (Tyr^{903}, Thr^{906}, Ser^{932}, Thr^{934}, Ser^{937}, Ser^{940}, Thr^{1007}, Thr^{1009}, and Tyr^{1087}) (Lee et al., 2007, 2010; Rinehart et al., 2009; Weber et al., 2014; Titz et al., 2015; Markkanen et al., 2017; Cordshagen et al., 2018; Zhang et al., 2020b). In addition, there are phospho-sites with no detectable effect so far on KCC2 activity (N-terminus: Ser^{25}, Ser^{26}, Ser^{31}, Thr^{34} and C-terminus: Ser^{728}, Thr^{787}, Thr^{999}, Ser^{1022}, Ser^{1025}, Ser^{1026}, Ser^{1034}) or which have not yet been functionally investigated (N-terminus: Thr^{32}, Ser^{55}, Ser^{60}, Thr^{69}, and C-terminus: Ser^{913}, Ser^{988}) (Lee et al., 2007; de Los Heros et al., 2014; Weber et al., 2014; Cordshagen et al., 2018; Zhang et al., 2020b). The difference in the location of

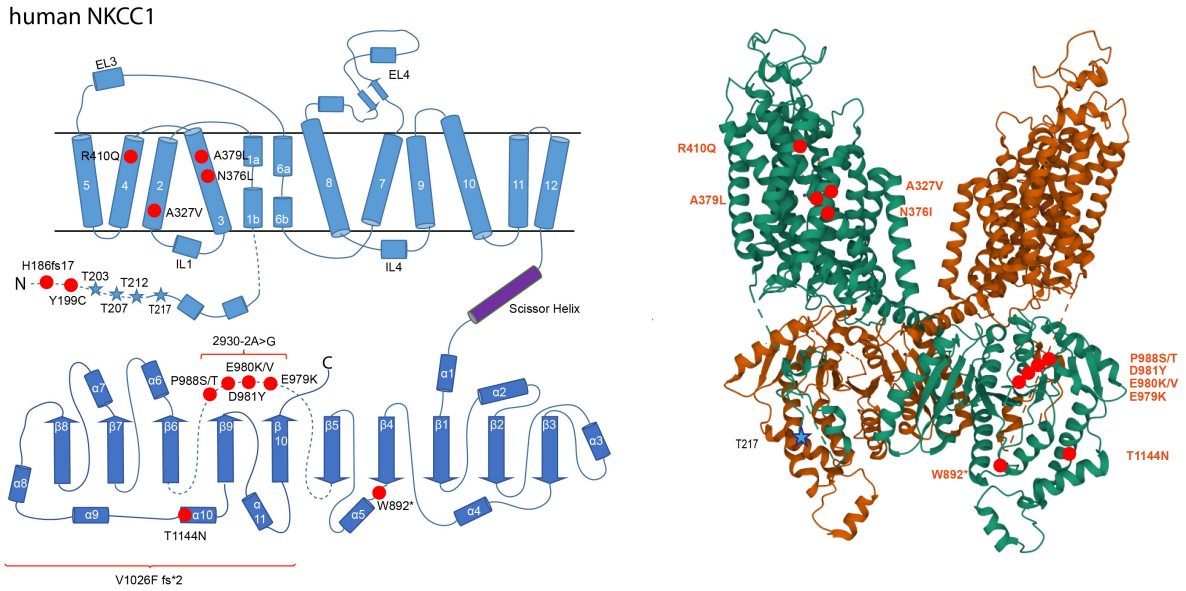

FIGURE 3
Structural organization of human NKCC1. 2-dimensional (left) and 3-dimensional (right) organization of human NKCC1 (A) according to Zhao et al. (2022) (PDB: 7S1X). NKCC1 consists of 12 transmembrane domains (TMs) and two intracellular termini. A large extracellular loop is located between transmembrane domains 7 and 8 (EL4). Phosphorylation sites that increase NKCC1 activity upon phosphorylation are marked as blue stars (Thr^{203}, Thr^{207}, Thr^{212}, and Thr^{217}). Human pathogenic variants of NKCC1 associated with autism spectrum disorder, schizophrenia, multisystem dysfunction, spastic quadriparesis, and hearing impairment are depicted as red dots in human NKCC1 ($His^{186\,fs\,17}$, $Tyr^{199\,Cys}$, $Ala^{327\,Val}$, $Asn^{376\,Leu}$, $Ala^{379\,Leu}$, $Arg^{410\,Glu}$, Trp^{892*}, $Gln^{979\,Lys}$, $Asn^{981\,Tyr}$, $Pro^{988\,Ser}$, $Pro^{988\,Thr}$, $Thr^{411\,Asn}$, 2930.2A > G, $Val^{1026\,Ffs*2}$). The 3D reconstruction of NKCC1 was generated using cryo-EM (Zhao et al., 2022). 3D visualization was performed using Mol* Viewer in PDB (Sehnal et al., 2021).

the phospho-sites between NKCC1 (N-terminus) and KCC2 (C-terminus) might relate to the presence of an autoinhibitory loop present in KCC2 (Chew et al., 2021; Zhang et al., 2021). This loop occludes the translocation pathway and thus locks the transporter in the inactive state (Zhang et al., 2021). The outward-open conformation of the human NKCC1 displays no autoinhibitory loop (**Figure 3**; Zhao et al., 2022). Although the presence of an auto-inhibitory loop in other conformations cannot be excluded, the current data suggests two distinct regulatory mechanisms in the N-terminus of CCC subfamilies: post-translational modification in NKCC1 and an autoinhibitory loop in KCC2 (Chew et al., 2021).

The high number of regulatory phospho-sites enables the transporters to sample across a multitude of signaling pathways, including with-no-lysine kinase (WNK) with their downstream kinase targets STE20/SP1-related proline/alanine rich kinase (SPAK) and oxidative stress response kinase (OSR1), protein kinase C (PKC), Src-tyrosine kinases, brain type creatine kinases and protein phosphatases (Liedtke et al., 2003; Korkhov et al., 2004; Inoue et al., 2006; Gagnon and Delpire, 2013; de Los Heros et al., 2014; Medina et al., 2014). The high number of phospho-sites might reflect the multi-compartmental organization of a neuron (e.g., soma vs. proximal vs. distal dendrites) and the different states a neuron or a synapse can adopt (see ionic plasticity). Future work should therefore aim to relate individual phospho-sites to specific forms of ionic plasticity. The increasing availability of mice with mutated phospho-sites (Silayeva et al., 2015; Moore et al., 2018, 2019; Pisella et al., 2019) will pave the avenue for such analyses.

WNK-SPAK/OSR1 mediated phosphorylation of NKCC1 and KCC2

Generally, phosphorylation of NKCC1 and dephosphorylation of KCC2 increase transport activity. The main mechanism that ensures reciprocal regulation is WNK-SPAK/OSR1 dependent phosphorylation of specific NKCC1 and KCC2 phospho-sites, thus activating NKCCs and inactivating KCCs (Darman and Forbush, 2002; Vitari et al., 2006; Richardson et al., 2008; Rinehart et al., 2009; Kahle et al., 2013; Alessi et al., 2014a; Titz et al., 2015; Markkanen et al., 2017; Zhang et al., 2020b). SPAK/OSR1, which is activated *via* WNK1, phosphorylates Thr^{6} and Thr^{1007} of KCC2 (Rinehart et al., 2009; de Los Heros et al., 2014; Conway et al., 2017; Heubl et al., 2017; Markkanen et al., 2017; Moore et al., 2018). WNKs also interact with a yet unknown kinase to phosphorylate Thr^{906} in the KCC2 C-terminus (de Los Heros et al., 2014; Conway et al., 2017). Site directed mutagenesis of Thr^{6} of KCC2a or Thr^{906} and Thr^{1007} of KCC2 to alanine (mimicking the dephosphorylated state)

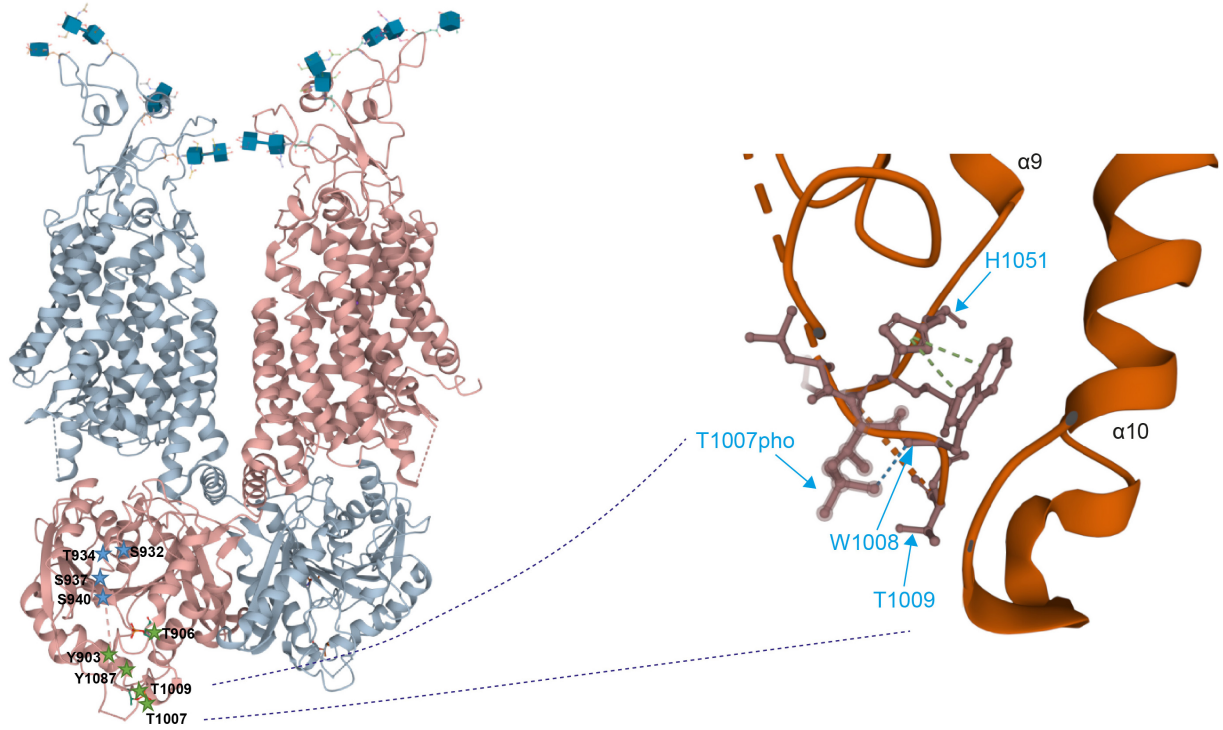

FIGURE 4
Detailed view on the 3D structure of the KCC2 C-terminus (Left). Overall 3-dimensional organization of human KCC2 (Right). Detailed view of the localization of phosphorylated Thr^{1007} and Thr^{1009}. Dashed lines indicate missing density and thus lack of structural information. The 3D reconstruction of KCC2 was generated using cryo-EM (Chi X. et al., 2020). 3D visualization was performed using Mol* Viewer in PDB (Sehnal et al., 2021).

results in activation of KCC2 as shown in cultured hippocampal neurons, cultured cortical neurons and slices, and HEK293 cells (Rinehart et al., 2009; Inoue et al., 2012; Weber et al., 2014; Friedel et al., 2015; Titz et al., 2015). The enhanced activation *via* dephosphorylation of Thr^{906} and Thr^{1007} is accompanied by an increase in cell surface expression in cultured hippocampal neurons (Friedel et al., 2015). Enhanced phosphorylation of Thr^{906} and Thr^{1007} increases in mature hippocampal neurons membrane diffusion resulting in cluster dispersion and enhanced membrane turnover (Heubl et al., 2017; Côme et al., 2019). This indicates that dephosphorylation of these residues increases KCC2 activity. WNK-SPAK/OSR1 mediates also the phosphorylation of human NKCC1 Thr^{203}, Thr^{207}, Thr^{212}, and Thr^{217} resulting in enhanced NKCC1 activity (Darman and Forbush, 2002; Dowd and Forbush, 2003; Moriguchi et al., 2005; Vitari et al., 2006; Gagnon et al., 2007; Richardson and Alessi, 2008; Geng et al., 2009; Thastrup et al., 2012; Alessi et al., 2014b; Hartmann and Nothwang, 2014; Heubl et al., 2017; Shekarabi et al., 2017). Thus, dephosphorylation (KCC2) and phosphorylation (NKCC1) reciprocally decrease the activity of the two Cl^- cotransporters (Zhang et al., 2020b).

The reciprocal phosphorylation of NKCC1 and KCC2 by the WNK-SPAK/OSR1-mediated pathway is involved in the regulation of the development-dependent D/H shift. In neurons, WNK1 phosphorylates SPAK at Ser^{373} and of OSR1 at Ser^{325}, thereby activating these kinases. This results in phosphorylation of NKCC1 (activation) and KCC2 (inactivation) and thus their reciprocal regulation (Vitari et al., 2005; Richardson and Alessi, 2008; de Los Heros et al., 2014; Moore et al., 2017; Zhang et al., 2020a). The action of WNK1 developmentally decreases, since phosphorylation of Ser^{382} in WNK1, and consequently of its targets Ser^{373} in SPAK and Ser^{325} in OSR1, decreases over time in cortical and hippocampal cultures (Friedel et al., 2015). This causes reduced phosphorylation of Thr^{906} and Thr^{1007} in KCC2 (Rinehart et al., 2009; Friedel et al., 2015; Moore et al., 2017). The developmental dependent dephosphorylation of Thr^{906} and Thr^{1007} activates KCC2 function, shifting E_{GABA} to more negative values (Friedel et al., 2015; Moore et al., 2017). This was corroborated by a dominant-negative WNK1 mutant or by genetic depletion of the kinase in immature neurons, as both manipulations cause an early hyperpolarizing action of GABA due to decreased phosphorylation of KCC2 Thr^{906} and Thr^{1007} (Friedel et al., 2015). Moreover, cultured hippocampal neurons derived from a mouse model, in which Thr^{906} and Thr^{1007} were mutated to alanine (mimicking the dephosphorylated state) show an accelerated D/H shift due to increased KCC2

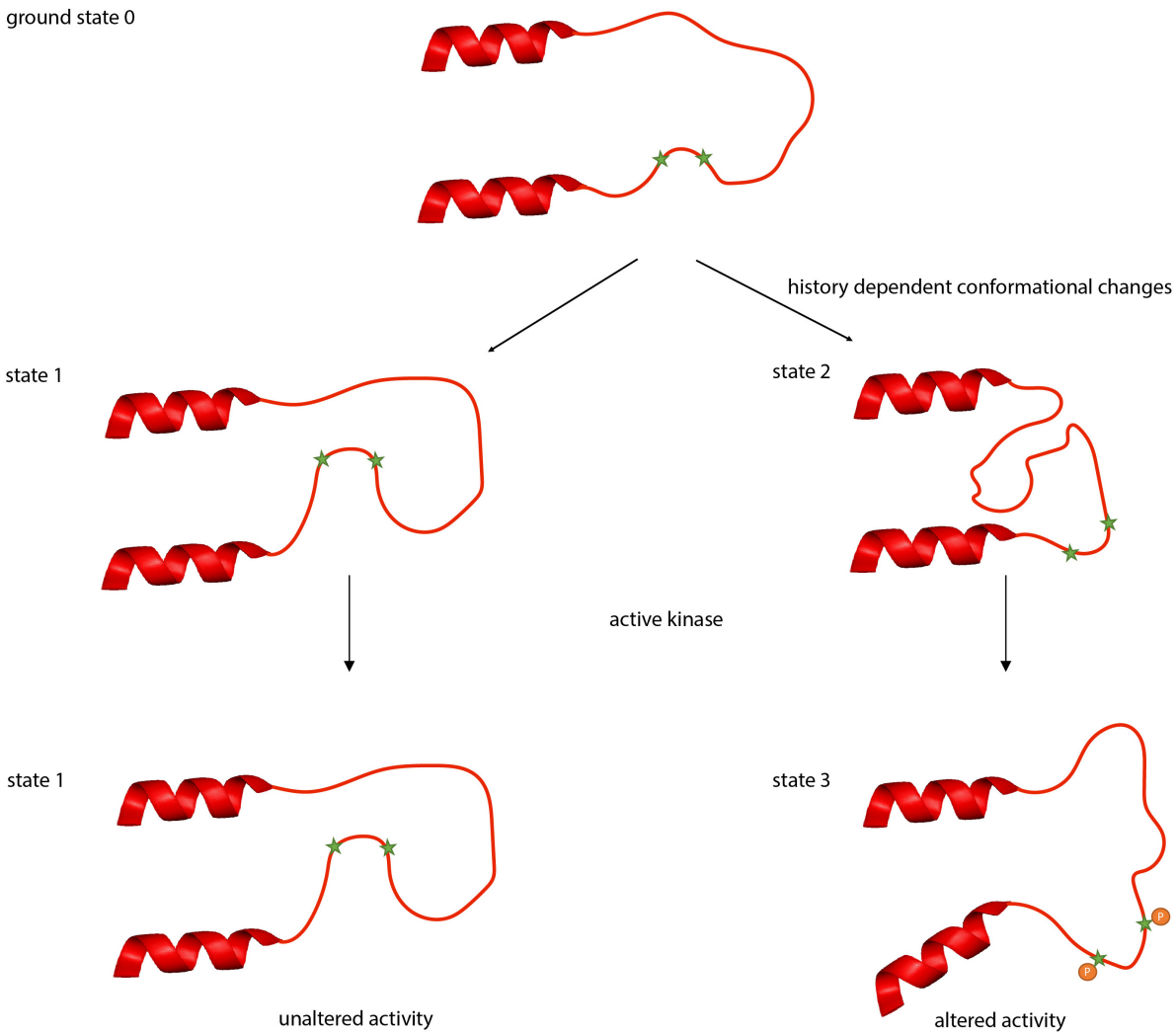

FIGURE 5
Putative conformational states of the intrinsically disordered regions between α8 and α9 helices in KCC2. Intrinsically disordered regions can adopt a variety of conformational states. Beginning with the ground state 0, different physiological conditions (activity, pH, temperature) can induce different conformational states (states 1 or 2). These conformational changes can result in occlusion (state 1) or deocclusion (state 2) of phospho-sites to signaling pathways. Phosphorylation in the deoccluded state results subsequently in altered transport activity.

function (Moore et al., 2019). In contrast, Thr^{906E}/Thr^{1007E} mice (mimicking phosphorylated states) showed a delayed D/H shift in CA3 pyramidal neurons and hippocampal slices (Pisella et al., 2019). These mice showed in addition long-term abnormalities in social behavior, memory retention and increased seizure susceptibility (Moore et al., 2019; Pisella et al., 2019). These data support the notion that post-translational regulation of KCC2 plays a central role in development-dependent regulation in the D/H shift in the central nervous system and that impairment of this regulatory mechanism entails neurodevelopmental disorders (Pisella et al., 2019).

Reciprocal regulation of NKCC1 and KCC2 is important not only in neuronal development but also in adult neurons. Inhibition of $GABA_AR$ *via* gabazine in mature neurons increases $[Cl^-]_i$. This activates WNK1 leading to phosphorylation of Thr^{906}/Thr^{1007} in KCC2 (inactivation) and phosphorylation of $Thr^{203}/Thr^{207}/Thr^{212}$ in NKCC1 (activation) (Heubl et al., 2017). This is important for "auto-tuning" GABAergic signaling *via* rapid regulation of KCC2-mediated Cl^- extrusion (Heubl et al., 2017).

Additional phosphorylation sites in KCC2

The principle that phosphorylation increases the activity of N(K)CCs and *de*phosphorylation that of KCCs is true

for N(K)CCs and KCC1, KCC3, and KCC4. Phospho-regulation in KCC2 is more complex since phosphorylation and dephosphorylation can both enhance its activity. Dephosphorylation of the following phospho-sites increases KCC2 activity: Thr^{6} (present only in KCC2a) and Thr^{906}, Thr^{1007}, Thr^{1009}, and Tyr^{1087} (present in both splice variants) (**Figure 2**). The mechanism leading to phosphorylated Thr^{6}, Thr^{906}, and Thr^{1007} by WNK1 mediated signaling was already described above. Dephosphorylation of the highly conserved Tyr^{1087} residue increases cell surface stability (Lee et al., 2010) and mutation of Tyr^{1087} to phenylalanine (mimicking the dephosphorylated state) does not alter KCC2 activity (Strange et al., 2000). In contrast, mutation of Tyr^{1087} into aspartate (mimicking the phosphorylated state) abolishes KCC2 activity (Strange et al., 2000; Akerman and Cline, 2006; Watanabe et al., 2009; Pellegrino et al., 2011). This indicates that KCC2 is dephosphorylated at Tyr^{1087} under basal conditions and that phosphorylation of this site decreases KCC2 activity. The highly conserved Thr^{1009} is another site that results in increased activity when dephosphorylated. Mutating this residue into alanine (mimicking the dephosphorylated state) intrinsically increases KCC2 activity without affecting cell surface expression (Cordshagen et al., 2018). The Thr^{1009} phosphorylating kinase has yet to be identified. Thus, several sites have been identified where dephosphorylation increases KCC2 activity.

In contrast, phosphorylation of the following residues activates KCC2: Ser^{932}, Thr^{934}, Ser^{937}, and Ser^{940} (**Figure 2**). These residues are all encoded by exon 22, which is only present in KCC2 and non-therian KCC4 (Hartmann and Nothwang, 2014). The most in-depth analyzed residue is Ser^{940}, which is phosphorylated *via* protein kinase C (PKC) and dephosphorylated *via* protein phosphatase 1 (PP1) (Lee et al., 2007, 2011). Phosphorylation of Ser^{940} increases cell surface expression, transport activity, and membrane clustering of KCC2 (Lee et al., 2007; Chamma et al., 2012), with most clusters found at both excitatory and inhibitory synapses in hippocampal cultures (Chamma et al., 2013; Côme et al., 2019). Accordingly, dephosphorylation of Ser^{940} increases membrane diffusion resulting in cluster dispersion and enhanced membrane turnover of KCC2 (Chamma et al., 2013; Côme et al., 2019). Consequently, its dephosphorylation inactivates KCC2 (Lee et al., 2011). Mutation of Ser^{940} to alanine results in transport activity that is equal or decreased compared to KCC2 wild type activity (Lee et al., 2007; Silayeva et al., 2015; Titz et al., 2015). These different outcomes likely reflect the different cellular systems used for the analyses (HEK293 cells, neuronal cell cultures, or knock-in mice) (Lee et al., 2007; Silayeva et al., 2015; Titz et al., 2015).

During development, phosphorylation of Ser^{940} increases concomitantly with KCC2 activity (Moore et al., 2019). Ser^{940Ala} knock-in mice show a delayed D/H shift, demonstrating that not only dephosphorylation of Thr^{906} and Thr^{1007} is important for the D/H shift, but also phosphorylation of Ser^{940} (Moore et al., 2019). Notably, these mice suffer from profound social interaction abnormalities (Moore et al., 2017, 2019). Furthermore, (de)phosphorylation of Ser^{940} is associated with epilepsy. Induction of status epilepticus using kainate causes dephosphorylation of Ser^{940} and internalization of KCC2 (Silayeva et al., 2015). This observation is supported by an analysis of the two human KCC2 pathogenic variants Arg^{952His} and $Arg^{1049Cys}$. Both variants are associated with idiopathic generalized seizure and decreased Ser^{940} phosphorylation (Kahle et al., 2014; Puskarjov et al., 2014; Silayeva et al., 2015). Phosphorylation of Ser^{940} therefore could provide an approach to limit the progress of status epilepticus (Silayeva et al., 2015).

In addition to Ser^{940}, exon 22 encodes the phosphorylation sites Ser^{932}, Thr^{934}, and Ser^{937}. Mutation of any of these residues to aspartate (mimicking the phosphorylated state) intrinsically increases KCC2 activity in HEK293 cells without affecting cell surface expression (Weber et al., 2014; Cordshagen et al., 2018). Mutation into alanine (mimicking the dephosphorylated state) has no effect in HEK293 cells (Weber et al., 2014; Cordshagen et al., 2018). Thus, both dephosphorylation and phosphorylation of specific phospho-sites can increase KCC2 activity. This peculiarity provides KCC2 with a rich regulatory tool-box for graded activity and integration of different signaling pathways (Cordshagen et al., 2018).

Phosphorylation affects conformation of NKCCs and KCCs

3D structure of the outward-open conformation of human NKCC1 (**Figure 3**) reveals that the dimeric interface is formed between the C-terminus and the N-terminal phosphoregulatory element and the C-terminus and the TMs (Zhao et al., 2022). These two domains define an allosteric interface that may transmit the impact of (de)phosphorylation of N-terminal phospho-sites, *via* the intervening C-terminal tail and the intracellular loop 1 (ICL1) to affect ion translocation (Zhao et al., 2022). Binding of kinases or phosphatases may form or disrupt these domain interactions (Zhao et al., 2022). However, FRET experiments in NKCC1 revealed that phosphorylation within the N-terminus affects movement of the C-terminus leading to a dissociation of the two monomers within the dimer (Monette and Forbush, 2012). Cross-linking studies support this conclusion. They showed that phosphorylation of residues within the N-terminus affects the localization of TM10 relative to TM12 thereby inducing movement of the C-terminus and disruption of dimerization (Monette et al., 2014; Zhang et al., 2021). Thus, phosphorylation of N-terminal phospho-sites in NKCC1 may induce long-range distance effects involving movement of the C-terminus. It is therefore an open question whether (de)phosphorylation of N-terminal NKCC1 phospho-sites cause disengagement of the TMs as described in the outward-facing cryo-EM of NKCC1 (Zhao et al., 2022) or

dissociation of the C-terminal domains (Monette and Forbush, 2012; Monette et al., 2014; Zhang et al., 2021).

(De)phosphorylation dependent conformational differences were also reported for KCC3. To examine the effect of phosphorylation on structural organization, two different KCC3 mutants were generated with triple substitutions of Ser^{45}, Thr^{940}, and Thr^{997} by either aspartate (KCC3-PM) or by alanine (KCC3-PKO). Analysis by cryo-EM revealed that the "dephosphorylated" KCC3-PKO is more dynamic in the scissor helix region and exhibits a greater rotational flexibility of the C-terminal dimer (Chi G. et al., 2021). The KCC3-PM mutant demonstrated more dynamic conformational changes within the ß7 strand and in the α8 and α10 helices (Chi G. et al., 2021). Multiple conformations for α7 were observed, in which the end of α7 moves 21° outward entailing conformational changes in the α7/ß6 loop (Chi G. et al., 2021). Cryo-EM identified also two conformational states in KCC1, as α8 was observed either above or below α10 (Chi G. et al., 2021). The first state matches the structures of $KCC3^{wt}$ and KCC3-PM (Chi G. et al., 2021). The second state is stabilized by polar interactions with glutamate residues in α11 (Chi G. et al., 2021). Thus, (de)phosphorylation of C-terminal phospho-sites results in substantial conformational reorganizations within the C-terminus in KCCs.

Notably, KCC2 Thr^{906} and Thr^{1007} correspond to the investigated Thr^{940}, and Thr^{997} amino acid residues in KCC3. Both amino acid residues are *bona fide* phospho-sites of KCC2 and targets of the WNK-SPAK/OSR1 signaling pathway with dephosphorylation resulting in increased transport activity (Rinehart et al., 2009; Inoue et al., 2012; de Los Heros et al., 2014; Titz et al., 2015; Markkanen et al., 2017). It is therefore tempting to speculate that changes in their phosphorylation pattern alter the C-terminal conformation of KCC2.

Intrinsically disordered regions of KCC2 as processors for ionic plasticity

The six KCC2 phosphorylation sites Ser^{932}, Thr^{934}, Ser^{937}, Ser^{940}, Thr^{1007}, and Thr^{1009}, which form a tight cluster, all reside in an intrinsically disordered region (IDR) between α8 and α9 helices according to the cryo-EM reconstruction of KCC2 (Chi G. et al., 2021; Chi X. et al., 2021). The presence of six out of ten (60%) known regulatory KCC2 phospho-sites within a stretch of 134 amino acid residues (12% of the total residues, Met^{919} to Ala^{1053} in *hs*KCC2b) (**Figure 2**) agrees well with the general enrichment of post-translational modification sites in such regions due to their increased surface area (Oldfield et al., 2008; Forman-Kay and Mittag, 2013; Hsu et al., 2013). In line with this, two further phospho-sites, Tyr^{903} and Thr^{906} are also located in a disordered region between ß8 strand and α8 helix (**Figure 2**).

Intrinsically disordered regions do not have a well-defined tertiary structure, instead they are in a dynamic equilibrium between different sets of conformational states (Boehr et al., 2009; Flock et al., 2014). It is thus likely that (de)phosphorylation of the amino acid residues within these regions will induce structural transitions with impact on the conformation of the entire C-terminus (and likely other regions as well). Indeed, phosphorylated Thr^{1007} forms main chain hydrogen bonds with Trp^{1008}, that itself has side chain interactions with His^{1051} (pi stacking), and Tyr^{903} forms a main chain hydrogen bond with Ser^{899} (**Figure 4**). Alterations in phosphorylation might affect these interactions thereby altering the organization and thus conformation of the C-terminus.

The clusters of phospho-sites might not only enable the transporters to integrate multiple signaling pathways but also to regulate activity in a history-dependent manner. Intrinsically disordered regions can adopt a variety of conformations each with distinct binding affinities and specificity properties (Oldfield et al., 2008; Forman-Kay and Mittag, 2013; Hsu et al., 2013; Flock et al., 2014). Thus, starting from a ground state 0, slightly different conformations named states 1 and 2 can be induced by two different physiological states, upon which a signaling pathway will act in different, history-dependent ways. This will induce in one instance a further conformational change resulting in state 3 whereas in the other instance, no further conformational change occurs (**Figure 5**).

Experiments with the kinase inhibitor staurosporine provide evidence for such different conformational states in KCC2. Mutation of the regulatory phospho-sites Ser^{932} and Thr^{1009} to either alanine or aspartate abrogates stimulation by staurosporine. In contrast, Ser^{31}, Thr^{34}, and Thr^{999} represent regulatory phospho-sites where only mutation into alanine or aspartate (Ser^{31Asp}, Thr^{34Ala}, and Thr^{999Ala}) abrogates stimulation, whereas substitution by the other amino acid residue (Ser^{31Ala}, Thr^{34Asp}, and Thr^{999Asp}) maintains sensitivity to staurosporine (Cordshagen et al., 2018; Zhang et al., 2020b). The change in phosphorylation of either of the three sites likely impacts the accessibility of other phospho-sites such as Ser^{932} and Thr^{1009} to the action of staurosporine (Cordshagen et al., 2018). One conformational state (state 1) might occlude hidden sites that are final targets of the action of staurosporine, resulting in no further activation of KCC2. The other conformational state (state 2) provides access to phospho-sites that are targeted by the action of this reagent, leading to state 3 (**Figure 5**). This can result in distinct Cl^- transport activities, reflecting the past history, and ultimately in different transformations of the neuronal input-output function (Currin et al., 2020), which relate to phenomena as important and diverse as synaptic integration, the flow of information through neuronal circuits, learning and memory, neural circuit development and diseases. The phospho-site enriched unstructured regions are therefore

ideally suited to act as a processor to regulate the output of the transporters by computing signaling from ongoing and past physiological states. This inherent feature of an intrinsically disordered region thus might provide a molecular basis for ionic plasticity.

Furthermore, the properties of intrinsically disordered regions might explain the surprising observation of decreased Ser^{940} phosphorylation in the presence of the two human pathogenic variants Arg^{952His} and $Arg^{1049Cys}$ (Kahle et al., 2014; Puskarjov et al., 2014; Silayeva et al., 2015; **Figure 2**). Both variants may cause altered conformation of the unstructured area, resulting in different binding affinities for PKC and PP1 that determine together the amount of Ser^{940} phosphorylation (Lee et al., 2007, 2011; Kahle et al., 2014). Finally, environmental factors, like changes in temperature, redox-potential and pH can induce conformational changes of intrinsically disordered regions (Kjaergaard et al., 2010; Flock et al., 2014; Jephthah et al., 2019). This might explain the temperature-dependency of KCC2, since increasing the temperature to 37°C decreases KCC2 activity (Hartmann and Nothwang, 2011).

Conclusion

(De)phosphorylation of phospho-sites most likely results in conformational reorganization as observed for other CCC family members. Many of the phospho-sites in the C-terminus of KCC2 are localized in an unstructured area. Due to biophysical properties of such areas, this part of KCC2 might serve a dual role. It might represent a platform for integrating different signaling pathways and simultaneously constitute a flexible, highly dynamic linker that can survey a wide variety of distinct conformations (Forman-Kay and Mittag, 2013). As each conformation can have distinct binding affinities and specificity properties, this may enable regulation of $[Cl^-]_i$ and thus the ionic driving force in a history-dependent way and explain long-range effects of mutations on phospho-sites.

Author contributions

A-MH and HN equally wrote the manuscript. A-MH generated all of the figures. Both authors contributed to the article and approved the submitted version.

Funding

The manuscript was supported by the funding of the DFG (grant numbers: HA6338/2-1 to A-MH and 428-4/1 and 428-4/2 to HN). Our institution has an open access for the publication (library).

Acknowledgments

A-MH and HN gratefully acknowledge long time support by the DFG.

Conflict of interest

The authors declare that the research was conducted in the absence of any commercial or financial relationships that could be construed as a potential conflict of interest.

Publisher's note

References

Achilles, K., Okabe, A., Ikeda, M., Shimizu-Okabe, C., Yamada, F., Fukuda, A., et al. (2007). Kinetic properties of Cl^- uptake mediated by Na^+-dependent K^+-$2Cl^-$ cotransport in immature rat neocortical neurons. *J. Neurosci.* 27, 8616–8627. doi: 10.1523/JNEUROSCI.5041-06.2007

Adadey, S. M., Schrauwen, I., Aboagye, E. T., Bharadwaj, T., Esoh, K. K., Basit, S., et al. (2021). Further confirmation of the association of SLC12A2 with non-syndromic autosomal-dominant hearing impairment. *J. Hum. Genet.* 66, 1169–1175. doi: 10.1038/s10038-021-00954-6

Akerman, C. J., and Cline, H. T. (2006). Depolarizing GABAergic conductances regulate the balance of excitation to inhibition in the developing retinotectal circuit in vivo. *J. Neurosci.* 26, 5117–5130. doi: 10.1523/JNEUROSCI.0319-06.2006

Alessi, D. R., Gourlay, R., Campbell, D. G., Deak, M., Macartney, T. J., Kahle, K. T., et al. (2014a). The WNK-regulated SPAK/OSR1 kinases directly phosphorylate and inhibit the K+–Cl- co-transporters. *Biochem. J.* 458(Pt 3), 559–573. doi: 10.1042/BJ20131478

Alessi, D. R., Zhang, J., Khanna, A., Hochdörfer, T., Shang, Y., and Kahle, K. T. (2014b). The WNK-SPAK/OSR1 pathway: master regulator of cation-chloride cotransporters. *Sci. Signal.* 7:re3. doi: 10.1126/scisignal.2005365

Arion, D., and Lewis, D. A. (2011). Altered expression of regulators of the cortical chloride transporters NKCC1 and KCC2 in schizophrenia. *Arch. Gen. Psychiatry* 68, 21–31. doi: 10.1001/archgenpsychiatry.2010.114

Balakrishnan, V., Becker, M., Löhrke, S., Nothwang, H. G., Güresir, E., and Friauf, E. (2003). Expression and function of chloride transportes during development of inhibitory neurotransmission in the auditory brainstem. *J. Neurosci.* 23, 4134–4145. doi: 10.1523/JNEUROSCI.23-10-04134.2003

Balena, T., and Woodin, M. A. (2008). Coincident pre-and postsynaptic activity downregulates NKCC1 to hyperpolarize ECl during development. *Eur. J. Neurosci.* 27, 2402–2412. doi: 10.1111/j.1460-9568.2008.06194.x

Ben-Ari, Y. (2017). NKCC1 chloride importer antagonists attenuate many neurological and psychiatric disorders. *Trends Neurosci.* 40, 536–554. doi: 10.1016/j.tins.2017.07.001

Ben-Ari, Y., Cherubini, E., Corradetti, R., and Gaiarsa, J.-L. (1983). Giant synaptic potentials in immature rat CA3 hippocampal neurones. *J. Physiol.* 416, 303–325. doi: 10.1113/jphysiol.1989.sp017762

Ben-Ari, Y., Gaiarsa, J.-L., Tyzio, R., and Khazipov, R. (2007). GABA: a pioneer transmitter that excites immature neurons and generates primitive oscillations. *Physiology* 87, 1215–1284. doi: 10.1152/physrev.00017.2006

Blaesse, P., Airaksinen, M. S., Rivera, C., and Kaila, K. (2009). Cation-chloride cotransporters and neuronal function. *Cell* 61, 820–838. doi: 10.1016/j.neuron.2009.03.003

Boehr, D. D., Nussinov, R., and Wright, P. E. (2009). The role of dynamic conformational ensembles in biomolecular recognition. *Nat. Chem. Biol.* 5, 789–796. doi: 10.1038/nchembio.232

Bormann, B. J., Hamill, O. P., and Sackmann, B. (1987). Mechanism of anion permeation through channels gated by glycine and y-aminobutyric acid in mouse cultured spinal neurones. *J. Physiol.* 385, 243–286. doi: 10.1113/jphysiol.1987.sp016493

Boulenguez, P., Liabeuf, S., Bos, R., Bras, H., Jean-Xavier, C., Brocard, C., et al. (2010). Down-regulation of the potassium-chloride cotransporter KCC2 contributes to spasticity after spinal cord injury. *Nat. Med.* 16, 302–307. doi: 10.1038/nm.2107

Chamma, I., Chevy, Q., Poncer, J. C., and Lévi, S. (2012). Role of the neuronal K-Cl co-transporter KCC2 in inhibitory and excitatory neurotransmission. *Front. Cell. Neurosci.* 6:5. doi: 10.3389/fncel.2012.00005

Chamma, I., Heubl, M., Chevy, Q., Renner, M., Moutkine, I., Eugène, E., et al. (2013). Activity-dependent regulation of the K/Cl transporter KCC2 membrane diffusion, clustering, and function in hippocampal neurons. *J. Neurosci.* 33, 15488–15503. doi: 10.1523/JNEUROSCI.5889-12.2013

Cherubini, E., Gaiarsa, J.-L., and Ben-Ari, Y. (1991). GABA: an excitatory transmitter in early postnatal life. *Trends Neurosci.* 14, 515–519. doi: 10.1016/0166-2236(91)90003-D

Cherubini, E., Rovira, C., Gaiarsa, J.-L., Corradetti, R., and Ben-Ari, Y. (1990). GABA mediated excitation in immature rat CA3 hippocampal neurons. *Int. J. Dev. Neurosci.* 8, 481–490. doi: 10.1016/0736-5748(90)90080-L

Chew, T. A., Zhang, J., and Feng, L. (2021). High-resolution views and transport mechanisms of the NKCC1 and KCC transporters. *J. Mol. Biol.* 433:167056. doi: 10.1016/j.jmb.2021.167056

Chi, G., Ebenhoch, R., Man, H., Tang, H., Tremblay, L. E., Reggiano, G., et al. (2021). Phospho-regulation, nucleotide binding and ion access control in potassium-chloride cotransporters. *EMBO J.* 40:e107294. doi: 10.15252/embj.2020107294

Chi, X., Li, X., Chen, Y., Zhang, Y., Su, Q., and Zhou, Q. (2020). Molecular basis for regulation of human potassium chloride cotransporters. *bioRxiv [Preprint]* doi: 10.1101/2020.02.22.960815

Chi, X., Li, X., Chen, Y., Zhang, Y., Su, Q., and Zhou, Q. (2021). Cryo-EM structures of the full-length human KCC2 and KCC3 cation-chloride cotransporters. *Cell Res.* 31, 482–484. doi: 10.1038/s41422-020-00437-x

Cohen, I., Navarro, V., Clemenceau, S., Baulac, M., and Miles, R. (2002). On the origin of interictal activity in human temporal lobe epilepsy in vitro. *Science* 298, 1418–1421. doi: 10.1126/science.1076510

Côme, E., Heubl, M., Schwartz, E. J., Poncer, J. C., and Lévi, S. (2019). Reciprocal regulation of KCC2 trafficking and synaptic activity. *Front. Cell. Neurosci.* 13:48. doi: 10.3389/fncel.2019.00048

Conway, L. C., Cardarelli, R. A., Moore, Y. E., Jones, K., McWilliams, L. J., Baker, D. J., et al. (2017). N-Ethylmaleimide increases KCC2 cotransporter activity by modulating transporter phosphorylation. *J. Biol. Chem.* 292, 21253–21263. doi: 10.1074/jbc.M117.817841

Cordshagen, A., Busch, W., Winklhofer, M., Nothwang, H. G., and Hartmann, A.-M. (2018). Phosphoregulation of the intracellular termini of K+-Cl-cotransporter 2 (KCC2) enables flexible control of its activity. *J. Biol. Chem.* 293, 16984–16993. doi: 10.1074/jbc.RA118.004349

Coull, J. A. M., Boudreau, D., Bachand, K., Prescott, S. A., Nault, F., Sik, A., et al. (2003). Trans-synaptic shift in anion gradient in spinal lamina I neurons as a mechanism of neuropathic pain. *Nature* 424, 938–942. doi: 10.1038/nature01868

Currin, C. B., Trevelyan, A. J., Akerman, C. J., and Raimondo, J. V. (2020). Chloride dynamics alter the input-output properties of neurons. *PLoS Comput. Biol.* 16:e1007932. doi: 10.1371/journal.pcbi.1007932

Darman, R. B., and Forbush, B. (2002). A regulatory locus of phosphorylation in the N terminus of the Na-K-Cl cotransporter, NKCC1. *J. Biol. Chem.* 277, 37542–37550. doi: 10.1074/jbc.M206293200

de Los Heros, P., Alessi, D. R., Gourlay, R., Campbell, D. G., Deak, M., Macartney, T. J., et al. (2014). The WNK-regulated SPAK/OSR1 kinases directly phosphorylate and inhibit the K^+-Cl^- co-transporters. *Biochem. J.* 458, 559–573. doi: 10.1042/BJ20131478

Delpire, E. (2000). Cation-chloride cotransporter in neuronal communication. *News Physiol. Sci.* 15, 309–312. doi: 10.1152/physiologyonline.2000.15.6.309

Delpire, E., Lu, J., England, R., Dull, C., and Thorne, T. (1999). Deafness and imbalance associated with inactivation of the secretory Na-K-2Cl co-transporter. *Nat. Genet.* 22, 192–195. doi: 10.1038/9713

Delpire, E., and Mount, D. B. (2002). Human and murine phenotypes associated with defects in cation-chloride-cotransporter. *Annu. Rev. Physiol.* 64, 803–843. doi: 10.1146/annurev.physiol.64.081501.155847

Delpire, E., Wolfe, L., Flores, B., Koumangoye, R., Schornak, C. C., Omer, S., et al. (2016). A patient with multisystem dysfunction carries a truncation mutation in human *SLC12A2*, the gene encoding the Na-K-2Cl cotransporter, NKCC1. *Cold Spring Harb. Mol. Case Stud.* 2:a001289. doi: 10.1101/mcs.a001289

Dowd, B. F. X., and Forbush, B. (2003). PASK (Proline-Alanine-rich-related Kinase), a regulatory kinase of the Na-K-Cl cotransporter (NKCC1). *J. Biol. Chem.* 278, 27347–27353. doi: 10.1074/jbc.M301899200

Doyon, N., Vinay, L., Prescott, S. A., and De Koninck, Y. (2016). Chloride regulation: a dynamic equilibrium crucial for synaptic inhibition. *Neuron* 89, 1157–1172. doi: 10.1016/j.neuron.2016.02.030

Dzhala, V. I., Talos, D. M., Sdrulla, D. A., Brumback, A. C., Mathews, G. C., Benke, T. A., et al. (2005). NKCC1 transporter facilitates seizures in the developing brain. *Nat. Med.* 11, 1205–1213. doi: izuresinthedevelopingbrai

Ehrlich, I., Löhrke, S., and Friauf, E. (1999). Shift from depolarizing to hyperpolarizing glycine action in rat auditory neurones is due to age-dependent Cl^- regulation. *J. Physiol.* 520, 121–137. doi: 10.1111/j.1469-7793.1999.00121.x

Eichler, S. A., and Meier, J. C. (2008). EI balance and human diseases-from molecules to networking. *Front. Mol. Neurosci.* 1:2. doi: 10.3389/neuro.02.002.2008

Flemmer, A. W., Gimenz, I., Dowd, B. F. X., Darman, R. B., and Forbush, B. (2002). Activation of the Na-K-Cl cotransporter NKCC1 detected with a Phospho-specific antibody. *J. Biol. Chem.* 277, 37551–37558. doi: 10.1074/jbc.M206294200

Flock, T., Weatheritt, R. J., Latysheva, N. S., and Babu, M. M. (2014). Controlling entropy to tune the functions of intrinsically disordered regions. *Curr. Opin. Struct. Biol.* 26, 62–72. doi: 10.1016/j.sbi.2014.05.007

Forman-Kay, J. D., and Mittag, T. (2013). From sequence and forces to structure, function, and evolution of intrinsically disordered proteins. *Structure* 21, 1492–1499.

Friedel, P., Kahle, K. T., Zhang, J., Hertz, N., Pisella, L. I., Buhler, E., et al. (2015). WNK1-regulated inhibitory phosphorylation of the KCC2 cotransporter maintains the depolarizing action of GABA in immature neurons. *Sci. Signal.* 8:ra65. doi: 10.1126/scisignal.aaa0354

Fukuda, A., and Watanabe, M. (2019). Pathogenic potential of human SLC12A5 variants causing KCC2 dysfunction. *Brain Res.* 1710, 1–7. doi: 10.1016/j.brainres.2018.12.025

Gagnon, K. B., and Delpire, E. (2013). Physiology of SLC12 transporters: lessons from inherited human genetic mutations and genetically engineered mouse knockouts. *Am. J. Physiol. Cell Physiol.* 304, C693–C714. doi: 10.1152/ajpcell.00350.2012

Gagnon, K. B., England, R., and Delpire, E. (2007). A single binding motif is required for SPAK activation of the Na-K-2Cl cotransporter. *Cell. Physiol. Biochem.* 20, 131–142. doi: 10.1159/000104161

Gagnon, K. B. E., England, R., and Delpire, E. (2006). Characterization of SPAK and OSR1, regulatory kinases of the Na-K-2Cl cotransporter. *Mol. Cell. Biol.* 26, 689–698. doi: 10.1128/MCB.26.2.689-698.2006

Geng, Y., Hoke, A., and Delpire, E. (2009). The Ste20 Kinases SPAK and OSR1 regulate NKCC1 function in sensory neurons. *J. Biol. Chem.* 284, 14020–14028. doi: 10.1074/jbc.M900142200

Hadjikhani, N., Johnels, J. Å., Lassalle, A., Zürcher, N. R., Hippolyte, L., Gillberg, C., et al. (2018). Bumetanide for autism: more eye contact, less amygdala activation. *Sci. Rep.* 8:3602. doi: 10.1038/s41598-018-21958-x

Hadjikhani, N., Zürcher, N. R., Rogier, O., Ruest, T., Hippolyte, L., Ben-Ari, Y., et al. (2015). Improving emotional face perception in autism with diuretic bumetanide: a proof-of-concept behavioral and functional brain imaging pilot study. *Autism* 19, 149–157. doi: 10.1177/1362361313514141

Hampel, P., Johne, M., Gailus, B., Vogel, A., Schidlitzki, A., Gericke, B., et al. (2021). Deletion of the Na-K-2Cl cotransporter NKCC1 results in a more severe epileptic phenotype in the intrahippocampal kainate mouse model of

temporal lobe epilepsy. *Neurobiol. Dis.* 152:105297. doi: 10.1016/j.nbd.2021.105297

Hartmann, A.-M., and Nothwang, H. G. (2011). Opposite temperature effect on transport activity of KCC2/KCC4 and N (K) CCs in HEK-293 cells. *BMC Res. Notes* 4:526. doi: 10.1186/1756-0500-4-526

Hartmann, A.-M., and Nothwang, H. G. (2014). Molecular and evolutionary insights into the structural organization of cation chloride cotransporters. *Front. Cell. Neurosci.* 8:470. doi: 10.3389/fncel.2014.00470

Henneberger, C., Bard, L., Panatier, A., Reynolds, J. P., Kopach, O., Medvedev, N. I., et al. (2020). LTP induction boosts glutamate spillover by driving withdrawal of perisynaptic astroglia. *Neuron* 108, 919–936.e11. doi: 10.1016/j.neuron.2020.08.030

Heubl, M., Zhang, J., Pressey, J. C., Al Awabdh, S., Renner, M., Gomez-Castro, F., et al. (2017). GABA A receptor dependent synaptic inhibition rapidly tunes KCC2 activity via the Cl–sensitive WNK1 kinase. *Nat. Commun.* 8:1776. doi: 10.1038/s41467-017-01749-0

Hsu, W. L., Oldfield, C. J., Xue, B., Meng, J., Huang, F., Romero, P., et al. (2013). Exploring the binding diversity of intrinsically disordered proteins involved in one-to-many binding. *Protein Sci.* 22, 258–273. doi: 10.1002/pro.2207

Huberfeld, G., Wittner, L., Clemenceau, S., Baulac, M., Kaila, K., Miles, R., et al. (2007). Perturbed chloride homeostasis and GABAergic signaling in human temporal lobe epilepsy. *J. Neurosci.* 27, 9866–9873. doi: 10.1523/JNEUROSCI.2761-07.2007

Hübner, C. A., Lorke, D. E., and Hermans-Borgmeyer, I. (2001a). Expression of the Na-K-2Cl-cotransporter NKCC1 during mouse development. *Mech. Dev.* 102, 267–269. doi: 10.1016/S0925-4773(01)00309-4

Hübner, C. A., Stein, V., Hermans-Borgmeyer, I., Meyer, T., Ballanyi, K., and Jentsch, T. J. (2001b). Disruption of KCC2 reveals an essential role of K-Cl cotransport already in early synaptic inhibition. *Neuron* 30, 515–524. doi: 10.1016/s0896-6273(01)00297-5

Hyde, T. M., Lipska, B. K., Ali, T., Mathew, S. V., Law, A. J., Metitiri, O. E., et al. (2011). Expression of GABA signaling molecules KCC2, NKCC1, and GAD1 in cortical development and schizophrenia. *J. Neurosci.* 31, 11088–11095. doi: 10.1523/JNEUROSCI.1234-11.2011

Ikeda, K., Onimaru, H., Yamada, J., Inoue, K., Ueno, S., Onaka, T., et al. (2004). Malfunction of respiratory-related neuronal activity in Na^+, K^+-ATPase L2 subunit-deficient mice is attributable to abnormal Cl^- homeostasis in brainstem neurons. *J. Neurosci.* 24, 10693–10701. doi: 10.1523/JNEUROSCI.2909-04.2004

Inoue, K., Furukawa, T., Kumada, T., Yamada, J., Wang, T., Inoue, R., et al. (2012). Taurine inhibits K+-Cl- cotransporter KCC2 to regulate embryonic Cl- homeostasis via With-no-lysine (WNK) protein kinase signaling pathway. *J. Biol. Chem.* 287, 20839–20850. doi: 10.1074/jbc.M111.319418

Inoue, K., Yamada, J., Ueno, S., and Fukuda, A. (2006). Brain-type creatine kinase activates neuron-specific K+-Cl- co-trasnporter KCC2. *J. Biochem.* 96, 598–608. doi: 10.1111/j.1471-4159.2005.03560.x

Jephthah, S., Staby, L., Kragelund, B., and Skepo, M. (2019). Temperature dependence of intrinsically disordered proteins in simulations: what are we missing? *J. Chem. Theory Comput.* 15, 2672–2683. doi: 10.1021/acs.jctc.8b01281

Kahle, K. T., Deeb, T. Z., Puskarjov, M., Silayeva, L., Liang, B., Kaila, K., et al. (2013). Modulation of neuronal activity by phosphorylation of the K–Cl cotransporter KCC2. *Trends Neurosci.* 36, 726–737. doi: 10.1016/j.tins.2013.08.006

Kahle, K. T., Merner, N. D., Friedel, P., Silayeva, L., Liang, B., Khanna, A., et al. (2014). Genetically encoded impairment of neuronal KCC2 cotransporter function in human idiopathic generalized epilepsy. *EMBO Rep.* 15, 766–774. doi: 10.15252/embr.201438840

Kaila, K. (1994). Ionic basis of GABA A receptor channel function in the nervous system. *Prog. Neurobiol.* 42, 489–537. doi: 10.1016/0301-0082(94)90049-3

Kaila, K., Price, T. J., Payne, J. A., Puskarjov, M., and Voipio, J. (2014). Cation-chloride cotransporters in neuronal development, plasticity and disease. *Nat. Rev. Neurosci.* 15, 637–654. doi: 10.1038/nrn3819

Kandler, K., and Friauf, E. (1995). Development of glycinergic and glutamatergic synaptic transmission on the auditory brainstem of perinatal rats. *J. Neurosci.* 15, 6890–6904. doi: 10.1523/JNEUROSCI.15-10-06890.1995

Khirug, S., Huttu, K., Ludwig, A., Smirnov, S., Voipo, J., Rivera, C., et al. (2005). Distinct properties of functional KCC2 expression in immature mouse hippocampal neurons in culture and in acute slices. *Eur. J. Neurosci.* 21, 899–904. doi: 10.1111/j.1460-9568.2005.03886.x

Kilb, W. (2020). "The relation between neuronal chloride transpor ter activities, GABA inhibition, and neuronal activity," in *Neuronal Chloride Transporters in Health and Disease*, ed. X. Tang (Amsterdam: Elsevier), 43–57. doi: 10.1016/B978-0-12-815318-5.00003-0

Kim, J. Y., Liu, C. Y., Zhang, F., Duan, X., Wen, Z., Song, J., et al. (2012). Interplay between DISC1 and GABA signaling regulates neurogenesis in mice and risk for schizophrenia. *Cell* 148, 1051–1064. doi: 10.1016/j.cell.2011.12.037

Kjaergaard, M., Nørholm, A. B., Hendus-Altenburger, R., Pedersen, S. F., Poulsen, F. M., and Kragelund, B. B. (2010). Temperature-dependent structural changes in intrinsically disordered proteins: formation of α−helices or loss of polyproline II? *Protein Sci.* 19, 1555–1564. doi: 10.1002/pro.435

Kopp-Scheinpflug, C., Tozer, A. J., Robinson, S. W., Tempel, B. L., Hennig, M. H., and Forsythe, I. D. (2011). The sound of silence: ionic mechanisms encoding sound termination. *Neuron* 71, 911–925. doi: 10.1016/j.neuron.2011.06.028

Korkhov, V. M., Farhan, H., Freissmuth, M., and Sitte, H. H. (2004). Oligomerization of the γ-aminobutyric acid transporter-1is driven by an interplay of polar and hydrophobic interactions in transmembrane helix II. *J. Biol. Chem.* 279, 55728–55736. doi: 10.1074/jbc.M409449200

Koumangoye, R., Bastarache, L., and Delpire, E. (2021). NKCC1: newly found as a human disease-causing ion transporter. *Function* 2:zqaa028. doi: 10.1093/function/zqaa028

Lamsa, K. P., Kullmann, D. M., and Woodin, M. A. (2010). Spike-timing dependent plasticity in inhibitory circuits. *Front. Synaptic Neurosci.* 2:8. doi: 10.3389/fnsyn.2010.00008

Lee, H. C., Jurd, R., and Moss, S. J. (2010). Tyrosine phosphorylation regulates the membrane trafficking of the potassium chloride co-transporter KCC2. *Mol. Cell. Neurosci.* 45, 173–179. doi: 10.1016/j.mcn.2010.06.008

Lee, H. H., Deeb, T. Z., Walker, J. A., Davies, P. A., and Moss, S. J. (2011). NMDA receptor activity downregulates KCC2 resulting in depolarizing GABA A receptor–mediated currents. *Nat. Neurosci.* 14, 736–743. doi: 10.1038/nn.2806

Lee, H. H. C., Walker, J. A., Jeffrey, R. W., Goodier, R. J., Payne, J. A., and Moss, S. J. (2007). Direct PKC-dependent phosphorylation regulates the cell surface stability and activity of the potassium chloride cotransporter, KCC2. *J. Biol. Chem.* 282, 29777–29784. doi: 10.1074/jbc.M705053200

Lemonnier, E., and Ben-Ari, Y. (2010). The diuretic bumetanide decreases autistic behaviour in five infants treated during 3 months with no side effects. *Acta Paediatr.* 99, 1885–1888. doi: 10.1111/j.1651-2227.2010.01933.x

Lemonnier, E., Degrez, C., Phelep, M., Tyzio, R., Josse, F., Grandgeorge, M., et al. (2012). A randomised controlled trial of bumetanide in the treatment of autism in children. *Transl. Psychiatry* 2:e202. doi: 10.1038/tp.2012.124

Lemonnier, E., Villeneuve, N., Sonie, S., Serret, S., Rosier, A., Roue, M., et al. (2017). Effects of bumetanide on neurobehavioral function in children and adolescents with autism spectrum disorders. *Transl. Psychiatry* 7:e1124. doi: 10.1038/tp.2017.101

Liedtke, C. M., Hubbard, M., and Wang, X. (2003). Stability of actin cytoskeleton and PKC-δ binding to actin regulate NKCC1 function in airway epithelial cells. *Am. J. Physiol. Cell Physiol.* 284, C487–C496. doi: 10.1152/ajpcell.00357.2002

Liu, R., Wang, J., Liang, S., Zhang, G., and Yang, X. (2020). Role of NKCC1 and KCC2 in epilepsy: from expression to function. *Front. Neurol.* 10:1407. doi: 10.3389/fneur.2019.01407

Löhrke, S., Srinivasan, G., Oberhofer, M., Doncheva, E., and Friauf, E. (2005). Shift from depolarizing to hyperpolarizing glycine action occurs at different perinatal ages in superior olivary complex nuclei. *Eur. J. Neurosci.* 22, 2708–2722. doi: 10.1111/j.1460-9568.2005.04465.x

Löscher, W., and Kaila, K. (2021). CNS pharmacology of NKCC1 inhibitors. *Neuropharmacology* 205:108910. doi: 10.1016/j.neuropharm.2021.108910

Luhmann, H. J., and Prince, D. A. (1991). Postnatal maturation of the GABAergic system in rat neocortex. *J. Neurophysiol.* 65, 247–263. doi: 10.1152/jn.1991.65.2.247

Mahadevan, V., and Woodin, M. A. (2016). Regulation of neuronal chloride homeostasis by neuromodulators. *J. Physiol.* 594, 2593–2605. doi: 10.1113/JP271593s

Markkanen, M., Ludwig, A., Khirug, S., Pryazhnikov, E., Soni, S., Khiroug, L., et al. (2017). Implications of the N-terminal heterogeneity for the neuronal K-Cl cotransporter KCC2 function. *Brain Res.* 1675, 87–101. doi: 10.1016/j.brainres.2017.08.034

McNeill, A., Iovino, E., Mansard, L., Vache, C., Baux, D., Bedoukian, E., et al. (2020). SLC12A2 variants cause a neurodevelopmental disorder or cochleovestibular defect. *Brain* 143, 2380–2387. doi: 10.1093/brain/awaa176

Medina, I., Friedel, P., Rivera, C., Kahle, K. T., Kourdougli, N., Uvarov, P., et al. (2014). Current view on the functional regulation of the neuronal K+-Cl- cotransporter KCC2. *Front. Cell. Neurosci.* 8:27. doi: 10.3389/fncel.2014.00027

Merner, N. D., Chandler, M. R., Bourassa, C., Liang, B., Khanna, A. R., Dion, P., et al. (2015). Regulatory domain or CpG site variation in SLC12A5, encoding

the chloride transporter KCC2, in human autism and schizophrenia. *Front. Cell. Neurosci.* 9:386. doi: 10.3389/fncel.2015.00386

Merner, N. D., Mercado, A., Khanna, A. R., Hodgkinson, A., Bruat, V., Awadalla, P., et al. (2016). Gain-of-function missense variant in SLC12A2, encoding the bumetanide-sensitive NKCC1 cotransporter, identified in human schizophrenia. *J. Psychiatr. Res.* 77, 22–26. doi: 10.1016/j.jpsychires.2016.02.016

Möhler, H. (2006). GABAA receptor diversity and pharmacology. *Cell Tissue Res.* 326, 505–516. doi: 10.1007/s00441-006-0284-3

Monette, M. Y., and Forbush, B. (2012). Regulatory activation is accompanied by movement in the C terminus of the Na-K-Cl cotransporter (NKCC1). *J. Biol. Chem.* 287, 2210–2220. doi: 10.1074/jbc.M111.309211

Monette, M. Y., Somasekharan, S., and Forbush, B. (2014). Molecular motions involved in Na-K-Cl cotransporter-mediated ion transport and transporter activation revealed by internal cross-linking between transmembrane domains 10 and 11/12. *J. Biol. Chem.* 289, 7569–7579. doi: 10.1074/jbc.M113.542258

Moore, Y. E., Conway, L. C., Wobst, H. J., Brandon, N. J., Deeb, T. Z., and Moss, S. J. (2019). Developmental regulation of KCC2 phosphorylation has long-term impacts on cognitive function. *Front. Mol. Neurosci.* 12:173. doi: 10.3389/fnmol.2019.00173

Moore, Y. E., Deeb, T. Z., Chadchankar, H., Brandon, N. J., and Moss, S. J. (2018). Potentiating KCC2 activity is sufficient to limit the onset and severity of seizures. *Proc. Natl. Acad. Sci. U.S.A.* 115, 10166–10171. doi: 10.1073/pnas.1810134115

Moore, Y. E., Kelley, M. R., Brandon, N. J., Deeb, T. Z., and Moss, S. J. (2017). Seizing control of KCC2: a new therapeutic target for epilepsy. *Trends Neurosci.* 40, 555–571. doi: 10.1016/j.tins.2017.06.008

Morgan, A., Pelliccione, G., Ambrosetti, U., Dell'Orco, D., and Girotto, G. (2020). SLC12A2: a new gene associated with autosomal dominant non-syndromic hearing loss in humans. *Hearing Balance Commun.* 18, 149–151. doi: 10.1038/s10038-021-00954-6

Moriguchi, T., Urushiyama, S., Hisamoto, N., Iemura, S.-I., Uchida, S., Natsume, T., et al. (2005). WNK1 regulates phosphorylation of cation-chloride-coupled cotransporters via the STE20-related kinases, SPAK and OSR1. *J. Biol. Chem.* 280, 42685–42693. doi: 10.1074/jbc.M510042200

Muñoz, A., Méndez, P., DeFelipe, J., and Alvarez-Leefmans, F. J. (2007). Cation-chloride cotransporters and GABA-ergic innervation in the human epileptic hippocampus. *Epilepsia* 48, 663–673. doi: 10.1111/j.1528-1167.2007.00986.x

Mutai, H., Wasano, K., Momozawa, Y., Kamatani, Y., Miya, F., Masuda, S., et al. (2020). Variants encoding a restricted carboxy-terminal domain of SLC12A2 cause hereditary hearing loss in humans. *PLoS Genet.* 16:e1008643. doi: 10.1371/journal.pgen.1008643

Muzyamba, M., Cossins, A., and Gibson, J. (1999). Regulation of Na+-K+-2Cl- cotransport in turkey red cells: the role of oxygen tension and protein phosphorylation. *J. Physiol.* 517, 421–429. doi: 10.1111/j.1469-7793.1999.0421t.x

Oldfield, C. J., Meng, J., Yang, J. Y., Yang, M. Q., Uversky, V. N., and Dunker, A. K. (2008). Flexible nets: disorder and induced fit in the associations of p53 and 14-3-3 with their partners. *BMC Genomics* 9(Suppl. 1):S1. doi: 10.1186/1471-2164-9-S1-S1

Ormond, J., and Woodin, M. A. (2009). Disinhibition mediates a form of hippocampal long-term potentiation in area CA1. *PLoS One* 4:e7224. doi: 10.1371/journal.pone.0007224

Owens, D. F., Boyce, L. H., Davis, M. B. E., and Kriegstein, A. R. (1996). Excitatory GABA responses in embryonic and neonatal cortical slices demonstrated by gramicidin perforated-patch recordings and calcium imaging. *J. Neurosci.* 16, 6416–6423. doi: 10.1523/JNEUROSCI.16-20-06414.1996

Palma, E., Amici, M., Sobrero, F., Spinelli, G., Di Angelantonio, S., Ragozzino, D., et al. (2006). Anomalous levels of Cl- transporters in the hippocampal subiculum from temporal lobe epilepsy patients make GABA excitatory. *Proc. Natl. Acad. Sci. U.S.A.* 103, 8465–8468. doi: 10.1073/pnas.0602979103

Papp, E., Rivera, C., Kaila, K., and Freund, T. F. (2008). Relationship between neuronal vulnerability and potassium-chloride cotransporter 2 immunoreactivity in hippocampus following transient forebrain ischemia. *Neuroscience* 154, 677–689. doi: 10.1016/j.neuroscience.2008.03.072

Payne, J. A., Rivera, C., Voipo, J., and Kaila, K. (2003). Cation-chloride cotransporters in neuronal communication, development and trauma. *Trends Neurosci.* 26, 199–206. doi: 10.1016/S0166-2236(03)00068-7

Pellegrino, C., Gubkina, O., Schaefer, M., Becq, H., Ludwig, A., Mukhtarov, M., et al. (2011). Knocking down of the KCC2 in rat hippocampal neurons increases intracellular chloride concentration and compromises neuronal survival. *J. Physiol.* 589, 2475–2496. doi: 10.1113/jphysiol.2010.203703

Pisella, L. I., Gaiarsa, J.-L., Diabira, D., Zhang, J., Khalilov, I., Duan, J., et al. (2019). Impaired regulation of KCC2 phosphorylation leads to neuronal network dysfunction and neurodevelopmental pathology. *Sci. Signal.* 12:eaay0300. doi: 10.1126/scisignal.aay0300

Puskarjov, M., Seja, P., Heron, S. E., Williams, T. C., Ahmad, F., Iona, X., et al. (2014). A variant of KCC 2 from patients with febrile seizures impairs neuronal Cl- extrusion and dendritic spine formation. *EMBO Rep.* 15, 723–729. doi: 10.1002/embr.201438749

Rahmati, N., Hoebeek, F. E., Peter, S., and De Zeeuw, C. I. (2018). Chloride homeostasis in neurons with special emphasis on the olivocerebellar system: differential roles for transporters and channels. *Front. Cell. Neurosci.* 12:101. doi: 10.3389/fncel.2018.00101

Randall, J., Thorne, T., and Delpire, E. (1997). Partial cloning and characterization of *Slc12a2*: the gene encoding the secretory Na^+-K^+-$2Cl^-$ cotransporter. *Am. J. Cell Physiol.* 273, 1267–1277. doi: 10.1152/ajpcell.1997.273.4.C1267

Richardson, C., and Alessi, D. R. (2008). The regulation of salt transport and blood pressure by the WNK-SPAK/OSR1 signalling pathway. *J. Cell Sci.* 121, 3293–3304. doi: 10.1242/jcs.029223

Richardson, C., Rafiqi, F. H., Karlsson, H. K. R., Moleleki, N., Vandewalle, A., Campbell, D. G., et al. (2008). Activation of the thiazide-sensitive Na+-Cl–cotransporter by the WNK-regulated kinases SPAK and OSR1. *J. Cell Sci.* 121, 675–684. doi: 10.1242/jcs.025312

Rinehart, J., Maksimova, Y. D., Tanis, J. E., Stone, K. L., Hodson, C. A., Zhang, J., et al. (2009). Sites of regulated phosphorylation that control K-Cl cotransporter activity. *Cell* 138, 525–536. doi: 10.1016/j.cell.2009.05.031

Rivera, C., Li, H., Thomas-Crussels, J., Lahtinen, H., Viitanen, T., Nanobashvili, A., et al. (2002). BDNF-induced TrkB activation down-regulates the K+-Cl-cotransporter KCC2 and impairs neuronal Cl- extrusion. *J. Cell Biol.* 159, 747–752. doi: 10.1083/jcb.200209011

Rivera, C., Voipo, J., and Kaila, K. (2005). Two developmental switches in GABAergic signalling: the K+-Cl- cotransporter KCC2 and carbonic anhydrase CAVII. *J. Physiol.* 562, 27–36. doi: 10.1113/jphysiol.2004.077495

Rivera, C., Voipo, J., Payne, J. A., Ruusuvuori, E., Lahtinen, H., Lamsa, K., et al. (1999). The K^+/Cl^- co-transporter KCC2 renders GABA hyperpolarizing during neuronal maturation. *Nature* 397, 251–255. doi: 10.1038/16697

Rohrbough, J., and Spitzer, N. C. (1996). Regulation of intracellular Cl- Levels by Na+-dependent Cl- cotransport distinguishes depolarizing from hyperpolarizing GABAA receptor-mediated responses in spinal neurons. *J. Neurosci.* 16, 82–91. doi: 10.1523/JNEUROSCI.16-01-00082.1996

Saitsu, H., Watanabe, M., Akita, T., Ohba, C., Sugai, K., Ong, W. P., et al. (2016). Impaired neuronal KCC2 function by biallelic SLC12A5 mutations in migrating focal seizures and severe developmental delay. *Sci. Rep.* 6:30072. doi: 10.1038/srep30072

Saraga, F., Balena, T., Wolansky, T., Dickson, C., and Woodin, M. (2008). Inhibitory synaptic plasticity regulates pyramidal neuron spiking in the rodent hippocampus. *Neuroscience* 155, 64–75. doi: 10.1016/j.neuroscience.2008.05.009

Savardi, A., Borgogno, M., De Vivo, M., and Cancedda, L. (2021). Pharmacological tools to target NKCC1 in brain disorders. *Trends Pharmacol. Sci.* 42, 1009–1034. doi: 10.1016/j.tips.2021.09.005

Sehnal, D., Bittrich, S., Deshpande, M., Svobodová, R., Berka, K., Bazgier, V., et al. (2021). Mol* Viewer: modern web app for 3D visualization and analysis of large biomolecular structures. *Nucleic Acids Res.* 49, W431–W437. doi: 10.1093/nar/gkab314

Shekarabi, M., Zhang, J., Khanna, A. R., Ellison, D. H., Delpire, E., and Kahle, K. T. (2017). WNK kinase signaling in ion homeostasis and human disease. *Cell Metab.* 25, 285–299. doi: 10.1016/j.cmet.2017.01.007

Shulga, A., Thomas-Crusells, J., Sigl, T., Blaesse, A., Mestres, P., Meyer, M., et al. (2008). Posttraumatic GABAA-mediated [Ca2+] i increase is essential for the induction of brain-derived neurotrophic factor-dependent survival of mature central neurons. *J. Neurosci.* 28, 6996–7005. doi: 10.1523/JNEUROSCI.5268-07.2008

Silayeva, L., Deeb, T. Z., Hines, R. M., Kelley, M. R., Munoz, M. B., Lee, H. H., et al. (2015). KCC2 activity is critical in limiting the onset and severity of status epilepticus. *Proc. Nat. Acad. Sci. U.S.A.* 112, 3523–3528. doi: 10.1073/pnas.1415126112

Stödberg, T., McTague, A., Ruiz, A. J., Hirata, H., Zhen, J., Long, P., et al. (2015). Mutations in SLC12A5 in epilepsy of infancy with migrating focal seizures. *Nat. Commun.* 6:8038. doi: 10.1038/ncomms9038

Strange, K., Singer, T. D., Morrison, R., and Delpire, E. (2000). Dependence of KCC2 K-Cl cotransporter activity on a conserved carboxy terminus tyrosine residue. *Am. J. Physiol. Cell Physiol.* 279, 860–867. doi: 10.1152/ajpcell.2000.279.3.C860

Su, G., Kintner, D. B., Flagella, M., Shull, G. E., and Sun, D. (2001). Astrocytes from Na-K-Cl cotransporter null mice exhibit an absence of high [K] o-induced swelling and a decrease in EAA release. *Am. J. Physiol. Cell Physiol.* 282, C1147–C1160. doi: 10.1152/ajpcell.00538.2001

Sung, K. W., Kirby, M., McDonald, M. P., Lovinger, D., and Delpire, E. (2000). Abnormal $GABA_A$ receptor-mediated currents in dorsal root ganglien neurons isolated from Na-K-2Cl cotransporter null mice. *J. Neurosci.* 20, 7531–7538. doi: 10.1523/JNEUROSCI.20-20-07531.2000

Thastrup, J. O., Rafiqi, F. H., Vitari, A. C., Pozo-Guisado, E., Deak, M., Mehellou, Y., et al. (2012). SPAK/OSR1 regulate NKCC1 and WNK activity: analysis of WNK isoform interactions and activation by T-loop trans-autophosphorylation. *Biochem. J.* 441, 325–337. doi: 10.1042/BJ20111879

Tillman, L., and Zhang, J. (2019). Crossing the chloride channel: the current and potential therapeutic value of the neuronal K+-Cl-cotransporter KCC2. *Biomed Res. Int.* 2019:8941046. doi: 10.1155/2019/8941046

Titz, S., Sammler, E. M., and Hormuzdi, S. G. (2015). Could tuning of the inhibitory tone involve graded changes in neuronal chloride transport? *Neuropharmacology* 95, 321–331. doi: 10.1016/j.neuropharm.2015.03.026

Tóth, K., Lénárt, N., Berki, P., Fekete, R., Szabadits, E., Pósfai, B., et al. (2022). The NKCC1 ion transporter modulates microglial phenotype and inflammatory response to brain injury in a cell-autonomous manner. *PLoS Biol.* 20:e3001526. doi: 10.1371/journal.pbio.3001526

Turrigiano, G. G., and Nelson, S. B. (2004). Homeostatic plasticity in the developing nervous system. *Nat. Rev. Neurosci.* 5, 97–107. doi: 10.1038/nrn1327

Tyzio, R., Nardou, R., Ferrari, D. C., Tsintsadze, T., Shahrokhi, A., Eftekhari, S., et al. (2014). Oxytocin-mediated GABA inhibition during delivery attenuates autism pathogenesis in rodent offspring. *Science* 343, 675–679. doi: 10.1126/science.1247190

Uvarov, P., Ludwig, A., Markkanen, M., Pruunsild, P., Kaila, K., Delpire, E., et al. (2007). A novel N-terminal isoform of the neuron-specific K-Cl cotransporter KCC2. *J. Biol. Chem.* 282, 30570–30576. doi: 10.1074/jbc.M705095200

Vanniya, S. P., Chandru, J., Jeffrey, J. M., Rabinowitz, T., Brownstein, Z., Krishnamoorthy, M., et al. (2022). PNPT1, MYO15A, PTPRQ, and SLC12A2-associated genetic and phenotypic heterogeneity among hearing impaired assortative mating families in Southern India. *Ann. Hum. Genet.* 86, 1–13. doi: 10.1111/ahg.12442

Virtanen, M. A., Uvarov, P., Hübner, C. A., and Kaila, K. (2020). NKCC1, an elusive molecular target in brain development: making sense of the existing data. *Cells* 9:2607. doi: 10.3390/cells9122607

Virtanen, M. A., Uvarov, P., Mavrovic, M., Poncer, J. C., and Kaila, K. (2021). The multifaceted roles of KCC2 in cortical development. *Trends Neurosci.* 44, 378–392. doi: 10.1016/j.tins.2021.01.004

Vitari, A. C., Deak, M., Morrice, N. A., and Alessi, D. R. (2005). The WNK1 and WNK4 protein kinases that are mutated in Gordon's hypertension syndrome phosphorylate and activate SPAK and OSR1 protein kinases. *Biochem. J.* 391, 17–24. doi: 10.1042/BJ20051180

Vitari, A. C., Thastrup, J., Rafiqi, F. H., Deak, M., Morrice, N. A., Karlsson, H. K., et al. (2006). Functional interactions of the SPAK/OSR1 kinases with their upstream activator WNK1 and downstream substrate NKCC1. *Biochem. J.* 397, 223–231. doi: 10.1042/BJ20060220

Wang, H., Yan, Y., Kintner, D. B., Lytle, C., and Sun, D. (2003). GABA-mediated trophic effect on oligodendrocytes requires Na-K-2Cl cotransport activity. *J. Neurophysiol.* 90, 1257–1265. doi: 10.1152/jn.01174.2002

Watanabe, M., Wake, H., Moorhouse, A. J., and Nabekura, J. (2009). Clustering of neuronal K+-Cl- cotransporter in lipid rafts by tyrosine phosphorylation. *J. Biochem.* 284, 27980–27988. doi: 10.1074/jbc.M109.043620

Weber, M., Hartmann, A.-M., Beyer, T., Ripperger, A., and Nothwang, H. G. (2014). A novel regulatory locus of phosphorylation in the C-terminus of the potassium chloride cotransporter KCC2 that interferes with N-ethylmaleimide or staurosporine mediated activation. *J. Biol. Chem.* 289, 18668–18679. doi: 10.1074/jbc.M114.567834

Woodin, M. A., Ganguly, K., and Poo, M.-M. (2003). Coincident pre-and postsynaptic activity modifies GABAergic synapses by postsynaptic changes in Cl-transporter activity. *Neuron* 39, 807–820. doi: 10.1016/s0896-6273(03)00507-5

Wu, W. I., Ziskind-Conhaim, L., and Sweet, M. A. (1992). Early development of Glycine- and GABA-mediated synapses in rat spinal cord. *J. Neurosci.* 12, 3935–3945. doi: 10.1523/JNEUROSCI.12-10-03935.1992

Xu, C., Zhao, M.-X., Poo, M.-M., and Zhang, X.-H. (2008). GABAB receptor activation mediates frequency-dependent plasticity of developing GABAergic synapses. *Nat. Neurosci.* 11, 1410–1418. doi: 10.1038/nn.2215

Zhang, B. L., Spigelman, I., and Carlen, P. L. (1991). Development of GABA-mediated, chloride dependent inhibition in CA1 pyramidal neurones of immature rat hippocampal slices. *J. Physiol.* 444, 25–49. doi: 10.1113/jphysiol.1991.sp018864

Zhang, J., Bhuiyan, M. I. H., Zhang, T., Karimy, J. K., Wu, Z., Fiesler, V. M., et al. (2020a). Modulation of brain cation-Cl- cotransport via the SPAK kinase inhibitor ZT-1a. *Nat. Commun.* 11:78. doi: 10.1038/s41467-019-13851-6

Zhang, J., Cordshagen, A., Medina, I., Nothwang, H. G., Wisniewski, J. R., Winklhofer, M., et al. (2020b). Staurosporine and NEM mainly impair WNK-SPAK/OSR1 mediated phosphorylation of KCC2 and NKCC1. *PLoS One* 15:e0232967. doi: 10.1371/journal.pone.0232967

Zhang, S., Zhou, J., Zhang, Y., Liu, T., Friedel, P., Zhuo, W., et al. (2021). The structural basis of function and regulation of neuronal cotransporters NKCC1 and KCC2. *Commun. Biol.* 4:226. doi: 10.1038/s42003-021-01750-w

Zhang, Y., Chen, K., Sloan, S. A., Bennett, M. L., Scholze, A. R., O'Keeffe, S., et al. (2014). An RNA-sequencing transcriptome and splicing database of glia, neurons, and vascular cells of the cerebral cortex. *J. Neurosci.* 34, 11929–11947. doi: 10.1523/JNEUROSCI.1860-14.2014

Zhao, Y., Roy, K., Vidossich, P., Cancedda, L., De Vivo, M., Forbush, B., et al. (2022). Structural basis for inhibition of the Cation-chloride cotransporter NKCC1 by the diuretic drug bumetanide. *Nat. Commun.* 13:2747. doi: 10.1038/s41467-022-30407-3

Zhu, L., Lovinger, D., and Delpire, E. (2005). Cortical neurons lacking KCC2 expression show impaired regulation of intracellular chloride. *J. Neurophysiol.* 93, 1557–1568. doi: 10.1152/jn.00616.2004

Zonouzi, M., Scafidi, J., Li, P., McEllin, B., Edwards, J., Dupree, J. L., et al. (2015). GABAergic regulation of cerebellar NG2 cell development is altered in perinatal white matter injury. *Nat. Neurosci.* 18, 674–682. doi: 10.1038/nn.3990

frontiers | Frontiers in Molecular Neuroscience

TYPE Original Research
PUBLISHED 11 August 2022
DOI 10.3389/fnmol.2022.979479

OPEN ACCESS

EDITED BY
Atsuo Fukuda,
Hamamatsu University School of Medicine, Japan

REVIEWED BY
Hajime Hirase,
University of Copenhagen, Denmark
Hiroki Toyoda,
Osaka University, Japan

*CORRESPONDENCE
Roustem Khazipov
roustem.khazipov@inserm.fr

SPECIALTY SECTION
This article was submitted to Methods and Model Organisms, a section of the journal Frontiers in Molecular Neuroscience

RECEIVED 27 June 2022
ACCEPTED 20 July 2022
PUBLISHED 11 August 2022

CITATION
Vazetdinova A, Valiullina-Rakhmatullina F, Rozov A, Evstifeev A, Khazipov R and Nasretdinov A (2022) On the accuracy of cell-attached current-clamp recordings from cortical neurons. *Front. Mol. Neurosci.* 15:979479. doi: 10.3389/fnmol.2022.979479

On the accuracy of cell-attached current-clamp recordings from cortical neurons

Alina Vazetdinova[1], Fliza Valiullina-Rakhmatullina[1], Andrei Rozov[1,2,3], Alexander Evstifeev[1], Roustem Khazipov[1,4]* and Azat Nasretdinov[1]

[1]Laboratory of Neurobiology, Kazan Federal University, Kazan, Russia, [2]Institut für Physiologie und Pathophysiologie, Heidelberg, Germany, [3]Federal Center of Brain Research and Neurotechnologies, Moscow, Russia, [4]INMED - INSERM, Aix-Marseille University, Marseille, France

Cell-attached current-clamp (CA/CC) recordings have been proposed to measure resting membrane potential and synaptic/agonist responses in neurons without disrupting the cell membrane, thus avoiding the intracellular dialysis that occurs in conventional whole-cell recordings (WC). However, the accuracy of CA/CC recordings in neurons has not been directly assessed. Here, we used concomitant CA and WC current clamp recordings from cortical neurons in brain slices. Resting membrane potential values and slow voltage shifts showed variability and were typically attenuated during CA/CC recordings by ∼10–20% relative to WC values. Fast signals were slowed down and their amplitude was greatly reduced: synaptic potentials by nearly 2-fold, and action potentials by nearly 10-fold in CA/CC mode compared to WC. The polarity of GABAergic postsynaptic responses in CA/CC mode matched the responses in WC, and depolarising GABAergic potentials were predominantly observed during CA/CC recordings of intact neonatal CA3 hippocampal pyramidal neurons. Similarly, CA/CC recordings reliably detected neuronal depolarization and excitation during network-induced giant depolarizing potentials in the neonatal CA3 hippocampus, and revealed variable changes, from depolarization to hyperpolarization, in CA1 pyramidal cells during sharp wave ripples in the adult hippocampus. Thus, CA/CC recordings are suitable for assessing membrane potential but signal distortion, probably caused by leakage via the seal contact and RC filtering should be considered.

KEYWORDS

patch-clamp technique, cell-attached, neurons, cortex, hippocampus, depolarizing action of GABA, giant depolarizing potentials (GDPs), sharp wave ripple

Introduction

Cell-attached patch-clamp recordings in voltage-clamp mode were pioneered for recording single ion channel activity and remain an unique technique (along with inside-out and outside-out) for exploring ion channel activity on the sub-millisecond time scale (Neher and Sakmann, 1976; Hamill et al., 1981). In addition, cell-attached

voltage-clamp recordings have been implemented for recording and evoking action potentials in neurons (Chavas and Marty, 2003; Perkins, 2006; Alcami et al., 2012; Khalilov et al., 2015), estimation of the resting membrane potential (E_m) from the reversal potential of the currents through potassium and NMDA channels (Khazipov et al., 1995; Verheugen et al., 1995, 1999; Fricker et al., 1999; Tyzio et al., 2003), and driving force acting on currents through GABA channels (Tyzio et al., 2006, 2008; Khazipov et al., 2008). An advantage of the cell-attached recording technique is that it allows access to neuronal functions without cell membrane rupture, thus avoiding an introduction of leakage conductance via the seal between the pipette and the membrane (Barry and Lynch, 1991; Tyzio et al., 2003) and without alteration in the intracellular medium caused by cell dialysis (Pusch and Neher, 1988). Performed in current-clamp mode, cell-attached recordings allow assessment of cell voltage including resting E_m, action potentials, synaptic events and agonist responses (Fenwick et al., 1982; Hayar et al., 2004; Mason et al., 2005; Perkins, 2006; Kirmse et al., 2015). The rationale for cell-attached current-clamp (CA/CC) recordings is that with seal resistance (R_{seal}) much greater than patch resistance (R_{patch}), the voltage at the cell-attached patch-pipette should approach the E_m value. Simultaneous whole-cell (WC) and CA/CC recordings from electrically compact rat basophilic leukemia cells and megakaryocytes revealed a high degree of accuracy in measuring E_m using the CA/CC approach and the ability of this technique to monitor dynamic changes in membrane potential in these non-excitable cells (Mason et al., 2005). However, it has been noted that the accuracy of the measurement of the dynamic changes in membrane potentials maybe limited by the filtering of fast signals by the membrane patch RC filter (Fenwick et al., 1982; Mason et al., 2005; Perkins, 2006). However, the accuracy with which CA/CC recordings measure E_m and its dynamic changes in neurons has not been directly addressed.

Here, were explored this issue using concomitant CA and WC recordings of neocortical and hippocampal neurons in mouse brain slices. We found that CA/CC recordings are suitable for assessing steady-state membrane potential, synaptic activity, action potentials, depolarizing and hyperpolarizing actions of GABA, and cellular behavior during network-driven activity, but with allowance for possible errors compromising signal amplitude and kinetics, including leakage of the seal and RC filtering.

Materials and methods

Ethical approval

The animal experiments were carried out in compliance with the ARRIVE guidelines. Animal care and procedures were in accordance with EU Directive 2010/63/EU for animal experiments, and all animal-use protocols were approved by the French National Institute of Health and Medical Research (APAFIS #16992-2020070612319346 v2) and the Local Ethical Committee of Kazan Federal University (No24/22.09.2020).

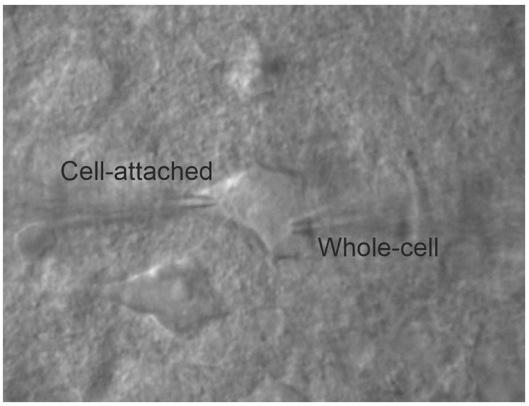

FIGURE 1
Dual whole-cell and cell-attached recordings from cortical neurons in brain slice. Differential interference contrast image of a L5 pyramidal cell in mouse somatosensory cortex. Cell-attached (left) and whole-cell patch electrodes (right) allow simultaneous recordings from the same neuron.

Brain slice preparation

C57BL/6 mice of both sexes aged from postnatal days [P] 5 to 60 were used. Animals were decapitated under isoflurane anesthesia (5%), the brain was rapidly removed and placed in ice-cold (2–5°C) slicing solution of the following composition (in mM): K-Gluconate 140, Na-Gluconate 15, NaCl 4, EGTA 0.2, D-AP5 50 μM and HEPES 10 (pH 7.4) (for cortical recordings) or NaCl, 125; $NaHCO_3$, 25; KCl 2.5; NaH_2PO_4 1,25; $MgCl_2$, 1; $CaCl_2$, 2; H D-glucose, 25 (for hippocampal recordings). Four hundred and fifty micrometer thick horizontal slices were cut using a PELCO easiSlicer™ vibratome (Ted Pella, Inc., Redding, CA, USA). Slices were first kept in oxygenated (95% O_2-5% CO_2) artificial cerebrospinal fluid (ACSF) of the following composition (in mM): NaCl 126, KCl 3.5, $CaCl_2$ 2, $MgCl_2$ 1.3, $NaHCO_3$ 25, NaH_2PO_4 1.2 and glucose 11 (pH 7.4) for 30 min at 32 °C and then at room temperature (20–22 °C) for at least 1 h before use.

Electrophysiological recordings

For recordings, slices were placed into a submerged chamber and superfused with oxygenated ACSF at 30–32°C at a flow rate of 2–3 ml/min. Individual neurons were identified using a vertical microscope (BX-51 WI; Olympus, Japan) at 40×

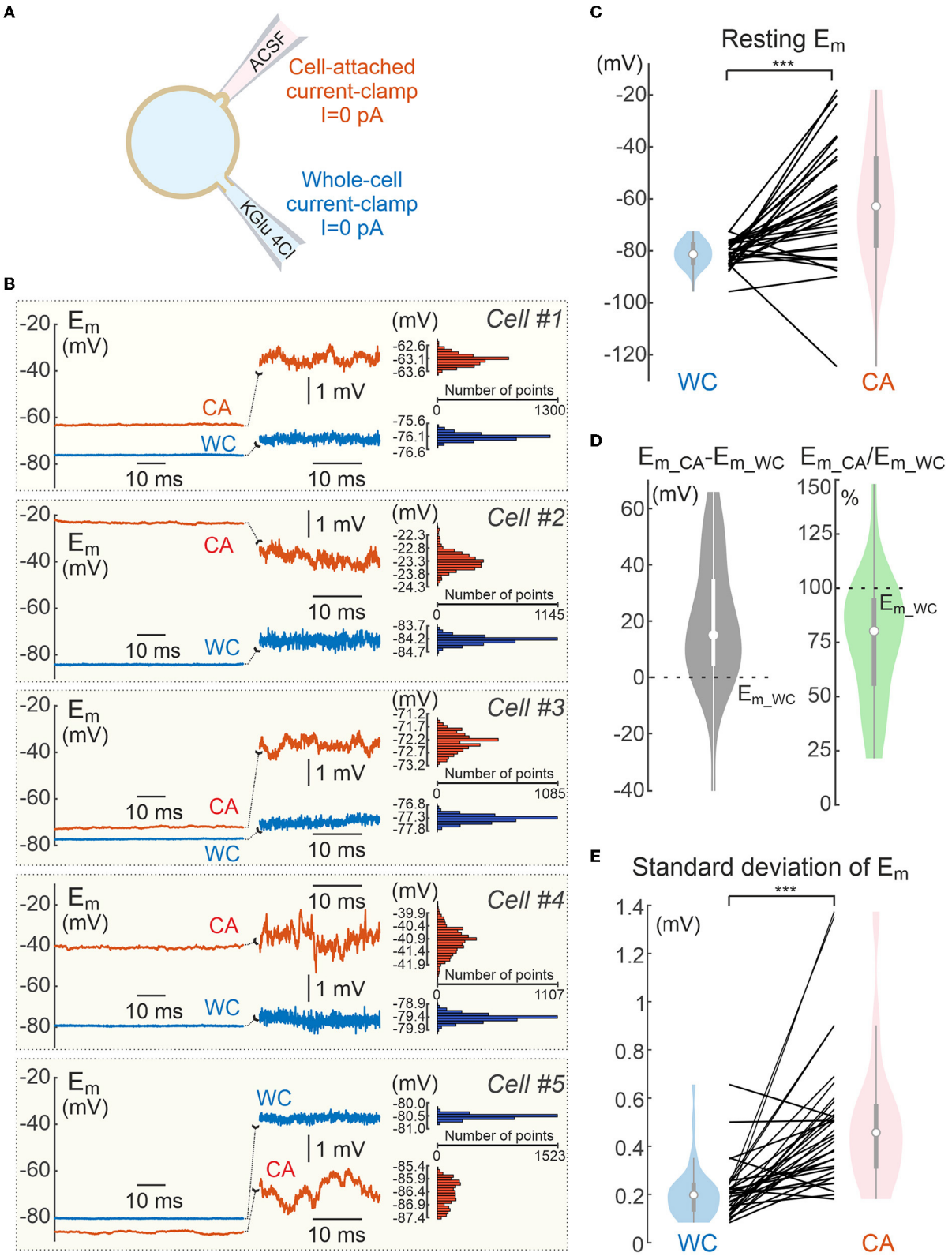

FIGURE 2
Resting membrane potential of L5 cortical neurons during dual cell-attached and whole-cell recordings in current-clamp mode. **(A)** Scheme of whole-cell and cell-attached recordings of the resting membrane potential. Null current (I = 0) is injected to either of electrodes. **(B)** Example

(Continued)

FIGURE 2
dual recordings of the resting membrane potential (E_{m_rest}) from five L5 pyramidal neurons in whole-cell (WC, blue traces) and cell-attached (CA, red traces) configurations in current-clamp mode with common E_m scale (left panels) and with expanded E_m scale (middle panels). The right panels show corresponding E_m all point histograms. **(C)** E_{m_rest} values measured in paired WC and CA recordings. Hereafter, each line represents paired WC and CA data from an individual neuron, violin plots show the probability density of the data at different values smoothed by a kernel density estimator, white dots show the median of the data, vertical gray bar indicates the interquartile range. **(D)** Difference between (left) and ratio of (right) CA and WC E_{m_rest} values. **(E)** Baseline noise assessed as standard deviation of E_m in CA and WC current-clamp recordings. **(C–E)** Pooled data from 32 L5 pyramidal cells of mouse somatosensory cortex and CA1 hippocampus (age P14–P30). ***$P < 0.001$.

magnification using infrared differential interference contrast microscopy (IR-DIC). Recordings were made from neurons of the neocortex (Figures 1–8), and CA1 (Figures 2, 9, 10, 13) and CA3 (Figures 11, 12) regions of the hippocampus. Whole-cell recordings were performed using electrodes prepared from borosilicate glass with resistance of 5–7 MOhm when filled with the pipette solution of the following composition (in mM): (1) K-Gluconate 144, KCl 4, MgATP 4, NaGTP 0.3, HEPES 10, phosphocreatine, or (2) K-Gluconate 105, KCl 30, MgATP 4, NaGTP 0.3, HEPES 10, phosphocreatine 10 (pH 7.26). For solutions 1 and 2, the equilibrium Nernst potentials for chloride were −92 and −39 mV, respectively. Cell-attached recordings were performed using electrodes of 10–17 MOhm when filled with the pipette solution containing (in mM): (3) NaCl 125; $NaHCO_3$ 25; KCl 2.5; NaH_2PO_4 1.25; $MgCl_2$ 1; $CaCl_2$ 2; H D-glucose, 25. E_m values obtained during WC recordings were corrected for the liquid junction potential of 16 mV and 12.5 mV for the pipette solutions containing 4 Cl^- and 30 Cl^-, respectively. Patch-clamp signals were recorded and digitized using EPC8 (HEKA electronics, Germany) with a sampling rate 50 kHz. For local field potential recordings, single-wire 50 μm tungsten electrodes or 16-channel iridium silicone probes were used. Signals were recorded and digitized using Open Ephys (Cambridge, Massachusetts) at a sampling rate of 30 kHz. The electrode of the silicone probe closest to the recorded cell was used for the analysis. GABAergic postsynaptic potentials were evoked by electrical stimulation in stratum radiatum of hippocampus in the presence of CNQX (10 μM) and APV (40 μM).

Data analysis

Data were analyzed using custom-written procedures in Matlab (MathWorks, Inc., Natick, MA, USA). Preprocessing, preliminary analysis and review of the data were performed using ExpressAnalysis and Eview tools (https://github.com/AndreyZakharovExp). In the recordings with current injection through the whole-cell pipette, off-line bridge compensation was made by subtracting a rectangular-shaped potential, at the boundaries of which the first derivative of the whole-cell potential exceeds the empirically determined threshold (30% of the derivative peak value during the ON-phase of the step). In the recordings with sinusoidal current injection, E_m signals recorded in CA and WC configurations were fit by sinusoids, from which the CA/WC amplitude ratio was estimated. To fit the experimental values of the amplitude response (AR), we used the function calculated from the circuit diagram of the model (Figure 5C):

$$AR(f) = \frac{\sqrt{(2 \cdot \pi \cdot K_R \cdot \tau \cdot f)^2 + K_R^2}}{\sqrt{(2 \cdot \pi \cdot (K_C + 1) \cdot K_R \cdot \tau \cdot f)^2 + (K_R + 1)^2}} \quad (1)$$

Where $K_R = R_{seal}/R_{patch}$, $K_C = C_{elec}/C_{patch}$, $\tau = R_{patch} \cdot C_{patch}$.

The amplitude of AP and PSP was calculated as the maximum value after subtraction of the mean E_m value in the interval of 1 and 5 ms before onset. APs in WC recordings were detected as events exceeding a threshold of 40 mV above the resting potential and spontaneous PSPs were detected as events exceeding the threshold of 1 mV/ms on the first derivative of the E_m signal. The onset of events was determined at a threshold of 10 mV/ms (for APs) or 0.1 mV/ms (for PSPs). The amplitude-to-noise ratio of the PSPs was calculated as average amplitude of the PSP divided by the standard deviation of the quietest 1 s interval in the recording. The amplitude of evoked GABA-PSPs was calculated as the maximum signal deflection reached within 200 ms after the stimulus in the average data, subtracting the corresponding E_m median baseline value within 200 ms before the stimulus. Sharp-wave ripples and Giant Depolarizing Potentials were detected from the 1–100 Hz band passed local field potential signal at the threshold of 3 standard deviations of the quietest 100 s episode in the recording. APs in CA recordings were detected from the first derivative of E_m at a threshold of 1 mV/ms. Extracellular multiple unit activity was detected from 300 to 2,500 Hz band passed local field potential signal at a threshold of 3 standard deviation of the quietest 100 s episode in the recording. Dominant frequency of APs and PSPs was calculated on the assumption that the half-width of the event is 1/3 of the period.

Statistical analysis

Statistical analysis was based on the non-parametric Wilcoxon signed rank and rank sum test (for paired and independent samples), or Kruskal-Wallis test with the significance level set at $p < 0.05$. Results are given as median [25th percentile; 75th percentile].

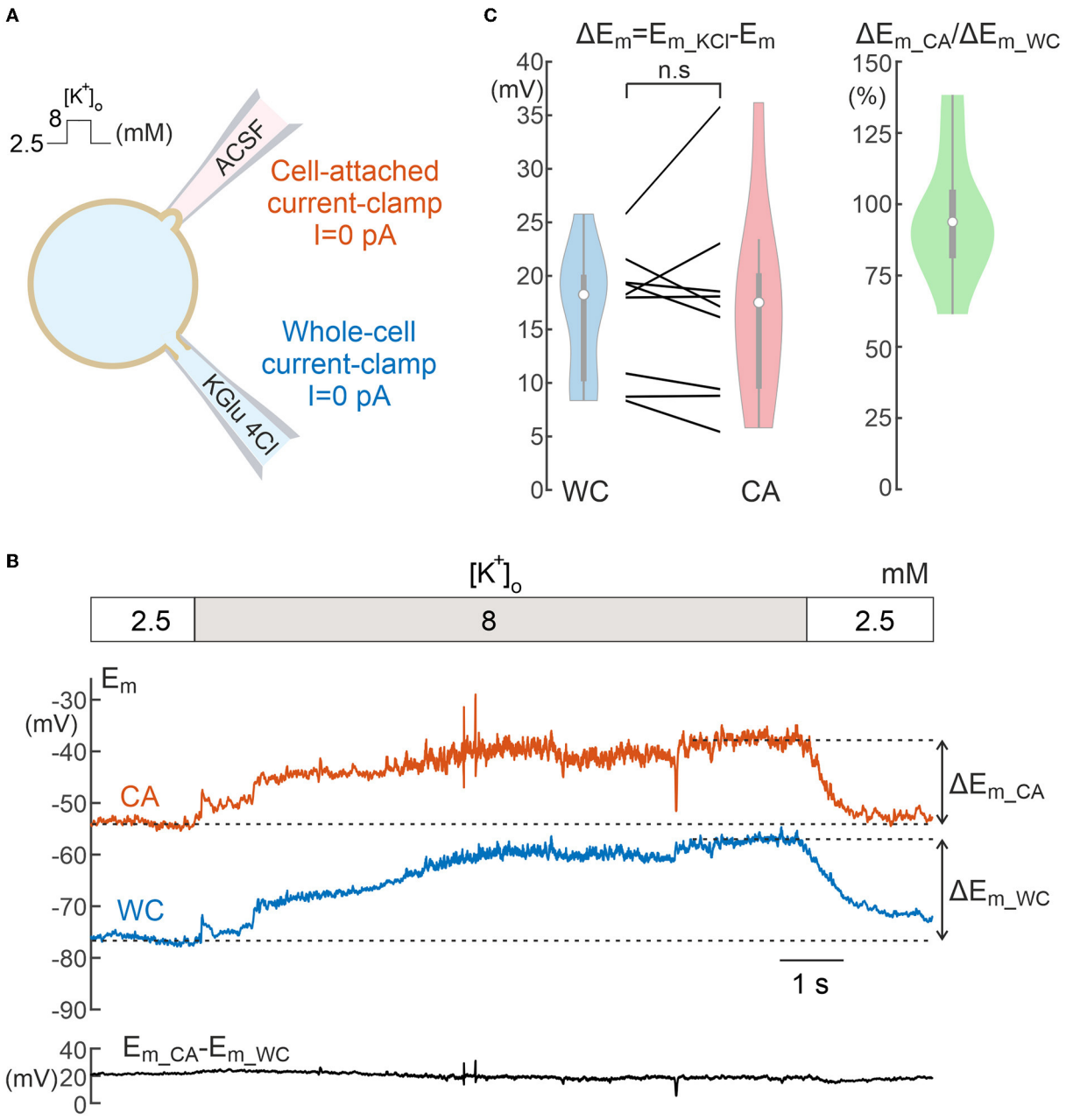

FIGURE 3
Comparison of neuronal depolarization induced by elevated potassium during cell-attached and whole-cell recordings. **(A)** Scheme of recordings. **(B)** Example of the response to an increase in $[K^+]_o$ from 2.5 to 8 mM in the bath solution during dual WC and CA recordings in a L5 pyramidal neuron. The dashed lines indicate the steady-state E_m levels used to calculate E_m depolarization during $[K^+]_o$ elevation. The trace below shows a difference between the E_m values in CA and WC throughout the experiment. **(C)** Neuronal depolarization in response to high potassium in paired WC and CA recordings (left) and corresponding CA/WC transfer coefficient (right). Pooled data from 9 L5 pyramidal cells of mouse somatosensory cortex. n.s, non-significant.

Results

Resting membrane potential

In the present study, we estimated the accuracy of CA/CC recordings of the membrane potential of cortical neurons in brain slices using dual CA and WC recordings from the same neurons (Figure 1). First, we compared resting membrane potential (E_m) values measured with CA and WC electrodes when zero current was injected into either electrode (Figure 2A). Figure 2B shows example traces of WC and CA recordings from five L5 neurons of mouse somatosensory cortex. E_m values

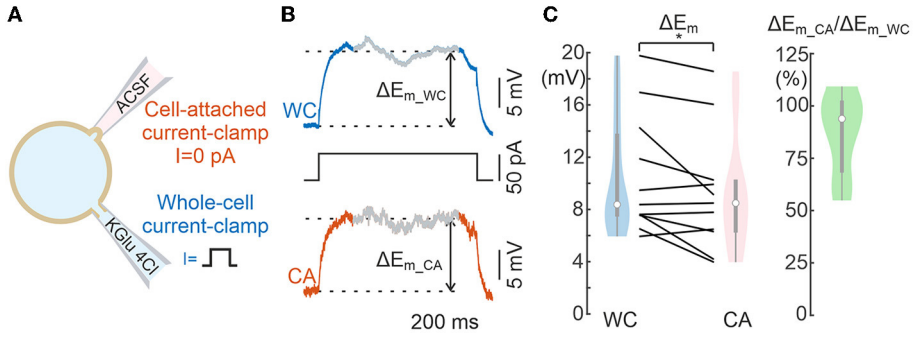

FIGURE 4
Comparison of voltage responses evoked by current steps during whole-cell and cell-attached recordings. **(A)** Scheme of recordings. **(B)** Example of the response to a current step applied to WC electrode during dual WC and CA recordings from a L5 pyramidal neuron. The section of the signal from which the response value was calculated is shaded. The dashed lines indicate E_m levels used to calculate the voltage response. **(C)** Neuronal depolarization in response to WC- current steps in paired WC and CA recordings. The left plot shows the absolute values and the right plot shows the corresponding CA/WC transfer coefficient. Pooled data from 11 L5 pyramidal cells of mouse somatosensory cortex. *$P < 0.05$.

obtained during WC recordings (E_{m_wc}) were −81.3 mV [-84.6 ÷ −77.3] mV (median [25th percentile 75th percentile]), range −95.7 to −72.5 mV (n = 32 cells) which is close to previously reported values (Gulledge and Stuart, 2003). E_m values obtained during CA recordings (E_{m_ca}) were on average more depolarized than E_{m_wc} values and showed higher variability, reaching −62.8 [−78.1 ÷ −44.3] mV, range −124.5 to −18.0 mV (Figure 2C; n = 32 cells, $p < 0.05$, Wilcoxon Signed Rank Test). It should be noted that, in general, E_m values were more frequently depolarized in CA relative to WC, but E_{m_ca} values more negative than E_{m_wc} were also observed. At the group level, the difference between E_m values in CA and WC was 16.0 [5.4 35.4] mV, range −39.4 to 66.9 mV (n = 32 cells). Accordingly, the E_m transfer coefficient, measured as the ratio E_{m_ca}/E_{m_wc}, was close to 0.8 and showed great variability (Figure 2D). Furthermore, CA records were characterized by larger baseline fluctuations (Figure 2B), with the standard deviation of E_m from the mean being more than twice as high (Figure 2E). Thus, CA recordings provided more variable and, on average, more depolarized E_m estimates compared to those obtained using WC recordings.

High potassium-induced depolarization

We further explored the responses evoked by bath application of high-potassium solution using CA and WC recordings from L5 neurons (Figure 3A). Increasing $[K^+]_o$ from control levels of 2.5 to 8 mM induced a slowly developing neuronal depolarization and neuronal firing in both WC and CA recordings (Figure 3B, note that APs are suppressed by <1 Hz low-pass median filtering for clarity). Despite any difference in initial resting E_m values during WC and CA recordings, the amplitude of depolarizing E_m shifts induced by high potassium was similar in CA and WC recordings, with the average CA/WC transfer coefficient close to 0.95 (Figure 3C; n = 9, $P > 0.05$, Wilcoxon Signed Rank Test).

Response to current steps

We next examined the voltage responses elicited by subthreshold square pulse current steps of 50 pA and 1 s duration injected into the cell via the WC patch pipette (Figure 4A). Figure 4B shows exemplary responses to current steps in WC and CA. The magnitude of E_m shifts during current steps was similar for CA and WC recordings, and analysis of group data revealed significant difference between CA and WC responses, and the amplitude of CA responses tended to be smaller than that of WC responses, with a mean CA/WC transfer coefficient of nearly 0.9 (Figure 4C; n = 11 L5 pyramidal cells; $P > 0.05$, Wilcoxon Signed Rank Test).

Responses to sinusoidal currents

The above results show that CA recordings estimate slow E_m changes in cortical neurons relatively reliably. Next, we examined the accuracy of cell-attached E_m measurements of voltage signals evoked by sinusoidal currents of different frequencies (from 0.1 to 100 Hz) injected into L5 pyramidal cells via the WC pipette (Figure 5A). As shown in Figure 5B, the voltage responses recorded in the CA configuration were similar to the WC response at low (0.1 Hz) frequency of the sinusoidal current. However, the amplitude of the CA voltage responses decreased more and more compared to the WC responses with an increase of the sinusoidal current frequency to 10 and 100 Hz. Figure 5D shows corresponding WC-to-CA transfer coefficient

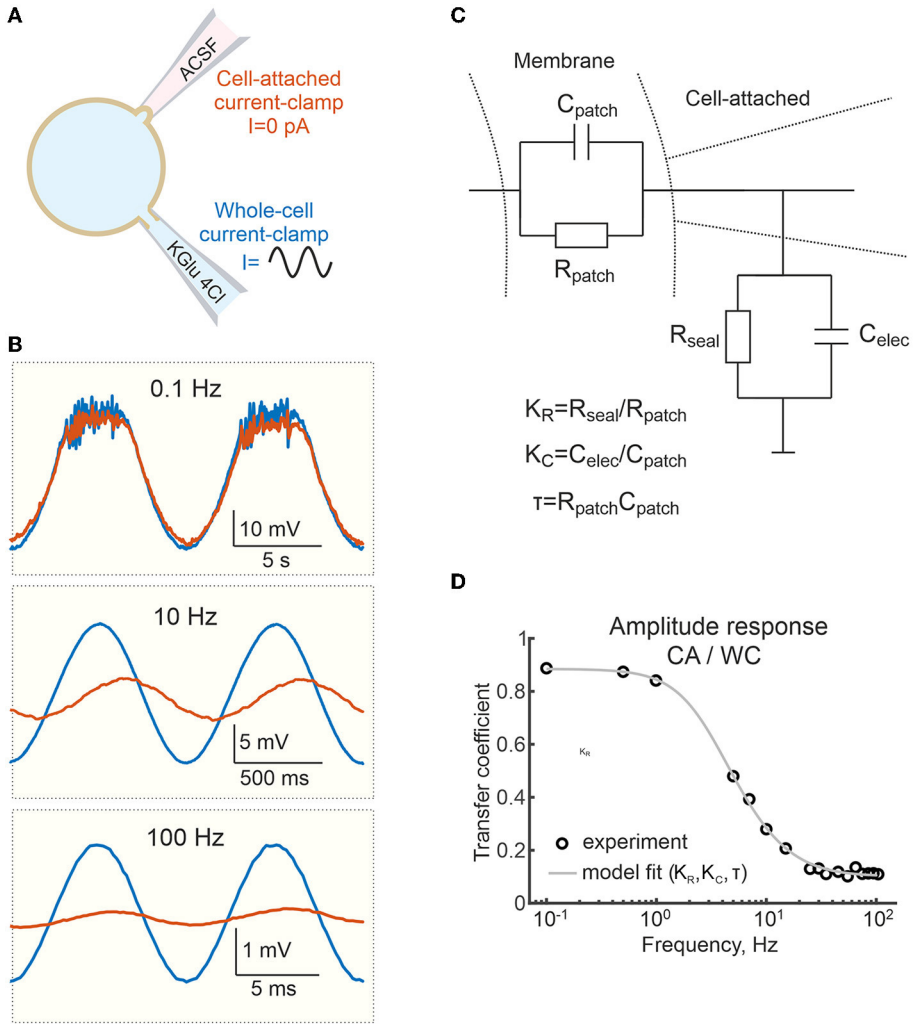

FIGURE 5
Frequency dependence of the voltage response to sinusoidal currents in cell-attached and whole-cell recordings. **(A)** Scheme of recordings. Sinusoidal currents of different frequencies are applied to the WC electrode. **(B)** Examples of responses to sinusoidal currents of different frequencies applied to WC electrode during dual WC and CA recordings from a L5 pyramidal neuron. **(C)** Electrical equivalent model of CA recordings. C_{patch} and R_{patch} are capacitance and resistance of the cell-attached membrane patch; C_{elec} and R_{seal} are capacitance of the patch pipette and seal resistance. **(D)** Transfer coefficient (amplitude response) during CA recordings relative to the WC response as a function of the frequency of the sinusoidal current applied to the WC- electrode. The circles are experimental data from a single cell, the gray line shows fit with a model on **(C)**.

estimated as the ratio of the oscillation amplitude in CA to WC recordings as a function of sinusoidal current frequency in the range 0.1 to 100 Hz. Note that for this neuron, the transfer coefficient approaches 0.9 at a frequency <1 Hz. At higher frequencies, CA/WC transfer coefficient gradually decreases and approaches the value of 0.1 at frequencies >10 Hz.

We fitted these data with an electrical equivalence model for CA/CC recordings that takes into account two RC chains made by the cell membrane patch under the electrode (R_{patch} and C_{patch}) and another by the electrode capacitance (C_{elec}) and the seal resistance (R_{seal}) (Figure 5C) (Fenwick et al., 1982; Tyzio et al., 2003; Mason et al., 2005; Perkins, 2006). In the low frequency range (from 0 to ~1 Hz) this filter mainly works as a voltage divider, with the transfer coefficient determined by the ratio $R_{seal}/(R_{seal}+R_{patch})$. In the high-frequency range (above 100 Hz), the filter mainly works as a capacitive voltage divider and the amplitude ratio is limited by the ratio $C_{patch}/(C_{patch}+C_{elec})$. The experimental data for amplitude response was fitted using function (1) (see Methods). The results of the fitting are shown as a gray line in Figure 5D. For C_{elec} of 7 pF, the best fit of the model to the experimental data for these recordings gave values of C_{patch} = 0.8 pF, R_{seal}=55.6 GOhm, R_{patch}=7.3 GOhm. The results of a similar analysis in a group of six L5 pyramidal cells are shown in Figure 6A, with

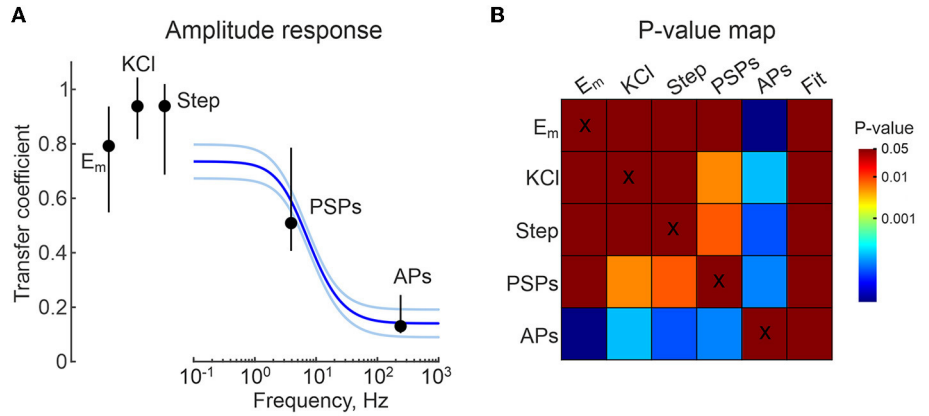

FIGURE 6
Group data on frequency dependence of CA/WC transfer coefficient. **(A)** Group data on the frequency dependence of the CA/WC amplitude transfer coefficient of sinusoidal signals obtained from 6 L5 neurons. The blue line shows the average fit, the iced blue lines show the standard errors. CA/WC transfer coefficients for E_{m_rest} values (from Figure 2), responses to high-potassium (from Figure 3) and current steps (from Figure 4), spontaneous postsynaptic potentials (from Figure 8) and APs (from Figure 7) are shown as median value ± interquartile range. **(B)** *P*-value map for comparison between all groups shown in **(A)**. The color of the cell at the row-column intersection shows the statistical significance (*p*-value) for the corresponding parameters. The last column shows the *p*-value for the corresponding comparison with the fitting results at the appropriate frequency (from the panel **A**). The dark red color corresponds to non-significant differences ($p > 0.05$), the other colors show different levels of significance of differences ($p < 0.05$) according to the color code (color bar on the right).

estimates of C_{patch} = 0.8 [0.4 1.6] pF, R_{seal} = 15.4 [8.2 23.6] GOhm, R_{patch}=4.9 [4.8 5.1] GOhm. The theoretical transfer coefficient approached values of 0.78 [0.63 0.85] at 0 Hz, which was close to the attenuation level of constant (resting E_m) and slow (responses to current steps and high-potassium) signals in CA mode (Figures 6A,B). Model data also agreed with the experimental results on the degree of suppression of the AP and PSP amplitude in the corresponding frequency ranges (Figures 6A,B and see below).

Action potentials and synaptic potentials

We further investigated the properties of fast physiological signals, action potentials (APs) and postsynaptic potentials (PSPs), during current-clamp CA recordings. L5 pyramidal cells were recorded with WC and CA electrodes, and APs were evoked in these neurons by suprathreshold depolarizing current steps at the WC electrode. Figure 7B shows examples of APs recorded in WC and CA configurations. Both the amplitude and the time course of the APs were severely distorted in CA recordings (Figure 7C). AP amplitude was reduced almost tenfold in CA recordings compared with WC recordings (CA/WC transfer coefficient: 0.13 [0.10 0.24], n = 12), whereas AP half-duration and onset-to-peak time were almost 2-fold longer in CA recordings (Figure 7D). Extremely low values of the CA/WC transfer coefficient of AP amplitude corresponded to the frequency response characteristics of the sinusoidal evoked responses at the dominant frequency of the AP waveform (240 [200 270]) Hz; n = 12) (Figures 6A,B).

Spontaneous postsynaptic potentials (sPSPs) were recorded from L5 pyramidal cells with WC and CA electrodes at the resting membrane potential. Since a WC pipette solution with low (4 mM) chloride content was used in these recordings and the GABAergic postsynaptic potentials reverse near the resting membrane potential (see below), most of the sPSPs were probably glutamatergic in nature. Figure 8A shows exemplary traces of sPSPs in CA and WC recordings. It is noteworthy that sPSPs were less visible in CA than WC recordings due to the higher baseline noise (see also Figures 1B,D) and the amplitude of sPSPs was smaller, resulting in almost 10-fold lower signal-to-noise ratio in CA mode (Figure 8D). Therefore, the sPSPs were detected from the WC recordings and compared with the corresponding voltage traces from the CA recordings. As shown by the average trace of sPSP in a L5 pyramidal neuron in Figure 8B, the amplitude of the CA-sPSPs was almost half of that of the WC-sPSPs (see also Figure 8C), and their time course was slowed down. At the same time there was a high correlation between the amplitudes of CA-sPSPs and WC-sPSPs (Figure 8C). At the population level (n = 10 L5 pyramidal cells), CA-sPSPs were 2-fold smaller in amplitude than WC-sPSPs (CA/WC transfer coefficient: 0.51 [0.41 0.79], n = 10), and their half-duration and rise time were significantly prolonged (Figure 8E). As with APs, the CA/WC transfer coefficient of the sPSPs amplitude corresponded to the frequency response characteristics of sinusoidal evoked responses at the dominant frequency of the sPSPs waveform (3.9 [2.2 4.5] Hz; n = 10) (Figures 6A,B).

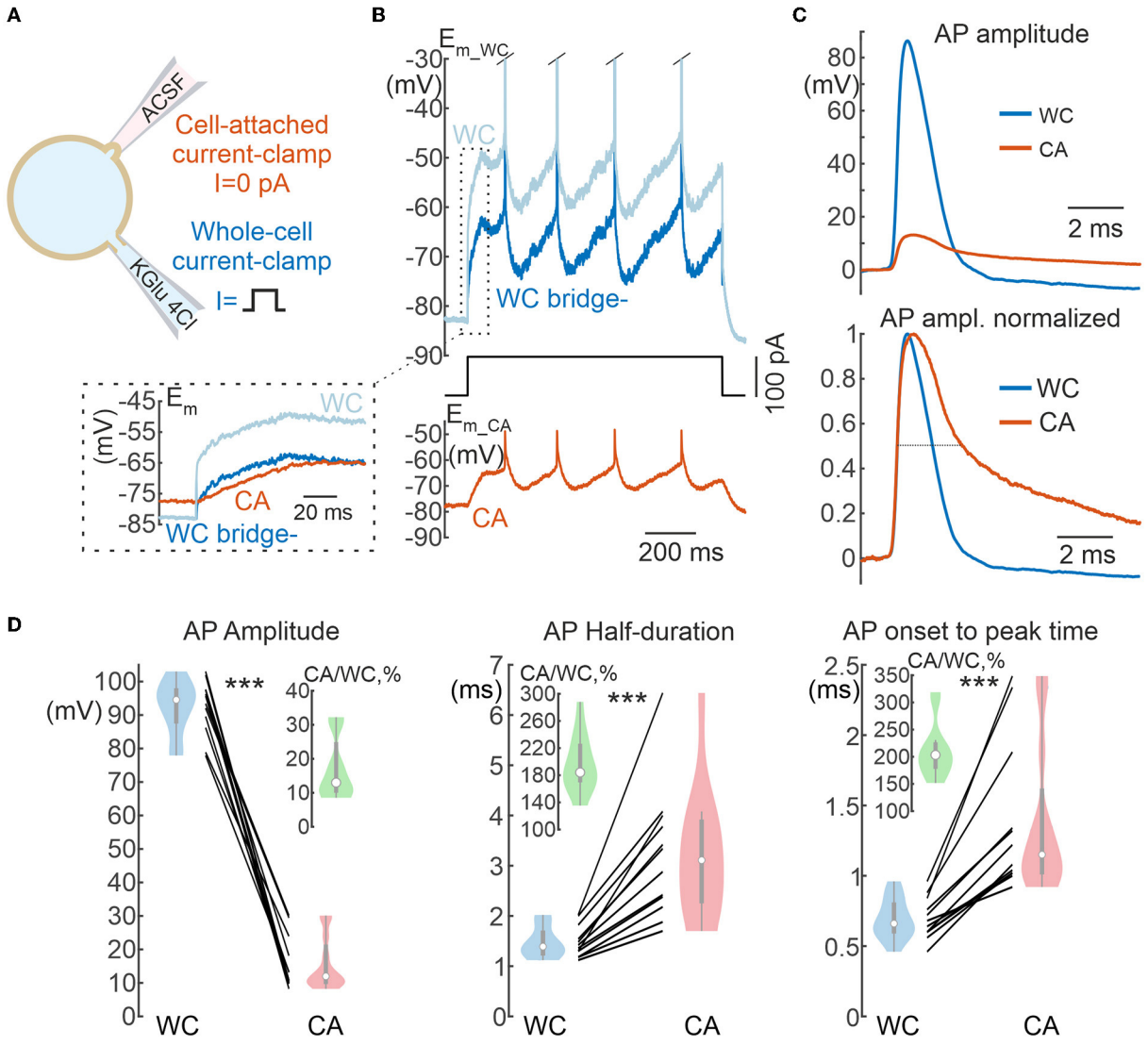

FIGURE 7
Action potentials in cell-attached and whole-cell recordings. **(A)** Scheme of recordings. APs are evoked by suprathreshold depolarizing current steps applied to the WC electrode. **(B)** Example of a response to a suprathreshold current step applied to the WC electrode during dual WC and CA recordings from a L5 pyramidal neuron. The ice-blue and blue traces show WC responses before (WC) and after (WC bridge -) bridge subtraction, respectively. Note that the bridge current is absent in the CA trace (inset). **(C)** APs in the CA and WC recordings with common voltage scale (top panel) and normalized to peak amplitude (bottom panel), dashed line is placed at half-amplitude. The resting membrane potential values were subtracted. **(D)** AP parameters in paired WC and CA recordings: AP amplitude (left), half-duration (middle), and time from onset to peak (right). The insets show in green the values of corresponding CA/WC transfer coefficients. Pooled data from 12 pyramidal cells in the L5 somatosensory cortex of the mouse. ***$P < 0.001$.

Dependence of GABAergic responses on membrane potential and intracellular chloride

In addition, we wanted to know how reliable CA recordings are for assessing the polarity (depolarising or hyperpolarising) of GABAergic responses. To this end, we examined the dependence of the polarity of GABA-PSPs in dual CA and WC current-clamp recordings of GABA-PSPs on membrane potential and intracellular chloride (Figure 9A). GABA-PSPs were evoked in CA1 pyramidal cells of juvenile (2–3 weeks old) mice by electrical stimulation of the stratum radiatum in the presence of the ionotropic glutamate receptors antagonists CNQX (10 μM) and d-APV (40 μM). Figure 9B shows examples of evoked GABA-PSPs during simultaneous CA and WC recordings with $[Cl^-]_i = 4$ and 30 mM in the WC pipette at different membrane potentials. Note that despite the different E_m values in CA and WC, the polarity of GABA-PSPs in both depolarizing and

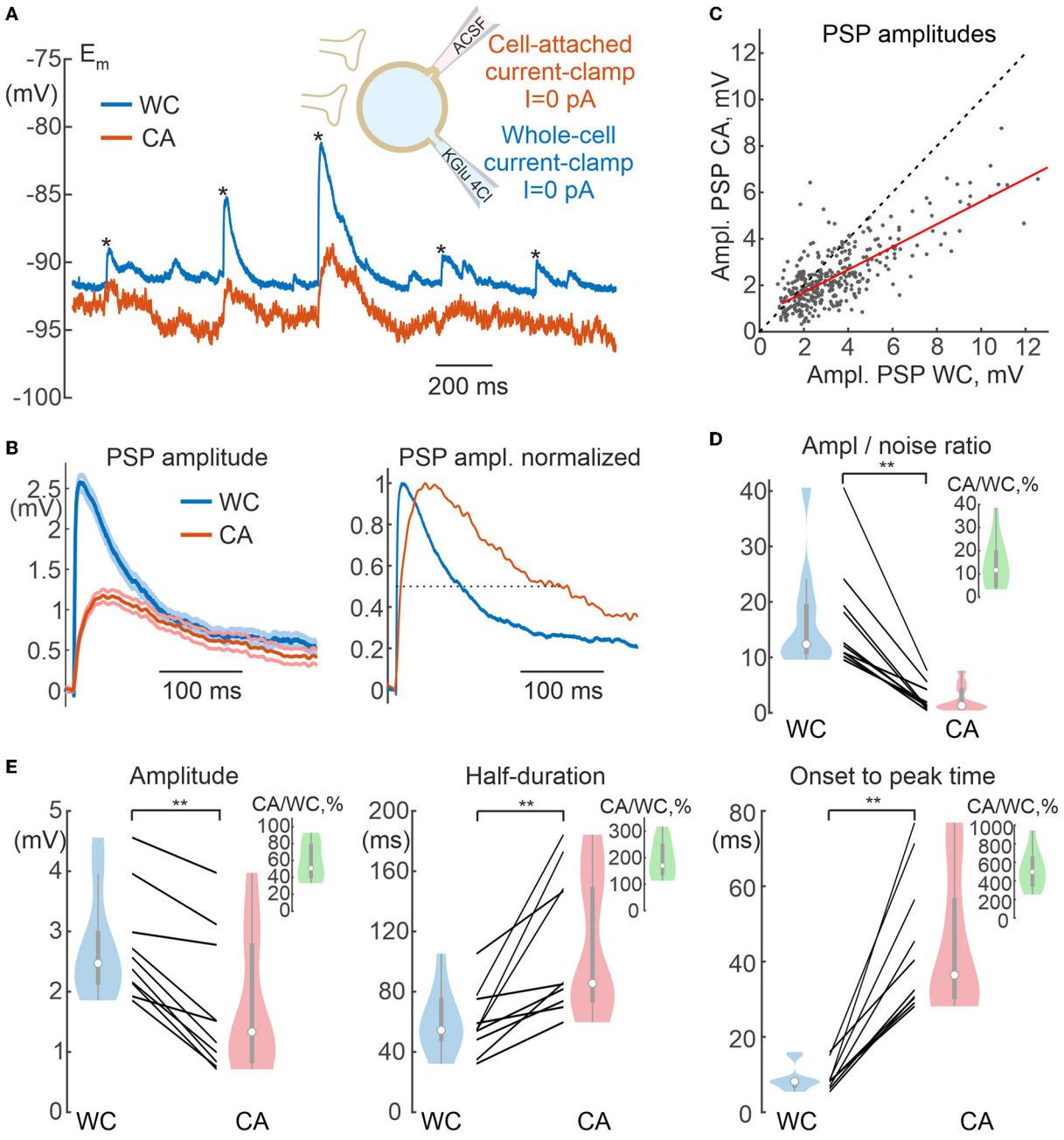

FIGURE 8
Spontaneous postsynaptic potentials in cell-attached and whole-cell recordings. **(A)** Scheme of recordings. Spontaneous postsynaptic potentials (sPSPs) are recorded using CA and WC electrodes from same neuron at resting membrane potential. WC electrode contains a low-chloride solution (4 mM), therefore most sPSPs are glutamatergic in nature. **(B)** Averaged sPSPs in WC and CA recordings with a common voltage scale (left panel) and normalized to peak amplitude (right panel), dashed line is placed at half-amplitude. The resting membrane potential values are subtracted. **(C)** Relationship between amplitudes of sPSPs in the WC and CA configurations for the cell shown in **(A)**. Each dot represents an individual sPSP. The red line shows a linear fit. **(D)** Amplitude to noise ratio for sPSPs in WC and CA recordings. The inset shows CA/WC transfer coefficient values. **(E)** Parameters of sPSPs in paired WC and CA recordings: amplitude of sPSPs (left), half-duration (middle), and time from onset to peak (right). The insets in green show the values of the respective CA/WC transfer coefficients. **(C,D)** Pooled data from 10 pyramidal cells in the L5 somatosensory cortex of the mouse. $^{**}P < 0.01$.

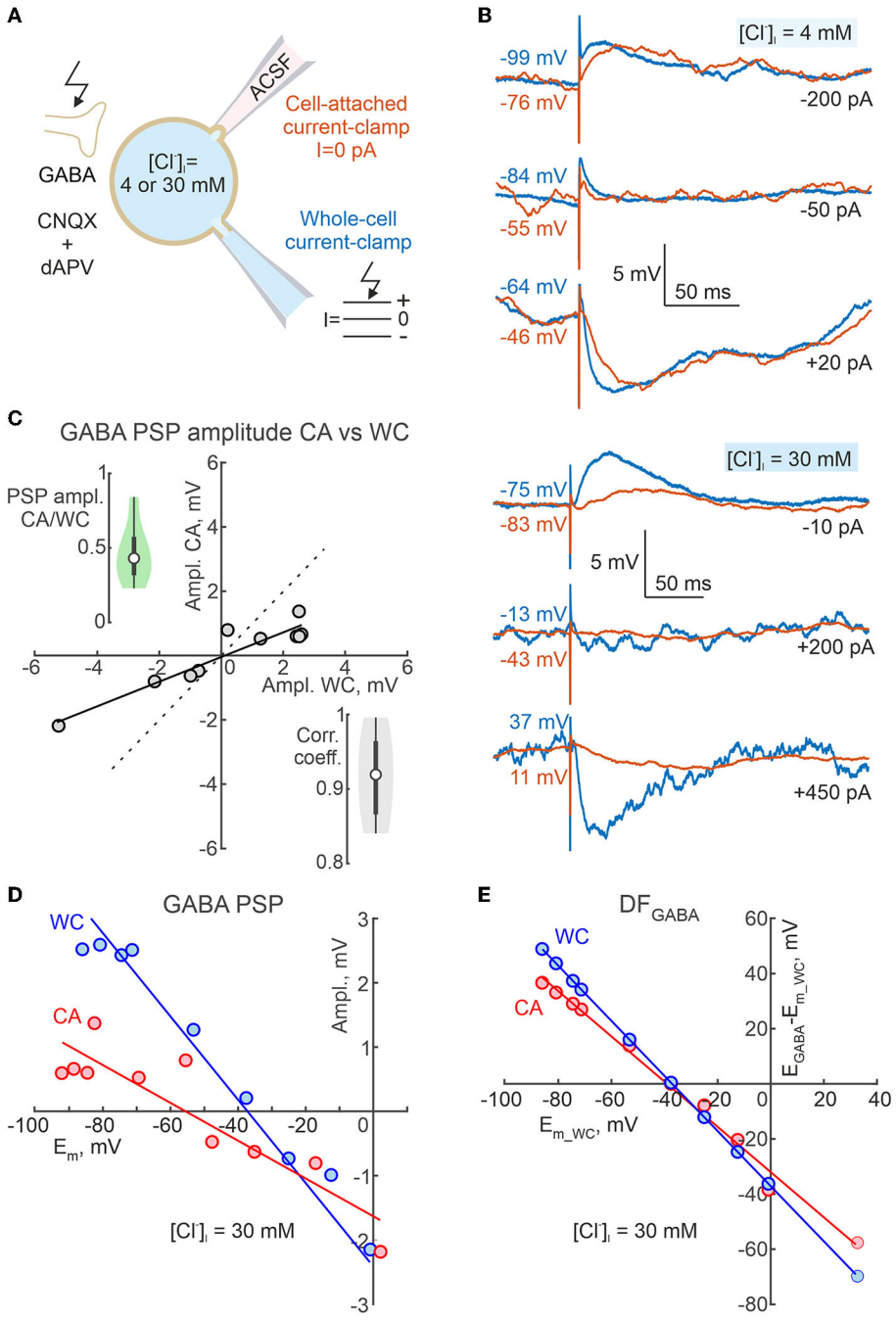

FIGURE 9
Dependence of the polarity of GABA-PSPs during cell-attached current clamp recordings on neuronal membrane potential and intracellular chloride. **(A)** Scheme of the experimental setup. Dual CA and WC current-clamp recordings of the pharmacologically isolated, electrically evoked GABA-PSPs were performed from adolescent CA1 pyramidal cells at different E_m values imposed by current injection into the WC electrode, and at various $[Cl^-]_i$ (4 mM and 30 mM) in the WC pipette solution. Ionotropic glutamate receptors were blocked by CNQX (10 μM) and d-APV (40 μM). **(B)** Examples of evoked GABA-PSPs during concomitant CA and WC recordings with $[Cl^-]_i = 4$ mM (top traces) and 30 mM (bottom traces) in the WC pipette at different membrane potentials. **(C)** Relationships between amplitudes of evoked GABA-PSPs in WC and CA configurations for a cell shown on **(B)** with $[Cl^-]_i = 30$ mM. The points represent the average of 10 GABA-PSP recorded at different E_{m_wc} values. Note that GABA-PSPs in WC and CA have similar polarity and that the conductance of GABA-PSPs in CA is smaller than in WC. The insets show group data on the CA/WC transfer coefficient of GABA-PSP amplitude (top left) and the correlation coefficient between GABA-PSP amplitude in CA and WC (bottom right) ($n = 8$ CA1 pyramidal cells from P15-19 mice). **(D)** Dependence of GABA-PSPs amplitude in WC and CA recordings on E_{m_wc} and E_{m_ca}, respectively for a CA1 pyramidal neuron recorded with $[Cl^-]_i = 30$ mM in the WC pipette solution. The E_m scale is the same for E_{m_wc} and E_{m_ca}. **(E)** Dependence of DF_{GABA} relative E_{m_wc} for GABA-PSPs recorded in CA and WC for a cell shown on **(D)**.

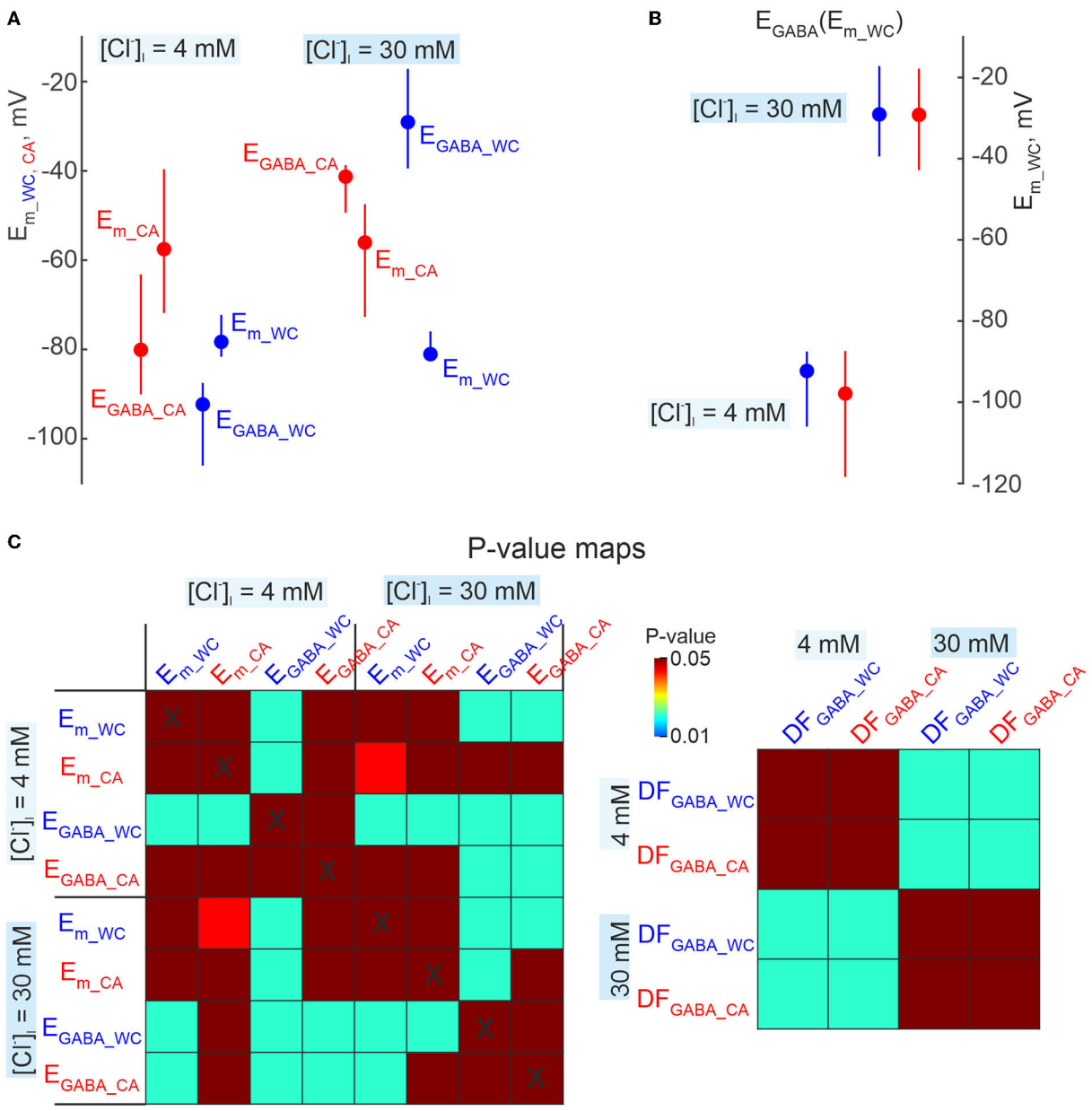

FIGURE 10
Comparisons of E_{GABA} derived from dual cell-attached and whole-cell recordings. **(A)** Summary plot of resting E_m and E_{GABA} obtained during CA and WC recordings of GABA-PSPs in CA1 pyramidal cells with $[Cl^-]_i = 4$ mM and 30 mM in the WC pipette solution. Note that E_{GABA} values were calculated relative to E_m values in CA and WC, respectively. The difference in resting E_m values results in an apparent difference in E_{GABA} estimates in CA and WC recordings. **(B)** E_{GABA} values from the same dataset as in **(A)**, recalculated as a function of E_m in WC both for WC and CA data. This approach minimizes the error caused by a difference in E_m values in CA and WC, and E_{GABA} values in CA and WC show no difference at both $[Cl^-]_i = 4$ mM and 30 mM. **(C)** Corresponding p-value maps for all parameters shown in **(A,B)**. The color of the cell at the row-column intersection shows the statistical significance (p-value) for the corresponding parameters. The dark red color corresponds to non-significant differences ($p > 0.05$), the other colors show different levels of significance of differences ($p < 0.05$) according to the color code (color bar on the right panel). **(A–C)** Pooled data from 8 pyramidal cells in the L5 somatosensory cortex of the mouse.

hyperpolarizing directions, as well as their reversal, were similar in WC and CA recordings. While the amplitudes of GABA-PSPs in the CA and WC recordings were highly correlated with a correlation coefficient >0.9, their amplitude in the CA recordings was on average twice as small as in the WC recordings (Figure 9C; $n = 8$ cells, $p < 0.05$; Wilcoxon Signed Rank test). As expected, a difference between resting E_m values in WC and CA recordings strongly biased GABA-PSPs reversal

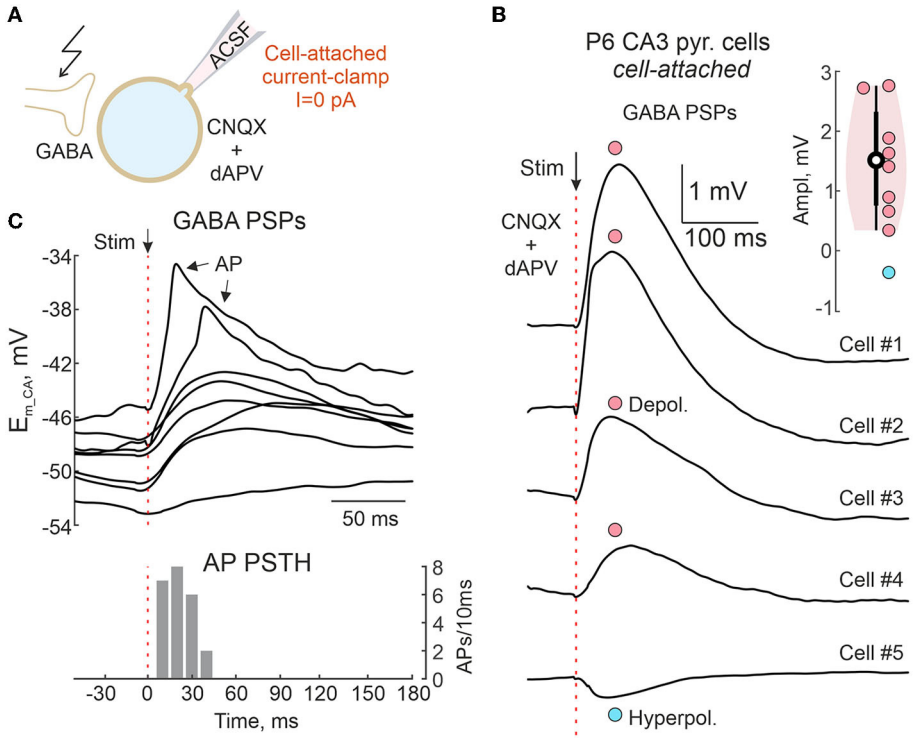

FIGURE 11
Cell-attached recordings of GABAergic postsynaptic responses in the neonatal hippocampus. **(A)** Scheme of the experimental setup. GABA-PSPs are evoked by electrical stimulation in the presence of the ionotropic glutamate antagonists CNQX (10 μM) and d-APV (40 μM) in a neonatal mouse hippocampal slice. Responses were recorded from CA3 pyramidal cells in CA/CC configuration without disturbance of intracellular chloride concentration. **(B)** Average evoked GABA-PSPs in five CA3 pyramidal cells, of which four show depolarizing responses (cells #1–4) and one (cell #5) shows a hyperpolarizing response. Inset shows group data on the amplitude of evoked GABA-PSPs recorded from 9 CA3 pyramidal cells of P6 mouse. **(C)** Example traces of evoked GABA-PSPs, some of which trigger APs. Below, a corresponding AP peristimulus time histogram.

potential (E_{GABA}) estimates from the relationships of GABA-PSPs amplitude from E_{m_ca} and E_{m_wc} (Figure 9D). However, both the E_{GABA} values and the GABA-driving force ($DF_{GABA} = E_{GABA} - E_m$) calculated from the E_{m_wc} values agreed between the CA and WC recordings and showed a similar dependence on $[Cl^-]_i$ (Figures 9E, 10).

Polarity of GABAergic responses in the neonatal hippocampus

The above results suggest that CA/CC recordings reliably report the polarity of GABAergic responses. We next tested this approach to characterize GABAergic responses in neonatal neurons from hippocampal slices, where depolarizing effects of GABA are well-documented (Ben-Ari et al., 1989; Ben Ari et al., 2007; Watanabe and Fukuda, 2015; Kirmse et al., 2018). Electrically evoked pharmacologically isolated GABA-PSPs were recorded from CA1 pyramidal neurons of neonatal (P6) mouse hippocampal slices in CA/CC configuration (Figure 11A). In contrast to the above experiments, no concomitant WC recordings were made to keep $[Cl^-]_i$ intact. Depolarizing GABA-PSPs with an average amplitude of +1.5 mV were recorded in eight cells under these conditions, and only one neuron showed slightly hyperpolarizing GABA-PSPs (Figure 11B). Depolarizing responses eventually triggered APs with delays similar to those reported with extracellular recordings (Figure 11C) (Valeeva et al., 2010).

Giant depolarizing potentials

Neuronal activity in hippocampal slices of neonatal rodents is characterized by recurrent Giant Depolarizing Potentials (GDPs), the generation of which is closely linked to the depolarizing effect of GABA on immature neurons (Ben-Ari et al., 1989; Garaschuk et al., 1998; Menendez de la Prida et al., 1998; Ben Ari et al., 2007; Griguoli and Cherubini, 2017; Cossart and Khazipov, 2022). Since GABAergic conductance dominates during GDPs, non-invasive CA/CC recordings can be potentially useful for GDPs assessment. To this end, we performed CA/CC recordings of CA3 pyramidal cells

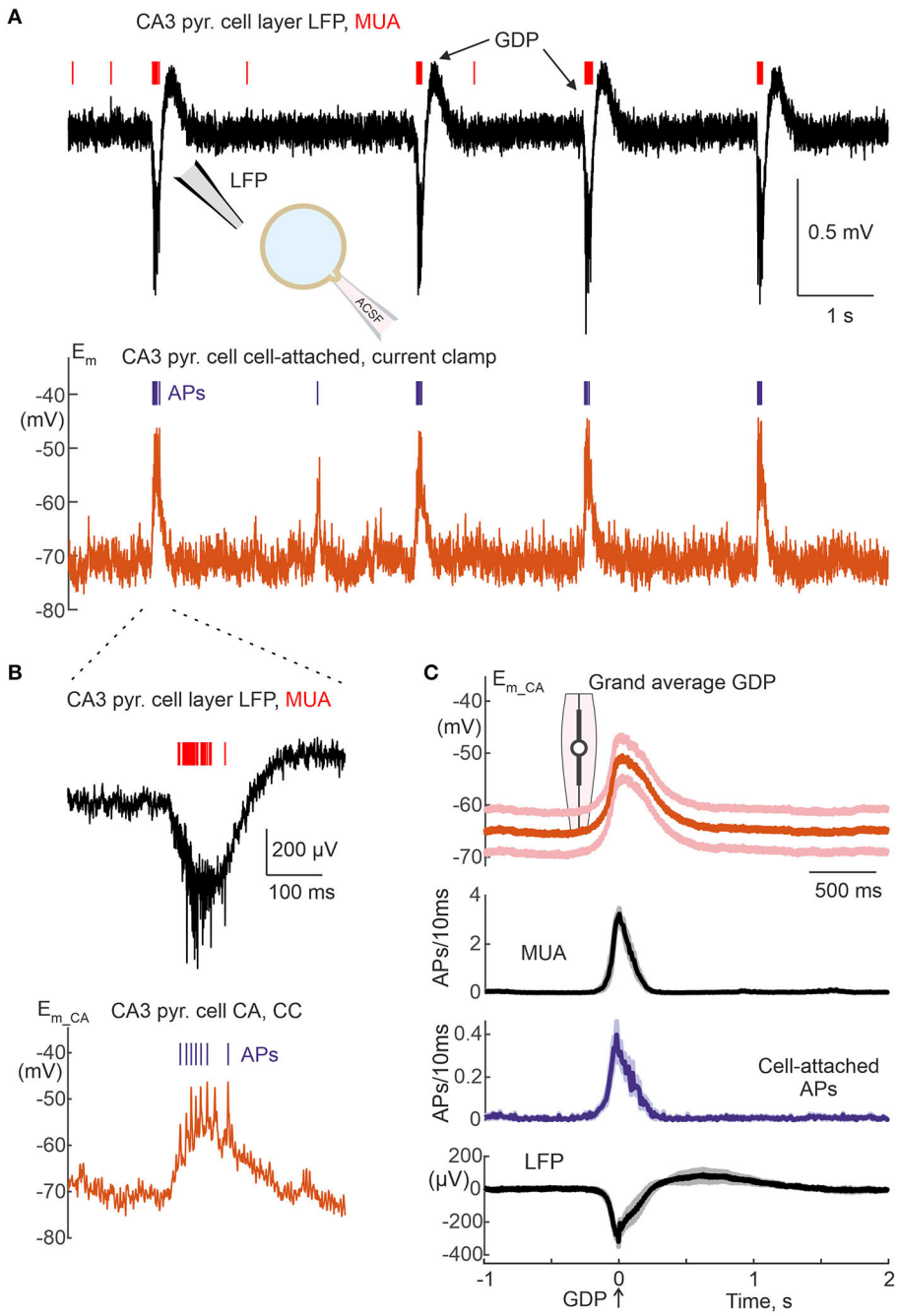

FIGURE 12
Cell-attached current-clamp recordings of Giant Depolarizing Potentials in the neonatal hippocampus. **(A)** Example recordings of local field potential (upper black trace) and MUA (red bars) from the CA3 pyramidal cell layer and CA/CC recordings from the CA3 pyramidal cell in a slice of neonatal (P5) mouse hippocampus showing spontaneous Giant Depolarizing Potentials (GDPs). **(B)** Example GDP from **(B)** on an expanded time scale. **(C)** Group data on average membrane potential changes and AP timing in CA3 pyramidal cells during CA/CC recordings, and extracellular MUA and LFP in the CA3 pyramidal cell layer during GDPs. The solid lines show the average, the shaded lines show ± SE. The violin plot shows the peak depolarization during GDPs. The peak negativity of the field GDP is taken as a time reference. Pooled data from 6 cells (37–92 GDPs/cell) from P5 mouse hippocampal slices.

from hippocampal slices of neonatal (P5) mice. Extracellular local field potential (LFP) and multiple unit activity (MUA) recordings from the CA3 pyramidal cell layer near the CA recordings were used to detect network-driven field GDPs (Figures 12A,B). We found that the GDPs and APs in the CA3 pyramidal cells were highly synchronized with field GDPs and

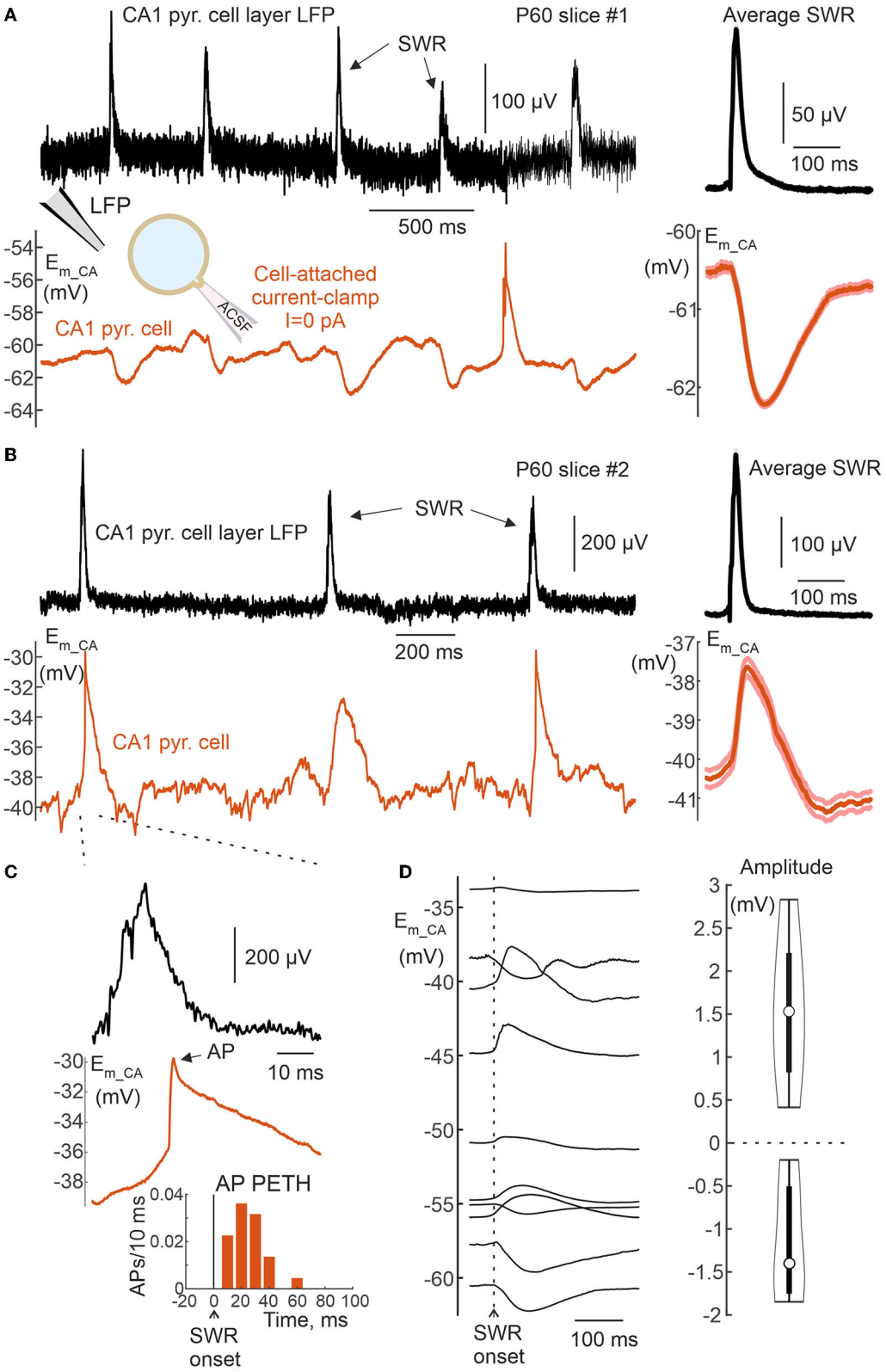

FIGURE 13
Cell-attached current-clamp recordings of Sharp Wave Ripples in the adult hippocampus. **(A,B)** Example recordings of the local field potential (upper black trace) from the CA1 pyramidal cell layer and CA/CC recordings from a CA1 pyramidal cell in a slice of the hippocampus of a

(Continued)

FIGURE 13
2-month-old mouse showing spontaneous Sharp Wave Ripples (SWRs) associated with neuronal hyperpolarization **(A)** and depolarization **(B)**. Averaged field and CA SWRs are shown on the right. **(C)** Example SWR from **(B)** on expanded time scale and corresponding peri-SWR AP histogram. **(D)** Average voltage change during SWR in 10 CA1 pyramidal cells, five of which show depolarization and another five hyperpolarization. On the right, the corresponding group data on the amplitude of E_m change during SWR recorded from 10 CA1 pyramidal cells of the 2-month-old mice.

MUA, and similar behavior was observed in all 6 neurons studied in this series, as shown by the grand average GDPs analysis in Figure 12C. During GDPs, CA3 pyramidal cells depolarized from resting E_{m_ca} −62.1 [−71.7 −57.9] mV to −49.0 [−55.4 −41.3] mV (i.e., by 16.3 [14.6 17.5] mV; $n = 6$ cells), which is close to GDP values reported in CA3 pyramidal cells using gramicidin perforated patch recordings (Khalilov et al., 2015) (Figure 12C). Maximal neuronal firing occurred at the peak of depolarization during GDPs, which coincided with MUA peak during extracellular recordings.

Hippocampal sharp waves

Adult rodent hippocampal slices show recurrent bursts of activity that share a number of similar features with Sharp Wave Ripples (SWRs) *in vivo* (Maier et al., 2003; Behrens et al., 2005; Hajos et al., 2009; Buzsaki, 2015; Norimoto et al., 2018). Interestingly, the behavior of CA1 pyramidal cells during SWRs is variable *in vitro*, with different cells showing depolarization, hyperpolarization or mixed responses during SWRs (Maier et al., 2003). Here, we approached the behavior of CA1 cells during SWRs by using CA/CC recordings from hippocampal slices of 2-month-old mice, using a similar experimental approach as for GDPs in the previous section. Unlike GDPs, SWRs were associated with positive LFP deflections in the CA1 pyramidal cell layer, and these were used for SWR detection (Figures 13A,B). Consistent with the results of a previous study using intracellular recordings (Maier et al., 2003), we found that half of the CA1 neurons (5 of 10) were hyperpolarized during SWRs (Figure 13A), while another half of the CA1 neurons (also 5 of 10) were depolarized during SWRs. Finally, in the case of depolarizations, the neurons also fired APs during SWRs (Figure 13C). Resting E_m was highly variable in this dataset, but we found no significant correlation between E_m and voltage response in CA1 neurons during SWRs, which average circa +1.5 mV and −1.5 mV in cells with depolarizing and hyperpolarizing SWR-driven responses, respectively (Figure 13D).

Discussion

The main aim of the present study was to determine the accuracy of the measurement of resting membrane potential and its dynamic changes in CA/CC recordings by comparing signals obtained in dual CA and WC recordings from the same neurons. Our overall conclusion is that CA/CC measurements are similar to WC recordings, have several advantages, including lack of cell dialysis, but also introduce several sources of error that should be considered when interpreting data obtained with CA/CC recordings.

Resting membrane potential

We found that the E_{m_rest} values obtained in CA/CC recordings are typically slightly more depolarized compared to WC-values (on average, by 19 mV). The depolarized E_{m_rest} values in CA/CC are consistent with theoretical model of CA/CC recordings, according to which E_{m_rest} in CA should be more depolarized than E_{m_rest} in WC, and its value critically depends on the R_{seal} / R_{patch} ratio. When $R_{seal} >> R_{patch}$, E_{m_rest} in CA approaches the true E_{m_rest} value. However, if R_{seal} is comparable to R_{patch}, electrical shunt across the seal causes a depolarization shift of E_{m_rest} in CA. Closer agreement than here between E_{m_rest} in CA and WC in megakariocytes (Mason et al., 2005) was probably due to higher R_{seal} contact between the patch pipette and cell membrane, which is easier to achieve when patching isolated cells than neurons in brain slices. Resting E_m in CA values (up to −120 mV) that were more negative than E_{m_rest} in WC, are hardly explained by the error introduced by leakage via R_{seal}, however. In addition, the CA/CC recordings were characterized by high levels of background noise. It is conceivable that these phenomena are caused by the high sensitivity of E_m in CA/CC to active currents across the patch membrane. It should be noted that the transmembrane potential in the attached membrane patch in CA/CC mode is nearly zero (because E_{m_ca} on the outer side of the membrane is close to the value of E_m inside the cell). Therefore, this highly depolarized membrane patch can be expected to exhibit activation of potassium channels and inactivation of sodium and calcium channels, as well as an increase in the driving force of outwardly directed currents through potassium and chloride channels, and a decrease in the driving force of inwardly directed currents through sodium and calcium channels. Thus, potassium conductance probably dominates in the membrane patch under these conditions, resulting in outwardly directed currents. These outward-directed currents, however, are seen as inward currents by the patch pipette attached to the cell, and thus should cause depolarizing signals in CA/CC contributing to depolarized E_{m_rest} values in CA/CC (in addition to the depolarization caused by leaky conductance via R_{seal}). Note that even small currents can cause significant voltage changes

in the patch. For example, opening a 100 pS potassium channel at a driving force for potassium of +90 mV generates a current of 9 pA, which induces a +9 mV depolarization of a 1GOhm patch. This active potassium conductance could contribute to depolarize E_{m_ca} relatively E_{m_wc}, in addition to leakage through R_{seal}. Less frequent but existing cases where E_{m_ca} values were more negative than E_{m_wc} are more difficult to explain. This could involve the presence of non-inactivating sodium or calcium channels in the patch mediating hyperpolarizing E_{m_ca} currents across the patch membrane, but this remains speculative. Sporadic opening and closing of ion channels also likely contributes to the high baseline fluctuations in the CA/CC recordings.

Dynamic changes in membrane potential

Dynamic changes in E_m evoked by current injection via the WC-electrode, elevation of extracellular potassium, and during synaptic activity and APs were also detected during CA/CC recordings, but their amplitude in CA/CC was smaller than in WC. Overall, faster events were strongly attenuated. Constant or very slow shifts in E_m occurring at <1 Hz had a transfer coefficient on the order of 0.8–0.9. Transfer coefficients for faster events reduced to nearly 0.5 for synaptic potentials and 0.1 for APs. From a practical point of view, detection of PSPs was more difficult in CA/CC recordings because of the low signal-to-noise ratio due to the reduced amplitude of PSPs and the larger baseline fluctuations. Besides reduction in the amplitude, fast signals were also slowed down in their kinetics. These modifications in E_m signals were in keeping with the frequency-dependent changes in the transfer coefficient of the responses evoked by injection of sinusoidal current at different frequency. These changes in the fast signals corresponded to frequency-dependent changes in the transfer coefficient in the responses evoked by sinusoidal current injection at different frequencies. The frequency dependence of the transfer coefficient could be fitted by a model (Figures 5, 6). In general, these observations are in agreement with the results of previous studies (Fenwick et al., 1982; Tyzio et al., 2003; Hayar et al., 2004; Mason et al., 2005; Perkins, 2006), but provide more quantitative descriptions of the accuracy of CA/CC recordings for the assessment of biologically relevant E_m changes during synaptic events and action potentials in neurons.

CA/CC recordings also revealed dynamic changes in E_m during network driven GDPs in CA3 neurons from neonatal rat hippocampal slices and during SWRs in CA1 cells from adult mouse hippocampal slices. All neonatal CA3 hippocampal neurons depolarized during GDPs, and the amplitude of GDPs (16 mV, on average) was comparable to that obtained during gramicidin perforated patch recordings (also 16 mV, on average). This is slightly different from a prediction of a slight attenuation of GDPs in CA/CC recordings, because CA/WC amplitude transfer coefficient at GDPs waveform at their dominant frequency (3 Hz) is ~ 0.6 (Figure 6A). In addition, CA3 neurons fired bursts of APs during GDPs, and APs rate was maximal at the peak of field GDP. The temporal distribution of APs during GDPs in CA/CC recordings corresponded to the firing of multiple units and was also similar to the AP firing of CA3 neurons in gramicidin perforated patch recordings and during CA voltage clamp recordings as reported previously (Leinekugel et al., 1997; Khalilov et al., 2015). This differs from intracellular recordings with high chloride solution, where the AP firing occurs mainly during the rising and falling phases of GDPs, and depolarization block of APs at the at the peak of GDPs probably due to chloride overload of the cells. In contrast to GDPs, behavior of CA1 pyramidal cells during SWRs in adult hippocampal slices was more heterogeneous. Whereas, half of CA1 neurons depolarized during SWRs, another half of CA1 pyramidal neurons hyperpolarized during SWRs. Of the neurons depolarized during SWRs, 2 out of 5 (40%) fired APs. These findings are in agreement with intracellular recordings, which revealed about the same distribution of CA1 pyramidal cells behaviors during SWRs *in vitro* (Maier et al., 2003). In the latter study, the amplitude of SWRs was approximately 3 to 5 mV (see Figure 12 from Maier et al., 2003). Because the CA/WC amplitude transfer coefficient at the dominant frequency of SWRs waveform (7 Hz) is close to 0.5 (Figure 6A), SWRs amplitude of ~1.5 mV obtained in the present study using CA/CC recordings should be about half of "true" SWR amplitude, which is thus in agreement with the results of previous intracellular recordings. Together, these findings suggest that CA/CC recordings are appropriate for non-invasive assessment of E_m changes during network-driven activities, but stronger attenuation of faster signals should be considered.

Polarity of GABAergic postsynaptic potentials

The undisturbed intracellular milieu is the main advantage of CA over WC recordings. In addition, despite artifacts affecting the measurement of E_{m_rest}, CA recordings affect the actual E_{m_rest} very little. These are the two major requirements for assessing the polarity of postsynaptic responses, whose reversal potential is close to E_{m_rest}, including those of GABA. Previously, CA/CC recordings have been used to demonstrate the predominantly positive polarity of puff-applied GABA responses in the L2/3 neocortical neurons of neonatal (P3–4) mice *in vivo*, and isoelectric responses to GABA in the presence of the membrane-permeable carbonic anhydrase inhibitor 6-ethoxy-2-benzothiazolesulfonamide in juvenile mice (P25–27) (Kirmse et al., 2015). Biphasic E_m shifts (hyperpolarizing to depolarizing) during GABA(A) receptor mediated giant postsynaptic potentials induced by 4-AP have also been described using CA/CC recordings from CA1 pyramidal cells in adult rat hippocampal slices

(Perkins, 2006). Our findings provide direct evidence for the accuracy of CA/CC recordings in assessing the polarity of GABAergic responses. Indeed, we found that during dual WC and CA recordings, GABAergic postsynaptic responses display concomitant E_m - dependent change in polarity and show a dependence on $[Cl^-]_i$. Furthermore, consistent with previous observations, GABAergic postsynaptic responses were predominantly depolarizing during CA/CC recordings of intact neonatal CA3 pyramidal cells. Of note, the latter findings of depolarizing action of GABA at P6 are more consistent with DF_{GABA} and E_{GABA} non-invasive estimates using cell-attached GABA and NMDA channel recordings, and gramicidin perforated patch recordings, rather than using intracellular recordings with sharp electrodes. Indeed, in P6 CA3 pyramidal neurons, GABA exerts hyperpolarizing action and GDPs are associated with large hyperpolarizing potentials in intracellular recordings (Ben-Ari et al., 1989). These apparent contradictions are likely due to neuronal depolarization caused by the introduction of a leak conductance (~500 MOhm) using sharp electrodes, and modifications of $[Cl^-]_i$ due to dialysis as discussed in detail elsewhere (Khazipov et al., 2015). Thus, affecting neither E_m nor $[Cl^-]_i$, CA/CC recordings appear to be reliable, simple and rapid for assessing the polarity of GABAergic responses, which could be useful in physiological and pathological conditions when GABA polarity is challenged (Miles et al., 2012; Kaila et al., 2014; Khazipov et al., 2015; Akita and Fukuda, 2020; Cherubini et al., 2021). Although not investigated in this paper, the CA/CC approach may prove particularly useful for non-invasive recordings of membrane potential and synaptic events in dendrites and axons as it allows the use of electrodes with a smaller tip than for conventional WC recordings from the neuronal body. Limitations of this approach are the inability to estimate E_{GABA} due to a lack of control over E_m, and relatively low signal-to-noise ratio.

Data availability statement

The original contributions presented in the study are included in the article/supplementary material, further inquiries can be directed to the corresponding author/s.

Ethics statement

The animal study was reviewed and approved by Local Ethical Committee of Kazan Federal University (No24/22.09.2020) French National Institute of Health and Medical Research (APAFIS #16992-2020070612319346 v2).

Author contributions

RK and AN conceived the project and wrote the paper. AV, FV-R, and AR performed the experiments. AN, AV, AE, and FV-R analyzed the data. All authors contributed to the article and approved the submitted version.

Funding

This work was supported by Russian Science Foundation # 20-75-00055 (experiments and analysis), subsidy allocated to Kazan Federal University for the state assignment # 0671-2020-0059 in the sphere of scientific activities (development of Eview software) and performed in the framework of the Kazan Federal University Strategic Academic Leadership Program (PRIORITY-2030).

Conflict of interest

The authors declare that the research was conducted in the absence of any commercial or financial relationships that could be construed as a potential conflict of interest.

Publisher's note

All claims expressed in this article are solely those of the authors and do not necessarily represent those of their affiliated organizations, or those of the publisher, the editors and the reviewers. Any product that may be evaluated in this article, or claim that may be made by its manufacturer, is not guaranteed or endorsed by the publisher.

References

Akita, T., and Fukuda, A. (2020). Intracellular Cl(-) dysregulation causing and caused by pathogenic neuronal activity. *Pflugers Arch. Eur. J. Physiol.* 472, 977–987. doi: 10.1007/s00424-020-02375-4

Alcami, P., Franconville, R., Llano, I., and Marty, A. (2012). Measuring the firing rate of high-resistance neurons with cell-attached recording. *J. Neurosci.* 32, 3118–3130. doi: 10.1523/JNEUROSCI.5371-11.2012

Barry, H., and Lynch, J. W. (1991). Liquid junction potentials and small cell effects in patch-clamp analysis. *J. Membrane Biol.* 121, 101–117. doi: 10.1007/BF01870526

Behrens, C. J., van den Boom, L. P., de Hoz, L., Friedman, A., and Heinemann, U. (2005). Induction of sharp wave-ripple complexes *in vitro* and reorganization of hippocampal networks. *Nat. Neurosci.* 8, 1560–1567. doi: 10.1038/nn1571

Ben Ari, Y., Gaiarsa, J. L., Tyzio, R., and Khazipov, R. (2007). GABA: a pioneer transmitter that excites immature neurons and generates primitive oscillations. *Physiol. Rev.* 87, 1215–1284. doi: 10.1152/physrev.00017.2006

Ben-Ari, Y., Cherubini, E., Corradetti, R., and Gaïarsa, J.-L. (1989). Giant synaptic potentials in immature rat CA3 hippocampal neurones. *J. Physiol.* 416, 303–325. doi: 10.1113/jphysiol.1989.sp017762

Buzsaki, G. (2015). Hippocampal sharp wave-ripple: a cognitive biomarker for episodic memory and planning. *Hippocampus* 25, 1073–1188. doi: 10.1002/hipo.22488

Chavas, J., and Marty, A. (2003). Coexistence of excitatory and inhibitory GABA synapses in the cerebellar interneuron network. *J. Neurosci.* 23, 2019–2031. doi: 10.1523/JNEUROSCI.23-06-02019.2003

Cherubini, E., Di, C. G., and Avoli, M. (2021). Dysregulation of GABAergic signaling in neurodevelomental disorders: targeting cation-chloride co-transporters to re-establish a proper E/I balance. *Front. Cell. Neurosci.* 15:813441. doi: 10.3389/fncel.2021.813441

Cossart, R., and Khazipov, R. (2022). How development sculpts hippocampal circuits and function. *Physiol. Rev.* 102, 343–378. doi: 10.1152/physrev.00044.2020

Fenwick, E. M., Marty, A., and Neher, E. (1982). Sodium and calcium channels in bovine chromaffin cells. *J. Physiol.* 331, 599–635. doi: 10.1113/jphysiol.1982.sp014394

Fricker, D., Verheugen, J. A., and Miles, R. (1999). Cell-attached measurements of the firing threshold of rat hippocampal neurones. *J.Physiol.* 517(Pt. 3), 791–804. doi: 10.1111/j.1469-7793.1999.0791s.x

Garaschuk, O., Hanse, E., and Konnerth, A. (1998). Developmental profile and synaptic origin of early network oscillations in the CA1 region of rat neonatal hippocampus. *J. Physiol.* 507, 219–236. doi: 10.1111/j.1469-7793.1998.219bu.x

Griguoli, M., and Cherubini, E. (2017). Early correlated network activity in the hippocampus: its putative role in shaping neuronal circuits. *Front. Cell. Neurosci.* 11:255. doi: 10.3389/fncel.2017.00255

Gulledge, A. T., and Stuart, G. J. (2003). Excitatory actions of GABA in the cortex. *Neuron* 37, 299–309. doi: 10.1016/S0896-6273(02)01146-7

Hajos, N., Ellender, T. J., Zemankovics, R., Mann, E. O., Exley, R., Cragg, S. J., et al. (2009). Maintaining network activity in submerged hippocampal slices: importance of oxygen supply. *Eur. J. Neurosci.* 29, 319–327. doi: 10.1111/j.1460-9568.2008.06577.x

Hamill, O. P., Marty, A., Neher, E., Sakmann, B., and Sigworth, F. J. (1981). Improved patch-clamp techniques for high-resolution current recording from cell-free membrane patches. *Pflugers Archiv.* 391, 85–100. doi: 10.1007/BF00656997

Hayar, A., Karnup, S., Shipley, M. T., and Ennis, M. (2004). Olfactory bulb glomeruli: external tufted cells intrinsically burst at theta frequency and are entrained by patterned olfactory input. *J. Neurosci.* 24, 1190–1199. doi: 10.1523/JNEUROSCI.4714-03.2004

Kaila, K., Price, T. J., Payne, J. A., Puskarjov, M., and Voipio, J. (2014). Cation-chloride cotransporters in neuronal development, plasticity and disease. *Nat. Rev. Neurosci.* 15, 637–654. doi: 10.1038/nrn3819

Khalilov, I., Minlebaev, M., Mukhtarov, M., and Khazipov, R. (2015). Dynamic changes from depolarizing to hyperpolarizing GABAergic actions during giant depolarizing potentials in the neonatal rat hippocampus. *J. Neurosci.* 35, 12635–12642. doi: 10.1523/JNEUROSCI.1922-15.2015

Khazipov, R., Ragozzino, D., and Bregestovski, P. (1995). Kinetics and Mg^{2+} block of *N*-methyl-D-aspartate receptor channels during postnatal development of hippocampal CA3 pyramidal neurons. *Neuroscience* 69, 1057–1065. doi: 10.1016/0306-4522(95)00337-I

Khazipov, R., Tyzio, R., and Ben Ari, Y. (2008). Effects of oxytocin on GABA signalling in the foetal brain during delivery. *Prog. Brain Res.* 170, 243–257. doi: 10.1016/S0079-6123(08)00421-4

Khazipov, R., Valeeva, G., and Khalilov, I. (2015). Depolarizing GABA and developmental epilepsies. *CNS Neurosci. Ther.* 21, 83–91. doi: 10.1111/cns.12353

Kirmse, K., Hubner, C. A., Isbrandt, D., Witte, O. W., and Holthoff, K. (2018). GABAergic transmission during brain development: multiple effects at multiple stages. *Neuroscientist* 24, 36–53. doi: 10.1177/1073858417701382

Kirmse, K., Kummer, M., Kovalchuk, Y., Witte, O. W., Garaschuk, O., and Holthoff, K. (2015). GABA depolarizes immature neurons and inhibits network activity in the neonatal neocortex *in vivo*. *Nat. Commun.* 6:7750. doi: 10.1038/ncomms8750

Leinekugel, X., Medina, I., Khalilov, I., Ben-Ari, Y., and Khazipov, R. (1997). Ca^{2+} oscillations mediated by the synergistic excitatory actions of $GABA_A$ and NMDA receptors in the neonatal hippocampus. *Neuron* 18, 243–255. doi: 10.1016/S0896-6273(00)80265-2

Maier, N., Nimmrich, V., and Draguhn, A. (2003). Cellular and network mechanisms underlying spontaneous sharp wave-ripple complexes in mouse hippocampal slices. *J. Physiol.* 550(Pt. 3), 873–887. doi: 10.1113/jphysiol.2003.044602

Mason, M. J., Simpson, A. K., Mahaut-Smith, M. P., and Robinson, H. P. (2005). The interpretation of current-clamp recordings in the cell-attached patch-clamp configuration. *Biophys. J.* 88, 739–750. doi: 10.1529/biophysj.104.049866

Menendez de la Prida, L., Bolea, S., and Sanchez-Andres, J. V. (1998). Origin of the synchronized network activity in the rabbit developing hippocampus. *Eur. J. Neurosci.* 10, 899–906. doi: 10.1046/j.1460-9568.1998.00097.x

Miles, R., Blaesse, P., Huberfeld, G., Wittner, L., and Kaila, K. (2012). "Chloride homeostasis and GABA signaling in temporal lobe epilepsy," in *Jasper's Basic Mechanisms of the Epilepsies*, 4 Edn, eds J. Nobels, M. Avoli, M. Rogawski, R. Olsen, and A. Delgado-Escueta (Oxford: Oxford University Press). doi: 10.1093/med/9780199746545.003.0045

Neher, E., and Sakmann, B. (1976). Single-channel currents recorded from membrane of denervated frog muscle fibres. *Nature* 260, 799–802. doi: 10.1038/260799a0

Norimoto, H., Makino, K., Gao, M., Shikano, Y., Okamoto, K., Ishikawa, T., et al. (2018). Hippocampal ripples down-regulate synapses. *Science* 359, 1524–1527. doi: 10.1126/science.aao0702

Perkins, K. L. (2006). Cell-attached voltage-clamp and current-clamp recording and stimulation techniques in brain slices. *J. Neurosci. Methods* 154, 1–18. doi: 10.1016/j.jneumeth.2006.02.010

Pusch, M., and Neher, E. (1988). Rates of diffusional exchange between small cells and a measuring patch pipette. *Pflugers Arch. Eur. J. Physiol.* 411, 204–211. doi: 10.1007/BF00582316

Tyzio, R., Cossart, R., Khalilov, I., Minlebaev, M., Hubner, C. A., Represa, A., et al. (2006). Maternal oxytocin triggers a transient inhibitory switch in GABA signaling in the fetal brain during delivery. *Science* 314, 1788–1792. doi: 10.1126/science.1133212

Tyzio, R., Ivanov, A., Bernard, C., Holmes, G. L., Ben Ari, Y., and Khazipov, R. (2003). Membrane potential of CA3 hippocampal pyramidal cells during postnatal development. *J. Neurophysiol.* 90, 2964–2972. doi: 10.1152/jn.00172.2003

Tyzio, R., Minlebaev, M., Rheims, S., Ivanov, A., Jorquera, I., Holmes, G. L., et al. (2008). Postnatal changes in somatic gamma-aminobutyric acid signalling in the rat hippocampus. *Eur. J. Neurosci.* 27, 2515–2528. doi: 10.1111/j.1460-9568.2008.06234.x

Valeeva, G., Abdullin, A., Tyzio, R., Skorinkin, A., Nikolski, E., Ben-Ari, Y., et al. (2010). Temporal coding at the immature depolarizing GABAergic synapse. *Front. Cell Neurosci.* 4:17. doi: 10.3389/fncel.2010.00017

Verheugen, J. A., Fricker, D., and Miles, R. (1999). Noninvasive measurements of the membrane potential and GABAergic action in hippocampal interneurons. *J. Neurosci.* 19, 2546–2555. doi: 10.1523/JNEUROSCI.19-07-02546.1999

Verheugen, J. A., Vijverberg, H. P., Oortgiesen, M., and Cahalan, M. D. (1995). Voltage-gated and Ca(2+)-activated K+ channels in intact human T lymphocytes. Noninvasive measurements of membrane currents, membrane potential, and intracellular calcium. *J. Gen. Physiol.* 105, 765–794. doi: 10.1085/jgp.105.6.765

Watanabe, M., and Fukuda, A. (2015). Development and regulation of chloride homeostasis in the central nervous system. *Front. Cell. Neurosci.* 9:371. doi: 10.3389/fncel.2015.00371

frontiers | Frontiers in Molecular Neuroscience

TYPE Original Research
PUBLISHED 29 September 2022
DOI 10.3389/fnmol.2022.990803

OPEN ACCESS

EDITED BY
Yonggang Gao,
China University of Geosciences Wuhan, China

REVIEWED BY
Andrzej T. Slominski,
University of Alabama at Birmingham, United States
Eunhee Kim,
University of Texas Health Science Center at Houston, United States

*CORRESPONDENCE
Atsuo Fukuda
axfukuda@hama-med.ac.jp

SPECIALTY SECTION
This article was submitted to Molecular Signalling and Pathways, a section of the journal Frontiers in Molecular Neuroscience

RECEIVED 10 July 2022
ACCEPTED 13 September 2022
PUBLISHED 29 September 2022

CITATION
Yesmin R, Watanabe M, Sinha AS, Ishibashi M, Wang T and Fukuda A (2022) A subpopulation of agouti-related peptide neurons exciting corticotropin-releasing hormone axon terminals in median eminence led to hypothalamic-pituitary-adrenal axis activation in response to food restriction.
Front. Mol. Neurosci. 15:990803.
doi: 10.3389/fnmol.2022.990803

A subpopulation of agouti-related peptide neurons exciting corticotropin-releasing hormone axon terminals in median eminence led to hypothalamic-pituitary-adrenal axis activation in response to food restriction

Ruksana Yesmin[1], Miho Watanabe[1], Adya Saran Sinha[1], Masaru Ishibashi[1], Tianying Wang[1] and Atsuo Fukuda[1,2]*

[1]Department of Neurophysiology, Hamamatsu University School of Medicine, Hamamatsu, Shizuoka, Japan, [2]Advanced Research Facilities and Services, Preeminent Medical Photonics Education and Research Center, Hamamatsu University School of Medicine, Hamamatsu, Japan

The excitatory action of gamma-aminobutyric-acid (GABA) in the median-eminence (ME) led to the steady-state release of corticotropin-releasing hormone (CRH) from CRH axon terminals, which modulates the hypothalamic-pituitary-adrenal (HPA) axis. However, in ME, the source of excitatory GABAergic input is unknown. We examined agouti-related peptide (AgRP) expressing neurons in the arcuate nucleus as a possible source for excitatory GABAergic input. Here, we show that a subpopulation of activated AgRP neurons directly project to the CRH axon terminals in ME elevates serum corticosterone levels in 60% food-restricted mice. This increase in serum corticosterone is not dependent on activation of CRH neuronal soma in the paraventricular nucleus. Furthermore, conditional deletion of Na^+-K^+-$2Cl^-$ cotransporter-1 (NKCC1), which promotes depolarizing GABA action, from the CRH axon terminals results in significantly lower corticosterone levels in response to food restriction. These findings highlight the important role of a subset of AgRP neurons in HPA axis modulation via NKCC1-dependent GABAergic excitation in ME.

KEYWORDS

CRH neuron, paraventricular nucleus, median eminence, AgRP neuron, arcuate nucleus, NKCC1, HPA axis, corticosterone

Introduction

The hypothalamic-pituitary-adrenal (HPA) axis consists of a cascade of endocrine pathways that maintain body homeostasis, including stress response modulation (Sheng et al., 2020). Corticotropin-releasing hormone (CRH) is a peptide hormone that regulates the HPA axis under both basal and stress-activated conditions. CRH is synthesized in the cell bodies of CRH neurons in the paraventricular nucleus (PVN) of the hypothalamus. Upon exposure to stress, CRH released from the axon terminals of CRH neurons in the median eminence (ME) (Palkovits, 1984), stimulates the anterior pituitary to release adrenocorticotropic hormone which activates the adrenal cortex to upregulate production of glucocorticoids (cortisol in human and corticosterone in mice) (Oakley and Cidlowski, 2013). Elevated glucocorticoid levels are regulated by a feedback mechanism (Vandenborne et al., 2005; Myers et al., 2012).

Multiple neurotransmitter systems, including noradrenergic, glutamatergic, and gamma-aminobutyric acid (GABA)-ergic synaptic inputs, regulate CRH neuronal activity. In the mature brain without stress, CRH neuronal soma receive robust GABAergic inhibition from the peri-PVN, anterior hypothalamic area, dorsomedial hypothalamic nucleus, medial preoptic area (mPOA), lateral hypothalamic area (LHA), and multiple nuclei within the bed nucleus of the stria terminalis (BNST). (Roland and Sawchenko, 1993; Tasker and Dudek, 1993; Bowers et al., 1998; Tasker et al., 1998; Miklos and Kovacs, 2002; Herman et al., 2004; Radley et al., 2009; Mody and Maguire, 2011; Levy and Tasker, 2012). However, during acute and chronic stress, GABA turns excitatory and increases CRH release (Hewitt et al., 2009; Sarkar et al., 2011; MacKenzie and Maguire, 2015; Kim et al., 2019). Inhibitory and excitatory effects of GABA are dependent on the electrochemical gradient of Cl^-, while inhibitory GABA function is dynamically mediated by a low intracellular Cl^- concentration, which is regulated by K^+-Cl^- co-transporter (KCC2) predominantly expressed in the cell body (Rivera et al., 1999). Conversely, under non-stressful condition in mature brain, we previously reported that excitatory GABAergic inputs originating from the arcuate nucleus (ARC) maintain steady-state CRH release from axon terminals of CRH neurons in the ME. While, excitatory GABA functions have been mediated by high intracellular Cl^- concentration in CRH axon terminals due to an abundance of Na^+-K^+-$2Cl^-$ cotransporter 1 (NKCC1) rather than KCC2 (Kakizawa et al., 2016). As a result of the differential intracellular Cl^- levels, GABA exerts diverse physiological roles on the somata and axon terminals of CRH neurons. However, the neuronal population in the ARC that sends excitatory GABAergic inputs to CRH neuron axon terminals in the ME is still unknown.

In ARC, agouti-related peptide (AgRP)-expressing neurons produce GABA (Tong et al., 2008; Wu et al., 2009) and send their axons to the median eminence. Diverse metabolic stimuli such as fasting and peripheral orexigenic signals like ghrelin (Cowley et al., 2003; Kohno et al., 2003) activate AgRP neurons. Besides stress, fasting or caloric restriction (CR) can increase serum cortisol or corticosterone (Champy et al., 2004; Jensen et al., 2013) implying that AgRP neuronal activity and corticosterone release may have a synergistic association. However, CR did not increase the activity of the CRH neuronal soma (Kenny et al., 2014) raising the possibility that CR activated the CRH axon terminal instead of the soma, resulting in an increase in corticosterone level, as we previously demonstrated. In line with our earlier findings, here we examine AgRP neurons as a putative GABAergic source that might activates the CRH axon terminals and upregulate the HPA axis.

Thus, the aforementioned AgRP neurons projecting to the ME may play a role in HPA axis activation in response to energy depletion. Here, we set out to characterize the neuronal population that specifically projects to the ME and affects corticosterone levels in response to 60% food restriction (60% amount of food was given; 60% FR). We examined physiological roles of AgRP neuronal activation by food restriction (FR) and observed increases in circulating corticosterone levels. Thereafter, we employed a retrograde tracer to identify a subset of AgRP neurons that directly project to the ME, respond to energy homeostasis, and modify HPA axis activity to increase serum corticosterone levels via excitatory GABA action at CRH nerve terminals in the ME.

Materials and methods

Animals

Adult male mice (8–12 weeks old) were used to avoid sex base difference in stress response. Mice were kept in groups of 3–4 per cage under a 12-h light-dark cycle (lights off from 19:00 to 07:00) with free access to water and food pellets. AgRP-Ires-Cre mice (Stock No. 012899), CRH-Ires-Cre mice (Stock No. 012704), Cre-dependent GCaMP3 reporter mice (Ai38, Stock No. 014538), and Cre-dependent Gq-DREADD mice (CAG-LSL-Gq-DREADD, Stock No. 026220) were purchased from the Jackson Laboratory and C57BL/6J (wild-type) mice was also used. $NKCC1^{flox/flox}$ mice (a gift from Prof. Christian A. Hübner) were previously described (Antoine et al., 2013). To visualize AgRP neurons, we crossed AgRP-Ires-Cre mice with Ai38 reporter mice to generate AgRP-Cre:GCaMP3 mice. For chemogenetic activation of AgRP neurons, we crossed AgRP-Ires-Cre mice with CAG-LSL-Gq-DREADD mice to generate AgRP Cre:DREADD mice. To generate CRH Cre:$NKCC1^{flox/flox}$ (NKCC1 KO^{CRH}) mice, we crossed CRH-Ires-Cre (NKCC1 WT) mice with $NKCC1^{flox/flox}$ mice. Animal identifiers and mouse genotype sequences were listed in **Supplementary Table 2**. All experiments were performed in accordance with guidelines issued by the Hamamatsu University School of Medicine on the ethical use of animals for experimentation, and were approved by the Committee for Animal Care and Use

(Approval Nos. 2017056, 2017057, 2018025, and 2020074). All efforts were made to minimize the number of animals used and their suffering.

Food restriction

All mice were individually housed and allowed to acclimatize for 7 days before experiments. To measure the average daily food consumption, daily food intake (*ad libitum*) and body weight of WT mice was monitored for 10 days. For FR experiments, mice were given a food pellet equal to 60% of average daily food intake (60% FR). Mice were assigned to *ad libitum* (Ad-lib) or 60% FR groups for 10 days and food was added to each cage in the afternoon prior to lights off. Water was freely available to both groups. To minimize the circadian variation in feeding and corticosterone levels, mice for all experiments were sacrificed between 09:00 and 11:00 a.m. Trunk blood was collected for hormone analysis, while brains were collected for c-Fos immunostaining.

Retrograde labeling

To label AgRP neurons sending axon terminals to the ME, AgRP-Cre:GCaMP3 mice received an intraperitoneal (i.p.) injection of the retrogradely transportable marker compound Fluoro-Gold (40 mg/kg; Fluorochrome). Because ME is the circumventricular organ, the uptake of the retrograde tracer and its accumulation in cell bodies occurs following injection into the bloodstream (Swanson and Kuypers, 1980). Four days after injection, mice were transcardially perfused with phosphate-buffered saline (PBS), followed by a 4% paraformaldehyde solution (PFA), and then brains were collected for immunohistochemistry.

Chemogenetic stimulation

For chemogenetic activation of AgRP neurons, AgRP-Cre:DREADD mice were treated with clozapine N-oxide (CNO; 1 mg/kg B.W.). For acute studies, food intake and body weight were measured at 0, 1, 2, and 24 h after saline/CNO injection. For the hormone assay, blood samples were collected 1 h after CNO or 0.9% saline i.p. injection between 09:00 and 11:00 a.m. For c-Fos immunohistochemistry, brain tissue was collected 90 min after CNO or 0.9% saline injection.

Immunohistochemistry

Mice were deeply anesthetized with sodium pentobarbital (50 mg/kg) and transcardially perfused with PBS, followed by ice-cold 4% PFA. Brains were collected and placed in 4% PFA for 2 h, followed by 20 and 30% sucrose in 0.1 M phosphate buffer (PB) at 4°C. Next, brains were frozen, coronally sectioned (30 μm), and processed for immunohistochemistry as previously described (Kakizawa et al., 2016). Free-floating sections were washed in 0.1% Tween 20 in PBS (PBS-T), and then blocked using 10% normal goat serum or normal donkey serum in PBS-T at room temperature. Subsequently, sections were incubated for 24–48 h with the following primary antibodies diluted in PBS-T at 4°C: guinea pig anti-CRH (1:800; Peninsula Laboratories, Carlos, CA, USA, T-5007), mouse anti-c-Fos (1:2000; Abcam, ab208942), chicken anti-GFP (1:1000; Abcam, ab13970), goat anti-AgRP (1:1000; R&D system, AF634), rabbit anti-TH (1:3000; Millipore, Ab152), mouse anti-HA (1:1000; Biolegend, 901501), rabbit anti-c-Fos (1:3000; Sigma-Aldrich, F7799), mouse monoclonal anti-NKCC1 (T4) (1:3000, DSHB), rabbit anti-POMC (1:2000; Phoenix Pharmaceuticals, Inc., Burlingame, CA, USA H-029-30), rabbit anti-Fluoro-Gold (1:500; Merck, AB 153-I). Antibody unique Identifiers and their resources were listed in **Supplementary Table 2**. Subsequently, all floating sections were washed several times with PBS-T and incubated with the following secondary antibodies: Alexa Fluor 488-conjugated goat anti-guinea pig IgG, Alexa Fluor 594-conjugated goat anti-guinea pig IgG, Alexa Fluor 594-conjugated goat anti-mouse IgG, Alexa Fluor 647-conjugated goat anti-mouse IgG, Alexa Fluor 488-conjugated goat anti-chicken IgG, Alexa Fluor 488-conjugated donkey anti-goat IgG, Alexa Fluor 488-conjugated goat anti-rabbit IgG, and Alexa Fluor 594-conjugated goat anti-rabbit IgG, (1:1000, all from Molecular Probes) at room temperature for 2 h. After several washes with PBS-T, sections were mounted and cover slipped. Confocal microscopy (Olympus FV1000-D or Leica TCS SP8) was used to capture images.

Cell counting

To determine whether FR induces c-Fos in AgRP neurons, AgRP-Cre:GCaMP3 mice were evaluated and CNO-mediated c-Fos induction was examined in AgRP-Cre:DREADD mice. For cell quantification, ImageJ (Fiji, NIH) was used to define a specific region of interest, such as the PVN or ARC. Four to five representative sections from one or both sides of the PVN and ARC of each mouse were included in this study. To distinguish cells from background, thresholding was adjusted to minimize non-specific background fluorescence. Individual neurons expressing AgRP or CRH were identified and counted by adjusting threshold values. c-Fos-positive cells were also counted in 30-μm coronal sections obtained serially across the anterior to posterior axis of the PVN and ARC of the hypothalamus using the "analyze particles" feature, such that consistent fluorescence and size thresholds were used throughout, as previously described (Grishagin, 2015).

Electron microscopic analysis

Mice were anesthetized with sodium pentobarbital (50 mg/kg) and perfused with 0.1 M PB containing 4% PFA and 0.5% glutaraldehyde. Following perfusion, the brain tissue was quickly cut into 1-mm square pieces with a razor and fixed with same solution for 2 h at 4°C. Next, the brain tissue was rinsed three times (10 min each) in 0.1 M PB to completely remove the fixative agents and post-fixed in 0.1 M PB containing 1% osmium tetroxide for 2 h at room temperature. Next, the fixed brain tissue was dehydrated by incubation in a series of ethanol solutions, followed by propylene oxide. Following dehydration, specimens were placed in a mold filled with liquid resin and cured into a hard block using heat. Samples embedded in London Resin (LR) white acrylic resin were subsequently polymerized at 48°C for 1 day and 60°C for 2 days. Each polymerized block was cut into semithin sections (1 μm) with a glass knife using an ultramicrotome. After staining the semithin sections with toluidine blue, trimming was performed and ultrathin (80-nm) sections made using a diamond knife were collected on nickel grids. Next, the ultrathin sections were subjected to double immunostaining for CRH and AgRP using gold-conjugated secondary antibodies. Primary antibodies and gold conjugates were diluted in Tris-buffered saline (TBS, pH 7.4) containing 1% bovine serum albumin (BSA) and 0.1% Tween 20. Grids with ultrathin section were placed on a drop of blocking solution in TBS containing 1% BSA, 0.1 M glycine, and 0.1% Tween 20 for 1 h at room temperature. Next, grids with sections were incubated overnight at 4°C with guinea pig anti-CRH (1:100; Peninsula Laboratories, Carlos, CA, USA, T-5007) and goat anti-AgRP (1:100; R&D Systems, AF634) antibodies. All grids were then washed with a few drops of TBS and incubated with 6-nm colloidal gold-donkey anti-goat IgG and 18-nm colloidal gold-donkey anti-guinea pig IgG secondary antibodies (Jackson Immuno Research Laboratories, West Grove, PA, USA) for 1 h at room temperature. Next, grids were stained with uranyl acetate for 5 min and lead citrate for 3 min. Observations were made with a transmission electron microscope (JEM 1400, JEOL) and images were recorded on a charge-coupled device camera.

Hormone assay

Adult mice were sacrificed by cervical dislocation. Mice were decapitated and the trunk blood was collected into polyethylene tubes containing EDTA-2K (Becton, Dickinson and Company, Franklin Lakes, NJ, USA) and centrifuged at 3000 rpm for 20 min at 4°C. Subsequently, serum was collected and stored at −80°C until use in the hormone assay. Samples were collected between 09:00 and 11:00 a.m. to minimize the effect of circadian rhythm. Plasma corticosterone levels were determined using a radioimmunoassay, as previously reported (Uchida et al., 2011). Briefly, a 25-μl sample of serum was boiled at 98°C for 5 min. Ice-cold radioimmunoassay buffer [0.1 M PB (pH 7.4) containing 0.05% NaN_3 and 0.1% Triton X-100] was used for dilution. ^{125}I-corticosterone (Institute of Isotopes) was used as the label. A mixture comprising 100 μl of corticosterone standard or sample, 100 μl of corticosterone antiserum, and 100 μl of ^{125}I-labeled corticosterone was incubated for 24 h at 4°C. Antibody-bound and antibody-free corticosterone were separated via incubation with 100 μl of a secondary antibody (bovine γ-globulin) and 400 μl of 25% polyethylene glycol, followed by centrifugation at 3000 rpm for 15 min at 4°C. Radioactivity of label bound to the antibody was counted using a γ-counter (ARC-7010, Aloka, Tokyo, Japan). The assay did not cross-react with other corticosteroids and the sensitivity was 2 pg/tube.

Statistics

Statistical analysis was performed using GraphPad Prism software. Data were first assessed for normality of distribution by the Kolmogorov-Smirnov test. For comparison of two groups, unpaired Student's *t* test was used. ANOVA (one- or two-way) followed by Tukey's or Bonferroni *post hoc* tests were used to analyze multiple comparisons. Statistical significance was defined as $P < 0.05$. All data are presented as the mean ± SEM.

Results

Agouti-related peptide and corticotropin-releasing hormone neuronal terminal juxtaposition in median-eminence

Emerging evidence suggests that AgRP neurons located in the ARC of the hypothalamus are GABAergic (Tong et al., 2008; Wu et al., 2009). Previously, we reported that GABAergic input originates from the ARC in the ME where the terminals of CRH neurons exist (Kakizawa et al., 2016). So, we postulated that if AgRP contributes to excitatory GABAergic input, it must project from the ARC to the ME, where it will be juxtaposed with the CRH axon terminal. Therefore, we examined the projection of AgRP neurons to ME. To visualize AgRP neurons in the ARC, we crossed AgRP-Cre mice with GCaMP3 (Ai38) reporter mice to generate AgRP-Cre:GCaMP3 mice expressing GCaMP3 with enhanced green fluorescent protein (EGFP) in Cre-expressing AgRP neurons. Fluoro-Gold, a retrograde tracer that does not penetrate the blood-brain barrier, was administered peripherally. Injection (i.p.) of Fluoro-Gold retrogradely labeled AgRP neurons in the ARC of AgRP-Cre:GCaMP3 mice ($n = 3$ mice; **Figure 1A**). Next, we performed

double immunostaining for EGFP (AgRP) and CRH. The results show that AgRP neurons densely projected over the internal layer of the ME with some projections extending to the external layer, whereby AgRP axon terminals were juxtaposed to CRH axon terminals (n = 4 mice; **Figure 1B**). For further confirmation, we performed immuno-electron microscopy. As shown in **Figure 1C**, the CRH neuron terminal (encircled with red) was juxtaposed to an AgRP neuron terminal (encircled with blue) in the external layer of ME. CRH immunoreactivity (large 18-nm gold particles) was confined to dense-core secretory granules, which have a mean diameter of approximately 90–100 nm. AgRP neuron terminals contained both large dense-core vesicles containing AgRP immunoreactivity (small 6-nm gold particles) and small clear vesicles, indicative of GABA vesicles. The higher magnification image shows that the AgRP neuron axon terminal had symmetric synaptic contact with the CRH neuronal terminal (n = 3 mice; **Figure 1C**). Together, these data suggest that GABA-containing AgRP neuronal terminals contact CRH axon terminals at the external layer of the ME.

Chemogenetic activation of agouti-related peptide neurons resulted in the increase in serum corticosterone levels

To test our hypothesis that AgRP neuronal activation contribute to increased serum corticosterone levels, we employed an excitatory hM3Dq designer receptor exclusively activated by designer drugs (DREADD)-mediated chemogenetic approach to specifically activate AgRP neurons. AgRP-Ires-Cre mice were crossed with hM3Dq DREADD mCitrine mice to generate AgRP-Cre:DREADD transgenic mice (**Supplementary Figure 1A**). To verify specific expression of hM3Dq DREADD in AgRP neurons after Cre recombination, brain sections of AgRP Cre:DREADD mice were immunohistochemically evaluated for expression of the yellow-green fluorescent protein mCitrine and hemagglutinin (HA) epitope tag. GFP antibody was used to stain mCitrine reporter (n = 4 mice for AgRP/GFP and n = 4 mice for HA/GFP; **Supplementary Figure 1B**).

Function of the excitatory DREADD was verified by specific expression of DREADD ligand clozapine N-oxide (CNO)-induced c-Fos expression in AgRP neurons. Following CNO administration, 91.1% ± 2% of AgRP neurons expressed c-Fos (195.08 ± 4.95 c-Fos-positive AgRP cells/214.04 ± 4.95 total AgRP cells), indicating good efficacy of our DREADD-mediated approach (saline, n = 3 mice, four sections per mouse; CNO, n = 5 mice, five sections per mouse; $P < 0.0001$, unpaired Student's t test; **Figures 2A,B**). We also observed that food intake was significantly increased by CNO administration without immediately significant body weight change (**Supplementary Figures 2A,B**). These results indicate that AgRP neurons were sufficiently activated. Next, we tested the potential involvement of AgRP neurons in increased levels of circulating corticosterone following i.p. injection of CNO or saline. We observed that CNO effectively increased serum corticosterone levels compared with the saline-treated group (saline, 92.84 ± 17.30 ng/ml; CNO, 326.5 ± 21.13 ng/ml; n = 10 mice per group; $P < 0.0001$, unpaired Student's t test; **Figure 2C**). These results demonstrate that the observed increase of serum corticosterone induced by CNO was dependent on ARC AgRP neuron activation.

Generally, increases in serum corticosterone levels are dependent on CRH neuronal activation of the PVN (Kim et al., 2019). Thus, we next examined c-Fos expression of CRH neurons in the PVN by chemogenetic activation of AgRP neurons. CNO administration significantly increased c-Fos expression in CRH neurons compared with saline administration, indicating that CRH neuronal activation caused corticosterone secretion. Indeed, we found that 45.58% ± 1.86% of CRH neurons in the PVN area were positive for c-Fos in the CNO-treated group, significantly more than observed in the saline-treated group 18.08% ± 1.20% ($P < 0.0001$; unpaired Student's t test; n = 5 mice, five sections per mouse; **Figures 2D,E**). This result indicates that chemogenetic activation of AgRP neurons activates CRH neuronal somata in the PVN.

Physiological activation of agouti-related peptide neurons activates the corticotropin-releasing hormone axon terminals, resulting in increased blood corticosterone levels

As AgRP neurons are progressively activated by energy deficient signal or FR (Betley et al., 2015; Chen et al., 2015), next as physiological stimulus we examined whether FR can increase serum corticosterone levels. In this study, we defined FR group mice as those who were only given 60% of the food compared to control (Ad-lib) mice (**Figure 3A**). As expected, when compared to the Ad-lib group, 60% of FR for 10 days resulted in a significant weight loss that was visible as early as the 2 day (n = 6 mice per group, $P < 0.005$; **Figure 3B**). Next, we investigated whether 60% FR had any effect on serum corticosterone levels via AgRP cell activation in adult wild-type mice. Consistent with a previous report (Allen et al., 2019) serum corticosterone levels were significantly increased following 60% FR compared with level of the Ad-lib group (Ad-lib, 43.93 ± 11.5 ng/ml; FR, 140.4 ± 18.6 ng/ml, n = 6 mice per group; $P < 0.0013$, unpaired Student's t test; **Figure 3C**). Increased serum corticosterone levels are generally dependent on CRH neuronal activation in the PVN (Parton et al., 2007). Accordingly, we examined c-Fos expression in CRH neuronal somata in the PVN. Interestingly, in contrast to chemogenetic activation of AgRP neurons, no c-Fos expression was observed in the PVN area (**Figure 3D**),

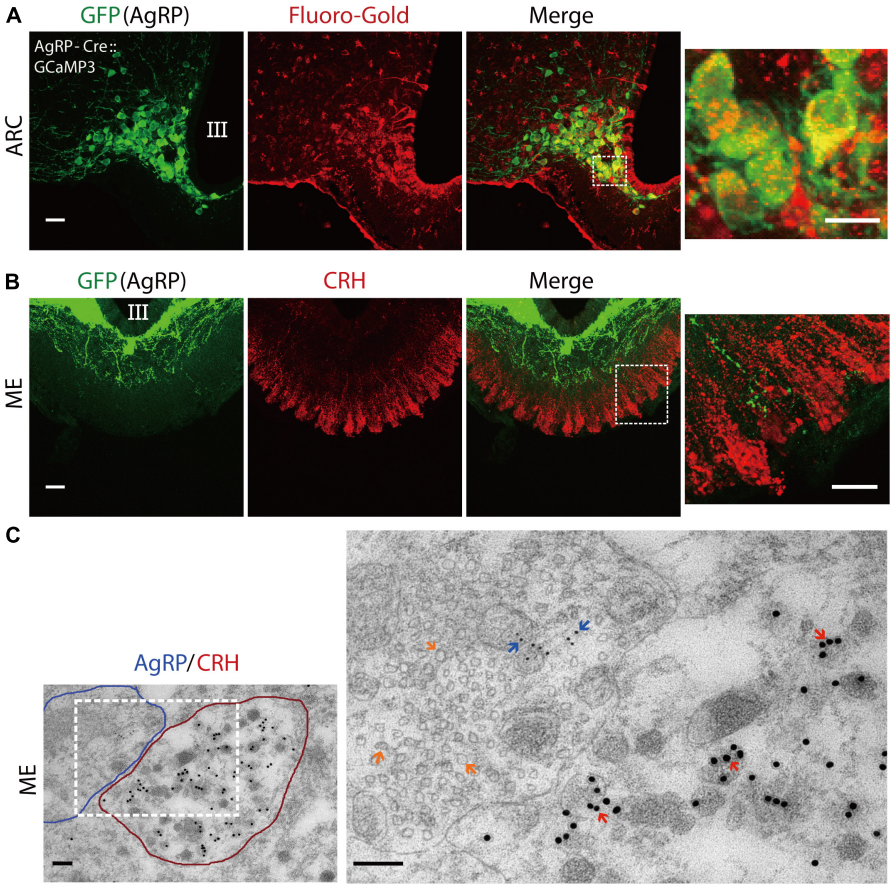

FIGURE 1
Agouti-related peptide (AgRP) neurons project to corticotropin-releasing hormone (CRH) neuronal terminals in the median eminence. **(A)** The retrograde tracer Fluoro-Gold was peripherally delivered in AgRP-Cre:GCaMP3 mice. Confocal image showing AgRP neurons in the arcuate nucleus (ARC) stained with an anti-GFP antibody (for GCaMP3; green) and anti-Fluoro-Gold antibody (red). The dotted boxed area indicates higher magnifications image. Scale bars, 40 and 10 μm (box). **(B)** Confocal image showing anti-GFP (green) and anti-CRH (red) immunoreactivity in the median-eminence (ME). Higher magnification image indicated by box shows AgRP and CRH neuronal axon terminals in the external layer of the ME. Scale bars, 40 and 10 μm (box). **(C)** Double immuno-electron microscopic images showing an AgRP nerve terminal (outlined in blue) contacting a CRH neuronal terminal (outlined in red) in the ME of wild-type mice. Note that the AgRP neuronal axon terminal makes direct contact to the axon terminal of the CRH neuron. Inset box image shows higher magnification image. AgRP immunoreactivity (6-nm gold particle) indicated by blue arrow and CRH immunoreactivity (18-nm gold particle) indicated by red arrow in the external layer of the ME. Large dense-core vesicles indicate CRH-containing vesicles, while small clear vesicles marked by orange arrows in AgRP neuronal terminal indicate gamma-aminobutyric-acid (GABA)-containing vesicles. Scale bars, 500 and 200 nm, respectively. III, third ventricle.

indicating that increased serum corticosterone by 60% FR does not result from somatic activation of CRH neurons in the PVN.

Fasting is a catabolic-metabolic state that causes several physiological changes in mice, such as activation of AgRP neurons in the ARC (Takahashi and Cone, 2005; Liu et al., 2012). CR upregulates AgRP mRNA expression level (Rogers et al., 2016). Thus, next we examined c-Fos expression in AgRP neurons to detect cells activated by FR. Following 60% FR in AgRP-Cre:GCaMP3 mice to clearly visualize AgRP neurons, c-Fos expression was significantly increased (**Figure 3E**). Specifically, we observed that 51.3% ± 1.7% of AgRP neurons (108.6 ± 4.73 c-Fos positive AgRP cells/211.76 ± 5.86 total AgRP cells) were activated (c-Fos positive; **Figure 3F**) and 68.53% ± 2.04% of c-Fos-positive cells were AgRP neurons under 60% FR (**Figure 3G**) ($n = 5$ mice, five sections per mouse; $P < 0.0001$, unpaired Student's t test).

We next evaluated proportions of activated AgRP neurons following CNO administration and FR. CNO treatment activated significantly more AgRP neurons (91.1% ± 2%) compared with 60% FR (51.3% ± 1.7%; $P < 0.0001$; unpaired Student's t test; $n = 5$ mice, five sections per mouse; **Figure 3H**). Furthermore, numbers of c-Fos-expressing neurons (CNO, 205.12 ± 5; FR, 159.6 ± 6.11; **Supplementary Figure 3B**), c-Fos-expressing AgRP neurons (CNO, 195.08 ± 4.95; FR, 108.6 ± 4.73; **Supplementary Figure 3C**) in the ARC and serum corticosterone levels (CNO, 326.50 ± 21.13 ng/ml; FR, 140.4 ± 18.64 ng/ml; **Supplementary Figure 3D**) were significantly higher in the CNO-treated group compared with

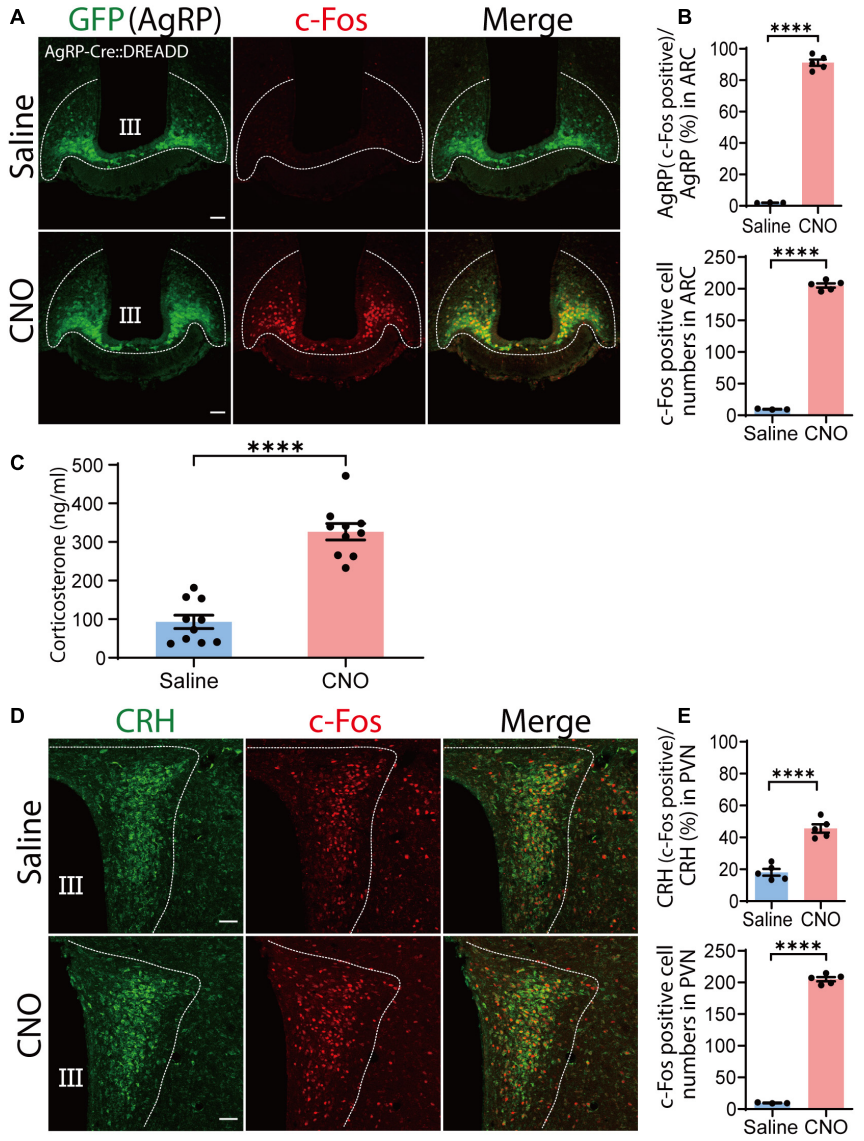

FIGURE 2
Chemogenetic activation of agouti-related peptide (AgRP) neurons by clozapine N-oxide (CNO) causes corticotropin-releasing hormone (CRH) neuronal somatic activation and increased serum corticosterone levels. **(A)** Injection of CNO i.p. induced c-Fos expression in the arcuate nucleus (ARC). Confocal image showing AgRP neurons stained with an anti-GFP antibody (green) and anti-c-Fos antibody (red). Scale bars, 50 μm. **(B)** Percentage of AgRP neurons expressing c-Fos in the ARC in upper panel; and total numbers of c-Fos-positive cells in the ARC in lower pannel; ****$P < 0.0001$, unpaired Student's *t* test. **(C)** Serum corticosterone level 1 h after CNO and saline injection; ****$P < 0.0001$, unpaired Student's *t* test. **(D)** Confocal image showing c-Fos expression in CRH neurons stained with an anti-CRH antibody (green) in the paraventricular nucleus (PVN) area after CNO and saline injection. Scale bars, 50 μm. **(E)** Proportion of CRH and c-Fos colocalization in the PVN **(upper panel)**. In total, 86.76 ± 3 CRH cells colocalized with c-Fos out of a total of 192 ± 3 CRH cells; ****$P < 0.0001$, unpaired Student's *t* test. Quantification of total c-Fos expression in the PVN; ****$P < 0.0001$, unpaired Student's *t* test **(lower panel)**. Error bars represent SEM. Dotted line indicate the area for counting of AgRP, CRH and c-Fos positive cells.

the 60% FR group. Collectively, these data indicate that about half of ARC AgRP neurons responded to FR and played an active role in modulation of circulating corticosterone levels. Because of the observed lack of activation of PVN CRH neurons by 60% FR, we hypothesize this subgroup may be responsible for modulating CRH release at the ME.

A subset of activated agouti-related peptide neurons directly project to the median eminence

Agouti-related peptide neurons can be subdivided based on their projection pattern (Betley et al., 2013). Thus, we examined the population of AgRP neurons that projected directly to the

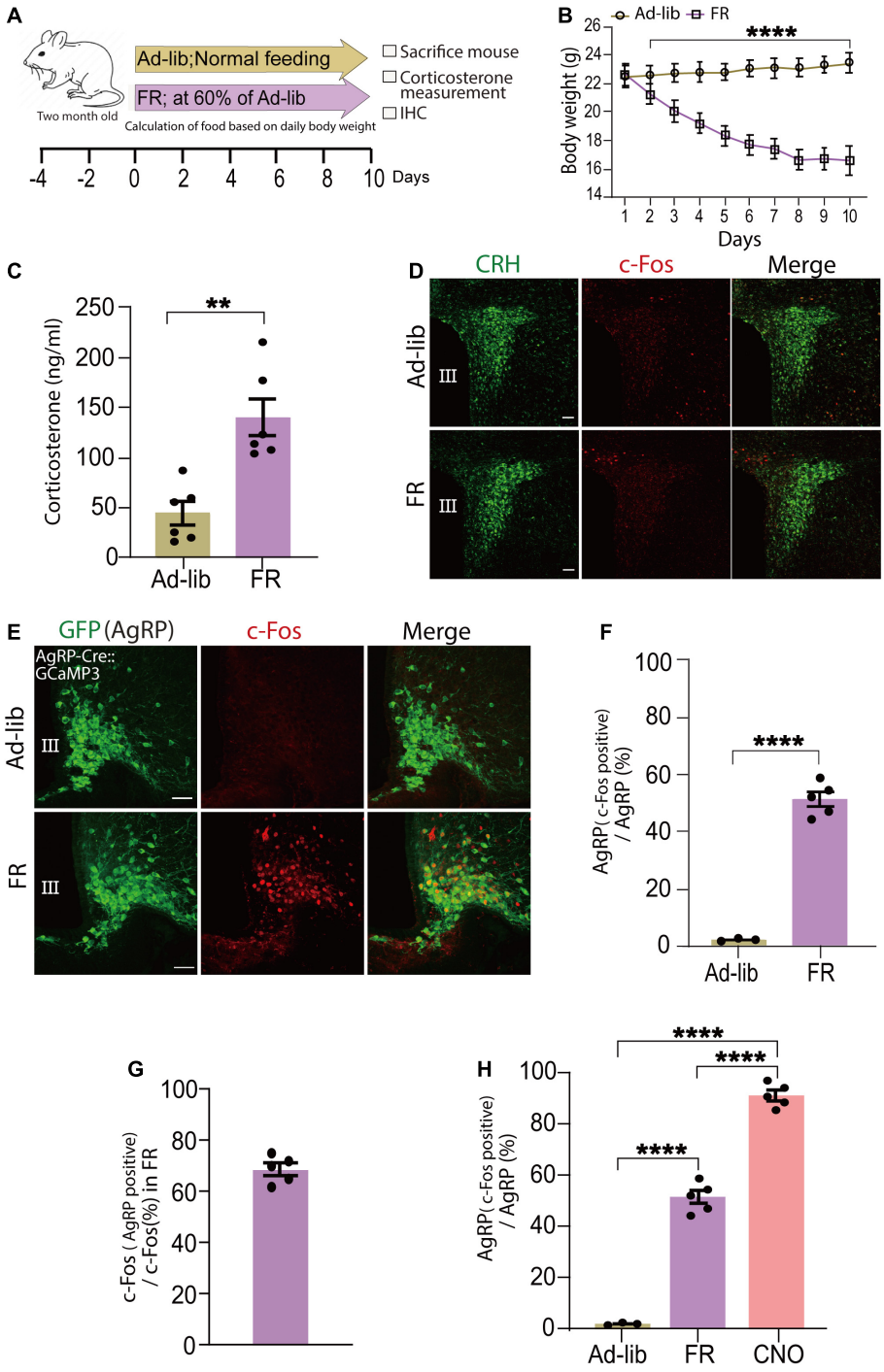

FIGURE 3
Food restriction (FR) activates agouti-related peptide (AgRP) neurons and increases serum corticosterone levels. **(A)** Schematic diagram of 60% FR for 10 days. FR was applied every day at 6 p.m. in wild-type adult male mice. **(B)** FR significantly decreased body weight; ****$P < 0.0001$, unpaired Student's *t* test. **(C)** Plasma corticosterone levels at 9.00 a.m.–11.00 a.m. was significantly increased in the FR group; **$P < 0.0013$; unpaired Student's *t* test. **(D)** c-Fos expression was not observed in the PVN area of *ad libitum* (Ad-Lib) or FR groups. Scale bars, 50 μm. **(E)** Confocal image showing c-Fos expression in AgRP neurons in the arcuate nucleus (ARC) stained with an anti-GFP antibody in AgRP-Cre:GCaMP3 mice. Scale bars, 40 μm. **(F)** Expression of c-Fos in AgRP neurons (51.3% ± 1.7%) was significantly increased by FR; ****$P < 0.0001$, unpaired Student's *t* test. **(G)** Approximately 68.53% ± 2.04% of c-Fos-expressing neurons were AgRP neurons in ARC of FR group. **(H)** AgRP neurons expressing c-Fos in the ARC after clozapine N-oxide (CNO) injection (91.1% ± 2%) were significantly more than that by FR; ****$P < 0.0001$; unpaired Student's *t* test. Error bars represent SEM.

ME. To reveal this, triple-immunostaining for AgRP, Fluoro-Gold, and c-Fos was performed (**Figure 4A**). We found that 19.49% ± 0.82% of AgRP neurons were double positive for Fluoro-Gold and c-Fos under 60% FR (**Figure 4B**). We also observed that 27.72% ± 0.95% of AgRP neurons were labeled by Fluoro-Gold in FR group (**Figure 4C**) as comparable to the control Ad-lib group, indicating that this population of AgRP neurons may directly project to the ME. We also observed that 53.43% ± 3% of AgRP neurons expressed c-Fos by 60% FR (**Figure 4D**). Thus, we found that 70.38% ± 2.54% of Fluoro-Gold-positive AgRP neurons were also positive for c-Fos after 60% FR (**Figure 4E**). In other words, most AgRP neurons directly projecting to the ME were activated by FR. Furthermore, 36.84% ± 2.58% of c-Fos-positive AgRP neurons were labeled by Fluoro-Gold (**Figure 4F**), indicating more than one third of FR-responding AgRP neurons are ME-projecting ones (n = 4 mice, five sections of one side of the ARC per mouse in each group from **Figures 4A–F**). Numbers of cells expressing: AgRP, c-Fos and AgRP, c-Fos, Fluoro-Gold and AgRP in FR group are shown in **Supplementary Table 1**.

It has been established that several types of GABAergic neurons in the ARC regulate energy homeostasis (Cone et al., 2001). Other studies show that tyrosine hydroxylase (TH)-positive ARC neurons are GABAergic and activated by overnight fasting (Zhang and van den Pol, 2015; Zhang and van den Pol, 2016). Following 60% FR, TH neurons exhibited almost no c-Fos expression (**Supplementary Figure 4A**). Proopiomelanocortin (POMC) neurons are the main anorexigenic neuronal population, thus we next examined c-Fos expression in POMC neurons (**Supplementary Figure 4B**). As expected, POMC neurons did not exhibit c-Fos expression after FR. Alternatively, our data suggest that 60% FR activated 31.47% ± 2.37% of non-AgRP neurons in the ARC, excluding TH and POMC neurons. However, these groups of c-Fos-positive non-AgRP neurons were not labeled by Fluoro-Gold (see **Figure 4A**; n = 4 mice, five sections per mouse) indicating no projection to the ME. All together, these data indicate that the majority of AgRP neurons directly projecting to the ME are activated under FR, whereby they may mediate FR-induced modulation of CRH release at ME.

Conditional deletion of NKCC1 from corticotropin-releasing hormone neuron terminals reduced serum corticosterone elevation induced by food restriction

Gamma-aminobutyric-acid-mediated depolarization is dependent on the high intracellular Cl^- concentration produced by NKCC1 (Yamada et al., 2004). CRH neuronal axon terminals, but not soma, express NKCC1. GABA evokes an increase of intracellular Ca^{2+} in CRH neuron terminals that is attenuated by the NKCC1 inhibitor bumetanide (Kakizawa et al., 2016). To establish whether NKCC1 is involved in CRH release from axon terminals of CRH neurons to cause FR-induced corticosterone increases, we generated conditional NKCC1-knockout mice by crossing CRH-Cre mice with $NKCC1^{flox/flox}$ mice. Using the resulting CRH-Cre:$NKCC1^{flox/flox}$ ($NKCC1\ KO^{CRH}$) mice, we confirmed deletion of NKCC1 from CRH axon terminals by immunohistochemical analysis (n = 3 mice; **Figure 5A**). Body weights were significantly decreased in both control (NKCC1 WT) and conditional NKCC1 KO^{CRH} groups following 60% FR (n = 6 mice per group; **Figure 5B**). Next, we measured serum corticosterone levels. Under *ad libitum* conditions, there were no differences in serum corticosterone levels between control and conditional NKCC1 KO^{CRH} groups (56.48 ± 10.13 ng/ml and 59.73 ± 9.67 ng/ml, respectively; n = 6 mice per group; $P > 0.999$; two-way ANOVA with Bonferroni's multiple comparisons test; **Figure 5C**). However, serum corticosterone levels in NKCC1 KO^{CRH} mice were significantly reduced compared with control mice following FR (186.03 ± 3.07 ng/ml and 273.8 ± 18.59 ng/ml, respectively; n = 6 mice per group; $P < 0.0003$, two-way ANOVA, Bonferroni's multiple comparisons test; **Figure 5C**). Together, these data indicate that NKCC1 at CRH axon terminals in the outer layer of the ME play a pivotal role in CRH release to increase serum corticosterone levels in response to hunger signals.

Discussion

The classical inhibitory action of GABA in CRH neuronal somata and its significance in regulation of the HPA axis have been studied extensively (Mody and Maguire, 2011; Levy and Tasker, 2012). Previously, we reported a novel excitatory action of GABA at the CRH neuronal axon terminals in the ME (Kakizawa et al., 2016). In addition, we demonstrated that this excitatory action of GABA is not involved in the physiological acute stress response, but rather in steady-state regulation of the HPA axis. Because of the close proximity of the ARC regulating energy balance and food intake (Minor et al., 2009) to the ME with its diverse GABAergic neuronal populations, we hypothesized that they may be involved in activation of the HPA axis by energy homeostasis and feeding responses (Makimura et al., 2003). In the present report, we demonstrate the possible involvement of AgRP-GABAergic neurons within the ARC in CRH release in response to dietary insufficiency.

To demonstrate an association between the HPA axis and energy metabolism, an FR protocol was used. Based on previous reports of FR affecting circulating corticosterone levels (Kenny et al., 2014; Allen et al., 2019) 60% FR for 10 days was performed, which caused increases in serum corticosterone levels (**Figure 3C**). To ascertain if the enhancement of corticosterone levels was dependent on CRH neuronal activation at the level of somata in the PVN, c-Fos

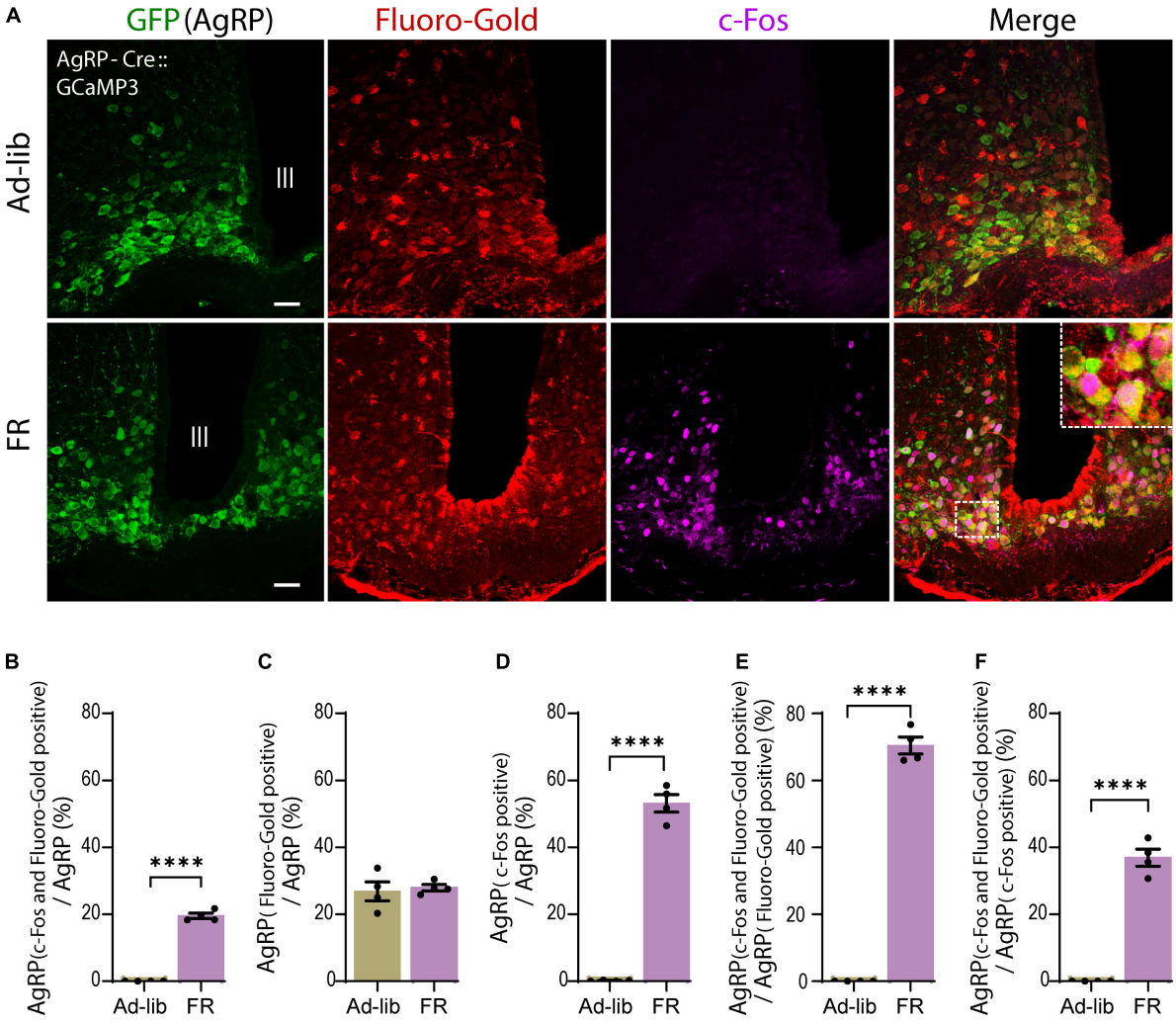

FIGURE 4
A subset of agouti-related peptide (AgRP) neurons directly projecting to the median eminence were activated by food restriction (FR). **(A)** Triple immunostaining of arcuate nucleus (ARC) with anti-GFP for AgRP (green), anti-Fluoro-Gold (red), and anti-c-Fos (magenta) antibodies in *ad libitum* (Ad-lib) **(upper panel)** and FR **(lower panel)** conditions. Note that no c-Fos signals were observed in Ad-lib group. The dotted boxed area indicates higher magnifications image (× 4). Scale bars, 40 μm. **(B)** A subset of AgRP neurons (19.49% ± 0.82%) co-express both Fluoro-Gold and c-Fos under FR. **(C)** In the FR, 27.72% ± 0.95% of AgRP neurons were labeled by Fluoro-Gold, while comparable proportion of AgRP neurons (26.76% ± 2.73%) were labeled by Fluoro-Gold in Ad-lib group ($P = 0.737$; unpaired Student's *t* test). **(D)** 53.43% ± 3% AgRP neurons were c-Fos positive in FR group. **(E)** 70.38% ± 2.54% of Fluro-Gold-positive AgRP neurons were also positive for c-Fos in FR group. **(F)** 36.84% ± 2.58% of c-Fos-positive AgRP neurons were Fluoro-Gold positive. ****$P < 0.0001$; unpaired Student's *t* test. Error bars represent SEM.

staining was performed. The absence of c-Fos expression in CRH neuronal somata in the PVN indicated CRH neuronal activation was not involved (**Figure 3D**), suggesting an altogether different mechanism for the observed increase in corticosterone levels.

Diverse GABAergic neurons in the ARC are involved in many critical homeostatic mechanisms, from food intake to fertility (Marshall et al., 2017; Suyama and Yada, 2018). Among them, almost all AgRP neuronal populations co-express GABA and are orexigenic (Horvath et al., 1997; Cowley et al., 2001). Various studies indicate that fasting induces strong activation of AgRP neurons (Takahashi and Cone, 2005; Liu et al., 2012) while FR significantly increases AgRP mRNA (Minor et al., 2009; Rogers et al., 2016). In the present study, 60% FR caused c-Fos activation in AgRP neurons in the ARC (**Figures 3E,F**), as well as increased circulating corticosterone levels (**Figure 3C**). However, c-Fos expression was absent in CRH neuronal somata (**Figure 3D**). Consistent with previous reports (Atasoy et al., 2012; Fan et al., 2021), *in vivo* CNO administration to selectively activate AgRP neurons also induced a clear enhancement of c-Fos expression in AgRP neurons in the ARC (**Figures 2A,B**) and increased circulating corticosterone levels

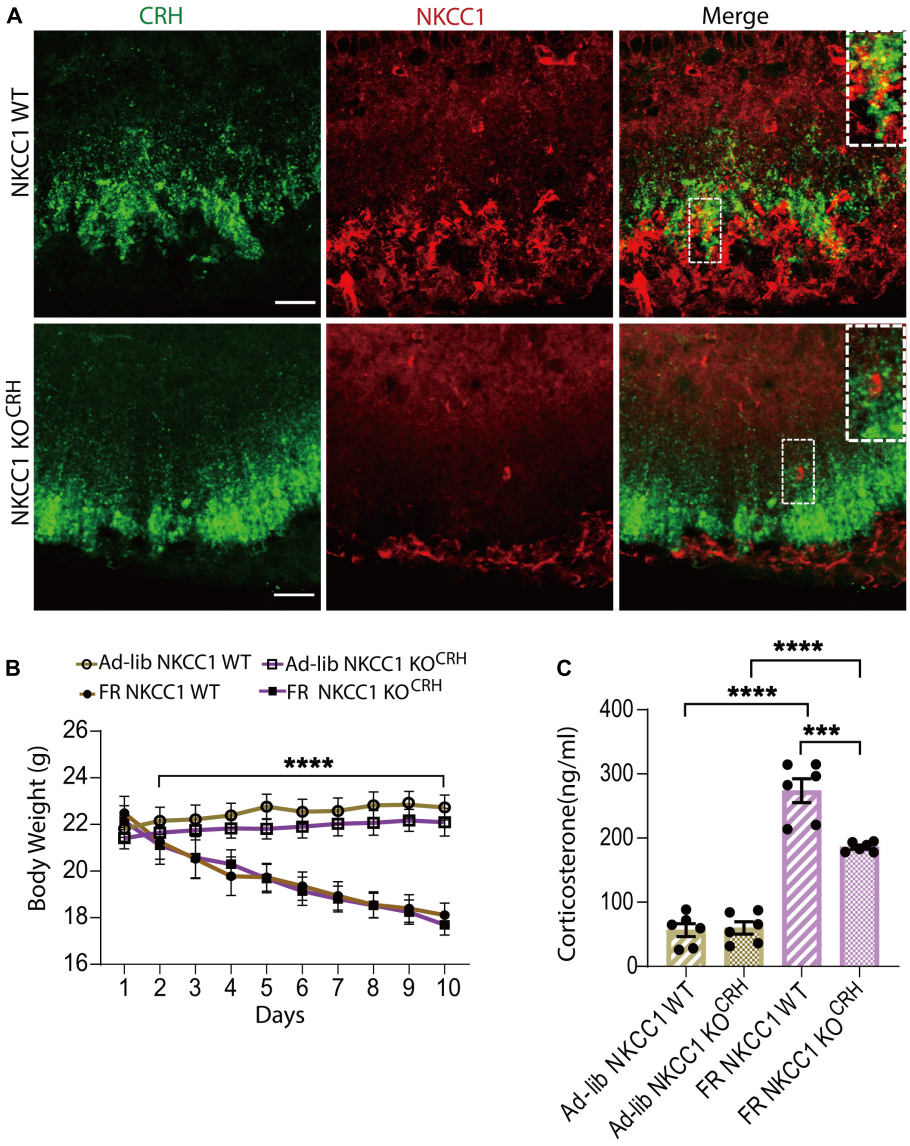

FIGURE 5
Conditional deletion of NKCC1 from corticotropin-releasing hormone (CRH) neuronal terminals reduced the elevation of serum corticosterone in response to food restriction. **(A)** Immunohistochemical staining with anti-CRH (green) and anti-NKCC1 (red) antibodies in CRH neuronal terminals in the median-eminence (ME). NKCC1 immunoreactivity was observed in the outer layer of the ME and colocalized with CRH (upper panel). In NKCC1 KO^{CRH} mice, NKCC1 immunoreactivity was not observed in CRH neuronal terminals (lower panel). Square areas at upper right corner are enlarged image of dotted area. Scale bars, 40 μm. **(B)** Temporal changes in body weight in *ad libitum* (Ad-lib) and food restriction (FR) conditions; ****$P < 0.0001$; two-way ANOVA with Tukey's multiple comparison test. **(C)** Concentrations of serum corticosterone at 9:00–11:00 a.m. in Ad-lib and FR groups, indicating a significant reduction in FR-induced corticosterone increases in NKCC1 KO^{CRH} compared with NKCC1 WT; ****$P < 0.0001$, ***$P < 0.0003$, two-way ANOVA with Bonferroni's multiple comparison test. Error bars represents SEM.

(Figure 2C), indicating a clear link between AgRP neuronal activation and increased serum corticosterone. In contrast to FR, activation of AgRP neurons by CNO was more robust and CRH neuronal somata were activated, as indicated by intense c-Fos expression in the PVN (Figures 2D,E). Clearly, only a portion of chemogenetically activated AgRP neurons were also activated by FR (compare Figures 2B, upper, 3F; Supplementary Figure 3C).

Thus, our results indicate that increases of serum corticosterone levels by chemogenetic and FR-mediated activation of AgRP neurons were different (compare Figures 2C, 3C; Supplementary Figure 3D). Specifically, we found that FR elevated serum corticosterone levels without affecting CRH neuronal somata in the PVN. Comparison of numbers of activated AgRP neurons and circulating corticosterone levels between chemogenetic activation and FR

groups revealed that a large proportion (91.1% ± 2%) of AgRP neurons were activated by CNO administration (**Figure 2B**, upper), whereas only half (51.3% ± 1.7%) of AgRP neurons were activated by FR (**Figure 3F**). Similarly, serum corticosterone levels were increased two-fold in CNO-treated group compared with the FR group (**Supplementary Figure 3D**). Our findings are consistent with the recent study (Fernandes et al., 2022) where they compared both a 24 h and a 36 h fasting protocol. 36 h fasting elevated the mRNA expression of CRH in the PVN and AgRP in the ARC like our CNO administration, whereas 24 h fasting increased AgRP mRNA in ARC but not CRH mRNA in PVN like our FR protocol. The increased corticosterone level is also higher in the 36 h fasting group than the 24 h group, Since the expression of AgRP mRNA in ARC is also higher in the 36 h fasting, the increased corticosterone level is dependent on AgRP neuronal activation. Thus, above difference between CNO and FR might be due to a difference in a population of activated AgRP neurons. Consistent with this, several previous reports using FR protocol found that CRH mRNA expression was not substantially different from the Ad-lib control group in PVN, while AgRP mRNA expression level was increased (de Rijke et al., 2005; Lindblom et al., 2005; Gallardo et al., 2014).

AgRP neuronal axon terminals project from the ARC to various brain regions, such as the PVN, LHA, BNST, raphe nuclei, nucleus accumbens, parabrachial nucleus, periaqueductal gray, paraventricular thalamic nucleus, central nucleus of the amygdala, and brainstem. Therefore, AgRP neurons may be further categorized into differential subpopulations based on their regions of projection (Betley et al., 2013). Indeed, it is quite possible that these projections are associated with different physiological functions and therefore, attributable to differential activation of AgRP neuronal subpopulations (Betley et al., 2013). As previously reported, chemogenetic activation of AgRP neurons may affect multiple downstream brain regions (Steculorum et al., 2016); i.e., CNO administration activates all the AgRP neuronal subpopulations and their downstream targets. CRH neurons in the PVN receive GABAergic input from the peri-PVN, LHA, mPOA, and BNST (Levy and Tasker, 2012). However, a direct synaptic connection between AgRP neuron terminals and CRH neuronal somata in the PVN has not been observed (Garfield et al., 2015). Thus, CRH neuronal somata in PVN could be indirectly activated via inhibition of local inhibitory interneurons by AgRP neurons, hence this disinhibition-dependent activation of CRH neurons may increase circulating corticosterone levels by chemogenetic stimulation (**Figure 6A**).

In contrast, 60% FR did not activate CRH neuronal somata in the PVN, although serum corticosterone levels were elevated. In addition, FR activated only a subset of AgRP neurons. Thus, it is quite likely that these activated neurons are exclusively involved in energy homeostasis triggered by FR, hence the projections from these neurons might not activate PVN CRH neurons (**Figure 6B**). Our data also indicate that FR activated ARC AgRP neurons in addition to other local neurons in the ARC. Several types of neurons besides AgRP neurons are present in the ARC, including subpopulations expressing POMC, TH, rat insulin II gene promoter, nitric oxide synthase, and prepronociceptin, which are all GABAergic and related to energy homeostasis. However, FR did not activate TH neurons or POMC neurons (**Supplementary Figure 4**). In addition, due to the extensive connections of AgRP neurons with other local cells in the ARC (Turi et al., 2003; Cone, 2005; Padilla et al., 2017; Jais et al., 2020; Smith et al., 2020; Varela et al., 2021), we cannot completely rule out the contribution of other neuronal populations in modulating circulating corticosterone levels under FR. Therefore, both the identities and overall function of other local neurons in the ARC interacting with AgRP neurons in response to FR remain to be elucidated.

Corticotropin-releasing hormone neuronal axon terminals exhibit very dense projections to the external layer of the ME (**Figure 1B**). Furthermore, CRH neuronal axon terminals in the ME express $GABA_A$ receptors, and GABAergic inputs to ME originate from the ARC (Kakizawa et al., 2016). AgRP neurons are GABAergic and retrogradely labeled by Fluoro-Gold, suggesting that AgRP neurons project to the ME (**Figure 1A**). Our findings that AgRP neuron terminals project to both the internal and external layers of the ME (**Figures 1B,C**) are corroborated by the previous report (Bagnol et al., 1999). Our double immuno-electron microscopic analysis further confirmed the presence of GABA vesicles in AgRP axons projecting to the external layer of the ME, whereby they formed symmetric synapses with CRH axon terminals (**Figure 1C**). We found that 27.72 ± 0.95% of AgRP neurons were labeled by Fluoro-Gold, indicating that a specific subgroup of AgRP neurons projects to the ME (**Figure 4C**). FR activated approximately half (53.43 ± 3%) of all AgRP neurons examined (**Figure 4D**), 36.84% ± 2.58% of which were retrogradely labeled by Fluoro-Gold (**Figure 4F**). These results indicate that this population of AgRP neurons directly projecting to the ME could contribute to modulation of CRH release from CRH neuronal axon terminals in response to FR (**Figure 6B**). This hypothesis has been supported by the very recent finding that inhibition of AgRP neurons in ARC in fasted animals increases CRH accumulation in the ME, indicating a reduction of release (Fernandes et al., 2022).

Gamma-aminobutyric-acid mediates either inhibition or excitation depending on KCC2 and NKCC1 expression, and functional balance (Rivera et al., 1999; Payne et al., 2003). We previously demonstrated that NKCC1, but not KCC2, was expressed in CRH axon terminals in the ME. In contrast, the somata of CRH neurons were enriched with KCC2 but not NKCC1 (Kakizawa et al., 2016). To evaluate whether AgRP neuronal activation caused GABA-mediated excitation of CRH neuronal terminals in an NKCC1-dependent manner to increase corticosterone levels, conditional knockout of NKCC1 in CRH

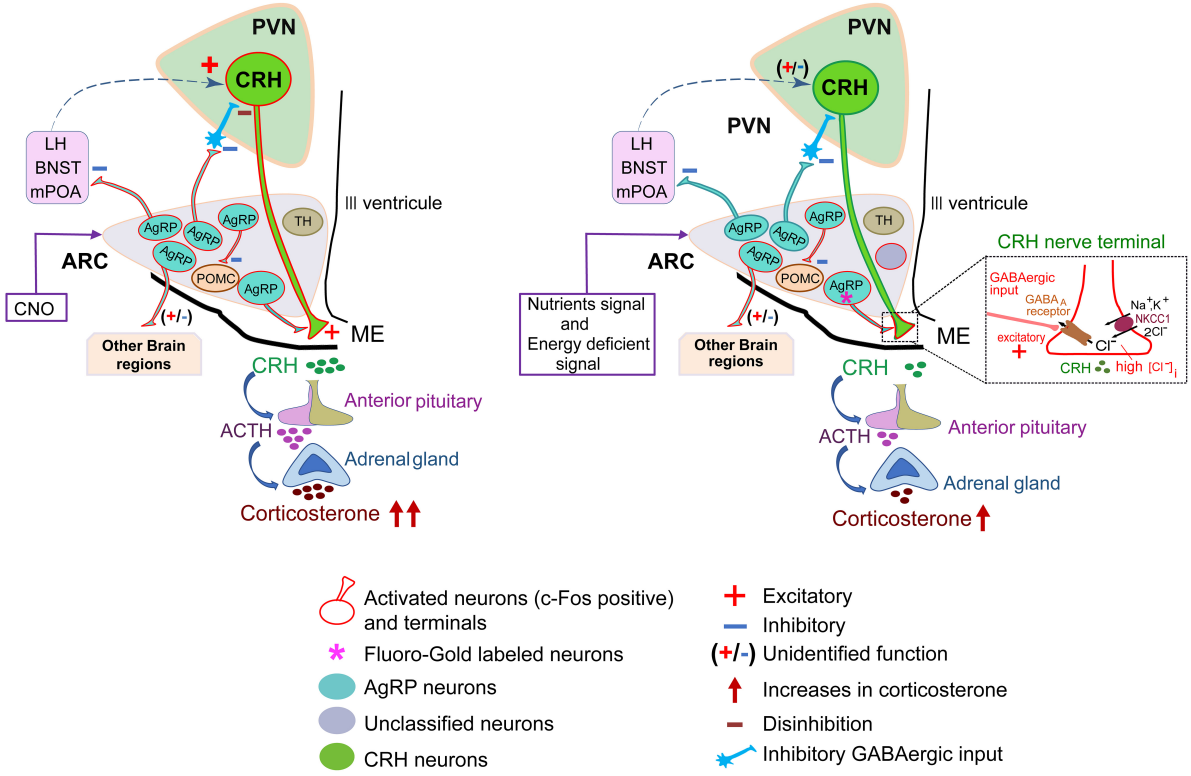

FIGURE 6
Hypothetical model of hypothalamic-pituitary-adrenal axis activation by food restriction. **(A)** Schematic diagram of CNO-mediated HPA-axis activation. Agouti-related peptide (AgRP) neurons project to diverse brain regions such as the PVN, BNST, LH, mPOA and some other regions. CNO activates almost all subsets of AgRP neurons (91.1% ± 2%; **Figure 2B**) in ARC to affect their downstream projecting neurons. As a result, about half of corticotropin-releasing hormone (CRH) neurons in the PVN (45.6% ± 1.9%; **Figure 2E**) were activated and serum corticosterone levels were increased (326.5 ± 21.1 ng/ml; **Figure 2C**). Dashed arrow line (blue) indicates proposed pathways of CRH neuronal activation. **(B)** Schematic diagram of food-restricted model: a subset of AgRP neurons in arcuate nucleus (ARC) (about 30%, **Figure 4C**) directly project to the ME. About half (51.3% ± 1.7%) of AgRP neurons are activated by FR (**Figure 3F**). Among them, about 70% of ME-projecting AgRP neurons were activated by FR (**Figure 4E**), exhibiting excitation of CRH terminals to increase CRH release and serum corticosterone levels (140.4 ± 18.6 ng/ml; **Figure 3C**). This excitatory gamma-aminobutyric-acid (GABA) action is promoted by NKCC1 at CRH neuronal terminals (Kakizawa et al., 2016), so that NKCC1 deletion resulted in significant depression of FR-induced corticosterone release (inset). AgRP, agouti-related peptide; BNST, bed nucleus of the stria terminalis; CNO, clozapine N-oxide; CRH, corticotropin-releasing hormone; FR, food restriction; HPA, hypothalamic-pituitary-adrenal axis; LH, lateral hypothalamus; ME, median eminence; mPOA, medial preoptic area; PVN, paraventricular nucleus; TH, tyrosine hydroxylase; POMC, Proopiomelanocortin.

neurons was performed (**Figure 5A**). NKCC1 KO^{CRH} mice showed equivalent body weight to WT mice under Ad-lib and 60% FR (**Figure 5B**). Moreover, the Ad-lib condition produced no difference in circulating serum corticosterone levels between WT and NKCC1 KO^{CRH} mice. Here, NKCC1 knockout was performed in developmental age, presenting a possibility that developmental compensatory mechanism may be involved. The similar serum corticosterone levels in WT littermates and NKCC1 knockout mice in *ad libitum* condition attest to such a possibility. However, the degree by which serum corticosterone levels increased was significantly reduced in NKCC1 KO^{CRH} mice compared with WT mice after FR (**Figure 5C**). Although AgRP neurons were similarly activated by FR and GABAergic transmission appears to be equivalent in both groups, the loss of NKCC1 in CRH neuron terminals resulted in reduced serum corticosterone secretion in response to FR (**Figure 5C**). Therefore, the excitatory action of GABA at axon terminals of CRH neurons must be dependent on NKCC1. Considering serum corticosterone levels were not different between WT and NKCC1 KO^{CRH} mice in Ad-lib condition, the GABAergic facilitation of CRH release at axon terminals in ME might be promoted exclusively by FR-induced AgRP neuronal activation in the ARC. But this requires further investigation for mechanistic details.

When the HPA axis functions properly, glucocorticoid deals with stress and has anti-inflammatory actions. However, overproduction can negatively impact metabolic, immune, and central nervous systems, subsequently causing physical

and psychiatric problems (Sapolsky et al., 2000; Raison and Miller, 2003). Circulating corticosterone concentrations may be influenced by a variety of factors including the time of day, season, age, sex, reproductive state, exercise, and ultraviolet B radiation (Romero, 2002; Dantzer et al., 2014; Slominski et al., 2018). For instance, a circadian rhythm of baseline glucocorticoid concentrations is found in most species (Romero and Remage-Healey, 2000; Chrousos et al., 2009). Interestingly, evidence suggests that corticosterone secretion is positively related to the diurnal rhythm of AgRP mRNA expression and food intake (Lu et al., 2002). In our study, both chemogenetic activation and FR-mediated activation of AgRP neurons increased corticosterone levels, confirming the involvement of AgRP neurons in corticosterone secretion. This role of AgRP neurons appears to be a critical link between energy demand dependent activation of HPA axis. The resulting disruption of several physiological processes, such as inflammatory response, autonomic function, and neuroendocrine dysregulation, predisposes to metabolic and stress-related disorders. (Harrell et al., 2016).

In the present study, we found that a subpopulation of AgRP neurons activated by FR is responsible for increasing serum corticosterone levels via GABAergic excitation at CRH neuron terminals in the ME (**Figure 6B**). AgRP neurons are related to feeding and energy homeostasis. Therefore, our novel finding that a specific group of ARC AgRP neurons directly projecting to the CRH axonal terminals in the ME are responsive to fasting signals and involved in reactive secretion of corticosterone via NKCC1-dependent excitatory GABA action sheds light on interactions between the HPA axis and food intake.

Data availability statement

The original contributions presented in this study are included in the article/**Supplementary material**, further inquiries can be directed to the corresponding author.

Ethics statement

All experiments were performed in accordance with guidelines issued by the Hamamatsu University School of Medicine on the ethical use of animals for experimentation, and were approved by the Committee for Animal Care and Use (Approval Nos. 2017056, 2017057, 2018025, and 2020074).

Author contributions

AF and RY contributed to the conceptualization of the study and wrote the original draft. RY performed the experiments. MW and RY generated the genetically modified mice. AF and MW supervised the study. RY, AF, and AS analyzed the data. AS, MW, MI, TW, AF, and RY contributed to the writing review and editing. All authors contributed to the article and approved the submitted version.

Funding

This work was supported by the Grant-in-Aid for Scientific Research (B) (no. 17H04025) from Japan Society for the Promotion of Science (AF); Research Grants from Smoking Research Foundation (AF); Research Grants (no. 2138) from The Salt Science Research Foundation (AF); Grant-in-Aid for Scientific Research on Innovative Areas (no. 21H05687) from Ministry of Education, Culture, Sports, and Science and Technology, Japan (AF); Grant-in-Aid for Scientific Research (B) (no. 21H02661) from Japan Society for the Promotion of Science (AF), and the Hamamatsu University School of Medicine Grant-in-Aid (RY).

Acknowledgments

We are grateful to Christian A. Hübner (University of Jena, Germany) for the gift of the NKCC1$^{flox/flox}$ mice. We also thank Isao Ohta and Yuhei Tokunaga (Advanced Research Facilities and Services of Hamamatsu University School of Medicine) for assistance with electron microscopy. We thank Edanz (https://jp.edanz.com/ac) for editing a draft of this manuscript.

Conflict of interest

The authors declare that the research was conducted in the absence of any commercial or financial relationships that could be construed as a potential conflict of interest.

Publisher's note

Supplementary material

The Supplementary Material for this article can be found online at: https://www.frontiersin.org/articles/10.3389/fnmol.2022.990803/full#supplementary-material

References

Allen, B. D., Liao, C. Y., Shu, J., Muglia, L. J., Majzoub, J. A., Diaz, V., et al. (2019). Hyperadrenocorticism of calorie restriction contributes to its anti-inflammatory action in mice. *Aging Cell* 18:e12944. doi: 10.1111/acel.12944

Antoine, M. W., Hübner, C. A., Arezzo, J. C., and Hébert, J. M. (2013). A causative link between inner ear defects and long-term striatal dysfunction. *Science* 341, 1120–1123. doi: 10.1126/science.1240405

Atasoy, D., Betley, J. N., Su, H. H., and Sternson, S. M. (2012). Deconstruction of a neural circuit for hunger. *Nature* 488, 172–177. doi: 10.1038/nature11270

Bagnol, D., Lu, X. Y., Kaelin, C. B., Day, H. E., Ollmann, M., Gantz, I., et al. (1999). Anatomy of an endogenous antagonist: Relationship between Agouti-related protein and proopiomelanocortin in brain. *J Neurosci.* 19:RC26. doi: 10.1523/JNEUROSCI.19-18-j0004.1999

Betley, J. N., Cao, Z. F., Ritola, K. D., and Sternson, S. M. (2013). Parallel, redundant circuit organization for homeostatic control of feeding behavior. *Cell* 155, 1337–1350. doi: 10.1016/j.cell.2013.11.002

Betley, J. N., Xu, S., Cao, Z. F. H., Gong, R., Magnus, C. J., Yu, Y., et al. (2015). Neurons for hunger and thirst transmit a negative-valence teaching signal. *Nature* 521, 180–185. doi: 10.1038/nature14416

Bowers, G., Cullinan, W. E., and Herman, J. P. (1998). Region-specific regulation of glutamic acid decarboxylase (GAD) mRNA expression in central stress circuits. *J. Neurosci.* 18, 5938–5947. doi: 10.1523/JNEUROSCI.18-15-05938.1998

Champy, M. F., Selloum, M., Piard, L., Zeitler, V., Caradec, C., Chambon, P., et al. (2004). Mouse functional genomics requires standardization of mouse handling and housing conditions. *Mamm. Genome* 15, 768–783. doi: 10.1007/s00335-004-2393-1

Chen, Y., Lin, Y. C., Kuo, T. W., and Knight, Z. A. (2015). Sensory detection of food rapidly modulates arcuate feeding circuits. *Cell* 160, 829–841. doi: 10.1016/j.cell.2015.01.033

Chrousos, G. P., Kino, T., and Charmandari, E. (2009). Evaluation of the hypothalamic-pituitary-adrenal axis function in childhood and adolescence. *Neuroimmunomodulation* 16, 272–283. doi: 10.1159/000216185

Cone, R. D. (2005). Anatomy and regulation of the central melanocortin system. *Nat. Neurosci.* 8, 571–578. doi: 10.1038/nn1455

Cone, R. D., Cowley, M. A., Butler, A. A., Fan, W., Marks, D. L., and Low, M. J. (2001). The arcuate nucleus as a conduit for diverse signals relevant to energy homeostasis. *Int. J. Obes. Relat. Metab. Disord.* 25, S63–S67. doi: 10.1038/sj.ijo.0801913

Cowley, M. A., Smart, J. L., Rubinstein, M., Cerdán, M. G., Diano, S., Horvath, T. L., et al. (2001). Leptin activates anorexigenic POMC neurons through a neural network in the arcuate nucleus. *Nature* 411, 480–484. doi: 10.1038/35078085

Cowley, M. A., Smith, R. G., Diano, S., Tschöp, M., Pronchuk, N., Grove, K. L., et al. (2003). The distribution and mechanism of action of ghrelin in the CNS demonstrates a novel hypothalamic circuit regulating energy homeostasis. *Neuron* 37, 649–661. doi: 10.1016/s0896-6273(03)00063-1

Dantzer, B., Fletcher, Q. E., Boonstra, R., and Sheriff, M. J. (2014). Measures of physiological stress: A transparent or opaque window into the status, management and conservation of species? *Conserv. Physiol.* 2:cou023. doi: 10.1093/conphys/cou023

de Rijke, C. E., Hillebrand, J. J., Verhagen, L. A., Roeling, T. A., and Adan, R. A. (2005). Hypothalamic neuropeptide expression following chronic food restriction in sedentary and wheel-running rats. *J. Mol. Endocrinol.* 35, 381–390. doi: 10.1677/jme.1.01808

Fan, S., Xu, Y., Lu, Y., Jiang, Z., Li, H., Morrill, J. C., et al. (2021). A neural basis for brain leptin action on reducing type 1 diabetic hyperglycemia. *Nat. Commun.* 12:2662. doi: 10.1038/s41467-021-22940-4

Fernandes, A., de Oliveira, F. P., Fernandez, G., da Guia Vieira, L., Rosa, C. G., do Nascimento, T., et al. (2022). Arcuate AgRP, but not POMC neurons, modulate paraventricular CRF synthesis and release in response to fasting. *Cell Biosci.* 12:118. doi: 10.1186/s13578-022-00853-z

Gallardo, C. M., Hsu, C. T., Gunapala, K. M., Parfyonov, M., Chang, C. H., Mistlberger, R. E., et al. (2014). Behavioral and neural correlates of acute and scheduled hunger in C57BL/6 mice. *PLoS One* 9:e95990. doi: 10.1371/journal.pone.0095990

Garfield, A. S., Li, C., Madara, J. C., Shah, B. P., Webber, E., Steger, J. S., et al. (2015). A neural basis for melanocortin-4 receptor-regulated appetite. *Nat. Neurosci.* 18, 863–871. doi: 10.1038/nn.4011

Grishagin, I. V. (2015). Automatic cell counting with ImageJ. *Anal. Biochem.* 473, 63–65. doi: 10.1016/j.ab.2014.12.007

Harrell, C. S., Gillespie, C. F., and Neigh, G. N. (2016). Energetic stress: The reciprocal relationship between energy availability and the stress response. *Physiol. Behav.* 166, 43–55. doi: 10.1016/j.physbeh.2015.10.009

Herman, J. P., Mueller, N. K., and Figueiredo, H. (2004). Role of GABA and glutamate circuitry in hypothalamo-pituitary-adrenocortical stress integration. *Ann. N. Y. Acad. Sci.* 1018, 35–45. doi: 10.1196/annals.1296.004

Hewitt, S. A., Wamsteeker, J. I., Kurz, E. U., and Bains, J. S. (2009). Altered chloride homeostasis removes synaptic inhibitory constraint of the stress axis. *Nat. Neurosci.* 12, 438–443. doi: 10.1038/nn.2274

Horvath, T. L., Bechmann, I., Naftolin, F., Kalra, S. P., and Leranth, C. (1997). Heterogeneity in the neuropeptide Y-containing neurons of the rat arcuate nucleus: GABAergic and non-GABAergic subpopulations. *Brain Res.* 756, 283–286. doi: 10.1016/s0006-8993(97)00184-4

Jais, A., Paeger, L., Sotelo-Hitschfeld, T., Bremser, S., Prinzensteiner, M., Klemm, P., et al. (2020). PNOC^{ARC} neurons promote hyperphagia and obesity upon high-fat-diet feeding. *Neuron* 106, 1009–1025.e10. doi: 10.1016/j.neuron.2020.03.022

Jensen, T. L., Kiersgaard, M. K., Sørensen, D. B., and Mikkelsen, L. F. (2013). Fasting of mice: A review. *Lab. Anim.* 47, 225–240. doi: 10.1177/0023677213501659

Kakizawa, K., Watanabe, M., Mutoh, H., Okawa, Y., Yamashita, M., Yanagawa, Y., et al. (2016). A novel GABA-mediated corticotropin-releasing hormone secretory mechanism in the median eminence. *Sci. Adv.* 2:e1501723. doi: 10.1126/sciadv.1501723

Kenny, R., Dinan, T., Cai, G., and Spencer, S. J. (2014). Effects of mild calorie restriction on anxiety and hypothalamic-pituitary-adrenal axis responses to stress in the male rat. *Physiol. Rep.* 2:e00265. doi: 10.1002/phy2.265

Kim, J. S., Han, S. Y., and Iremonger, K. J. (2019). Stress experience and hormone feedback tune distinct components of hypothalamic CRH neuron activity. *Nat. Commun.* 10:5696. doi: 10.1038/s41467-019-13639-8

Kohno, D., Gao, H. Z., Muroya, S., Kikuyama, S., and Yada, T. (2003). Ghrelin directly interacts with neuropeptide-Y-containing neurons in the rat arcuate nucleus: Ca2+ signaling via protein kinase A and N-type channel-dependent mechanisms and cross-talk with leptin and orexin. *Diabetes* 52, 948–956. doi: 10.2337/diabetes.52.4.948

Levy, B. H., and Tasker, J. G. (2012). Synaptic regulation of the hypothalamic-pituitary-adrenal axis and its modulation by glucocorticoids and stress. *Front. Cell. Neurosci.* 6:24. doi: 10.3389/fncel.2012.00024

Lindblom, J., Haitina, T., Fredriksson, R., and Schiöth, H. B. (2005). Differential regulation of nuclear receptors, neuropeptides and peptide hormones in the hypothalamus and pituitary of food restricted rats. *Brain Res. Mol. Brain Res.* 133, 37–46. doi: 10.1016/j.molbrainres.2004.09.025

Liu, T., Kong, D., Shah, B. P., Ye, C., Koda, S., Saunders, A., et al. (2012). Fasting activation of AgRP neurons requires NMDA receptors and involves spinogenesis and increased excitatory tone. *Neuron* 73, 511–522. doi: 10.1016/j.neuron.2011.11.027

Lu, X. Y., Shieh, K. R., Kabbaj, M., Barsh, G. S., Akil, H., and Watson, S. J. (2002). Diurnal rhythm of agouti-related protein and its relation to corticosterone and food intake. *Endocrinology* 143, 3905–3915. doi: 10.1210/en.2002-220150

MacKenzie, G., and Maguire, J. (2015). Chronic stress shifts the GABA reversal potential in the hippocampus and increases seizure susceptibility. *Epilepsy Res.* 109, 13–27. doi: 10.1016/j.eplepsyres.2014.10.003

Makimura, H., Mizuno, T. M., Isoda, F., Beasley, J., Silverstein, J. H., and Mobbs, C. V. (2003). Role of glucocorticoids in mediating effects of fasting and diabetes on hypothalamic gene expression. *BMC Physiol.* 3:5. doi: 10.1186/1472-6793-3-5

Marshall, C. J., Desroziers, E., McLennan, T., and Campbell, R. E. (2017). Defining subpopulations of arcuate nucleus GABA neurons in male, female, and prenatally androgenized female mice. *Neuroendocrinology* 105, 157–169. doi: 10.1159/000452105

Miklos, I. H., and Kovacs, K. J. (2002). GABAergic innervation of corticotropin-releasing hormone (CRH)-secreting parvocellular neurons and its plasticity as demonstrated by quantitative immunoelectron microscopy. *Neuroscience* 113, 581–592. doi: 10.1016/s0306-4522(02)00147-1

Minor, R. K., Chang, J. W., and de Cabo, R. (2009). Hungry for life: How the arcuate nucleus and neuropeptide Y may play a critical role in mediating the benefits of calorie restriction. *Mol. Cell. Endocrinol.* 299, 79–88. doi: 10.1016/j.mce.2008.10.044

Mody, I., and Maguire, J. (2011). The reciprocal regulation of stress hormones and GABA(A) receptors. *Front. Cell. Neurosci.* 6:4. doi: 10.3389/fncel.2012.00004

Myers, B., McKlveen, J. M., and Herman, J. P. (2012). Neural regulation of the stress response: The many faces of feedback. *Cell. Mol. Neurobiol.* 32, 683–694. doi: 10.1007/s10571-012-9801-y

Oakley, R. H., and Cidlowski, J. A. (2013). The biology of the glucocorticoid receptor: New signaling mechanisms in health and disease. *J. Allergy Clin. Immunol.* 132, 1033–1044. doi: 10.1016/j.jaci.2013.09.007

Padilla, S. L., Qiu, J., Nestor, C. C., Zhang, C., Smith, A. W., Whiddon, B. B., et al. (2017). AgRP to Kiss1 neuron signaling links nutritional state and fertility. *Proc. Natl. Acad. Sci. U.S.A.* 114, 2413–2418. doi: 10.1073/pnas.1621065114

Palkovits, M. (1984). Neuropeptides in the hypothalamo-hypophyseal system: Lateral retrochiasmatic area as a common gate for neuronal fibers towards the median eminence. *Peptides* 5, 35–39. doi: 10.1016/0196-9781(84)90262-6

Parton, L. E., Ye, C. P., Coppari, R., Enriori, P. J., Choi, B., Zhang, C. Y., et al. (2007). Glucose sensing by POMC neurons regulates glucose homeostasis and is impaired in obesity. *Nature* 449, 228–232. doi: 10.1038/nature06098

Payne, J. A., Rivera, C., Voipio, J., and Kaila, K. (2003). Cation-chloride co-transporters in neuronal communication, development and trauma. *Trends Neurosci.* 26, 199–206. doi: 10.1016/S0166-2236(03)00068-7

Radley, J. J., Gosselink, K. L., and Sawchenko, P. E. (2009). A discrete GABAergic relay mediates medial prefrontal cortical inhibition of the neuroendocrine stress response. *J. Neurosci.* 29, 7330–7340. doi: 10.1523/JNEUROSCI.5924-08.2009

Raison, C. L., and Miller, A. H. (2003). When not enough is too much: The role of insufficient glucocorticoid signaling in the pathophysiology of stress-related disorders. *Am. J. Psychiatry* 160, 1554–1565. doi: 10.1176/appi.ajp.160.9.1554

Rivera, C., Voipio, J., Payne, J. A., Ruusuvuori, E., Lahtinen, H., Lamsa, K., et al. (1999). The K+/Cl- co-transporter KCC2 renders GABA hyperpolarizing during neuronal maturation. *Nature* 397, 251–255. doi: 10.1038/16697

Rogers, N. H., Walsh, H., Alvarez-Garcia, O., Park, S., Gaylinn, B., Thorner, M. O., et al. (2016). Metabolic benefit of chronic caloric restriction and activation of hypothalamic AGRP/NPY neurons in male mice is independent of ghrelin. *Endocrinology* 157, 1430–1442. doi: 10.1210/en.2015-1745

Roland, B. L., and Sawchenko, P. E. (1993). Local origins of some GABAergic projections to the paraventricular and supraoptic nuclei of the hypothalamus in the rat. *J. Comp. Neurol.* 332, 123–143. doi: 10.1002/cne.903320109

Romero, L. M. (2002). Seasonal changes in plasma glucocorticoid concentrations in free-living vertebrates. *Gen. Comp. Endocrinol.* 128, 1–24. doi: 10.1016/s0016-6480(02)00064-3

Romero, L. M., and Remage-Healey, L. (2000). Daily and seasonal variation in response to stress in captive starlings (Sturnus vulgaris): Corticosterone. *Gen. Comp. Endocrinol.* 119, 52–59. doi: 10.1006/gcen.2000.7491

Sapolsky, R. M., Romero, L. M., and Munck, A. U. (2000). How do glucocorticoids influence stress responses? Integrating permissive, suppressive, stimulatory, and preparative actions. *Endocr. Rev.* 21, 55–89. doi: 10.1210/edrv.21.1.0389

Sarkar, J., Wakefield, S., MacKenzie, G., Moss, S. J., and Maguire, J. (2011). Neurosteroidogenesis is required for the physiological response to stress: Role of neurosteroid-sensitive GABAA receptors. *J. Neurosci.* 31, 18198–18210. doi: 10.1523/JNEUROSCI.2560-11.2011

Sheng, J. A., Bales, N. J., Myers, S. A., Bautista, A. I., Roueinfar, M., Hale, T. M., et al. (2020). The hypothalamic-pituitary-adrenal axis: Development, programming actions of hormones, and maternal-fetal interactions. *Front. Behav. Neurosci.* 14:601939. doi: 10.3389/fnbeh.2020.601939

Slominski, A. T., Zmijewski, M. A., Plonka, P. M., Szaflarski, J. P., and Paus, R. (2018). How UV light touches the brain and endocrine system through skin, and why. *Endocrinology* 159, 1992–2007. doi: 10.1210/en.2017-03230

Smith, M. A., Choudhury, A. I., Glegola, J. A., Viskaitis, P., Irvine, E. E., de Campos Silva, P. C. C., et al. (2020). Extrahypothalamic GABAergic nociceptin-expressing neurons regulate AgRP neuron activity to control feeding behavior. *J. Clin. Invest.* 130, 126–142. doi: 10.1172/JCI130340

Steculorum, S. M., Ruud, J., Karakasilioti, I., Backes, H., Engström Ruud, L., Timper, K., et al. (2016). AgRP neurons control systemic insulin sensitivity via myostatin expression in brown adipose tissue. *Cell* 165, 125–138. doi: 10.1016/j.cell.2016.02.044

Suyama, S., and Yada, T. (2018). New insight into GABAergic neurons in the hypothalamic feeding regulation. *J. Physiol. Sci.* 68, 717–722. doi: 10.1007/s12576-018-0622-8

Swanson, L. W., and Kuypers, H. G. (1980). The paraventricular nucleus of the hypothalamus: Cytoarchitectonic subdivisions and organization of projections to the pituitary, dorsal vagal complex, and spinal cord as demonstrated by retrograde fluorescence double-labeling methods. *J. Comp. Neurol.* 194, 555–570. doi: 10.1002/cne.901940306

Takahashi, K. A., and Cone, R. D. (2005). Fasting induces a large, leptin-dependent increase in the intrinsic action potential frequency of orexigenic arcuate nucleus neuropeptide Y/Agouti-related protein neurons. *Endocrinology* 146, 1043–1047. doi: 10.1210/en.2004-1397

Tasker, J. G., and Dudek, F. E. (1993). Local inhibitory synaptic inputs to neurones of the paraventricular nucleus in slices of rat hypothalamus. *J. Physiol.* 469, 179–192. doi: 10.1113/jphysiol.1993.sp019810

Tasker, J. G., Boudaba, C., and Schrader, L. A. (1998). Local glutamatergic and GABAergic synaptic circuits and metabotropic glutamate receptors in the hypothalamic paraventricular and supraoptic nuclei. *Adv. Exp. Med. Biol.* 449, 117–121. doi: 10.1007/978-1-4615-4871-3_11

Tong, Q., Ye, C. P., Jones, J. E., Elmquist, J. K., and Lowell, B. B. (2008). Synaptic release of GABA by AgRP neurons is required for normal regulation of energy balance. *Nat. Neurosci.* 11, 998–1000. doi: 10.1038/nn.2167

Turi, G. F., Liposits, Z., Moenter, S. M., Fekete, C., and Hrabovszky, E. (2003). Origin of neuropeptide Y-containing afferents to gonadotropin-releasing hormone neurons in male mice. *Endocrinology* 144, 4967–4974. doi: 10.1210/en.2003-0470

Uchida, T., Oki, Y., Yanagawa, Y., and Fukuda, A. (2011). A heterozygous deletion in the glutamate decarboxylase 67 gene enhances maternal and fetal stress vulnerability. *Neurosci. Res.* 69, 276–282. doi: 10.1016/j.neures.2010.12.010

Vandenborne, K., De Groef, B., Geelissen, S. M., Kühn, E. R., Darras, V. M., and Van der Geyten, S. (2005). Corticosterone-induced negative feedback mechanisms within the hypothalamo-pituitary-adrenal axis of the chicken. *J. Endocrinol.* 185, 383–391. doi: 10.1677/joe.1.05969

Varela, L., Stutz, B., Song, J. E., Kim, J. G., Liu, Z. W., Gao, X. B., et al. (2021). Hunger-promoting AgRP neurons trigger an astrocyte-mediated feed-forward autoactivation loop in mice. *J. Clin. Invest.* 131:e144239. doi: 10.1172/JCI144239

Wu, Q., Boyle, M. P., and Palmiter, R. D. (2009). Loss of GABAergic signaling by AgRP neurons to the parabrachial nucleus leads to starvation. *Cell* 137, 1225–1234. doi: 10.1016/j.cell.2009.04.022

Yamada, J., Okabe, A., Toyoda, H., Kilb, W., Luhmann, H. J., and Fukuda, A. (2004). Cl- uptake promoting depolarizing GABA actions in immature rat neocortical neurones is mediated by NKCC1. *J. Physiol.* 557, 829–841. doi: 10.1113/jphysiol.2004.062471

Zhang, X., and van den Pol, A. N. (2015). Dopamine/tyrosine hydroxylase neurons of the hypothalamic arcuate nucleus release GABA, communicate with dopaminergic and other arcuate neurons, and respond to dynorphin, Met-Enkephalin, and Oxytocin. *J. Neurosci.* 35, 14966–14982. doi: 10.1523/JNEUROSCI.0293-15.2015

Zhang, X., and van den Pol, A. N. (2016). Hypothalamic arcuate nucleus tyrosine hydroxylase neurons play orexigenic role in energy homeostasis. *Nat. Neurosci.* 19, 1341–1347. doi: 10.1038/nn.4372

frontiers | Frontiers in Molecular Neuroscience

TYPE Original Research
PUBLISHED 30 September 2022
DOI 10.3389/fnmol.2022.959224

OPEN ACCESS

EDITED BY
Lorenz S. Neuwirth,
State University of New York at Old Westbury, United States

REVIEWED BY
Juan Hong,
Washington University in St. Louis, United States
Daniela Neuhofer,
Medical University of South Carolina, United States
Pavel Ivanovich Ortinski,
University of Kentucky, United States
Uwe Rudolph,
University of Illinois at Urbana-Champaign, United States
Wenfeng Yu,
Guizhou Medical University, China

*CORRESPONDENCE
Sha Sha
shashass@njmu.edu.cn
Lei Chen
chenl@njmu.edu.cn

SPECIALTY SECTION
This article was submitted to Brain Disease Mechanisms, a section of the journal Frontiers in Molecular Neuroscience

RECEIVED 01 June 2022
ACCEPTED 25 August 2022
PUBLISHED 30 September 2022

CITATION
Qin Y, Xu W, Li K, Luo Q, Chen X, Wang Y, Chen L and Sha S (2022) Repeated inhibition of sigma-1 receptor suppresses $GABA_A$ receptor expression and long-term depression in the nucleus accumbens leading to depressive-like behaviors. Front. Mol. Neurosci. 15:959224. doi: 10.3389/fnmol.2022.959224

Repeated inhibition of sigma-1 receptor suppresses $GABA_A$ receptor expression and long-term depression in the nucleus accumbens leading to depressive-like behaviors

Yaoyao Qin, Weixing Xu, Kunpeng Li, Qi Luo, Xi Chen, Yue Wang, Lei Chen* and Sha Sha*

Department of Physiology, Nanjing Medical University, Nanjing, China

Sigma-1 receptor (σ_1R) downregulation in male mice is known to cause a depressive-like phenotype. The nucleus accumbens (NAc), a region associated with affective regulation, has high levels of σ_1R. Here, we investigated the effect of repeated inhibition of σ_1R in the NAc on depressive-like behaviors and synaptic plasticity by microinjecting σ_1R antagonist NE-100 into NAc nuclei in mice (NE-100 mice); this was followed by behavioral tests and field potentials recordings. We first examined the effect of NE-100 administration on σ_1R expression and found that cell surface levels of σ_1R were significantly reduced in the NAc of NE-100 mice. Compared to control mice, NE-100 mice exhibited significantly prolonged immobility in forced swim test (FST) and tail suspension test (TST), impaired long-term depression (LTD) as well as multi-spike waveform field excitatory postsynaptic potential (fEPSP) with an extended duration and an increased paired-pulse ratio (PPR). Reduced levels of $GABA_A$ receptor ($GABA_A$R)-α1, -α2, -β2, and -β3 subunits, membrane D2R, and PKC phosphorylation in the NAc were observed in NE-100 mice. Activation of $GABA_A$R by muscimol corrected the extended fEPSP duration and increased PPR, restored LTD maintenance as well as alleviated depressive-like behaviors in NE-100 mice. The decline of PKC phosphorylation in the NAc of NE-100 mice was corrected by injecting NAc with quinpirole, a D2R agonist. Injections of quinpirole or PMA (a PKC activator) into NAc of NE-100 mice rescued the expression levels of $GABA_A$R, and alleviated the increase in PPR and impairment in LTD; these effects were sensitive to GF109203X, a PKC inhibitor. Furthermore, injecting NAc with quinpirole or PMA relieved depressive-like behaviors in NE-100 mice.

Collectively, these results indicate that repeated inhibition of σ_1R in the NAc reduces D2R-mediated PKC phosphorylation and suppresses $GABA_AR$ expression, thus impairing LTD maintenance and leading to depressive-like behaviors.

KEYWORDS

sigma-1 receptor (σ_1R), nucleus accumbens (NAc), $GABA_A$ receptor ($GABA_AR$), depressive-like behaviors, long-term depression (LTD)

Introduction

Sigma-1 receptors (σ_1Rs) are highly expressed in regions of the brain involved in emotion and neuropsychiatric disorders (Maurice et al., 2002; Lan et al., 2019). Animal models and clinical trials have confirmed that σ_1R agonists exert antidepressant effects (Hayashi et al., 2011) and that mice with σ_1R deficiency exhibit a depressive-like phenotype (Sabino et al., 2009; Sha et al., 2015; Zhang S. et al., 2017). However, the mechanisms underlying these effects have yet to be fully elucidated.

Several lines of investigation indicate that σ_1Rs are involved in the activities of multiple neurotransmitter systems in the brain. Agonists of σ_1R can influence intracellular Ca^{2+} levels by regulating Gq-coupled receptors and by mediating the steady-state balance of dopaminergic neurons (Hayashi and Su, 2007; Ryskamp et al., 2017). Interactions of σ_1R and dopamine receptors or dopamine receptor-containing heteromers can indirectly regulate food-seeking behavior (Aguinaga et al., 2019). Brünig et al. (1999) reported that D2 receptor (D2R) activation results in an enhancement of GABAergic transmission involving the protein kinase C (PKC) pathway in the olfactory bulb. GABAergic neurons have been found to play a major role in controlling mood and stress. Deficits in the functionality of the cortical GABAergic system resulting from exposure to chronic stress can compromise the integrity of neurocircuits and lead to depression and other stress-related disorders (Fogaça and Duman, 2019). The σ_1R has been reported to modulate GABA release, GABA transport at the presynaptic level, and the activity of the GABA type A receptor ($GABA_AR$; Mtchedlishvili and Kapur, 2003; Pozdnyakova et al., 2020).

A significant level of σ_1R has been reported in the nucleus accumbens (NAc; Hayashi et al., 2010; Delint-Ramirez et al., 2020), a region that is critical for reward and motivation. Alterations in the NAc have been implicated in the pathophysiology of depression (Bagot et al., 2015). GABAergic medium spiny neurons (MSNs), which co-express D1 and D2 receptors (D1R and D2R), are the major cell type in the NAc and receive glutamatergic inputs from the ventral hippocampus (vHIP) and basolateral amygdala (BLA) amongst many other inputs (Nicola et al., 2000). Projections from the vHIP-NAc and BLA-NAc have been shown to regulate emotional behavior, social interaction behavior, and sensitivity to depression in mice (Sesack and Grace, 2010; Bagot et al., 2015; Muir et al., 2020). Exposure to stress has been shown to impair long-term depression (LTD) in the NAc and induces depressive-like behaviors in mice (Wang et al., 2010). Our previous studies confirmed that in the BLA of mice, a reduction of dopaminergic function suppresses $GABA_AR$ (Zhang T. et al., 2017). Furthermore, σ_1R knockout weakens the $GABA_AR$-mediated inhibition and leads to impaired synaptic plasticity and depressive-like behaviors (Zhang B. et al., 2017). Therefore, it is of great interest to investigate whether a reduction of σ_1R in the NAc would affect the functionality of local GABAergic and dopaminergic neurons, and thus impact depressive-like behaviors. Our previous study demonstrated that the intracerebroventricular injection of NE-100 for 3 days in wild-type mice results in the same biological changes as in the σ_1R knockout mice (Di et al., 2017). It has been shown that activated σ_1R dissociates from the chaperone-binding immunoglobulin protein and is transferred from the mitochondria-associated endoplasmic reticulum membrane to other sites, such as the cell surface, or cytoplasm. NE-100 as an antagonist of σ_1R can prevent this process (Hayashi and Su, 2007). In the present study, we used σ_1R antagonists to microinject NAc nuclei in male ICR mice and assayed σ_1R expression to clarify its activity; then investigated the influence of NAc-injection with NE-100 in the NAc on depressive-like behaviors and synaptic plasticity. To investigate the mechanisms underlying these effects, we also investigated the expression levels of $GABA_AR$ and dopamine receptors as well as the phosphorylation of PKC in the NAc. Finally, we analyzed the causal link between synaptic plasticity and the depressive-like phenotype in mice receiving repeated inhibition of σ_1R. Collectively, our results indicate that repeated inhibition of σ_1R in the NAc reduces the expression levels of $GABA_AR$ and impairs the maintenance of LTD, thus causing a depressive-like phenotype.

Material and methods

Animals

All animal experiments were performed in accordance with the ARRIVE guidelines of Laboratory Animal Care (Kilkenny et al., 2012). All mice were handled in accordance with the experimental animal guidelines of the Laboratory Animal Research Institute and Ethical Committee of Nanjing Medical University (No. 2016-110). All efforts were made to minimize animal suffering and to reduce the number of animals used. For instance, laboratory personnel handled these mice carefully, used appropriate anesthesia during surgery, and kept the mice warm on a constant temperature blanket following surgery. Twelve-week-old male ICR mice (Animal Core facility of Nanjing Medical University) were maintained under constant environmental conditions (temperature 23 ± 2°C, humidity 55% ± 5%, and a 12:12 h light/dark cycle) with free access to water and food. The study had not been pre-registered with a pre-specified endpoint. This study was exploratory and there were no pre-determined exclusion criteria for the animals.

Reagents and antibodies

σ_1R antagonist NE-100 (Tocris Cat#3133), PKC activator phorbol 12-myristate 13-acetate (PMA; Sigma-Aldrich Cat#P1585), PKC inhibitor GF109302X (Tocris Cat#0741), D2R antagonist L-sulpiride (Sigma-Aldrich Cat#S7771), D2R agonist quinpirole (Sigma-Aldrich Cat#Q102), $GABA_AR$ agonist muscimol (Alomone Labs Cat#M-240), $GABA_AR$ antagonist bicuculline(Sigma-Aldrich Cat#14340), D1R agonist SKF38393 (Sigma-Aldrich Cat#S101), D1R antagonist SCH23390 (TocrisCat#No. 0925), NMDA receptor (NMDAR) agonist NMDA (Sigma-Aldrich Cat#M3262) and CB1 receptor agonist WIN55, 212-2 (MedChemExpress Cat#HY-13291) were dissolved in dimethyl sulfoxide (DMSO) and diluted by sterile saline or artificial cerebrospinal fluid (ACSF; in mM: 124 NaCl, 2 $CaCl_2$, 4.5 KCl, 1.0 $MgCl_2$, 1.2 NaH_2PO_4, 10 D-glucose, and 26 $NaHCO_3$, pH7.4) to a final concentration of 0.1% DMSO. We used triple antibiotic ointment containing 400 units of bacitracin Zinc, 5 mg of neomycin dulfate, and 5,000 units of polymyxin B sulfate (WATER-JEL Technologies Cat#22405). Several antibodies were used in this study: anti-D2R (1:1,000; Millipore Cat#AB5084p, RRID:AB_2094980), anti-$GABA_AR$-α1 (Sigma Cat#G4416, RRID:AB_477016), anti-$GABA_AR$-α2(AbcamCat#ab72445, RRID:AB_1268929), anti-$GABA_AR$-β2 (Affinity Biosciences Cat#DF6671, RRID:AB_2838633), anti-$GABA_AR$-β3 (Abcam Cat#ab98968, RRID:AB_10670809), anti-phosphorylation PKC (Epsilon Ser729; Abcam Cat#ab63387, RRID:AB_1142277), anti-PKC (Abcam Cat#ab253274, RRID:AB_2827663), anti-σ_1R (B5; Santa Cruz Biotechnology Cat#sc-137075, RRID:AB_2285870), anti-Na^+-K^+ ATPase (Cell Signaling Technology Cat#3010, RRID:AB_2060983) and anti-GAPDH (Abcam Cat#ab181602, RRID:AB_2630358).

Drug administration

For NAc micro-injections, mice were anesthetized with an injection (i.p) of ketamine (100 mg/kg)/xylazine (10 mg/kg; Kroeger et al., 2017) in accordance with institutional guidelines and then placed in a stereotaxic instrument (Stoelting, Wood Dale, IL, USA). A 26-gauge stainless-steel guide cannula (Plastics One, Roanoke, VA, USA) was implanted into the unilateral NAc shell (anterior to the bregma: +1.54 mm; middle lateral: ±0.7 mm; dorsal ventral: −4.5 mm; Zhang et al., 2021). On the third postoperative day, the dummy cannula was removed from the guide cannula and then replaced by an infusion cannula (30 gauge) connected by polyethylene tubing (PE10; Becton Dickinson, Sparks, MD, USA) with a stepper motorized micro-syringe (Stoelting). NE-100 (0.15 nmol/mouse), L-sulpiride (0.25 μg/mouse), quinpirole (0.5 μg/mouse), PMA (48 pmol/mouse), GF109203X (5 ng/mouse), muscimol (4 nmol/mouse), NMDA (5 nmol/mouse) or WIN55, 212-2 (1.5 μg/mouse) was injected in a volume of 0.25 μl/side NAc (Yang et al., 2011; Madronal et al., 2012; Zhang T. et al., 2017; Zhang B. et al., 2017). Control mice were given an equal volume of vehicle. Only the administered NAc regions were used for mRNA and protein tests, as well as electrophysiological experiments. The micro-injection sites were validated postmortem by an injection with 2% Evans Blue followed by histological detection. After surgery, a triple antibiotic ointment was applied copiously on the closure site for three consecutive days.

For bath applications involving brain slices, the mice were decapitated under deep anesthesia with isoflurane (5%; Di et al., 2020). Then, the brains were rapidly removed and coronal brain slices containing the NAc region (350 μm) were cut using a vibrating microtome (Microslicer DTK 1500, Dousaka EM Co, Kyoto, Japan) in an ice-cold oxygenated (95% O_2/5% CO_2) cutting solution composed of (in mM): 94 sucrose, 30 NaCl, 4.5 KCl, 1.0 $MgCl_2$, 26 $NaHCO_3$, 1.2 NaH_2PO_4, and 10 D-glucose (pH 7.4). Our previous studies reported that the bath-application of muscimol (10 μM) and bicuculline (10 μM) to brain slices for 30 min could alter synaptic transmission in field potential recordings (Zhang T. et al., 2017; Di et al., 2020). Thus, in this study, the brain slices were treated with muscimol (10 μM) or bicuculline (10 μM) for 30 min. In all pharmacological experiments, the control slices were treated with an equal volume of vehicle.

Experimental design and groups

In total, we used 260 mice: control mice (n = 120) and NE-100 mice (n = 140). The mice were divided into three experimental groups. The first group (12 + 12 control mice and 12 + 12 NE-100 mice) was used to examine the influence of inhibiting σ_1R in the NAc on depressive-like behaviors, the electrophysiological characteristics of the NAc, and the expression levels of $GABA_A$R and the dopamine receptor. At the end of the behavioral tests, the mice were divided into two cohorts, one cohort for field potential recording and the other for the detection of mRNA and protein. The second group (48 control mice and 48 + 20 NE-100 mice) was used to test whether reduced levels of σ_1R in the NAc altered the expression levels of $GABA_A$R *via* D2R-mediated PKC activity; this group was also used to examine the effect of suppressed D2R/PKC/$GABA_A$R levels on LTD. The third group (48 control mice and 48 NE-100 mice) was used to investigate the effect of suppressed D2R/PKC/$GABA_A$R levels on mouse affective disorder. The second and the third groups of control mice received either non-coadministered quinpirole, L-sulpiride, GF109203X, PMA, or muscimol; NE-100 mice received non-coadministered uinpirole, L-sulpiride, PMA, or muscimol, orcoadministered quinpirole and GF109203X. The volume of the microinjected drug was limited to 0.25 μl.

Field potential recording

Brain slices were transferred to a recording chamber and continuously perfused with oxygenated ACSF and maintained at 30 ± 1°C. Field potential recordings were performed in the NAc, the area immediately surrounding the anterior commissure. Field excitatory postsynaptic potentials (fEPSPs) were evoked by a concentric bipolar stimulation electrode (FHC, St Bowdoin, ME, USA) that was placed 300–500 μm away from the recording electrode (Wang et al., 2010; White et al., 2016). Constant current pulses (0.1 ms, 0.05 Hz) were supplied by a stimulator (SEN-3301, Nihon Kohden, Japan). To record the fEPSPs, glass pipettes (4–5 MΩ) were filled with 2 M NaCl and connected to a neutralized, high input-impedance preamplifier with a high-pass filter at 5 kHz. Signals were amplified by a differential AC amplifier (A-M Systems, model 1700, Seattle, WA, USA) and were digitized and saved using the pCLAMP system (Axon Instrument Inc., Sunnyvale, CA, USA). A stable baseline of fEPSPs was recorded for at least 20 min by using a stimulus intensity adjusted to elicit approximately 50% of its maximal amplitude, before applying drugs or delivering low-frequency stimulation (LFS; 10 Hz, 10 min; Wang et al., 2010). Baseline synaptic transmission was assessed by averaging the response to six pulses (from 0.1 to 1.1 mA). The fEPSP slope was calculated as the absolute value of the rising phase between 10% and 90% of the first negative peak response, by using Clampfit 10.0 (Molecular Devices; White et al., 2016). The paired-pulse ratio (PPR) was measured by using the intensity of the test stimulus with an inter-pulse interval (IPI) of 15–100 ms. For LTD evaluation, pre-train responses were recorded for 20 min (baseline); this was followed by LFS. Single-pulse recording resumed immediately after the LFS-train had been delivered and continued for 60 min.

Reverse transcription polymerase chain reaction (RT-PCR)

Mice were anesthetized with ketamine (100 mg/kg)/xylazine (10 mg/kg) and the brains were quickly removed. Then, coronal sections (500 μm in thickness) from +1.5 mm to +0.5 mm relative to the bregma were cut using a cryostat microtome (CM1900, Wetzlar, Hessen, Germany) according to the Mouse Brain Atlas (Paxinos and Franklin, 2001). The region containing the NAc was then harvested using a 15-gauge needle (inner diameter: 1.5 mm) and RNA was extracted using TRIzol reagent kit (Invitrogen, Camarillo, CA, USA). Total RNA was then reverse transcribed into cDNA using a Prim Script RT reagent kit (TaKaRa, China) for quantitative PCR (ABI Step One Plus, Foster City, CA, United States) in the presence of a fluorescent dye (SYBR Green I; Takara, China). The primer sets used for σ_1R, $GABA_AR$-α*1*, $GABA_AR$-α*2*, $GABA_AR$-α*3*, $GABA_AR$-α*4*, $GABA_AR$-α*5*, $GABA_AR$-β*1*, $GABA_AR$-β*2*, $GABA_AR$-β*3*, $GABA_AR$-γ*1*, $GABA_AR$-γ*2*, $GABA_AR$-γ*3*, $GABA_AR$-δ, *D1R*, and *D2R* were designed according to previous publications (Nakai et al., 2014; Pan et al., 2017; Chen et al., 2018). The relative expression of genes was determined using the $2^{-\Delta\Delta Ct}$ method and normalized to *GAPDH* expression. Final values were averaged from four sets of independent experiments and were expressed as a percentage of control mice.

Cell-surface biotinylation

NAc slices were placed on a 6-well plate and washed with frozen ACSF for 5 min. Then, the slices were incubated with ACSF containing EZ-link Sulfo-NHS-SS-Biotin (0.5 mg/ml, Pierce, Northumberland, UK) for 25 min at 4°C. Next, the slices were washed three times with ACSF containing 50 mM NH_4Cl (5 min per wash) at 4°C to remove excess biotin. After biotinylation, the NAc region was removed by dissection and homogenized with lysis buffer containing 50 mM Tris-HCl (pH 7.4), 150 mM NaCl, 1.5 mM $MgCl_2$, 1 mM EGTA, 0.5 mM DTT, 50 mM NaF, 2 mM sodium pyruvate, 25% glycerol, 1% Triton X-100, 0.5% sodium deoxycholate, and 1% protease inhibitor cocktail. After centrifugation at 20,000× *g* for 20 min at 4°C, the supernatants were collected as the source of protein and the final protein concentration was determined using a bicinchoninic acid (BCA) protein assay kit (Pierce Biotechnology, Rockford,

IL, USA). Biotinylated proteins (50 μg) were then incubated with streptavidin-coated magnetic beads (30 μl) on a head-over-head shaker for 45 min at room temperature. The streptavidin beads to which the biotinylated proteins had adhered were washed three times with lysis buffer containing 0.1% sodium dodecyl sulfate (SDS) and then separated with a magnet. The biotinylated proteins were eluted into sample buffer (62.5 mM Tris-HCl, 2% SDS, 5% glycerol, 5% 2-mercaptoethanol) at 100°C for 5 min. The protein lysates and biotinylated proteins (cell surface) were then frozen until analysis.

Western blotting analysis

Proteins from the NAc region were separated by 10% SDS-polyacrylamide gel electrophoresis and transferred onto a polyvinylidene difluoride membrane (Millipore, MA, USA). Non-specific binding sites were blocked with 5% non-fat milk in tris-buffered saline containing 0.1% Tween-20 (TBST) for 1 h. Then, the membranes were incubated at 4°C overnight with a monoclonal antibody to D2R (1:1,000), antibodies to $GABA_AR$-α1 (1:1,000), $GABA_AR$-α2 (1:1,000), $GABA_AR$-β2 (1:1,000), $GABA_AR$-β3 (1:1,000), an antibody to phosphorylated PKC (1:1,000), an antibody to σ_1R (1:500), and an antibody to Na^+-K^+ ATPase (1:1,000). After rinsing in TBST buffer, the membranes were incubated with horseradish peroxidase-labeled secondary antibodies and developed using an enhanced chemiluminescence detection kit (Millipore, Billerica, MA, USA). Following visualization, the blots were stripped by incubation in stripping buffer (Restore; Pierce Biotechnology, Rockford, IL, USA) and then incubated with antibodies against PKC (1:1,000) or GAPDH (1:5,000). Western blot bands were then scanned and analyzed by Image J analysis software package (NIH). The optical density of specific bands was first normalized to the corresponding level of Na^+-K^+ ATPase or GAPDH and then normalized according to control levels.

Behavioral investigations

Three different behavioral tests were carried out (09:00–14:00 h) under the following test sequence: open-field test (OFT) → forced swim test (FST) → tail suspension test (TST). The order of testing was chosen such that the test involving low-stress levels (OFT) took precedence over tests involving medium-stress levels (FST) and high-stress levels (TST; Di et al., 2017). The FST and OFT were performed at least 24 h apart while the TST and FST were performed at least 48 h apart, as previously reported (Di et al., 2017). These behavioral tests were captured by a video-monitor, and the data were analyzed using TopScan Lite 2.0 (Clever Sys., Reston, VA, USA).

Before the OFT, mice were moved to the testing area in their home cages and allowed to adapt to their new environment for at least 1 h. Each mouse was placed in a cuboid Plexiglas box (60 × 60 × 40 cm) with 15 lux lighting and allowed to explore freely for 5 min. The distance traveled within 5 min was measured to assess the state of movement (Dere et al., 2004).

The FST was performed as described previously (Zhang B. et al., 2017). In brief, swim sessions were conducted by placing mice in plastic cylinders (diameter: 12 cm; height: 24 cm) filled with water (23–25°C) to a height of 20 cm. The total duration of immobility during a 6-min test was then scored. A mouse was judged to be immobile when it stopped any movements except those that were necessary to keep its head above water.

The TST was carried out by taping the tail of a mouse onto a rod 60 cm above the floor, as described previously (Zhou et al., 2014).

Data analysis/statistics

All outcome analyses were carried out by an independent investigator who was blinded to the treatment conditions and animal groupings. All data were retrieved and processed using the Microcal Origin 9.1 software program (Origin Lab, Northampton, MA, USA). All data were expressed as means ± standard error (SE) and were analyzed by SPSS software (SPSS, RRID: SCR-002865, version 18.0). All normally distributed data (determined by the Shapiro-Wilk test) were performed by the Grubb's test to determine outliers ($p < 0.01$), and outliers in **Figures 1G**, **6B**, and **6C** were removed from the analysis. Differences between two groups were evaluated by the Student's *t*-test (for normally distributed data). One-way analysis of variance (ANOVA) and two-way ANOVA were used to detect statistical significance between two or more groups on a single independent variable or two independent variables, respectively. With regards to the analysis of electrophysiological data: (1) input-output (I-O) function was assessed by measuring fEPSP slopes evoked by stimulating intensities from 0.1 to 1.1 mA. The duration of fEPSPs was measured as the time between the stimulus (measured at the midpoint of the stimulus artifact) to the time when the fEPSP amplitude decayed to half that of the maximal amplitude (**Figure 2B**; Yang et al., 2014); (2) the PPR was calculated with the following formula: $(fEPSP_{S2}/fEPSP_{S1}) \times 100$, in which $fEPSP_{S1}$ and $fEPSP_{S2}$ represented the fEPSP slopes evoked by the first and second stimulations, respectively; and (3) for LTD analysis, the fEPSP slopes were normalized to the mean baseline slope over the last 10 min before LFS and plotted over time. The 20% lower values of the fEPSP slopes 50–60 min after delivering LFS than baseline was considered as maintenance of LTD. The effects of control and NE-100, along with the drugs applied in different groups, were determined by testing data from the last 10 min of recordings with the Mann-Whitney U test (as the data were not normally distributed). Repeated-measures ANOVA (with Greenhouse-Geisser corrections if necessary) was used to

analyze I-O data and PPR. ANOVA, followed by Bonferroni's *post-hoc* test, was performed when data showed homogeneity of variance. *P*-values < 0.05 were considered statistically different.

Results

Repeated injection of NE-100 into NAc leads to reduced surface expression of σ_1r and depressive-like behaviors

In our previous study, we reported that σ_1R gene knockout or the systematic administration of the σ_1R inhibitor NE-100 induced or worsened depressive-like behaviors in mice (Sha et al., 2015; Zhang B. et al., 2017; Zhang S. et al., 2017). To test the specific effect of σ_1R antagonist in the NAc on depressive-like behaviors in mice, we microinjected the NAc region of 12-week-old mice with NE-100 (0.15 nmol/mouse/day) for 3 days (NE-100 mice; **Figures 1A,B**). To clarify the effect of NE-100 administration on σ_1R expression, we examined the level of σ_1R in the NAc of control mice and NE-100 mice at the end of the behavioral tests. RT-PCR results showed that the administration of NE-100 did not affect the mRNA levels of σ_1R in the NAc of mice ($t_{(14)} = 0.511$, $p = 0.618$; **Figure 1C**). The σ_1R protein at approximately 25 kDa was observed in the NAc of control and NE-100 mice. In comparison with control mice, the total amount of σ_1R protein was not significantly altered in NE-100 mice ($t_{(14)} = -0.155$, $p = 0.879$; **Figure 1D**), notably, the cell surface protein level of σ_1R was significantly reduced in NE-100 mice ($t_{(14)} = 4.939$, $p < 0.001$), suggesting a downregulation of σ_1R activity in the cell membrane.

We then examined spontaneous activity and depressive-like behaviors by the open-field test (OFT), forced swim test (FST), and tail suspension test (TST). As shown in **Figure 1E**, the total distance traveled in the OFT was not significantly different when compared between control mice and NE-100 mice ($t_{(22)} = -0.419$, $p = 0.679$). In comparison with control mice, the NE-100 mice exhibited prolongation of immobility time in the FST ($t_{(22)} = -3.862$, $p < 0.001$; **Figure 1F**) and TST ($t_{(21)} = -4.444$, $p < 0.001$; **Figure 1G**), thus indicating a state of despair. These results indicate that the impairment of σ_1R in the NAc induces depressive-like behaviors in mice.

Impaired synaptic function involved with $GABA_A$R in NE-100 mice

Synaptic plasticity in the NAc is involved in depressive-like behavior caused by chronic unpredictable stress (Wang et al., 2010). To determine whether an impairment of σ_1R function affects synaptic function in the NAc, we recorded field excitatory postsynaptic potentials (fEPSPs) by stimulating the NAc in brain slices obtained from control and NE-100 mice (**Figure 2B**). The mice were decapitated on day 2.5 after the last administration of NE-100 (at the end of the behavioral tests; **Figure 2A**) and brain slices were prepared to record field potentials. To evaluate the basal properties of the NAc, an I-O curve was generated by plotting fEPSP slopes against stimulation intensities from 0.1 mA to 1.1 mA. Repeated measures ANOVA found no significant interactions for the control mice and NE-100 mice over six different stimulation intensities on the fEPSP slope ($F_{(5,35)} = 0.430$, $p = 0.824$; **Figure 2C**). Interestingly, when compared with the single fEPSP waveform in control mice, the same stimulation elicited a multi-spike fEPSP waveform in the NAc of NE-100 mice (upper right panel in **Figure 2C**). The duration of fEPSP in NE-100 mice was significantly longer than that in control mice ($t_{(14)} = -3.094$, $p = 0.008$; **Figure 2D**). In addition, the paired-pulse ratio (PPR) in NE-100 mice was significantly larger than those in control mice with an interpulse interval (IPI) of 15–25 ms (15 ms IPI: $p = 0.025$; 25 ms IPI: $p = 0.045$; **Figure 2E**); values with the different IPIs (50–100 ms) showed no change ($p > 0.05$). Notably, the fEPSP slopes reduced by approximately 35% following the delivery of low-frequency stimulation (LFS) over 60 min in control slices, indicating LTD maintenance. The same LFS protocol did not induce a stable reduction of the fEPSP slopes in brain slices from NE-100 mice ($U_{(8,8)} = 0$, $p < 0.001$; **Figure 2F**).

According to our previous studies, the increased PPR indicates dysfunctional $GABA_A$R-mediated inhibition (Zhang T. et al., 2017). To test the involvement of $GABA_A$R in synaptic dysfunction in the NAc region of NE-100 mice, the NAc slices were treated with the $GABA_A$R antagonist bicuculine (10 mM) or agonist muscimol (10 mM) for 30 min. The application of bicuculine caused an increase in the duration of fEPSP ($p = 0.001$; **Figure 2Gi**) and PPR value (IPI: 25 ms; $p = 0.006$; **Figure 2Gii**) in control mice. In addition, the application of muscimol led to the decrease in the duration of fEPSP ($p = 0.001$; **Figure 2Ii**) and PPR ($p = 0.002$; **Figure 2Iii**) in NE-100 mice. Furthermore, the application of bicuculline caused LTD to be unsustainable in control mice ($p < 0.001$; **Figure 2H**), while the application of muscimol recovered LTD in NE-100 mice ($p < 0.001$; **Figure 2J**). Therefore, these findings indicate that an impairment of σ_1R function in the NAc attenuates synaptic plasticity and $GABA_A$R-mediated inhibition.

Reduced $GABA_A$R and D2R expression in NE-100 mice

$GABA_A$R-α2, -α4, -δ, and other α and β subunits were reported to be expressed at levels ranging from strong to weak in the NAc region of male mice (Hortnagl et al., 2013). To investigate the mechanisms underlying the abnormal

10.3389/fnmol.2022.959224

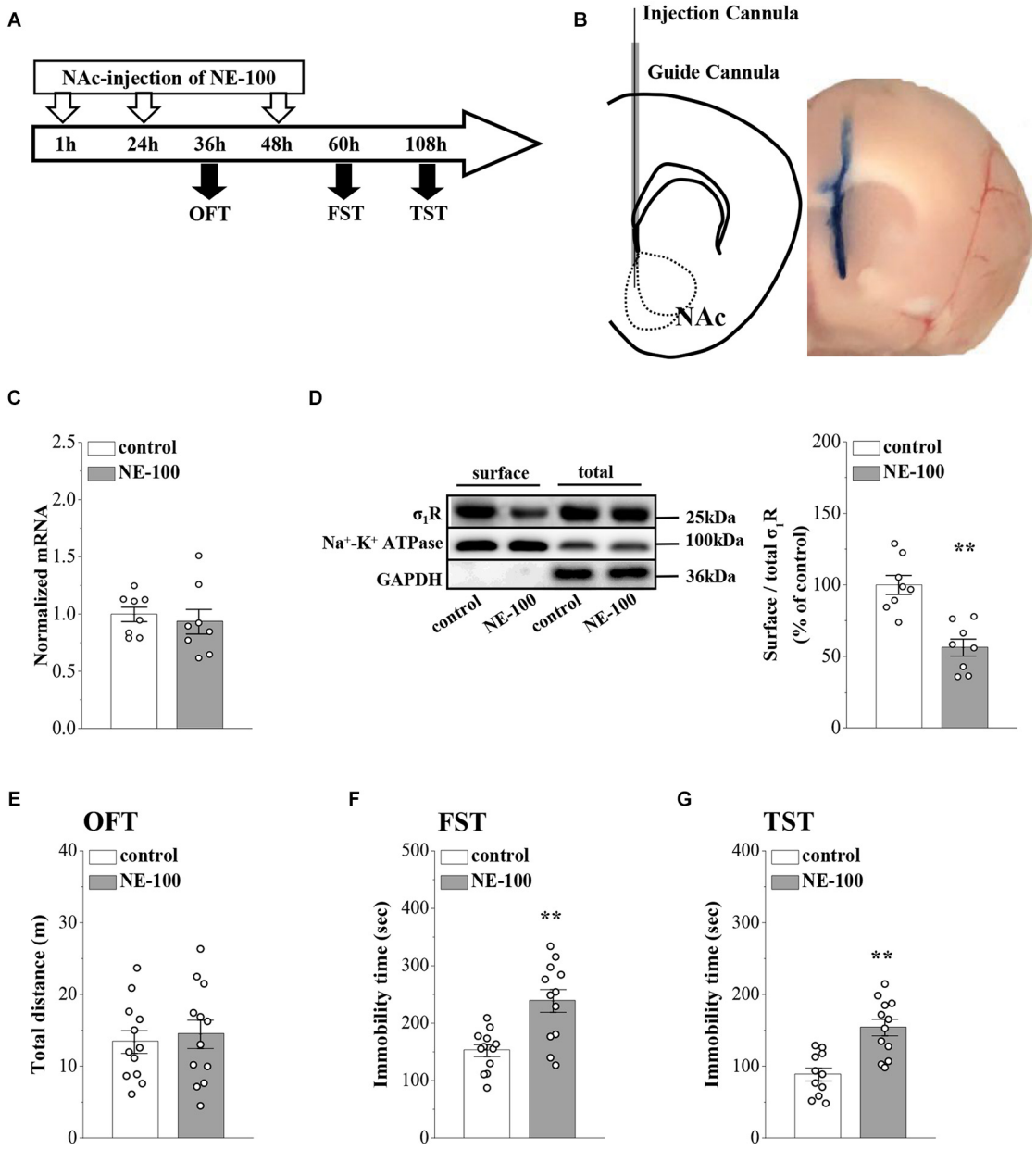

FIGURE 1
Repeated injection of NE-100 in the NAc induces depressive-like behaviors. **(A)** The time course of the experimental procedure. **(B)** Schematic diagram of the NAc (left panel) and image of the NAc injected with Evans-blue (right panel). **(C)** The level of $\sigma_1 R$ mRNA in the NAc was examined at the end of the behavioral tests (n = 8 mice per group; Student's t-test). **(D)** Representative Western blots of biotin-labeled surface proteins (surface) and total proteins (total) σ_1R in the NAc. Na^+-K^+ ATPase served as internal control and GAPDH served as a negative control. Bar graphs indicate the ratio of proteins at the cell surface to their total levels. $^{**}p < 0.01$ vs. control mice (n = 8 mice per group; Student's t-test). **(E)** Bar graphs show the distance traveled in OFT in control mice and NE-100 mice (n = 12 mice per group; Student's t-test). **(F,G)** Bar graphs show the immobility time of FST and TST in control mice and NE-100 mice. $^{**}p < 0.01$ vs. control mice (n = 11 mice in control group of TST and n = 12 mice in other groups; Student's t-test).

synaptic properties and plasticity in the NAc of NE-100 mice, we investigated the expression of $GABA_AR$ and D1 and D2 receptors (D1R and D2R) in the NAc by RT-PCR and Western blotting, respectively, on day 2.5 after the last administration of NE-100 (timeline see Figure 2A). For mRNA levels, the results of a two-way ANOVA revealed a significant main effect of repeated NE-100 treatment ($F_{(1,196)}$ = 18.235, $p < 0.001$; Figure 3A). The main effect of genes ($F_{(13,196)}$ = 1.721, $p > 0.05$) or NE-100 treatment × genes interaction was not significant ($F_{(13,196)}$ = 1.721, $p > 0.05$). Bonferroni *post-hoc*

10.3389/fnmol.2022.959224

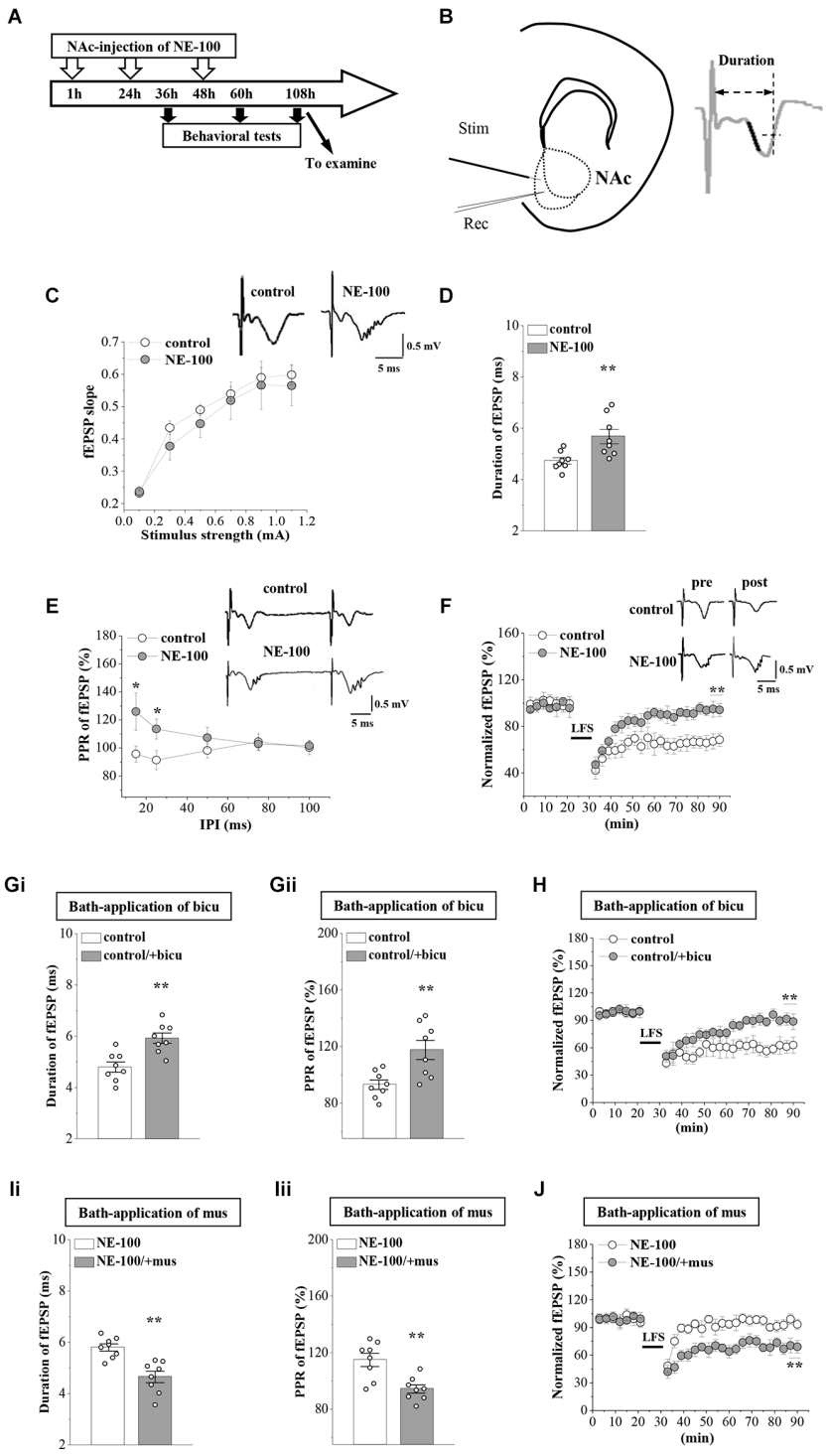

FIGURE 2
Repeated injection of NE-100 leads to synaptic dysfunction. **(A)** The timecourse of the experimental procedure. **(B)** Schematic illustrating sites of stimulating electrode (Stim) and recording electrode (Rec) in the shell of NAc (left panel). The right panel shows a typical trace. The dark mark of the initial descending phase indicates the 10% to 90% data points of the slope, and the two-way arrow indicates the duration. **(C)** Input-output (I-O) curve in the NAc. Each point represents the group mean value of fEPSP slopes against stimulus intensity from 0.1 mA to 1.1 mA in control mice and NE-100 mice. Representative traces of fEPSP evoked at 0.5 mA stimulus intensity in control mice and NE-100 mice (n = 8 slices/4 mice per group; repeated-measures ANOVA). **(D)** Bar graphs show the duration (ms) of fEPSP in control mice and NE-100 mice. $^{**}p < 0.01$ vs. control mice (n = 8 slices/4 mice per group; Student's-t test). **(E)** PPR (%) of fEPSP slopes was plotted against interpulse intervals (IPIs) ranging from
(*Continued*)

FIGURE 2 (Continued)
15 ms to 100 ms. Traces represent fEPSPs evoked by stimulation pulses delivered with a 25 ms IPI. *$p < 0.05$ vs. control mice ($n = 8$ slices/4 mice per group; repeated-measures ANOVA). **(F)** LTD induction by delivering low-frequency stimulation (LFS) in control mice and NE-100 mice. A solid line indicates when LFS was given. Traces show fEPSPs pre- and post-LFS. **$p < 0.01$ vs. control mice ($n = 8$ slices/4 mice per group; Mann-Whitney U test). **(Gi,Gii)** Bar graphs show the duration (ms) of fEPSP and the PPR value (25 ms IPI) in vehicle-treated and bicuculline (bicu)-treated control mice. **$p < 0.01$ vs. vehicle-treated mice ($n = 8$ slices/4 mice per group; Student's t-test). **(H)** LTD induction by LFS in slices of control mice treated with bicuculline (bicu). **$p < 0.01$ vs. vehicle-treated mice ($n = 8$ slices/4 mice per group; Mann-Whitney U test). **(Ii,Iii)** Bar graphs show the duration (ms) of fEPSP and the PPR value (25 ms IPI) in vehicle-treated and muscimol (mus)-treated NE-100 mice. **$p < 0.01$ vs. vehicle-treated mice ($n = 8$ slices/4 mice per group; Student's t-test). **(J)** LTD induction in slices of NE-100 mice treated with muscimol (mus). **$p < 0.01$ vs. vehicle-treated mice ($n = 8$ slices/4 mice per group; Mann-Whitney U test).

analyses revealed that the levels of *$GABA_AR$-α1* ($p = 0.048$), *$GABA_AR$-α2* ($p = 0.017$), *$GABA_AR$-β2* ($p = 0.010$), and *$GABA_AR$-β3* ($p = 0.014$) mRNA in NE-100 mice were significantly reduced when compared to those in control mice. There were no significant differences between control mice and NE-100 mice with respect to the other *$GABA_AR$* subunits or *D1R* and *D2R* mRNA ($p > 0.05$). Furthermore, the results of a two-way ANOVA revealed a significant main effect of repeated NE-100 treatment on the protein levels of $GABA_AR$ subunits ($F_{(1,56)} = 27.563$, $p < 0.001$; **Figure 3B**). The main effect of the $GABA_AR$ subunits ($F_{(3,56)} = 0.138$, $p > 0.05$)as well as the interaction ($F_{(3,56)} = 0.138$, $p > 0.05$)were not significant. Bonferroni *post-hoc* analyses revealed that the levels of $GABA_AR$-α1 ($p = 0.031$), $GABA_AR$-α2 ($p = 0.017$), $GABA_AR$-β2 ($p = 0.011$) and $GABA_AR$-β3 ($p = 0.030$) protein in NE-100 mice were significantly lower than those in control mice.

σ_1R can be complex with D2R on the cell membrane (Borroto-Escuela et al., 2020). To analyze whether inhibition of σ_1R in the NAc affects D2R internalization, we investigated the distribution of D2R on the membrane surface by using a cell surface biotinylation approach. The level of D2R at the cell surface in the NAc of NE-100 mice was significantly reduced when compared to controls ($t_{(14)} = 3.448$, $p = 0.004$; **Figure 3C**). Quantification of the total amount of D2Rs in the NAc revealed no difference between the NE-100 mice and control mice ($p > 0.05$).

Reduced D2R-mediated PKC activity suppresses $GABA_AR$ expression in NE-100 mice

In our previous studies, we showed that the inhibition of D2R indirectly suppresses the GABAergic inhibitory circuit by affecting the activity of PKC (Zhang T. et al., 2017). Here, we further examined the levels of PKC phosphorylation (phospho-PKC) within the NAc (**Figure 4A**). For the level of phospho-PKC, the results of a two-way ANOVA revealed significant main effects of repeated NE-100 treatment ($F_{(1,42)} = 8.934$, $p = 0.005$; **Figure 4B**) and drug treatment ($F_{(2,42)} = 18.099$, $p < 0.001$), but the interaction was not significant ($F_{(2,42)} = 2.013$, $p > 0.05$). Bonferroni *post-hoc* analyses revealed that the level of phospho-PKC was significantly reduced in NE-100 mice than in control mice ($p = 0.025$); this was rescued by injecting the NAc with quinpirole, a D2R agonist ($p = 0.045$), yet quinpirole had no effect on the level of phospho-PKC in control mice ($p > 0.05$). Administration of the D2R antagonist L-sulpiride significantly reduced the levels of phospho-PKC in control mice ($p = 0.014$), but not in NE-100 mice ($p > 0.05$). There was no significant difference in the levels of PKC proteins when compared between control mice and NE-100 mice ($p > 0.05$).

Next, we microinjected the NAc region of control and NE-100 mice with D2R agonist quinpirole or PKC activator PMA (**Figure 4A**) to examine the effects on the level of $GABA_AR$ subunits. The results of a two-way ANOVA revealed significant main effects of drug treatment on the protein level of $GABA_AR$ subunits (α1: $F_{(2,42)} = 7.762$, $p < 0.001$; **Figure 4C**; α2: $F_{(2,42)} = 4.752$, $p = 0.014$; **Figure 4D**; β2: $F_{(2,42)} = 4.411$, $p = 0.018$; **Figure 4E**; β3: $F_{(2,42)} = 3.502$, $p = 0.041$; **Figure 4F**), but not the interaction (α1: $F_{(2,42)} = 1.286$, $p > 0.05$; α2: $F_{(2,42)} = 2.320$, $p > 0.05$; β2: $F_{(2,42)} = 2.325$, $p > 0.05$; β3: $F_{(2,42)} = 3.050$, $p > 0.05$). Bonferroni *post-hoc* analyses revealed that in NE-100 mice, injecting the NAc with quinpirole or the PKC activator PMA rescued the protein levels of $GABA_AR$-α1 (quinpirole: $p = 0.037$; PMA: $p = 0.010$), along with the -α2 (quinpirole: $p = 0.014$; PMA: $p = 0.011$), -β2 (quinpirole: $p = 0.010$; PMA: $p = 0.011$), and -β3 (quinpirole: $p = 0.017$; PMA: $p = 0.011$) subunits. In contrast, neither quinpirole nor PMA had a significant effect on the level of $GABA_AR$ subunits in the NAc of the control mice ($p > 0.05$).

Mechanisms involved in the synaptic dysfunction in NE-100 mice

To test the involvement of D2R-mediated PKC activity in synaptic dysfunction caused by reduced $GABA_AR$ in the NAc, the NE-100 mice were treated with NAc-injection of quinpirole, PMA, or coadministered quinpirole and GF109203X for 3 days (for a time chart of the experimental procedure, see **Figure 4A**). The results of a one-way ANOVA revealed a significant main effect of drug treatment ($F_{(3,28)} = 5.724$, $p = 0.003$; **Figure 5A**). Bonferroni *post-hoc* analyses revealed that the application of quinpirole or PMA led to a significant reduction in the PPR ($p < 0.05$). In parallel, quinpirole or PMA resulted in an approximately 35% reduction in the fEPSP slopes over 60 min

10.3389/fnmol.2022.959224

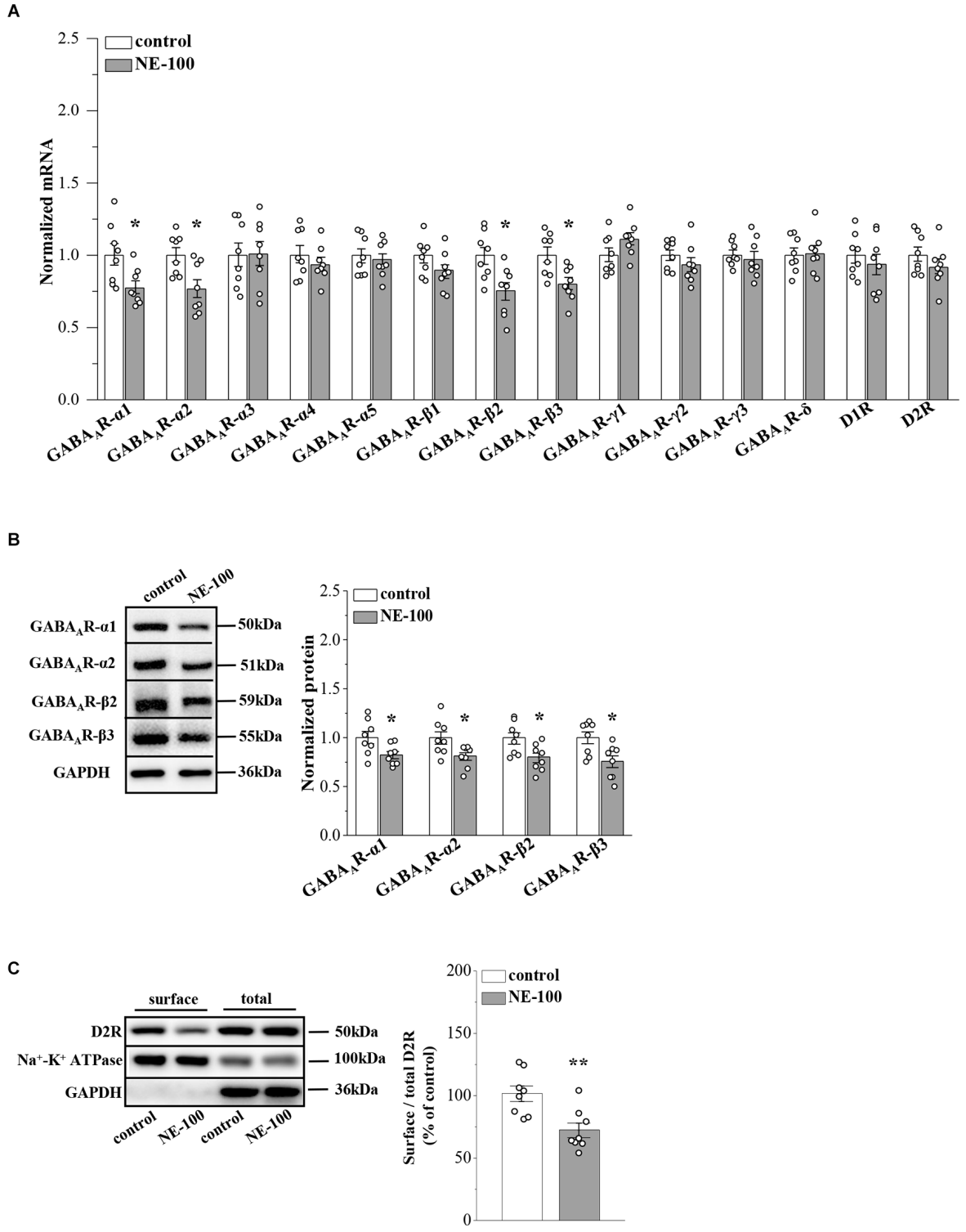

FIGURE 3
Repeated injection of NE-100 suppresses GABA$_A$R and D2R expression. **(A)** The levels of *GABA$_A$R-α1-5, -β1-3, -γ1-3,* -δ subunits, and *D1R, D2R* mRNA in the NAc were examined at the end of the behavioral tests. *$p < 0.05$ vs. control mice ($n = 8$ mice per group; two-way ANOVA). **(B)** Bar graphs show levels of GABA$_A$R-α1, GABA$_A$R-α2, GABA$_A$R-β2, and GABA$_A$R-β3 protein in the NAc normalized by the level of GAPDH were normalized by control levels. *$p < 0.05$ vs. control mice ($n = 8$ mice per group; two-way ANOVA). **(C)** Representative Western blots of biotin-labeled surface proteins (surface) and total proteins (total) D2R in the NAc. Na$^+$-K$^+$ ATPase served as internal control and GAPDH served as a negative control. Bar graphs indicate the ratio of proteins at the cell surface to their total levels. **$p < 0.01$ vs. control mice ($n = 8$ mice per group; Student's *t* -test).

10.3389/fnmol.2022.959224

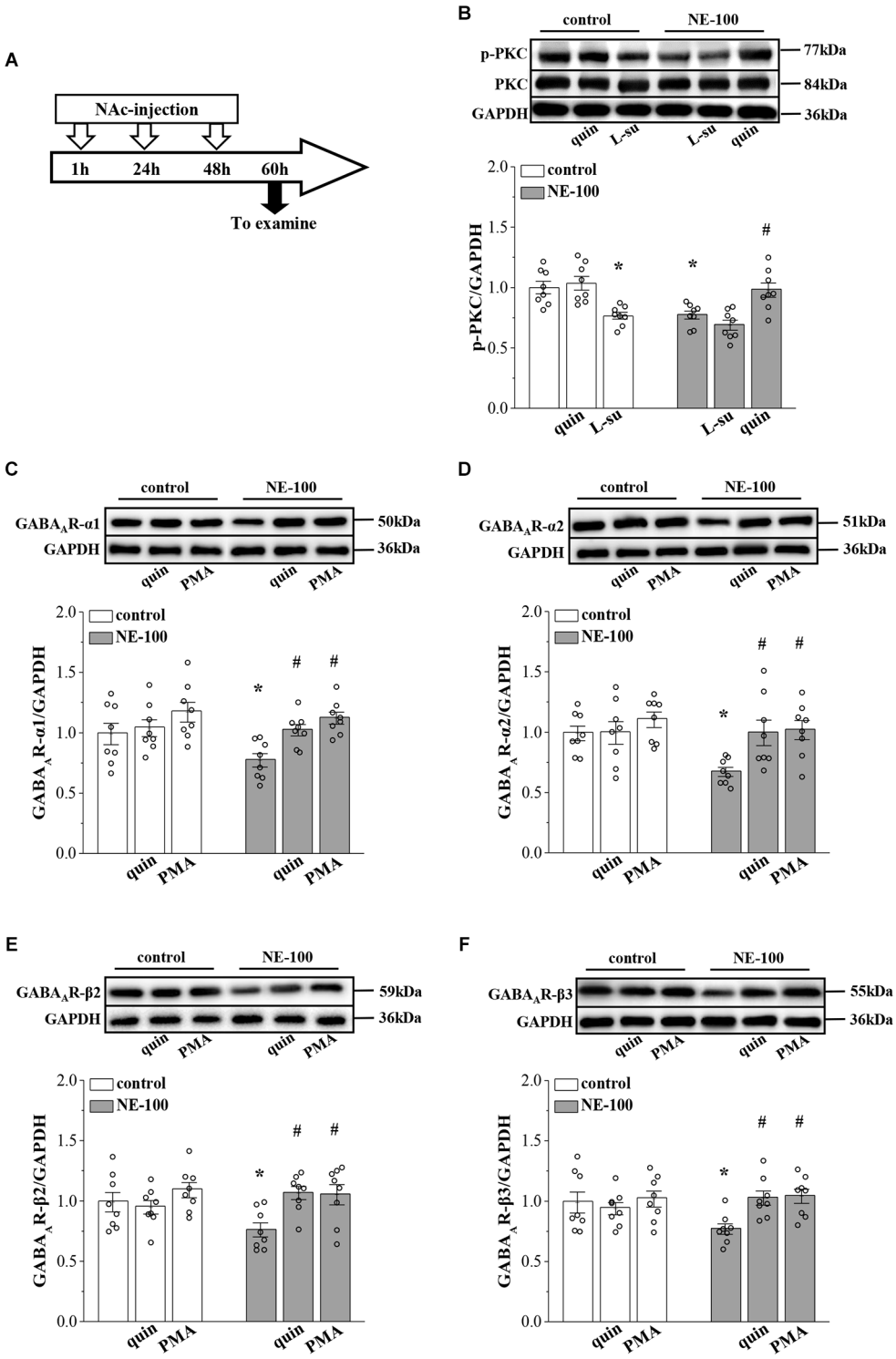

FIGURE 4
Repeated injection of NE-100 reduces PKC signaling leading to decreased GABA$_A$R expression. **(A)** Time chart of the experimental procedure. **(B)** Representative blots of phospho-PKC in the NAc of control mice treated with quinpirole (quin) or L-sulpiride (L-su), and NE-100 mice treated with L-sulpiride (L-su) or quinpirole (quin). Densitometric values of phospho-PKC normalized by the PKC protein were normalized by control levels. *$p < 0.05$ vs. control mice; $^{\#}p < 0.05$ vs. NE-100 mice ($n = 8$ mice per group; two-way ANOVA). **(C–F)** Bar graphs show levels of GABA$_A$R-α1, GABA$_A$R-α2, GABA$_A$R-β2, and GABA$_A$R-β3 protein in the NAc of control mice and NE-100 mice treated with NAc-injection of quinpirole (quin) or PMA. Densitometric values normalized by the level of GAPDH were normalized by control levels. *$p < 0.05$ vs. control mice; $^{\#}p < 0.05$ vs. vehicle-treated NE-100 mice ($n = 8$ mice per group; two-way ANOVA).

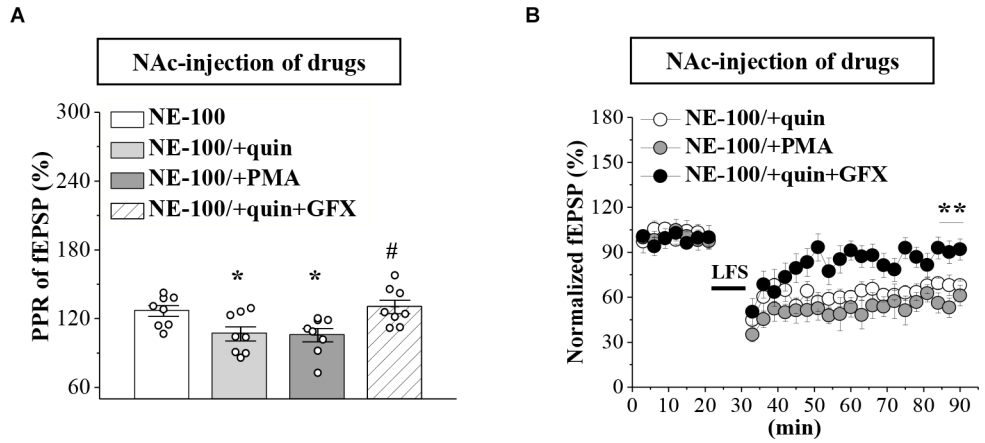

FIGURE 5
Repeated injection of NE-100 impairs $GABA_AR$-regulated LTD through reduced PKC activity. **(A)** Bar graphs show the PPR (25 ms IPI) in the slices of NE-100 mice treated with NAc-injection of quinpirole (quin), PMA, or the co-administration of quinpirole and GF109203X (quin+GFX). $^*p < 0.05$ vs. vehicle-treated mice; $^{\#}p < 0.05$ vs. quin-treated mice (n = 8 slices/4 mice per group; one-way ANOVA). **(B)** LTD induction in NE-100 mice treated with NAc-injection of quinpirole (quin), PMA, or the co-administration of quinpirole and GF109203X (quin+GFX). $^{**}p < 0.01$ vs. quin-treated mice (n = 8 slices/4 mice per group; Mann-Whitney U test).

post-LFS (Figure 5B). In addition, the effects of quinpirole on the PPR ($p < 0.05$) or LTD ($p < 0.01$) were sensitive to the co-injection of GF109203X.

Impaired LTD is involved in depressive-like behaviors of NE-100 mice

To investigate the relationship between altered synaptic function and depressive-like behaviors, we conducted OFT, FST, and TST evaluations on days 2–4 after the administration of NE-100 and drugs (for a time chart of the experimental procedure, see Figure 1A). For OFT (Figure 6A), the results of a two-way ANOVA revealed no significant main effect of repeated NE-100 treatment ($F_{(1,88)} = 0.216$, $p > 0.05$), drug treatment ($F_{(3,88)} = 1.105$, $p > 0.05$), or the interaction ($F_{(3,88)} = 0.429$, $p > 0.05$). Bonferroni *post-hoc* analyses revealed that the distance traveled in the OFT did not differ significantly between control and NE-100 mice and of the drugs applied groups ($p > 0.05$). For FST (Figure 6B) and TST (Figure 6C), the main effect of repeated NE-100 treatment (FST: $F_{(1,86)} = 12.89$, $p = 0.001$; TST: $F_{(1,86)} = 19.433$, $p < 0.001$), drug treatment (FST: $F_{(3,86)} = 3.974$, $p = 0.011$; TST: $F_{(3,86)} = 5.391$, $p = 0.002$) and the interaction (FST: $F_{(3,86)} = 3.206$, $p = 0.027$; TST: $F_{(3,86)} = 3.014$, $p = 0.047$) were significant. Bonferroni *post-hoc* analyses revealed that injecting the NAc with quinpirole (FST:$p = 0.034$; TST: $p = 0.015$), PMA (FST: $p = 0.010$; TST: $p = 0.011$), and muscimol (FST: $p = 0.012$; TST: $p = 0.010$) rescued the prolongation of immobility time in the FSTand TSTin NE-100 mice. Nevertheless, neither quinpirole, PMA, nor muscimol had a significant effect on the immobility time in FST ($p > 0.05$) and TST ($p > 0.05$) in control mice.

Discussion

In this study, we investigated the influence of σ_1R antagonist NE-100 in the NAc on synaptic plasticity and depressive-like behaviors. Microinjection of NE-100 into the NAc for 3 days did not affect the total amount of σ_1R, whereas it caused a decrease in σ_1R surface expression, suggesting downregulation of its activity in the cell membrane. As a result, our findings provide the first *in vivo* evidence that inhibition of σ_1R in the NAc impairs LTD by reducing $GABA_AR$ expression, leading to depressive-like behaviors. Besides, there is a difference when compared to previous results: we reported that the GABA-activated current remained unaltered in the hippocampal dentate gyrus (DG) of σ_1R knockout mice, while the NMDA-activated current was reduced (Sha et al., 2013). Our present results showed that repeated inhibition of σ_1R in the NAc caused a reduction in the expression of $GABA_AR$ subunits. In addition, an NMDAR agonist did not rescue LTD in NE-100 mice (Supplementary Figure S1B). Possible explanations for these conflicting data are that the cellular properties of the NAc differ from those of immature cells in the DG, and that there may be key differences between experiments involving gene knockouts and pharmacological inhibitors. Further studies on the effects of downregulated σ_1R on NMDAR, $GABA_AR$, and $GABA_BR$ in the NAc MSNs are in progress.

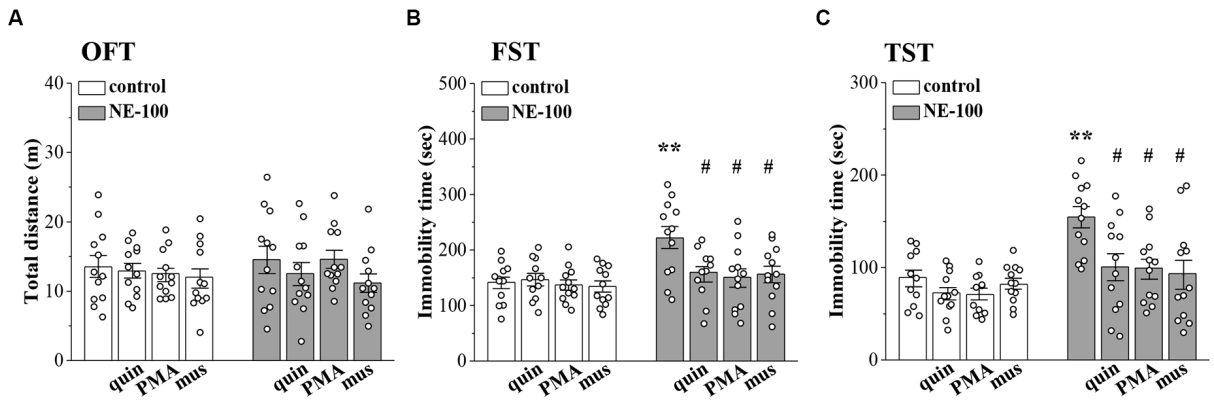

FIGURE 6
Involvement of impaired LTD in the NAc in depressive-like behaviors. **(A–C)** Bar graphs show the distance traveled in OFT, and the immobility time in FST and in TST of control mice, NE-100 mice, and mice treated with NAc-injection of quinpirole (quin), PMA, or muscimol (mus). $^{**}p < 0.01$ vs. control mice; $^{\#}p < 0.05$ vs. vehicle-treated NE-100 mice (n = 11 mice of quin-treated group in FST, n = 11 mice of vehicle-treated control group and PMA-treated control group in TST, and n = 12 mice in the other groups; two-way ANOVA).

A principal finding in the present study is that the membrane levels of D2R were reduced in the NAc when σ_1R was deficient. The activity of σ_1R is closely related to the function of dopamine receptors. It has been found that in cultured cells, and in animal striatum, σ_1R can complex with D2R to form a heterodimer, thus maintaining its stability and acting as a target for D2R ligands to activate or inhibit downstream signaling pathways (Borroto-Escuela et al., 2019, 2020). Our results showed that repeated inhibition of σ_1R in the NAc did not affect the transcriptional and total protein levels of D2R; however, membrane protein expression was significantly reduced, thus suggesting that downregulated σ_1R in the NAc causes a reduction in D2R-mediated downstream signaling. The activation of σ_1R prevents intracellular calcium dysregulation and increases intracellular calcium responses (Katnik et al., 2006; Choi et al., 2022). Intracellular Ca^{2+} signals can affect the activity of neuronal calcium sensor-1 (NCS-1); NCS-1 inhibits the internalization and desensitization of D2R in a Ca^{2+}-dependent manner (Kabbani et al., 2002). Therefore, we hypothesize that σ_1R complexes with D2R to form heterodimers that stabilize the membrane by anchoring D2R and that downregulated σ_1R causes an imbalance in the distribution of D2R in cells, thus resulting in the reduced expression of D2R in the membrane. Another explanation is that repeated inhibition of σ_1R indirectly causes the abnormal distribution of D2R in cells by reducing intracellular Ca^{2+} signaling, thus resulting in a reduction in the endogenous ligand binding sites and overall functionality.

A previous study reported that σ_1R agonists induce the activation of PKC (Morin-Surun et al., 1999). In the present study, we found that the levels of phospho-PKC in the NAc of NE-100 mice were lower than those in control mice. The D2R agonist could recover the level of phospho-PKC in NE-100 mice, without affecting the activation of PKC in control mice; the D2R antagonist caused the decline of phospho-PKC in control mice, but not in NE-100 mice. Moreover, neither agonist nor antagonist of D1R, have these effects (**Supplementary Figures S2Ai and Aii**), suggesting that σ_1R regulates PKC activity by affecting D2R. Hong et al. (2016) reported that agonists of D2R enhanced PKC signaling. In our previous study, we demonstrated that D2R downregulation in BLA caused a reduction in PKC phosphorylation levels (Zhang T. et al., 2017). D2R activates the downstream phospholipase C (PLC)-diacylglycerol (DAG)-PKC signaling pathway *via* Gαi proteins (Yao et al., 2008). Thus, inhibition of σ_1R in the NAc leads to reduced levels of PKC phosphorylation *via* the downregulation of D2R.

Electrophysiological results showed that inhibition of σ_1R in the NAc caused multi-peak-like change, a prolonged duration in the fEPSP, and an increased PPR; collectively, these results indicated a weakening in the functionality of the $GABA_A$R-mediated inhibitory circuit in amygdale (Delaney and Sah, 2001; Zhang T. et al., 2017). In line with our results showing that inhibition of $GABA_A$R resulted in an increased PPR value and extended fEPSP duration in the NAc of control mice, and activation of $GABA_A$R corrected the increased PPR and extended fEPSP duration in the NAc of NE-100 mice. The expression levels of $GABA_A$R-α1, along with the -α2, -β2, and -β3 subunits were all decreased in NE-100 mice. Previous immunocytochemical studies revealed that the rodent brain the NAc expresses high levels of $GABA_A$R-α1, along with the -α2, -β2, and -β3 subunits, with MSN dendrites expressing α2 and β3 subunits and interneurons expressing α1 and β2 subunits (Schwarzer et al., 2001; Boyes and Bolam, 2007). Thus, the reduced expression of these subunits causes the functionality of the $GABA_A$R inhibitory

circuit to be diminished. It was previously demonstrated that activation of D2R promotes the embedding of $GABA_AR$ in protrusions and the formation of new inhibitory synapses (Li et al., 2011). D2R knockout mice exhibit attenuated GABAergic neurotransmission (An et al., 2004); the long-term activation of D2R has been shown to increase postsynaptic $GABA_AR$ cluster density in striatal MSNs (Lalchandani et al., 2013). The present results showed that D2R activation increased the expression levels of $GABA_AR$ subunits and restored the PPR in the NAc of NE-100 mice; these effects were blocked by PKC inhibition (**Supplementary Figures S3Aii–Dii**). Activation of the PKC increased the expression of $GABA_AR$ subunits and restored PPR of the NAc in NE-100 mice. In contrast, no obvious effect of either activation of D2R or PKC on the $GABA_AR$ subunits in the NAc of control mice was found. The inhibition of D2R and PKC reduced the expression of $GABA_AR$ in control mice (**Supplementary Figures S3Ai–Di**), thus suggesting that D2R exerts a regulatory effect on $GABA_AR$ *via* PKC signaling. Activated PKC is known to contribute to $GABA_AR$ function, transport, and cell surface stability (Field et al., 2021). The activation of PKC promotes phosphorylation of α and β subunits to increase the surface expression of $GABA_AR$ (Luscher et al., 2011; Nakamura et al., 2015). Consistent with the present results, our previous study confirmed that the inhibition of PKC reduces the expression levels of $GABA_AR$ subunits, which consequently leads to a functional downregulation of $GABA_AR$ in BLA (Zhang T. et al., 2017). Collectively, these results indicate thatinhibition of σ_1R in the NAc causes the reduction of $GABA_AR$ subunits expression *via* downregulation of D2R-mediated PKC signaling, which further leads to a downgrade in $GABA_AR$ function.

Basal synaptic transmission in the NAc was not affected in NE-100 mice. However, the maintenance of LTD was impaired in the NAc of NE-100 mice. The activation of $GABA_AR$ restored LTD maintenance in NE-100 mice while the inhibition of $GABA_AR$ resulted in impaired LTD in control mice. A previous study showed that D2R inhibition affects LTP in the BLA by influencing presynaptic CB1R activation; however, the current results suggest that CB1R activation did not affect LTD in the NAc of NE-100 mice (**Supplementary Figure S1C**). The activation of D2R and GABAR facilitates the inwards flow of Ca^{2+} mediated by voltage-gated calcium channels (Guatteo et al., 2004). Consistent with this observation, the administration of the $GABA_AR$ agonist muscimol in the NAc brain slices in adolescent mice was found to depolarize neuronal membrane projection and promote the maintenance of LTD (Zhang et al., 2016). Thus, repeated inhibition of σ_1R in the NAc impairs LTD by reducing GABAergic function. GABAergic inhibition participates in regulating depressive-like states: male α2 subunit knockout mice appear depressive-like behavior (Vollenweider et al., 2011); in male mice, α2-containing $GABA_ARs$ on D2R-positive but not on D1R-positive neurons promote resiliency to chronic social defeat stress (Benham et al., 2021). Additionally, similar to the effects of $GABA_AR$ agonists, the activation of D2R or PKC restored LTD maintenance in the NAc while also correcting depressive-like behaviors in NE-100 mice; and yet these agonists had no significant effect on the behaviors of control mice. These results suggest that the LTD of synaptic plasticity in the NAc is closely related to depression. Impaired LTD in the NAc is known to contribute to depressive-like behaviors induced by chronic unpredictable stress in mice (Wang et al., 2010). In a mouse model of chronic mild stress, excessive activation of glycogen synthase kinase-3β led to decreased synaptic plasticity in the NAc; this subsequently led to reduced adaptive flexibility to stress and induced depressive disorders (Aceto et al., 2020). A reduction in the GABAergic synapses of the NAc was previously correlated with depressive-like behaviors and stress susceptibility (Heshmati et al., 2020).

Conclusions

The results from the present study indicate that inhibition of σ_1R in the NAc led to the suppression of $GABA_AR$ expression through a reduction in D2R/PKC activation, thus impairing LTD and leading to depressive-like behaviors. The present study provides a new insight into the mechanisms underlying depressive disorders and identifies potential therapeutic targets.

Data availability statement

The original contributions presented in the study are included in the article/**Supplementary material**, further inquiries can be directed to the corresponding author/s.

Ethics statement

The animal study was reviewed and approved by Animal Research Institute and Ethical Committee of Nanjing Medical University.

Author contributions

SS conceived and designed the experiments. YQ and WX performed the field potential recording, Western blotting, and all statistical analysis. KL and QL undertook the RT-PCR analysis. XC and YW carried out the animal care and behavioral examination. LC and SS drafted the manuscript.

All authors contributed to the article and approved the submitted version.

Funding

This study was supported by the National Natural Science Foundation of China (31600835).

Conflict of interest

The authors declare that the research was conducted in the absence of any commercial or financial relationships that could be construed as a potential conflict of interest.

Publisher's note

Supplementary material

The Supplementary Material for this article can be found online at: https://www.frontiersin.org/articles/10.3389/fnmol.2022.959224/full#supplementary-material.

References

Aceto, G., Colussi, C., Leone, L., Fusco, S., Rinaudo, M., Scala, F., et al. (2020). Chronic mild stress alters synaptic plasticity in the nucleus accumbens through GSK3β-dependent modulation of Kv4.2 channels. *Proc. Natl. Acad. Sci. U S A* 117, 8143–8153. doi: 10.1073/pnas.1917423117

Aguinaga, D., Casanovas, M., Rivas-Santisteban, R., Reyes-Resina, I., Navarro, G., and Fransco, R. (2019). The sigma-1 receptor as key common factor in cocaine and food-seeking behaviors. *J. Mol. Endocrinol.* 63, R81–R92. doi: 10.1530/JME-19-0138

An, J. J., Bae, M. H., Cho, S. R., Lee, S. H., Choi, S. H., Lee, B. H., et al. (2004). Altered GABAergic neurotransmission in mice lacking dopamine D2 receptors. *Mol. Cell. Neurosci.* 25, 732–741. doi: 10.1016/j.mcn.2003.12.010

Bagot, R. C., Parise, E. M., Peña, C. J., Zhang, H. X., Maze, I., Chaudhury, D., et al. (2015). Ventral hippocampal afferents to the nucleus accumbens regulate susceptibility to depression. *Nat. Commun.* 6:7062. doi: 10.1038/ncomms8062

Benham, R. S., Choi, C., Hodgson, N. W., Hewage, N. B., Kastli, R., Donahue, R. J., et al. (2021). α2-containing γ-aminobutyric acid type A receptors promote stress resiliency in male mice. *Neuropsychopharmacology* 46, 2197–2206. doi: 10.1038/s41386-021-01144-w

Borroto-Escuela, D. O., Narvaez, M., Romero-Fernandez, W., Pinton, L., Wydra, K., Filip, M., et al. (2019). Acute cocaine enhances dopamine D_2R recognition and signaling and counteracts D_2R internalization in sigma1R-D_2R heteroreceptor complexes. *Mol. Neurobiol.* 56, 7045–7055. doi: 10.1007/s12035-019-1580-8

Borroto-Escuela, D. O., Romero-Fernandez, W., Wydra, K., Zhou, Z., Suder, A., Filip, M., et al. (2020). OSU-6162, a sigma1R ligand in low doses, can further increase the effects of cocaine self-administration on accumbal D2R heteroreceptor complexes. *Neurotox. Res.* 37, 433–444. doi: 10.1007/s12640-019-00134-7

Boyes, J., and Bolam, J. P. (2007). Localization of GABA receptors in the basal ganglia. *Prog. Brain Res.* 160, 229–243. doi: 10.1016/S0079-6123(06)60013-7

Brünig, I., Sommer, M., Hatt, H., and Bormann, J. (1999). Dopamine receptor subtypes modulate olfactory bulb γ-aminobutyric acid type A receptors. *Proc. Natl. Acad. Sci. U S A* 96, 2456–2460. doi: 10.1073/pnas.96.5.2456

Chen, C.-Y., Di Lucente, J., Lin, Y.-C., Lien, C.-C., Rogawski, M. A., Maezawa, I., et al. (2018). Defective GABAergic neurotransmission in the nucleus tractus solitarius in Mecp2 -null mice, a model of Rett syndrome. *Neurobiol. Dis.* 109, 25–32. doi: 10.1016/j.nbd.2017.09.006

Choi, J. G., Choi, S. R., Kang, D. W., Kim, J., Park, J. B., Lee, J. H., et al. (2022). Sigma-1 receptor increases intracellular calcium in cultured astrocytes and contributes to mechanical allodynia in a model of neuropathic pain. *Brain Res. Bull.* 178, 69–81. doi: 10.1016/j.brainresbull.2021.11.010

Delaney, A. J., and Sah, P. (2001). Pathway-specific targeting of $GABA_A$ receptor subtypes to somatic and dendritic synapses in the central amygdala. *J. Neurophysiol.* 86, 717–723. doi: 10.1152/jn.2001.86.2.717

Delint-Ramirez, I., Garcia-Oscos, F., Segev, A., and Kourrich, S. (2020). Cocaine engages a non-canonical, dopamine-independent, mechanism that controls neuronal excitability in the nucleus accumbens. *Mol. Psychiatry* 25, 680–691. doi: 10.1038/s41380-018-0092-7

Dere, E., De Souza-Silva, M. A., Spieler, R. E., Lin, J. S., Ohtsu, H., Haas, H. L., et al. (2004). Changes in motoric, exploratory and emotional behaviours and neuronal acetylcholine content and 5-HT turnover in histidine decarboxylase-KO mice. *Eur. J. Neurosci.* 20, 1051–1058. doi: 10.1111/j.1460-9568.2004.03546.x

Di, T., Wang, Y., Zhang, Y., Sha, S., Zeng, Y., and Chen, L. (2020). Dopaminergic afferents from midbrain to dorsolateral bed nucleus of stria terminalis inhibit release and expression of corticotropin-releasing hormone in paraventricular nucleus. *J. Neurochem.* 154, 218–234. doi: 10.1111/jnc.14992

Di, T., Zhang, S., Hong, J., Zhang, T., and Chen, L. (2017). Hyperactivity of hypothalamic-pituitary-adrenal axis due to dysfunction of the hypothalamic glucocorticoid receptor in sigma-1 receptor knockout mice. *Front. Mol. Neurosci.* 10:287. doi: 10.3389/fnmol.2017.00287

Field, M., Dorovykh, V., Thomas, P., and Smart, T. G. (2021). Physiological role for $GABA_A$ receptor desensitization in the induction of long-term potentiation at inhibitory synapses. *Nat. Commun.* 12:2112. doi: 10.1038/s41467-021-22420-9

Fogaça, M. V., and Duman, R. S. (2019). Cortical GABAergic dysfunction in stress and depression: new insights for therapeutic interventions. *Front. Cell. Neurosci.* 13:87. doi: 10.3389/fncel.2019.00087

Guatteo, E., Bengtson, C. P., Bernardi, G., and Mercuri, N. B. (2004). Voltage-gated calcium channels mediate intracellular calcium increase in weaver dopaminergic neurons during stimulation of D_2 and $GABA_B$ receptors. *J. Neurophysiol.* 92, 3368–3374. doi: 10.1152/jn.00602.2004

Hayashi, T., Justinova, Z., Hayashi, E., Cormaci, G., Mori, T., Tsai, S. Y., et al. (2010). Regulation of sigma-1 receptors and endoplasmic reticulum chaperones in the brain of methamphetamine self-administering rats. *J. Pharmacol. Exp. Ther.* 332, 1054–1063. doi: 10.1124/jpet.109.159244

Hayashi, T., and Su, T. P. (2007). Sigma-1 receptor chaperones at the ER-mitochondrion interface regulate Ca^{2+} signaling and cell survival. *Cell* 131, 596–610. doi: 10.1016/j.cell.2007.08.036

Hayashi, T., Tsai, S. Y., Mori, T., Fujimoto, M., and Su, T. P. (2011). Targeting ligand-operated chaperone sigma-1 receptors in the treatment of neuropsychiatric disorders. *Expert Opin. Ther. Targets* 15, 557–577. doi: 10.1517/14728222.2011.560837

Heshmati, M., Christoffel, D. J., LeClair, K., Cathomas, F., Golden, S. A., Aleyasin, H., et al. (2020). Depression and social defeat stress are associated with inhibitory synaptic changes in the nucleus accumbens. *J. Neurosci.* 40, 6228–6233. doi: 10.1523/JNEUROSCI.2568-19.2020

Hong, S. I., Kwon, S. H., Hwang, J. Y., Ma, S. X., Seo, J. Y., Ko, Y. H., et al. (2016). Quinpirole increases melatonin-augmented pentobarbital sleep via cortical ERK, p38 MAPK and PKC in mice. *Biomol. Ther. (Seoul)* 24, 115–122. doi: 10.4062/biomolther.2015.097

Hortnagl, H., Tasan, R. O., Wieselthaler, A., Kirchmair, E., Sieghart, W., and Sperk, G. (2013). Patterns of mRNA and protein expression for 12 $GABA_A$

receptor subunits in the mouse brain. *Neuroscience* 236, 345–372. doi: 10.1016/j.neuroscience.2013.01.008

Kabbani, N., Negyessy, L., Lin, R., Goldman-Rakic, P., and Levenson, R. (2002). Interaction with neuronal calcium sensor NCS-1 mediates desensitization of the D2 dopamine receptor. *J. Neurosci.* 22, 8476–8486. doi: 10.1523/JNEUROSCI.22-19-08476.2002

Katnik, C., Guerrero, W. R., Pennypacker, K. R., Herrera, Y., and Cuevas, J. (2006). Sigma-1 receptor activation prevents intracellular calcium dysregulation in cortical neurons during in vitro ischemia. *J. Pharmacol. Exp. Ther.* 319, 1355–1365. doi: 10.1124/jpet.106.107557

Kilkenny, C., Browne, W. J., Cuthill, I. C., Emerson, M., and Altman, D. G. (2012). Improving bioscience research reporting: the ARRIVE guidelines for reporting animal research. *Osteoarthritis Cartilage* 20, 256–260. doi: 10.1016/j.joca.2012.02.010

Kroeger, D., Ferrari, L. L., Petit, G., Mahoney, C. E., Fuller, P. M., Arrigoni, E., et al. (2017). Cholinergic, glutamatergic and GABAergic neurons of the pedunculopontine tegmental nucleus have distinct effects on sleep/wake behavior in mice. *J. Neurosci.* 37, 1352–1366. doi: 10.1523/JNEUROSCI.1405-16.2016

Lalchandani, R. R., van der Goes, M. S., Partridge, J. G., and Vicini, S. (2013). Dopamine D_2 receptors regulate collateral inhibition between striatal medium spiny neurons. *J. Neurosci.* 33, 14075–14086. doi: 10.1523/JNEUROSCI.0692-13.2013

Lan, Y., Bai, P., Chen, Z., Neelamegam, R., Placzek, M. S., Wang, H., et al. (2019). Novel radioligands for imaging sigma-1 receptor in brain using positron emission tomography (PET). *Acta Pharm. Sin. B* 9, 1204–1215. doi: 10.1016/j.apsb.2019.07.002

Li, Y. C., Kellendonk, C., Simpson, E. H., Kandel, E. R., and Gao, W. J. (2011). D2 receptor overexpression in the striatum leads to a deficit in inhibitory transmission and dopamine sensitivity in mouse prefrontal cortex. *Proc. Natl. Acad. Sci. U S A* 108, 12107–12112. doi: 10.1073/pnas.1109718108

Luscher, B., Fuchs, T., and Kilpatrick, C. L. (2011). $GABA_A$ receptor trafficking-mediated plasticity of inhibitory synapses. *Neuron* 70, 385–409. doi: 10.1073/pnas.1109718108

Madronal, N., Gruart, A., Valverde, O., Espadas, I., Moratalla, R., and Delgado-Garcia, J. M. (2012). Involvement of cannabinoid CB1 receptor in associative learning and in hippocampal CA3-CA1 synaptic plasticity. *Cereb. Cortex* 22, 550–566. doi: 10.1093/cercor/bhr103

Maurice, T., Martin-Fardon, R., Romieu, P., and Matsumoto, R. R. (2002). $Sigma_1$ (σ_1) receptor antagonists represent a new strategy against cocaine addiction and toxicity. *Neurosci. Biobehav. Rev.* 26, 499–527. doi: 10.1016/s0149-7634(02)00017-9

Morin-Surun, M. P., Collin, T., Denavit-Saubie, M., Baulieu, E. E., and Monnet, F. P. (1999). Intracellular sigma1 receptor modulates phospholipase C and protein kinase C activities in the brainstem. *Proc. Natl. Acad. Sci. U S A* 96, 8196–8199. doi: 10.1073/pnas.96.14.8196

Mtchedlishvili, Z., and Kapur, J. (2003). A presynaptic action of the neurosteroid pregnenolone sulfate on GABAergic synaptic transmission. *Mol. Pharmacol.* 64, 857–864. doi: 10.1124/mol.64.4.857

Muir, J., Tse, Y. C., Iyer, E. S., Biris, J., Cvetkovska, V., Lopez, J., et al. (2020). Ventral hippocampal afferents to nucleus accumbens encode both latent vulnerability and stress-induced susceptibility. *Biol. Psychiatry* 88, 843–854. doi: 10.1016/j.biopsych.2020.05.021

Nakai, T., Nagai, T., Wang, R., Yamada, S., Kuroda, K., Kaibuchi, K., et al. (2014). Alterations of GABAergic and dopaminergic systems in mutant mice with disruption of exons 2 and 3 of the Disc1 gene. *Neurochem. Int.* 74, 74–83. doi: 10.1016/j.neuint.2014.06.009

Nakamura, Y., Darnieder, L. M., Deeb, T. Z., and Moss, S. J. (2015). Regulation of $GABA_A$Rs by phosphorylation. *Adv. Pharmacol.* 72, 97–146. doi: 10.1016/bs.apha.2014.11.008

Nicola, S. M., Surmeier, J., and Malenka, R. C. (2000). Dopaminergic modulation of neuronal excitability in the striatum and nucleus accumbens. *Annu. Rev. Neurosci.* 23, 185–215. doi: 10.1146/annurev.neuro.23.1.185

Pan, L., Pasternak, D. A., Xu, J., Xu, M., Lu, Z., Pasternak, G. W., et al. (2017). Isolation and characterization of alternatively spliced variants of the mouse sigma1 receptor gene, Sigmar1. *PLoS One* 12:e174694. doi: 10.1371/journal.pone.0174694

Paxinos, G., and Franklin, K. B. J. (2001). *The Mouse Brain In Stereotaxic Coordinates.* San Diego, CA: Academic Press.

Pozdnyakova, N., Krisanova, N., Dudarenko, M., Vavers, E., Zvejniece, L., Dambrova, M., et al. (2020). Inhibition of sigma-1 receptors substantially modulates GABA and glutamate transport in presynaptic nerve terminals. *Exp. Neurol.* 333:113434. doi: 10.1016/j.expneurol.2020.113434

Ryskamp, D., Wu, J., Geva, M., Kusko, R., Grossman, I., Hayden, M., et al. (2017). The $sigma_1$ receptor mediates the beneficial effects of pridopidine in a mouse model of Huntington disease. *Neurobiol. Dis.* 97, 46–59. doi: 10.1016/j.nbd.2016.10.006

Sabino, V., Cottone, P., Parylak, S. L., Steardo, L., and Zorrilla, E. P. (2009). Sigma-1 receptor knockout mice display a depressive-like phenotype. *Behav. Brain Res.* 198, 472–476. doi: 10.1016/j.bbr.2008.11.036

Schwarzer, C., Berresheim, U., Pirker, S., Wieselthaler, A., Fuchs, K., Sieghart, W., et al. (2001). Distribution of the major γ-aminobutyric $acid_A$ receptor subunits in the basal ganglia and associated limbic brain areas of the adult rat. *J. Comp. Neurol.* 433, 526–549. doi: 10.1002/cne.1158

Sesack, S. R., and Grace, A. A. (2010). Cortico-basal ganglia reward network: microcircuitry. *Neuropsychopharmacology* 35, 27–47. doi: 10.1038/npp.2009.93

Sha, S., Hong, J., Qu, W.-J., Lu, Z.-H., Li, L., Yu, W.-F., et al. (2015). Sex-related neurogenesis decrease in hippocampal dentate gyrus with depressive-like behaviors in sigma-1 receptor knockout mice. *Eur. Neuropsychopharmacol.* 25, 1275–1286. doi: 10.1016/j.euroneuro.2015.04.021

Sha, S., Qu, W.-J., Li, L., Lu, Z.-H., Chen, L., Yu, W.-F., et al. (2013). Sigma-1 receptor knockout impairs neurogenesis in dentate gyrus of adult hippocampus via down-regulation of NMDA receptors. *CNS Neurosci. Ther.* 19, 705–713. doi: 10.1111/cns.12129

Vollenweider, I., Smith, K. S., Keist, R., and Rudolph, U. (2011). Antidepressant-like properties of α2-containing $GABA_A$ receptors. *Behav. Brain Res.* 217, 77–80. doi: 10.1016/j.bbr.2010.10.009

Wang, W., Sun, D., Pan, B., Roberts, C. J., Sun, X., Hillard, C. J., et al. (2010). Deficiency in endocannabinoid signaling in the nucleus accumbens induced by chronic unpredictable stress. *Neuropsychopharmacology* 35, 2249–2261. doi: 10.1038/npp.2010.99

White, A. O., Kramar, E. A., Lopez, A. J., Kwapis, J. L., Doan, J., Saldana, D., et al. (2016). BDNF rescues BAF53b-dependent synaptic plasticity and cocaine-associated memory in the nucleus accumbens. *Nat. Commun.* 7:11725. doi: 10.1038/ncomms11725

Yang, J., Harte-Hargrove, L. C., Siao, C. J., Marinic, T., Clarke, R., Ma, Q., et al. (2014). proBDNF negatively regulates neuronal remodeling, synaptic transmission and synaptic plasticity in hippocampus. *Cell Rep.* 7, 796–806. doi: 10.1016/j.celrep.2014.03.040

Yang, R., Zhou, R., Chen, L., Cai, W., Tomimoto, H., Sokabe, M., et al. (2011). Pregnenolone sulfate enhances survival of adult-generated hippocampal granule cells via sustained presynaptic potentiation. *Neuropharmacology* 60, 529–541. doi: 10.1016/j.neuropharm.2010.11.017

Yao, L., Fan, P., Jiang, Z., Gordon, A., Mochly-Rosen, D., and Diamond, I. (2008). Dopamine and ethanol cause translocation of epsilonPKC associated with epsilonRACK: cross-talk between cAMP-dependent protein kinase A and protein kinase C signaling pathways. *Mol. Pharmacol.* 73, 1105–1112. doi: 10.1124/mol.107.042580

Zhang, T., Chen, T., Chen, P., Zhang, B., Hong, J., and Chen, L. (2017). MPTP-induced dopamine depletion in basolateral amygdala via decrease of D2R activation suppresses $GABA_A$ receptors expression and LTD induction leading to anxiety-like behaviors. *Front. Mol. Neurosci.* 10:247. doi: 10.3389/fnmol.2017.00247

Zhang, Y., Gui, H., Hu, L., Li, C., Zhang, J., and Liang, X. (2021). Dopamine D1 receptor in the NAc shell is involved in delayed emergence from isoflurane anesthesia in aged mice. *Brain Behav.* 11:e1913. doi: 10.1002/brb3.1913

Zhang, S., Hong, J., Zhang, T., Wu, J., and Chen, L. (2017). Activation of sigma-1 receptor alleviates postpartum estrogen withdrawal-induced "Depression" through restoring hippocampal nNOS-NO-CREB activities in mice. *Mol. Neurobiol.* 54, 3017–3030. doi: 10.1007/s12035-016-9872-8

Zhang, B., Wang, L., Chen, T., Hong, J., Sha, S., Wang, J., et al. (2017). Sigma-1 receptor deficiency reduces GABAergic inhibition in the basolateral amygdala leading to LTD impairment and depressive-like behaviors. *Neuropharmacology* 116, 387–398. doi: 10.1016/j.neuropharm.2017.01.014

Zhang, X., Yao, N., and Chergui, K. (2016). The $GABA_A$ receptor agonist muscimol induces an age- and region-dependent form of long-term depression in the mouse striatum. *Learn. Mem.* 23, 479–485. doi: 10.1101/lm.043190.116

Zhou, L., Yin, J., Wang, C., Liao, J., Liu, G., and Chen, L. (2014). Lack of seipin in neurons results in anxiety- and depression-like behaviors via down regulation of PPARγ. *Hum. Mol. Genet.* 23, 4094–4102. doi: 10.1093/hmg/ddu126

frontiers | Frontiers in Molecular Neuroscience

TYPE Original Research
PUBLISHED 13 October 2022
DOI 10.3389/fnmol.2022.856262

OPEN ACCESS

EDITED BY
Jean Christophe Poncer,
Institut National de la Santé et de la Recherche Médicale (INSERM), France

REVIEWED BY
Marianne Renner,
Sorbonne Universités, France
Vivek Mahadevan,
National Institutes of Health (NIH), United States

*CORRESPONDENCE
Atsuo Fukuda
axfukuda@hama-med.ac.jp

SPECIALTY SECTION
This article was submitted to Neuroplasticity and Development, a section of the journal Frontiers in Molecular Neuroscience

RECEIVED 17 January 2022
ACCEPTED 22 September 2022
PUBLISHED 13 October 2022

CITATION
Sinha AS, Wang T, Watanabe M, Hosoi Y, Sohara E, Akita T, Uchida S and Fukuda A (2022) WNK3 kinase maintains neuronal excitability by reducing inwardly rectifying K^+ conductance in layer V pyramidal neurons of mouse medial prefrontal cortex.
Front. Mol. Neurosci. 15:856262.
doi: 10.3389/fnmol.2022.856262

WNK3 kinase maintains neuronal excitability by reducing inwardly rectifying K^+ conductance in layer V pyramidal neurons of mouse medial prefrontal cortex

Adya Saran Sinha[1], Tianying Wang[1], Miho Watanabe[1], Yasushi Hosoi[1], Eisei Sohara[2], Tenpei Akita[1], Shinichi Uchida[2] and Atsuo Fukuda[1]*

[1]Department of Neurophysiology, Hamamatsu University School of Medicine, Hamamatsu, Japan, [2]Department of Nephrology, Graduate School of Medical and Dental Sciences, Tokyo Medical and Dental University, Tokyo, Japan

The with-no-lysine (WNK) family of serine-threonine kinases and its downstream kinases of STE20/SPS1-related proline/alanine-rich kinase (SPAK) and oxidative stress-responsive kinase-1 (OSR1) may regulate intracellular Cl^- homeostasis through phosphorylation of cation-Cl^- co-transporters. WNK3 is expressed in fetal and postnatal brains, and its expression level increases during development. Its roles in neurons, however, remain uncertain. Using WNK3 knockout (KO) mice, we investigated the role of WNK3 in the regulation of the intracellular Cl^- concentration ($[Cl^-]_i$) and the excitability of layer V pyramidal neurons in the medial prefrontal cortex (mPFC). Gramicidin-perforated patch-clamp recordings in neurons from acute slice preparation at the postnatal day 21 indicated a significantly depolarized reversal potential for $GABA_A$ receptor-mediated currents by 6 mV, corresponding to the higher $[Cl^-]_i$ level by ∼4 mM in KO mice than in wild-type littermates. However, phosphorylation levels of SPAK and OSR1 and those of neuronal Na^+-K^+-$2Cl^-$ co-transporter NKCC1 and K^+-Cl^- co-transporter KCC2 did not significantly differ between KO and wild-type mice. Meanwhile, the resting membrane potential of neurons was more hyperpolarized by 7 mV, and the minimum stimulus current necessary for firing induction was increased in KO mice. These were due to an increased inwardly rectifying K^+ (IRK) conductance, mediated by classical inwardly rectifying (Kir) channels, in KO neurons. The introduction of an active form of WNK3 into the recording neurons reversed these changes. The potential role of KCC2 function in the observed changes of KO neurons was investigated by applying a selective KCC2 activator, CLP290. This reversed the enhanced IRK conductance in KO neurons, indicating that both WNK3 and KCC2 are intimately linked in the regulation of resting K^+ conductance. Evaluation of synaptic properties revealed that the frequency of miniature excitatory postsynaptic currents (mEPSCs) was reduced, whereas that of inhibitory currents (mIPSCs) was slightly increased in KO neurons. Together, the impact of these developmental changes on the membrane and synaptic properties

was manifested as behavioral deficits in pre-pulse inhibition, a measure of sensorimotor gating involving multiple brain regions including the mPFC, in KO mice. Thus, the basal function of WNK3 would be the maintenance and/or development of both intrinsic and synaptic excitabilities.

KEYWORDS

WNK3 kinase, brain development, chloride homeostasis, neuronal excitability, inwardly rectifying K^+ channel, KCC2

Introduction

The with-no-lysine (WNK) kinase subfamily of serine/threonine kinases is characterized by the absence of the critical ATP-binding lysine residue in the subdomain II of these kinases. Instead, the kinase function is mediated by a lysine residue in subdomain I (Xu et al., 2000). In mammals, the WNK family of kinases comprises four gene products (WNK1-WNK4) with defined spatiotemporal expression patterns (reviewed in McCormick and Ellison, 2011). Though pleiotropic in their functions, the primary physiological role ascribed to the WNK family is its phosphorylation of downstream signaling cascades integral to the maintenance of Cl^- homeostasis (Alessi et al., 2014). In neurons, intracellular Cl^- concentrations ($[Cl^-]_i$) are critical for neuronal excitability (Blaesse et al., 2009; Raimondo et al., 2017) and cell volume regulation (Akita and Okada, 2014; Huang et al., 2019). It was first reported that WNK1 phosphorylates downstream SPS1-related proline/alanine-rich kinase (SPAK) and its homolog oxidative stress-responsive kinase (OSR1) (Moriguchi et al., 2005). These kinases catalyze post-translational phosphorylation of cation-Cl^- co-transporters. The phosphorylation of residues Thr^{212} and Thr^{217} of human Na^+-K^+-$2Cl^-$ co-transporter (NKCC1) increases its activation leading to intracellular Cl^- accumulation (Flemmer et al., 2002; Kahle et al., 2005). In striking contrast, activation of the WNK- SPAK/OSR1 cascade inhibits neuron-specific K^+-Cl^- co-transporter (KCC2) by phosphorylation of residues Thr^{906} and Thr^{1007} in immature neurons (Inoue et al., 2012). Perinatally, the WNK/SPAK-OSR1 cascade exerts tight control on the relative functionalities of NKCC1 and KCC2 to set the level of Cl^- (Kahle et al., 2013). The Cl^- reported around this period is ~30 mM (Achilles et al., 2007). The significance of Cl^- values is that it determines the equilibrium potential (E_{Cl}) of Cl^-. Therefore, E_{Cl} values positive to resting membrane potential (RMP) cause depolarizing action of the neurotransmitter γ -aminobutyric acid (GABA) on binding to ligand-gated Cl^- channels ($GABA_A$ receptors) in immature neurons (Ben-Ari, 2002). However, at later time points when E_{Cl} values are more negative to RMP, the classical hyperpolarizing action of GABA is observed (Yamada et al., 2004). This dependence on E_{Cl} also underlies the initial excitatory action mediated through glycine receptors (GlyR) during cortical development (Flint et al., 1998) and subsequent inhibitory neurotransmission after maturation. Thus, the regulatory changes affecting E_{Cl} prompting the remarkable switch from excitation to inhibition mediated by both $GABA_A$Rs and GlyRs, represents a key event in the developmental trajectory of the brain. Accordingly, this posits the role of the WNK-SPAK/OSR1 cascade to be of utmost importance during brain development (Watanabe and Fukuda, 2015).

More recent investigations on the role of WNK kinases in neurons have confirmed WNK1 kinase functioning as a Cl^- sensor (Piala et al., 2014). The binding of Cl^- inactivates WNK1 by inhibiting its autophosphorylation. Recent experiments have revealed that WNK1 forms a physical complex with KCC2 (Friedel et al., 2015) and confirmed inhibitory phosphorylation of C-terminal threonine residues ($Thr^{906/1007}$) restricting KCC2 activity. Furthermore, constitutive phosphorylation of these threonine residues ($KCC2^{T906E/T1007E}$) in a mice model caused early postnatal death due to respiratory arrest (Watanabe et al., 2019). These accumulating evidences underline the importance of WNK1 in normal brain development. Surprisingly, given its importance, the only pathology of nervous tissue associated with WNK1 are rare forms of hereditary sensory and autonomic neuropathy (Lafreniere et al., 2004).

On the contrary, mounting evidence from clinics indicates another member of the WNK family, WNK3, to be associated with diverse pathologies of the central nervous system. In brief, the expression of WNK3 transcripts was found to be significantly higher in the prefrontal cortex (PFC) area of subjects with schizophrenia (Arion and Lewis, 2011). Furthermore, an increase in WNK3 was reported from dispersed granule cells of subjects presenting a pathology of hippocampal sclerosis associated with mesial temporal lobe epilepsy (Jeong et al., 2018). Incidentally, WNK3 loci are on the X-chromosome (Holden et al., 2004) and within the critical linkage zone associated with several monogenic intellectual disability disorders. In fact, one report (Qiao et al., 2008) correlates microdeletion of this region Xp11.22 with autistic behavioral phenotype. More recently, using exome sequencing analysis, multiple pathogenic missense variants for WNK3 were identified (Küry et al., 2022). All the

individuals were affected with developmental delay and showed intellectual disability with 38% of them exhibiting epilepsy. Surprisingly, all these rare variants are predicted to cause loss of function of WNK3. In the fetal brain, strong expression of WNK3 mRNA transcripts was observed. Subsequently, expression was observed to be weak around postnatal day 7 with transcripts almost undetectable by postnatal day 10. Following this period, the WNK3 expression increased again plateauing around postnatal day 21 (Kahle et al., 2005). This increase of WNK3 transcripts from postnatal day 10 to 21 leads to earlier reports drawing parallels with the KCC2 expression pattern (Lu et al., 1999; Kahle et al., 2005, 2013). However, a more recent report (Küry et al., 2022) indicates that postnatal period WNK3 levels are significantly lower in comparison to their fetal expression levels. In addition, it has also been observed that the expression level of WNK1 is 10-fold higher than that observed in WNK3 postnatally (Heubl et al., 2017). Therefore, comparisons of expression patterns of WNK3 and KCC2 commencing from early development to the postnatal period actually are divergent (Küry et al., 2022). The earliest investigation (Kahle et al., 2005) probing the physiological role of WNK3 earmarks it as a key effector of Cl^--dependent volume regulation. This result was supported by recent experimental findings using stroke models as below. While activated WNK3 function exacerbates brain injury after cerebral hemorrhage (Wu et al., 2020), either inhibition of WNK3 function (Begum et al., 2015) or deletion of WNK3-SPAK complex reduced brain damage and accelerated neurological recovery (Zhao et al., 2017). Furthermore, its pleiotropic nature was revealed by biochemical investigations reporting WNK3-dependent suppression of neuronal splicing factor Rbfox1 (Lee et al., 2012). Interestingly, Rbfox1 is a nodal point in the signaling pathways altered in autistic brains (Voineagu et al., 2011) and implicated in synaptic dysfunctions (Gehman et al., 2011; Lee et al., 2016).

Based on these findings, it is probable that WNK3 plays an important role during fetal development and postnatally affects neuronal excitability during brain development. We therefore used a constitutive WNK3 knockout (KO) mouse (Oi et al., 2012) and investigated this possibility. Our results suggest that WNK3 in pyramidal neurons plays a more critical role in the maintenance of neuronal excitability by reducing resting membrane K^+ conductance and increasing the number of excitatory synaptic inputs. It also impacts ionic plasticity albeit weakly by regulating intracellular Cl^- homeostasis. The impact of these developmental changes in membrane and synaptic properties of pyramidal neurons in WNK3 KO mice together with yet uninvestigated changes in other neuronal subtypes and cells alters information processing in the mPFC. Together, these changes manifested as behavioral deficits in pre-pulse inhibition, a measure of sensorimotor gating involving multiple brain regions including the mPFC. Thus, the basal function of WNK3 would be the maintenance and/or development of both intrinsic and synaptic excitabilities.

Materials and methods

WNK3 knockout mice

The WNK3 knockout mice were generated as explained earlier elsewhere (Oi et al., 2012). In brief, the Cre-Lox recombination system was used to target the WNK3 gene for deletion. Experimental mice were generated by mating $WNK3^{+/-}$ heterozygous female mice with male (>10 weeks) $WNK3^{-/-}$ mice to obtain both constitutive knockout (KO) and wild-type (WT) littermates. All experiments were planned to minimize the number of animals used. The procedures used were in accordance with the guidelines issued by the Hamamatsu University School of Medicine and were approved by the Committee for Animal Care and Use (No. 2018048).

Slice preparation

Postnatal day (P) 21–27 old male mice comprising WNK3 KO and WT littermate were anesthetized with 50–90 mg/Kg intraperitoneal injection (i. p.) of pentobarbital and cardially perfused with ice-cold oxygenated, modified artificial cerebrospinal fluid (ACSF; in mM, 220 sucrose, 2.5 KCl, 1.25 NaH_2PO_4, 2.0 $MgSO_4$, 0.5 $CaCl_2$, 26.0 $NaHCO_3$, and 30.0 glucose at pH 7.4). After perfusion, the mice were decapitated, and the brains were quickly dissected out. Coronal slices containing the prefrontal cortex with a thickness of 350 μm were prepared in modified ACSF using a vibratome (Campden Instruments, Loughborough, Leicestershire, UK). Slices were allowed to recover for 60 min on nylon meshes (with 1 mm pores) placed on dishes and submerged in standard ACSF consisting of (in mM) 126 NaCl, 2.5 KCl, 1.25 NaH_2PO_4, 2.0 $MgSO_4$, 2.0 $CaCl_2$, 26.0 $NaHCO_3$, and 20.0 glucose, with osmolarity value of 310-312 mOsm and saturated with 95% O_2 and 5% CO_2 at room temperature (RT).

Solutions for recordings

All recordings were performed in standard ACSF as bath solution at RT. The electrode was filled with solutions of different compositions depending on the experiments performed. Current-clamp recordings for evaluation of passive and active properties were performed using an internal solution containing (in mM) 140.0 potassium methane sulfonate (CH_3SO_3K), 10.0 KCl, 2.0 $MgCl_2$, 10.0 HEPES, 3.0 Na_2-ATP, 0.2 Na-GTP, and 1.0 EGTA with pH adjusted to 7.3 with KOH and osmolarity value of 310 mOsm. The liquid junction potential (LJP) was calculated to be 4.8 mV and was corrected during recordings. Recordings were performed in the presence of

bath-applied ionotropic glutamate receptor blockers, 10 μM 6-cyano-7-nitroquinoxaline-2,3-dione (CNQX), 50 μM 2-amino-5-phosphonopentanoic acid (D-AP5), and 50 μM picrotoxin (PTX, Tocris), a $GABA_A$ receptor antagonist. Miniature excitatory post-synaptic currents (mEPSCs) were recorded using the same internal solution with bath-applied 50 μM PTX and 0.5 μM TTX (Tetrodotoxin, Wako). The Ba^{2+}-sensitive inward rectifier currents were isolated in the presence of 200 μM $BaCl_2$-$2H_2O$ and 1 μM TTX. In a subset of experiments for recording inward rectifier potassium conductance (IRK), the active form of WNK3 kinase (Eurofins) was dissolved in the CH_3SO_3K-based normal Cl^- internal solution. The final concentration of the WNK3 active peptide fragment in the internal solution was 3.4 ng/μl. In addition, to investigate the role of KCC2 function on IRK conductance, we used KCC2 antagonist [(dihydroindenyl)oxy] acetic acid (DIOA, Sigma) dissolved in DMSO. A final concentration of 30 μM in the internal solution was used. This strategy was utilized to reduce the off-target effects of DIOA, as a recent report (Chi et al., 2021) suggests the binding of DIOA closer to the CTD region of KCC2 transmembrane assembly. After whole-cell patch-clamp recordings, we allowed a period of 20 min for DIOA action all the while monitoring for stable recording. The effect of antagonizing KCC2 function on WT neurons was evaluated by a subsequent application of Ba^{2+} block and IRK current recordings. To investigate if KCC2 membrane expression and stability exerted an effect on IRK currents as reported earlier (Goutierre et al., 2019), we incubated acute mPFC slices from both WT and KO mice with selective KCC2 activator drug CLP 290 (30 μM) for 1 h at 30–32°C. This was followed by recording Ba^{2+}-sensitive IRK currents. For recording miniature inhibitory post-synaptic currents (mIPSCs), a high [Cl^-] internal solution of the following composition (in mM) was used: 150.0 CsCl, 2.0 $MgCl_2$, 10.0 HEPES, 3.0 Na_2-ATP, 0.2 Na-GTP, and 1.0 EGTA with pH adjusted to 7.3 with CsOH and osmolarity of 305 mOsm. The E_{Cl} was calculated to be −3.9 mV. The corresponding calculated LJP value of 4.6 mV was corrected during recordings. The bath solution contained 10 μM CNQX, 50 μM D-AP5, and 0.5 μM TTX. For estimation of $[Cl^-]_i$, gramicidin-perforated patch-clamp recordings were performed. The electrode solution comprised 150.0 mM KCl and 10.0 mM HEPES with pH adjusted to 7.3 using KOH. On the day of the experiment, gramicidin (Sigma) was dissolved in solvent methanol to obtain a stock. Subsequently, aliquots of this stock were used every 2 h and added to a fresh aliquot of KCl-based internal solution with a final concentration of 50 μg/ml gramicidin in the electrode solution. To the bath solution, excitatory synaptic blockers CNQX (10 μM) and D-AP5 (50 μM) were added. In addition, TTX (1 μM) and CGP55845 (3 μM) were applied to block Na^+-dependent action potentials and $GABA_B$ receptors, respectively. The calculated LJP of −3.6 mV was not corrected, as it was negated by the E_K of approximately +4 mV owing to the higher K^+ ion concentration in the electrode solution in comparison to that of the cytosol (Kim and Trussell, 2007).

Whole-cell patch-clamp recordings

Slices thus obtained were then transferred to an imaging chamber on the stage of an upright microscope (BX51WI; Olympus Tokyo, Japan) and continuously perfused with oxygenated standard ACSF at a flow rate of 2 mL/min at RT. The electrode resistance ranged from 3 to 5 MΩ. Whole-cell patch-clamp recordings were made from layer V pyramidal neurons of the medial prefrontal cortex (mPFC). The neurons were identified based on their pyramidal shape and long apical dendrites. The soma was located at a distance of >500 μm from the medial midline. Voltage changes were recorded by a multiclamp 700B amplifier (Axon Instruments, Sunnyvale, CA, USA) with a Bessel pre-filter at 5 kHz and digitized at 25 kHz using a Digidata 1440A data-acquisition system (Axon instruments, Sunnyvale, CA, USA).

For current-clamp recordings to study passive and active properties, step current injections of Δ 20 pA starting from −60 pA to +540 pA with a duration of 1,000 ms were made. A short pulse (2 ms) protocol for eliciting single action potential (AP) was used for the evaluation of the AP waveform. The bridge balance circuit was applied while recording the voltage changes. Voltage clamp recordings were performed for evaluating synaptic physiology. In brief, both mIPSCs and mEPSCs were recorded at a holding voltage ($\mathbf{V_H}$) of −70 mV using the aforementioned internal solutions. Voltage steps for isolating inward rectifying K^+ (IRK) currents were of 500 ms duration starting from $\mathbf{V_H}$ of −50 mV to −120 mV with a step size of Δ10 mV. The series resistance ($\mathbf{R_S}$) compensation circuit was applied at 70% during recordings. Recordings from neurons with R_s exceeding 25 MΩ were not used. The GABA reversal potential (E_{GABA}) measurements were performed from layer V pyramidal neurons at P 21 by using the gramicidin-perforated patch-clamp technique. In brief, the tip of the patch electrodes was filled by capillary action with a gramicidin-free KCl-based solution as described above. The gramicidin-containing electrode solution was back-filled. This allowed the formation of tight gigaseal >8 GΩ. In 1–1.15 h, the gramicidin diffused forming perforations on the neuronal membrane such that Rs changed to <100 MΩ. An additional 10 min were allowed to confirm a stable recording condition. Starting from a set voltage of −60 mV ($\mathbf{V_H}$), a voltage ramp of 300 ms long from −90 mV to −30 mV was applied. Matched with the ramp protocol, a 300 μM GABA puff was applied for a duration of 1 s. The holding current levels immediately before and after the voltage ramp were unchanged. The R_s compensation at 70% was applied. Each measurement was repeated two times following an interval of 5 min, and if the differences in the obtained E_{GABA} values were > ±1 mV, the data were discarded.

Electrophysiological analysis

The data were acquired using a pCLAMP suite comprising Clampex 10.7 for acquisition, and analysis was performed using Clampfit 10.4 software. In brief, to evaluate the input resistance ($\mathbf{R}_{In}$) of neurons recorded, small hyperpolarizing current injections of 1,000 ms duration were applied starting from −60 pA. The voltage responses obtained were plotted to their corresponding current injection amplitudes to generate current-voltage relationships. The data points were subsequently fitted by linear regression analysis. The calculated slope value indicated the $\mathbf{R}_{In}$ of the recorded neuron. The membrane time constant ($\boldsymbol{\tau}_m$) was estimated by the single exponential fitting of the membrane charge phase in response to the −40 pA current injection. The cell capacitance (C_m) value was thereafter calculated from the relationship ($\boldsymbol{\tau}_m = C_m R_m$). The rheobase current, i.e., the current injection at which the neuron fired a single AP was estimated by applying depolarizing current steps 1,000 ms long with step increments of 20 pA. Single APs were elicited by the application of a short (2 ms) depolarizing pulse protocol, and its waveform parameters like AP amplitude, half-width, maximum rise, and decay slope were analyzed. Resting membrane potential (RMP) was calculated from traces at zero current injection (I = 0) levels preceding the application of the short pulse protocol. AP amplitude was calculated from RMP to AP peak voltage. AP threshold voltages were determined by phase plane plot analysis. Furthermore, repetitive AP firing elicited by depolarizing current steps was used to investigate the spike number output to current injection relationship (I-O curves) of recorded neurons. In addition, a comparison of frequency-current injection (F/I) plots (number of spikes at 1X, 2X, and 3X rheobase currents) was used to evaluate gain. Adaption parameters of repetitive firing were compared between groups at 3X rheobase currents. In brief, all parameters were compared by normalizing to the first AP evoked during a spike train. AP amplitude values were calculated from threshold voltage to peak amplitudes for adaptation parameters. The E_{GABA} values were calculated as voltage values at which the $GABA_A$ receptor-mediated current reverses direction and ascertained the intersection of current responses' before and during 300 μM GABA puff application. The voltage shifts due to 30% of uncompensated R_s were corrected to calculate the exact values. For each cell, the E_{GABA} values were calculated from an average of two repeated measurements. In addition, approximate internal chloride concentrations were back-calculated using the Nernst equation.

Analysis of mIPSC events was performed using the threshold-based event detection suite of clampfit. A single epoch of 60 s was selected for analysis. The threshold was set at three times the standard deviation (3 S.D.) of the baseline noise. Likewise, an analysis of mEPSCs was performed. Analysis of IRK currents was performed by subtracting current responses in the presence of Ba^{2+} block from control responses to voltage commands. I-V plots were constructed for different treatments and compared.

Immunoblotting

Under deep anesthesia, mPFC was removed, homogenized, and lysed in a buffer containing 50 mM Tris-HCl (pH 7.5), 150 mM NaCl, 1% (v/v), Triton X-100, 5 mM EDTA, protease inhibitors (Roche complete protease inhibitor cocktail tablets, 1 tablet per 50 ml), and phosphatase inhibitor cocktail 3 (P0044, Sigma). Tween–tris-buffered saline (TTBS) contained 50 mM Tris-HCl (pH 7.5), 0.15 M NaCl, and 0.1% (v/v) Tween 20. A 2x SDS sample buffer consisted of 0.1 M Tris-HCl, pH 6.8, 4% SDS, 20% glycerol, 1% (v/v) 2-mercaptoethanol, and 0.01% bromphenol blue. After centrifugation at 12,000 g for 10 min at 4 °C, supernatants were collected, and protein concentration was determined using the Bradford method with bovine serum albumin (BSA) as the standard. Aliquots of 30 μg of protein were mixed with sample buffer and boiled at 95 °C for 10 min. Samples were resolved by SDS-polyacrylamide gel electrophoresis and transferred to polyvinylidene difluoride membranes. The membranes were incubated for 1 h with blocking buffer containing 3% (w/v) BSA in TTBS and then immunoblotted in blocking buffer with indicated primary antibodies overnight at 4°C. Blots were probed with antibodies to WNK1 phospho-Ser-382, total WNK1, SPS1-related proline/alanine-rich kinase (SPAK) phospho-Ser-373, total SPAK, total oxidative stress response 1 (OSR1), NKCC1, NKCC1 phospho-Thr-206, KCC2, and actin, and then detected using HRP-conjugated secondary antibodies and an ECL kit (Amersham Biosciences). The amount of protein loaded was monitored by immunoblotting for actin. The KCC2 antibody (1:1,000) was purchased from Millipore and the actin antibody (1:10,000) from Sigma. NKCC1 phospho-Thr-206 antibody (1:400) was previously reported (Yang et al., 2010). The remaining antibodies used for Western blots were raised in sheep and affinity-purified on the appropriate antigen and were kindly provided by Dr. Alessi, University of Dundee. Antibodies prepared in sheep were used at a concentration of 1 μg/ml. The incubation with phosphorylation site-specific sheep antibodies was performed with the addition of 10 μg/ml of the non-phosphorylated peptide antigen used to raise the antibody. In order to evaluate the phosphorylation levels of KCC2 at the residue Thr1007, cortical tissue was homogenized in ice-cold lysis buffer containing 50 mM Tris-HCl, pH 7.5, 150 mM NaCl, 1% Nonidet P40, and 0.5% sodium deoxycholate, supplemented with protease inhibitor mixture (Roche) and phosphatase inhibitor cocktail 3 (Sigma-Aldrich). The lysates were centrifuged at 12,000 g for 10 min at 4°C. Immunoprecipitation was performed using the immunoprecipitation kit (Roche) according to the manufacturer's protocol. Briefly, 3.5 mg of lysate was

precipitated with 5 μg of phospho-specific KCC2 antibody (Dundee) in the presence of 10 μg of the dephosphorylated form of the phosphopeptide antigen for 1 h at 4°C followed by incubation with protein G-Sepharose overnight at 4°C. The immunoprecipitates were washed in triplicate with the above buffer solution before being diluted in the SDS sample buffer and analyzed by immunoblotting using the KCC2 antibody. Relative intensities of immunoblot bands were determined using densitometry analysis with ImageJ software, and expression levels were compared between the groups as fold changes against actin. The phosphorylated KCC2 band intensity was normalized to the KCC2 band intensity.

Behavioral test

A series of behavioral assays were conducted with male mice aged 8–10 weeks. The mice weighed 20 ± 2 g [$n = 8$(WT) and 4(WNK3KO)] on average at the beginning of the tests.

Open field test

The apparatus used consisted of a square base (42 × 40 cm) surrounded by a 22 cm wall. The testing arena was divided into 16 squares. The "border" is defined as the 12 outer periphery squares and the "center" as the 4 central squares. Each mouse was placed individually in the center of the open-field apparatus. Testing was conducted over 5 min and recorded with the detection of multiple body points (nose, middle, and tail) of the mice using a video tracking system (SMART v3.0; Panlab/Harvard Apparatus, Barcelona, Spain). The walls and floors of the apparatus were cleaned thoroughly with 10% ethanol between tests. The total distance and the time spent in the center were calculated.

Social interaction and social recognition memory test

The three-chamber test of social interaction and social novelty recognition was performed as described previously (Silverman et al., 2010) with a slight modification. The apparatus consisted of three compartments (40 × 20 × 22 cm) made of clear plexiglass, each separated by side doors. The social communication activities were also measured by using the SMART video tracking system. The task included four sessions. In the first session, a test mouse was habituated to the center chamber for 5 min. In the second session, a test mouse was allowed to explore all three chambers for 10 min. Before the third session, an unfamiliar mouse (Stranger 1, S1) was placed in a steel cage (11 cm D × 25 cm H) enclosure in the left or right chamber, chosen randomly to avoid side preference. In the third session, the subject mouse was allowed to explore all three chambers and cages. Social interaction was determined by measuring the length of time spent by the test mouse exploring the chamber holding the unfamiliar Stranger 1 vs. the empty chamber (E). To measure the social novelty, a new unfamiliar mouse (Stranger 2, S2) was placed in the steel enclosure in the previously empty chamber, and the existing unfamiliar Stranger 1 was retained in the same chamber. The experimental mouse was left to freely explore the chambers for 10 min. The amount of time spent by the test mouse for exploring the chamber containing the familiar Stranger 1 and the novel unfamiliar Stranger 2 mouse was measured to determine the social memory or social novelty. The preference index (%) was calculated from the time spent as (S1 – E)/(S1 + E) × 100 for social interaction, where E denotes empty cage, and (S2 – S1)/(S2 + S1) × 100 for social novelty recognition. The apparatus was cleaned with 70% ethanol between each trial.

Pre-pulse inhibition test

Pre-pulse inhibition (PPI) experiments were conducted with a Panlab System (San Diego Instruments, Inc., San Diego, CA). Each PPI session began with a 5 min habituation period (no stimuli). The test sessions consisted of a series of 5 pulse-only trials (120 dB) for habituation purposes followed by six repetitions of a 9 trial block for a total of 59 trials. The nine trial types included one blank trial (no stimuli), two startle pulse (110 and 120 dB; 40 ms) trials, two pre-pulse (74 and 78 dB; 40 ms) trials, and four pre-pulse + pulse trials [74/78 dB (40 ms) + 110/120 dB (40ms)] and were pseudo-randomized with a 10–20s inter-trial variable interval. All tests were fully computerized by the PACKWIN v2.0 software package (Panlab/Harvard Apparatus, Barcelona Spain). PPI was calculated as a percent score (% PPI) using the following formula: 1–(average startle response on prepulse + pulse trials/average startle response on pulse-alone trials) ×100.

Statistical analysis

For analysis of data obtained by patch-clamp experiments, statistical analysis was performed using IBM SPSS Ver.23 software. In brief, data were tested for normality using the *Kolmogorov–Smirnov* (K-S) test, upon both non-significant K-S statistic and *Levene's statistic* confirming normal distribution and equality of variance, respectively. Independent samples *t-test* was used for comparison of the two groups. However, if the K-S statistic confirmed non-normal distribution, then for two groups *Mann–Whitney U test* and for multiple groups *Kruskal–Wallis test* followed by *post-hoc* stepwise stepdown test was employed. Distributions of miniature events from WT and WNK3 KO were compared by the K-S test. Data are presented as the mean ± standard error of the mean (SEM). Statistical significance was presented using the following rules: $^{*}P < 0.05$, $^{**}P < 0.01$, $^{***}P < 0.001$, and ns represents not significant.

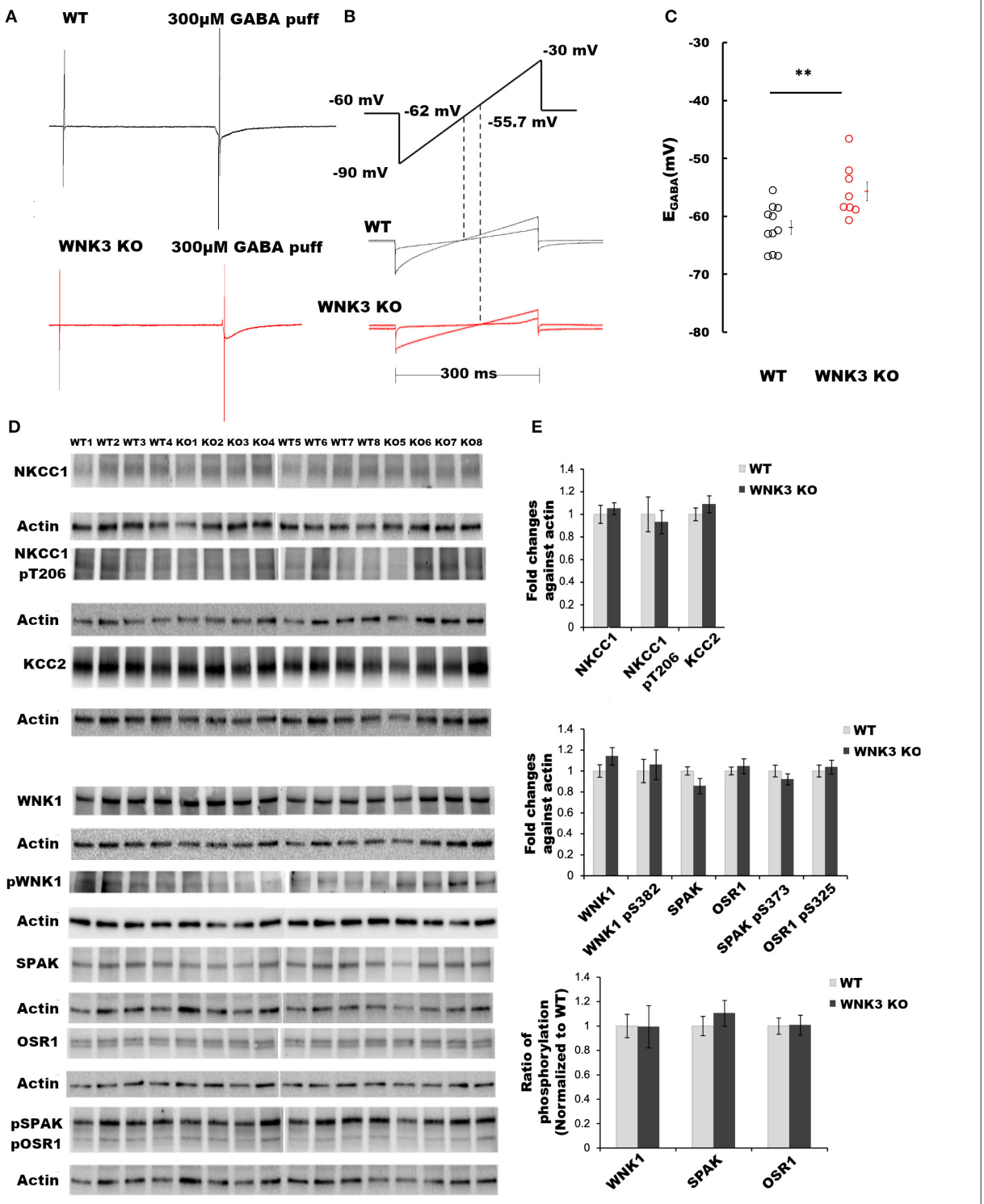

FIGURE 1
WNK 3 loss depolarizes GABA reversal potential in layer V pyramidal neurons at postnatal day 21. **(A)** Gramicidin-perforated patch recordings showing current traces in WT (black) and WNK3 KO neurons (red). The voltage ramps were applied before and during 300 μM GABA application to determine the GABA reversal potential (E_{GABA}). The rise and decay phase of the current response to GABA puff application were unchanged by the ramp protocol **(B)**. Voltage ramp protocol was performed to determine E_{GABA} (upper panel). The holding voltage was clamped at −60 mV. Two voltage ramps starting from −90 mV to −30 mV of 300 ms duration in the absence and presence of GABA (1s) were applied. The middle and lower panels show representative current responses to these two ramp protocols in WT (black) and WNK3 KO neurons (red), respectively. Dashed lines indicate the corresponding voltage level at which the two responses intersect indicating the E_{GABA} values. **(C)** Quantitative analysis

(Continued)

FIGURE 1 (Continued)
of E_{GABA} of layer V pyramidal neurons from the mPFC at P 21. WT (black open circles) and WNK3 KO (red open circles) indicate individual data points. The mean values are indicated with solid bars next to the data points (WT = −61.95 ± 1.16 mV, n = 11 cells, 6 mice; WNK3 KO = −55.70 ± 1.64 mV, n = 8 cells, 6 mice; t-test ** $P < 0.01$). **(D)** Immunoblots for evaluating changes in WNK1-SPAK/OSR1 cascade and cation- Cl^- cotransporters. Protein blots for total NKCC1, pNKCC1, and total KCC2 protein levels (upper panel) followed by protein blots of WNK1, pWNK1, total SPAK, total OSR1, and pSPAK1/pOSR1 (lower panel) are shown. Actin was used as a loading control. **(E)** Densitometric analysis for NKCC1, pNKCC1, and KCC2 (upper panel) and WNK1, pWNK1, total SPAK/OSR1, and pSPAK/pOSR1 (lower panel) showed no significant differences between WT (Gray bars) and WNK3 KO (Black bars) at P 21. Intensities were normalized to WT levels. N = 8 mice in each group. Error bars represent SEM.

Results

WNK3 loss depolarizes GABA reversal potential in layer V pyramidal neurons

The primary function of the WNK subfamily of kinases is the regulation of Cl^- homeostasis. The expression levels of WNK3 kinase peak at P21 (Kahle et al., 2005). Therefore, using acute slice preparation at P21, we performed gramicidin-perforated patch-clamp recordings from layer V pyramidal neurons to understand the effect of WNK3 knockout on E_{GABA} values. We used a ramp protocol to determine the E_{GABA} values. Examples of current recordings from WT (black) and WNK3 KO (red) neurons to voltage ramps (−90 mv to −30 mV, 300 ms) in the absence and the presence of 300 μM GABA are shown in Figure 1A. The representative ramp responses from WT and WNK3 neurons, with corresponding intersection voltage values marked on the ramp protocol, are illustrated in Figure 1B. Statistical comparisons of recorded E_{GABA} values indicate a significant depolarization shift of reversal potentials by 6 mV in WNK3 KO neurons (WT = −61.95 ± 1.16 mV, n = 11 cells, 6 mice; WNK3 KO = −55.70 ± 1.64 mV, n = 8 cells, 6 mice; t-test, $P = P = 0.0050$) as shown in Figure 1C. This depolarization corresponds to a 4 mM increase in resting $[Cl^-]_i$ levels in WNK3 KO pyramidal neurons when compared to WT neurons. The observed increase in $[Cl^-]_i$ levels following the loss of WNK3 may correspond to a compensatory increase in the activity of WNK1 as observed in the mouse kidney (Mederle et al., 2013). The possibility of such occurrences has also been proposed in mature neurons (Heubl et al., 2017). Incidentally, in mature neurons, the mRNA transcripts of WNK1 and WNK3 are more abundant than other isoforms (Heubl et al., 2017). Therefore, to confirm this possibility, immunoblotting experiments evaluating compensatory activation of WNK1-SPAK/OSR1 cascade onto NKCC1 and KCC2 were performed. However, the phosphorylation levels of residue Thr-206 (pNKCC1), a marker for increased NKCC1 function (Rinehart et al., 2009; Yang et al., 2010), were similar between groups. Total KCC2 protein levels were also observed to be not significantly different (Figures 1D,E). We observed no significant difference in the expression levels of total WNK1 levels (Figures 1D,E) between the WT and WNK3 KO groups. The activation of WNK1 requires autophosphorylation of Ser-382 (De Los Heros et al., 2014). The phosphorylation levels of residue Ser-382 (pWNK1) between WT and WNK3 KO were observed to be similar. Another possibility would be that loss of WNK3 directly alters the phosphorylation status of downstream signaling kinases SPAK/OSR1. We therefore evaluated changes in total SPAK/OSR1 protein levels, as well as phosphorylated SPAK/OSR1 (Inoue et al., 2012). The total protein levels of SPAK/OSR1 were not significantly altered in the KO mice (Figures 1D,E). In addition, phosphoantibodies against Ser-373 (pSPAK) and Ser-325 (pOSR1) revealed no significant differences (Figures 1D,E).

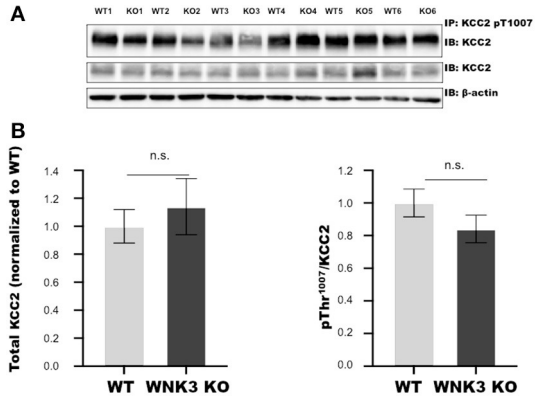

FIGURE 2
WNK 3 KO mice cortex show no change in KCC2 pT1007 levels at postnatal day (P) 21 in comparison to WT littermates. **(A)** Immunoblots for pThr1007 KCC2 and total KCC2 protein levels following immunoprecipitation from postnatal day 21 cortex. Actin was used as a loading control. **(B)** Densitometric analysis for total KCC2 (left panel) and $pThr^{1007}$/KCC2 (right panel) showed no significant differences between WT (Gray bars) and WNK3 KO (Black bars) at P 21. Intensities were normalized to WT levels. N = 6 mice in each group. Error bars represent SEM.

The WNK- SPAK/OSR1 signaling cascade also exerts a regulatory role on KCC2 function by inhibitory phosphorylation of C-terminal residue Thr1007. The progressive downregulation of this posttranslational modification in the course of development is essential for mouse survival (Watanabe et al., 2019). Alterations in this programmed downregulation in pT1007 KCC2 levels may contribute to the depolarizing shift of E_{GABA} (Figures 1B,C) in WNK3 KO neurons. We

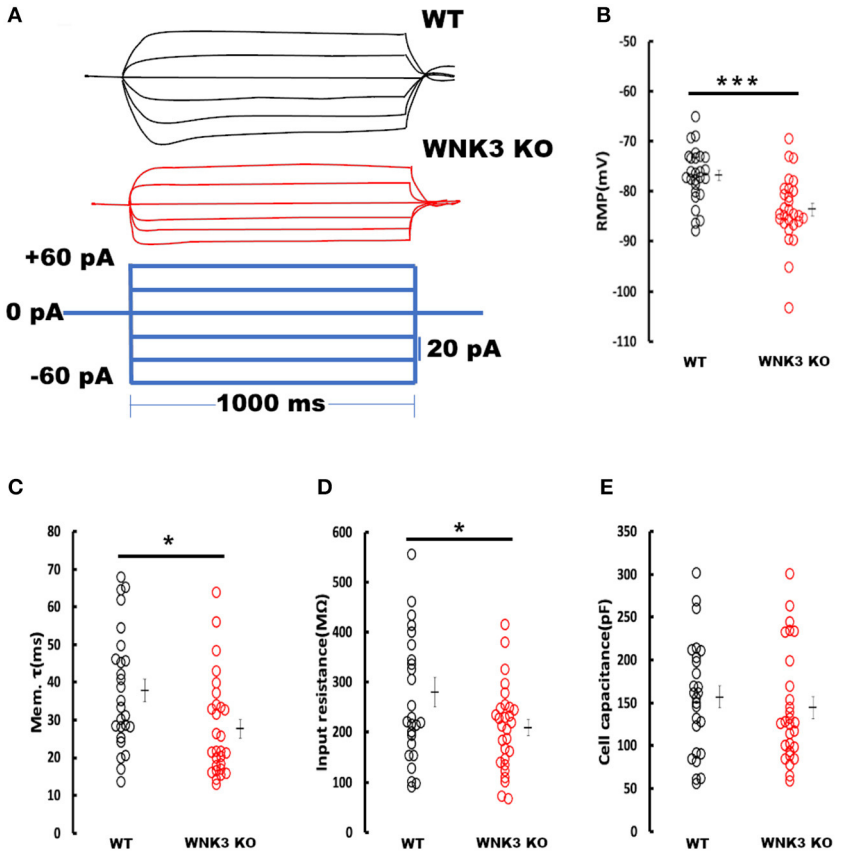

FIGURE 3
Enhanced resting membrane conductance in WNK3 KO neurons alter passive membrane properties. **(A)** Representative current-clamp recordings at small hyperpolarizing and depolarizing current steps. Step current injections of Δ 20 pA starting from −60 pA to +40 pA (lower panel, blue current step) and corresponding membrane voltage changes recorded from WT (upper panel, black traces) and WNK3 KO (middle panel, red traces) neurons are illustrated. The duration of the step pulse was 1,000 ms. **(B)** Quantitative analysis of RMP values indicate significantly hyperpolarized membrane potential in WNK3 KO neurons (WT = −76.81 ± 1.07 mV, $n = 26$ cells, 7 mice; WNK3 KO = −83.60 ± 1.26 mV, $n = 28$ cells, 7 mice; *t*-test *** $P < 0.001$). **(C)** Comparison of membrane time constant (τ_m) values are significantly decreased (WT = 37.93 ± 3.05 ms; WNK3 KO = 27.68 ± 2.48 ms; *Mann–Whitney U* test, * $P < 0.05$). **(D)** Quantitative analysis of input resistance of layer V pyramidal neurons from the mPFC. The input resistance of pyramidal neurons is significantly reduced in the WNK3 KO group (WT = 280.4 ± 29.15 MΩ; WNK3 KO = 209.03 ± 16.02 MΩ; *t*-test, *$P < 0.05$). **(E)** Plots of calculated cell capacitance values were similar in WT and WNK3 KO neurons (WT = 156.86 ± 12.98 pF; WNK3 KO = 144.31 ± 12.39 pF; *Mann–Whitney U* test, *ns*). Individual data points are plotted as WT (black open circles) and WNK3 KO (red open circles). The mean values are indicated with solid bars next to the data points. Error bars represent SEM.

therefore evaluated if the loss of WNK3 all throughout the fetal and postnatal developmental period disrupts this phenomenon. We immunoprecipitated pT1007 KCC2 using a phospho-specific antibody as reported earlier (Zhang et al., 2016) followed by immunoblotting. We observed no significant differences in the phosphorylation levels of Thr1007 residue in the C-terminal region of native KCC2 between the WT and WNK3 KO groups (Figures 2A,B). Together, these results suggest that the ∼4 mM enhancement of resting $[Cl^-]_i$ level was not dependent on compensatory overactivation of the WNK1-SPAK/OSR1 cascade.

Enhanced resting membrane conductance in WNK3 KO neurons alters passive membrane properties

We next investigated the effect of WNK3 loss on passive membrane properties of layer V pyramidal neurons in the mPFC. Representative voltage responses from WT and WNK3 KO neurons to small hyperpolarizing and depolarizing current steps are depicted in Figure 3A. These traces indicate a notable reduction in voltage responses to the same current injection intensities in WNK3 KO neurons. A comparison of membrane

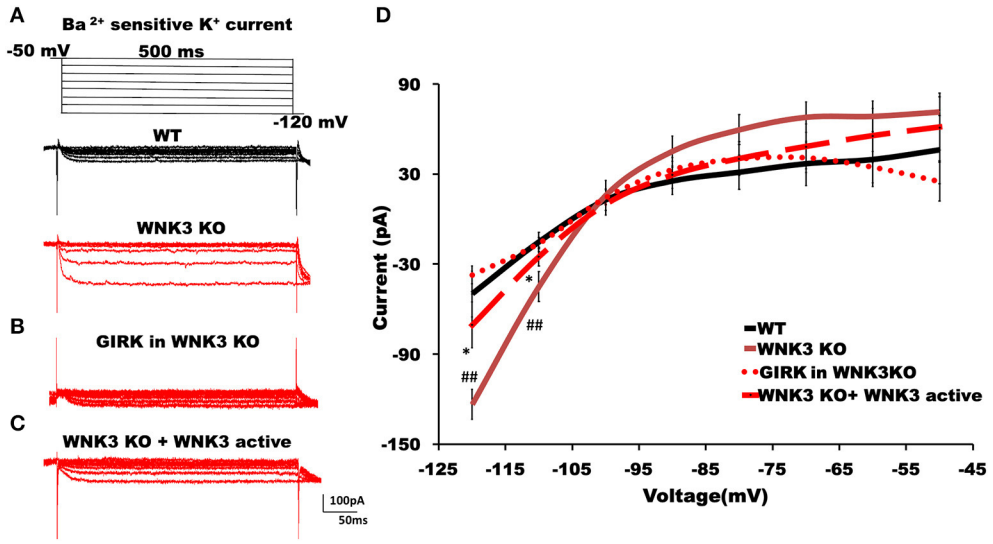

FIGURE 4
WNK3 kinase regulates classical inwardly rectifying potassium channels through kinase activity. **(A)** Representative traces of Ba^{2+}-sensitive inward rectifying potassium (IRK) currents from layer V pyramidal neurons of the mPFC. Upper panel illustrates the voltage clamp protocol. WT neuron (black), WNK3 KO neuron (red), **(B)** Weak GIRK-mediated K^+ currents in WNK3 KO neuron(red) isolated after the application of $GABA_B$ receptor antagonist CGP55845 (3μM). **(C)** Reduction of IRK currents in WNK3 KO neuron following the introduction of WNK3 active fragment in the internal solution. Scale bar as shown in inset (100 pA, 50 ms). **(D)** I-V relationship of IRK currents recorded from layer V pyramidal neurons in the mPFC. Plots of mean IRK currents at different voltages are labeled as follows: WT (solid black line; $n = 11$ cells, 4 mice); WNK3 KO (solid red line; $n = 12$ cells, 4 mice); CGP55845-sensitive GIRK in WNK3 KO (dotted red line; $n = 12$ cells, 4 mice); and WNK3 KO+ WNK3 active (dashed red line; $n = 10$ cells, 4 mice). Data are represented as mean ± SEM (*K-W test, post-hoc stepwise stepdown method.* $^{\#\#}P < 0.01$, $^{*}P < 0.05$).

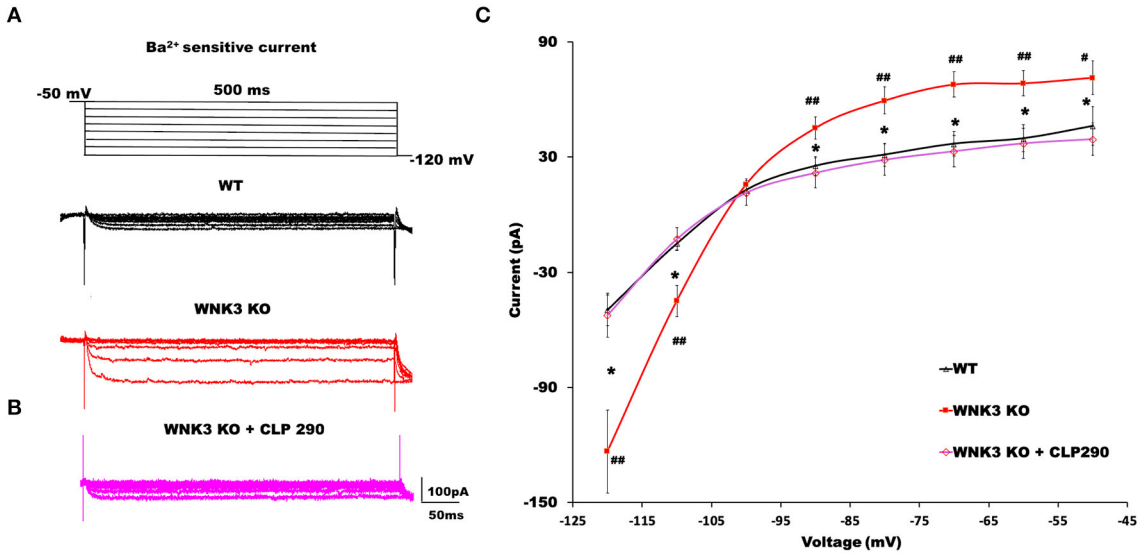

FIGURE 5
KCC2 activator CLP290 reverses increased IRK currents in WNK3 KO layer V pyramidal neurons. **(A)** Representative traces of Ba^{2+}-sensitive inward rectifying potassium (IRK) currents from layer V pyramidal neurons of the mPFC. Upper panel illustrates the voltage clamp protocol. WT neuron (black), WNK3 KO neuron (red). **(B)** Representative trace of Ba^{2+}-sensitive inward rectifying potassium (IRK) currents from WNK3 KO layer V pyramidal neurons after preincubation with CLP 290 (magenta). **(C)** I-V relationship of IRK currents recorded from layer V pyramidal neurons in the mPFC. Plots of mean IRK currents at different voltages are labeled as follows: WT (solid black line; $n = 11$ cells, 4 mice); WNK3 KO (solid red line; $n = 12$ cells, 4 mice); and WNK3 KO after preincubation with CLP290 (30 μM) (magenta; $n = 12$ cells, 4 mice). Data are represented as mean ± SEM (*ANOVA, post-hoc R-E-G-W F test.* $^{\#\#}P < 0.01$, $^{\#}P < 0.05$, $^{*}P < 0.05$).

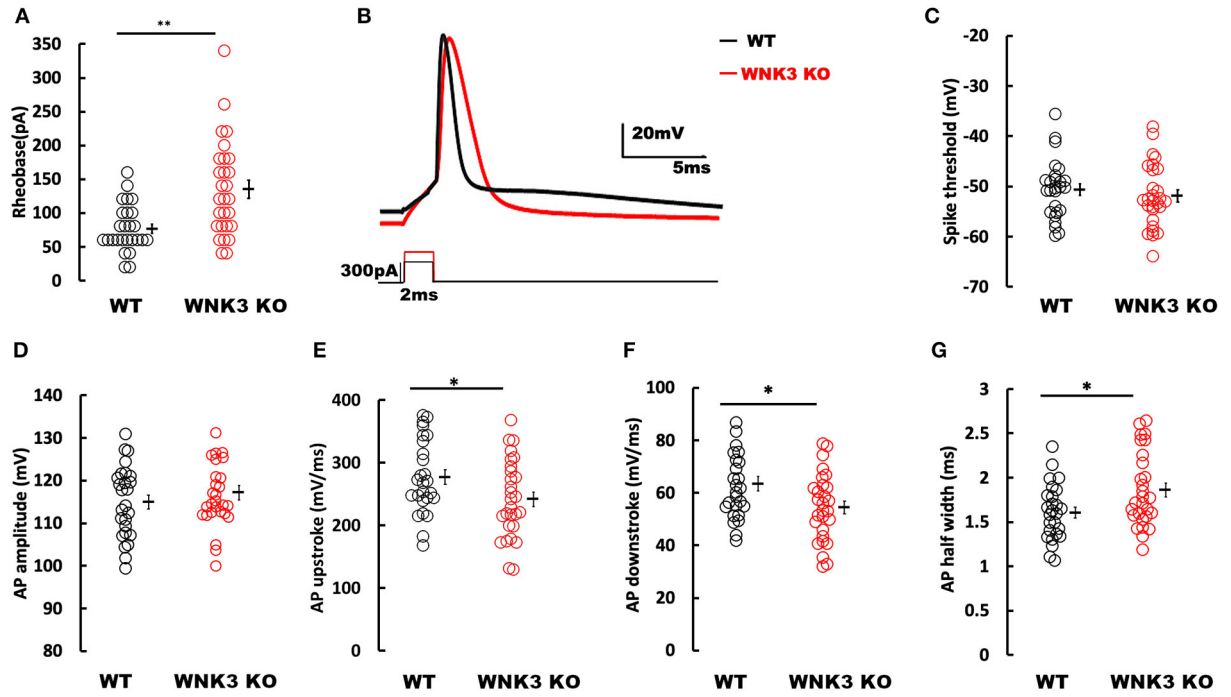

FIGURE 6
Loss of WNK3 reduces intrinsic excitability and increases single action potential (AP) duration of layer V pyramidal neurons in the mPFC. **(A)** Quantitative analysis of rheobase currents. Rheobase currents from layer V pyramidal neurons are significantly increased in the WNK3 KO group when compared to the WT group (black, WT = 76.92 ± 6.8pA, $n = 26$; red, WNK3 KO = 135 ± 13.4 pA, $n = 28$; *Mann–Whitney U* test, $^{**}P < 0.01$). **(B)** Representative single AP waveforms elicited by a short pulse (2 vms) protocol (black, WT; red, WNK3 KO). Note that both the rise slope and decay slope are slower in WNK3 KO, leading to an increase in AP half-width. Scale bar as shown in inset (20 mV, 5 ms). **(C)** Quantitative analysis of AP threshold voltages shows no significant differences within groups (WT = −50.61 ± 1.14 mV; WNK3 KO = −51.93 ± 1.18 mV; *t*-test, *ns*). **(D)** AP amplitudes are not significantly different between groups (WT =114.98 ± 1.64 mV; WNK3 KO = 117.16 ± 1.66 mV; *t*-test, *ns*). **(E)** AP upstrokes are significantly slower in WNK3 KO neurons (WT = 276.85 ± 11.53 mV/ms; WNK3 KO = 241.52 ± 11.78 mV/ms; *t*-test, $^{*}P < 0.05$). **(F)** AP downstrokes are significantly slower in WNK3 KO neurons (WT = 63.42 ± 2.78 mV/ms; WNK3 KO = 54.49 ± 2.42 mV/s; *t*-test, $^{*}P < 0.05$). **(G)** AP half-maximal widths are significantly prolonged in the WNK3 KO group (WT = 1.61 ± 0.06 ms; WNK3 KO = 1.86 ± 0.08 ms; *t*-test, $^{*}P < 0.05$). Individual data points are plotted as WT (black open circles) and WNK3 KO (red open circles). Mean values are indicated with solid bars next to the data points. Error bars represent SEM.

potential values calculated from zero current injection (I = 0) traces exhibited a significantly hyperpolarized RMP in WNK3 KO neurons (WT = −76.81 ± 1.07 mV, $n = 26$ cells, 7 mice; WNK3 KO = −83.60 ± 1.26 mV, $n = 28$ cells, 7 mice; $P = 0.000158$) as plotted in Figure 3B. The membrane time constants estimated by the single exponential fitting of the charging phase were observed to be significantly decreased (WT = 37.93 ± 3.05 ms; WNK3 KO = 27.68 ± 2.48 ms; $P = 0.011$) as plotted in Figure 3C. In addition, estimation of the input resistance of layer V pyramidal neurons revealed a significant reduction in the WNK3 KO in comparison to WT (WT = 280.4 ± 29.15 MΩ; WNK3 KO = 209.03 ± 16.02 MΩ; $P = 0.038$, Figure 3D). However, the calculated cell capacitance values calculated using the relationship ($C_m = R_m/\tau_m$) showed no difference between the neurons of WT and WNK3 KO mice (WT = 156.86 ± 12.98 pF; WNK3 KO = 144.31 ± 12.39 pF; $P = 0.359$, Figure 3E). These results indicate enhancement of ionic conductance at resting states, leading to hyperpolarization of RMP and significant reduction of input resistance.

WNK3 kinase regulates classical inwardly rectifying potassium channels through kinase activity

The hyperpolarized RMP values indicate a possible increase in the leak and inward rectifying K^+ conductance (IRK) in WNK3 KO neurons. We therefore explored this possibility further by performing voltage-clamp recordings to measure IRK. The Ba^{2+}-sensitive IRK component was isolated by subtracting current responses after the Ba^{2+} block (200 μM) from basal currents. The representative Ba^{2+}-sensitive IRK recorded from WT and WNK3 KO neurons are shown in Figure 4A. Notably, the evoked currents are larger in WNK3 KO neurons. The current-voltage relationships (I-V plot) indicate a significant enhancement of inward rectification in WNK3 KO neurons (Figure 4D). This enhancement of IRK currents explains the hyperpolarized RMP values in these neurons. The layer V pyramidal neurons in the mPFC are previously reported to express $GABA_B$-activated G

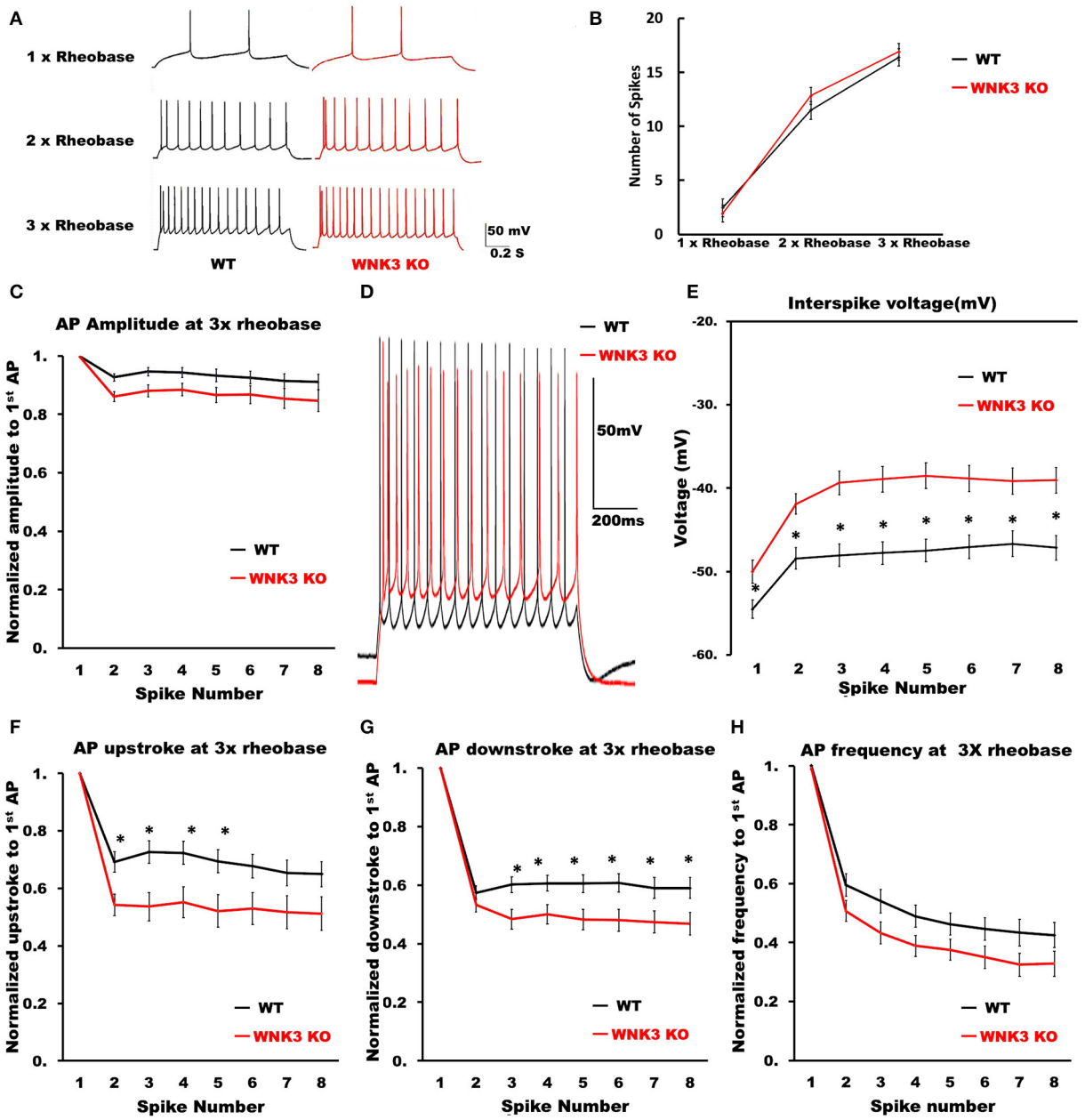

FIGURE 7
Repetitive firing frequencies are not affected in WNK3 KO neurons at multiples of rheobase currents. **(A)** Representative traces for repetitive firing at 1X, 2X, and 3X rheobase currents. WT (black) and WNK3 KO (red). The current injection duration is 1,000 ms. Scale bar as in figure inset (50 mV, 200 ms). **(B)** Plot of the relationship between the number of spikes and current injection at 1X, 2X, and 3X rheobase currents; WT (black) and WNK3 KO (red). **(C)** Normalized to first AP amplitude for first eight spikes at 3X rheobase. **(D)** Representative repetitive firing traces for 1,000 ms current injection at 3X rheobase currents for layer V pyramidal neurons (WT, black and WNK3 KO, red). Note the persistent depolarized interspike voltage in WNK3 KO neuron. Scale bar as in figure inset (50 mV, 200 ms). **(E)** Quantitative analysis of interspike voltage at 3 X rheobase (*t*-test, $^*P < 0.05$). **(F)** Normalized AP upstroke for the first eight spikes at 3X rheobase indicates a significant reduction in upstroke during repetitive firing (*t*-test, $^*P < 0.05$). **(G)** Normalized AP downstroke at 3X rheobase is significantly slower (*t*-test, $^*P < 0.05$). **(H)** However, normalized instantaneous frequencies at 3X rheobase are not affected.

protein-gated inwardly rectifying potassium channels (GIRK) (Takigawa and Alzheimer, 1999). Evidence also suggests that $GABA_B$ receptor-dependent regulation of network excitability of mPFC (Wang et al., 2010) is important in limiting network upstates. A recent report using an ASD mice model showed hyperexcitability due to a reduction of GIRK currents (Bassetti et al., 2020). We therefore investigated the possibility of $GABA_B$ receptor-mediated enhancement of GIRK currents in the WNK3

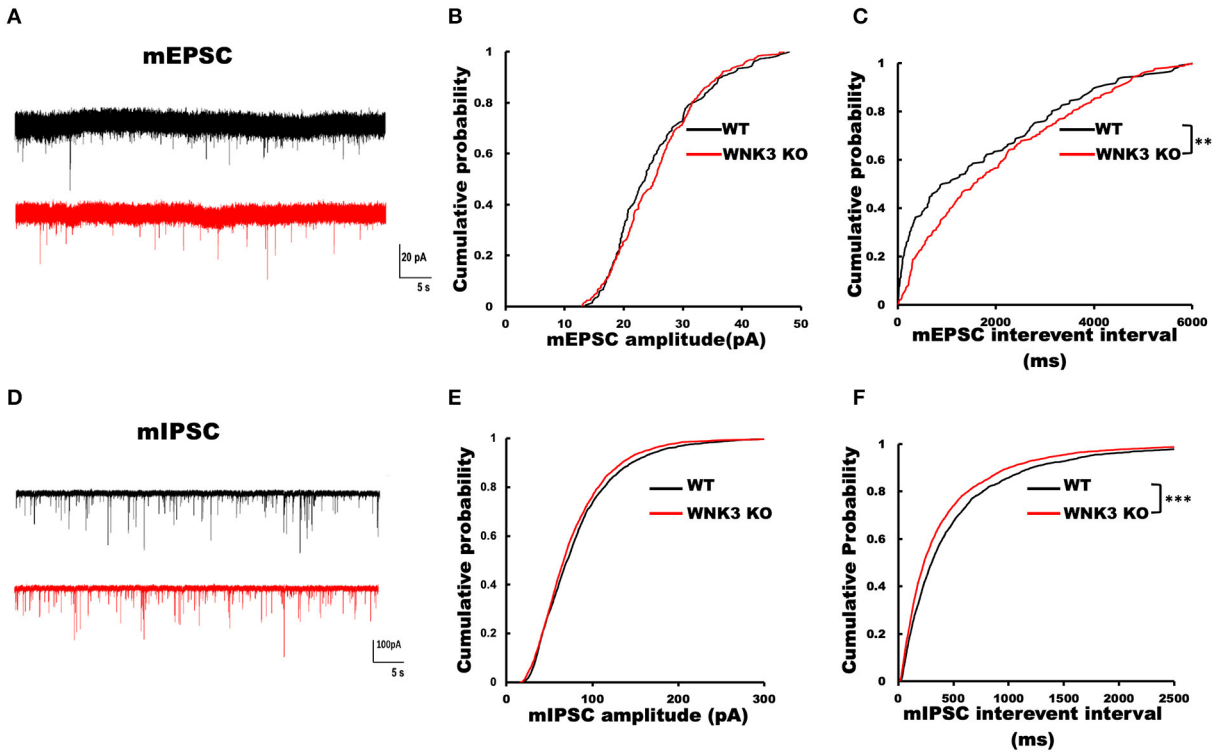

FIGURE 8
Loss of WNK3 kinase leads to simultaneous reduction and increment of excitatory and inhibitory inputs, respectively, to layer V pyramidal neurons in the mPFC. **(A)** Representative mEPSC current traces recorded from layer V pyramidal neurons, WT (black) and WNK3 KO (red). Holding voltage was set at −70 mV with a CH_3SO_3K-based normal Cl^- internal solution (see Methods section for composition). Scale bar as in figure inset (20 pA, 5 s). **(B)** Cumulative probability plot of amplitude distribution of mEPSC events. **(C)** Cumulative probability plot of interevent intervals (IEIs) of mEPSC events, indicating a reduction in the frequency of mEPSC recorded from WNK3 KO neurons ($N = 24$ cells; *K-S test*, $^{**}P < 0.01$). **(D)** Representative mIPSC current traces recorded from layer V pyramidal neurons, WT (black) and WNK3 KO (red). Holding voltage was set at −70 mV with a 150.0 mM CsCl-based solution (see Methods section for composition). Scale bar as in figure inset (100 pA, 5 s). **(E)** Cumulative probability plot of the amplitude distribution of mIPSC events. **(F)** Cumulative probability plot of IEI of mIPSC events. Note the leftward shift of IEI cumulative distribution of mIPSC events recorded from WNK3 KO neurons clearly indicating an increase in mIPSC frequency ($N = 25$ cells; *K-S test*, $^{***}P < 0.001$). Cumulative plots are color coded as WT (black) and WNK3 KO (red).

KO mice. We blocked $GABA_B$ receptors by the application of CGP55845 (3 μM) and isolated the CGP-sensitive GIRK current from WNK3 KO neurons. The representative GIRK currents are shown in Figure 4B. The I-V plot of isolated GIRK currents from WNK3 KO neurons rules out the role of GIRK channels as mediators of enhanced inward rectification (Figure 4D). The WNK3 KO neurons exhibit large current amplitudes at more negative holding potentials, suggesting the enhancement of K^+ conductance through classical inward rectifier channels (Kir 2.X). WNK3 being a kinase, we next investigated the possibility of its kinase function in the regulation of IRK in these neurons. We included an active fragment of WNK3 with intact kinase function into the internal solution and recorded IRK currents from WNK3 KO neurons. The representative Ba^{2+}-sensitive current traces are shown in Figure 4C. Quantification of observed responses indicates a significant reduction of IRK conductance in these neurons (Figure 4D), suggesting WNK3 kinase-dependent regulation of Kir channels. Together, our results indicate an important role of WNK3 kinase in the maintenance of intrinsic excitability of layer V pyramidal neurons in the mPFC.

WNK3 and KCC2 in tandem regulate classical Kir and leak K^+ channel membrane expression

The RMP is an important determinant in the driving force of GABAergic inhibition or excitation. A recent finding suggests knockdown of KCC2 reduced the membrane expression of a two-pore leak (TASK-3) K^+ channels (Goutierre et al., 2019) depolarizing both E_{GABA} and RMP. Though we observed a depolarized E_{GABA} (Figures 1B,C), RMP was hyperpolarized (Figure 3B) in WNK3 KO neurons. We therefore next investigated the possible link between KCC2 and IRK

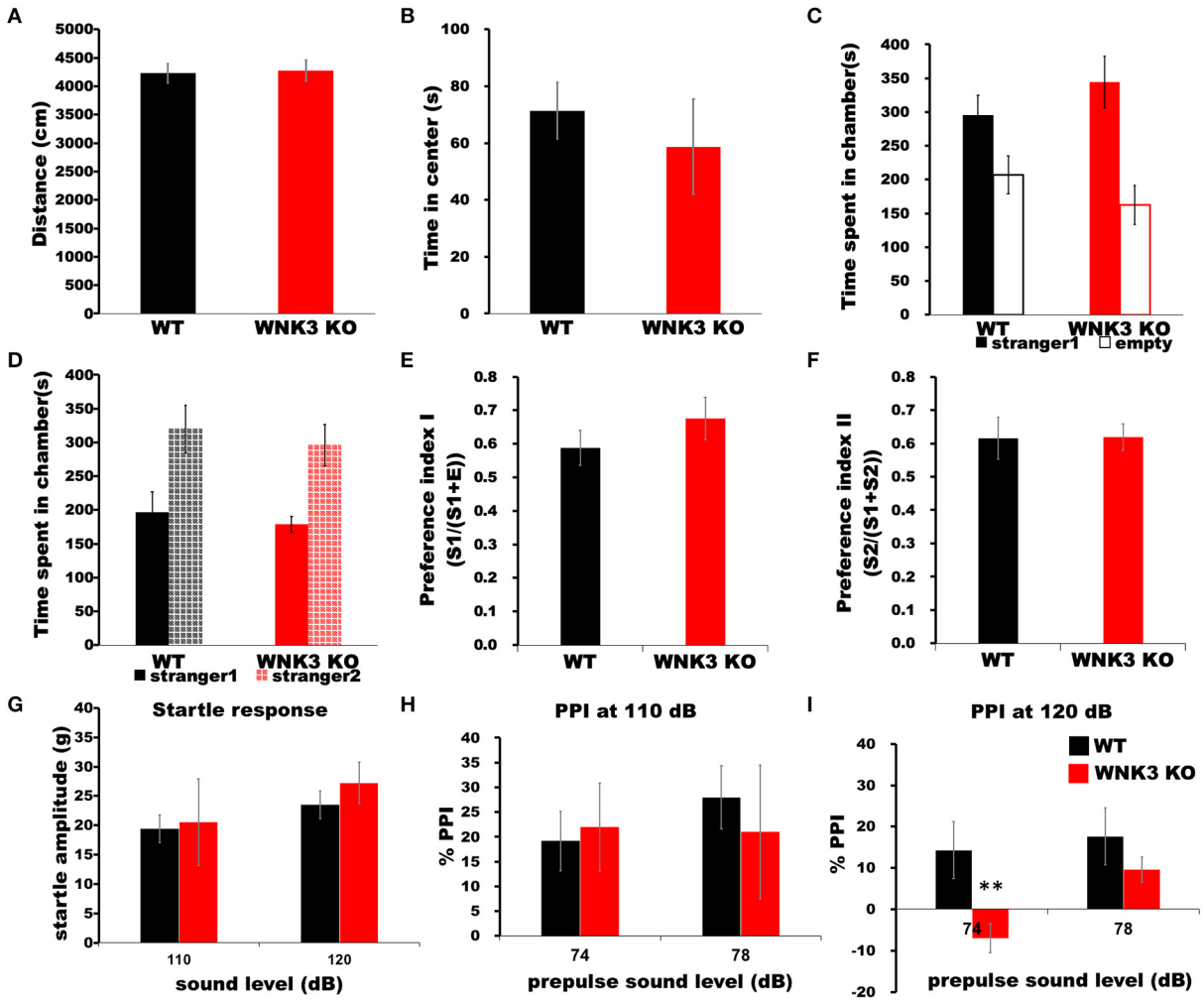

FIGURE 9
WNK3 KO mice exhibit normal locomotion and social behavior but deficits in prepulse inhibition. **(A)** Open field test show no difference in total distance traveled (WT = 4,229.71 ± 170.84 cm, $n = 8$ mice; WNK3 KO = 4,271.45 ± 186.62 cm, $n = 4$ mice) indicating normal exploratory and locomotor activity. **(B)** Time spent in the center of the open field arena is similar between WT and WNK3 KO mice indicating anxiety levels are similar (WT = 71.39 ± 8.82 s; WNK3 KO = 58.73 ± 6.13 s). **(C)** No alterations in sociability were observed between WT and WNK3 KO mice. **(D)** Social novelty recognition was not affected in WNK3KO. Preference indices for **(E)** social interaction and **(F)** social memory were also not affected by WNK3 deletion. **(G)** Startle response amplitudes at 110 dB and 120 dB were not different between groups **(H)**. Percent PPI at 110 dB to prepulse of 74 and 78 dB was not affected. **(I)** Percent PPI at 120 dB to prepulse of 74 dB was significantly reduced in WNK3 KO (*t*-test ** $P <$ 0.01) and with the extent of PPI showing reduction at 78 dB does not reach significance.

conductance in pyramidal neurons. We blocked KCC2 activity in WT neurons by including KCC2 antagonist DIOA (30 μM) in the internal solution and recorded Ba^{2+}-sensitive K^+ currents. DIOA at this concentration has multiple off-target effects and therefore is not an ideal KCC2 antagonist. However, as a previous report observed, at reduced time scales (<1h), it acts primarily as a KCC2 antagonist (Pellegrino et al., 2011). The representative current traces and their I-V characteristic are shown in Supplementary Figures 1B,D. We observed that on acute antagonism of KCC2 function per se, IRK currents remain unaffected as reported earlier (Goutierre et al., 2019). We then proceeded to evaluate if the application of the KCC2 activator may affect IRK currents. For this purpose, we pre-incubated acute slices with a selective KCC2 activator CLP290 (30 μM) for 1 h before recording IRK currents from WT neurons. At this concentration, this drug increases KCC2 expression, and it has been suggested that this action may be dependent on the slightly enhanced phosphorylation levels of Ser-940 of KCC2 observed after treatment (Sullivan et al., 2021). Interestingly, the CLP290 treatment produced a weak but significant enhancement of IRK currents in WT neurons (Supplementary Figures 1C,D). Similarly, experiments combining pre-incubation with CLP290 followed by IRK recordings from KO neurons were performed.

The representative IRK current traces are shown in Figure 5B. We observed that instead of showing further enhancement, the recorded, IRK currents exhibited a complete reversal receding to basal current levels comparable to those recorded from WT neurons (Figure 5A). Thus, after enhancing KCC2 membrane stability with CLP290 application, normalization of IRK conductance I-V relationship was evidenced (Figure 5C). These results indicate that WNK3 and KCC2 are involved in the regulation of membrane expression of both Kir and leak K^+ channels in layer V pyramidal neurons of mPFC.

Loss of WNK3 reduces intrinsic excitability of layer V pyramidal neurons in the mPFC

Following the elucidation of WNK3 action on the regulation of membrane excitability, we evaluated its effect on action potential firing in these neurons. We observed that the mean rheobase currents were significantly higher for WNK3 KO neurons (WT = 76.92 ± 6.8 pA, n = 26; WNK3 KO = 135 ± 13.4 pA, n = 28; P = 0.001; Figure 6A). Thereafter, the effect of WNK3 loss on AP waveform was analyzed from a single action potential (AP) elicited by a short pulse (2 ms) protocol. The representative traces for the AP waveform are illustrated in Figure 6B. Phase-plane analysis revealed no clear differences in threshold voltages at which AP was triggered (WT = −50.61 ± 1.14 mV; WNK3 KO = −51.93 ± 1.18 mV; P =0.424; Figure 6C). The mean amplitude of AP was observed to be similar between groups (WT = 114.98 ± 1.64 mV; WNK3 KO = 117.16 ± 1.66 mV; P = 0.356; Figure 6D). In addition, both upstroke (WT = 276.85 ± 11.53 mV/ms; WNK3 KO = 241.52 ± 11.78 mV/ms; P = 0.037; Figure 6E) and downstroke (WT = 63.42 ± 2.78 mV/ms; WNK3 KO = 54.49 ± 2.42 mV/s; P = 0.018; Figure 6F) of AP waveform were significantly slower in WNK3 KO neurons. As a consequence, mean duration of AP half-width was significantly prolonged in WNK3 KO neurons (WT = 1.61 ± 0.06 ms; WNK3 KO = 1.86 ± 0.08 ms; P = 0.015; Figure 6G). Thus, loss of WNK3 function significantly reduced intrinsic excitability of layer V pyramidal neurons.

Repetitive firing frequencies are not affected in WNK3 KO neurons at multiples of rheobase currents

We then examined the repetitive firing and its adaptation parameters following 1 s long step current injections. In view of the significant reduction in input resistance and increase of rheobase currents in WNK3 KO neurons, the input-output relationship was significantly reduced (data not shown). Therefore, to estimate if the neuronal gain was affected, we compared AP firing frequencies at multiples of rheobase current injections (1x, 2x, and 3x rheobase). The repetitive firing patterns at these current injections are illustrated in Figure 7A. Statistical analysis revealed no significant differences between WT and WNK3 KO neurons, suggesting no effect of WNK3 loss on neuronal gain (Figure 7B). The assessment of repetitive firing and adaptation was performed at three times rheobase current. The comparison between amplitudes of the first eight spikes normalized to the peak amplitude of the first AP showed no significant difference between WT and WNK3 KO groups (Figure 7C). In addition, interspike voltages (ISV) were found to be significantly depolarized in WNK3 KO neurons (Figures 7D,E). Also, comparisons of AP upstroke and downstroke revealed significant decrements in WNK3 KO neurons (Figures 7F,G). Sluggish upstroke and downstroke of spikes would predict a reduction in the frequencies of spikes. Instead, interestingly, the comparison between normalized instantaneous frequencies (Figure 7H) and firing frequencies (Figure 7B) showed no significant differences between WT and WNK3 KO neurons.

Loss of WNK3 kinase leads to simultaneous reduction of excitatory inputs and increment of inhibitory inputs to layer V pyramidal neurons

To understand the role of WNK3 in the development of neural circuits in the mPFC, we performed recordings for both excitatory and inhibitory miniature postsynaptic currents (mEPSCs and mIPSCs) from layer V pyramidal neurons. The representative mEPSC current traces recorded from WT and WNK3 KO neurons are shown in Figure 8A. Analysis of mEPSC event distributions for amplitude and interevent intervals was restricted to events within 50 pA. Comparisons of mEPSC amplitude distributions show no differences between WT and WNK3 KO neurons (P = 0.1516, n = 24; Figure 8B). The distribution of interevent intervals was significantly right-shifted for WNK3 KO neurons, indicating a decrease in the frequency of mEPSC events (P = 0.0046, n = 24; Figure 8C). On the other hand, evaluation of mIPSC events revealed a contrasting phenomenon. The representative mIPSC recordings for each group are shown in Figure 8D. The comparison between the distribution of mIPSC interevent intervals showed a significant leftward shift for WNK3 KO neurons, indicating the enhanced frequency of mIPSCs (P = 0.000001, n = 25; Figure 8F). The mIPSC amplitudes were apparently affected in the cumulative distribution plots (P =0.0002, n = 25; Figure 8E).

WNK3 KO mice exhibit normal locomotion and social behavior but deficits in prepulse inhibition

Finally, we assessed the impact of a decrease in neuronal excitability and alterations on mPFC cortical circuits during development by evaluating behavioral changes in WNK3 KO mice. The time spent in the center of the arena and total distance traveled within a period of 5 min in an open-field apparatus were not significantly different between WNK3 KO and WT littermates, indicating no changes in anxiety levels (Figure 9A) and locomotor activities, respectively (Figure 9B). No alterations in sociability (Figure 9C) and social novelty (Figure 9D) were observed, resulting in similar preference indices for social interaction (Figure 9E) and social memory (Figure 9F) between groups. We also evaluated startle response and prepulse inhibition (PPI), a measure of sensorimotor gating (Swerdlow and Geyer, 1998), in these mice. Interestingly, while startle response was unchanged (Figure 9G), we observed a deficit in PPI response after a prepulse of 74 dB in WNK3 KO mice at 120 dB (Figure 9I) but not at 110 dB (Figure 9H), which showed no significant differences. These results indicate a deficit in sensorimotor gating in WNK3 KO mice without compromising social behavior. In addition, locomotion and anxiety levels are unaffected by the loss of WNK3 function.

Discussion

In the present study, using a constitutive WNK3 KO mouse, we investigated the role of WNK3 kinase in brain development. In particular, we examined its role in the regulation of chloride homeostasis in pyramidal neurons, its function in the control of neuronal excitability, and the effect on the development of neural circuits governing synaptic connectivity in the mPFC. Furthermore, we analyzed the behavioral impact of changes on brain development manifested by WNK3 loss. Our findings indicate a significantly depolarized reversal potential for $GABA_A$ receptor-mediated currents by 6 mV at P 21. This corresponded to higher resting $[Cl^-]_i$ level of ∼4 mM in KO mice than in WT littermates. However, expected alterations in the phosphorylation levels of the WNK1-SPAK/OSR1 signaling cascade and their downstream targets NKCC1 and KCC2 were not observed in KO mice. Meanwhile, the RMP of neurons was more hyperpolarized by 7 mV, and the rheobase current necessary for firing induction was increased in KO mice. These were due to an increase in IRK currents. Investigations ruled out the possibility of increased activation of GIRK-mediated reduction in neuronal excitability; instead, this reduction was mediated by Kir channels. Interestingly, supplementation of an active form of WNK3 with intact kinase function reversed these changes. We also observed a novel association between KCC2 and WNK3 affecting the IRK currents mediated by Kir and leak K^+ channels suggestive of their important role in the regulation of the RMP. Analysis of individual action potential spikes indicated prolonged half widths in KO neurons. Evaluation of repetitive action potential firing at three times rheobase current surprisingly showed no effect on instantaneous firing frequencies and neuronal gain. Moreover, synaptic current recordings from KO neurons revealed that the frequency of mEPSCs was reduced, whereas those of mIPSCs were increased. These developmental changes in membrane and synaptic properties of pyramidal neurons in unison with yet-to-be elucidated changes in other cellular subtypes culminated as deficits in PPI, a measure of sensorimotor gating involving multiple brain regions including the mPFC, in WNK3 KO mice.

The primary physiological role ascribed to the WNK-SPAK/OSR1 signaling cascade is its maintenance of chloride homeostasis by phosphorylation-dependent regulation of cation-Cl^-co-transporters (Alessi et al., 2014). In neurons, $[Cl^-]_i$ levels are critical for determining GABA action (Ben-Ari, 2002) and cell volume regulation (Akita and Okada, 2014; Huang et al., 2019). Our gramicidin-perforated patch-clamp recordings of layer V pyramidal neurons from WNK3 KO mice at P21 revealed average E_{GABA} values depolarized by 6 mV (Figure 1C). This corresponds to a weak increase in resting $[Cl^-]_i$ levels by 4 mM. However, this enhancement was not paralleled by an increase in WNK1-SPAK/OSR1 signaling, because no changes in activated pWNK1, pSPAK, and pOSR1 protein levels were observed (Figure 1). The pNKCC1 levels were also not affected, ruling out an indirect effect on the NKCC1 Cl^- import function. We also investigated if there is a more pronounced effect of WNK3 loss of function on the phosphorylation level of Thr1007 residue in the C-terminal domain of KCC2, which may explain the elevated resting $[Cl^-]_I$ levels. However, we observed no significant differences when compared to the WT group (Figure 2). Our observations are not in agreement with a recent report (Lim et al., 2021). In this study, employing a primary hippocampal neuronal culture, a knockdown of WNK3 using lentiviral-mediated shRNA at DIV 1 was established, a time point at which the fetal phase of development nears completion. This produced a reduction in the WNK3 protein levels between 60 and 80% of control levels. This also reduced the pThr1007 KCC2 levels and contributed to a hyperpolarized E_{GABA}. These findings fit the dogma that loss of WNK-SPAK/OSR1 regulation would facilitate the enhancement of GABAergic inhibition. However, whether loss of WNK3 leads to regulation of WNK1 activity by changes in $[Cl^-]_i$ as predicted earlier (Heubl et al., 2017) was not explored. If one were to make a reasoned argument, the main difference between our approach and that of Lim et al. (2021) is that we used constitutive KO of *WNK3* in contrast to a knockdown approach with a reported 60–80% efficiency. This may contribute to differences. It would be noteworthy that high expression of WNK3 in the fetal developmental phase, as reported by Küry et al. (2022), would remain unaffected in the knockdown model. In contrast, a constitutive KO

would affect both phases of brain development. The WNK-SPAK/OSR1 cascade is one of the regulatory pathways affecting the downstream functions of both NKCC1 and KCC2, and their disruption may trigger an alteration in other regulatory pathways. The KCC2 function-mediated lowering of $[Cl^-]_i$ in mature neurons is subject to regulation by multiple mechanisms controlling its membrane expression and stability (Côme et al., 2019). Furthermore, changes in phosphorylation-dependent posttranslational regulation of KCC2 at other amino acid residues in its C-terminal region are quite possible. In addition to these possibilities, Cl^- movement across the neuronal membrane is also facilitated by Ca^{2+}-activated Cl^- channel (TMEM6B), volume-regulated anion channels (VSOR), and a novel voltage-gated Cl^- channel (SLC26A11) (Akita and Fukuda, 2020). If the WNK3 function entails regulation of any of these Cl^- channels, the weak enhancement of $[Cl^-]_i$ remains a possibility in the WNK3 KO mice. More importantly, the functional impact of WNK3-mediated regulation of $[Cl^-]_i$, independent of activation of WNK1-SPAK/OSR1 cascade, would require careful examination.

The membrane properties of layer V pyramidal neurons rapidly change during the second postnatal week with adult-like properties observed by P21 (Zhang, 2004). In our mouse model, WNK3 deletion led to multiple changes in membrane excitability. The RMP was significantly hyperpolarized. In addition, input resistance values were significantly reduced. During normal development, the decrease in input resistance leading to deeper RMP between P14 and P21 is attributed to the enhancement of leak K^+ conductance mediated by KCNK channels (Goldstein et al., 2001). Incidentally, expression of TWIK1 and TASK-3, two-pore leak K^+ channels, increases during this phase (Aller and Wisden, 2008). Previous recordings from layer V pyramidal neurons of the mouse mPFC observed two distinct K^+ conductance systems attributed to leak K^+ channels and IRK channels (Day et al., 2005). These neurons are reported to express a $GABA_B$ receptor-dependent GIRK conductance as well (Takigawa and Alzheimer, 1999). To confirm the enhancement of resting K^+ currents in KO neurons, the Ba^{2+}-sensitive inward K^+ current component was isolated by subtracting current responses after Ba^{2+} block (200 μM) from basal currents (Figure 4). The K^+ currents were larger in WNK3 KO neurons confirming our hypothesis. Furthermore, these currents showed strong inward rectification at voltages deeper than the E_K value of−103 mV ruling out the enhancement of leak conductance which is characterized by linear I-V characteristics (Goldstein et al., 2001; Day et al., 2005). In addition, isolated GIRK currents were minimal (∼37.2 pA; GIRK vs ∼ 123.5 pA; total IRK at −120mV) in comparison to total IRK currents recorded in WNK3 KO neurons. The observed small peak amplitudes of GIRK currents at P21 are in agreement with previous results which show enhancement of $GABA_B$-dependent GIRK conductance in rodent mPFC only after P25-P36 (Wang et al., 2010; Bassetti et al., 2020). Thus, the observed strong inward rectification in WNK3 KO neurons is ascribed to enhanced classical inward rectifier channel function (Kir 2.X) that is expressed in these neurons (Day et al., 2005). The classical inward rectifier channels are regulated by multiple mechanisms (see review Hibino et al., 2010). More recent reports have shown that the WNK-SPAK/OSR1 cascade also plays a regulatory role in Kir channel functions. Both WNK1 and WNK4 in a kinase-independent manner reduce the surface expression of ROMK (Kir1.1) channels (Liu et al., 2009). Another report finds that activated OSR1 increased membrane stabilization of specific Kir channel subtypes (Kir2.1 and Kir2.3) (Taylor et al., 2018). However, till now, there are no reports suggesting direct regulation of inward rectification in neurons by WNK3. Based on our loss of function and rescue experiments with kinase-active WNK3 fragment in the internal solution, we can confirm that normal WNK3 activity would reduce the strong inward rectification. This result implies that endogenous WNK3 may either directly phosphorylate classical Kir channels attenuating IRK currents in pyramidal neurons or indirectly modulate another regulatory sequence involved in the membrane expression of these channels. We therefore explored the possibility of indirect modulation of IRK currents by WNK3. It has recently been reported that only reduced membrane expression of KCC2 and not reduced transport activity led to a robust decrease in the membrane expression of two-pore leak (TASK-3) K^+ channels in the dentate gyrus granule cells and in CA1 pyramidal neurons (Goutierre et al., 2019). The layer V pyramidal neurons in the adult rodent cortex show moderate levels of TASK-3 transcripts when compared to granule cells (Talley et al., 2001), suggesting a lesser fraction of IRK currents would be mediated by leak K^+ channels currents (Day et al., 2005). We confirmed that blocking KCC2 transporter activity per se in WT neurons did not reduce IRK currents (Supplementary Figure 1). Instead, increasing the membrane stability of KCC2 with pre-incubation with CLP290 produced a slight but significant enhancement of IRK currents, corroborating that an increase in KCC2 membrane stability enhances IRK currents (Seja et al., 2012; Goutierre et al., 2019). This linear increase may occur after changes in the membrane localization of TASK-3 channels and would require additional experiments. In stark contrast, a similar pretreatment with CLP290 in WNK3 KO neurons produced a reversal of IRK currents to levels similar to WT neurons (Figure 5). This would indicate that the enhanced IRK currents are mediated by a probable increase in classical Kir channel membrane expression in WNK3 KO neurons, in addition to the fact that WNK3 kinase activity would depend on KCC2 membrane stability or vice versa. Delving deeper, it might also be speculated that WNK3 plays a role in the interaction between KCC2 and TASK-3 channels. Conversely, an increase in KCC2 membrane expression inhibits classical Kir channel membrane expression, but increases TASK-3 channel membrane expression. In addition, our result could also imply

that constitutive WNK3 loss may reduce the membrane stability of KCC2 by mechanisms other than regulation of pThr1007 KCC2 levels. This could also explain the weak increase in resting $[Cl^-]_i$ levels in WNK3 KO neurons; however, confirmation of this assumption would require further investigation. Overall, in the context of regulation of IRK currents in neurons, among the different possible mechanisms, we hypothesize that WNK3 and KCC2 in tandem regulate the expression of Kir channels and leak K^+ channels (TASK-3 channels), thus maintaining their relative proportions in the membrane. This regulating cascade would possess the wherewithal to control the RMP and thereby act as a restraint to exaggerated shifts in the driving force of Cl^-. Furthermore, it would be interesting to examine how different pathological conditions affect this regulatory mechanism. Our findings therefore assign a novel function to WNK3 in tandem with KCC2 in the regulation of RMP and thereby neuronal excitability.

The waveform analysis of single AP elicited by a short pulse protocol indicates no differences in AP threshold voltage and single AP amplitude between the genotypes. The observed reduction in input resistance and membrane time constant (Figure 3) due to the enhancement of IRK currents (Figure 4) explains the significant increase in rheobase currents (Figure 6) recorded in KO neurons. Our analysis of a single AP waveform shows slower AP upstroke and downstroke prolonging the AP duration. The slower AP decay in KO neurons suggests changes in K^+ currents during the repolarization phase. During the sustained neuronal activity, as in repetitive firing, these effects are accentuated as significant decrements in AP downstrokes and relatively slower upstrokes in KO neurons (Figures 6E,F). This reduction would predict greater adaptation in KO neurons. However, surprisingly, no effects on firing frequencies were observed in KO neurons (Figures 7B,H). The repolarization of spikes in pyramidal neurons is primarily contributed by the delayed rectifier K^+ channels (K_V2) forming heteromeric channels in association with other K_V channels (Misonou et al., 2005). However, for these channels to maintain activity, sufficient membrane depolarization for activation is required. Functionally, these assemblies contribute to maintaining repetitive firing in pyramidal neurons by regulation of the interspike trough voltages (Liu and Bean, 2014; Saitsu et al., 2015). In our findings, though the ISV levels are significantly depolarized in comparison to WT, uniform trough voltages are maintained (Figure 7). This suggests that during repetitive firing, another repolarizing conductance in concurrence mediated by delayed rectifier K^+ channels sustains repetitive firing in the KO neurons. This may occur as a compensatory mechanism to counter changes in predicted changes in adaptation parameters or occur due to the absence of WNK3 regulating these channels. If we were to speculate, a candidate could be BK-type Ca^{2+}-activated K^+ channels. Both experimental and biophysical modeling data indicate a facilitatory role of BK channels in high-frequency firing in pyramidal neurons (Gu et al., 2007). The prolongation of spike duration as observed (Figure 6) may contribute to increased Ca^{2+} entry into the KO neurons. This enhanced $[Ca^{2+}]_i$ may affect the BK channel function. Recent evidence, utilizing artificial expression systems in HEK cells, indicated that WNK-SPAK/OSR1 cascade affects the BK channel function (Liu et al., 2015).

We further assessed the role of WNK3 in the development of cortical networks by recording mPSCs from pyramidal neurons. Our results indicate a significant reduction in excitatory inputs to layer V pyramidal neurons in KO mice (Figure 8C). On the contrary, inhibitory inputs to these neurons were enhanced (Figure 8F). Incidentally, shRNA knockdown of WNK3 showed an increase in mEPSC amplitudes from hippocampal culture neurons (Lim et al., 2021). The possible mechanisms underlying this dichotomy in the synaptic connectivity pattern between constitutive KO and knockdown of WNK3 warrants further investigation. The functional maturation and integration of distinct GABAergic interneuron subtypes in the cortical circuitry (Lim et al., 2018) also coincide with changes in WNK3 expression. In this period, both rapid modifications of layer V pyramidal neuron morphology (Zhang, 2004; Romand et al., 2011) and layer-specific synaptic inputs in the mPFC (Zhang, 2004; Kroon et al., 2019) have been observed. Moreover, circuit refinements during this period are neuronal activity-dependent (Burrone et al., 2002). In the constitutive WNK3 KO mice, the intrinsic excitability of pyramidal neurons is significantly reduced (Figure 3), which may contribute to differences in synaptic inputs when compared to WT littermates. In addition, KCC2 membrane expression is an important regulator of excitatory synapse formation (Watanabe and Fukuda, 2015). Thus, differences in KCC2 membrane stability between WT and WNK3 KO neurons, which may be implied from our results (Figure 5), also need to be considered as a probable mechanism. As the mIPSC frequencies are increased, additional experiments would be necessary to ascertain if this presynaptic change is due to enhanced intrinsic excitability of gabaergic neurons or at the level of gabaergic terminals with changes in release probability and enhancement of synaptic boutons. The gabaergic interneurons would also normally express WNK3, and it would be important to examine if interneuron-specific loss of WNK3 exhibits the same electrophysiological characteristics. In the scenario of a similar enhancement of IRK conductance in inhibitory neurons, the input resistance ($\mathbf{R}_{In}$) would be decreased and might affect the low threshold spiking neurons with reportedly higher $\mathbf{R}_{In}$ to a greater extent than mature parvalbumin-positive fast-spiking interneurons.

The cumulative effect of these developmental changes in WNK3 KO mice manifests as deficits in PPI, an indicator of abnormal information processing during sensorimotor gating (Figure 7G). Deficits in PPI are a hallmark feature in patients presenting with varied neuropsychiatric disorders, including schizophrenia (Kohl et al., 2013). The neural circuit

modulating PPI is the cortico-striatal-pallido-thalamic (CSPT) circuit comprising multiple brain regions including the mPFC and hippocampus (Swerdlow and Geyer, 1998). Several reports indicate that either increase or decrease in mPFC activity leads to deficits in PPI (Tapias-Espinosa et al., 2019). In addition, disruptions in neurodevelopmental sequelae of mPFC by different strategies like isolation rearing (Day-Wilson et al., 2006) and prenatal exposure to drugs (Toriumi et al., 2016) and toxins (Wischhof et al., 2015) all produce PPI deficits. The loss of WNK3 regulation reducing neuronal excitability of pyramidal neurons in the mPFC and yet unidentified effects on other neuronal subtypes leading to observed changes in synaptic connectivity could disrupt the functional development of the mPFC, thereby affecting the CSPT circuit and resulting in PPI deficits.

It has been proposed that the downregulation of the WNK-SPAK/OSR1 signaling cascade may work as a therapeutic strategy in disorders of altered inhibition, such as epilepsy, schizophrenia, and autism spectrum disorders (Kahle and Delpire, 2016; Côme et al., 2019). Incidentally, preliminary investigations examining the effects of the rare WNK3 variants predicted to produce loss of function (Küry et al., 2022) when expressed in a HEK293T cell line reported a 60% reduction in WNK3 protein levels and reduction of pThr1007 KCC2 levels. This reduction would facilitate an increase in inhibitory tone and in all probability produce a shift in the E/I balance toward enhanced inhibition. However, interestingly, the behavioral assessments of these subjects revealed that 38% showed seizures. Some of them manifested attention deficit hyperactivity disorders (ADHD) and auto-aggressiveness with profound intellectual disabilities observed in all affected individuals. Clinically, these phenotypes are normally associated with increased excitability of brain function. These observations of functional dichotomy may hold the key to explaining the variance of our findings. All the affected individuals underwent developmental sequalae with the predicted loss of function produced by the WNK3 variants. The developmental phase of brain development is a labile period, and loss of WNK3 function may trigger parallel compensatory mechanisms possible due to the great complexity and multiple redundancies inherent in the system with some of them being beneficial and others detrimental to the long-term health of the brain manifesting as disease phenotypes. Future studies with animal models incorporating the human WNK3 variants would be essential in elucidating and reconciling these reported differences.

To conclude, our findings suggest that constitutive loss of WNK3 in pyramidal neurons plays a critical role in the maintenance of neuronal excitability by reducing resting membrane K^+ conductance and increasing the number of excitatory synaptic inputs, with a weak effect on intracellular Cl^- homeostasis. Thus, the basal function of WNK3 would be the maintenance and/or development of both intrinsic and synaptic excitabilities.

Data availability statement

The original contributions presented in the study are included in the article/Supplementary material, further inquiries can be directed to the corresponding author/s.

Ethics statement

The animal study was reviewed and approved by Committee for Animal Care and Use (No. 2018048) Hamamatsu University School of Medicine.

Author contributions

AS, TW, and MW performed experiments. AS, TW, MW, and YH performed analysis. AS, TA, and AF designed experiments. ES and SU generated mice and contributed with suggestions on the manuscript. AS and AF wrote the manuscript. All authors contributed to the article and approved the submitted version.

Funding

This work was supported by Grants-in-Aid for Scientific Research on Innovative Areas (Non-linear oscillology) #15H05872 from the Ministry of Education, Culture, Sports, Science and Technology of Japan (to AF), Grants-in-Aid for Scientific Research (B) #21H02661 from the Japan Society for the Promotion of Science, and Grant-in-Aid for Transformative Research Areas (A) #21H05687 from the Ministry of Education, Culture, Sports, Science and Technology of Japan.

Acknowledgments

We would like to thank Dr. Kyohei Watanabe, Department of Urology, HUSM for providing us with CLP290. We would also like to thank all the members of Neurophysiology Lab, HUSM (past and present) for their insightful comments and assistance during the course of our experiments.

Conflict of interest

The authors declare that the research was conducted in the absence of any commercial or financial relationships that could be construed as a potential conflict of interest.

Publisher's note

All claims expressed in this article are solely those of the authors and do not necessarily represent those

of their affiliated organizations, or those of the publisher, the editors and the reviewers. Any product that may be evaluated in this article, or claim that may be made by its manufacturer, is not guaranteed or endorsed by the publisher.

Supplementary material

The Supplementary Material for this article can be found online at: https://www.frontiersin.org/articles/10.3389/fnmol.2022.856262/full#supplementary-material

References

Achilles, K., Okabe, A., Ikeda, M., Shimizu-Okabe, C., Yamada, J., Fukuda, A., et al. (2007). Kinetic properties of Cl uptake mediated by Na+-dependent K+-2Cl cotransport in immature rat neocortical neurons. *J. Neurosci.* 27, 8616–27. doi: 10.1523/JNEUROSCI.5041-06.2007

Akita, T., and Fukuda, A. (2020). Intracellular Cl^-dysregulation causing and caused by pathogenic neuronal activity. *Pflugers Arch.* 472, 977–987. doi: 10.1007/s00424-020-02375-4

Akita, T., and Okada, Y. (2014). Characteristics and roles of the volume-sensitive outwardly rectifying (VSOR) anion channel in the central nervous system. *Neuroscience* 275, 211–31. doi: 10.1016/j.neuroscience.2014.06.015

Alessi, D. R., Zhang, J., Khanna, A., Hochdörfer, T., Shang, Y., and Kahle, K. T. (2014). The WNK-SPAK/OSR1 pathway: master regulator of cation-chloride cotransporters. *Sci. Signal.* 7, re3. doi: 10.1126/scisignal.2005365

Aller, M. I., and Wisden, W. (2008). Changes in expression of some two-pore domain potassium channel genes (KCNK) in selected brain regions of developing mice. *Neuroscience.* 151, 1154–1172. doi: 10.1016/j.neuroscience.2007.12.011

Arion, D., and Lewis, D. A. (2011). Altered expression of regulators of the cortical chloride transporters NKCC1 and KCC2 in schizophrenia. *Arch. Gen. Psychiatry.* 68, 21–31. doi: 10.1001/archgenpsychiatry.2010.114

Bassetti, D., Lombardi, A., Kirischuk, S., and Luhmann, H. J. (2020). Haploinsufficiency of Tsc2 leads to hyperexcitability of medial prefrontal cortex via weakening of tonic GABAB receptor-mediated inhibition. *Cereb. Cortex.* 30, 6313–6324. doi: 10.1093/cercor/bhaa187

Begum, G., Yuan, H., Kahle, K. T., Li, L., Wang, S., Shi, Y., et al. (2015). Inhibition of WNK3 kinase signaling reduces brain damage and accelerates neurological recovery after stroke. *Stroke.* 46, 1956–1965. doi: 10.1161/STROKEAHA.115.008939

Ben-Ari, Y. (2002). Excitatory actions of gaba during development: the nature of the nurture. *Nat. Rev. Neurosci.* 3, 728–739. doi: 10.1038/nrn920

Blaesse, P., Airaksinen, M. S., Rivera, C., and Kaila, K. (2009). Cation-chloride cotransporters and neuronal function. *Neuron.* 61, 820–38. doi: 10.1016/j.neuron.2009.03.003

Burrone, J., O'Byrne, M., and Murthy, V. N. (2002). Multiple forms of synaptic plasticity triggered by selective suppression of activity in individual neurons. *Nature.* 420, 414–8. doi: 10.1038/nature01242

Chi, X., Li, X., Chen, Y., Zhang, Y., Su, Q., and Zhou, Q. (2021). Cryo-EM structures of the full-length human KCC2 and KCC3 cation-chloride cotransporters. *Cell Res.* 31, 482–484. doi: 10.1038/s41422-020-00437-x

Côme, E., Heubl, M., Schwartz, E. J., Poncer, J. C., and Lévi, S. (2019). Reciprocal regulation of KCC2 trafficking and synaptic activity. *Front. Cell Neurosci.* 13, 48. doi: 10.3389/fncel.2019.00048

Day, M., Carr, D. B., Ulrich, S., Ilijic, E., Tkatch, T., and Surmeier, D. J. (2005). Dendritic excitability of mouse frontal cortex pyramidal neurons is shaped by the interaction among HCN, Kir2, and Kleak channels. *J. Neurosci.* 25, 8776–87. doi: 10.1523/JNEUROSCI.2650-05.2005

Day-Wilson, K. M., Jones, D. N., Southam, E., Cilia, J., and Totterdell, S. (2006). Medial prefrontal cortex volume loss in rats with isolation rearing-induced deficits in prepulse inhibition of acoustic startle. *Neuroscience.* 141, 1113–21. doi: 10.1016/j.neuroscience.2006.04.048

De Los Heros, P., Alessi, D. R., Gourlay, R., Campbell, D. G., Deak, M., Macartney, T. J., et al. (2014). The WNK-regulated SPAK/OSR1 kinases directly phosphorylate and inhibit the K+-Cl- co-transporters. *Biochem. J.* 458, 559–73. doi: 10.1042/BJ20131478

Flemmer, A. W., Gimenez, I., Dowd, B. F., Darman, R. B., and Forbush, B. (2002). Activation of the Na-K-Cl cotransporter NKCC1 detected with a phospho-specific antibody. *J. Biol. Chem.* 277, 37551–8. doi: 10.1074/jbc.M206294200

Flint, A. C., Liu, X., and Kriegstein, A. R. (1998). Nonsynaptic glycine receptor activation during early neocortical development. *Neuron.* 20, 43–53. doi: 10.1016/S0896-6273(00)80433-X

Friedel, P., Kahle, K. T., Zhang, J., Hertz, N., Pisella, L. I., Buhler, E., et al. (2015). WNK1-regulated inhibitory phosphorylation of the KCC2 cotransporter maintains the depolarizing action of GABA in immature neurons. *Sci. Signal.* 8, ra65. doi: 10.1126/scisignal.aaa0354

Gehman, L. T., Stoilov, P., Maguire, J., Damianov, A., Lin, C. H., Shiue, L., et al. (2011). The splicing regulator Rbfox1 (A2BP1) controls neuronal excitation in the mammalian brain. *Nat. Genet.* 43, 706–11. doi: 10.1038/ng.841

Goldstein, S. A., Bockenhauer, D., O'Kelly, I., and Zilberberg, N. (2001). Potassium leak channels and the KCNK family of two-P-domain subunits. *Nat. Rev. Neurosci.* 2, 175–84. doi: 10.1038/35058574

Goutierre, M., Al Awabdh, S., Donneger, F., François, E., Gomez-Dominguez, D., Irinopoulou, T., et al. (2019). KCC2 Regulates Neuronal Excitability and Hippocampal Activity via Interaction with Task-3 Channels. *Cell Rep.* 28, 91–103.e7. doi: 10.1016/j.celrep.2019.06.001

Gu, N., Vervaeke, K., and Storm, J. F. (2007). BK potassium channels facilitate high-frequency firing and cause early spike frequency adaptation in rat CA1 hippocampal pyramidal cells. *J. Physiol.* 580, 859–82. doi: 10.1113/jphysiol.2006.126367

Heubl, M., Zhang, J., Pressey, J. C., Al Awabdh, S., Renner, M., Gomez-Castro, F., et al. (2017). $GABA_A$ receptor dependent synaptic inhibition rapidly tunes KCC2 activity via the Cl^--sensitive WNK1 kinase. *Nat. Commun.* 8, 1776. doi: 10.1038/s41467-017-01749-0

Hibino, H., Inanobe, A., Furutani, K., Murakami, S., Findlay, I., and Kurachi, Y. (2010). Inwardly rectifying potassium channels: their structure, function, and physiological roles. *Physiol. Rev.* 90, 291–366. doi: 10.1152/physrev.00021.2009

Holden, S., Cox, J., and Raymond, F. L. (2004). Cloning, genomic organization, alternative splicing and expression analysis of the human gene WNK3 (PRKWNK3). *Gene* 335, 109–119. doi: 10.1016/j.gene.2004.03.009

Huang, H., Song, S., Banerjee, S., Jiang, T., Zhang, J., Kahle, K. T., et al. (2019). The WNK-SPAK/OSR1 kinases and the cation-chloride cotransporters as therapeutic targets for neurological diseases. *Aging Dis.* 10, 626–636. doi: 10.14336/AD.2018.0928

Inoue, K., Furukawa, T., Kumada, T., Yamada, J., Wang, T., Inoue, R., et al. (2012). Taurine inhibits K+-Cl- cotransporter KCC2 to regulate embryonic Cl- homeostasis via with-no-lysine (WNK) protein kinase signaling pathway. *J. Biol. Chem.* 287, 20839–50. doi: 10.1074/jbc.M111.319418

Jeong, K. H., Kim, S. H., Choi, Y. H., Cho, I., and Kim, W. J. (2018). Increased expression of WNK3 in dispersed granule cells in hippocampal sclerosis of mesial temporal lobe epilepsy patients. *Epilepsy Res.* 147, 58–61. doi: 10.1016/j.eplepsyres.2018.09.006

Kahle, K. T., Deeb, T. Z., Puskarjov, M., Silayeva, L., Liang, B., Kaila, K., et al. (2013). Modulation of neuronal activity by phosphorylation of the K-Cl cotransporter KCC2. *Trends Neurosci.* 36, 726–737. doi: 10.1016/j.tins.2013.08.006

Kahle, K. T., and Delpire, E. (2016). Kinase-KCC2 coupling: Cl^- rheostasis, disease susceptibility, therapeutic target. *J. Neurophysiol.* 115, 8–18. doi: 10.1152/jn.00865.2015

Kahle, K. T., Rinehart, J., de Los Heros, P., Louvi, A., Meade, P., Vazquez, N., et al. (2005). WNK3 modulates transport of Cl- in and out of cells: implications for control of cell volume and neuronal excitability. *Proc. Natl. Acad. Sci. U S A.* 102, 16783–8. doi: 10.1073/pnas.0508307102

Kim, Y., and Trussell, L. O. (2007). Ion channels generating complex spikes in cartwheel cells of the dorsal cochlear nucleus. *J. Neurophysiol.* 97, 1705–25. doi: 10.1152/jn.00536.2006

Kohl, S., Heekeren, K., Klosterkötter, J., and Kuhn, J. (2013). Prepulse inhibition in psychiatric disorders- apart from schizophrenia. *J. Psychiatr. Res.* 47, 445–52. doi: 10.1016/j.jpsychires.2012.11.018

Kroon, T., van Hugte, E., van Linge, L., Mansvelder, H. D., and Meredith, R. M. (2019). Early postnatal development of pyramidal neurons across layers of the mouse medial prefrontal cortex. *Sci. Rep.* 9, 5037. doi: 10.1038/s41598-019-41661-9

Küry, S., Zhang, J., Besnard, T., Caro-Llopis, A., Zeng, X., Robert, S. M., et al. (2022). Rare pathogenic variants in WNK3 cause X-linked intellectual disability. *Genet. Med.* 24, 1941–1951. doi: 10.1016/j.gim.2022.05.009

Lafreniere, R. G., MacDonald, M. L., Dube, M. P., MacFarlane, J., O'Driscoll, M., Brais, B., et al. (2004). Identification of a novel gene (HSN2) causing hereditary sensory and autonomic neuropathy type II through the Study of Canadian Genetic Isolates. *Am. J. Hum. Genet.* 74, 1064–73. doi: 10.1086/420795

Lee, A. Y., Chen, W., Stippec, S., Self, J., Yang, F., Ding, X., et al. (2012). Protein kinase WNK3 regulates the neuronal splicing factor Fox-1. *Proc. Natl. Acad. Sci. U S A.* 109, 16841–6. doi: 10.1073/pnas.1215406109

Lee, J. A., Damianov, A., Lin,. C. H., Fontes, M., Parikshak, N. N., Anderson, E. S., et al. (2016). Cytoplasmic rbfox1 regulates the expression of synaptic and autism-related genes. *Neuron*. 89, 113–28. doi: 10.1016/j.neuron.2015.11.025

Lim, L., Mi, D., Llorca, A., and Marín, O. (2018). Development and functional diversification of cortical interneurons. *Neuron.* 100, 294–313. doi: 10.1016/j.neuron.2018.10.009

Lim, W. M., Chin, E. W. M., Tang, B. L., Chen, T., and Goh, E. L. K. (2021). WNK3 maintains the GABAergic inhibitory tone, synaptic excitation and neuronal excitability *via* regulation of kcc2 cotransporter in mature neurons. *Front. Mol. Neurosci.* 14, 762142. doi: 10.3389/fnmol.2021.762142

Liu, P. W., and Bean, B. P. (2014). Kv2 channel regulation of action potential repolarization and firing patterns in superior cervical ganglion neurons and hippocampal CA1 pyramidal neurons. *J. Neurosci*. 34, 4991–5002. doi: 10.1523/JNEUROSCI.1925-13.2014

Liu, Y., Song, X., Shi, Y., Shi, Z., Niu, W., Feng, X., et al. (2015). WNK1 activates large-conductance Ca2+-activated K+ channels through modulation of ERK1/2 signaling. *J. Am. Soc. Nephrol.* 26, 844–54. doi: 10.1681/ASN.2014020186

Liu, Z., Wang, H. R., and Huang, C. L. (2009). Regulation of ROMK channel and K+ homeostasis by kidney-specific WNK1 kinase. *J. Biol. Chem.* 284, 12198–206. doi: 10.1074/jbc.M806551200

Lu, J., Karadsheh, M., and Delpire, E. (1999). Developmental regulation of the neuronal-specific isoform of K-Cl cotransporter KCC2 in postnatal rat brains. *J. Neurobiol.* 39, 558–68. doi: 10.1002/(SICI)1097-4695(19990615)39:4<558::AID-NEU9>3.0.CO;2-5

McCormick, J. A., and Ellison, D. H. (2011). The WNKs: atypical protein kinases with pleiotropic actions. *Physiol. Rev.* 91, 177–219. doi: 10.1152/physrev.00017.2010

Mederle, K., Mutig, K., Paliege, A., Carota, I., Bachmann, S., Castrop, H., et al. (2013). Loss of WNK3 is compensated for by the WNK1/SPAK axis in the kidney of the mouse. *Am. J. Physiol. Renal Physiol.* 304, F1198–209. doi: 10.1152/ajprenal.00288.2012

Misonou, H., Mohapatra, D. P., and Trimmer, J. S. (2005). Kv2.1: a voltage-gated k+ channel critical to dynamic control of neuronal excitability. *Neurotoxicology.* 26, 743–52. doi: 10.1016/j.neuro.2005.02.003

Moriguchi, T., Urushiyama, S., Hisamoto, N., Iemura, S., Uchida, S., Natsume, T., et al. (2005). WNK1 regulates phosphorylation of cation-chloride-coupled cotransporters via the STE20-related kinases, SPAK and OSR1. *J. Biol. Chem.* 280, 42685–93. doi: 10.1074/jbc.M510042200

Oi, K., Sohara, E., Rai, T., Misawa, M., Chiga, M., Alessi, D. R., et al. (2012). A minor role of WNK3 in regulating phosphorylation of renal NKCC2 and NCC co-transporters in vivo. *Biol. Open.* 1, 120–7. doi: 10.1242/bio.2011048

Pellegrino, C., Gubkina, O., Schaefer, M., Becq, H., Ludwig, A., Mukhtarov, M., et al. (2011). Knocking down of the KCC2 in rat hippocampal neurons increases intracellular chloride concentration and compromises neuronal survival. *J. Physiol.* 589, 2475–96. doi: 10.1113/jphysiol.2010.203703

Piala, A. T., Moon, T. M., Akella, R., He, H., Cobb, M. H., and Goldsmith, E. J. (2014). Chloride sensing by WNK1 involves inhibition of autophosphorylation. *Sci. Signal.* 7, ra41. doi: 10.1126/scisignal.2005050

Qiao, Y., Liu, X., Harvard, C., Hildebrand, M. J., Rajcan-Separovic, E., Holden, J. J., et al. (2008). Autism-associated familial microdeletion of Xp11.22. *Clin. Genet.* 74, 134–44. doi: 10.1111/j.1399-0004.2008.01028.x

Raimondo, J. V., Richards, B. A., and Woodin, M. A. (2017). Neuronal chloride and excitability - the big impact of small changes. *Curr. Opin. Neurobiol.* 43, 35–42. doi: 10.1016/j.conb.2016.11.012

Rinehart, J., Maksimova, Y. D., Tanis, J. E., Stone, K. L., Hodson, C. A., Zhang, J., et al. (2009). Sites of regulated phosphorylation that control K-Cl cotransporter activity. *Cell.* 138, 525–36. doi: 10.1016/j.cell.2009.05.031

Romand, S., Wang, Y., Toledo-Rodriguez, M., and Markram, H. (2011). Morphological development of thick-tufted layer v pyramidal cells in the rat somatosensory cortex. *Front. Neuroanat.* 5, 5. doi: 10.3389/fnana.2011.00005

Saitsu, H., Akita, T., Tohyama, J., Goldberg-Stern, H., Kobayashi, Y., Cohen, R., et al. (2015). De novo KCNB1 mutations in infantile epilepsy inhibit repetitive neuronal firing. *Sci. Rep.* 5, 15199. doi: 10.1038/srep15199

Seja, P., Schonewille, M., Spitzmaul, G., Badura, A., Klein, I., Rudhard, Y., et al. (2012). Raising cytosolic Cl- in cerebellar granule cells affects their excitability and vestibulo-ocular learning. *EMBO J.* 31, 1217–30. doi: 10.1038/emboj.2011.488

Silverman, J. L., Yang, M., Lord, C., and Crawley, J. N. (2010). Behavioural phenotyping assays for mouse models of autism. *Nat. Rev. Neurosci.* 11, 490–502. doi: 10.1038/nrn2851

Sullivan, B. J., Kipnis, P. A., Carter, B. M., Shao, L. R., and Kadam, S. D. (2021). Targeting ischemia-induced KCC2 hypofunction rescues refractory neonatal seizures and mitigates epileptogenesis in a mouse model. *Sci. Signal.* 14, eabg2648. doi: 10.1126/scisignal.abg2648

Swerdlow, N. R., and Geyer, M. A. (1998). Using an animal model of deficient sensorimotor gating to study the pathophysiology and new treatments of schizophrenia. *Schizophr. Bull.* 24, 285–301. doi: 10.1093/oxfordjournals.schbul.a033326

Takigawa, T., and Alzheimer, C. (1999). Variance analysis of current fluctuations of adenosine- and baclofen-activated GIRK channels in dissociated neocortical pyramidal cells. *J. Neurophysiol.* 82, 1647–50. doi: 10.1152/jn.1999.82.3.1647

Talley, E. M., Solorzano, G., Lei, Q., Kim, D., and Bayliss, D. A. (2001). CNS distribution of members of the two-pore-domain (KCNK) potassium channel family. *J. Neurosci.* 21, 7491–505. doi: 10.1523/JNEUROSCI.21-19-07491.2001

Tapias-Espinosa, C., Río-Álamos, C., Sánchez-González, A., Oliveras, I., Sampedro-Viana, D., Castillo-Ruiz, M. D. M., et al. (2019). Schizophrenia-like reduced sensorimotor gating in intact inbred and outbred rats is associated with decreased medial prefrontal cortex activity and volume. *Neuropsychopharmacology.* 44, 1975–1984. doi: 10.1038/s41386-019-0392-x

Taylor, C. A. 4th., An, S. W., Kankanamalage, S. G., Stippec, S., Earnest, S., Trivedi, A. T., et al. (2018). OSR1 regulates a subset of inward rectifier potassium channels via a binding motif variant. *Proc. Natl. Acad. Sci. U S A.* 115, 3840–3845. doi: 10.1073/pnas.1802339115

Toriumi, K., Oki, M., Muto, E., Tanaka, J., Mouri, A., Mamiya, T., et al. (2016). Prenatal phencyclidine treatment induces behavioral deficits through impairment of GABAergic interneurons in the prefrontal cortex. *Psychopharmacology (Berl).* 233, 2373–81. doi: 10.1007/s00213-016-4288-8

Voineagu, I., Wang, X., Johnston, P., Lowe, J. K., Tian, Y., Horvath, S., et al. (2011). Transcriptomic analysis of autistic brain reveals convergent molecular pathology. *Nature.* 474, 380–4. doi: 10.1038/nature10110

Wang, Y., Neubauer, F. B., Lüscher, H. R., and Thurley, K. (2010). GABAB receptor-dependent modulation of network activity in the rat prefrontal cortex in vitro. *Eur. J. Neurosci.* 31, 1582–94. doi: 10.1111/j.1460-9568.2010.07191.x

Watanabe, M., and Fukuda, A. (2015). Development and regulation of chloride homeostasis in the central nervous system. *Front. Cell Neurosci. Sep* 24; 9, 371. doi: 10.3389/fncel.2015.00371

Watanabe, M., Zhang, J., Mansuri, M. S., Duan, J., Karimy, J. K., Delpire, E., et al. (2019). Developmentally regulated KCC2 phosphorylation is essential for dynamic GABA-mediated inhibition and survival. *Sci. Signal.* 12, eaaw9315. doi: 10.1126/scisignal.aaw9315

Wischhof, L., Irrsack, E., Osorio, C., and Koch, M. (2015). Prenatal LPS-exposure- a neurodevelopmental rat model of schizophrenia–differentially affects cognitive functions, myelination and parvalbumin expression in male and female offspring. *Prog. Neuropsychopharmacol. Biol. Psychiatry.* 57, 17–30. doi: 10.1016/j.pnpbp.2014.10.004

Wu, D., Lai, N., Deng, R., Liang, T., Pan, P., Yuan, G., et al. (2020). Activated WNK3 induced by intracerebral hemorrhage deteriorates brain injury maybe via WNK3/SPAK/NKCC1 pathway. *Exp. Neurol.* 332, 113386. doi: 10.1016/j.expneurol.2020.113386

Xu, B., English, J. M., Wilsbacher, J. L., Stippec, S., Goldsmith, E. J., and Cobb, M. H. (2000). WNK1, a novel mammalian serine/threonine protein kinase lacking the catalytic lysine in subdomain II. *J. Biol. Chem.* 275, 16795–801. doi: 10.1074/jbc.275.22.16795

Yamada, J., Okabe, A., Toyoda, H., Kilb, W., Luhmann, H. J., and Fukuda, A. (2004). Cl- uptake promoting depolarizing GABA actions in immature rat neocortical neurones is mediated by NKCC1. *J. Physiol.* 557, 829–41. doi: 10.1113/jphysiol.2004.062471

Yang, S. S., Lo, Y. F., Wu, C. C., Lin, S. W., Yeh, C. J., Chu, P., et al. (2010). SPAK-knockout mice manifest Gitelman syndrome and impaired vasoconstriction. *J. Am. Soc. Nephrol.* 21, 1868–77. doi: 10.1681/ASN.2009121295

Zhang, J., Gao, G., Begum, G., Wang, J., Khanna, A. R., Shmukler, B. E., et al. (2016). Functional kinomics establishes a critical node of volume-sensitive cation-Cl^- cotransporter regulation in the mammalian brain. *Sci. Rep.* 6, 35986. doi: 10.1038/srep35986

Zhang, Z. W. (2004). Maturation of layer V pyramidal neurons in the rat prefrontal cortex: intrinsic properties and synaptic function. *J. Neurophysiol.* 91, 1171–82. doi: 10.1152/jn.00855.2003

Zhao, H., Nepomuceno, R., Gao, X., Foley, L. M., Wang, S., Begum, G., et al. (2017). Deletion of the WNK3-SPAK kinase complex in mice improves radiographic and clinical outcomes in malignant cerebral edema after ischemic stroke. *J. Cereb. Blood Flow Metab.* 37, 550–563. doi: 10.1177/0271678X16631561

frontiers | Frontiers in Molecular Neuroscience

TYPE Original Research
PUBLISHED 17 November 2022
DOI 10.3389/fnmol.2022.806798

OPEN ACCESS

EDITED BY
Yuchio Yanagawa,
Gunma University,
Japan

REVIEWED BY
Yasuhiko Saito,
Nara Medical University,
Japan
Tatsumi Hirata,
National Institute of Genetics, Japan

*CORRESPONDENCE
Tenpei Akita
tenpak@hama-med.ac.jp
Atsuo Fukuda
axfukuda@hama-med.ac.jp

SPECIALTY SECTION
This article was submitted to Neuroplasticity and Development, a section of the journal Frontiers in Molecular Neuroscience

RECEIVED 01 November 2021
ACCEPTED 27 October 2022
PUBLISHED 17 November 2022

CITATION
Hosoi Y, Akita T, Watanabe M, Ito T, Miyajima H and Fukuda A (2022) Taurine depletion during fetal and postnatal development blunts firing responses of neocortical layer II/III pyramidal neurons. *Front. Mol. Neurosci.* 15:806798. doi: 10.3389/fnmol.2022.806798

Taurine depletion during fetal and postnatal development blunts firing responses of neocortical layer II/III pyramidal neurons

Yasushi Hosoi[1,2], Tenpei Akita[1,3]*, Miho Watanabe[1], Takashi Ito[4], Hiroaki Miyajima[2] and Atsuo Fukuda[1]*

[1]Department of Neurophysiology, Hamamatsu University School of Medicine, Hamamatsu, Japan, [2]First Department of Medicine, Hamamatsu University School of Medicine, Hamamatsu, Japan, [3]Division of Health Science, Department of Basic Nursing, Hamamatsu University School of Medicine, Hamamatsu, Japan, [4]Department of Biosciences and Biotechnology, Fukui Prefectural University, Fukui, Japan

Fetal and infant brains are rich in maternally derived taurine. We previously demonstrated that taurine action regulates the cation-chloride cotransporter activity and the differentiation and radial migration of pyramidal neuron progenitors in the developing neocortex of rodent fetuses. Here we examined the effects of fetal and infantile taurine depletion caused by knockout of the taurine transporter Slc6a6 on firing properties of layer II/III pyramidal neurons in the mouse somatosensory cortex at 3weeks of postnatal age, using the whole-cell patch-clamp technique. The membrane excitability under resting conditions was similar between the neurons in knockout mice and those in wildtype littermates. However, the frequency of repetitive spike firing during moderate current injection was significantly lower, along with lower membrane voltage levels during interspike intervals in knockout neurons. When strong currents were injected, by which repetitive firing was rapidly abolished due to inactivation of voltage-gated Na^+ channels in wildtype neurons, the firing in knockout neurons lasted for a much longer period than in wildtype neurons. This was due to much lower membrane voltage levels during interspike intervals in knockout neurons, promoting greater recovery of voltage-gated Na^+ channels from inactivation. Thus, taurine depletion in pyramidal neurons blunted neuronal responses to external stimuli through increasing the stability of repetitive firing, presumably mediated by larger increases in membrane K^+ conductance during interspike intervals.

KEYWORDS

taurine, neocortex, pyramidal neurons, action potentials, taurine transporter-knockout mouse

Introduction

The central nervous system during fetal and postnatal development is rich in maternally supplied taurine. Taurine is supplied to fetuses from maternal blood through the placenta and to offspring after birth through breast milk (Miyamoto et al., 1988; Sturman, 1993). The taurine transporter SLC6A6 (TauT) is responsible for its transport into the body and cells. As the action of taurine in the central nervous system, activation of $GABA_A$, $GABA_B$, and glycine receptors as a partial agonist has been known (Kilb and Fukuda, 2017). Moreover, we previously demonstrated that taurine incorporated into the progenitors of glutamatergic neurons, mainly pyramidal neurons, in the developing neocortex of fetal rats activates the with-no-lysine (WNK) protein kinase system that phosphorylates the neuron-specific type 2 K^+-Cl^- cotransporter KCC2 (Inoue et al., 2012). The phosphorylation suppresses the Cl^- transporter activity of KCC2, thereby maintaining a high intracellular Cl^- level at ~30 mM made by the type 1 Na^+-K^+-$2Cl^-$ cotransporter NKCC1 and confirming the depolarizing effect of the opening of $GABA_A$ and glycine receptor Cl^- channels in these progenitors (Akita and Fukuda, 2020).

It has long been known that activation of $GABA_A$ receptors on pyramidal neuron progenitors promotes differentiation of the progenitors and terminates their radial migration during fetal neocortical development (Wang and Kriegstein, 2009; Luhmann et al., 2015; Akita and Fukuda, 2020). We recently revealed that taurine plays important roles as an activator of $GABA_A$ receptors in regulating both the differentiation (Tochitani et al., 2021) and the radial migration (Furukawa et al., 2014). About the differentiation, we found that the $GABA_A$ receptor-mediated differentiation of progenitors from radial glia during early embryonic development was delayed by administration of an inhibitor of taurine synthesis, D-cysteine acid (D-CSA), to maternal mice or by knocking out the TauT gene (Tochitani et al., 2021). Similarly, about the radial migration, the acceleration of migration caused by blockade of $GABA_A$ receptors was mimicked by the taurine depletion with D-CSA, in parallel with reduction of tonic $GABA_A$ receptor currents in migrating progenitors (Furukawa et al., 2014). These findings indicated that the $GABA_A$ receptor activation by taurine does facilitate progenitor differentiation and slow the speed of radial migration during normal fetal development. Nevertheless, the final proportion and destination of differentiated progenitors after migration were unaffected by taurine depletion, suggesting that a small amount of GABA in the fetal neocortex still has a significant role in these processes (Furukawa et al., 2014; Tochitani et al., 2021). The significance of taurine-mediated regulation of differentiation and migration in the following maturation of pyramidal neurons is yet unknown.

To examine the effect of taurine depletion during fetal and postnatal neocortical development on the functions of differentiated pyramidal neurons, here we used TauT knockout (KO) mice and compared intrinsic passive membrane properties and firing properties of layer II/III pyramidal neurons in the somatosensory cortex between wildtype (WT) and KO littermates at 3 weeks of postnatal age, using the whole-cell patch-clamp technique. We found that taurine depletion during development significantly altered the firing responses of pyramidal neurons to external stimuli.

Materials and methods

Ethical approval

All experiments were conducted according to the guidelines for Proper Conduct of Animal Experiments issued by Science Council of Japan, and the experimental procedures were reviewed and approved by the Institutional Animal Care and Use Committee of Hamamatsu University School of Medicine.

Animals

Heterozygous (*Slc6a6*$^{+/-}$; HT) and homozygous (*Slc6a6*$^{-/-}$; Homo) TauT KO mice with a C57BL/6 background were produced as described previously (Ito et al., 2008; Tochitani et al., 2021). Six mice of each of the genotypes (WT, HT, and Homo) were used for electrophysiological experiments. These mice were littermates born to the same pairs of HT parents. This number of mice was minimal and sufficient to reach conclusions.

Acute brain slice preparation

Coronal brain slices (300 μM in thickness) including the somatosensory cortex were obtained from male and female mice at the postnatal age of 19–23 days (P19-23). Mice were deeply anesthetized by intraperitoneal injection of pentobarbital and transcardially perfused with the cold (4°C) modified artificial cerebrospinal fluid (ACSF), whose composition was (in mM): 220 sucrose, 2.5 KCl, 1.25 NaH_2PO_4, 10 $MgSO_4$, 0.5 $CaCl_2$, 26 $NaHCO_3$, 30 glucose, oxygenated with 95% O_2/5% CO_2. After full replacement of the blood with the ACSF, mice were decaptitated and brains were removed. Slices were made in the cold modified ACSF using a VT-1000 vibratome (Leica, Wetzlar, Germany) and incubated at room temperature for 1 h prior to experiments in the standard ACSF consisting of (in mM): 126 NaCl, 2.5 KCl, 1.25 NaH_2PO_4, 2 $MgSO_4$, 2 $CaCl_2$, 26 $NaHCO_3$, 20 glucose bubbled with 95% O_2/5% CO_2.

Electrophysiology

Electrophysiological recording of action potentials (APs) was done in layer II/III pyramidal neurons in the somatosensory cortex under current-clamp conditions with the whole-cell patch-clamp technique, using a MultiClamp 700B amplifier (Molecular Devices,

San Jose, CA, United States). Membrane voltage records were lowpass filtered at 6 kHz and digitized at 20 kHz through a Digidata 1550 (Molecular Devices, San Jose, CA, United States). Recordings were made at 30°C in the standard ACSF supplemented with 10 μM CNQX, 50 μM D-AP5 and 50 μM picrotoxin to block AMPA- and NMDA-type glutamate receptors and $GABA_A$ receptors, respectively. The drugs were purchased from Sigma-Aldrich. Patch electrodes were fabricated from borosilicate glass capillaries (1.5 mm in outer diameter; GD-1.5; Narishige, Tokyo, Japan) using a P-97 puller (Sutter Instrument, Novato, CA, United States). Electrodes were filled with the solution containing (in mM): 140 K-methanesulfonate, 10 KCl, 2 $MgCl_2$, 10 HEPES, 3 Na_2ATP, 0.2 NaGTP, 1 EGTA, pH 7.3, and had a pipette resistance of 3–4 MΩ. The liquid junction potential between the solutions was 4.8 mV and corrected online. The whole-cell patch was made onto the somata of pyramidal neurons under the guidance of infrared differential interference contrast imaging.

Resting membrane potential (RMP) was determined as the mean membrane voltage level for 300 ms before current injection. Cellular membrane capacitance around the soma (C_m) was calculated from the time constant (τ) and the maximum amplitude of a membrane voltage change (ΔV) from RMP induced by injection of a hyperpolarizing current of −60 pA (I), using the equation $\tau = C_m(\Delta V/I)$, i.e., $C_m = \tau I/\Delta V$. Input resistance was determined as the linear regression slope of the I-ΔV relationship obtained by injection of currents from −60 to +60 pA in 20 pA increments. Threshold voltage level for single AP generation was determined as the level from which the slope of voltage changes (dV/dt) became >3 times larger than the slope during injection of a 2 ms current pulse. The amplitude of a single AP spike evoked by the 2 ms current pulse was defined as the difference between the peak of the AP and either RMP or the most negative voltage level during afterhyperpolarization (AHP) if it existed. The amplitudes of repetitive APs during current injection for 1 s were defined as the differences between the peaks and the following minimum voltage levels during interspike intervals.

Western blotting

The posterior halves of the cerebral cortex including the somatosensory area were collected from six WT and six Homo KO mice each. The cortices were homogenized and lysed in the lysis buffer containing (in mM) 150 NaCl, 50 Tris–HCl, 0.1% SDS, 1% NP-40, 0.5% sodium deoxycholate, added with protease inhibitors (#1697498; Roche, Basel, Switzerland). The supernatant after centrifugation was collected, separated by SDS-PAGE and transferred to a nitrocellulose membrane. Blots were blocked with 1% bovine serum albumin and incubated overnight at 4°C with the following primary antibodies: mouse anti-KCNB1 (Kv2.1) (1:1000, #SAB5200077, Sigma-Aldrich) or rabbit anti-KCNN2 (SK2) (1:1000, #APC-028, Alomone Labs, Jerusalem, Israel), and mouse anti-β actin (1:5000, #A5441, Sigma-Aldrich). The blots were then incubated with horseradish peroxidase-conjugated secondary antibody (GE Healthcare, Chicago, IL, United States) for 1 h at room temperature. Immunoblots were visualized with ECL (GE Healthcare) and photographed using a ChemiDoc Touch imaging system (Bio-Rad, Hercules, CA, United States). Band intensities of the blots were measured using Image Lab software (Bio-Rad).

Statistics

Statistical comparisons were made using SPSS software (IBM, Armonk, NY, United States). Data normality was first assessed with the Kolmogorov–Smirnov test. When the normality was confirmed, multiple comparisons were made with one-way ANOVA followed *post hoc* by Ryan–Einot–Gabriel–Welsch F (REGW-F) or Dunnett's T3 test, depending on whether equal variances could be assumed or not, respectively, from Levene statistic. When the normality was rejected, comparisons were made with the Kruskal–Wallis test (K-W) followed by the stepwise stepdown comparisons. The comparison of the proportions of neurons generating AHP after a single AP between genotypes was made with Pearson's chi-square test. The amplitude and the peak time of AHP were compared only between HT and Homo neurons, because AHP was generated only in 3 of 24 WT neurons. The comparisons were made with Student's *t* test or the Mann–Whitney *U* test, according to the data normality. Expression levels of Kv2.1 and SK2 measured by Western blotting were compared using the Mann–Whitney *U* test. $p < 0.05$ was considered significant. Data are presented as mean ± standard error of the mean (SEM).

Results

Broadening of single action potential spike in neocortical pyramidal neurons of TauT knockout mice

We previously confirmed that the taurine content in the telencephalon of TauT KO fetuses was reduced to 70% in HT and < 5% in Homo, compared with that in WT littermates, at embryonic day 12 (Tochitani et al., 2021). Since the capacity of taurine biosynthesis is still low in young animals (Hayes and Sturman, 1981), similar taurine levels would have been maintained in the brains of breast-fed infant mice (P19-23) used in this study. Indeed, in another TauT KO mouse line, the taurine content in the neocortex at 6–11 weeks of postnatal age was reported to be 57% in HT and 2% in Homo (Sergeeva et al., 2003). In the adult brain at 3 months age in our mouse line, the taurine content in Homo is increased to 15% (Ito et al., 2008).

Membrane voltage changes induced by current injection under current-clamp conditions were analyzed in neocortical somatosensory layer II/III pyramidal neurons in acute brain slice preparations. About passive membrane properties of neurons, we found no significant differences in cellular membrane

capacitance around the soma (Figure 1A), RMP (Figure 1B) and input resistance at around RMP (Figure 1C) between genotypes, although some decreasing trends in RMP and input resistance were seen in KO neurons. About a single AP spike evoked by a 2 ms brief current pulse, we found broadening of the spike in KO neurons (Figure 2A). The half-width of the spike in Homo neurons was significantly prolonged, compared with WT neurons (WT: 2.60 ± 0.06 ms, $n = 24$ from 6 mice, HT: 2.91 ± 0.12 ms, $n = 23$ from 6 mice, Homo: 2.87 ± 0.06 ms, $n = 25$ from 6 mice; $p = 0.013$, WT vs. Homo; $p = 0.074$, WT vs. HT by Dunnett's T3; Figure 2F). This was due to the reduction in speed of spike downstroke (dV/dt down; WT: −40.7 ± 1.1 mV/ms, HT: −37.6 ± 1.7 mV/ms, Homo: −36.8 ± 1.0 mV/ms; $p = 0.033$, WT vs. HT and Homo by K-W; Figure 2E) without significant changes in speed of spike upstroke (dV/dt up; Figure 2D). In addition to the broadening, the threshold voltage level for spike generation was significantly lowered in KO neurons (WT: −45.4 ± 1.3 mV, HT: −50.6 ± 1.5 mV, Homo: −51.8 ± 1.7 mV; $p = 0.035$, WT vs. HT and Homo by REGW-F; Figure 2B). The AP amplitude was slightly larger only in HT neurons (WT: 120.4 ± 1.0 mV, HT: 123.8 ± 1.0 mV, Homo: 120.5 ± 1.1 mV; $p = 0.048$, HT vs. WT and Homo by REGW-F; Figure 2C). The AHP of a single AP (not shown) was generated only in 3 of 24 WT neurons, whereas it was noticeable in 8 of 23 HT neurons and in 8 of 25 Homo neurons. However, the chi-square test did not indicate significant differences in the proportion of AHP-positive neurons between genotypes ($p = 0.163$). The amplitude of AHP (WT: −0.60 ± 0.18 mV, HT: −0.44 ± 0.09 mV, Homo: −0.92 ± 0.25 mV; $p = 0.100$, HT vs. Homo by t test) and the peak time of AHP from the AP spike peak (WT: 340.0 ± 115.9 ms, HT: 236.2 ± 35.0 ms, Homo: 488.5 ± 193.9 ms; $p = 0.574$, HT vs. Homo by Mann–Whitney U test) were similar between genotypes.

Lower frequency of repetitive action potential firing during moderate current injection in TauT knockout pyramidal neurons

We next examined the properties of repetitive AP firing induced by current injection for 1 s. The lower AP threshold level in KO neurons (Figure 2B) had implications for enhanced excitability in these neurons. Nevertheless, the minimum strength of the current required for eliciting at least one AP, called rheobase, did not differ between genotypes (Figure 3C). This means that the membrane excitability under resting conditions was not significantly altered by the lower threshold level in KO neurons. When repetitive AP firing was induced by injection of two times the rheobase current (2 × rheobase), the number of spikes in HT and Homo neurons was significantly smaller than that in WT neurons, despite no difference between HT and Homo neurons (WT: 11.4 ± 0.5 spikes/s, HT: 9.0 ± 0.6 spikes/s, Homo: 8.8 ± 0.5 spikes/s; $p = 0.001$, WT vs. HT and Homo by K-W; Figures 3A,D). This reduction in firing frequency in HT and Homo neurons was accompanied by lower membrane voltage levels during interspike intervals in these neurons, compared with WT neurons (e.g., the 5th interspike minimum voltage level, WT: −45.6 ± 1.3 mV, HT: −53.2 ± 1.8 mV, Homo: −54.1 ± 1.8 mV; $p = 0.001$, WT vs. HT and Homo by REGW-F; Figures 3A, 4A). The spike amplitude, dV/dt up and dV/dt down of APs were reduced during repetitive firing in all genotypes, and we found that all the reductions in HT and Homo neurons were significantly smaller than those in WT neurons (Figures 4B–D). The smaller reductions resulted in smaller increases in spike half-width during repetitive firing despite the wider first AP in KO neurons than in WT neurons (Supplementary Figure S1A). These indicate that the lower

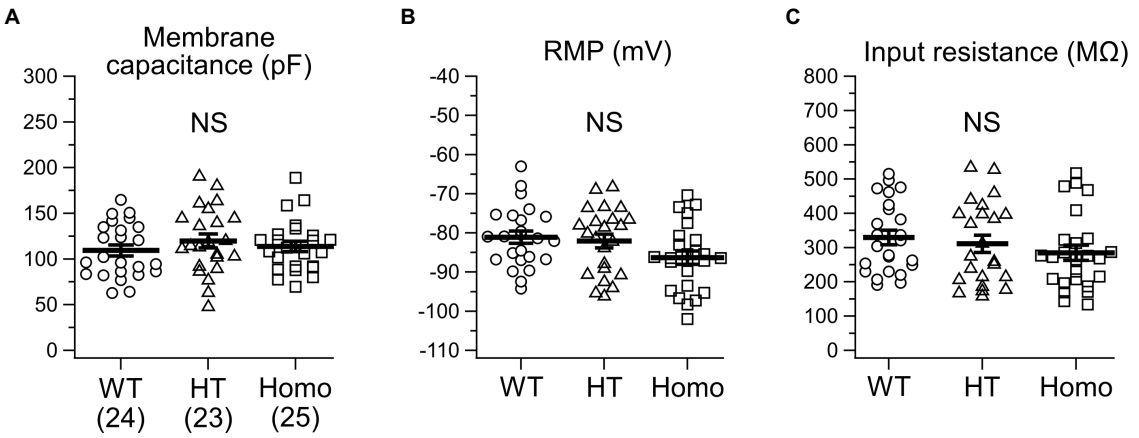

FIGURE 1
Passive membrane properties of somatosensory layer II/III pyramidal neurons in heterozygous (HT) and homozygous (Homo) TauT KO mice and wildtype (WT) littermates. **(A)** Comparison of cellular membrane capacitance around the soma. The numbers in brackets indicate the numbers of neurons analyzed. These are the same in all the figures except Figure 6 in this study. WT: 109.4±6.1pF, HT: 119.8±7.6pF, Homo: 113.9±5.6pF, $p = 0.535$ by ANOVA. **(B)** RMP. WT: −81.1±1.6mV, HT: −82.1±1.8mV, Homo: −86.3±1.7mV, $p = 0.067$ by ANOVA. **(C)** Input resistance. WT: 329.3±21.2MΩ, HT: 311.2±25.1MΩ, Homo: 284.8±22.1MΩ, $p = 0.379$ by ANOVA. NS, not significant. **(A–C)** Symbols indicate the values in individual neurons, and thick horizontal bars with error bars indicate means ± SEMs.

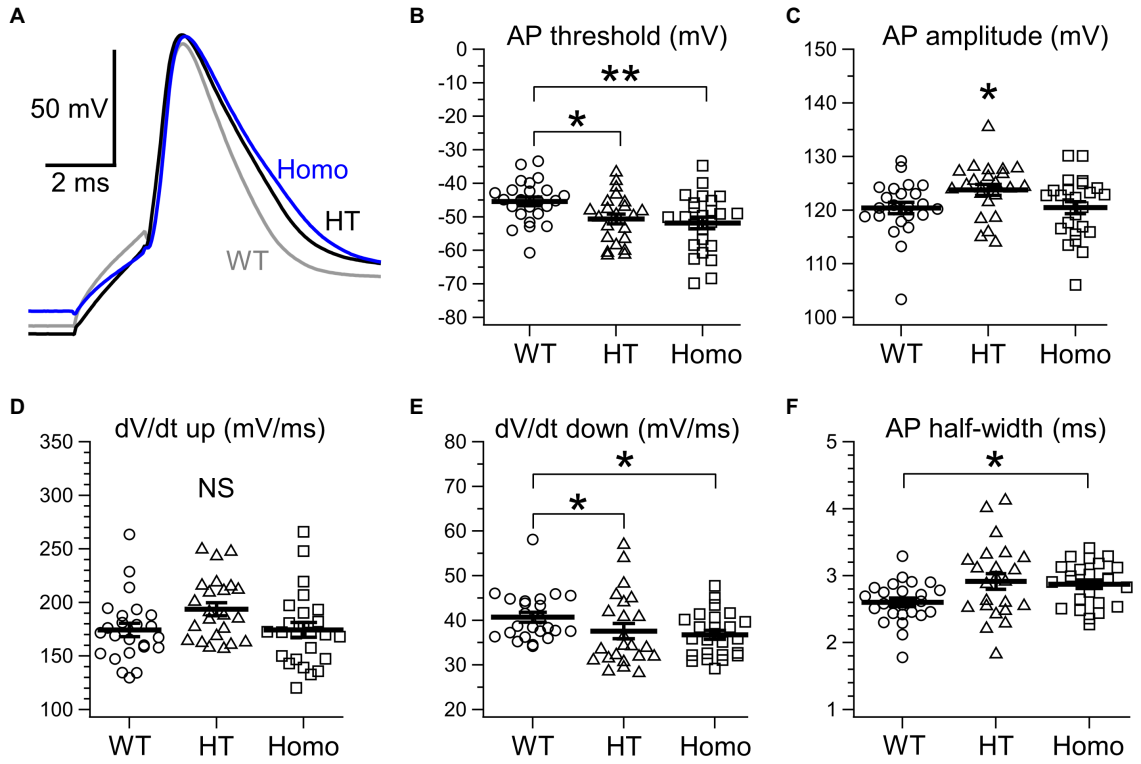

FIGURE 2
Properties of a single AP spike evoked by brief current injection. **(A)** Representative traces of a single AP evoked by a 2ms current pulse. The gray trace obtained from a WT neuron, the black from a HT neuron and the blue from a Homo neuron are superimposed. **(B)** Threshold voltage level for an AP. *p<0.05, **p<0.01 by REGW-F. See text for the values of mean±SEM. **(C)** AP spike amplitude. *p<0.05 by REGW-F. See text for the values of mean±SEM. **(D)** The maximum dV/dt during spike upstroke (dV/dt up). WT: 174.4±6.2mV/ms, HT: 193.7±6.1mV/ms, Homo: 174.4±6.9mV/ms; p=0.062 by ANOVA. **(E)** The maximum negative dV/dt during spike downstroke (dV/dt down). Plots indicate absolute values of the dV/dt. *p<0.05 by K-W. See text for the values of mean±SEM. **(F)** The width at half-maximal spike amplitude. *p<0.05 by Dunnett's T3. See text for the values of mean±SEM. **(B–F)** Symbols indicate the values in individual neurons, and thick bars with error bars indicate means ± SEMs.

interspike membrane voltage levels in KO neurons allowed voltage-gated Na^+ channels (Nav) to recover more from inactivation that occurred at AP peaks, resulting in larger repetitive APs, which in turn activated more the voltage-gated K^+ channels (Kv) that caused spike repolarization, resulting in narrower repetitive APs. Spike frequency adaptation was assessed as the gradual reduction in instantaneous frequency (the reciprocal of the interspike interval) during repetitive firing. The first instantaneous frequency, i.e., the reciprocal of the interval between the first and the second APs, did not significantly differ between genotypes (Figure 4E), although the mean value of the frequency in HT neurons was somewhat smaller than the others. The frequency reduction during repetitive firing, i.e., the adaptation, was found to be significantly faster in Homo neurons than the others (Figure 4F). Thus, these results imply that the K^+ conductance during interspike intervals would have been more increased in TauT KO neurons, thereby counteracting more strongly the depolarization caused by current injection and delaying repetitive AP generation. For the AHP generated after the end of current injection, there were no significant differences in its amplitude between genotypes (WT: −2.65 ± 0.23 mV, HT: −2.03 ± 0.23 mV, Homo: −2.44 ± 0.42 mV; p = 0.362 by ANOVA).

Sustained repetitive action potential firing during strong current injection in TauT knockout neurons

When much stronger currents of 4× and 5× rheobase were injected into WT neurons, the injection produced less than five of rapidly damping APs at the beginning of the injection, whereas the same current injection into HT and Homo neurons produced much larger numbers of repetitive APs (WT: 2.3 ± 0.1 spikes/s, HT: 5.9 ± 1.1 spikes/s, Homo: 6.4 ± 1.3 spikes/s induced by 5× rheobase; p = 0.004, WT vs. HT and Homo by K-W; Figures 3B,D) for longer periods. These differences in spike number were accompanied by much higher membrane voltage levels during interspike intervals in WT neurons, compared with KO neurons (Figures 3B, 5A). The reductions in spike amplitude, dV/dt up and dV/dt down and the increase in spike half-width during repetitive firing were still clearly smaller in KO neurons (Figures 5B–D; Supplementary Figure S1B). The first instantaneous frequency and the spike frequency adaptation under this condition were similar between genotypes (Figures 5E,F). The AHP amplitude after the end of current injection were also similar (WT: −2.64 ± 0.27 mV, HT: −1.91 ± 0.23 mV, Homo: −2.42 ± 0.45 mV; p = 0.320 by ANOVA).

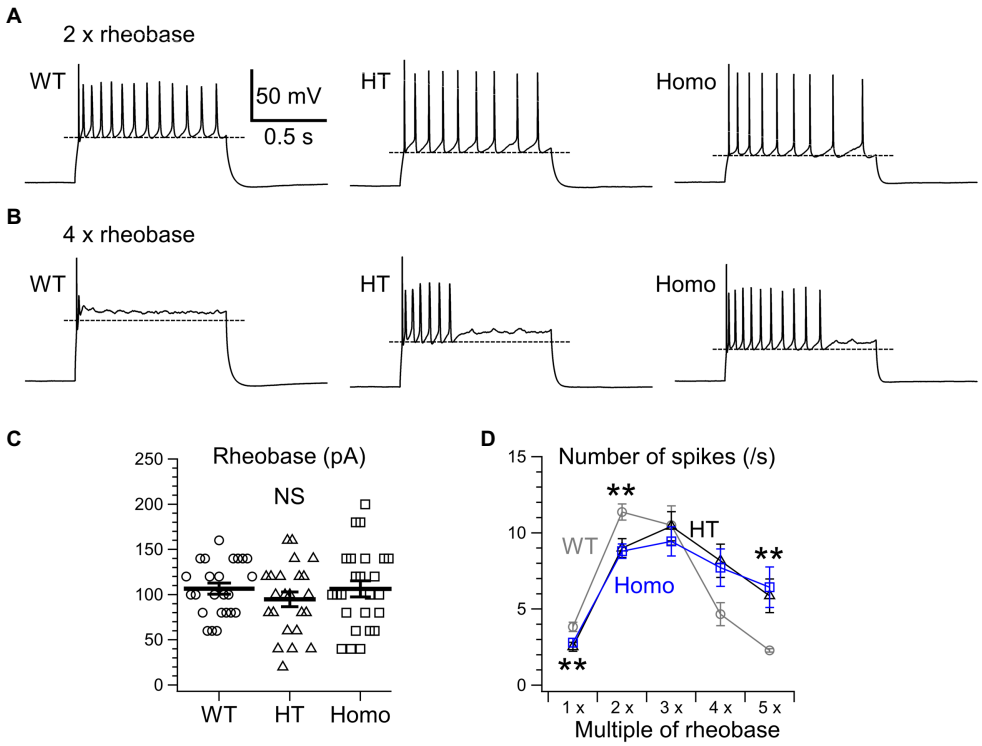

FIGURE 3
Repetitive AP firing induced by current injection for 1s. **(A)** Representative traces of repetitive firing induced by injection of two times the rheobase current (2×rheobase) in WT, HT, and Homo neurons. **(B)** The traces induced by 4×rheobase in the same neurons as in **(A)**. Broken lines in **(A,B)** indicate mean minimum membrane voltage levels during interspike intervals in these examples. **(C)** Rheobase was determined by applying current steps in 20 pA increments. WT: 106.7±6.1 pA, HT: 94.8±8.2 pA, Homo: 106.4±8.9 pA, p=0.485 by ANOVA. Symbols indicate the values in individual neurons, and thick bars with error bars indicate means ± SEMs. NS, not significant. **(D)** The numbers of AP spikes induced by 1–5×rheobase for 1s in WT (gray), HT (black), and Homo (blue) neurons. Symbols with error bars indicate means ± SEMs. **p<0.01, WT vs. HT and Homo by K-W.

These results are consistent with the idea that the more increased K^+ conductance during interspike intervals in TauT KO neurons produced lower membrane voltage levels during the intervals and promoted greater recovery of Nav from inactivation, and that this resulted in more sustained repetitive AP firing in KO neurons than in WT neurons, in which the firing was rapidly abolished through the inactivation, during strongly depolarizing current injection.

Similar protein expression levels of Kv2.1 and SK2 channels in the neocortex of wildtype and TauT knockout mice

Candidate K^+ channels responsible for the K^+ conductance during interspike intervals in neocortical pyramidal neurons are delayed rectifier Kv2 channels (Guan et al., 2013) and Ca^{2+}-activated SK-type K^+ channels (Gill and Hansel, 2020). Among these, we focused on the Kv2.1 and SK2 subtypes, which have been reported to be expressed in layer II/III (Gymnopoulos et al., 2014; Bishop et al., 2015), and compared their protein expression levels in WT and TauT KO mice. However, Western blotting of lysates from the posterior half of the neocortex showed no clear differences in the expression levels of both Kv2.1 and SK2 between WT and Homo KO mice (Figure 6).

Discussion

In this study, we found that taurine depletion during fetal and postnatal development caused by knockout of TauT significantly altered the intrinsic firing properties of neocortical layer II/III pyramidal neurons in the somatosensory cortex. The main finding was that, in TauT KO neurons, the frequency of repetitive AP firing induced by moderate stimulation with 2 × rheobase was lower than that in WT neurons, whereas the firing was sustained even during strongly depolarizing stimulation with >4 × rheobase, by which the firing in WT neurons was rapidly abolished due to Nav inactivation. These differences between KO and WT neurons were made by the lower membrane voltage levels during interspike intervals of repetitive APs in KO neurons. The lower interspike voltage levels delay the subsequent Nav activation and also promote greater recovery of Nav from inactivation occurring at AP peaks. The larger the proportion of recovered Nav, the faster spike upstrokes and the larger amplitudes of subsequent APs are generated, and these further enhance the opening of Kv responsible for spike downstroke. These were indeed indicated by the smaller reductions of these parameters during repetitive firing in KO neurons than in WT neurons. Therefore, the taurine depletion was found to blunt the responses of pyramidal neurons to external stimuli through increasing the

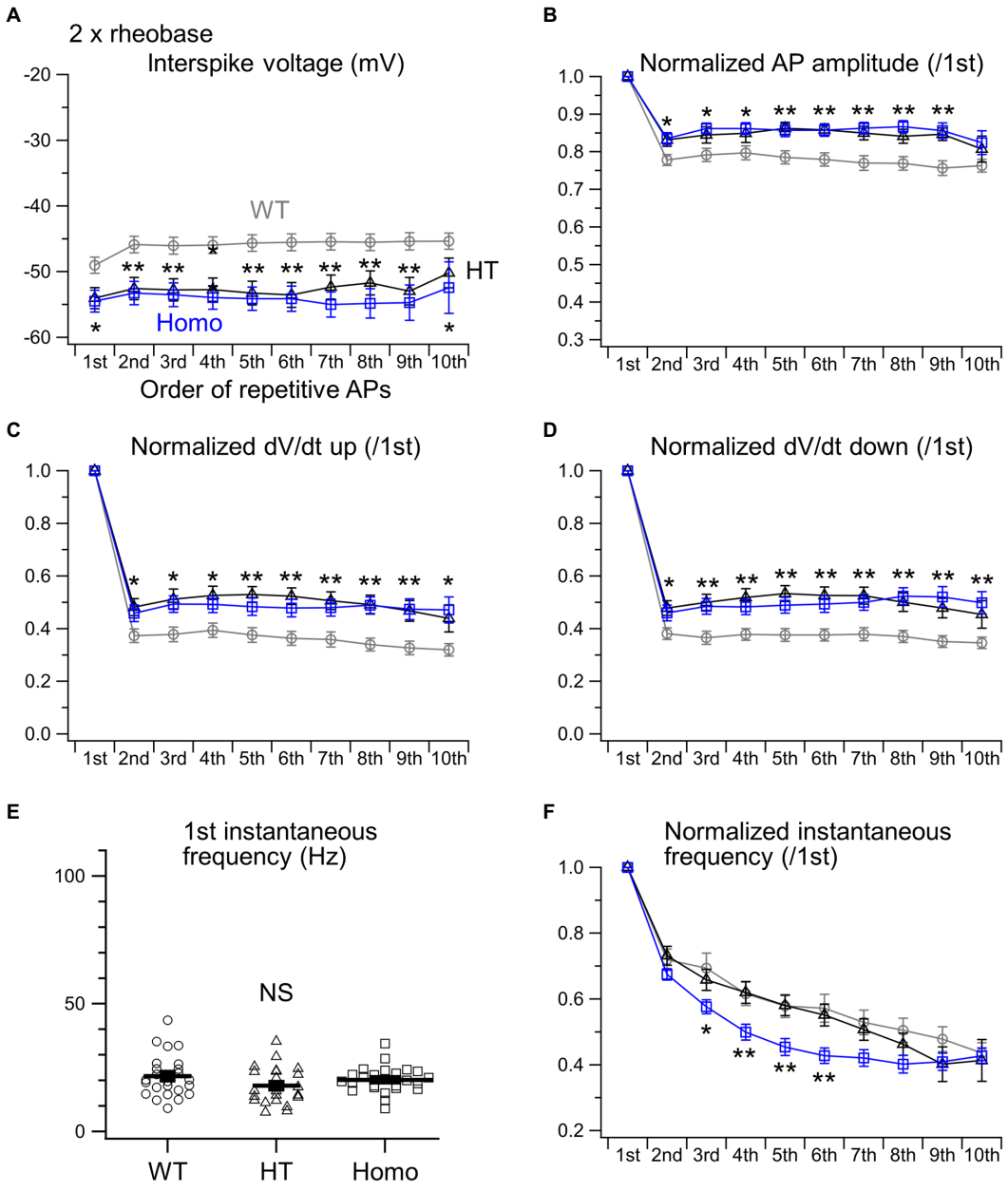

FIGURE 4
Properties of repetitive AP firing induced by 2×rheobase. **(A)** Interspike voltage levels were defined as the minimum membrane voltage levels between adjacent AP spikes. The initial 10 interspike voltages were compared between WT (gray), HT (black) and Homo (blue) neurons. **(B)** The amplitudes of initial 10 APs were normalized to that of the first AP. **(C)** dV/dt ups of initial 10 APs were normalized to the first. **(D)** dV/dt downs of initial 10 APs were normalized to the first. *p<0.05, **p<0.01, WT vs. HT and Homo by REGW-F. **(E)** Comparison of the first instantaneous frequency. Symbols indicate the values in individual neurons, and thick bars with error bars indicate means ± SEMs. WT: 21.7±1.7Hz, HT: 17.9±1.5Hz, Homo: 20.2±1.0Hz, p=0.184 by ANOVA. NS, not significant. **(F)** The initial 10 instantaneous frequencies were normalized to the first. * at 3rd, p<0.05, WT vs. HT and Homo by K-W. ** at 4th, p<0.01, WT vs. HT and Homo by Dunnett's T3. ** at 5th, p<0.01, WT vs. HT and Homo by REGW-F. ** at 6th, p<0.01, WT vs. HT and Homo by K-W.

stability of repetitive firing, presumably mediated by larger increases in membrane K^+ conductance during interspike intervals.

Despite the significantly lower threshold voltage level for single AP generation in KO neurons, the rheobase in these neurons was not smaller than that in WT neurons. This implies that the threshold reduction was so small and/or offset by different factors. Rheobase is determined not only by the AP threshold, but also by RMP and input resistance. Although the differences in RMP and input resistance between genotypes did not reach statistical significance, there were the trends of lower RMP and lower input resistance in KO neurons compared with WT neurons (Figures 1B,C). Because both the trends are the factors increasing rheobase, the trends might have canceled out the effect of the lower AP threshold in KO neurons.

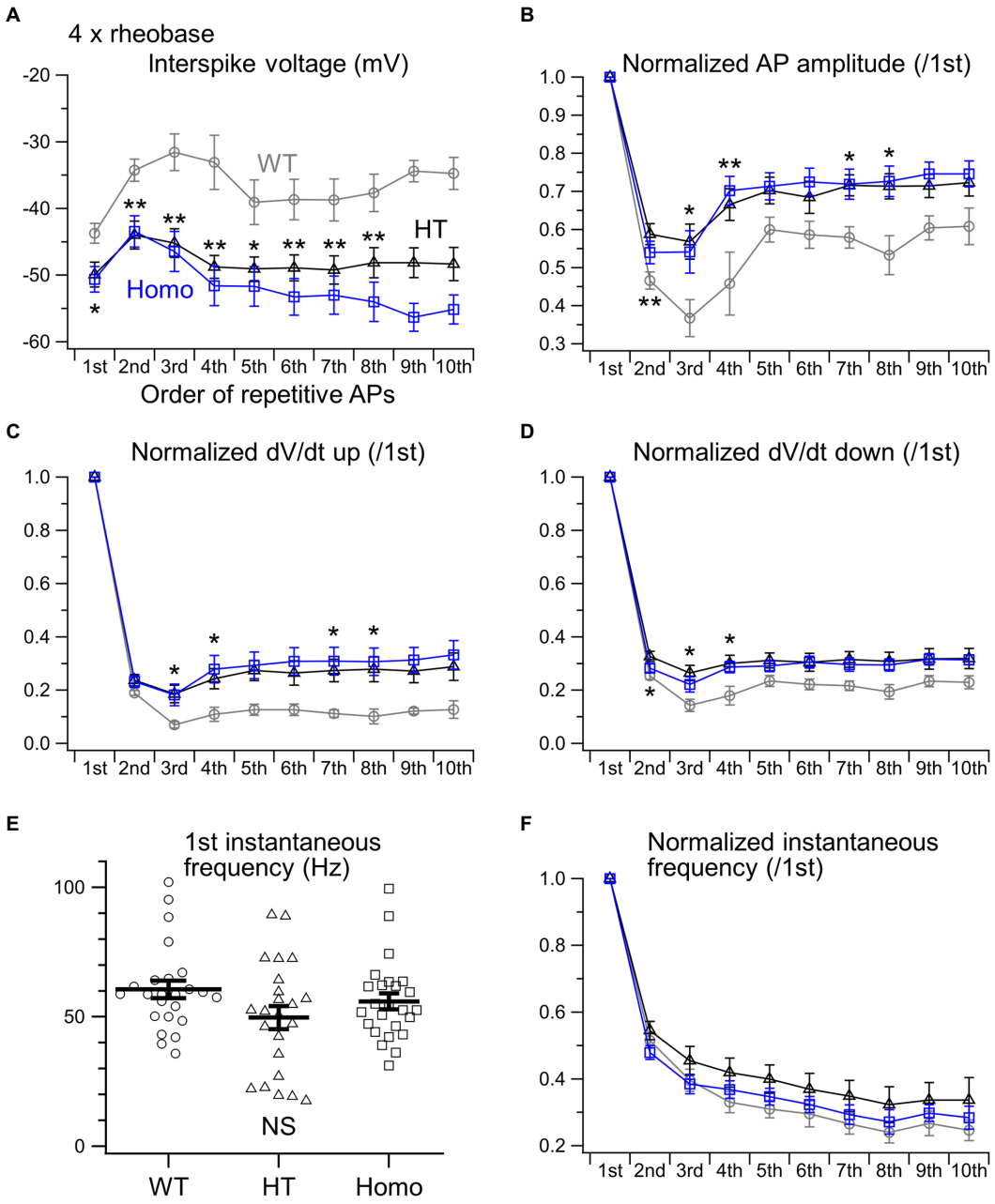

FIGURE 5
Properties of repetitive AP firing induced by 4×rheobase. **(A)** The initial 10 interspike voltage levels were compared between WT (gray), HT (black) and Homo (blue) neurons. **(B)** Normalized AP amplitudes of the initial 10 APs. **(C)** Normalized dV/dt ups. **(D)** Normalized dV/dt downs. *p<0.05, **p<0.01, WT vs. HT and Homo by REGW-F. **(E)** The first instantaneous frequency. Symbols indicate the values in individual neurons, and thick bars with error bars indicate means ± SEMs. WT: 60.6±3.4Hz, HT: 49.7±4.5Hz, Homo: 55.9±3.1Hz, p=0.220 by K-W. NS, not significant. **(F)** The initial 10 instantaneous frequencies were normalized to the first. **(A–D,F)** The parameters of the 9th and 10th APs were not compared statistically, because the number of spikes induced by 4×rheobase in WT neurons was so small (4.7±0.8 spikes/s) that the sample sizes of the 9th and 10th APs in WT neurons were less than 5.

The membrane voltage levels during interspike intervals in cortical pyramidal neurons are mainly determined by the activities of delayed rectifier Kv2 channels (Guan et al., 2013; Bishop et al., 2015) and Ca^{2+}-activated SK- and KCa3.1-types of K^+ channels (Gymnopoulos et al., 2014; Gill and Hansel, 2020; Roshchin et al., 2020), all of which do not open under resting conditions and open after AP peaks. Therefore, these K^+ channel activities would be enhanced without affecting the input resistance under resting conditions in TauT KO neurons. The comparable protein expression levels of Kv2.1 and SK2, representative subtypes of the K^+ channels, in WT and TauT KO neocortex suggest the possibility that expression levels of other subtypes such as Kv2.2 (Bishop et al., 2015), SK1, SK3 (Gymnopoulos et al., 2014) and KCa3.1 (SK4 or IK; Roshchin et al., 2020) might be elevated in TauT KO neurons. It is also possible that

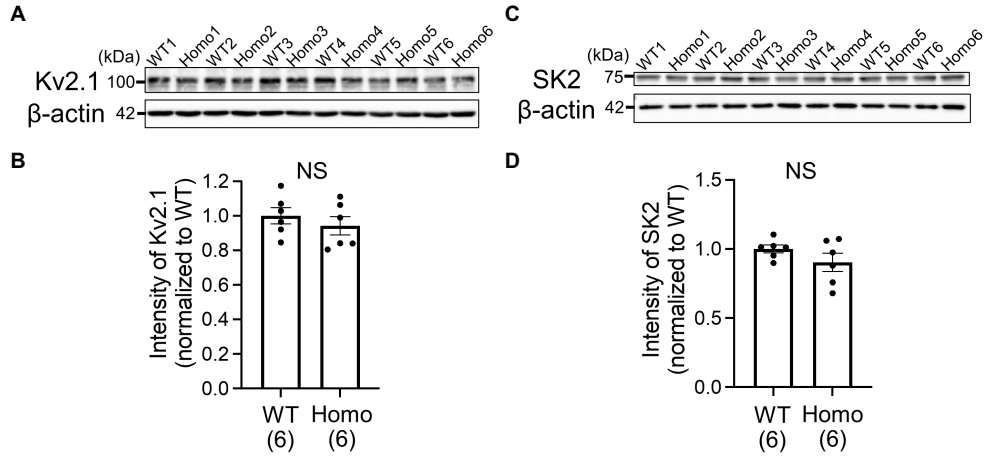

FIGURE 6
Comparison of protein expression levels of Kv2.1 and SK2 channels in the neocortex of WT and TauT Homo KO mice by Western blot analysis. **(A)** Immunoblots indicating the levels of Kv2.1 and β-actin in individual neocortices of WT and Homo KO mice. Lysates from six WT (WT1-WT6) and six Homo (Homo1-Homo6) mice were loaded onto the same polyacrylamide gel and blotted onto the same membrane. **(B)** Statistical comparison of Kv2.1 levels between WT and Homo mice. The ratio of Kv2.1 band intensity to β-actin band intensity in each lane was normalized to the mean of the ratios in the six WT lanes. Normalized ratios are plotted for each group of WT and Homo, with the height of the bar representing the mean in each group. Error bars indicate SEMs. The numbers in brackets indicate the numbers of mice analyzed. $p=0.394$ by Mann–Whitney *U* test. NS, not significant. **(C)** Immunoblots for SK2 made in the same way as in **(A)**. **(D)** Comparison of SK2 levels. The ratio of SK2 intensity to β-actin intensity in each lane was normalized to the mean of the ratios in the six WT lanes. $p=0.394$ by Mann–Whitney *U* test.

the voltage dependence, Ca^{2+} dependence or both of these K^+ channels in TauT KO neurons may differ from WT neurons due to differences in the phosphorylation state of the channels (Bishop et al., 2015; Gill and Hansel, 2020). On the other hand, the lower AP threshold and the spike broadening of isolated single APs in KO neurons suggest the reduced activities of other types of K^+ channels, like Ca^{2+}-activated BK (Bock and Stuart, 2016), Kv1 (Kole et al., 2007) and Kv4 (Carrasquillo and Nerbonne, 2014). Therefore, it is very likely that multiple types of K^+ channels are differentially modulated in TauT KO neurons. The mechanisms by which taurine depletion induces such modulation need further investigation. One possibility is the reduced signaling through the WNK kinase system under taurine-depleted conditions, because the WNK kinase and its downstream kinases of the SPS1-related proline/alanine-rich kinase (SPAK) and the oxidative stress-responsive kinase 1 (OSR1) have been reported to regulate several types of K^+ channels in other tissues (Elvira et al., 2016; Taylor et al., 2018; Bi et al., 2020). In our recent microarray assay of signal transduction proteins in WT and TauT Homo KO brains (Watanabe et al., 2022), the protein expression levels of the major WNK isoforms WNK1, WNK2 and WNK3, and the phosphorylation level of WNK1 at serine 382 were comparable between them (Supplementary Table S1), although the phosphorylation levels of the other WNK isoforms were not investigated. Furthermore, the assay revealed significantly increased expression levels of 17 proteins and phosphorylation levels of 4 proteins in TauT KO brains (Supplementary Table S1; Watanabe et al., 2022). Of these, the increased phosphorylation level of STAT3 (signal transducer and activator of transcription 3) at tyrosine 705 was particularly noticeable. STAT3 is involved in leptin signaling in the central nervous system and regulates energy metabolism in animals (Liu et al., 2021). Further studies are needed to determine whether this and the other signaling proteins may modulate K^+ channel activity in pyramidal neurons. The broadening of AP spikes with maintained peak AP levels increases the amount of Ca^{2+} entry and the subsequent Ca^{2+}-induced Ca^{2+} release from sub-plasma membrane ryanodine receptors during the spikes (Akita and Kuba, 2000; Sahu et al., 2019). The resulting enhancement of intracellular Ca^{2+} rises would contribute to the increased activity of Ca^{2+}-activated K^+ channels during the initial AP generation in TauT KO neurons. During subsequent repetitive AP spikes, the broadening was greater in WT neurons, but this was accompanied by greater reductions in AP amplitude. The amplitude reduction reduces the Ca^{2+} entry, and this would have led to weaker activation of Ca^{2+}-activated K^+ channels during repetitive APs in WT neurons than in TauT KO neurons.

The intensity of sensation to sensory stimuli is encoded by firing frequency. Therefore, the stimulus range < 3 × rheobase in this study, in which the firing rate increased with increasing current, could be regarded as the physiological range of sensory stimuli. In this range, our results imply that taurine depletion during brain development reduces the sensitivity of mice to somatosensory stimuli. In other words, taurine action in the developing brain plays a role in enhancing the somatosensory sensitivity. If the firing frequency of pyramidal neurons in other neocortical areas is also reduced in TauT KO mice, it might be reflected as the dullness or slowness of other neocortical functions, such as thinking or motor execution, of the KO mice. Indeed, our recent behavioral analysis of the KO mice revealed that, during the elevated plus maze test, Homo KO mice spent significantly less time in the closed arm and more time in the center region, with a tendency of spending more time in the open arm, although the total distance of movement during the test was similar between genotypes (Watanabe et al., 2022). This indicated that KO mice exhibited reduced anxiety-like behavior and

had difficulty making judgements regarding potential risk assessment, suggesting blunted frontal lobe function. Nevertheless, conventional TauT KO mice used in this and our recent studies show a variety of impairments in many organs including skeletal muscles (Warskulat et al., 2007; Ito et al., 2008, 2014, 2015; Qvartskhava et al., 2019; Watanabe et al., 2022). Therefore, it is difficult to precisely assess the impact of altered pyramidal neuron responses through behavioral analysis of the mice. For that purpose, conditional KO mice of TauT in pyramidal neurons would be useful.

The differences in firing properties between HT and Homo neurons were not significant in this study. This means that only 30–40% reduction in taurine content had nearly the maximum effect on the firing properties. Thus, some low-affinity taurine-sensing system would be involved in the firing regulation. Our results suggest the possibility that dietary restriction of taurine during the fetal and infantile period may cause such a reduction in taurine content that it significantly reduces the sensitivity of pyramidal neurons to external stimuli, especially in the species with a low capacity for taurine biosynthesis, like humans (Hayes and Sturman, 1981).

Studies on the effects of taurine depletion on neocortical neurons at the cellular level were largely limited to their developmental period (Furukawa et al., 2014; Kilb and Fukuda, 2017; Tochitani et al., 2021). Therefore, this study firstly reports one of the consequences of taurine depletion during development on the properties of differentiated neocortical neurons. The more stable repetitive firing of TauT KO neurons may suggest the possibility of its antiepileptic effect. This idea appears to be controversial, given the partial agonist action of taurine on $GABA_A$ and glycine receptors. Effects of taurine on epileptic seizures have long been discussed, but there have been both types of reports supportive and unsupportive of its antiepileptic effects (Oja and Saransaari, 2013). In addition, we have never seen spontaneous seizures in our TauT KO mice. The properties of interneurons, synaptic connections and glial contributions are also involved in epileptogenesis, and thus the assessment of these properties in TauT KO mice is necessary. In the striatum of another TauT KO mouse line, reduced agonist sensitivity of synaptic and extrasynaptic $GABA_A$ receptors was reported (Sergeeva et al., 2007), although it was not examined in the neocortex. We are now striving to identify other properties of neocortical neurons in our TauT KO mice, and we will report them elsewhere.

Data availability statement

The original data on which the figures in this article are based can be made available by the corresponding authors upon reasonable request.

Ethics statement

The animal study was reviewed and approved by the Institutional Animal Care and Use Committee of Hamamatsu University School of Medicine.

Author contributions

YH, TA, HM, and AF conceived and designed the study. TI produced TauT knockout mice. YH performed electrophysiological experiments. YH and TA analyzed the data. MW performed Western blotting. TA wrote the manuscript. All authors contributed to the article and approved the submitted version.

Funding

This work was supported by Grants-in-Aid for Scientific Research (B) (#25293052, #21H02661), and for Challenging Exploratory Research (#24659508) from the Japan Society for the Promotion of Science, and Grants-in-Aid for Scientific Research on Innovative Areas (Sugar Chain and Neuronal Functions #26110705 and Neuro-oscillology #15H05872) from the Ministry of Education, Culture, Sports, Science and Technology of Japan.

Acknowledgments

We thank Tomonori Furukawa in Hirosaki University for his initial technical assistance and all the members of Department of Neurophysiology in Hamamatsu University School of Medicine for fruitful discussions and suggestions on this work.

Conflict of interest

The authors declare that the research was conducted in the absence of any commercial or financial relationships that could be construed as a potential conflict of interest.

Publisher's note

Supplementary material

The Supplementary material for this article can be found online at: https://www.frontiersin.org/articles/10.3389/fnmol.2022.806798/full#supplementary-material

References

Akita, T., and Fukuda, A. (2020). "Regulation of neuronal cell migration and cortical development by chloride transporter activities," in *Neuronal Chloride Transporters in Health and Disease*. ed. X. Tang (Cambridge, MA, United States: Elsevier), 89–100.

Akita, T., and Kuba, K. (2000). Functional triads consisting of ryanodine receptors, Ca^{2+} channels, and Ca^{2+}-activated K^+ channels in bullfrog sympathetic neurons: plastic modulation of action potential. *J. Gen. Physiol.* 116, 697–720. doi: 10.1085/jgp.116.5.697

Bi, Y., Li, C., Zhang, Y., Wang, Y., Chen, S., Yue, Q., et al. (2020). Stimulatory role of SPAK signaling in the regulation of large conductance Ca^{2+}-activated potassium (BK) channel protein expression in kidney. *Front. Physiol.* 11, 1–10. doi: 10.3389/fphys.2020.00638

Bishop, H. I., Guan, D., Bocksteins, E., Parajuli, L. K., Murray, K. D., Cobb, M. M., et al. (2015). Distinct cell- and layer-specific expression patterns and independent regulation of Kv2 channel subtypes in cortical pyramidal neurons. *J. Neurosci.* 35, 14922–14942. doi: 10.1523/JNEUROSCI.1897-15.2015

Bock, T., and Stuart, G. J. (2016). The impact of BK channels on cellular excitability depends on their subcellular location. *Front. Cell. Neurosci.* 10:206. doi: 10.3389/fncel.2016.00206

Carrasquillo, Y., and Nerbonne, J. M. (2014). I_A channels: diverse regulatory mechanisms. *Neuroscientist* 20, 104–111. doi: 10.1177/1073858413504003

Elvira, B., Singh, Y., Warsi, J., Munoz, C., and Lang, F. (2016). OSR1 and SPAK sensitivity of large-conductance Ca^{2+} activated K^+ channel. *Cell. Physiol. Biochem.* 38, 1652–1662. doi: 10.1159/000443105

Furukawa, T., Yamada, J., Akita, T., Matsushima, Y., Yanagawa, Y., and Fukuda, A. (2014). Roles of taurine-mediated tonic $GABA_A$ receptor activation in the radial migration of neurons in the fetal mouse cerebral cortex. *Front. Cell. Neurosci.* 8, 1–18. doi: 10.3389/fncel.2014.00088

Gill, D. F., and Hansel, C. (2020). Muscarinic modulation of SK2-type K^+ channels promotes intrinsic plasticity in L2/3 pyramidal neurons of the mouse primary somatosensory cortex. *eNeuro* 7:2020. doi: 10.1523/ENEURO.0453-19.2020

Guan, D., Armstrong, W. E., and Foehring, R. C. (2013). Kv2 channels regulate firing rate in pyramidal neurons from rat sensorimotor cortex. *J. Physiol.* 591, 4807–4825. doi: 10.1113/jphysiol.2013.257253

Gymnopoulos, M., Cingolani, L. A., Pedarzani, P., and Stocker, M. (2014). Developmental mapping of small-conductance calcium-activated potassium channel expression in the rat nervous system. *J. Comp. Neurol.* 522, 1072–1101. doi: 10.1002/cne.23466

Hayes, K. C., and Sturman, J. A. (1981). Taurine in metabolism. *Annu. Rev. Nutr.* 1, 401–425. doi: 10.1146/annurev.nu.01.070181.002153

Inoue, K., Furukawa, T., Kumada, T., Yamada, J., Wang, T., Inoue, R., et al. (2012). Taurine inhibits K^+-cl^- cotransporter KCC2 to regulate embryonic cl^- homeostasis via with-no-lysine (WNK) protein kinase signaling pathway. *J. Biol. Chem.* 287, 20839–20850. doi: 10.1074/jbc.M111.319418

Ito, T., Kimura, Y., Uozumi, Y., Takai, M., Muraoka, S., Matsuda, T., et al. (2008). Taurine depletion caused by knocking out the taurine transporter gene leads to cardiomyopathy with cardiac atrophy. *J. Mol. Cell. Cardiol.* 44, 927–937. doi: 10.1016/j.yjmcc.2008.03.001

Ito, T., Yoshikawa, N., Inui, T., Miyazaki, N., Schaffer, S. W., and Azuma, J. (2014). Tissue depletion of taurine accelerates skeletal muscle senescence and leads to early death in mice. *PLoS One* 9:e107409. doi: 10.1371/journal.pone.0107409

Ito, T., Yoshikawa, N., Ito, H., and Schaffer, S. W. (2015). Impact of taurine depletion on glucose control and insulin secretion in mice. *J. Pharmacol. Sci.* 129, 59–64. doi: 10.1016/j.jphs.2015.08.007

Kilb, W., and Fukuda, A. (2017). Taurine as an essential neuromodulator during perinatal cortical development. *Front. Cell. Neurosci.* 11:328. doi: 10.3389/fncel.2017.00328

Kole, M. H. P., Letzkus, J. J., and Stuart, G. J. (2007). Axon initial segment Kv1 channels control axonal action potential waveform and synaptic efficacy. *Neuron* 55, 633–647. doi: 10.1016/j.neuron.2007.07.031

Liu, H., Du, T., Li, C., and Yang, G. (2021). STAT3 phosphorylation in central leptin resistance. *Nutr. Metab.* 18:39. doi: 10.1186/s12986-021-00569-w

Luhmann, H. J., Fukuda, A., and Kilb, W. (2015). Control of cortical neuronal migration by glutamate and GABA. *Front. Cell. Neurosci.* 9:4. doi: 10.3389/fncel.2015.00004

Miyamoto, Y., Balkovetz, D. F., Leibach, F. H., Mahesh, V. B., and Ganapathy, V. (1988). Na^+ + cl^- −gradient-driven, high-affinity, uphill transport of taurine in human placental brush-border membrane vesicles. *FEBS Lett.* 231, 263–267. doi: 10.1016/0014-5793(88)80744-0

Oja, S. S., and Saransaari, P. (2013). Taurine and epilepsy. *Epilepsy Res.* 104, 187–194. doi: 10.1016/j.eplepsyres.2013.01.010

Qvartskhava, N., Jin, C. J., Buschmann, T., Albrecht, U., Bode, J. G., Monhasery, N., et al. (2019). Taurine transporter (TauT) deficiency impairs ammonia detoxification in mouse liver. *Proc. Natl. Acad. Sci. U. S. A.* 116, 6313–6318. doi: 10.1073/pnas.1813100116

Roshchin, M.v., Ierusalimsky, V. N., Balaban, P. M., and Nikitin, E. S. (2020). Ca^{2+}-activated KCa3.1 potassium channels contribute to the slow afterhyperpolarization in L5 neocortical pyramidal neurons. *Sci. Rep.* 10:14484. doi: 10.1038/s41598-020-71415-x

Sahu, G., Wazen, R.-M., Colarusso, P., Chen, S. R. W., Zamponi, G. W., and Turner, R. W. (2019). Junctophilin proteins tether a Cav1-RyR2-KCa3.1 tripartite complex to regulate neuronal excitability. *Cell Rep.* 28, 2427–2442.e6. doi: 10.1016/j.celrep.2019.07.075

Sergeeva, O. A., Chepkova, A. N., Doreulee, N., Eriksson, K. S., Poelchen, W., Mönnighoff, I., et al. (2003). Taurine-induced long-lasting enhancement of synaptic transmission in mice: role of transporters. *J. Physiol.* 550, 911–919. doi: 10.1113/jphysiol.2003.045864

Sergeeva, O. A., Fleischer, W., Chepkova, A. N., Warskulat, U., Häussinger, D., Siebler, M., et al. (2007). $GABA_A$-receptor modification in taurine transporter knockout mice causes striatal disinhibition. *J. Physiol.* 585, 539–548. doi: 10.1113/jphysiol.2007.141432

Sturman, J. A. (1993). Taurine in development. *Physiol. Rev.* 73, 119–148. doi: 10.1152/physrev.1993.73.1.119

Taylor, C. A., An, S.-W., Kankanamalage, S. G., Stippec, S., Earnest, S., Trivedi, A. T., et al. (2018). OSR1 regulates a subset of inward rectifier potassium channels via a binding motif variant. *Proc. Natl. Acad. Sci. U. S. A.* 115, 3840–3845. doi: 10.1073/pnas.1802339115

Tochitani, S., Furukawa, T., Bando, R., Kondo, S., Ito, T., Matsushima, Y., et al. (2021). $GABA_A$ receptors and maternally derived taurine regulate the temporal specification of progenitors of excitatory glutamatergic neurons in the mouse developing cortex. *Cereb. Cortex* 31, 4554–4575. doi: 10.1093/cercor/bhab106

Wang, D. D., and Kriegstein, A. R. (2009). Defining the role of GABA in cortical development. *J. Physiol.* 587, 1873–1879. doi: 10.1113/jphysiol.2008.167635

Warskulat, U., Heller-Stilb, B., Oermann, E., Zilles, K., Haas, H., Lang, F., et al. (2007). Phenotype of the taurine transporter knockout mouse. *Methods Enzymol.* 428, 439–458. doi: 10.1016/S0076-6879(07)28025-5

Watanabe, M., Ito, T., and Fukuda, A. (2022). Effects of taurine depletion on body weight and mouse behavior during development. *Meta* 12:631. doi: 10.3390/metabo12070631

frontiers | Frontiers in Molecular Neuroscience

TYPE Review
PUBLISHED 01 February 2023
DOI 10.3389/fnmol.2023.1052288

OPEN ACCESS

EDITED BY
Lorenz S. Neuwirth,
State University of New York at Old Westbury, United States

REVIEWED BY
Nicole Ferrara,
Rosalind Franklin University of Medicine and Science, United States
Robert Perna,
University of Michigan Medical Center, United States
Ansab Akhtar,
University of Petroleum and Energy Studies, India

*CORRESPONDENCE
Kangrong Lu
✉ 261267443@qq.com
Wanshan Wang
✉ wws@smu.edu.cn

†These authors have contributed equally to this work and share first authorship

SPECIALTY SECTION
This article was submitted to Brain Disease Mechanisms, a section of the journal Frontiers in Molecular Neuroscience

RECEIVED 23 September 2022
ACCEPTED 16 January 2023
PUBLISHED 01 February 2023

CITATION
Huang J, Xu F, Yang L, Tuolihong L, Wang X, Du Z, Zhang Y, Yin X, Li Y, Lu K and Wang W (2023) Involvement of the GABAergic system in PTSD and its therapeutic significance. *Front. Mol. Neurosci.* 16:1052288. doi: 10.3389/fnmol.2023.1052288

Involvement of the GABAergic system in PTSD and its therapeutic significance

Junhui Huang[1†], Fei Xu[1†], Liping Yang[2], Lina Tuolihong[3], Xiaoyu Wang[4], Zibo Du[4], Yiqi Zhang[4], Xuanlin Yin[3], Yingjun Li[5], Kangrong Lu[6*] and Wanshan Wang[7*]

[1]Southern Medical University, Guangzhou, China, [2]Department of Applied Psychology of School of Public Health, Southern Medical University, Guangzhou, China, [3]Department of Basic Medical of Basic Medical College, Southern Medical University, Guangzhou, China, [4]Eight-Year Master's and Doctoral Program in Clinical Medicine of the First Clinical Medical College, Southern Medical University, Guangzhou, China, [5]Department of Medical Laboratory Science, School of Laboratory Medicine and Biotechnology, Southern Medical University, Guangzhou, China, [6]Guangdong Provincial Key Laboratory of Construction and Detection in Tissue Engineering, Southern Medical University, Guangzhou, China, [7]Department of Laboratory Animal Center, Southern Medical University, Guangzhou, China

The neurobiological mechanism of post-traumatic stress disorder (PTSD) is poorly understood. The inhibition of GABA neurons, especially in the amygdala, is crucial for the precise regulation of the consolidation, expression, and extinction of fear conditioning. The GABAergic system is involved in the pathophysiological process of PTSD, with several studies demonstrating that the function of the GABAergic system decreases in PTSD patients. This paper reviews the preclinical and clinical studies, neuroimaging techniques, and pharmacological studies of the GABAergic system in PTSD and summarizes the role of the GABAergic system in PTSD. Understanding the role of the GABAergic system in PTSD and searching for new drug targets will be helpful in the treatment of PTSD.

KEYWORDS

post-traumatic stress disorder, GABA, fear memory, amygdala, neurotransmitter

1. Introduction

Post-traumatic stress disorder (PTSD) refers to a delayed and persistent mental disorder that is caused by an individual's experience of a sudden and traumatic event, such as war, earthquake, car accident, sexual assault, or exposure to extreme stress (Battle, 2013). More than 70% of adults worldwide have experienced at least one traumatic event in their lifetime, and 31% have experienced four or more (Benjet et al., 2016). The lifetime prevalence of PTSD varies by social background and country of residence, ranging from 1.3 to 12.2%, and the 1-year prevalence ranges from 0.2 to 3.8% (Karam et al., 2014). As PTSD was originally thought to be a physiological disorder rather than a mental one, some early studies used physiological methods to explore the physical abnormalities of patients, such as heart rate, skin conductance, and facial electromyography (EMG). These measures have been widely used in PTSD studies and have strongly demonstrated high emotional responses to trauma-related cues and excessive startle responses (Vasterling and Brewin, 2005). One of the earliest and most common findings of PTSD studies is the autonomic reactivity of patients to traumatic stimuli (e.g., heart rate and

skin conductance) and facial EMG. Studies have demonstrated that the response to trauma-related cues is related to the severity of the disease (Wilson and Keane, 1997; Wolfe et al., 2000; Suendermann et al., 2010). In addition, the exaggerated startle response of PTSD patients has been documented in numerous blinks and electromyogram measurements (Orr et al., 1997, 2003; Pole, 2007; Pole et al., 2009). In mammalian studies (Koch and Schnitzler, 1997), the acoustic startle response may be a valuable model for studying the general principles of sensorimotor-motivational information processing at the behavioral and neurophysiological levels. Besides, studies of acoustic startle responses in rodents have shown that phasic fear is mediated by the amygdala, which sends outputs to the hypothalamus and brainstem to produce fear symptoms (Davis et al., 2010). However, it is still not clear whether this represents an increased neurological sensitivity to situational threats in people with PTSD. According to the latest Diagnostic and Statistical Manual of Mental Disorders by the American Psychiatric Association (DSM-5, 5th edition) (Battle, 2013) and the International Classification of Diseases, 11th Edition (ICD-11) published by the World Health Organization (Almeida et al., 2020), the core features of PTSD include intrusive symptoms, avoidance symptoms, and excessive alertness. According to ICD-11, these three symptom groups are also part of the complex post-traumatic stress disorder (CPTSD) diagnosis. Additionally, In CPTSD three other symptom groups can be summarized as disturbances in self-organization: Emotion regulation difficulties, relationship difficulties, and negative self-concept (Maercker, 2021). The DSM-5 also emphasizes cognitive and emotional changes, and patients may experience cognitive decline, depression, loss of interest, indifference, and other manifestations. The clinical diagnosis of PTSD is established when these symptoms persist for more than 1 month.

At present, the neurobiological mechanism of PTSD has not been confirmed, and the research directions mainly include four aspects: (1) Genes involved with monoamine and the hypothalamic-pituitary-adrenal (HPA) axis function have been examined extensively in epigenetic and genetic studies of PTSD risk and separately in studies of disease risk and response to treatments for mood disorders (Kato and Serretti, 2010; Domschke et al., 2014; Zannas et al., 2015; Smoller, 2016). Two of the most commonly characterized genes in this regard are the serotonin transporter (SLC6A4) and FK506 binding protein 5 (FKBP5) (Bishop et al., 2021); (2) neuroendocrine dysfunction, such as the increased secretion of catecholamines (Olson et al., 2011) and decreased secretion of 5-hydroxytryptamine (5-HT) hormones (Liu et al., 2018) and corticosterone (Geracioti et al., 2008); (3) changes in the neural structure and circuitry. Basic and clinical studies have demonstrated that structural and functional abnormalities in the hippocampus, prefrontal cortex (PFC), amygdala, and other brain areas were observed in both animal models and individuals with PTSD (Rauch et al., 2006; Hayes et al., 2012; Disner et al., 2018).

Gamma-aminobutyric acid (GABA) is an important inhibitory neurotransmitter in the central nervous system (CNS), which can reduce neuronal activity, prevent nerve cells from overheating, and calm nerves. Besides, GABA is also an active amino acid that plays an important role in the process of energy metabolism in the human brain. For example, GABA participates in the tricarboxylic acid cycle in the brain and promotes the metabolism of brain cells. At the same time, GABA can also improve the activity of glucose phosphatase during glucose metabolism, increase the generation of acetylcholine, expand blood vessels to increase blood flow, and reduce blood ammonia to promote brain metabolism and restore the function of brain cells (Petroff, 2002). As one of the inhibitory neurotransmitters of the CNS, GABA plays an essential role in regulating the stress response, emotion, and registration and encoding of fear memory (Corcoran and Maren, 2001). Dysfunction of the GABAergic system has been proven to be one of the mechanisms of PTSD, with several studies demonstrating that PTSD can reduce the levels of GABA and its receptors in some brain regions. Positron emission tomography (PET) was used to identify post-war PTSD patients, and it was observed that the distribution of benzodiazepine-GABA receptors decreased in the PFC, as well as the entire cortex, hippocampus, and thalamus (Geuze et al., 2008). Other studies have shown that the levels of GABA in the occipital and temporal lobes of PTSD patients were significantly decreased compared to controls, resulting in sleep disorders (Meyerhoff et al., 2014). Studies on animals have shown that the anxiety and fear behaviors of mouse models of PTSD improved after the administration of exogenous tetrahydroprogesteroneal, which may be induced by the enhancement of GABA function mediated by allopregnanolone (Evans et al., 2012).

Recent preclinical and clinical data indicate that GABA, which is a major inhibitory neurotransmitter involved in the pathophysiology of PTSD, plays an important role in stress. Changes in the GABA system are related to the pathogenesis of PTSD. Understanding the systemic changes in GABA in PTSD will not only contribute to the diagnosis of PTSD but also reveal new targets for pharmacological intervention.

In this review, we review the role of the GABAergic system from the phenomenon to the mechanism, and then to the clinical guidance in PTSD. We discuss fear memory, an important component of PTSD, and the role of GABA receptors in fear memory formation and extinction. By reviewing the changes in the GABA system in different brain regions in PTSD, we state the ubiquitous and heterogeneous nature of GABA in the brain. Furthermore, the role of GABA in PTSD and its mechanism were further discussed, which involved how the GABA system interacts with other systems, including the HPA axis and the endocannabinoid system (ECS), as well as the role of glutamate (Glu) and GABA signal imbalance in the brain in PTSD. Finally, we bring together the clinical, preclinical and neuroimaging evidence of changes in the GABA system in PTSD, as well as GABA mechanisms of several clinical drugs. We treat the "GABAergic system" as a single unified neurotransmitter system. It is useful to highlight large-scale, non-specific changes in GABA signaling to establish the importance of dysregulation of GABA function in PTSD.

2. GABAergic system and PTSD

The GABAergic system plays a certain role in the onset of depression, anxiety, and other mental disorders. Clinical and preclinical studies have shown that the inhibitory effect of the GABAergic system in anxiety patients is reduced (Domschke and Zwanzger, 2008). The receptor of GABA refers to the part of the postsynaptic membrane that can recognize and bind GABA. When it binds to GABA, it can cause changes in membrane ion permeability. The expression or dysfunction of GABA receptors is associated with mental illness. Three main subtypes of GABA receptors, namely, GABA-A, GABA-B, and GABA-C, have been identified so far. Among them, GABA-A and GABA-C receptors are ligand-gated ion channels. The transmembrane receptor GABA-B binds with the G protein to activate the second messenger system (Chebib and Johnston, 1999). GABA-A receptors are widely

distributed throughout the nervous system and peripheral tissues. GABA-B receptors are found in the olfactory bulb, neocortex, hippocampus, thalamus and cerebellum of mammals (Lujan and Ciruela, 2012). GABA-C receptors are found mainly in the retina, which is also distributed in the spinal cord, thalamus, pituitary gland, and intestine of mammals (Zhang et al., 2001). The rapid inhibition of the neurotransmitter GABA is mediated by GABA-A receptors. Furthermore, various subtypes of the GABA-A receptor have been identified, including α1–6, β1–3, γ1–3, δ, ε1–3, θ, and π (Jacob et al., 2008). The main receptors mediating neural inhibition in the brain are GABA-A receptors, and changes in the expression or function of these receptors in patients are increasingly related to the etiology of anxiety and depression (Merali et al., 2004; Sanacora et al., 2004; Bhagwagar et al., 2008; Poulter et al., 2008; Klempan et al., 2009; Sequeira et al., 2009; Craddock et al., 2010; Levinson et al., 2010; **Figure 1**). In particular, the changes in GABA-A receptor subunits play an important role in the amygdala and PFC mediating fear memory, as detailed in section "2.1.2. Effects of the GABAergic system on fear memory in specific brain regions." In addition, decreased levels of GABA are associated with stress responses (Dolfen et al., 2021), and GABA transmitters mediate stress and fear responses mainly by binding to their receptors.

2.1. Fear memory

Generally, PTSD is regarded as a high fear response to a threat. Thus, fear is an important target in the neurobiology of PTSD. The process of fear memory is divided into several stages, including fear acquisition, fear consolidation, fear destabilization/reconsolidation and fear extinction (Liberzon and Abelson, 2016; **Figure 2**).

Classical (or Pavlovian) fear conditioning is an effective behavioral paradigm for studying the mechanisms of associative fear learning and memory processes. In rodents, fear indicators are typically assessed by freezing behaviors (Bouton and Bolles, 1980), which is characterized by immobility and the absence of any movement except for breathing. Freezing is a potent conditioned fear response in rats and mice. And it has a great advantage over many other fear measures because freezing is not a typical response of rats or mice to ordinary new stimuli (Anagnostaras et al., 2010). A computerized method based on latency between photobeam interruption measures is used as a reliable scoring criterion in mice, which can reduce bias or inconsistencies (Valentinuzzi et al., 1998). It is important to note that when testing different strains of mice, it would be essential to validate the testing or scoring procedure (Valentinuzzi et al., 1998). To avoid artificially inflated lighting sources and thus ensure freezing behavior is induced in a well-controlled manner, it is suggested to report Lux and control the lighting properly (Neuwirth et al., 2022). When a neutral cue or context [a sound, light, or conditioned stimulus (CS)] occurs with a highly aversive signal or unconditioned stimuli (US) and leads to fear behaviors or conditioned fear responses (CRs), which include freezing, a systemic response to behavior besides breathing, fear acquisition arises [47]. The training box used in the Pavlov paradigm itself can be used as an environmental situational stimulus (CS), which is matched with an aversive plantar shock (US) multiple times. Animals learn the connection between the CS and the US and obtain the fear response (CR) to the environment. This process is called contextual fear conditioning (CFC). If a cue [usually an auditory stimulus (CS)] is matched with a foot shock (US) multiple times during the training, the auditory stimulus (CS) will be separated from the environment and associated with the foot shock (US) to form the CR to the auditory stimulus (CS). This process is called cued fear conditioning (Maren et al., 2001). The exposure of an individual to CS stimulation is sufficient to trigger a fear response (CR). This process is called retrieval of fear memory (Pape and Pare, 2010). Following retrieval, previously formed memory is destabilized, which is similar to the unstable state when the memory has just been acquired, and requires new protein synthesis to restabilize, a process referred to as reconsolidation. Reconsolidation acts to stabilize, update, or integrate new information into long-term memories (Izquierdo et al., 2016). Memory-dependent reconsolidation modification may serve as a therapeutic target to modulate the enhanced fear response commonly associated with debilitating mental disorders. People with PTSD are

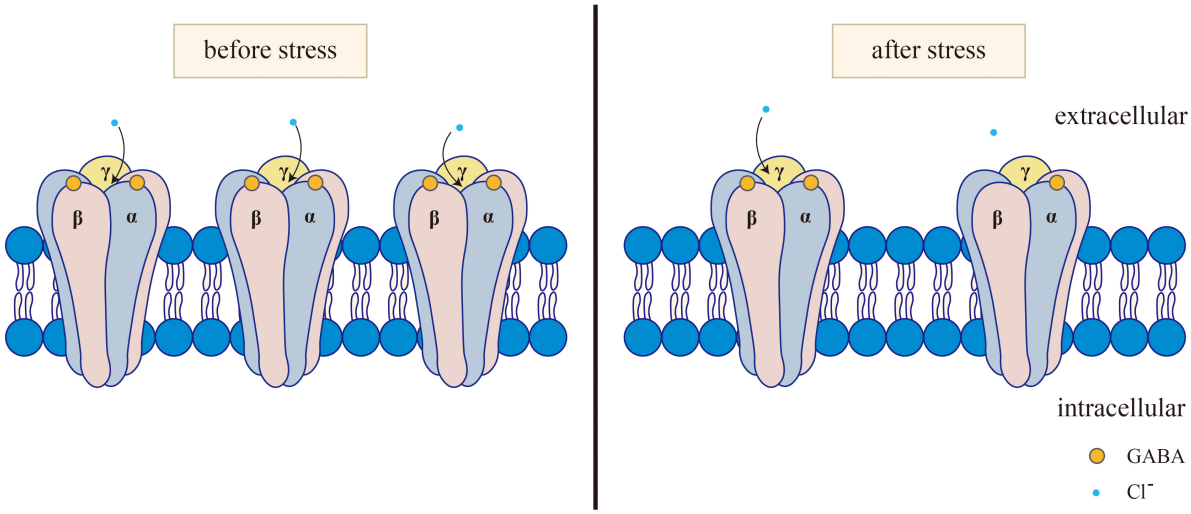

FIGURE 1
Changes of GABAA receptor before and after stress. Normally, GABA activates the opening of GABAA receptors. After the GABAA receptor is activated, it can selectively let Cl^- through, causing the hyperpolarization of neurons. After stress, GABA levels and GABA-A receptors decrease, and GABA binding to GABA-A receptors subsequently decreases, resulting in reduced Cl- influx.

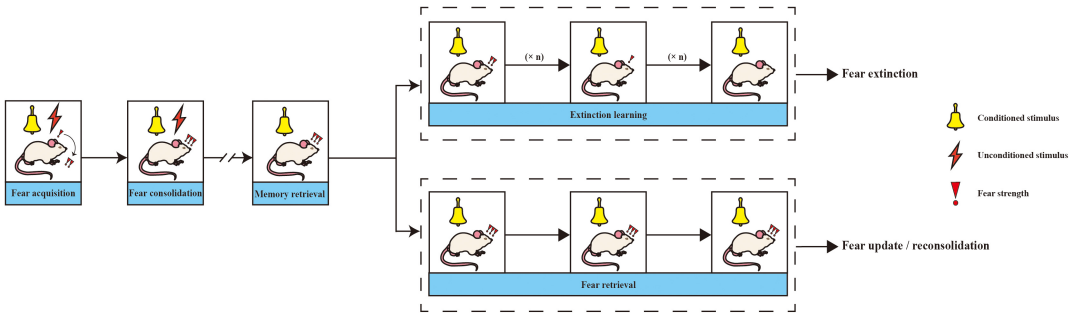

FIGURE 2
The process of fear memory. When a neutral cue or context [a sound, light, or conditioned stimulus (CS)] occurs with a highly aversive signal or unconditioned stimuli (US) and leads to fear behaviors or conditioned fear responses (CRs), fear acquisition arises. Fear memory will be consolidated within a few hours to a day of fear acquisition. When CS occurs alone, the animal will retrieve the fear memory and lead to CR. After that, if CS has been presented alone without US, fear memory becomes unstable and two different processes could occur. One is called fear extinction, which occurs after CS appears alone repeatedly many times. As a result, fear strength will decrease. The other is reconsolidation, where the fear the memory can be updated or left intact.

unable to modify or weaken memories through the reconsolidation process (Ferrara et al., 2019). Once the animals have acquired a CR, repetition of the CS alone without the US usually reduces the CR: this is called extinction. Fear extinction indicates the formation of a new competing memory, which is similar to fear conditioning, rather than the elimination of the original fear memory. In this process, the organism is enabled to acquire an association between CS and no-US, which competes with the conditioned fear memory (Bouton and Bolles, 1980). It is known that extinction generates a new memory engram, so it can be regarded as a process of active learning (Maddox et al., 2019).

2.1.1. The interplay between GABA and fear memory

Exposure to trauma can not only damage the body's physiological and psychological adaptation to stress (Lissek and van Meurs, 2015; Hill et al., 2018) but also alter to the formation and consolidation of associative fear memories (Parsons and Ressler, 2013; Elms et al., 2019). Frequent exposure to fear-related cues can impact the initial consolidation and subsequent retrieval of memory (Maddox et al., 2019), causing anxiety and trauma-related ailments such as PTSD. The persistent presence of negative cognition will impair the inhibition of invasive memory (Meiser-Stedman et al., 2009; Catarino et al., 2015). Thus, memories related to traumatic events will be repeated, while frequent flashbacks and avoidance behaviors will, in turn, worsen negative cognition, resulting in anxiety and depressive symptoms. Thus, a vicious cycle is formed.

Fear conditioning is a highly conservative form of emotional learning that occurs when an environmental stimulus predicts aversive events. This type of learning allows a previously neutral stimulus to trigger a fear response that prepares the animal for the threat and helps it escape (LeDoux et al., 1988; Blanchard and Blanchard, 1989; Fendt and Fanselow, 1999; Babaev et al., 2018). Neural circuits and cellular mechanisms that mediate fear conditioning have been extensively described, among which the inhibitory regulation of GABA neurons is crucial for the precise regulation of the consolidation, expression, and extinction of fear conditioning (Fendt and Fanselow, 1999; Zhang and Cranney, 2008; Makkar et al., 2010). The antagonists of GABA such as bicuculline (Castellano and McGaugh, 1990) have been demonstrated to enhance memory consolidation, while GABA agonists such as muscimol (Akirav et al., 2006) inhibit memory consolidation. These data suggest the involvement of GABA receptors in memory acquisition and consolidation. The role and mechanism of GABA in PTSD and fear memory extinction are still unclear. A study indicated that GABA signals promoted extinction (Berlau and McGaugh, 2006), while another study found that the activation of GABA signals prevented extinction (Singewald et al., 2015). The divergent role of GABA in extinction may be related to the different distribution of GABAergic neurons in the brain, but this still needs further explanation.

2.1.2. Effects of the GABAergic system on fear memory in specific brain regions

Most commonly, studies involved in fear memory include the PFC, amygdala and hippocampus. A summary of the changes and effects of the GABAergic system in specific brain regions can be seen in **Figure 3**. Under normal conditions, the PFC exerts inhibitory control over the amygdala. When the inhibitory effect of the PFC on the amygdala is weakened, it leads to excessive activation of the amygdala. This reduction in top-down control leads to impaired fear extinction. Michels et al. (2014) found increased GABA in the dorsolateral PFC of PTSD patients, indicating an overall shift toward inhibitory tone. Schneider et al. (2016) also showed similar changes in PFC inhibitory tone. GABA was increased in the PFC, but Glu was not changed. This change in GABA may indicate reduced excitatory activity of the PFC. A temporary increase of GABA in PFC can initiate long-term plasticity of the PFC. This change in PFC may affect the activity of the network, transmit through connections to the midline thalamus or entorhinal cortex, and ultimately affect the excitability of the hippocampus (Kyd and Bilkey, 2005). The increased excitatory tone in the hippocampus may lead to impaired fear extinction. The ventral hippocampus (vHPC) can directly project to the PFC and amygdala, affecting their activity (Ishikawa and Nakamura, 2006; Sierra-Mercado et al., 2011). The vHPC projections to the PFC can activate GABAergic neurons in the dorsal PFC and anterior cingulate.

2.1.2.1. Amygdala

Previous studies have used specific agonists of GABA receptors to inhibit the function of specific brain regions, aiming to clarify the role of each brain region in behavior. The amygdala is crucial for fear conditioning and is a key brain structure for the acquisition and expression of conditioned fear responses

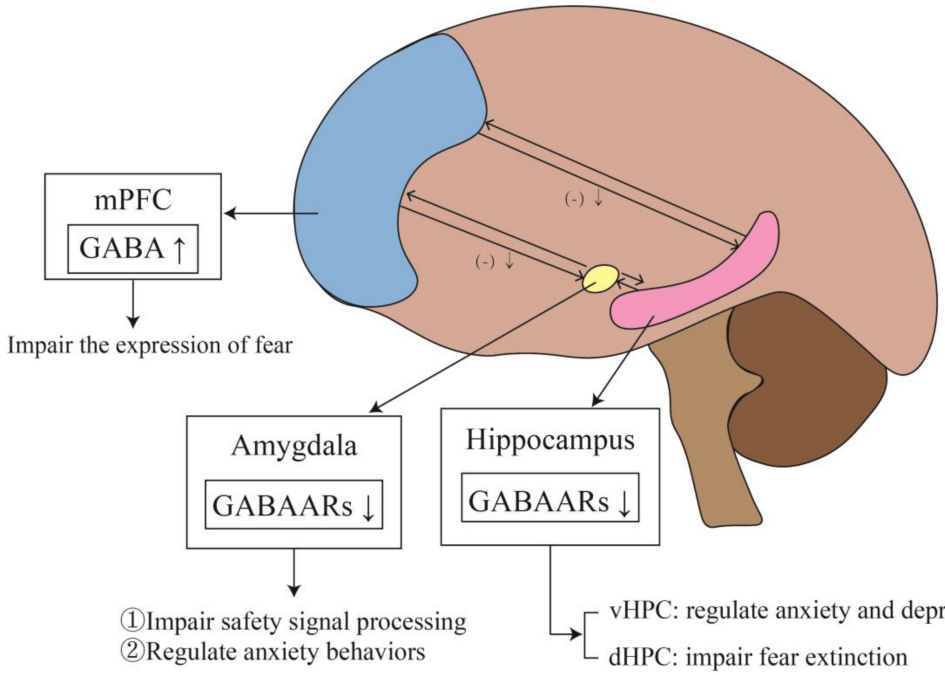

FIGURE 3
The changes and effects of the GABAergic system in specific brain regions. The outputs of mPFC to the amygdala and hippocampus are inhibitory. When PTSD develops, the level of GABA in mPFC rises, which weakens the inhibition of mPFC to amygdala and hippocampus, affecting fear memory. Meanwhile, elevated GABA level in mPFC impairs fear expression. In addition, the reduction of GABAARs in the amygdala impairs safety signal processing and regulates anxiety behaviors. The expression of GABAARs also decreases in the hippocampus. In vHPC, it leads to anxiety and depression, while in dHPC affected fear extinction.

(LeDoux, 2000; Sah et al., 2003; Chen et al., 2006). The amygdala consists of the basolateral amygdala (BLA) and the central amygdala (CeA). The BLA can be subdivided into the lateral amygdala (LA), basal amygdala (BA), and basal medial amygdala (BMA), while CeA can be further subdivided into lateral CEA (CEl) and medial CEA (CEm) (Tovote et al., 2015). The BLA and the CeA are the main research objects of fear memory, and both receive input from the cortex. The BLA consists of glutamatergic spiny projection neurons (approximately 80%) and GABAergic interneurons (McDonald, 1982; McDonald and Augustine, 1993). In contrast, the CeA is composed of GABAergic medium spiny neurons (Sah et al., 2003). In addition, there is a class of GABAergic neuronuclear nuclei between the BLA and CeA that provide feedforward inhibition signals for the BLA and CeA (Tovote et al., 2015). When the amygdala was inactivated with the GABA-A agonist muscimol, the inactivation of the amygdala resulted in deficits in situational and delayed conditioning (Raybuck and Lattal, 2011). Conversely, hyperactivity of the amygdala may be associated with impaired safety signal processing in PTSD (Christianson et al., 2012). In the classical fear conditioning circuit model, the LA is the main part of the formation and storage association of CS and US (LeDoux, 2000; Maren and Quirk, 2004; Chen et al., 2006; Sigurdsson et al., 2007; Sah et al., 2008). Besides, CeA is involved not only in fear expression but also in the learning and consolidation of Pavlovian fear conditioning (Wilensky et al., 2006). Conditioned fear can activate the inhibitory network in the CeA, inhibit the CeA-periaqueduct gray pathway, and finally promote fear (Ball et al., 2017). Conditioned fear was observed to reduce the frequency of miniature inhibitory postsynaptic current (mIPSC), as well as the expression levels of GABA type-A (GABAAR) γ2 and β2 receptors of the amygdala (Lin et al., 2011). Moreover, α2 receptors in the amygdala are involved in the regulation of anxiety behaviors (Lehner et al., 2010).

2.1.2.2. Hippocampus

The hippocampus plays a key role in the encoding, storage, and retrieval of fear memories (Anagnostaras et al., 1999; Bast et al., 2001). The vHPC inputting directly into prelimbic cortex enables to form contextual fear memory, which is necessary for the subsequent rapid expression of a fear response (Twining et al., 2020). Contextual fear conditioning was impaired after unilateral microinjection of GABAA agonist muscimol into the vHPC (Gilmartin et al., 2012). Another study (Herbst et al., 2022) showed that shock encoding in the vHPC modulated the expression of learned fear in a sex-specific manner, i.e., preventing hippocampal shock-evoked firing led to a more prolonged expression of CS freezing across test trials, an effect observed in males but not in females. Moreover, Almada et al. (2013) reported that the injection of the GABAA agonist muscimol into the dorsal hippocampus (dHPC) of mice impaired the expression of situation-associated fear memory. Similarly, another experiment revealed that the injection of muscimol into the dHPC inhibited the retrieval of short-term fear memory but not long-term fear memory (Raybuck and Lattal, 2014). This may be because the enhanced transmission of GABAergic signals can inhibit excitatory pyramidal neurons and prevent them from participating in the encoding and storage of fear memories. For example, the inhibition of hippocampal CA1 pyramidal neurons can impair the expression of fear memories associated with recent situations (Sakaguchi et al., 2015). In addition, one study showed that after stress exposure, the expression of the α1 and α2 subunits of GABA-A receptors in the vHPC is increased, contributing to stress recovery in rats (Ardi et al., 2016).

Stress and stress hormones such as corticosterone affect long-term potentiation (LTP) differently in the ventral and dorsal hippocampus. Maggio's study (Maggio and Segal, 2007) found that the magnitude of LTP in the vHPC was significantly smaller than that elicited in the dHPC. However, stress actually enhanced LTP in the vHPC, which is unlike the case in the dHPC. This different property is controlled by a metabolic Glu receptor (Sakaguchi et al., 2015). Glucocorticoid receptor (GR) and mineralocorticoid receptor (MR) antagonists blocked the stress on dHPC and vHPC, respectively. The vHPC and dHPC are distinguished not only by differences in anatomical structure but also by differences in function and gene expression. The vHPC is more involved in anxiety and emotional processing, while the dHPC is more involved in learning and memory (Fanselow and Dong, 2010). People with PTSD may suffer from anxiety and depression, and the neurobiological mechanism of PTSD involves fear learning and fear memory. Therefore, it may be difficult to distinguish the role between the vHPC and dHPC in PTSD, and further research is needed in the future.

2.1.2.3. Prefrontal cortex

Early studies on the connection between the medial prefrontal cortex (mPFC) and fear have been conducted through damage experiments. Morgan and LeDoux (1995) demonstrated that the overall damage to the mPFC, including the anterior cingulate cortex (ACC), prelimbic cortex (PL), and infralimbic cortex (IL), impaired fear acquisition rather than fear extinction. Subsequent studies have shown that damage to PL alone (mainly the dorsomedial region) enhances the acquisition of fear memories and prevents fear extinction (Davidson et al., 2000). The expression of fear was also impaired by the injection of muscimol to reduce the activity of PL neurons before extinction training (Marquis et al., 2007). Another study revealed that specific damage to the ventromedial prefrontal cortex (vmPFC) is necessary for recalling a previously learned extinction memory, rather than learning extinction *per se* (Quirk et al., 2000). These studies suggest that PL is involved in the expression of extinction learning, whereas the vmPFC is in extinction consolidation. Additionally, different subregions of the mPFC play different roles in fear expression, which may be related to differences in the distribution of GABA receptor subtypes.

Moreover, the PFC controls the stress response and participates in the regulation of emotion through inhibitory GABAergic projection to the amygdala (Davidson et al., 2000). The findings of Lu et al. (2017) indicate that early traumatic stress can increase the expression of the α2 subunit in the PFC. Deficiency of GABAAR in the PFC will weaken its control over downstream neuroanatomical regions and increase the expression of the γ2 subunit in the amygdala, leading to defective GABAergic neurotransmission. This fails to erase fear-related memories (Koenigs and Grafman, 2009; Milad et al., 2009) and impairs the control of fear responses in PTSD (Aupperle et al., 2012), thereby increasing susceptibility to PTSD in adulthood.

2.2. Changes in the GABAergic system in PTSD

Exposure to war or other traumatic events is associated with a higher risk of mental health problems, including PTSD. The clinical symptoms of these stress-related anxiety disorders are associated with the long-term dysfunction of inhibitory and excitatory neurotransmission and potential neuronal damage (Hageman et al., 2001; Charney, 2004). Both GABA and Glu are important neurotransmitters that are associated with general neurological function, memory registration, and encoding of emotional and fearful memories in anxiety disorders, especially anxiety (Pham et al., 2009). Chronic stress reduces the activity of the neurotransmitter GABA in the hippocampus and PFC, as well as the inhibition of the HPA axis, resulting in anxiety and depression (Mikkelsen et al., 2008). In previous neuroimaging studies, concentrations of these amino acids (in addition to the density and activity of neurotransmitter receptors and transporters) have been associated with mood disorders and memory dysfunction (Krystal et al., 2002). It is suggested that the normal excitation-inhibition balance in the CNS is broken between excitatory glutamatergic neurons and inhibitory GABAergic neurons due to the weakened function of GABAergic neurons, which may lead to the onset of mental disorders. The decrease in plasma GABA levels after trauma can predict the development of PTSD (Vaiva et al., 2004), suggesting that the GABAergic system is involved in the pathophysiology of PTSD. Various studies, including preclinical and clinical studies, neuroimaging techniques, and pharmacological studies, have reported the involvement of the GABAergic system in PTSD.

2.2.1. Preclinical and clinical evidence

Preclinical and clinical data indicate that GABA plays an important role in stress and that changes in the GABAergic system are related to the pathogenesis of PTSD, as it is the main inhibitory neurotransmitter involved in the pathophysiology of PTSD (Shin and Liberzon, 2010; Averill et al., 2017; Ghosal et al., 2017). Increasing evidence has suggested that the overactivation of the amygdala in PTSD patients is associated with a decreased inhibitory function of GABA (Pitman et al., 2012). Decreased inhibitory function of GABA thus plays an important role in the expression of stress-induced fear memory and the production of neuronal LTP. Reduced binding of GABA-A receptors in the cortex, hippocampus, and thalamus has been reported in veterans with PTSD, and the overall inhibitory function of the brain is deficient (Geuze et al., 2008). In victims of traffic accidents that meet the criteria of trauma exposure, a lower level of post-traumatic plasma GABA predicts the development and more chronic course of PTSD (Vaiva et al., 2006). In addition, PET studies have demonstrated that the binding of hippocampal GABAARs to benzodiazepine (BDZ) in PTSD patients is reduced (Geuze et al., 2008; Möller et al., 2016). These studies suggest that the increased expression of GABA-A receptors under stress may contribute to stress adaptation, while decreased expression of GABA-A receptors may contribute to PTSD susceptibility. Consistent with this view, a recent study in the ventral tegmental region reported that the mRNA levels of GABAergic genes were down-regulated in stress-prone mice but not in stress-adapted mice (Sun et al., 2018). Other clinical studies have reported that PTSD patients have impaired recognition of environmental cues, suggesting that impaired hippocampal function may play an important role in the development of PTSD. Exposure to unavoidable foot shock results in reduced GABA-A receptor function, as well as cortical and hippocampal binding (Lippa et al., 1978; Medina et al., 1983; Drugan et al., 1986). In the stress-restress paradigm, an animal model exhibits a similar pattern as PTSD, wherein stress causes a sustained decline in hippocampal GABA levels (Harvey et al., 2004). Animal experiments have demonstrated that chronic stress can reduce the number of GABA neurons in the hippocampal CA1 and

CA3 regions (Megahed et al., 2015). Chronic exposure to stress levels of adrenal corticosteroids leads to the abnormal expression of GABA and receptor subunits in the hippocampal CA1 and CA3 regions, although the changes in the expression of different subunits follow different patterns in the CA1 and CA3 regions (Orchinik et al., 1995). Moreover, the expression of the GABAA α2 and γ2 receptors in the PFC of adult rats decreased after shock stress in childhood, indicating that traumatic stress may reduce the activity of GABA in PFC, thus reducing the inhibition of amygdala (Lu et al., 2017). Rodent models are usually used to study social behavior disorders because they can simulate human social behavior and provide guiding information for the treatment of human social-emotional disorders. However, current rodent models of PTSD are still unable to simulate real PTSD patients well and can only simulate some features of PTSD. Therefore, more suitable animal models of PTSD still need to be explored.

In addition, several other studies have linked the GABAergic system to PTSD. Spivak et al. (2000) reported significantly elevated levels of dehydroepiandrosterone and dehydroepiandrosterone sulfate in response to GABAARs in the blood of patients with war-related chronic PTSD. These results strongly suggested that the increase in steroids and the inhibition of GABAARs are closely related to the delayed recovery of PTSD patients. A molecular genetic study reported that the polymorphism of the microsatellite sequence at the third end of the GABA β3 subunit is correlated with the incidence of PTSD (Feusner et al., 2001).

2.2.2. Neuroimaging evidence

Currently, intracranial GABA levels can be measured using proton magnetic resonance spectroscopy. Neuroimaging studies of BDZ-GABAA receptors in PTSD are rare. The GABAAR complex includes the GABAergic postsynaptic membrane, GABA receptor and chloride ion channel. When BDZ binds to BDZ receptors on the GABAAR complex, chloride channels open, and GABA binds to GABAAR to increase the frequency of chloride channel opening, which promotes chloride influx in a dual way to enhance central inhibition. Bremner et al. (2000) examined the distribution of benzodiazepine receptor recognition sites (a recognition site on the GABAAR complex) in the PFC of PTSD patients and observed that the density was significantly lower than that of normal controls. It has been suggested that changes in the function of GABAAR in this region may underlie several symptoms of PTSD. However, one study (Randall et al., 1995) showed no increase in anxiety and PTSD symptoms in PTSD patients treated with the GABAAR antagonist flumazenil. Flumazenil can reverse the central sedative effects of BDZ, but the results of this study suggest that PTSD and panic disorder (a type of anxiety disorder) differ in BDZ/GABAA system function. This may indicate the complexity of the pathological mechanism of PTSD. Changes in GABA have also been reported in Magnetic resonance spectroscopy studies on the *in vivo* neurochemistry of PTSD. Rosso et al. (2014) reported a 30% decrease in the insular GABA/creatine ratio in 13 adults with PTSD compared to healthy controls. Male veterans and civilians exhibited lower levels of GABA in the parietal occipital cortex (POC) and the proximal temporal lobe than trauma-exposed controls, while POC-GABA levels were inversely correlated with the severity of sleep symptoms (Meyerhoff et al., 2014). Sheth et al. (2019) observed that the exposure of veterans to trauma might be related to lower GABA/H_2O and glutamine (Gln)/H_2O levels in the dorsal ACC (dACC), indicating the interruption of the GABA-Gln-Glu cycle. Moreover, changes in Glu/GABA in the dACC in the PTSD group may indicate an excitation-inhibition (E-I) imbalance (Sheth et al., 2019). The E-I balance can represent the ratio of excitatory and inhibitory inputs to a neuron, and the E-I balance of a single neuron is viewed as a combination of two reaction forces projected on the neuron: excitatory and inhibitory. That is, if the excitatory input level increases, the firing rate of the neuron will increase, and if the inhibitory input level increases, the firing rate of the neuron will decrease accordingly. Furthermore, reduced GABA/H_2O in the ACC was associated with poor sleep quality in the PTSD group (Meyerhoff et al., 2014). Treatments that restore the GABAergic balance may be particularly effective in reducing sleep symptoms of PTSD. Reduction in GABAergic tone may also disturb the E/I balance, which disrupts not only regional neural activity but also functional connections in large-scale brain networks (Gu et al., 2019). These studies collectively suggest that reduced GABAergic activity may underlie the symptoms of PTSD.

2.2.3. Pharmacological evidence

Pharmacological studies also support the involvement of the GABAergic system in PTSD. Potential drugs targeting the GABAergic system can be seen in **Table 1**.

Neurosteroids, including 5-dihydro-progesterone (5-DHP), allopregnanolone (ALLO), and their stereoisomers, such as progesterone, are synthesized directly by brain neurons (glutamatergic and GABAergic long-projection neurons) in the CNS (Baulieu and Robel, 1990; Agís-Balboa et al., 2006, 2007). Neurosteroids not only act on classical steroid hormone receptors (which regulate gene expression and have long-term effects) but also rapidly regulate neuronal excitability by binding membrane receptors to ion channels. They effectively modulate GABAARs (Belelli and Lambert, 2005). Neurosteroid levels and the expression of GABAARs are affected by normal physiological changes, such as pregnancy and the ovarian cycle (Concas et al., 1998; Maguire et al., 2005), as well as by pathological conditions caused by delayed or traumatic stress, such as anxiety, depression, and PTSD (Romeo et al., 1998; Uzunova et al., 1998; Rasmusson et al., 2006). In a physiological state, the mRNA expression level of the GABAAR γ2 L subunit in the cerebral cortex and hippocampus decreased during pregnancy and recovered to the control level 2 days after delivery. Subchronic administration of finasteride (a 5α-reductase inhibitor) in pregnant rats reduced ALLO in the brain to a greater extent than in plasma and prevented the observed decline in γ2S mRNA during pregnancy (Belelli and Lambert, 2005). Pollack et al. (2008) demonstrated

TABLE 1 Potential drugs targeting GABAergic system.

Category	Medicine	Associated studies
Neurosteroids	Allopregnanolone	Almeida et al., 2021; Chen et al., 2021
Benzodiazepines	Flumazenil	Randall et al., 1995
	Alprazolam	Matar et al., 2009
	Clonazepam	Sutherland and Davidson, 1994; Cates et al., 2004
	Midazolam	Gilbert et al., 2020
GABA re-uptake inhibitor	Tiagabine	Connor et al., 2006; Davidson et al., 2007
GABA-A receptor agonist	Eszopiclone	Pollack et al., 2008
GABA-mimetic	Phenibut	Lapin, 2001
	Piracetam	Uniyal et al., 2019

that periodic changes in the specific GABAAR subunit during the estrous cycle in mice lead to periodic changes in the tonic inhibition of hippocampal neurons. In late diabetes (the high progesterone phase), tonic inhibition was increased by increased expression of deltaGABA(A)Rs, and decreased neuronal excitability was reflected in decreased susceptibility to epilepsy and anxiety. Elimination of the circulation of deltaGABA(A)Rs by antisense RNA treatment or gene knockout may prevent decreased excitability in diabetes. In a pathological state, Szabó et al. (2014) found that low levels of ALLO in the cerebrospinal fluid of premenopausal women with PTSD may lead to an imbalance between inhibitory and excitatory neurotransmitters, leading to PTSD re-experience and increased depressive symptoms. Romeo et al. (1998) found that GABA receptor positive modulators 3α,5α-tetrahydrogestrone (3α,5α-THP) and 3α,5β-THP concentrations decreased significantly during depression, while 3β,5α-THP levels increased. This imbalance of neuroactive steroids can be corrected with different antidepressant medications. Moreover, ALLO (3α5α and 3α5β isomers) has a high affinity for GABAAR and promotes the action of GABA at these receptors. In one study (Kamprath et al., 2006), SSRIs treatment induced a normal increase in ALLO levels in the cerebrospinal fluid of depressed patients. Normalization of ALLO levels in the cerebrospinal fluid of depressed patients appears to be sufficient to mediate fluoxetine or fluvoxamine to modulate the antianxiety effects of positive allosteric modulation of GABAAR. Progesterone or its neuroactive metabolite tetrahydrogestrinone can produce anti-anxiety, sedation, anesthesia, analgesic, and anticonvulsant effects in rodents and humans by effectively increasing the flux of Cl^- by binding GABA to GABAARs (Belelli et al., 2009). Allopregnanolone regulates neuroendocrine changes induced by the stress response, especially in combination with the GABAAR-mediated feedback mechanism that regulates the HPA axis (Almeida et al., 2021). Studies have demonstrated that low levels of allopregnanolone can improve PTSD symptoms by regulating the activity of GABAARs (Schüle et al., 2014).

Generally, BDZ is widely used to treat anxiety disorders, including PTSD, because of its quick-relief properties. In animal studies, BDZ regulates the function of GABAARs and inhibits the "startle" response caused by the threat from predators (Adamec et al., 2006). The role of GABA in PTSD is also supported by studies on treatment using other GABAergic compounds, such as the selective GABA re-uptake inhibitor tiagabine (Taylor, 2003; Connor et al., 2006). In addition, pharmacological studies have found that the combination of piracetam (a GABA derivative drug) and risperidone can enhance the therapeutic of PTSD (Uniyal et al., 2019). Insomnia is among the main features of PTSD, and pharmacological drugs that regulate GABA effectively alleviate insomnia (Randall et al., 1995; Krystal et al., 2014). Although BDZ effectively reduces anxiety in PTSD patients, it do not affect the core symptoms of the disorder, such as intrusive thinking, numbness, and hyperarousal (Gelpin et al., 1996; Viola et al., 1997; Davidson, 2004). This suggests that drugs targeting GABAA receptors may not be effective in the treatment of PTSD, so future studies could explore drugs targeting other targets of the GABAergic system, such as GABA reuptake inhibitors.

2.3. How does the GABAergic system change in PTSD?

2.3.1. HPA axis

Stress responses mediated by the HPA axis are most closely related to psychiatric disorders, such as PTSD and depression (Almeida et al., 2021). There are intricate afferent and efferent connections between the hypothalamus and other brain regions of CNS. Neuroendocrine cells in the hypophysiotrophic area of the hypothalamus have endocrine functions and can produce peptide neurohormones to be transported to the adenohypophysis to regulate the secretion of corresponding hormones (Clarke, 2015). Activation of the HPA axis originates from the release of corticotropin-releasing hormone (CRH) from the paraventricular nucleus (PVN) of the hypothalamus, then CRH induces the release of adrenocorticotropic hormone (ACTH), which stimulates the adrenal gland to release glucocorticoid (de Kloet et al., 2005). Glucocorticoid inhibits the release of CRH in the hypothalamus by activating MR and GR with negative feedback (de Kloet et al., 2005). During acute stress, the HPA axis is activated, which plays an important role in mobilizing energy and maintaining homeostasis. However, exposure to a single but extremely intense traumatic event, combined with chronic stress conditions, can lead to anxiety spectrum disorders or induce PTSD. Patients with PTSD showed abnormal regulation of the HPA axis, such as altered cortisol levels or failure to suppress cortisol release during dexamethasone suppression tests (Almeida et al., 2021). Preclinical and clinical studies have demonstrated that continuous activation of the HPA axis leads to elevated levels of corticosterone, which is strongly associated with stress-related psychiatric disorders (Ouellet-Morin et al., 2011; Rasmusson and Pineles, 2018). In addition, the HPA axis and GABAergic system have mutual regulatory effects.

First, changes in GABA signaling cause HPA axis dysfunction in fear memory. GABAergic connects the brain regions involved in the HPA axis and the PVN, as well as its surrounding regions, including the subventricular area, the anterior hypothalamic area, the dorsomedial nucleus of the hypothalamus, the medial preoptic area, the lateral hypothalamic area, and some subnuclei of the bed nucleus of the stria terminalis. Thus, CRH neurons receive several GABAergic inputs (Cullinan et al., 2008). The fear response is regulated by GABAergic signaling through the HPA axis, mainly through the activation of GABAARs (Brickley and Mody, 2012). Previous studies have demonstrated that CRF plays a part in fear extinction learning. Ouellet-Morin et al. (2011) reported that the absence of either GABAAα1 or NMDAR1 gene expression in CRFergic neurons results in significant and long-term deficiency of fear extinction rather than acquisition or retention.

Besides, the HPA axis regulates stress by regulating GABAergic signaling (Mikkelsen et al., 2008). Studies have reported that the injection of metyrapone, an inhibitor of corticosterone synthesis, can prevent the enhancement of intrinsic excitability in BLA→vHPC pyramidal neurons caused by foot shock. Moreover, the overexpression of GR and MR in amygdala neurons provides the basis for corticosterone regulation of BLA neurons (Kohda et al., 2007; Deppermann et al., 2014). Furthermore, changes in the intrinsic excitability of neurons are regulated by several factors, among which the weakening of inhibitory signals by the GABAAR antagonist bicuculline is an important factor (Song et al., 2017). Long-term corticosterone feeding has been observed to decrease GABAAR-mediated tonic inhibition in amygdala neurons. Moreover, corticosterone can alter the expression and function of GABAAR and drive the GABAAR-mediated chloride current (Liu et al., 2017). Liu et al. (2017) found that the recruitment of GABAA(δ)R by researchers through pharmacological and physiological methods leads to the weakening of GABAergic transmission in LA projection neurons, which indicates the disinhibition of GABAA(δ)R. Activation of GABAA(δ)R reduces the input resistance of local interneurons

and inhibits the activation of local interneurons. Deletion of the GABAA(δ)R gene weakened its inhibitory effect on LA interneurons. Therefore, corticosterone may enhance the intrinsic excitability of BLA→vHPC pyramidal neurons by reducing their inhibitory signals. In addition, studies have found that (Verkuyl and Joëls, 2003), parvocellular neurons in the PVN receive hormonal inputs mediated by corticosterone as well as GABAergic inhibitory projection. It has been proven that increases in glucocorticoid levels due to stress can inhibit GABAergic tone on parvocellular hypothalamic neurons (Verkuyl et al., 2005). Interestingly, some current studies (Hartmann et al., 2017) suggest that the regulation of fear and stress-related behaviors by corticosterone and glucocorticoids in the forebrain is mediated more by glutamatergic neurons than by GABA. Therefore, there may be two different explanations for the enhancement of neuronal excitability caused by the HPA axis in different brain regions, and more studies are needed to show which mechanism plays a dominant role in other brain regions in the future.

2.3.2. Endocannabinoid system

The endocannabinoid system (ECS) plays an important role in regulating behaviors such as fear and anxiety (Lafenêtre et al., 2007; Ruehle et al., 2012; Gunduz-Cinar et al., 2013; McLaughlin et al., 2014). Moreover, the abnormal function of this system can cause a series of neuropsychiatric disorders, such as depression and anxiety (Hillard et al., 2012; Mechoulam and Parker, 2013). Studies in the past decade have reported the relationship between The ECS and traumatic stress disorder. Piomelli (2003) and Neumeister et al. (2013) found abnormal levels of endocannabinoids in the blood and their receptors in PTSD patients, suggesting possible changes in the function of the ECS in PTSD patients.

Endocannabinoids mainly include N-arachidonoylethanolamine (AEA) and 2-arachidonoylglycerol (2-AG), which are mainly synthesized at the postsynaptic and serve as retrograde first messengers. It regulates the release of neurotransmitters by activating cannabinoid receptors located in the presynaptic membrane (Piomelli, 2003). Endocannabinoids primarily regulate the transport of GABA and Glu neurotransmitters. In addition, they also regulate the release of acetylcholine, biogenic amines noradrenaline and serotonin, and the neuropeptide CCK-8 (Piomelli, 2003).

There are two main types of cannabinoid receptors in the human body, the CB1 receptor and CB2 receptor, both of which are G-protein-coupled receptors that can activate intracellular signal transduction pathways and regulate the release of neurotransmitters and synaptic function (Adolphs et al., 2002). Animal studies have observed that the knockdown of CB1 receptors or the inhibition of CB1 receptor signaling with drugs can cause anxiety symptoms (Haller et al., 2002, 2004). The CB1 receptor-knockout mice could not eliminate fear memory after fear extinction training, indicating that the CB1 receptor plays an important role in the process of fear extinction (Marsicano et al., 2002; Cannich et al., 2004; Dubreucq et al., 2012). The agonists of CB1 such as nabilone and △9-THC can relieve some of the clinical symptoms of PTSD, such as over-stress, forgetfulness, nightmares, and pain (Bremner et al., 1996; Fraser, 2009; Passie et al., 2012). These findings suggest that the CB1 receptor is involved in regulating the transmission of neural information in the PTSD brain and plays an important role in the pathogenesis of PTSD.

Recent studies have reported that endocannabinoids regulate the processing of fear memory (Marsicano et al., 2002; Barad et al., 2006; Mahan and Ressler, 2012; Drumond et al., 2017). They are involved in the acquisition, consolidation, retrieval, and extinction of fear memories, as well as in the regulation of emotional states (Ruehle et al., 2012; Trezza and Campolongo, 2013; Xu and Südhof, 2013). In the hippocampus and amygdala, the activation of GABAergic presynaptic CB1 receptors decreases the release of GABA transmitters, thereby modulating the processing of fear memories (Morales et al., 2004; Szabó et al., 2014). The CB1 receptors are located in the presynaptic membranes of glutamatergic and GABAergic neurons, and their activation inhibits the release of Glu (Kamprath et al., 2006; Hoffman et al., 2010) and GABA (Laaris et al., 2010). Several researchers have suggested that there exists a dynamic balance system that is composed of Glu and GABA in the brain, which jointly maintains a balance between the inhibition and excitation of nerve cells. Once this dynamic balance is broken, anxiety, depression, and other emotional-related behaviors may occur (Martin et al., 2002; Haller et al., 2004), and the ECB system is an important part of the regulation of this balance. Studies have demonstrated that activation of the CB1 receptor in the dorsolateral periaqueductal gray can induce anxiety-like effects in the elevated plus maze, while the CB1 receptor antagonist AM251 prevents anxiety-like behaviors resulting from the Vogel conflict test (Lisboa et al., 2008). The activation of CB1 receptors on GABAergic neurons leads to the reduced release of GABA transmitters, resulting in anxiety-like responses (Roohbakhsh et al., 2009).

2.3.3. Imbalance between excitatory (Glu) and inhibitory (GABA) transmitters

The main inhibitory neurotransmitter in the brain is GABA, acting along with Glu to control the balance of excitation and inhibition in several brain circuits (Petroff, 2002). The neurotoxicity of Glu not only leads to the apoptosis and necrosis of brain neurons in patients with ischemic cerebrovascular disease (Sun et al., 2015) but also affects synaptic plasticity in the brains of patients with PTSD (Stachowicz, 2018). The GABAergic system is an important inhibitory system in the CNS that can protect the normal regulatory function of the nervous system by inhibiting the hyper-excitatory effect of Glu. During the metabolic switch between Glu and GABA, two pathways eliminate excess Glu in the synaptic cleft or mitigate its neurotoxicity (Gao et al., 2014).

The production of GABA from Glu promotes the release of more Glu, which is mediated by glutamic acid decarboxylase (GAD). The GAD is the key rate-limiting enzyme in GABA synthesis. There are two kinds of isoenzymes of GAD, GAD65 and GAD67. Abnormal function of GAD65/67 can also lead to decreased GABA levels. Generally, GAD65 is primarily responsible for the synthesis of GABA that is released at synapses, while GAD67 is the 67 kDa isoform of GAD (GABA synthase), which is responsible for the synthesis of GABA in the metabolic pool of neurons. The distribution of GAD is consistent with that of GABAergic neurons, which makes GAD an excellent marker enzyme for GABAergic neurons, with the functional status of GABAergic neurons in the CNS being often reflected by measuring the activity of GAD in brain tissue. It was reported that chronic adverse stimulation further decreased the expression level of GAD67 and the number of GAD67-positive neurons, suggesting that stress impaired the conversion of Glu to GABA by reducing the level of GAD, thereby limiting GABA synthesis (Fogaça and Duman, 2019). The levels of GAD67 in the hippocampus, amygdala, and PFC of PTSD rats were decreased, suggesting that the reduction in GABA content could weaken the central inhibitory function and disrupt the balance between GABA and Glu. The results of autopsies of patients with major depressive disorder showed significant reductions in the activity of GAD65

in the PFC brain region (Karolewicz et al., 2010), as well as the density of GAD65/67 in the PVN of the hypothalamus (Gao et al., 2013). Similarly, the expression of GAD67 was downregulated in the PFC (Pochwat et al., 2016) in both mouse and rat models of depression. The GAD65 knockout mice showed fear generalization and fear resolution disorders in preclinical trials (Sangha et al., 2009), suggesting an important role for GAD65 in preventing anxiety-like behaviors, fear memory extinction, and resilience to the development of contextual fear generalization.

The GABA transporter (GAT) may play an important role in mental disorders such as anxiety and depression by affecting GABAergic transmission. However, evidence for this hypothesis is scarce, with studies reporting that patients with anxiety disorders exhibit positive clinical responses to the selective GAT-1 inhibitor tiagabine (Schwartz and Nihalani, 2006). In the study of Liu et al. (2007) the researchers used the forced swimming test and the tail suspension test to model depression and anxiety in mice and measured resilience through the open field test, the dark light exploration test, the emergence test and the elevated plus maze (EPM) behavior test. The GAT-1-deficient mice exhibit increased resilience to acute stress in response to behavioral paradigms such as antidepressant- and antianxiety-like activities (Liu et al., 2007; Gong et al., 2015), which substantiates the role of GAT-1 in mood disorders. However, the role of GAT in PTSD needs investigation. The concentration of GABA in the extra-synaptic space is regulated in several ways. In addition to GAT-1, the GABA transporters GAT-2 and betaine/GABA transporter 1 (BGT-1) are located on astrocytes that recycle GABA. Additionally, GABA in astrocytes can enter the intercellular space through the bestrophin channel as a non-vesicular release (Brickley and Mody, 2012), and these regulatory mechanisms maintain the concentration of GABA at a stable level outside synapses. However, there are very few studies linking GABA-astrocytes to PTSD, which gives us an indication that future studies may focus on this aspect.

Psychological stress can cause an imbalance between excitatory Glu and inhibitory GABA neurotransmitters, which can lead to a series of neurochemical changes. First, the increased expression of apoptotic markers in the muscle, thymus, and nervous system is related to stress. Moreover, the survival and apoptosis of neurons are related to the mechanism of the balance between Glu and GABA (Engelbrecht et al., 2010). The glutamate/gamma-aminobutyric acid-glutamine metabolic circuit in the CNS is the main pathway that regulates the metabolism of Glu and GABA, which is important to maintain the dynamic balance between excitatory and inhibitory systems in the brain (Jiang et al., 2022). During the metabolic conversion of Glu to GABA, excess Glu in the synaptic cleft can be eliminated or reduced through the excitatory amino acid transporters (EAATs) and GAD pathways. In other words, when the conversion level of Glu to GABA is insufficient, resulting in too much Glu and too little GABA in the CNS, an imbalance of excitation and inhibition can occur. The elevation or accumulation of Glu can induce apoptosis in sensitive neural cells. When GABA is catalyzed by Glu and directed by GAD, it has positive feedback on its own release. Such imbalance further leads to dysfunctional excitatory spasms. The findings of Fogaça and Duman (2019) suggest that the imbalance between the excitatory (Glu) and inhibitory (GABA) transmitters may promote apoptosis in the hippocampal neurons and play an important role in the pathogenesis of PTSD. However, this finding is inconsistent with the brain imaging results of patients, which may indicate that humans and rodents have different responses to PTSD-like stress. Therefore, the specific reasons for this need further investigation.

3. Clinical directions

Several types of drugs, mainly antidepressants, antipsychotics, and anticonvulsants, target PTSD. However, anti-stress drugs are not widely used in PTSD, although they can regulate the GABAergic system, stimulate GABA receptors, inhibit GABA transporters, and restore the function of the GABAergic system in the brain.

As anti-anxiety agents, BDZ is widely used clinically. For instance, BDZ such as diazepam, flurazepam, clorazepate, oxazepam, and triazolam, is also used in the treatment of PTSD symptoms, but prolonged use of these agents can cause dizziness, drowsiness, fatigue, and other adverse effects. In addition, BDZ promotes GABA-mediated neural transmission in the CNS (Mao et al., 1975). Such drugs do not directly excite GABA recognition sites and accelerate the release of GABA but increase the affinity of low-affinity GABAAR or the number of GABAARs through allosteric regulation to enhance the inhibitory function of GABA. Promoting the E-I balance caused by stress produces anti-anxiety and sedative effects. Studies on the GABAAR family reported that the α2 and α3 subunits are closely related to anxiety behaviors under the effect of BDZ (Dias et al., 2005). The α5 subunit is involved in hippocampus-associated associative memory (Rudolph et al., 1999; Rudolph and Möhler, 2004). The γ^2 subunit is extensively regulated by BDZ in the brain (Günther et al., 1995).

Topiramate is an anticonvulsant, which is also among the supplementary drugs in the clinical use of PTSD (Khan and Liberzon, 2004). Topiramate enhances the function of the GABA receptor and induces the influx of chloride ions. It is also involved in the intervention of PTSD symptoms by regulating and restoring the content of GABA in the brain and maintaining the excitation-inhibitory stability of Glu and GABA in the CNS (Berlant, 2001). In clinical studies on PTSD, it was observed that the rate of relief from PTSD symptoms in the topiramate-treatment group was significantly higher than that in the control group. Topiramate has been proven to relieve the symptoms of recurrent traumatic experiences, nightmares, and other PTSD symptoms, such as high arousal, although these drugs also have significant side effects, including dizziness and lethargy.

Studies have also found that neurosteroids have an anti-anxiety effect by acting on the GABAergic system, as they can directly act on the GABAAR, prolong the opening time and increase the opening frequency of its chloride channel, thus increasing the inhibitory effect of GABA (Lambert et al., 1995).

4. Conclusion

The GABAergic system is significant in the regulation of PTSD. After traumatic events, the formation of fear memory and synaptic plasticity are affected by the GABA inhibition system, and the balance in excitation-inhibition homeostasis between neural networks is destroyed, resulting in complex changes in the thoughts, feelings, and behaviors of the subject. Anti-stress drugs that regulate the GABAergic system restore GABA function in the brain by stimulating GABA receptors or inhibiting GABA transporters. Although such drugs can relieve PTSD symptoms, they can also have side effects such as dizziness, drowsiness, and fatigue. Future research is needed

to further explore the common mechanisms underlying the core symptoms of PTSD to guide the discovery of ideal targets for the treatment of PTSD. In summary, the consequence of PTSD may be related to the downregulation of GABAergic system. However, although patients with PTSD have been found reduced GABAARs, the GABAergic system has weaker pharmacodynamics at the receptor level.

Author contributions

JH and FX conceived and designed the study and wrote the draft. LY and LT collected the literature and organized the structure. XW, ZD, and YZ contributed to the supervision. XY and YL used software to do the drawing. KL and WW reviewed and revised the manuscript. All authors contributed to the article and approved the submitted version.

Conflict of interest

The authors declare that the research was conducted in the absence of any commercial or financial relationships that could be construed as a potential conflict of interest.

Publisher's note

References

Adamec, R., Strasser, K., Blundell, J., Burton, P., and McKay, D. W. (2006). Protein synthesis and the mechanisms of lasting change in anxiety induced by severe stress. *Behav. Brain Res.* 167, 270–286. doi: 10.1016/j.bbr.2005.09.019

Adolphs, R., Baron-Cohen, S., and Tranel, D. (2002). Impaired recognition of social emotions following amygdala damage. *J. Cogn. Neurosci.* 14, 1264–1274. doi: 10.1162/089892902760807258

Agís-Balboa, R. C., Pinna, G., Pibiri, F., Kadriu, B., Costa, E., and Guidotti, A. (2007). Down-regulation of neurosteroid biosynthesis in corticolimbic circuits mediates social isolation-induced behavior in mice. *Proc. Natl. Acad. Sci. U.S.A.* 104, 18736–18741. doi: 10.1073/pnas.0709419104

Agís-Balboa, R. C., Pinna, G., Zhubi, A., Maloku, E., Veldic, M., Costa, E., et al. (2006). Characterization of brain neurons that express enzymes mediating neurosteroid biosynthesis. *Proc. Natl. Acad. Sci. U.S.A.* 103, 14602–14607. doi: 10.1073/pnas.0606544103

Akirav, I., Raizel, H., and Maroun, M. (2006). Enhancement of conditioned fear extinction by infusion of the GABA(A) agonist muscimol into the rat prefrontal cortex and amygdala. *Eur. J. Neurosci.* 23, 758–764. doi: 10.1111/j.1460-9568.2006.04603.x

Almada, R. C., Albrechet-Souza, L., and Brandão, M. L. (2013). Further evidence for involvement of the dorsal hippocampus serotonergic and γ-aminobutyric acid (GABA)ergic pathways in the expression of contextual fear conditioning in rats. *J. Psychopharmacol. (Oxford, England)* 27, 1160–1168. doi: 10.1177/0269881113482840

Almeida, F. B., Pinna, G., and Barros, H. M. T. (2021). The role of HPA axis and allopregnanolone on the neurobiology of major depressive disorders and PTSD. *Int. J. Mol. Sci.* 22:5495. doi: 10.3390/ijms22115495

Almeida, M., Sousa Filho, L. F., Rabello, P. M., and Santiago, B. M. (2020). International classification of diseases - 11th revision: From design to implementation. *Rev. Saude Publica* 54:104. doi: 10.11606/s1518-8787.2020054002120

Anagnostaras, S. G., Maren, S., and Fanselow, M. S. (1999). Temporally graded retrograde amnesia of contextual fear after hippocampal damage in rats: Within-subjects examination. *J. Neurosci.* 19, 1106–1114. doi: 10.1523/JNEUROSCI.19-03-01106.1999

Anagnostaras, S. G., Wood, S. C., Shuman, T., Cai, D. J., Leduc, A. D., Zurn, K. R., et al. (2010). Automated assessment of pavlovian conditioned freezing and shock reactivity in mice using the video freeze system. *Front. Behav. Neurosci.* 4:158. doi: 10.3389/fnbeh.2010.00158

Ardi, Z., Albrecht, A., Richter-Levin, A., Saha, R., and Richter-Levin, G. (2016). Behavioral profiling as a translational approach in an animal model of posttraumatic stress disorder. *Neurobiol. Dis.* 88, 139–147. doi: 10.1016/j.nbd.2016.01.012

Aupperle, R. L., Melrose, A. J., Stein, M. B., and Paulus, M. P. (2012). Executive function and PTSD: Disengaging from trauma. *Neuropharmacology* 62, 686–694. doi: 10.1016/j.neuropharm.2011.02.008

Averill, L. A., Purohit, P., Averill, C. L., Boesl, M. A., Krystal, J. H., and Abdallah, C. G. (2017). Glutamate dysregulation and glutamatergic therapeutics for PTSD: Evidence from human studies. *Neurosci. Lett.* 649, 147–155. doi: 10.1016/j.neulet.2016.11.064

Babaev, O., Piletti Chatain, C., and Krueger-Burg, D. (2018). Inhibition in the amygdala anxiety circuitry. *Exp. Mol. Med.* 50, 1–16. doi: 10.1038/s12276-018-0063-8

Ball, T. M., Knapp, S. E., Paulus, M. P., and Stein, M. B. (2017). Brain activation during fear extinction predicts exposure success. *Depress. Anxiety* 34, 257–266. doi: 10.1002/da.22583

Barad, M., Gean, P. W., and Lutz, B. (2006). The role of the amygdala in the extinction of conditioned fear. *Biol. Psychiatry* 60, 322–328. doi: 10.1016/j.biopsych.2006.05.029

Bast, T., Zhang, W. N., and Feldon, J. (2001). The ventral hippocampus and fear conditioning in rats. Different anterograde amnesias of fear after tetrodotoxin inactivation and infusion of the GABA(A) agonist muscimol. *Exp. Brain Res.* 139, 39–52. doi: 10.1007/s002210100746

Battle, D. E. (2013). Diagnostic and statistical manual of mental disorders (DSM). *CoDAS* 25, 191–192. doi: 10.1590/s2317-17822013000200017

Baulieu, E. E., and Robel, P. (1990). Neurosteroids: A new brain function? *J. Steroid Biochem. Mol. Biol.* 37, 395–403. doi: 10.1016/0960-0760(90)90490-c

Belelli, D., and Lambert, J. J. (2005). Neurosteroids: Endogenous regulators of the GABA(A) receptor. *Nat. Rev. Neurosci.* 6, 565–575. doi: 10.1038/nrn1703

Belelli, D., Harrison, N. L., Maguire, J., Macdonald, R. L., Walker, M. C., and Cope, D. W. (2009). Extrasynaptic GABAA receptors: Form, pharmacology, and function. *J. Neurosci.* 29, 12757–12763. doi: 10.1523/JNEUROSCI.3340-09.2009

Benjet, C., Bromet, E., Karam, E. G., Kessler, R. C., McLaughlin, K. A., Ruscio, A. M., et al. (2016). The epidemiology of traumatic event exposure worldwide: results from the World Mental Health Survey Consortium. *Psychol. Med.* 46, 327–343. doi: 10.1017/S0033291715001981

Berlant, J. L. (2001). Topiramate in posttraumatic stress disorder: Preliminary clinical observations. *J. Clin. Psychiatry* 62 Suppl 17, 60–63.

Berlau, D. J., and McGaugh, J. L. (2006). Enhancement of extinction memory consolidation: The role of the noradrenergic and GABAergic systems within the basolateral amygdala. *Neurobiol. Learn. Mem.* 86, 123–132. doi: 10.1016/j.nlm.2005.12.008

Bhagwagar, Z., Wylezinska, M., Jezzard, P., Evans, J., Boorman, E., Matthews, P., et al. (2008). Low GABA concentrations in occipital cortex and anterior cingulate cortex in medication-free, recovered depressed patients. *Int. J. Neuropsychopharmacol.* 11, 255–260. doi: 10.1017/S1461145707007924

Bishop, J. R., Lee, A. M., Mills, L. J., Thuras, P. D., Eum, S., Clancy, D., et al. (2021). Corrigendum: Methylation of FKBP5 and SLC6A4 in relation to treatment response to mindfulness based stress reduction for posttraumatic stress disorder. *Front. Psychiatry* 12:642245. doi: 10.3389/fpsyt.2021.642245

Blanchard, R. J., and Blanchard, D. C. (1989). Attack and defense in rodents as ethoexperimental models for the study of emotion. *Prog. Neuro Psychopharmacol. Biol. Psychiatry* 13 Suppl, S3–S14. doi: 10.1016/0278-5846(89)90105-x

Bouton, M., and Bolles, R. (1980). Conditioned fear assessed by freezing and by the suppression of three different baselines. *Anim. Learn. Behav.* 8, 429–434.

Bremner, J. D., Innis, R. B., Southwick, S. M., Staib, L., Zoghbi, S., and Charney, D. S. (2000). Decreased benzodiazepine receptor binding in prefrontal cortex in combat-related posttraumatic stress disorder. *Am. J. Psychiatry* 157, 1120–1126. doi: 10.1176/appi.ajp.157.7.1120

Bremner, J. D., Southwick, S. M., Darnell, A., and Charney, D. S. (1996). Chronic PTSD in Vietnam combat veterans: Course of illness and substance abuse. *Am. J. Psychiatry* 153, 369–375. doi: 10.1176/ajp.153.3.369

Brickley, S. G., and Mody, I. (2012). Extrasynaptic GABA(A) receptors: Their function in the CNS and implications for disease. *Neuron* 73, 23–34. doi: 10.1016/j.neuron.2011.12.012

Cannich, A., Wotjak, C. T., Kamprath, K., Hermann, H., Lutz, B., and Marsicano, G. (2004). CB1 cannabinoid receptors modulate kinase and phosphatase activity during extinction of conditioned fear in mice. *Learn. Mem. (Cold Spring Harbor, N.Y.)* 11, 625–632. doi: 10.1101/lm.77904

Castellano, C., and McGaugh, J. L. (1990). Effects of post-training bicuculline and muscimol on retention: Lack of state dependency. *Behav. Neural Biol.* 54, 156–164. doi: 10.1016/0163-1047(90)91352-c

Catarino, A., Küpper, C. S., Werner-Seidler, A., Dalgleish, T., and Anderson, M. C. (2015). Failing to forget: Inhibitory-control deficits compromise memory suppression in posttraumatic stress disorder. *Psychol. Sci.* 26, 604–616. doi: 10.1177/0956797615569889Meiser-Stedman

Cates, M. E., Bishop, M. H., Davis, L. L., Lowe, J. S., and Woolley, T. W. (2004). Clonazepam for treatment of sleep disturbances associated with combat-related posttraumatic stress disorder. *Ann. Pharmacother.* 38, 1395–1399. doi: 10.1345/aph.1E043

Charney, D. S. (2004). Psychobiological mechanisms of resilience and vulnerability: Implications for successful adaptation to extreme stress. *Am. J. Psychiatry* 161, 195–216. doi: 10.1176/appi.ajp.161.2.195

Chebib, M., and Johnston, G. A. (1999). The 'ABC' of GABA receptors: A brief review. *Clin. Exp. Pharmacol. Physiol.* 26, 937–940. doi: 10.1046/j.1440-1681.1999.03151.x

Chen, S. W., Shemyakin, A., and Wiedenmayer, C. P. (2006). The role of the amygdala and olfaction in unconditioned fear in developing rats. *J. Neurosci.* 26, 233–240. doi: 10.1523/JNEUROSCI.2890-05.2006

Chen, S., Gao, L., Li, X., and Ye, Y. (2021). Allopregnanolone in mood disorders: Mechanism and therapeutic development. *Pharmacol. Res.* 169:105682. doi: 10.1016/j.phrs.2021.105682

Christianson, J., Fernando, A., Kazama, A., Jovanovic, T., Ostroff, L., and Sangha, S. (2012). Inhibition of fear by learned safety signals: A mini-symposium review. *J. Neurosci.* 32, 14118–14124. doi: 10.1523/JNEUROSCI.3340-12.2012

Clarke, I. J. (2015). Hypothalamus as an endocrine organ. *Compr. Physiol.* 5, 217–253. doi: 10.1002/cphy.c140019

Concas, A., Mostallino, M. C., Porcu, P., Follesa, P., Barbaccia, M. L., Trabucchi, M., et al. (1998). Role of brain allopregnanolone in the plasticity of gamma-aminobutyric acid type A receptor in rat brain during pregnancy and after delivery. *Proc. Natl. Acad. Sci. U.S.A.* 95, 13284–13289. doi: 10.1073/pnas.95.22.13284

Connor, K. M., Davidson, J. R., Weisler, R. H., Zhang, W., and Abraham, K. (2006). Tiagabine for posttraumatic stress disorder: Effects of open-label and double-blind discontinuation treatment. *Psychopharmacology* 184, 21–25. doi: 10.1007/s00213-005-0265-3

Corcoran, K. A., and Maren, S. (2001). Hippocampal inactivation disrupts contextual retrieval of fear memory after extinction. *J. Neurosci.* 21, 1720–1726. doi: 10.1523/JNEUROSCI.21-05-01720.2001

Craddock, N., Jones, L., Jones, I. R., Kirov, G., Green, E. K., Grozeva, D., et al. (2010). Strong genetic evidence for a selective influence of GABAA receptors on a component of the bipolar disorder phenotype. *Mol. Psychiatry* 15, 146–153. doi: 10.1038/mp.2008.66

Cullinan, W. E., Ziegler, D. R., and Herman, J. P. (2008). Functional role of local GABAergic influences on the HPA axis. *Brain Struct. Funct.* 213, 63–72. doi: 10.1007/s00429-008-0192-2

Davidson, J. R. (2004). Use of benzodiazepines in social anxiety disorder, generalized anxiety disorder, and posttraumatic stress disorder. *J. Clin. Psychiatry* 65 Suppl 5, 29–33.

Davidson, J. R., Brady, K., Mellman, T. A., Stein, M. B., and Pollack, M. H. (2007). The efficacy and tolerability of tiagabine in adult patients with post-traumatic stress disorder. *J. Clin. Psychopharmacol.* 27, 85–88. doi: 10.1097/JCP.0b013e31802e5115

Davidson, R. J., Putnam, K. M., and Larson, C. L. (2000). Dysfunction in the neural circuitry of emotion regulation–A possible prelude to violence. *Science (New York, N.Y.)* 289, 591–594. doi: 10.1126/science.289.5479.591

Davis, M., Walker, D. L., Miles, L., and Grillon, C. (2010). Phasic vs sustained fear in rats and humans: Role of the extended amygdala in fear vs anxiety. *Neuropsychopharmacology* 35, 105–135. doi: 10.1038/npp.2009.109

de Kloet, E. R., Joëls, M., and Holsboer, F. (2005). Stress and the brain: From adaptation to disease. *Nat. Rev. Neurosci.* 6, 463–475. doi: 10.1038/nrn1683

Deppermann, S., Storchak, H., Fallgatter, A. J., and Ehlis, A. C. (2014). Stress-induced neuroplasticity: (Mal)adaptation to adverse life events in patients with PTSD–a critical overview. *Neuroscience* 283, 166–177. doi: 10.1016/j.neuroscience.2014.08.037

Dias, R., Sheppard, W. F., Fradley, R. L., Garrett, E. M., Stanley, J. L., Tye, S. J., et al. (2005). Evidence for a significant role of alpha 3-containing GABAA receptors in mediating the anxiolytic effects of benzodiazepines. *J. Neurosci.* 25, 10682–10688. doi: 10.1523/JNEUROSCI.1166-05.2005

Disner, S. G., Marquardt, C. A., Mueller, B. A., Burton, P. C., and Sponheim, S. R. (2018). Spontaneous neural activity differences in posttraumatic stress disorder: A quantitative resting-state meta-analysis and fMRI validation. *Hum. Brain Mapp.* 39, 837–850. doi: 10.1002/hbm.23886

Dolfen, N., Veldman, M. P., Gann, M. A., von Leupoldt, A., Puts, N. A. J., Edden, R. A. E., et al. (2021). A role for GABA in the modulation of striatal and hippocampal systems under stress. *Commun. Biol.* 4:1033. doi: 10.1038/s42003-021-02535-x

Domschke, K., and Zwanzger, P. (2008). GABAergic and endocannabinoid dysfunction in anxiety – Future therapeutic targets? *Curr. Pharm. Design* 14, 3508–3517. doi: 10.2174/138161208786848784

Domschke, K., Tidow, N., Schwarte, K., Deckert, J., Lesch, K., Arolt, V., et al. (2014). Serotonin transporter gene hypomethylation predicts impaired antidepressant treatment response. *Int. J. Neuropsychopharmacol.* 17, 1167–1176. doi: 10.1017/S146114571400039X

Drugan, R. C., Basile, A. S., Crawley, J. N., Paul, S. M., and Skolnick, P. (1986). Inescapable shock reduces [3H]Ro 5-4864 binding to "peripheral-type" benzodiazepine receptors in the rat. *Pharmacol. Biochem. Behav.* 24, 1673–1677. doi: 10.1016/0091-3057(86)90504-6

Drumond, A., Madeira, N., and Fonseca, R. (2017). Endocannabinoid signaling and memory dynamics: A synaptic perspective. *Neurobiol. Learn. Mem.* 138, 62–77. doi: 10.1016/j.nlm.2016.07.031

Dubreucq, S., Matias, I., Cardinal, P., Häring, M., Lutz, B., Marsicano, G., et al. (2012). Genetic dissection of the role of cannabinoid type-1 receptors in the emotional consequences of repeated social stress in mice. *Neuropsychopharmacology* 37, 1885–1900. doi: 10.1038/npp.2012.36

Elms, L., Shannon, S., Hughes, S., and Lewis, N. (2019). Cannabidiol in the treatment of post-traumatic stress disorder: A case series. *J. Altern. Complement. Med.* 25, 392–397.

Engelbrecht, A. M., Smith, C., Neethling, I., Thomas, M., Ellis, B., Mattheyse, M., et al. (2010). Daily brief restraint stress alters signaling pathways and induces atrophy and apoptosis in rat skeletal muscle. *Stress (Amsterdam, Netherlands)* 13, 132–141. doi: 10.3109/10253890903089834

Evans, J., Sun, Y., McGregor, A., and Connor, B. (2012). Allopregnanolone regulates neurogenesis and depressive/anxiety-like behaviour in a social isolation rodent model of chronic stress. *Neuropharmacology* 63, 1315–1326. doi: 10.1016/j.neuropharm.2012.08.012

Fanselow, M. S., and Dong, H. W. (2010). Are the dorsal and ventral hippocampus functionally distinct structures? *Neuron* 65, 7–19. doi: 10.1016/j.neuron.2009.11.031

Fendt, M., and Fanselow, M. S. (1999). The neuroanatomical and neurochemical basis of conditioned fear. *Neurosci. Biobehav. Rev.* 23, 743–760. doi: 10.1016/s0149-7634(99)00016-0

Ferrara, N. C., Jarome, T. J., Cullen, P. K., Orsi, S. A., Kwapis, J. L., Trask, S., et al. (2019). GluR2 endocytosis-dependent protein degradation in the amygdala mediates memory updating. *Sci. Rep.* 9:5180. doi: 10.1038/s41598-019-41526-1

Feusner, J., Ritchie, T., Lawford, B., Young, R. M., Kann, B., and Noble, E. P. (2001). GABA(A) receptor beta 3 subunit gene and psychiatric morbidity in a post-traumatic stress disorder population. *Psychiatry Res.* 104, 109–117. doi: 10.1016/s0165-1781(01)00296-7

Fogaça, M. V., and Duman, R. S. (2019). Cortical GABAergic dysfunction in stress and depression: New insights for therapeutic interventions. *Front. cell. Neurosci.* 13:87. doi: 10.3389/fncel.2019.00087

Fraser, G. A. (2009). The use of a synthetic cannabinoid in the management of treatment-resistant nightmares in posttraumatic stress disorder (PTSD). *CNS Neurosci. Ther.* 15, 84–88. doi: 10.1111/j.1755-5949.2008.00071.x

Gao, J., Wang, H., Liu, Y., Li, Y. Y., Chen, C., Liu, L. M., et al. (2014). Glutamate and GABA imbalance promotes neuronal apoptosis in hippocampus after stress. *Med. Sci. Monit.* 20, 499–512. doi: 10.12659/MSM.890589

Gao, S. F., Klomp, A., Wu, J. L., Swaab, D. F., and Bao, A. M. (2013). Reduced GAD(65/67) immunoreactivity in the hypothalamic paraventricular nucleus in depression: A postmortem study. *J. Affect. Disord.* 149, 422–425. doi: 10.1016/j.jad.2012.12.003

Gelpin, E., Bonne, O., Peri, T., Brandes, D., and Shalev, A. Y. (1996). Treatment of recent trauma survivors with benzodiazepines: A prospective study. *J. Clin. Psychiatry* 57, 390–394.

Geracioti, T. D. Jr., Baker, D. G., Kasckow, J. W., Strawn, J. R., Jeffrey Mulchahey, J., Dashevsky, B. A., et al. (2008). Effects of trauma-related audiovisual stimulation on cerebrospinal fluid norepinephrine and corticotropin-releasing hormone concentrations in post-traumatic stress disorder. *Psychoneuroendocrinology* 33, 416–424. doi: 10.1016/j.psyneuen.2007.12.012

Geuze, E., van Berckel, B. N., Lammertsma, A. A., Boellaard, R., de Kloet, C. S., Vermetten, E., et al. (2008). Reduced GABAA benzodiazepine receptor binding in veterans with post-traumatic stress disorder. *Mol. Psychiatry* 13, 74–83, 3. doi: 10.1038/sj.mp.4002054

Ghosal, S., Hare, B., and Duman, R. S. (2017). Prefrontal cortex GABAergic deficits and circuit dysfunction in the pathophysiology and treatment of chronic stress and depression. *Curr. Opin. Behav. Sci.* 14, 1–8. doi: 10.1016/j.cobeha.2016.09.012

Gilbert, M., Dinh La, A., Romulo Delapaz, N., Kenneth Hor, W., Fan, P., Qi, X., et al. (2020). An emulation of randomized trials of administrating benzodiazepines in PTSD patients for outcomes of suicide-related events. *J. Clin. Med.* 9:3492. doi: 10.3390/jcm9113492

Gilmartin, M. R., Kwapis, J. L., and Helmstetter, F. J. (2012). Trace and contextual fear conditioning are impaired following unilateral microinjection of muscimol in the ventral hippocampus or amygdala, but not the medial prefrontal cortex. *Neurobiol. Learn. Mem.* 97, 452–464. doi: 10.1016/j.nlm.2012.03.009

Gong, X., Shao, Y., Li, B., Chen, L., Wang, C., and Chen, Y. (2015). γ-aminobutyric acid transporter-1 is involved in anxiety-like behaviors and cognitive function in knockout mice. *Exp. Ther. Med.* 10, 653–658. doi: 10.3892/etm.2015.2577

Gu, H., Hu, Y., Chen, X., He, Y., and Yang, Y. (2019). Regional excitation-inhibition balance predicts default-mode network deactivation via functional connectivity. *NeuroImage* 185, 388–397. doi: 10.1016/j.neuroimage.2018.10.055

Gunduz-Cinar, O., Hill, M. N., McEwen, B. S., and Holmes, A. (2013). Amygdala FAAH and anandamide: Mediating protection and recovery from stress. *Trends Pharmacol. Sci.* 34, 637–644. doi: 10.1016/j.tips.2013.08.008

Günther, U., Benson, J., Benke, D., Fritschy, J. M., Reyes, G., Knoflach, F., et al. (1995). Benzodiazepine-insensitive mice generated by targeted disruption of the gamma 2 subunit gene of gamma-aminobutyric acid type A receptors. *Proc. Natl. Acad. Sci. U.S.A.* 92, 7749–7753. doi: 10.1073/pnas.92.17.7749

Hageman, I., Andersen, H. S., and Jørgensen, M. B. (2001). Post-traumatic stress disorder: A review of psychobiology and pharmacotherapy. *Acta Psychiatr. Scand.* 104, 411–422. doi: 10.1034/j.1600-0447.2001.00237.x

Haller, J., Bakos, N., Szirmay, M., Ledent, C., and Freund, T. F. (2002). The effects of genetic and pharmacological blockade of the CB1 cannabinoid receptor on anxiety. *Eur. J. Neurosci.* 16, 1395–1398. doi: 10.1046/j.1460-9568.2002.02192.x

Haller, J., Varga, B., Ledent, C., and Freund, T. F. (2004). CB1 cannabinoid receptors mediate anxiolytic effects: Convergent genetic and pharmacological evidence with CB1-specific agents. *Behav. Pharmacol.* 15, 299–304. doi: 10.1097/01.fbp.0000135704.56422.40

Hartmann, J., Dedic, N., Pöhlmann, M. L., Häusl, A., Karst, H., Engelhardt, C., et al. (2017). Forebrain glutamatergic, but not GABAergic, neurons mediate anxiogenic effects of the glucocorticoid receptor. *Mol. Psychiatry* 22, 466–475. doi: 10.1038/mp.2016.87

Harvey, B. H., Oosthuizen, F., Brand, L., Wegener, G., and Stein, D. J. (2004). Stress-restress evokes sustained iNOS activity and altered GABA levels and NMDA receptors in rat hippocampus. *Psychopharmacology* 175, 494–502. doi: 10.1007/s00213-004-1836-4

Hayes, J. P., Hayes, S. M., and Mikedis, A. M. (2012). Quantitative meta-analysis of neural activity in posttraumatic stress disorder. *Biol. Mood Anxiety Disord.* 2:9. doi: 10.1186/2045-5380-2-9

Herbst, M. R., Twining, R. C., and Gilmartin, M. R. (2022). Ventral hippocampal shock encoding modulates the expression of trace cued fear. *Neurobiol. Learn. Mem.* 190:107610. doi: 10.1016/j.nlm.2022.107610

Hill, M. N., Campolongo, P., Yehuda, R., and Patel, S. (2018). Integrating endocannabinoid signaling and cannabinoids into the biology and treatment of posttraumatic stress disorder. *Neuropsychopharmacology* 43, 80–102. doi: 10.1038/npp.2017.162

Hillard, C. J., Weinlander, K. M., and Stuhr, K. L. (2012). Contributions of endocannabinoid signaling to psychiatric disorders in humans: Genetic and biochemical evidence. *Neuroscience* 204, 207–229. doi: 10.1016/j.neuroscience.2011.11.020

Hoffman, A. F., Laaris, N., Kawamura, M., Masino, S. A., and Lupica, C. R. (2010). Control of cannabinoid CB1 receptor function on glutamate axon terminals by endogenous adenosine acting at A1 receptors. *J. Neurosci.* 30, 545–555. doi: 10.1523/JNEUROSCI.4920-09.2010

Ishikawa, A., and Nakamura, S. (2006). Ventral hippocampal neurons project axons simultaneously to the medial prefrontal cortex and amygdala in the rat. *J. Neurophysiol.* 96, 2134–2138. doi: 10.1152/jn.00069.2006

Izquierdo, I., Furini, C. R., and Myskiw, J. C. (2016). Fear memory. *Physiol. Rev.* 96, 695–750. doi: 10.1152/physrev.00018.2015

Jacob, T. C., Moss, S. J., and Jurd, R. (2008). GABA(A) receptor trafficking and its role in the dynamic modulation of neuronal inhibition. *Nat. Rev. Neurosci.* 9, 331–343. doi: 10.1038/nrn2370

Jiang, C., Wang, H., Qi, J., Li, J., He, Q., Wang, C., et al. (2022). Antidepressant effects of cherry leaf decoction on a chronic unpredictable mild stress rat model based on the Glu/GABA-Gln metabolic loop. *Metab. Brain Dis.* 37, 2883–2901. doi: 10.1007/s11011-022-01081-7

Kamprath, K., Marsicano, G., Tang, J., Monory, K., Bisogno, T., Di Marzo, V., et al. (2006). Cannabinoid CB1 receptor mediates fear extinction via habituation-like processes. *J. Neurosci.* 26, 6677–6686. doi: 10.1523/JNEUROSCI.0153-06.2006

Karam, E. G., Friedman, M. J., Hill, E. D., Kessler, R. C., McLaughlin, K. A., Petukhova, M., et al. (2014). Cumulative traumas and risk thresholds: 12-month PTSD in the World Mental Health (WMH) surveys. *Depress. Anxiety* 31, 130–142. doi: 10.1002/da.22169

Karolewicz, B., Maciag, D., O'Dwyer, G., Stockmeier, C. A., Feyissa, A. M., and Rajkowska, G. (2010). Reduced level of glutamic acid decarboxylase-67 kDa in the prefrontal cortex in major depression. *Int. J. Neuropsychopharmacol.* 13, 411–420. doi: 10.1017/S1461145709990587

Kato, M., and Serretti, A. (2010). Review and meta-analysis of antidepressant pharmacogenetic fifindings in major depressive disorder. *Mol. Psychiatry* 15, 473–500. doi: 10.1038/mp.2008.116

Khan, S., and Liberzon, I. (2004). Topiramate attenuates exaggerated acoustic startle in an animal model of PTSD. *Psychopharmacology* 172, 225–229. doi: 10.1007/s00213-003-1634-4

Klempan, T. A., Sequeira, A., Canetti, L., Lalovic, A., Ernst, C., ffrench-Mullen, J., et al. (2009). Altered expression of genes involved in ATP biosynthesis and GABAergic neurotransmission in the ventral prefrontal cortex of suicides with and without major depression. *Mol. Psychiatry* 14, 175–189. doi: 10.1038/sj.mp.4002110

Koch, M., and Schnitzler, H. U. (1997). The acoustic startle response in rats–circuits mediating evocation, inhibition and potentiation. *Behav. Brain Res.* 89, 35–49. doi: 10.1016/s0166-4328(97)02296-1

Koenigs, M., and Grafman, J. (2009). Posttraumatic stress disorder: The role of medial prefrontal cortex and amygdala. *Neuroscientist* 15, 540–548.

Kohda, K., Harada, K., Kato, K., Hoshino, A., Motohashi, J., Yamaji, T., et al. (2007). Glucocorticoid receptor activation is involved in producing abnormal phenotypes of single-prolonged stress rats: A putative post-traumatic stress disorder model. *Neuroscience* 148, 22–33. doi: 10.1016/j.neuroscience.2007.05.041

Krystal, A. D., Zhang, W., Davidson, J. R., and Connor, K. M. (2014). The sleep effects of tiagabine on the first night of treatment predict post-traumatic stress disorder response at three weeks. *J. Psychopharmacol. (Oxford, England)* 28, 457–465. doi: 10.1177/0269881113509903

Krystal, J. H., Sanacora, G., Blumberg, H., Anand, A., Charney, D. S., Marek, G., et al. (2002). Glutamate and GABA systems as targets for novel antidepressant and mood-stabilizing treatments. *Mol. Psychiatry* 7 Suppl 1, S71–S80. doi: 10.1038/sj.mp.4001021

Kyd, R. J., and Bilkey, D. K. (2005). Hippocampal place cells show increased sensitivity to changes in the local environment following prefrontal cortex lesions. *Cereb.Cortex (New York, N.Y. : 1991)* 15, 720–731. doi: 10.1093/cercor/bhh173

Laaris, N., Good, C. H., and Lupica, C. R. (2010). Delta9-tetrahydrocannabinol is a full agonist at CB1 receptors on GABA neuron axon terminals in the hippocampus. *Neuropharmacology* 59, 121–127. doi: 10.1016/j.neuropharm.2010.04.013

Lafenêtre, P., Chaouloff, F., and Marsicano, G. (2007). The endocannabinoid system in the processing of anxiety and fear and how CB1 receptors may modulate fear extinction. *Pharmacol. Res.* 56, 367–381. doi: 10.1016/j.phrs.2007.09.006

Lambert, J. J., Belelli, D., Hill-Venning, C., and Peters, J. A. (1995). Neurosteroids and GABAA receptor function. *Trends Pharmacol. Sci.* 16, 295–303. doi: 10.1016/s0165-6147(00)89058-6

Lapin, I. (2001). Phenibut (beta-phenyl-GABA): A tranquilizer and nootropic drug. *CNS Drug Rev.* 7, 471–481. doi: 10.1111/j.1527-3458.2001.tb00211.x

LeDoux, J. E. (2000). Emotion circuits in the brain. *Annu. Rev. Neurosci.* 23, 155–184. doi: 10.1146/annurev.neuro.23.1.155

LeDoux, J. E., Iwata, J., Cicchetti, P., and Reis, D. J. (1988). Different projections of the central amygdaloid nucleus mediate autonomic and behavioral correlates of conditioned fear. *J. Neurosci.* 8, 2517–2529. doi: 10.1523/JNEUROSCI.08-07-02517.1988

Lehner, M., Wisłowska-Stanek, A., Skórzewska, A., Maciejak, P., Szyndler, J., Turzyńska, D., et al. (2010). Differences in the density of GABA-A receptor alpha-2 subunits and gephyrin in brain structures of rats selected for low and high anxiety in basal and fear-stimulated conditions, in a model of contextual fear conditioning. *Neurobiol. Learn. Mem.* 94, 499–508. doi: 10.1016/j.nlm.2010.09.001

Levinson, A. J., Fitzgerald, P. B., Favalli, G., Blumberger, D. M., Daigle, M., and Daskalakis, Z. J. (2010). Evidence of cortical inhibitory deficits in major depressive disorder. *Biol. Psychiatry* 67, 458–464. doi: 10.1016/j.biopsych.2009.09.025

Liberzon, I., and Abelson, J. L. (2016). Context processing and the neurobiology of post-traumatic stress disorder. *Neuron* 92, 14–30. doi: 10.1016/j.neuron.2016.09.039

Lin, H. C., Tseng, Y. C., Mao, S. C., Chen, P. S., and Gean, P. W. (2011). GABAA receptor endocytosis in the basolateral amygdala is critical to the reinstatement of fear memory measured by fear-potentiated startle. *J. Neurosci.* 31, 8851–8861. doi: 10.1523/JNEUROSCI.0979-11.2011

Lippa, A. S., Klepner, C. A., Yunger, L., Sano, M. C., Smith, W. V., and Beer, B. (1978). Relationship between benzodiazepine receptors and experimental anxiety in rats. *Pharmacol. Biochem. Behav.* 9, 853–856. doi: 10.1016/0091-3057(78)90368-4

Lisboa, S. F., Resstel, L. B., Aguiar, D. C., and Guimarães, F. S. (2008). Activation of cannabinoid CB1 receptors in the dorsolateral periaqueductal gray induces anxiolytic effects in rats submitted to the Vogel conflict test. *Eur. J. Pharmacol.* 593, 73–78. doi: 10.1016/j.ejphar.2008.07.032

Lissek, S., and van Meurs, B. (2015). Learning models of PTSD: Theoretical accounts and psychobiological evidence. *Int. J. Psychophysiol.* 98(3 Pt 2), 594–605. doi: 10.1016/j.ijpsycho.2014.11.006

Liu, G. X., Cai, G. Q., Cai, Y. Q., Sheng, Z. J., Jiang, J., Mei, Z., et al. (2007). Reduced anxiety and depression-like behaviors in mice lacking GABA transporter subtype 1. *Neuropsychopharmacology* 32, 1531–1539. doi: 10.1038/sj.npp.1301281

Liu, L., Wang, L., Cao, C., Cao, X., Zhu, Y., Liu, P., et al. (2018). Serotonin transporter 5-HTTLPR genotype is associated with intrusion and avoidance symptoms of DSM-5 posttraumatic stress disorder (PTSD) in Chinese earthquake survivors. *Anxiety Stress Coping* 31, 318–327. doi: 10.1080/10615806.2017.1420174

Liu, Z. P., He, Q. H., Pan, H. Q., Xu, X. B., Chen, W. B., He, Y., et al. (2017). Delta subunit-containing gamma-aminobutyric acid a receptor disinhibits lateral amygdala and facilitates fear expression in mice. *Biol. Psychiatry* 81, 990–1002. doi: 10.1016/j.biopsych.2016.06.022

Lu, C. Y., Liu, X., Jiang, H., Pan, F., Ho, C. S., and Ho, R. C. (2017). Effects of traumatic stress induced in the juvenile period on the expression of gamma-aminobutyric acid receptor type a subunits in adult rat brain. *Neural Plast.* 2017:5715816. doi: 10.1155/2017/5715816

Lujan, R., and Ciruela, F. (2012). GABAB receptors-associated proteins: Potential drug targets in neurological disorders? *Curr. Drug Targets* 13, 129–144. doi: 10.2174/138945012798868425

Maddox, S. A., Hartmann, J., Ross, R. A., and Ressler, K. J. (2019). Deconstructing the gestalt: Mechanisms of fear, threat, and trauma memory encoding. *Neuron* 102, 60–74. doi: 10.1016/j.neuron.2019.03.017

Maercker, A. (2021). Development of the new CPTSD diagnosis for ICD-11. *Borderline Pers. Disord. Emot. Dysregul.* 8:7. doi: 10.1186/s40479-021-00148-8

Maggio, N., and Segal, M. (2007). Striking variations in corticosteroid modulation of long-term potentiation along the septotemporal axis of the hippocampus. *J. Neurosci.* 27, 5757–5765. doi: 10.1523/JNEUROSCI.0155-07.2007

Maguire, J. L., Stell, B. M., Rafizadeh, M., and Mody, I. (2005). Ovarian cycle-linked changes in GABA(A) receptors mediating tonic inhibition alter seizure susceptibility and anxiety. *Nat. Neurosci.* 8, 797–804. doi: 10.1038/nn1469

Mahan, A. L., and Ressler, K. J. (2012). Fear conditioning, synaptic plasticity and the amygdala: Implications for posttraumatic stress disorder. *Trends Neurosci.* 35, 24–35. doi: 10.1016/j.tins.2011.06.007

Makkar, S. R., Zhang, S. Q., and Cranney, J. (2010). Behavioral and neural analysis of GABA in the acquisition, consolidation, reconsolidation, and extinction of fear memory. *Neuropsychopharmacology* 35, 1625–1652. doi: 10.1038/npp.2010.53

Mao, C. C., Guidotti, A., and Costa, E. (1975). Evidence for an involvement of GABA in the mediation of the cerebellar cGMP decrease and the anticonvulsant action diazepam. *Naunyn Schmiedebergs Arch. Pharmacol.* 289, 369–378. doi: 10.1007/BF00508411

Maren, S., and Quirk, G. J. (2004). Neuronal signalling of fear memory. *Nat. Rev. Neurosci.* 5, 844–852. doi: 10.1038/nrn1535

Maren, S., Yap, S. A., and Goosens, K. A. (2001). The amygdala is essential for the development of neuronal plasticity in the medial geniculate nucleus during auditory fear conditioning in rats. *J. Neurosci.* 21:RC135. doi: 10.1523/JNEUROSCI.21-06-j0001.2001

Marquis, J. P., Killcross, S., and Haddon, J. E. (2007). Inactivation of the prelimbic, but not infralimbic, prefrontal cortex impairs the contextual control of response conflict in rats. *Eur. J. Neurosci.* 25, 559–566. doi: 10.1111/j.1460-9568.2006.05295.x

Marsicano, G., Wotjak, C. T., Azad, S. C., Bisogno, T., Rammes, G., Cascio, M. G., et al. (2002). The endogenous cannabinoid system controls extinction of aversive memories. *Nature* 418, 530–534. doi: 10.1038/nature00839

Martin, M., Ledent, C., Parmentier, M., Maldonado, R., and Valverde, O. (2002). Involvement of CB1 cannabinoid receptors in emotional behaviour. *Psychopharmacology* 159, 379–387. doi: 10.1007/s00213-001-0946-5

Matar, M. A., Zohar, J., Kaplan, Z., and Cohen, H. (2009). Alprazolam treatment immediately after stress exposure interferes with the normal HPA-stress response and increases vulnerability to subsequent stress in an animal model of PTSD. *Eur. Neuropsychopharmacol.* 19, 283–295. doi: 10.1016/j.euroneuro.2008.12.004

McDonald, A. J. (1982). Neurons of the lateral and basolateral amygdaloid nuclei: A Golgi study in the rat. *J. Comp. Neurol.* 212, 293–312. doi: 10.1002/cne.902120307

McDonald, A. J., and Augustine, J. R. (1993). Localization of GABA-like immunoreactivity in the monkey amygdala. *Neuroscience* 52, 281–294. doi: 10.1016/0306-4522(93)90156-a

McLaughlin, R. J., Hill, M. N., and Gorzalka, B. B. (2014). A critical role for prefrontocortical endocannabinoid signaling in the regulation of stress and emotional behavior. *Neurosci. Biobehav. Rev.* 42, 116–131. doi: 10.1016/j.neubiorev.2014.02.006

Mechoulam, R., and Parker, L. A. (2013). The endocannabinoid system and the brain. *Annu. Rev. Psychol.* 64, 21–47. doi: 10.1146/annurev-psych-113011-143739

Medina, J. H., Novas, M. L., Wolfman, C. N., Levi de Stein, M., and De Robertis, E. (1983). Benzodiazepine receptors in rat cerebral cortex and hippocampus undergo rapid and reversible changes after acute stress. *Neuroscience* 9, 331–335. doi: 10.1016/0306-4522(83)90298-1

Megahed, T., Hattiangady, B., Shuai, B., and Shetty, A. K. (2015). Parvalbumin and neuropeptide Y expressing hippocampal GABA-ergic inhibitory interneuron numbers decline in a model of Gulf War illness. *Front. Cell. Neurosci.* 8:447. doi: 10.3389/fncel.2014.00447

Meiser-Stedman, R., Dalgleish, T., Glucksman, E., Yule, W., and Smith, P. (2009). Maladaptive cognitive appraisals mediate the evolution of posttraumatic stress reactions: A 6-month follow-up of child and adolescent assault and motor vehicle accident survivors. *J. Abnorm. Psychol.* 118, 778–787. doi: 10.1037/a0016945

Merali, Z., Du, L., Hrdina, P., Palkovits, M., Faludi, G., Poulter, M. O., et al. (2004). Dysregulation in the suicide brain: mRNA expression of corticotropin-releasing hormone receptors and GABA(A) receptor subunits in frontal cortical brain region. *J. Neurosci.* 24, 1478–1485. doi: 10.1523/JNEUROSCI.4734-03.2004

Meyerhoff, D. J., Mon, A., Metzler, T., and Neylan, T. C. (2014). Cortical gamma-aminobutyric acid and glutamate in posttraumatic stress disorder and their relationships to self-reported sleep quality. *Sleep* 37, 893–900. doi: 10.5665/sleep.3654

Michels, L., Schulte-Vels, T., Schick, M., O'Gorman, R. L., Zeffiro, T., Hasler, G., et al. (2014). Prefrontal GABA and glutathione imbalance in posttraumatic stress disorder: Preliminary findings. *Psychiatry Res.* 224, 288–295. doi: 10.1016/j.pscychresns.2014.09.007

Mikkelsen, J. D., Bundzikova, J., Larsen, M. H., Hansen, H. H., and Kiss, A. (2008). GABA regulates the rat hypothalamic-pituitary-adrenocortical axis via different GABA-A receptor alpha-subtypes. *Ann. N. Y. Acad. Sci.* 1148, 384–392. doi: 10.1196/annals.1410.044

Milad, M. R., Pitman, R. K., Ellis, C. B., Gold, A. L., Shin, L. M., Lasko, N. B., et al. (2009). Neurobiological basis of failure to recall extinction memory in posttraumatic stress disorder. *Biol. Psychiatry* 66, 1075–1082. doi: 10.1016/j.biopsych.2009.06.026

Möller, A. T., Bäckström, T., Nyberg, S., Söndergaard, H. P., and Helström, L. (2016). Women with PTSD have a changed sensitivity to GABA-A receptor active substances. *Psychopharmacology* 233, 2025–2033. doi: 10.1007/s00213-014-3776-y

Morales, M., Wang, S. D., Diaz-Ruiz, O., and Jho, D. H. (2004). Cannabinoid CB1 receptor and serotonin 3 receptor subunit A (5-HT3A) are co-expressed in GABA neurons in the rat telencephalon. *J. Comp. Neurol.* 468, 205–216. doi: 10.1002/cne.10968

Morgan, M. A., and LeDoux, J. E. (1995). Differential contribution of dorsal and ventral medial prefrontal cortex to the acquisition and extinction of conditioned fear in rats. *Behav. Neurosci.* 109, 681–688. doi: 10.1037//0735-7044.109.4.681

Neumeister, A., Normandin, M. D., Pietrzak, R. H., Piomelli, D., Zheng, M. Q., Gujarro-Anton, A., et al. (2013). Elevated brain cannabinoid CB1 receptor availability in post-traumatic stress disorder: a positron emission tomography study. *Mol. Psychiatry* 18, 1034–1040. doi: 10.1038/mp.2013.61

Neuwirth, L. S., Verrengia, M. T., Harikinish-Murrary, Z. I., Orens, J. E., and Lopez, O. E. (2022). Under or absent reporting of light stimuli in testing of anxiety-like behaviors in rodents: the need for standardization. *Front. Mol. Neurosci.* 15:912146. doi: 10.3389/fnmol.2022.912146

Olson, V. G., Rockett, H. R., Reh, R. K., Redila, V. A., Tran, P. M., Venkov, H. A., et al. (2011). The role of norepinephrine in differential response to stress in an animal model of posttraumatic stress disorder. *Biol. Psychiatry* 70, 441–448. doi: 10.1016/j.biopsych.2010.11.029

Orchinik, M., Weiland, N. G., and McEwen, B. S. (1995). Chronic exposure to stress levels of corticosterone alters GABAA receptor subunit mRNA levels in rat hippocampus. *Brain Res. Mol. Brain Res.* 34, 29–37. doi: 10.1016/0169-328x(95)00118-c

Orr, S. P., Lasko, N. B., Metzger, L. J., and Pitman, R. K. (1997). Physiologic responses to non-startling tones in Vietnam veterans with post-traumatic stress disorder. *Psychiatry Res.* 73, 103–107. doi: 10.1016/s0165-1781(97)00110-8

Orr, S. P., Metzger, L. J., Lasko, N. B., Macklin, M. L., Hu, F. B., Shalev, A. Y., et al. (2003). Physiologic responses to sudden, loud tones in monozygotic twins discordant for combat exposure: Association with posttraumatic stress disorder. *Arch. Gene. Psychiatry* 60, 283–288. doi: 10.1001/archpsyc.60.3.283

Ouellet-Morin, I., Odgers, C. L., Danese, A., Bowes, L., Shakoor, S., Papadopoulos, A. S., et al. (2011). Blunted cortisol responses to stress signal social and behavioral problems among maltreated/bullied 12-year-old children. *Biol. Psychiatry* 70, 1016–1023. doi: 10.1016/j.biopsych.2011.06.017

Pape, H. C., and Pare, D. (2010). Plastic synaptic networks of the amygdala for the acquisition, expression, and extinction of conditioned fear. *Physiol. Rev.* 90, 419–463. doi: 10.1152/physrev.00037.2009

Parsons, R., and Ressler, K. (2013). Implications of memory modulation for post-traumatic stress and fear disorders. *Nat. Neurosci.* 16, 146–153. doi: 10.1038/nn.3296

Passie, T., Emrich, H. M., Karst, M., Brandt, S. D., and Halpern, J. H. (2012). Mitigation of post-traumatic stress symptoms by *Cannabis resin*: A review of the clinical and neurobiological evidence. *Drug Test. Anal.* 4, 649–659. doi: 10.1002/dta.1377

Petroff, O. A. (2002). GABA and glutamate in the human brain. *Neuroscientist* 8, 562–573. doi: 10.1177/1073858402238515

Pham, X., Sun, C., Chen, X., van den Oord, E. J., Neale, M. C., Kendler, K. S., et al. (2009). Association study between GABA receptor genes and anxiety spectrum disorders. *Depression Anxiety* 26, 998–1003. doi: 10.1002/da.20628

Piomelli, D. (2003). The molecular logic of endocannabinoid signalling. *Nat. Rev. Neurosci.* 4, 873–884. doi: 10.1038/nrn1247

Pitman, R. K., Rasmusson, A. M., Koenen, K. C., Shin, L. M., Orr, S. P., Gilbertson, M. W., et al. (2012). Biological studies of post-traumatic stress disorder. *Nat. Rev. Neurosci.* 13, 769–787. doi: 10.1038/nrn3339

Pochwat, B., Nowak, G., and Szewczyk, B. (2016). Brain glutamic acid decarboxylase-67kDa alterations induced by magnesium treatment in olfactory bulbectomy and chronic mild stress models in rats. *Pharmacol. Rep.* 68, 881–885. doi: 10.1016/j.pharep.2016.04.011

Pole, N. (2007). The psychophysiology of posttraumatic stress disorder: A meta-analysis. *Psychol. Bull.* 133, 725–746. doi: 10.1037/0033-2909.133.5.725

Pole, N., Neylan, T. C., Otte, C., Henn-Hasse, C., Metzler, T. J., and Marmar, C. R. (2009). Prospective prediction of posttraumatic stress disorder symptoms using fear potentiated auditory startle responses. *Biol. Psychiatry* 65, 235–240. doi: 10.1016/j.biopsych.2008.07.015

Pollack, M. H., Jensen, J. E., Simon, N. M., Kaufman, R. E., and Renshaw, P. F. (2008). High-field MRS study of GABA, glutamate and glutamine in social anxiety disorder: Response to treatment with levetiracetam. *Prog. Neuro Psychopharmacol. Biol. Psychiatry* 32, 739–743. doi: 10.1016/j.pnpbp.2007.11.023

Poulter, M. O., Du, L., Weaver, I., Palkovits, M., Faludi, G., Merali, Z., et al. (2008). GABAA receptor promoter hypermethylation in suicide brain: Implications for the involvement of epigenetic processes. *Biol. Psychiatry* 64, 645–652. doi: 10.1016/j.biopsych.2008.05.028

Quirk, G. J., Russo, G. K., Barron, J. L., and Lebron, K. (2000). The role of ventromedial prefrontal cortex in the recovery of extinguished fear. *J. Neurosci.* 20, 6225–6231. doi: 10.1523/JNEUROSCI.20-16-06225.2000

Randall, P. K., Bremner, J. D., Krystal, J. H., Nagy, L. M., Heninger, G. R., Nicolaou, A. L., et al. (1995). Effects of the benzodiazepine antagonist flumazenil in PTSD. *Biol. Psychiatry* 38, 319–324. doi: 10.1016/0006-3223(94)00306-n

Rasmusson, A. M., and Pineles, S. L. (2018). Neurotransmitter, peptide, and steroid hormone abnormalities in PTSD: Biological endophenotypes relevant to treatment. *Curr. Psychiatry Rep.* 20:52. doi: 10.1007/s11920-018-0908-9

Rasmusson, A. M., Pinna, G., Paliwal, P., Weisman, D., Gottschalk, C., Charney, D., et al. (2006). Decreased cerebrospinal fluid allopregnanolone levels in women with posttraumatic stress disorder. *Biol. Psychiatry* 60, 704–713. doi: 10.1016/j.biopsych.2006.03.026

Rauch, S. L., Shin, L. M., and Phelps, E. A. (2006). Neurocircuitry models of posttraumatic stress disorder and extinction: Human neuroimaging research–Past, present, and future. *Biol. Psychiatry* 60, 376–382. doi: 10.1016/j.biopsych.2006.06.004

Raybuck, J. D., and Lattal, K. M. (2011). Double dissociation of amygdala and hippocampal contributions to trace and delay fear conditioning. *PLoS One* 6:e15982. doi: 10.1371/journal.pone.0015982

Raybuck, J. D., and Lattal, K. M. (2014). Differential effects of dorsal hippocampal inactivation on expression of recent and remote drug and fear memory. *Neurosci. Lett.* 569, 1–5. doi: 10.1016/j.neulet.2014.02.063

Romeo, E., Ströhle, A., Spalletta, G., di Michele, F., Hermann, B., Holsboer, F., et al. (1998). Effects of antidepressant treatment on neuroactive steroids in major depression. *Am. J. Psychiatry* 155, 910–913. doi: 10.1176/ajp.155.7.910

Roohbakhsh, A., Keshavarz, S., Hasanein, P., Rezvani, M. E., and Moghaddam, A. H. (2009). Role of endocannabinoid system in the ventral hippocampus of rats in the modulation of anxiety-like behaviours. *Basic Clin. Pharmacol. Toxicol.* 105, 333–338. doi: 10.1111/j.1742-7843.2009.00449.x

Rosso, I. M., Weiner, M. R., Crowley, D. J., Silveri, M. M., Rauch, S. L., and Jensen, J. E. (2014). Insula and anterior cingulate GABA levels in posttraumatic stress disorder: Preliminary findings using magnetic resonance spectroscopy. *Depression Anxiety* 31, 115–123. doi: 10.1002/da.22155

Rudolph, U., and Möhler, H. (2004). Analysis of GABAA receptor function and dissection of the pharmacology of benzodiazepines and general anesthetics through mouse genetics. *Annu. Rev. Pharmacol. Toxicol.* 44, 475–498. doi: 10.1146/annurev.pharmtox.44.101802.121429

Rudolph, U., Crestani, F., Benke, D., Brünig, I., Benson, J. A., Fritschy, J. M., et al. (1999). Benzodiazepine actions mediated by specific gamma-aminobutyric acid(A) receptor subtypes. *Nature* 401, 796–800. doi: 10.1038/44579

Ruehle, S., Rey, A. A., Remmers, F., and Lutz, B. (2012). The endocannabinoid system in anxiety, fear memory and habituation. *J. Psychopharmacol. (Oxford, England)* 26, 23–39. doi: 10.1177/0269881111408958

Sah, P., Faber, E. S., Lopez De Armentia, M., and Power, J. (2003). The amygdaloid complex: Anatomy and physiology. *Physiol. Rev.* 83, 803–834. doi: 10.1152/physrev.00002.2003

Sah, P., Westbrook, R. F., and Lüthi, A. (2008). Fear conditioning and long-term potentiation in the amygdala: What really is the connection? *Ann. N. Y. Acad. Sci.* 1129, 88–95. doi: 10.1196/annals.1417.020

Sakaguchi, M., Kim, K., Yu, L. M., Hashikawa, Y., Sekine, Y., Okumura, Y., et al. (2015). Inhibiting the activity of CA1 hippocampal neurons prevents the recall of contextual fear memory in inducible ArchT transgenic mice. *PLoS One* 10:e0130163. doi: 10.1371/journal.pone.0130163

Sanacora, G., Gueorguieva, R., Epperson, C. N., Wu, Y. T., Appel, M., Rothman, D. L., et al. (2004). Subtype-specific alterations of gamma-aminobutyric acid and glutamate in patients with major depression. *Arch. Gen. Psychiatry* 61, 705–713. doi: 10.1001/archpsyc.61.7.705

Sangha, S., Narayanan, R. T., Bergado-Acosta, J. R., Stork, O., Seidenbecher, T., and Pape, H. C. (2009). Deficiency of the 65 kDa isoform of glutamic acid decarboxylase impairs extinction of cued but not contextual fear memory. *J. Neurosci.* 29, 15713–15720. doi: 10.1523/JNEUROSCI.2620-09.2009

Schneider, B. L., Ghoddoussi, F., Charlton, J. L., Kohler, R. J., Galloway, M. P., Perrine, S. A., et al. (2016). Increased cortical gamma-aminobutyric acid precedes incomplete extinction of conditioned fear and increased hippocampal excitatory tone in a mouse model of mild traumatic brain injury. *J. Neurotrauma* 33, 1614–1624. doi: 10.1089/neu.2015.4190

Schüle, C., Nothdurfter, C., and Rupprecht, R. (2014). The role of allopregnanolone in depression and anxiety. *Prog. Neurobiol.* 113, 79–87. doi: 10.1016/j.pneurobio.2013.09.003

Schwartz, T. L., and Nihalani, N. (2006). Tiagabine in anxiety disorders. *Expert Opin. Pharmacother.* 7, 1977–1987. doi: 10.1517/14656566.7.14.1977

Sequeira, A., Mamdani, F., Ernst, C., Vawter, M. P., Bunney, W. E., Lebel, V., et al. (2009). Global brain gene expression analysis links glutamatergic and GABAergic alterations to suicide and major depression. *PLoS One* 4:e6585. doi: 10.1371/journal.pone.0006585

Sheth, C., Prescot, A. P., Legarreta, M., Renshaw, P. F., McGlade, E., and Yurgelun-Todd, D. (2019). Reduced gamma-amino butyric acid (GABA) and glutamine in the anterior cingulate cortex (ACC) of veterans exposed to trauma. *J. Affect. Disord.* 248, 166–174. doi: 10.1016/j.jad.2019.01.037

Shin, L. M., and Liberzon, I. (2010). The neurocircuitry of fear, stress, and anxiety disorders. *Neuropsychopharmacology* 35, 169–191. doi: 10.1038/npp.2009.83

Sierra-Mercado, D., Padilla-Coreano, N., and Quirk, G. J. (2011). Dissociable roles of prelimbic and infralimbic cortices, ventral hippocampus, and basolateral amygdala in the expression and extinction of conditioned fear. *Neuropsychopharmacology* 36, 529–538. doi: 10.1038/npp.2010.184

Sigurdsson, T., Doyère, V., Cain, C. K., and LeDoux, J. E. (2007). Long-term potentiation in the amygdala: A cellular mechanism of fear learning and memory. *Neuropharmacology* 52, 215–227. doi: 10.1016/j.neuropharm.2006.06.022

Singewald, N., Schmuckermair, C., Whittle, N., Holmes, A., and Ressler, K. J. (2015). Pharmacology of cognitive enhancers for exposure-based therapy of fear, anxiety and trauma-related disorders. *Pharmacol. Ther.* 149, 150–190. doi: 10.1016/j.pharmthera.2014.12.004

Smoller, J. (2016). The genetics of stress-related disorders: PTSD, depression, and anxiety disorders. *Neuropsychopharmacology* 41, 297–319. doi: 10.1038/npp.2015.266

Song, C., Zhang, W. H., Wang, X. H., Zhang, J. Y., Tian, X. L., Yin, X. P., et al. (2017). Acute stress enhances the glutamatergic transmission onto basoamygdala neurons embedded in distinct microcircuits. *Mol. Brain* 10:3. doi: 10.1186/s13041-016-0283-6

Spivak, B., Maayan, R., Kotler, M., Mester, R., Gil-Ad, I., Shtaif, B., et al. (2000). Elevated circulatory level of GABA(A)–antagonistic neurosteroids in patients with combat-related post-traumatic stress disorder. *Psychol. Med.* 30, 1227–1231. doi: 10.1017/s0033291799002731

Stachowicz, K. (2018). The role of DSCAM in the regulation of synaptic plasticity: Possible involvement in neuropsychiatric disorders. *Acta Neurobiol. Exp.* 78, 210–219.

Suendermann, O., Ehlers, A., Boellinghaus, I., Gamer, M., and Glucksman, E. (2010). Early heart rate responses to standardized trauma-related pictures predict posttraumatic stress disorder: A prospective study. *Psychosom. Med.* 72, 301–308. doi: 10.1097/PSY.0b013e3181d07db8

Sun, K., Fan, J., and Han, J. (2015). Ameliorating effects of traditional Chinese medicine preparation, Chinese materia medica and active compounds on ischemia/reperfusion-induced cerebral microcirculatory disturbances and neuron damage. *Acta Pharm. Sin. B* 5, 8–24. doi: 10.1016/j.apsb.2014.11.002

Sun, X., Song, Z., Si, Y., and Wang, J. H. (2018). microRNA and mRNA profiles in ventral tegmental area relevant to stress-induced depression and resilience. *Prog. Neuro Psychopharmacol. Biol. Psychiatry* 86, 150–165. doi: 10.1016/j.pnpbp.2018.05.023

Sutherland, S. M., and Davidson, J. R. (1994). Pharmacotherapy for post-traumatic stress disorder. *Psychiatric Clin. North Am.* 17, 409–423.

Szabó, G. G., Lenkey, N., Holderith, N., Andrási, T., Nusser, Z., and Hájos, N. (2014). Presynaptic calcium channel inhibition underlies CB_1 cannabinoid receptor-mediated suppression of GABA release. *J. Neurosci.* 34, 7958–7963. doi: 10.1523/JNEUROSCI.0247-14.2014

Taylor, F. B. (2003). Tiagabine for posttraumatic stress disorder: A case series of 7 women. *J. Clin. Psychiatry* 64, 1421–1425. doi: 10.4088/jcp.v64n1204

Tovote, P., Fadok, J. P., and Lüthi, A. (2015). Neuronal circuits for fear and anxiety. *Nat. Rev. Neurosci.* 16, 317–331. doi: 10.1038/nrn3945

Trezza, V., and Campolongo, P. (2013). The endocannabinoid system as a possible target to treat both the cognitive and emotional features of post-traumatic stress disorder (PTSD). *Front. Behav. Neurosci.* 7:100. doi: 10.3389/fnbeh.2013.00100

Twining, R. C., Lepak, K., Kirry, A. J., and Gilmartin, M. R. (2020). Ventral hippocampal input to the prelimbic cortex dissociates the context from the cue association in trace fear memory. *J. Neurosci.* 40, 3217–3230. doi: 10.1523/JNEUROSCI.1453-19.2020

Uniyal, A., Singh, R., Akhtar, A., Bansal, Y., Kuhad, A., and Sah, S. P. (2019). Co-treatment of piracetam with risperidone rescued extinction deficits in experimental paradigms of post-traumatic stress disorder by restoring the physiological alterations in cortex and hippocampus. *Pharmacol. Biochem. Behav.* 185:172763. doi: 10.1016/j.pbb.2019.172763

Uzunova, V., Sheline, Y., Davis, J. M., Rasmusson, A., Uzunov, D. P., Costa, E., et al. (1998). Increase in the cerebrospinal fluid content of neurosteroids in patients with unipolar major depression who are receiving fluoxetine or fluvoxamine. *Proc. Natl. Acad. Sci. U.S.A.* 95, 3239–3244. doi: 10.1073/pnas.95.6.3239

Vaiva, G., Boss, V., Ducrocq, F., Fontaine, M., Devos, P., Brunet, A., et al. (2006). Relationship between posttrauma GABA plasma levels and PTSD at 1-year follow-up. *Am. J. Psychiatry* 163, 1446–1448. doi: 10.1176/ajp.2006.163.8.1446

Vaiva, G., Thomas, P., Ducrocq, F., Fontaine, M., Boss, V., Devos, P., et al. (2004). Low posttrauma GABA plasma levels as a predictive factor in the development of acute posttraumatic stress disorder. *Biol. Psychiatry* 55, 250–254. doi: 10.1016/j.biopsych.2003.08.009

Valentinuzzi, V. S., Kolker, D. E., Vitaterna, M. H., Shimomura, K., Whiteley, A., Low-Zeddies, S., et al. (1998). Automated measurement of mouse freezing behavior and its

use for quantitative trait locus analysis of contextual fear conditioning in (BALB/cJ x C57BL/6J)F2 mice. *Learn. Mem. (Cold Spring Harbor, N.Y.)* 5, 391–403.

Vasterling, J., and Brewin, C. R. (2005). *Neuropsychology of PTSD : Biological, cognitive, and clinical perspectives*. New York, NY: Guilford Press.

Verkuyl, J. M., and Joëls, M. (2003). Effect of adrenalectomy on miniature inhibitory postsynaptic currents in the paraventricular nucleus of the hypothalamus. *J. Neurophysiol.* 89, 237–245. doi: 10.1152/jn.00401.2002

Verkuyl, J. M., Karst, H., and Joëls, M. (2005). GABAergic transmission in the rat paraventricular nucleus of the hypothalamus is suppressed by corticosterone and stress. *Eur. J. Neurosci.* 21, 113–121. doi: 10.1111/j.1460-9568.2004.03846.x

Viola, J., Ditzler, T., Batzer, W., Harazin, J., Adams, D., Lettich, L., et al. (1997). Pharmacological management of post-traumatic stress disorder: clinical summary of a five-year retrospective study, 1990-1995. *Military Med.* 162, 616–619.

Wilensky, A. E., Schafe, G. E., Kristensen, M. P., and LeDoux, J. E. (2006). Rethinking the fear circuit: the central nucleus of the amygdala is required for the acquisition, consolidation, and expression of Pavlovian fear conditioning. *J. Neurosci.* 26, 12387–12396. doi: 10.1523/JNEUROSCI.4316-06.2006

Wilson, J., and Keane, T. M. (1997). *Assessing psychological trauma and PTSD*. New York, NY: Guilford Press.

Wolfe, J., Chrestman, K. R., Ouimette, P. C., Kaloupek, D., Harley, R. M., and Bucsela, M. (2000). Trauma-related psychophysiological reactivity in women exposed to war-zone stress. *J. Clin. Psychol.* 56, 1371–1379. doi: 10.1002/1097-4679(200010)56:10<1371::AID-JCLP8<3.0.CO;2-X

Xu, W., and Südhof, T. C. (2013). A neural circuit for memory specificity and generalization. *Science (New York, N.Y.)* 339, 1290–1295. doi: 10.1126/science.1229534

Zannas, A., Provençal, N., and Binder, E. (2015). Epigenetics of posttraumatic stress disorder: Current evidence, challenges, and future directions. *Biol. Psychiatry* 78, 327–335. doi: 10.1016/j.biopsych.2015.04.003

Zhang, D., Pan, Z. H., Awobuluyi, M., and Lipton, S. A. (2001). Structure and function of GABA(C) receptors: A comparison of native versus recombinant receptors. *Trends Pharmacol. Sci.* 22, 121–132. doi: 10.1016/s0165-6147(00)01625-4

Zhang, S., and Cranney, J. (2008). The role of GABA and anxiety in the reconsolidation of conditioned fear. *Behav. Neurosci.* 122, 1295–1305. doi: 10.1037/a0013273

Frontiers in
Molecular Neuroscience

Leading research into the brain's molecular structure, design and function

Part of the most cited neuroscience series, this journal explores and identifies key molecules underlying the structure, design and function of the brain across all levels.

Discover the latest Research Topics

See more →

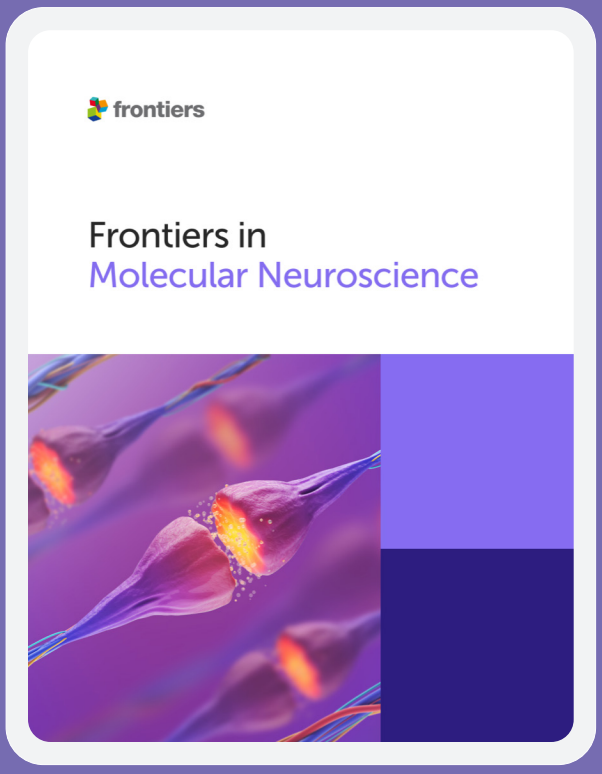

Frontiers

Avenue du Tribunal-Fédéral 34
1005 Lausanne, Switzerland
frontiersin.org

Contact us

+41 (0)21 510 17 00
frontiersin.org/about/contact